Research Topics

Exercise and biomechanical intervention in the prevention, management and rehabilitation of neuro-musculoskeletal disorders

Edited by
Qichang Mei, Yumeng Li and Kwong Ming Tse

Published in
Frontiers in Bioengineering and Biotechnology
Frontiers in Physiology
Frontiers in Sports and Active Living

ISSN 1664-8714
ISBN 978-2-8325-3226-3
DOI 10.3389/978-2-8325-3226-3

About Frontiers

Frontiers is more than just an open access publisher of scholarly articles: it is a pioneering approach to the world of academia, radically improving the way scholarly research is managed. The grand vision of Frontiers is a world where all people have an equal opportunity to seek, share and generate knowledge. Frontiers provides immediate and permanent online open access to all its publications, but this alone is not enough to realize our grand goals.

Frontiers journal series

The Frontiers journal series is a multi-tier and interdisciplinary set of open-access, online journals, promising a paradigm shift from the current review, selection and dissemination processes in academic publishing. All Frontiers journals are driven by researchers for researchers; therefore, they constitute a service to the scholarly community. At the same time, the *Frontiers journal series* operates on a revolutionary invention, the tiered publishing system, initially addressing specific communities of scholars, and gradually climbing up to broader public understanding, thus serving the interests of the lay society, too.

Dedication to quality

Each Frontiers article is a landmark of the highest quality, thanks to genuinely collaborative interactions between authors and review editors, who include some of the world's best academicians. Research must be certified by peers before entering a stream of knowledge that may eventually reach the public - and shape society; therefore, Frontiers only applies the most rigorous and unbiased reviews. Frontiers revolutionizes research publishing by freely delivering the most outstanding research, evaluated with no bias from both the academic and social point of view. By applying the most advanced information technologies, Frontiers is catapulting scholarly publishing into a new generation.

What are Frontiers Research Topics?

Frontiers Research Topics are very popular trademarks of the *Frontiers journals series*: they are collections of at least ten articles, all centered on a particular subject. With their unique mix of varied contributions from Original Research to Review Articles, Frontiers Research Topics unify the most influential researchers, the latest key findings and historical advances in a hot research area.

Find out more on how to host your own Frontiers Research Topic or contribute to one as an author by contacting the Frontiers editorial office: frontiersin.org/about/contact

Exercise and biomechanical intervention in the prevention, management and rehabilitation of neuro-musculoskeletal disorders

Topic editors
Qichang Mei — Ningbo University, China
Yumeng Li — Texas State University, United States
Kwong Ming Tse — Swinburne University of Technology, Australia

Citation
Mei, Q., Li, Y., Tse, K. M., eds. (2023). *Exercise and biomechanical intervention in the prevention, management and rehabilitation of neuro-musculoskeletal disorders*. Lausanne: Frontiers Media SA. doi: 10.3389/978-2-8325-3226-3

Table of contents

frontiers | Frontiers in Physiology

TYPE Editorial
PUBLISHED 31 July 2023
DOI 10.3389/fphys.2023.1260147

Check for updates

OPEN ACCESS

EDITED AND REVIEWED BY
Giuseppe D'Antona,
University of Pavia, Italy

*CORRESPONDENCE
Qichang Mei,
qmei907@aucklanduni.ac.nz

RECEIVED 17 July 2023
ACCEPTED 20 July 2023
PUBLISHED 31 July 2023

CITATION
Mei Q (2023), Editorial: Exercise and biomechanical intervention in the prevention, management and rehabilitation of neuro-musculoskeletal disorders.
Front. Physiol. 14:1260147.
doi: 10.3389/fphys.2023.1260147

Editorial: Exercise and biomechanical intervention in the prevention, management and rehabilitation of neuro-musculoskeletal disorders

Qichang Mei[1,2,3]*

[1]Faculty of Sports Science, Ningbo University, Ningbo, China, [2]Research Academy of Grand Health, Ningbo University, Ningbo, China, [3]Auckland Bioengineering Institute, The University of Auckland, Auckland, New Zealand

KEYWORDS

sport injury, spine biomechanics, lower extremity, ACL, foot and ankle, computational biomechanics, rehabilitation

Editorial on the Research Topic
Exercise and biomechanical intervention in the prevention, management and rehabilitation of neuro-musculoskeletal disorders

Neuromusculoskeletal biomechanics has been a popular tool for understanding the disorders of the human motor system in everyday and sports-specific activities and clinical practice. Recently, the interdisciplinary fusion of techniques has been widely employed in the prevention, management, and rehabilitation of neuromusculoskeletal disorders. With the rapid development of technologies over the past decades, cross-platform challenges have been overcome, specifically from subject-specific to population-based studies, from exercise intervention and rigid dynamics to continuum mechanical loading, training adaptability, and local tissue damage. The interest in promoting neuromusculoskeletal health with either experimental or computational techniques, or even combining the approaches, would offer promising plausibility for the prevention and rehabilitation of motor disorders or diseases.

With this in mind, the editorial team organized this Research Topic (RT) to serve as a compendium of the above-mentioned techniques for understanding neuromusculoskeletal disorders. A total of 20 studies, including 16 original articles and four review articles, were collected for publication in the current Research Topic, entitled "*Exercise and Biomechanical Intervention in the Prevention, Management, and Rehabilitation of Neuromusculoskeletal Disorders*".

The exercise intervention studies covered gait retraining to facilitate arch function Shen et al. and found that a 12-week forefoot running program together with foot core exercises increases arch height and hallux strength. Prolonged static stretching can reduce quadriceps stiffness (particularly the rectus femoris and proximal patellar tendon) and improve knee range of motion Zhu et al. As with the Achilles tendon, a systematic review was conducted and found that eccentric strength training can improve power generation, and concentric strength training would improve balance and postural control for the rehabilitation of mid-portion Achilles tendinopathy (AT) Kim et al. Meanwhile, for a specific cohort, a systematic review of the physical exercise would improve muscle strength and reduce the pain in military pilots with neck and shoulder pain Heng et al. A combination of conventional and functional strength training showed benefits in the prevention of back pain in emergency responders Kong et al.

In order to address foot posture changes during running (Mei et al., 2019), an orthotic intervention for runners with pronated foot posture was developed to prevent potential running-related injuries (Cheng et al.; Zhang and Vanwanseele), and the center of pressure path was altered with redistributed plantar pressure loads and reduced forefoot motion in the pronated foot. Kinesio-type (KT) interventions have been used as an acute strategy to assist postural control after fatigue in athletes with functional ankle instability (FAI) Li et al. showing improved dynamic postural control and reduced risk of re-injury. ACL (anterior cruciate ligament) injury, with high risks in the knee joint, has attracted excellent studies, specifically the development of a Ligs digital arthrometer to investigate mechanical stresses and rupture mechanisms Li et al. In terms of functional recovery, an *in-vivo* evaluation of multiplanar kinematics in the knee joint during hopping activities Zhou et al. Other well-designed interventions involving strength training, proprioception, and sensation were conducted to support rehabilitation after ACL reconstruction Hu et al.; Ma et al. as different strategies for return-to-sport in patients.

Considering the pivotal role of the spine and trunk in the entire motor chain, any deformity, such as Adolescent Idiopathic Scoliosis (AIS), would lead to compensation in postural stability and gait performance Liu et al. showing the altered center of pressure trajectory patterns, pelvic motion, and gait spatiotemporal features. Computational finite element (FE) modeling, which has the advantage of being non-invasive and subject-specific, has been conducted mainly in spinal (thoracic or lumbar) disorders, with an evaluation of different fixations in the upper instrumented vertebra Pan et al. multiple pelvic screws and multirod construct Yang et al. and pedicle screw and cortical bone trajectory fixation Pei et al. The digitization of the different designs and the efficacy feedback from computational modeling could provide important clinical guidance prior to surgical correction. Furthermore, computational FE analysis for knee arthroplasty was systematically introduced and discussed, covering aspects of design and material selection and understanding of kinetic alignment and unilateral and total knee arthroplasty Zhang et al.

Neuromuscular control plays a crucial role in motor control during the execution of various tasks. Meanwhile, the disorders in the neural system, which were assessed and diagnosed using muscle synergies, have been systematically reviewed in the literature, covering the methodological Research Topic and clinical implications Beltrame et al. The handgrip task evaluation was measured with a novel sensor-embedded digital device to monitor upper extremity function and provide clinical implications for stroke and age-related function decline Ma et al. Hanger reflex intervention was performed to stimulate cervical muscle activation for rehabilitation Wang and Liu, reporting that cervical activities were substantially improved, with bilateral hanger reflex intervention showing a greater effect than unilateral hanger reflex intervention.

This Research Topic published the latest approaches to exercise and biomechanical intervention for neuromusculoskeletal disorders and several findings of practical and clinical importance. Due to the popularity of this Research Topic, we are currently organizing a second volume as a compendium for the multidisciplinary community, with a particular interest in the application of data-driven and Digital Twin (DT) technologies to understand neuromusculoskeletal disorders.

Author contributions

QM: Writing–original draft, Writing–review and editing.

Conflict of interest

The authors declare that the research was conducted in the absence of any commercial or financial relationships that could be construed as a potential conflict of interest.

Publisher's note

All claims expressed in this article are solely those of the authors and do not necessarily represent those of their affiliated organizations, or those of the publisher, the editors and the reviewers. Any product that may be evaluated in this article, or claim that may be made by its manufacturer, is not guaranteed or endorsed by the publisher.

References

Mei, Q., Gu, Y., Xiang, L., Baker, J. S., and Fernandez, J. (2019). Foot pronation contributes to altered lower extremity loading after long distance running. *Front. Physiology* 10, 573. doi:10.3389/fphys.2019.00573

frontiers | Frontiers in Bioengineering and Biotechnology

TYPE Original Research
PUBLISHED 15 August 2022
DOI 10.3389/fbioe.2022.958242

OPEN ACCESS

EDITED BY
Qichang Mei,
Ningbo University, China

REVIEWED BY
Ryoichi Ema,
Shizuoka Sangyo University, Japan
Tunc Akbas,
Harvard University, United States

*CORRESPONDENCE
Zhijie Zhang,
sportspt@163.com

SPECIALTY SECTION
This article was submitted to Biomechanics,
a section of the journal
Frontiers in Bioengineering and Biotechnology

RECEIVED 31 May 2022
ACCEPTED 11 July 2022
PUBLISHED 15 August 2022

CITATION
Zhu Y, Feng Y, Huang F, Li Y, Wang W, Wang X, Cao X and Zhang Z (2022), Changes in stiffness of the specific regions of knee extensor mechanism after static stretching.
Front. Bioeng. Biotechnol. 10:958242.
doi: 10.3389/fbioe.2022.958242

Changes in stiffness of the specific regions of knee extensor mechanism after static stretching

Yuanchun Zhu[1], Yanan Feng[2], Fangchao Huang[2], Yapeng Li[2], Wenjing Wang[1], Xueqiang Wang[1], Xiangyang Cao[2] and Zhijie Zhang[2]*

[1]Department of Sport Rehabilitation, Shanghai University of Sport, Shanghai, China, [2]Rehabilitation Therapy Center, Luoyang Orthopedic Hospital of Henan Province, Orthopedic Hospital of Henan Province, Luoyang, China

Decreased muscle stiffness could reduce musculotendinous injury risk in sports and rehabilitation settings. Static stretching (SS) has been used to increase the flexibility of muscles and reduce muscle stiffness, but the effects of SS on the stiffness of specific regions of the knee extensor mechanism are unclear. The quadriceps femoris and patellar tendon are essential components of the knee extensor mechanism and play an important role in knee motion. Therefore, we explored the acute and prolonged effects of SS on the stiffness of the quadriceps femoris and patellar tendon and knee flexion range of motion (ROM). Thirty healthy male subjects participated in the study. Three 60-s SS with 30-s intervals were conducted in right knee flexion with 30° hip extension. We measured the ROM and stiffness of the vastus medialis (VM), vastus lateralis (VL), and rectus femoris (RF) and the proximal-(PPT), middle-(MPT), and distal-(DPT) region stiffness of the patellar tendon before and immediately after SS intervention, or 5 and 10 min after SS. The stiffness of the quadriceps muscle and patellar tendon were measured using MyotonPRO, and the knee flexion ROM was evaluated using a medical goniometer. Our outcomes showed that the ROM was increased after SS intervention in all-time conditions ($p < 0.01$). Additionally, the results showed that the stiffness of RF ($p < 0.01$) and PPT ($p = 0.03$) were decreased immediately after SS intervention. These results suggested that SS intervention could be useful to increase knee flexion ROM and temporarily reduce the stiffness of specific regions of the knee extensor mechanism.

KEYWORDS

stiffness, knee extensor mechanism, quadriceps, patellar tendon, static stretching, range of motion (ROM)

Introduction

The knee extensor mechanism refers to the convergence of the four quadriceps muscles into the quadriceps tendon, which is attached to the proximal patella and extends distally to the tibial tuberosity through the patellar tendon (Dan et al., 2018). The muscle and tendon play a crucial role in the extension and flexion of the knee joint, which enables the efficient functioning of the knee extensor mechanism in stabilization and locomotion (Ostlere, 2013). Regarding muscle strain incidence, quadriceps femoris [especially the rectus femoris (RF)] is one of the most frequently affected (Cross et al., 2004; Orchard et al., 2020). Previous studies found that higher muscle–tendon unit stiffness could contribute to impaired function and decreased range of motion (ROM) (Watsford et al., 2010; Geertsen et al., 2015). Stiffness is one of the mechanical properties associated with the muscle and tendon adaptation process, representing the relationship between the force imposed on soft tissue and the deformation it applies (Bohm et al., 2015). To reduce muscle strain and improve joint ROM, it is crucial to reduce the stiffness of muscle and tendon (Watsford et al., 2010; Geertsen et al., 2015).

Static stretching (SS) is commonly utilized to increase muscle flexibility, decrease muscle stiffness, and reduce musculotendinous injury risk in sports and rehabilitation settings (Malliaropoulos et al., 2004; Morse et al., 2008; Konrad et al., 2017). A systematic review revealed that the four factors related to the impact of stretching on flexibility are intervention frequency, duration, position, and intensity (Apostolopoulos et al., 2015). Flexibility is usually assessed by measuring the ROM. Recently, Nakamura et al. reported the acute effect of 180-s of three different SS intensities on the ROM and the passive stiffness of quadriceps muscles, with results showing that the ROM was increased after 100% and 120% (high) intensities of SS intervention and only the RF stiffness was reduced significantly after 100% intensity SS (Nakamura et al., 2020). However, this study has a limitation: only acute effects were investigated. Past studies reported that SS acutely reduces the stiffness of gastrocnemius (Konrad et al., 2019) and hamstrings (Hatano et al., 2019). Hatano et al. (2019) reported that hamstrings stiffness decreased significantly 20 min after SS, and knee ROM increased significantly 30 min after SS. A limited number of research studies have explored the acute effect of SS on quadriceps stiffness and knee flexion ROM (Nakamura et al., 2020; Takeuchi et al., 2021). Nevertheless, none of the studies examined the chronic effects of SS on quadriceps stiffness and knee flexion ROM.

In addition, muscular function and integrity are close-knit and are related to variations in the mechanical properties of tendons (McCrum et al., 2018). Some researchers reported that tendon stiffness reduced after 300 s of SS (Kubo et al., 2002; Burgess et al., 2009). However, Kay et al. found that 3 min of SS decreased muscle stiffness but there was no change in Achilles tendon stiffness (Kay and Blazevich, 2009). Thus, the effects of SS interventions on tendon properties remain unclear. Moreover, to the best of our knowledge, no study has explored the acute and prolonged effects of SS on specific regions of patellar tendon stiffness. Thus, the purpose of our study was to investigate 1) the acute and prolonged effects of SS intervention on the knee flexion ROM and 2) the acute and prolonged effects of SS intervention on the stiffness of the proximal (PPT), middle (MPT), and distal (DPT) regions of the patellar tendon and the vastus medialis (VM), vastus lateralis (VL), and RF. We hypothesized that there would be a significant decrease in RF stiffness and a significant increase in knee ROM, both of which would persist for all testing periods after stretching. Furthermore, we hypothesized that the stiffness of the patellar tendon does not change before and after stretching. We believed that significant ROM and RF stiffness changes after SS might reduce the risk of knee extensor mechanism injuries such as RF strain in physical therapy and rehabilitation practice.

Materials and methods

Experimental design

A repeated measures experimental design was conducted to examine the acute and prolonged impacts of SS protocol (100% intensity and 3 min duration) on ROM, stiffness of the quadriceps (VM, VL, and RF), and patellar tendon (PPT, MPT, and DPT) in the lead extremity (ball kicking preference). Our SS intensity and duration option refers to a previous study (Nakamura et al., 2020). The dominant extremity of all participants was the right leg. In this study, the ROM and stiffness of the quadriceps muscles and patellar tendon were examined before (PRE) and immediately after SS (POST), or 5 (POST 5) and 10 (POST 10) min after SS. As for this measurement sequence, we measured the knee flexion ROM first and then assessed the stiffness.

Participants

Thirty healthy male volunteers (21.5 ± 1.2 years, 176.5 ± 5.2 cm, and 70.4 ± 6.3 kg) were recruited for this experiment. Participants who regularly performed strength and flexibility training or had a history of neuromuscular diseases and lower limb musculoskeletal system injuries were excluded. All volunteers were requested not to conduct flexibility or resistance training of the lower extremities for the duration of the experiment. All volunteers signed written informed consent to participate in the present study. This research was approved by the Ethics Committee of the Luoyang Orthopedic Hospital of Henan Province (KY 2020-003-02), China, and conformed to the Declaration of Helsinki.

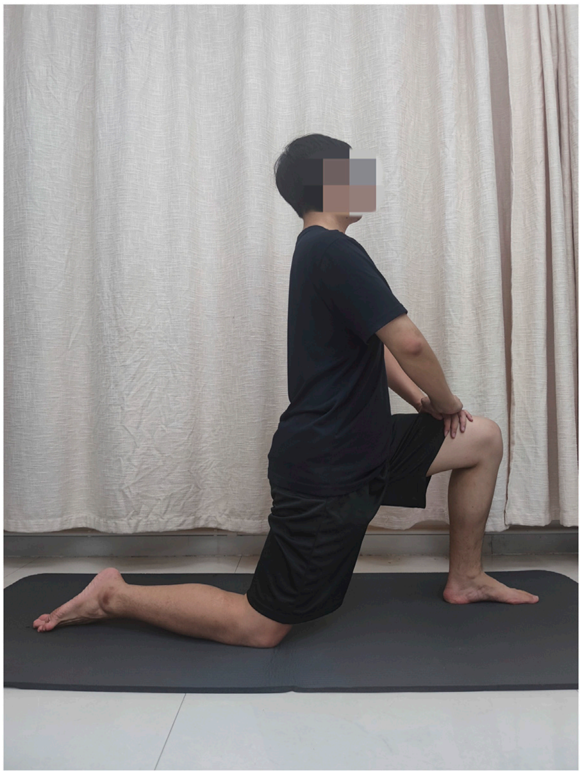

FIGURE 1
Reference extremity posture of static stretching (SS).

Knee flexion ROM

The methodology for assessing ROM was the same as that of the previous study (Takeuchi et al., 2021). Subjects were positioned with the left hip and knee flexed at 90° and the right limb with the knee flexed and the hip extended at 30° as the reference extremity posture (Figure 1). Then, the researcher flexed the knee slowly and passively from the reference extremity posture to the angle just before the volunteers began to feel pain or discomfort (Nakamura et al., 2020). We used a medical goniometer to measure the ROM twice and the mean value for the subsequent analysis.

Equipment

The MyotonPRO (Myoton AS, Tallinn, Estonia) is a non-invasive portable machine utilized to quantify tendon and muscle stiffness in this study. The device works by exerting a small mechanical impact on the tissue of interest area, perpendicular to the skin surfaces. The probe's tip is then pushed to the measured site to reach the desired depth. After the red light turns green, the machine automatically implements five short pulses (0.8 s between taps) to cause mechanical oscillations of the tissue. According to the previous study, we found good intra- and inter-tester reliability for measuring the stiffness of the quadricep muscles and patellar tendon using the MyotonPRO (Chen et al., 2019). MyotonPRO recorded the parameters of stiffness. Stiffness was described as newtons/meter (N/m). The higher the value, the stiffer the soft tissue.

Stiffness measurements of quadriceps muscle and patellar tendon

We measured the stiffness of the VM, VL, RF, PPT, MPT, and DPT using MyotonPRO. All subjects were tested in the same physical therapy room, and measurements were performed at the ambient temperature of 25°C in a relaxed position with knee and hip flexed at 90°. The stiffness of the RF at the reproducible location is about two-thirds of the distance between the anterior superior iliac spine and the patella apex (Agyapong-Badu et al., 2016). In order to locate the VM and VL's muscular abdomen more accurately, participants were asked to actively extend their hip and knee joints. The most prominent site of each muscle belly was used as a measurement point (Chen et al., 2019). The stiffness of the patellar tendon was measured at defined anatomic areas (PPT, the patella apex as a superior landmark; MPT, the middle of the patellar tendon between the patella apex and tibial insertion; and DPT, tibial insertion as a distal landmark) (Dickson et al., 2020). All testing sites were marked on the skin by Yuanchun Zhu using a non-toxic pen. We measured the stiffness of each position five times and used the average value for analysis.

Before the SS intervention maneuver, we randomly examined the test–retest reliability of stiffness measurement for the quadriceps femoris and patellar tendon using ten limbs in ten healthy male subjects.

Static stretching

The SS maneuver was conducted similar to the ROM measurement. The 100% intensity of SS intervention was determined by the ROM in the PRE value just before the volunteers began to feel pain or discomfort (Nakamura et al., 2020). Three 60-s SS with 30-s intervals were conducted with the same knee flexion angle. Subjects were required to remain relaxed and hold their trunk upright during SS duration. During the rest period of each SS, the subjects lay on the treatment couch in the supine position and remained completely relaxed.

Statistical analyses

All descriptive data are presented as means ± standard deviation. The statistical analyses were conducted using SPSS (version 26.0, IBM, United States). The Shapiro–Wilk test was utilized to examine the normality of all data. Measurement

TABLE 1 Reliability assessment of stiffness measurements (Mean ± SD).

	Test	Retest	ICC (95%CI)	CV (%)
RF (N/m)	268.3 ± 34.3	268.4 ± 34.0	0.950 (0.810–0.987)	12.4
VM (N/m)	292.3 ± 34.0	288.7 ± 37.3	0.985 (0.923–0.996)	12.0
VL (N/m)	385.6 ± 56.4	382.4 ± 58.4	0.993 (0.971–0.998)	14.6
PPT (N/m)	821.1 ± 117.1	821.8 ± 126.4	0.983 (0.933–0.996)	14.4
MPT (N/m)	620.2 ± 105.7	622.7 ± 106.2	0.991 (0.966–0.998)	16.6
DPT (N/m)	714.5 ± 123.7	723.6 ± 131.4	0.979 (0.924–0.995)	17.3

RF, rectus femoris; VM, vastus medialis; VL, vastus lateralis; PPT, proximal patellar tendon; MPT, middle patellar tendon; DPT, distal patellar tendon; ICC, intraclass correlation coefficient; CV, coefficient variation.

TABLE 2 Changes in RF, VM, VL, PPT, MPT, and DPT stiffness and knee flexion ROM before and after the static stretching intervention (Mean ± SD).

	PRE	POST	POST 5	POST 10
RF (N/m)	274.7 ± 39.1	258.4 ± 38.2**	266.4 ± 38.7##	270.0 ± 37.4##
VM (N/m)	295.4 ± 43.8	292.1 ± 40.9	293.9 ± 39.7	298.3 ± 40.5
VL (N/m)	366.2 ± 51.2	363.5 ± 48.4	364.4 ± 51.2	367.1 ± 50.7
PPT (N/m)	858.3 ± 92.2	831.0 ± 90.9*	849.4 ± 100.7	852.7 ± 96.2#
MPT (N/m)	635.7 ± 109.7	641.4 ± 113.1	646.9 ± 116.3	642.2 ± 107.2
DPT (N/m)	744.1 ± 114.2	754.5 ± 105.7	755.2 ± 104.3	753.1 ± 104.5
ROM (°)	123.2 ± 7.1	132.9 ± 5.1**	127.7 ± 5.6**,##	125.2 ± 5.9**,##,†

PRE, before the SS; POST, immediately after the SS; POST 5, 5 min after the SS; POST 10, 10 min after the SS; RF, rectus femoris; VM, vastus medialis; VL, vastus lateralis; PPT, proximal patellar tendon; MPT, middle patellar tendon; DPT, distal patellar tendon; ROM, range of motion.
*$p < 0.05$; significant difference with PRE.
**$p < 0.01$; significant difference with PRE.
#$p < 0.05$; significant difference with POST.
##$p < 0.01$; significant difference with POST.
†$p < 0.01$; significant difference with POST 5.

test–retest reliability was analyzed using the intraclass correlation coefficient and coefficient variation. We executed a one-way repeated measure analysis of variance (ANOVA) to assess time effects (PRE vs POST vs POST 5 vs POST 10) for the ROM. For the stiffness, a two-way repeated measure ANOVA was utilized to evaluate [time (PRE vs POST vs POST 5 vs POST 10) and regions (RF vs VM vs VL vs PPT vs MPT vs DPT)] and analyze the main and interaction effect. Post-hoc analyses using Bonferroni multiple comparison tests were performed if a significant interaction effect was detected. Statistical significance was considered as p values <0.05.

Results

Reliability of the stiffness measurements

Good test–retest reliability (ICC, CV) was found for the stiffness measurements of the quadriceps and patellar tendon (Table 1).

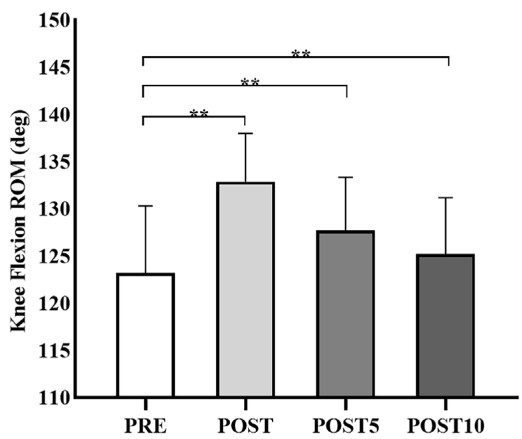

FIGURE 2
Knee flexion range of motion (ROM) changes before (PRE) and immediately after static stretching (POST), or 5 (POST 5) and 10 (POST 10) min after static stretching. **$p < 0.01$.

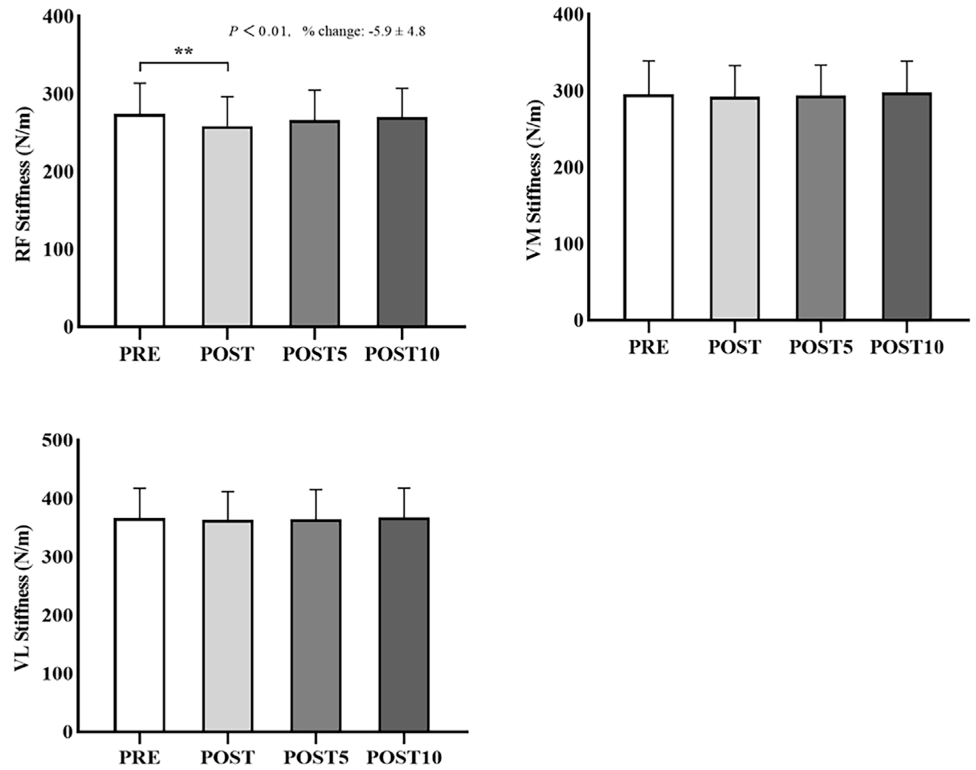

FIGURE 3
Stiffness changes of the rectus femoris (RF), vastus medialis (VM), and vastus lateralis (VL) muscles before (PRE) and immediately after static stretching (POST), or 5 (POST 5) and 10 (POST 10) min after static stretching. $**p < 0.01$.

Changes in the knee flexion ROM

The changes in the ROM before and after SS are shown in Table 2 and Figure 2. The ROM after SS in all-time conditions was greater than that before SS intervention ($p < 0.01$). There was a significant increase in knee flexion ROM after the SS intervention ($p < 0.01$). In addition, the post-hoc test revealed that the knee flexion ROM was significantly higher in POST and POST 5 than in POST 10 ($p < 0.01$).

Changes in the stiffness

The stiffness changes of the patellar tendon and quadriceps muscles before and after SS are shown in Table 2 and Figures 3 and 4. The two-way repeated ANOVA revealed a significant interaction effect ($p = 0.02$, F = 2.00, $\eta_p^2 = 0.05$) and the significant time effect in the stiffness of RF and PPT ($p < 0.01$, F = 16.93, $\eta_p^2 = 0.65$; $p = 0.03$, F = 3.87, $\eta_p^2 = 0.30$, respectively). When comparing time points between PRE and POST in the SS intervention, the Bonferroni's test revealed a significant decrease in the stiffness of RF and PPT ($p < 0.01$, 95% confidence interval, 9.0–23.6; $p = 0.03$, 95% confidence interval, 2.0–52.7), whereas no significant differences were found in POST 5 and POST 10 compared with PRE stiffness. In addition, there was no significant change in VM, VL, MPT, and DPT stiffness after the SS intervention compared with PRE stiffness.

Discussion

The present research study explored the acute and prolonged effects of SS intervention on the ROM and VM, VL, and RF muscle stiffness and PPT, MPT, and DPT tendon stiffness. Accordingly, the major findings of our study were that 1) the SS intervention increased the knee flexion ROM, and this change was continued till 10 min after SS; and 2) the RF stiffness and PPT stiffness significantly decreased after the SS, whereas this reduction was not sustained till 5 min after SS. Although some studies have investigated the effects of SS intervention on the gastrocnemius (Nakamura et al., 2011; Sato et al., 2020), hamstring (Hatano et al., 2019; Fukaya et al., 2021), and the quadriceps femoris (Nakamura et al., 2020; Takeuchi et al., 2021). Moreover, this is the first study to investigate the acute and prolonged effects of SS intervention on ROM and specific regions of stiffness of the patellar tendon and quadriceps muscle.

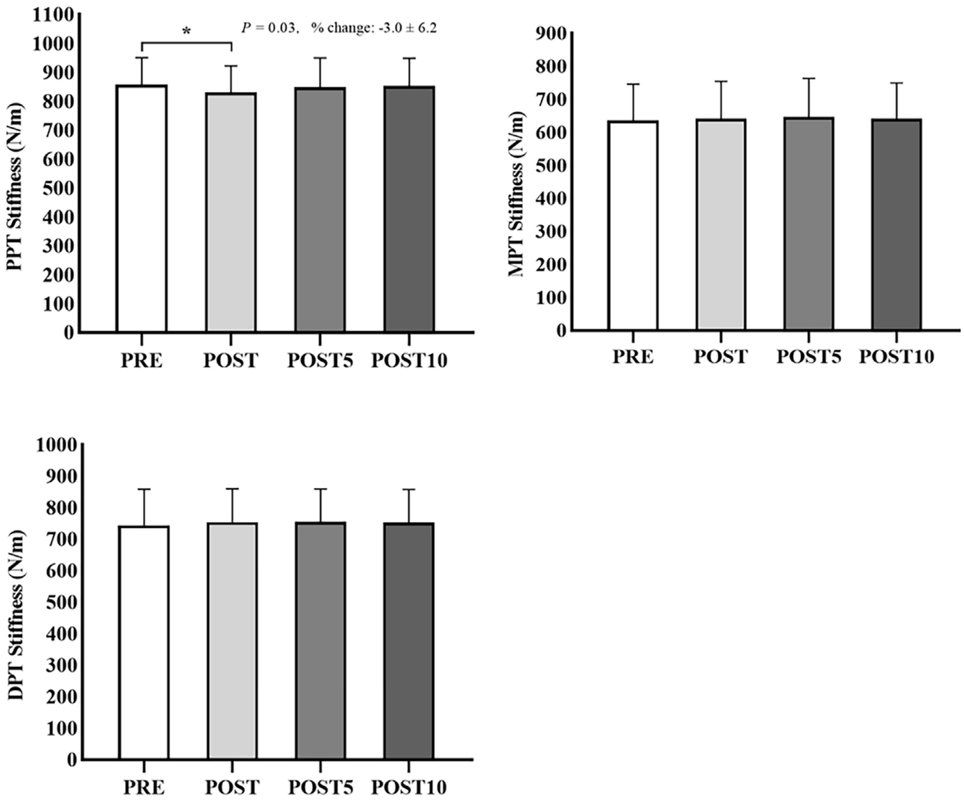

FIGURE 4
Stiffness changes of the proximal (PPT), middle (MPT), and distal (DPT) regions of the patellar tendon before (PRE) and immediately after static stretching (POST), or 5 (POST 5) and 10 (POST 10) min after static stretching. $^{*}p < 0.05$.

According to the study results, knee flexion ROM increased for 10 or more minutes after 100% intensity SS intervention. This acute effect was in alignment with the previous research (Nakamura et al., 2020), which revealed that 100% and 120% intensities of SS intervention immediately increased the knee flexion ROM. Kataura et al. (2017) found that high-intensity SS is more effective for decreasing stiffness and increasing ROM than low-intensity SS. Additionally, recent research explored the influences of SS with low intensity and long duration (50% and 240 s) or high intensity and short duration (120% and 100 s) on ankle dorsiflexion ROM, and results revealed that the ROM was significantly higher at (120% and 100 s) than that of (50% and 240 s) conditions after SS intervention (Fukaya et al., 2020). Therefore, the SS at greater intensity (100% intensity) performed in our study may reduce the SS duration required to decrease stiffness. A change in ROM after SS is related to changes in stretching tolerance (peak passive torque) and muscle stiffness (Behm et al., 2016). Recent studies have reported that the proposed mechanisms of ROM increase could be related to increased stretch tolerance modulation and the stretching sensation of the participants (Kay et al., 2015; Freitas et al., 2018). Previous studies have proposed increased stretch tolerance due to the reduction of the sensations of discomfort and pain accompanied by the modulation of neuropsychological factors after stretching (Folpp et al., 2006; Law et al., 2009). Similarly, Hatano et al. (2019) reported the chronic influence of 5 min of SS on hamstrings muscles and revealed that the increase in knee extension ROM lasted 30 or more minutes after SS intervention. Nevertheless, due to the differences in mechanical properties and muscle structure, the effects of SS on different muscles and joint ROM are still unclear and need to be investigated further, even when SS intervention of equal intensity and duration is performed.

The results of our study showed that RF muscle and PPT stiffness significantly decreased after SS, whereas there were no significant alterations in the VM, VL, MPT, and DPT stiffness. A previous study examined the effects of the 120% intensity with two different durations (1 and 3 min) and 110% intensity with 3-min duration SS intervention on RF muscle stiffness, and the authors reported a significant reduction in the 110% intensity SS group, but the stiffness of RF muscle was not changed in 120% intensity SS group (Takeuchi et al., 2021). These results revealed that the SS intensity is more crucial than duration in decreasing the RF stiffness (Takeuchi et al., 2021). Moreover, a recent study investigated the effects of three different SS intensities (80 vs 100 vs 120%) on the RF stiffness. Results showed that the RF stiffness decreased only after 100% intensity SS (Nakamura et al., 2020). Therefore, we used SS at 100% intensity for 3 min as our intervention parameters for this study. At 100% intensity, the RF stiffness was reduced significantly after the SS maneuver, with no changes in the stiffness of the VM and VL, which could be associated with the structural differences between the biarticular and monoarticular muscles. We used a flexed knee and extended hip stretch position, and the RF as a biarticular muscle may have been stretched more fully compared to the VM and VL muscles, resulting in the stiffness decrease. The stiffness changes after SS differed from what we hypothesized; according to the outcomes of the present study, the decreased RF stiffness recovered to baseline within 5 min. Assuming that the reduction in muscle stiffness is based on a stretch-induced increase in resting sarcomere length (Gajdosik, 2002), these results may be due to the impact of the sarcomere length recovered 5 min after SS. Therefore, the effect of SS interventions on the constitutive muscles of the quadriceps may be different. More investigation is needed on the influence of various types of stretching on the stiffness of each muscle that makes up the quadriceps.

Interestingly, the SS intervention only significantly decreased the PPT stiffness, whereas there were no significant alterations in the MPT and DPT stiffness. Decreased tendon stiffness after SS training was also reported by Kubo et al. (2002). Nakamura et al. (2013) reported that 5 min SS increased the tendon stiffness. However, other researchers found unchanged tendon stiffness after a single SS intervention (Kay and Blazevich, 2009; Kay et al., 2015). Indeed, the change in tendon stiffness induced by SS has been debated among investigators. One possible interpretation for the contradictory results of the effect of SS on changes in tendon stiffness could be the methodological differences (e.g., measurement area, stretching time, stretching method, and strength). Moreover, the patellar tendon architecture of humans is depicted as viscoelastic, which is sensitive to increased mechanical loading environment and adapts by altering its material, morphological, and mechanical properties (Kongsgaard et al., 2007; Seynnes et al., 2009). Indeed, a previous study has demonstrated that the prominent histopathological changes of the patellar tendon typically occur in the proximal region accompanied by reduced tendon stiffness (Wiesinger et al., 2020), which may present a deficit concerning muscle function (Pearson and McMahon, 2012; Pearson and Hussain, 2014). Previous studies have reported a possible increase in tendon displacement during stretching, resulting in decreased tendon stiffness (Kubo et al., 2002; Burgess et al., 2009). We also considered that the difference in stress applied to the patellar tendon during the SS intervention might decrease PPT stiffness. Nevertheless, the mechanism of this temporary decrease in stiffness in specific areas of the patellar tendon after SS remains unclear, and whether this change in stiffness is associated with pathological changes in the patellar tendon requires further study. Previous studies found that the higher muscle–tendon unit stiffness could contribute to impaired function and decreased ROM (Watsford et al., 2010; Geertsen et al., 2015). SS is commonly utilized to increase muscle flexibility, decrease muscle stiffness, and reduce musculotendinous injury risk in exercise and rehabilitation settings (Malliaropoulos et al., 2004; Konrad et al., 2017). Additionally, flexibility is usually assessed by measuring the ROM. Our study showed that knee ROM was significantly increased after SS, and stiffness of RF and PPT was significantly decreased after SS. This suggested that when we intervene with 3 min of 100% intensity SS in physical therapy and rehabilitation practice, it may reduce the risk of knee extensor mechanism injuries such as RF strains.

There were several limitations in this study. First, the subjects were not regular exercisers. Thus, it is necessary to investigate the influences of SS intervention in athletes who regularly perform exercise training. Second, we did not consider female subjects in the study, although it is well known that there are differences in structure and function between the sexes. Third, the SS intensity was determined by reference to ROM (Nakamura et al., 2020; Takeuchi et al., 2021). However, ROM is influenced by subjective factors of stretching tolerance. Fourth, we did not include a control group without SS intervention. Thus, future studies should investigate the effect of SS on the stiffness of specific regions of the knee extensor mechanism in gender-specific athletes and sedentary populations.

Conclusion

The results showed that the SS intervention increased the knee flexion ROM, and this change was continued till 10 min after SS; the RF stiffness and PPT stiffness significantly decreased after the SS intervention, whereas this reduction was not sustained till 5 min after SS. It is suggested that SS intervention could be useful to increase ROM and temporarily reduce the stiffness of specific regions of the knee extensor mechanism. However, SS interventions with different stretching intensities and durations for further studies are necessary to investigate whether they effectively prevent injuries related to the quadriceps and patellar tendon.

Data availability statement

The original contributions presented in the study are included in the article/Supplementary Material; further inquiries can be directed to the corresponding author.

Ethics statement

The studies involving human participants were reviewed and approved by The Ethics Committee of the Luoyang Orthopedic Hospital of Henan Province (KY 2020-003-02). The patients/ participants provided their written informed consent to participate in this study.

Author contributions

Y-CZ, X-QW, X-YC, and Z-JZ designed this study. Y-CZ, Y-NF, F-CH, and W-JW performed the experiments and collected data. Y-CZ, Y-NF, Z-JZ, and Y-PL analyzed the experimental data. Y-CZ and Y-NF drafted the manuscript. All authors agreed with the submission of this manuscript.

Funding

This research was supported by the Project of Science Research of Traditional Chinese Medicine of Henan Province of China (2019ZY1028).

Acknowledgments

This study was supported by the rehabilitation therapy center of Luoyang Orthopedic Hospital in Henan Province.

Conflict of interest

The authors declare that the research was conducted in the absence of any commercial or financial relationships that could be construed as a potential conflict of interest.

Publisher's note

All claims expressed in this article are solely those of the authors and do not necessarily represent those of their affiliated organizations, or those of the publisher, the editors, and the reviewers. Any product that may be evaluated in this article, or claim that may be made by its manufacturer, is not guaranteed or endorsed by the publisher.

References

Agyapong-Badu, S., Warner, M., Samuel, D., and Stokes, M. (2016). Measurement of ageing effects on muscle tone and mechanical properties of rectus femoris and biceps brachii in healthy males and females using a novel hand-held myometric device. *Arch. Gerontol. Geriatr.* 62, 59–67. doi:10.1016/j.archger.2015.09.011

Apostolopoulos, N., Metsios, G. S., Flouris, A. D., Koutedakis, Y., and Wyon, M. A. (2015). The relevance of stretch intensity and position-a systematic review. *Front. Psychol.* 6, 1128. doi:10.3389/fpsyg.2015.01128

Behm, D. G., Blazevich, A. J., Kay, A. D., and McHugh, M. (2016). Acute effects of muscle stretching on physical performance, range of motion, and injury incidence in healthy active individuals: A systematic review. *Appl. Physiol. Nutr. Metab.* 41 (1), 1–11. doi:10.1139/apnm-2015-0235

Bohm, S., Mersmann, F., and Arampatzis, A. (2015). Human tendon adaptation in response to mechanical loading: A systematic review and meta-analysis of exercise intervention studies on healthy adults. *Sports Med. Open* 1 (1), 7. doi:10.1186/s40798-015-0009-9

Burgess, K. E., Graham-Smith, P., and Pearson, S. J. (2009). Effect of acute tensile loading on gender-specific tendon structural and mechanical properties. *J. Orthop. Res.* 27 (4), 510–516. doi:10.1002/jor.20768

Chen, G., Wu, J., Chen, G., Lu, Y., Ren, W., Xu, W., et al. (2019). Reliability of a portable device for quantifying tone and stiffness of quadriceps femoris and patellar tendon at different knee flexion angles. *PLoS One* 14 (7), e0220521. doi:10.1371/journal.pone.0220521

Cross, T. M., Gibbs, N., Houang, M. T., and Cameron, M. (2004). Acute quadriceps muscle strains: Magnetic resonance imaging features and prognosis. *Am. J. Sports Med.* 32 (3), 710–719. doi:10.1177/0363546503261734

Dan, M., Parr, W., Broe, D., Cross, M., and Walsh, W. R. (2018). Biomechanics of the knee extensor mechanism and its relationship to patella tendinopathy: A review. *J. Orthop. Res.* 36 (12), 3105–3112. doi:10.1002/jor.24120

Dickson, D. M., Fawole, H. O., Hendry, G. J., and Smith, S. L. (2020). Intermachine variation of ultrasound strain elastographic measures of the quadriceps and patellar tendons in healthy participants: Implications for clinical practice. *J. Ultrasound Med.* 39 (7), 1343–1353. doi:10.1002/jum.15228

Folpp, H., Deall, S., Harvey, L. A., and Gwinn, T. (2006). Can apparent increases in muscle extensibility with regular stretch be explained by changes in tolerance to stretch? *Aust. J. Physiother.* 52 (1), 45–50. doi:10.1016/s0004-9514(06)70061-7

Freitas, S. R., Mendes, B., Le Sant, G., Andrade, R. J., Nordez, A., Milanovic, Z., et al. (2018). Can chronic stretching change the muscle-tendon mechanical properties? A review. *Scand. J. Med. Sci. Sports* 28 (3), 794–806. doi:10.1111/sms.12957

Fukaya, T., Kiyono, R., Sato, S., Yahata, K., Yasaka, K., Onuma, R., et al. (2020). Effects of static stretching with high-intensity and short-duration or low-intensity and long-duration on range of motion and muscle stiffness. *Front. Physiol.* 11, 601912. doi:10.3389/fphys.2020.601912

Fukaya, T., Matsuo, S., Iwata, M., Yamanaka, E., Tsuchida, W., Asai, Y., et al. (2021). Acute and chronic effects of static stretching at 100% versus 120% intensity on flexibility. *Eur. J. Appl. Physiol.* 121 (2), 513–523. doi:10.1007/s00421-020-04539-7

Gajdosik, R. L. (2002). Relationship between passive properties of the calf muscles and plantarflexion concentric isokinetic torque characteristics. *Eur. J. Appl. Physiol.* 87 (3), 220–227. doi:10.1007/s00421-002-0624-2

Geertsen, S. S., Kirk, H., Lorentzen, J., Jorsal, M., Johansson, C. B., Nielsen, J. B., et al. (2015). Impaired gait function in adults with cerebral palsy is associated with reduced rapid force generation and increased passive stiffness. *Clin. Neurophysiol.* 126 (12), 2320–2329. doi:10.1016/j.clinph.2015.02.005

Hatano, G., Suzuki, S., Matsuo, S., Kataura, S., Yokoi, K., Fukaya, T., et al. (2019). Hamstring stiffness returns more rapidly after static stretching than range of motion, stretch tolerance, and isometric peak torque. *J. Sport Rehabil.* 28 (4), 325–331. doi:10.1123/jsr.2017-0203

Kataura, S., Suzuki, S., Matsuo, S., Hatano, G., Iwata, M., Yokoi, K., et al. (2017). Acute effects of the different intensity of static stretching on flexibility and isometric muscle force. *J. Strength Cond. Res.* 31 (12), 3403–3410. doi:10.1519/jsc.0000000000001752

Kay, A. D., and Blazevich, A. J. (2009). Moderate-duration static stretch reduces active and passive plantar flexor moment but not Achilles tendon stiffness or active muscle length. *J. Appl. Physiol. (1985).* 106 (4), 1249–1256. doi:10.1152/japplphysiol.91476.2008

Kay, A. D., Husbands-Beasley, J., and Blazevich, A. J. (2015). Effects of contract-relax, static stretching, and isometric contractions on muscle-tendon mechanics. *Med. Sci. Sports Exerc.* 47 (10), 2181–2190. doi:10.1249/mss.0000000000000632

Kongsgaard, M., Reitelseder, S., Pedersen, T. G., Holm, L., Aagaard, P., Kjaer, M., et al. (2007). Region specific patellar tendon hypertrophy in humans following resistance training. *Acta Physiol. (Oxf).* 191 (2), 111–121. doi:10.1111/j.1748-1716.2007.01714.x

Konrad, A., Reiner, M. M., Thaller, S., and Tilp, M. (2019). The time course of muscle-tendon properties and function responses of a five-minute static stretching exercise. *Eur. J. Sport Sci.* 19 (9), 1195–1203. doi:10.1080/17461391.2019.1580319

Konrad, A., Stafilidis, S., and Tilp, M. (2017). Effects of acute static, ballistic, and PNF stretching exercise on the muscle and tendon tissue properties. *Scand. J. Med. Sci. Sports* 27 (10), 1070–1080. doi:10.1111/sms.12725

Kubo, K., Kanehisa, H., and Fukunaga, T. (2002). Effects of transient muscle contractions and stretching on the tendon structures *in vivo*. *Acta Physiol. Scand.* 175 (2), 157–164. doi:10.1046/j.1365-201X.2002.00976.x

Law, R. Y., Harvey, L. A., Nicholas, M. K., Tonkin, L., De Sousa, M., Finniss, D. G., et al. (2009). Stretch exercises increase tolerance to stretch in patients with chronic musculoskeletal pain: A randomized controlled trial. *Phys. Ther.* 89 (10), 1016–1026. doi:10.2522/ptj.20090056

Malliaropoulos, N., Papalexandris, S., Papalada, A., and Papacostas, E. (2004). The role of stretching in rehabilitation of hamstring injuries: 80 athletes follow-up. *Med. Sci. Sports Exerc.* 36 (5), 756–759. doi:10.1249/01.mss.0000126393.20025.5e

McCrum, C., Leow, P., Epro, G., König, M., Meijer, K., Karamanidis, K., et al. (2018). Alterations in leg extensor muscle-tendon unit biomechanical properties with ageing and mechanical loading. *Front. Physiol.* 9, 150. doi:10.3389/fphys.2018.00150

Morse, C. I., Degens, H., Seynnes, O. R., Maganaris, C. N., and Jones, D. A. (2008). The acute effect of stretching on the passive stiffness of the human gastrocnemius muscle tendon unit. *J. Physiol.* 586 (1), 97–106. doi:10.1113/jphysiol.2007.140434

Nakamura, M., Ikezoe, T., Takeno, Y., and Ichihashi, N. (2011). Acute and prolonged effect of static stretching on the passive stiffness of the human gastrocnemius muscle tendon unit *in vivo*. *J. Orthop. Res.* 29 (11), 1759–1763. doi:10.1002/jor.21445

Nakamura, M., Ikezoe, T., Takeno, Y., and Ichihashi, N. (2013). Time course of changes in passive properties of the gastrocnemius muscle-tendon unit during 5 min of static stretching. *Man. Ther.* 18 (3), 211–215. doi:10.1016/j.math.2012.09.010

Nakamura, M., Sato, S., Murakami, Y., Kiyono, R., Yahata, K., Sanuki, F., et al. (2020). The comparison of different stretching intensities on the range of motion and muscle stiffness of the quadriceps muscles. *Front. Physiol.* 11, 628870. doi:10.3389/fphys.2020.628870

Orchard, J. W., Chaker Jomaa, M., Orchard, J. J., Rae, K., Hoffman, D. T., Reddin, T., et al. (2020). Fifteen-week window for recurrent muscle strains in football: A prospective cohort of 3600 muscle strains over 23 years in professional Australian rules football. *Br. J. Sports Med.* 54 (18), 1103–1107. doi:10.1136/bjsports-2019-100755

Ostlere, S. (2013). The extensor mechanism of the knee. *Radiol. Clin. North Am.* 51 (3), 393–411. doi:10.1016/j.rcl.2012.11.006

Pearson, S. J., and Hussain, S. R. (2014). Region-specific tendon properties and patellar tendinopathy: A wider understanding. *Sports Med.* 44 (8), 1101–1112. doi:10.1007/s40279-014-0201-y

Pearson, S. J., and McMahon, J. (2012). Lower limb mechanical properties: Determining factors and implications for performance. *Sports Med.* 42 (11), 929–940. doi:10.1007/bf03262304

Sato, S., Kiyono, R., Takahashi, N., Yoshida, T., Takeuchi, K., Nakamura, M., et al. (2020). The acute and prolonged effects of 20-s static stretching on muscle strength and shear elastic modulus. *PLoS One* 15 (2), e0228583. doi:10.1371/journal.pone.0228583

Seynnes, O. R., Erskine, R. M., Maganaris, C. N., Longo, S., Simoneau, E. M., Grosset, J. F., et al. (2009). Training-induced changes in structural and mechanical properties of the patellar tendon are related to muscle hypertrophy but not to strength gains. *J. Appl. Physiol. (1985).* 107 (2), 523–530. doi:10.1152/japplphysiol.00213.2009

Takeuchi, K., Sato, S., Kiyono, R., Yahata, K., Murakami, Y., Sanuki, F., et al. (2021). High-intensity static stretching in quadriceps is affected more by its intensity than its duration. *Front. Physiol.* 12, 709655. doi:10.3389/fphys.2021.709655

Watsford, M. L., Murphy, A. J., McLachlan, K. A., Bryant, A. L., Cameron, M. L., Crossley, K. M., et al. (2010). A prospective study of the relationship between lower body stiffness and hamstring injury in professional Australian rules footballers. *Am. J. Sports Med.* 38 (10), 2058–2064. doi:10.1177/0363546510370197

Wiesinger, H. P., Seynnes, O. R., Kösters, A., Müller, E., and Rieder, F. (2020). Mechanical and material tendon properties in patients with proximal patellar tendinopathy. *Front. Physiol.* 11, 704. doi:10.3389/fphys.2020.00704

frontiers | Frontiers in Physiology

TYPE Original Research
PUBLISHED 30 August 2022
DOI 10.3389/fphys.2022.980438

OPEN ACCESS

EDITED BY
Qichang Mei,
Ningbo University, China

REVIEWED BY
Javad Sarvestan,
Newcastle University, United Kingdom
Milad Gholami,
Arak University of Medical Sciences, Iran

*CORRESPONDENCE
Lin Wang,
wanglin@sus.edu.cn

SPECIALTY SECTION
This article was submitted to Exercise Physiology,
a section of the journal
Frontiers in Physiology

RECEIVED 28 June 2022
ACCEPTED 05 August 2022
PUBLISHED 30 August 2022

CITATION
Li P, Wei Z, Zeng Z and Wang L (2022), Acute effect of kinesio tape on postural control in individuals with functional ankle instability following ankle muscle fatigue.
Front. Physiol. 13:980438.
doi: 10.3389/fphys.2022.980438

Acute effect of kinesio tape on postural control in individuals with functional ankle instability following ankle muscle fatigue

Pan Li, Zhen Wei, Ziwei Zeng and Lin Wang*

Key Laboratory of Exercise and Health Sciences, Shanghai University of Sport, Ministry of Education, Shanghai, China

Background: Kinesio taping (KT) is one of the therapeutic interventions in sports medicine practice. The study aims to assess the acute effect of different KT methods on postural control in individuals with functional ankle instability (FAI) after ankle muscle fatigue.

Methods: Twenty-eight participants with FAI were recruited to complete maximum voluntary isometric contraction (MVIC) and proprioception of ankle using isokinetic dynamometer, dynamic postural control using Y-balance test and static postural control using a force platform after a fatigue protocol in four taping conditions: facilitatory KT (FKT), ankle balance taping (ABT), sham taping (ST) and no taping (NT).

Results: No significant difference was observed for the data MVIC and proprioception after ankle muscle fatigue amongst the four taping treatments. A significant difference in Y-Balance Test was observed amongst the four taping treatments at posterolateral direction ($p < 0.001$) and posteromedial direction ($p < 0.001$), suggesting that KT may significantly improve dynamic postural control following ankle muscle fatigue. For Center of pressure (COP) measurements, the mediolateral COP sway range of NT was significantly larger than that of FKT ($p = 0.003$) and ST ($p < 0.001$), suggesting that the placebo effect of KT was inevitable.

Conclusion: The effect of KT seems increased dynamic postural control in individuals with FAI after ankle muscle fatigue, and this effect is not strongly related to the taping methods. By preventing fatigue-related impairments of postural control, KT may help reduce the risk of injury in individuals with FAI.

KEYWORDS

functional ankle instability, kinesio tape, fatigue, postural control, short term

Introduction

Lateral ankle sprain has a high occurrence, not only in physically active patients but also in the general populations (Gribble et al., 2016). Despite the high prevalence, people rarely seek interventions after a first sprain (Feger et al., 2017). The high rate of reinjury leads to chronic ankle instability (CAI), characterised by persistent ankle pain, swelling, self-reported instability and feelings of “giving way” (Gribble et al., 2014). Repeated ankle sprains increase the physical and mental burden on patients. Hiller et al. (2011) proposed a model of CAI involving mechanical ankle instability, functional ankle instability and recurrent ankle sprain independently or in combination. Functional ankle instability (FAI) refers to the tendency of the ankle to sprain or the feeling of “giving way” after an initial ankle sprain.

Previous research has indicated that FAI is associated with neuromuscular deficit, including a decrease in muscle strength, proprioception and postural control (Hertel, 2002). In addition, most ankle injuries occur during the last third of each half of matches, where athletes have insufficient rest (Woods et al., 2003). This phenomenon may indicate that ankle sprain may be related to fatigue state. Fatigue is defined as the inability to maintain the required or expected strength (Edwards, 1981). It is a major factor increasing the risk of falls and acute injury which has been well documented (Paquette et al., 2017). Possible contributions of fatigue in performance have been attributed to decreases in postural control and proprioception (Verschueren et al., 2020). In addition, compared with healthy people, fatigue is more harmful to people with FAI (Jahjah et al., 2018). Therefore, it is very important to potentially decrease fatigue in sport.

Kinesio taping (KT) is one of the therapeutic interventions in sports medicine practice. Previous studies have attempted to explain the benefits of KT on muscle strength, range of motion, proprioception, functional performance, pain and postural control (Binaei et al., 2021; Biz et al., 2022). KT is also used to prevent ankle sprain and as an intervention to improve function in individuals with CAI (Sarvestan et al., 2020). However, the results of many studies evaluating the efficacy of KT for CAI are controversial. In a systematic review, Wang et al. (2018) concluded that KT was superior to other taping methods in ankle functional performance and it may be useful to athletes with ankle sprains. In another systematic review published in the same journal, Nunes et al. (2021) did not obtain sufficient evidence to encourage using KT for functional performance in people with or without ankle sprain. One of the main reasons for these conflict results may be the huge differences in recruited participants. The first review included only 10 studies (233 participants), while the second included 84 studies (2684 participants) and discussed the different populations separately. Another reason for these conflict results could be the inconsistent techniques of KT (Lim and Tay, 2015). Therefore, it is difficult to draw a definite conclusion for CAI individuals.

In relation to the application of KT on the ankle joint, some studies have used facilitatory KT (FKT) (Halseth et al., 2004) and some have used ankle balance taping (ABT) (Yin et al., 2021), but few studies have compared the effects of the two taping methods. In addition, a dearth of determining the possible benefits of KT on postural control in people with FAI after muscle fatigue still exists. Thus, this study aimed to assess the acute effect of different KT methods on postural control in individuals with FAI after ankle muscle fatigue.

Materials and methods

Participants

The G-Power was used to perform a priori power analysis. Considering the effective size of 0.25 (Cohen, 1988), the power of 0.8, and alpha level of 0.05, twenty-eight participants (15 males, 13 females; age, 21.2 ± 2.0 years; body height, 172.3 ± 8.0 cm; body weight, 64.1 ± 10.1 kg) were recruited in this study. The inclusion criteria (Wu et al., 2022) are as follows: 1) a history of at least one significant ankle sprain (initial must have occurred at least 1 year prior to study enrolment); 2) feelings of “giving way” of the ankle joint, and/or recurrent sprain, and/or “feeling of instability”; 3) a score of Identification of Functional Ankle Instability of at least 11 (Simon et al., 2012) (if both feet match, the less stable side is chosen); 4) negative anterior drawer test and talar tilt test; and 5) not allergic to KT. The participants were free of lower extremity musculoskeletal surgeries, operation, nervous and vestibular system disease or any other conditions that could affect to postural control. Those who had an acute ankle sprain within 3 months prior to the study, resulting in cessation of physical activity for at least 1 day, were excluded (Yin et al., 2021). All participants were asked to provide consent before the experiments. This study was approved by the Human Ethics Committee of the Shanghai University of Sport.

Taping methods

Before taping, the skin of taping area was shaved and wiped with 70% alcohol (Saltan et al., 2019). Each participant randomly experienced four taping conditions as follows: 1) FKT (Halseth et al., 2004); 2) ABT (Lee and Lee, 2015); 3) sham taping, (ST) (Lee and Lee, 2015), and 4), no taping (NT, Figure 1). The taping (LP 670 MAXTAPING) was applied before the fatigue protocol. Additionally, a wash-out phase of 1 week was performed between each taping treatment to relieve any learning effect.

All tapes were accomplished by a single experienced physical therapist who was not involved in the recruitment and assessment. The FKT and ABT consistency with 50% tension was maintained using the following equation (Wei et al., 2020), and the ST was applied without tension.

$$\text{Actual length of tape to cut (cm)} = \left[\frac{x-4}{1.5}+4\right] \times 1.1$$

where x is the actual length measured from the origin and insertion and the anchor length of the KT was set to 4 cm (2 cm each for the proximal and distal sites).

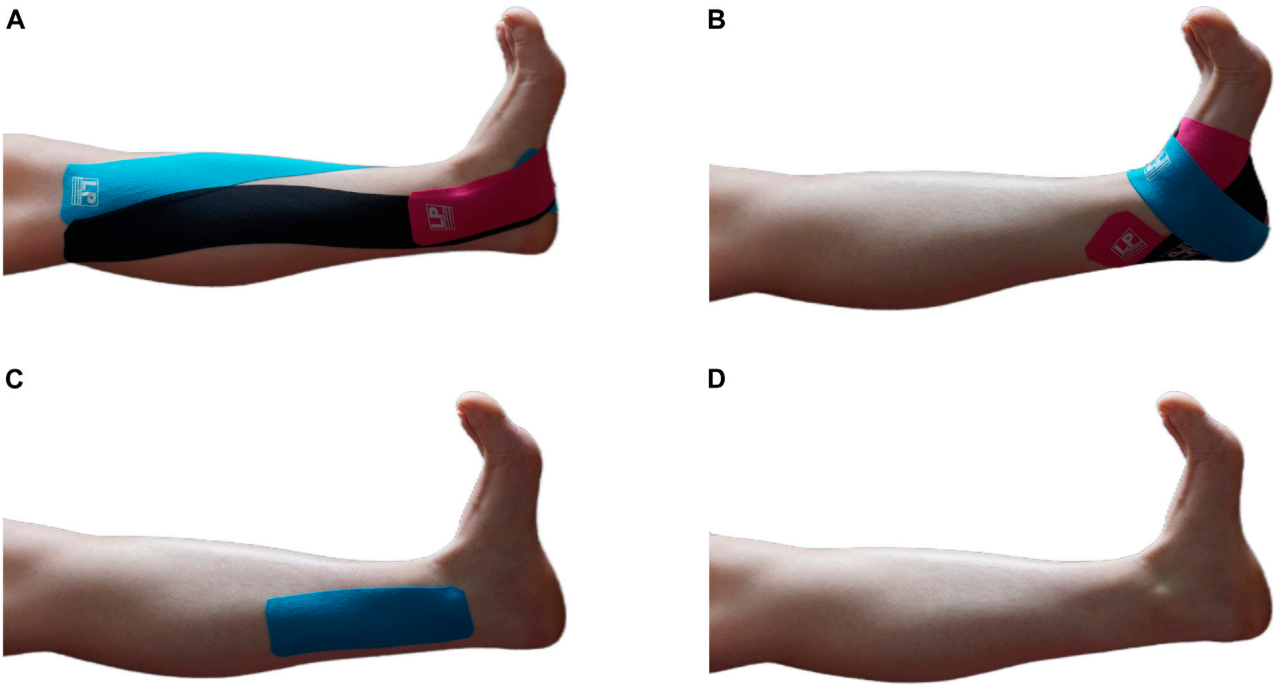

FIGURE 1
Four treatments in this study. **(A)** FKT, facilitatory Kinesio taping; **(B)** ABT, ankle balance taping; **(C)** ST, sham taping; **(D)** NT, no taping.

Fatigue protocol and maximum voluntary isometric contraction measurement

The fatigue protocol was performed on a CONTREX isokinetic dynamometer (PHYSIOMED CON-TREX TP1000, Germany) in accordance with previous studies (Gribble et al., 2007). The participants were instructed to avoid muscle fatigue 48 h prior to assessment. They were secured in the isokinetic device with their ankle at neutral position and they were stabilised with two straps around the abdomen. The movement pattern was set at concentric/concentric mode and the angular velocity at 60°/s. Prior to fatigue protocol, the participants performed 10 repetitions of consecutive maximal concentric/concentric contractions of the ankle to familiarise the device. Then, they rested for 5 min to restore muscle strength. The maximum voluntary isometric contraction (MVIC) of plantarflexion and dorsiflexion for 5 s was measured three times by a rest period of 30 s before inducing the ankle muscle fatigue. The highest value of the MVIC was taken as a parameter for inducing fatigue. Next, each participant was asked to perform plantarflexion and dorsiflexion contractions at maximal effort. Verbal encouragement was given by the examiner. According to previous studies (Flevas et al., 2017), the point of muscle fatigue must meet the following two criteria: 1) three consecutives of the peak torque reaching below 50% MVIC of the first measured and 2) the participants reported they were no longer able to complete any repetitions. After the fatigue protocol was conducted, three times of 5 s of MVIC of plantarflexion and dorsiflexion by a rest period of 30 s were performed once again and used in data analysis.

Joint position sense measurement

Ankle proprioception is an important component of postural control in movement because in most physical activities, the ankle-foot complex is the only part of the body that touches the ground (Han et al., 2015). The ankle proprioceptive tests in the current study included Joint position sense (JPS) and force sense (FS) measurements. JPS was assessed using CONTREX and tested at 5° of plantarflexion and 5° of dorsiflexion. Firstly, the participant's ankle was passively moved from the neutral position by the isokinetic force measurement system to one of two target positions randomly and stayed for 10 s. The participants were then asked to concentrate on the feeling of position of this angle and then took the initiative to acquire the angle of practice twice. Before the test, the participants were instructed to avoid active muscle contraction and blindfolded, with ears covered throughout the examination. The participants held the hand-held switch and actively started to move from the neutral position of the ankle joint. When the participants felt that the ankle joint reached the target angle, the switch was pressed and the tester recorded the actual angle. This experiment was repeated in three trials, and the experimental results of each trial were not fed back to the participants.

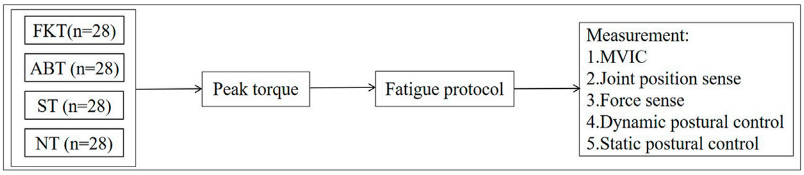

FIGURE 2
A flowchart of the experimental procedures.

TABLE 1 Comparison of parameters in JPS, FS and MVIC among four taping treatments.

	NT	FKT	ABT	ST	F	P	η^2
PF-AEJPS(°)	1.33 ± 0.77	1.33 ± 0.63	1.23 ± 0.69	1.30 ± 0.59	0.152	0.928	0.006
DF-AEJPS(°)	1.50 ± 0.91	1.31 ± 0.82	1.54 ± 0.86	1.40 ± 0.63	0.792	0.502	0.280
PF-VEJPS(°)	0.62 ± 0.29	0.50 ± 0.26	0.60 ± 0.44	0.51 ± 0.37	0.777	0.510	0.028
DF-VEJPS(°)	0.47 ± 0.29	0.53 ± 0.35	0.41 ± 0.20	0.57 ± 0.39	1.448	0.235	0.510
PF-RAEFS(°/N)	1.33 ± 0.77	1.33 ± 0.63	1.23 ± 0.69	1.30 ± 0.59	0.152	0.928	0.006
DF-RAEFS(°/N)	1.50 ± 0.91	1.31 ± 0.82	1.54 ± 0.86	1.40 ± 0.63	0.792	0.502	0.028
PF-RVEFS(°/N)	2.11 ± 1.43	2.02 ± 1.39	2.21 ± 1.42	1.96 ± 1.26	0.221	0.881	0.008
DF-RVEFS(°/N)	0.94 ± 0.67	0.83 ± 0.51	0.72 ± 0.58	2.60 ± 9.14	1.063	0.313	0.038
PF-MIVC(N)	83.04 ± 25.56	89.46 ± 30.29	87.71 ± 26.45	88.39 ± 31.68	1.672	0.179	0.058
DF-MIVC(N)	25.87 ± 8.21	24.86 ± 7.71	24.76 ± 7.51	25.68 ± 8.53	0.524	0.667	0.019

Note: Values are means ± standard deviation (SD); Significant differences ($p < 0.05$); PF, plantarflexion; DF, dorsiflexion; MVIC, maximum voluntary isometric contraction; AEJPS, absolute error of joint position sense; VEJPS, variable error of joint position sense; RAEFS, relative absolute error of force sense; RVEFS, relative variable error of force sense; NT, no taping; FKT, facilitatory kinesio taping; ABT, ankle balance taping; ST, sham taping.

The accuracy of JPS was inversely proportional to the absolute error (AE) and variable error (VE) scores. AE is a measure of the overall accuracy of the positioning and VE is a measure of the variability of the positioning (Jahjah et al., 2018). The formulas are as follows:

$$AE = \frac{\sum_{i=1}^{3} |a_i - a|}{3} \quad (1)$$

$$VE = \sqrt{\frac{\sum_{i=1}^{3} a_i^2 - \frac{\left(\sum_{i=1}^{3} a_i\right)^2}{3}}{2}} \quad (2)$$

The actual measured value is a_i and the target value is a.

Force sense measurement

All participants were placed in the same position as in JPS measurement. The main purpose was to examine the ability of the participant's ankle joint to replicate the torque value of 25% MVIC. Before the force sense test was performed, the participants were asked to plantarflex/dorsiflex to a torque of 25% MVIC, with looking at a monitor showing the torque, and keep the position for 10 s. The participants had to concentrate on the feeling of target force and then withdraw from the monitor. The participants were asked to relax and close their eyes. Next, they were asked to reproduce that target force and maintain this force for 10 s. The CONTREX device marked the data. This procedure was repeated three times, with a rest period of 30 s in between trials. The results of each experimental test were not fed back to the participants.

For force sense data, the relative values of VE and AE were used for representation and the formulas are as follows:

$$RAEFS = \frac{AE}{25\%MVIC} \quad (3)$$

$$RVEFS = \frac{VE}{25\%MVIC} \quad (4)$$

Notes: RAEFS: relative absolute error of force sense; RVEFS: relative variable error of force sense.

Dynamic postural control-Dynamic postural control was evaluated using the Y-balance test (Move2Perform, Evansville, IN, United States), which was verified to have good interrater test-retest reliability (Overmoyer and Reiser., 2015). The participants stood barefoot at the centre joint of the standing board whilst their toe was pointed at the red line for maintaining the position of the foot. Their

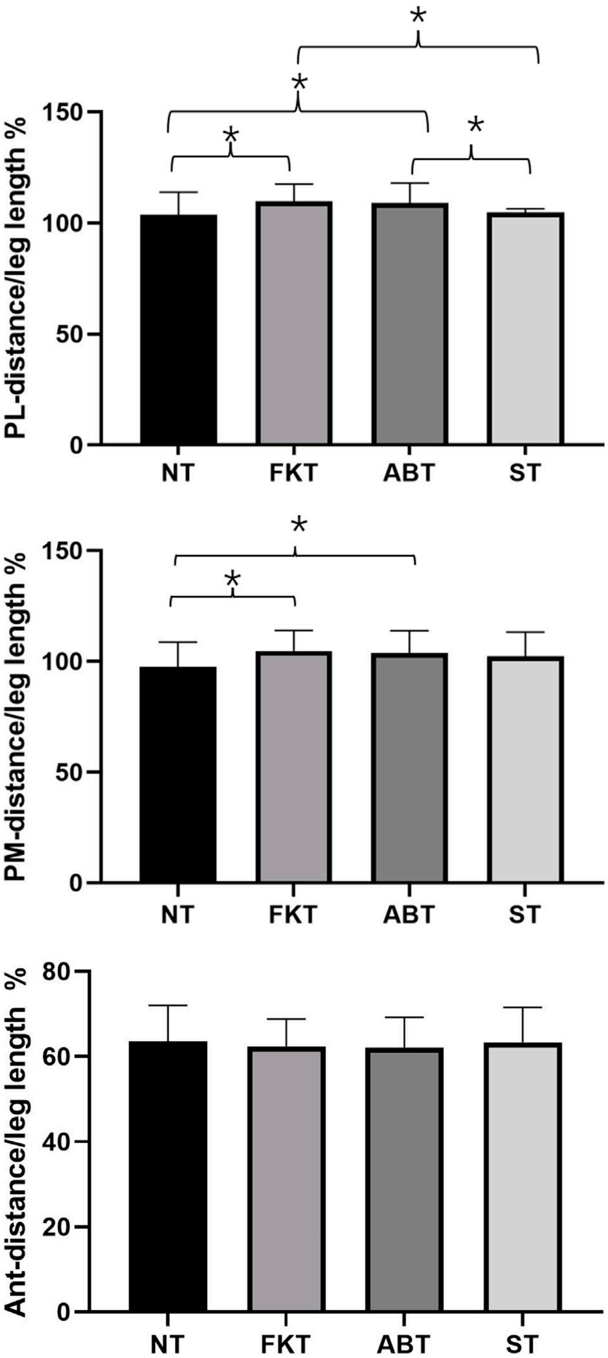

FIGURE 3
Comparison of parameters in Y-Balance scores amongst four taping treatments. *$p < 0.05$, Ant, anterior; PL, posterolateral; PM, posteromedial.

hands were placed on the hips during the test. They were instructed to reach as far as possible with the non-supporting legs in the anterior, posterolateral and posteromedial directions. The participants performed six trials to eliminate the learning effect before the testing procedure. When a participant had the following conditions, the trial must be retested: 1) fails to keep balance during the test; 2) the heel of the supporting leg is lifted off the ground and 3) unable to return to the initial position after reaching. The average reach distance was then normalised to leg length, which measured from the anterior superior iliac spine to medial malleolus.

Static postural control

For static postural control tasks, the participants were asked to keep standardised unilateral stance with barefoot on a force platform (KForce, KINVENT, United States) for 30 s. During the test, the participants stood on the test limb and kept their hands on their hips and their non-test limb maintained hip flexion at 30° and knee flexion at 45°. Subsequently, the tests were performed with the participants' eyes closed. All values were collected at a sample rate of 75 Hz. The Center of pressure (COP) data generated from the force platform were analysed using the code written in Matlab (Mathworks Inc., Natik, MA), which included 1) mediolateral COP sway range (mm); 2) anteroposterior COP sway range (mm); 3) mean velocity of mediolateral COP sway (mm/s); 4) mean velocity of anteroposterior COP sway (mm/s) and 5) sway area (mm^2), which is the elliptical area of the COP points. The above tests were performed in random order. Figure 2 presents a schematic flowchart of the entire procedure.

Statistical analysis

Data were presented as mean and standard deviation (SD). The normality of distribution of data was tested using Shapiro–Wilk test. One-way repeated measures ANOVA was used in determining whether a significant difference exists amongst the taping conditions. Statistical significance was set at alpha <0.05. Bonferroni tests were conducted for post-hoc analysis when the effect of the test was significant. All data were analysed with SPSS 26 (IBM Corp., Armonk, NY, United States).

Results

The results showed no significant difference in the four taping treatments in JPS and FS measurements. Similarly, no significant difference was found for the MVIC of plantarflexion and dorsiflexion in all four taping treatments (Table 1).

For Y-balance test, a significant difference was observed amongst the four taping treatments in posterolateral direction [$F(3,81) = 11.9$, $p < 0.001$, $\eta^2 = 0.291$]. Post-hoc analysis showed that the mean of normalised reach distance of NT was significantly lower than that of FKT [$p < 0.001$, $d = -6.099$, 95% confidence interval (CI) = −9.839, −2.360%] and ABT ($p < 0.001$, $d = -5.439$, 95% CI = −8.941, −1.937%). The mean of normalised reach distance of ST was significantly lower than that of FKT ($p < 0.001$, $d = -5.095$, 95%

TABLE 2 Comparison of parameters in COP for different conditions.

	NT	FKT	ABT	ST	F	P	η^2
ML COP sway range (mm)	13.72 ± 6.22	9.97 ± 4.22	11.55 ± 5.31	10.17 ± 4.36	9.116	<0.001	0.252
AP COP sway range (mm)	12.22 ± 3.16	13.08 ± 5.41	13.14 ± 5.43	14.08 ± 6.14	1.041	0.379	0.037
ML COP velocity (mm/s)	8.53 ± 7.51	8.55 ± 9.89	8.61 ± 9.19	6.12 ± 7.46	0.657	0.545	0.024
AP COP velocity (mm/s)	7.75 ± 6.24	13.41 ± 18.60	11.26 ± 15.45	8.39 ± 6.60	1.153	0.323	0.41
Sway area (mm^2)	114.92 ± 60.65	86.51 ± 69.30	101.22 ± 63.55	94.00 ± 50.00	1.465	0.23	0.051

Note: Values are means ± standard deviation (SD); Significant differences ($p < 0.05$); ML, mediolateral; COP, left of pressure; AP, anteroposterior; NT, no taping; FKT, facilitatory kinesio taping; ABT, ankle balance taping; ST, sham taping.

CI = −7.777, −2.413%) and ABT ($p < 0.001$, d = −4.435, 95% CI = −7.075, −1.796%). Similarly, a significant difference was found amongst the four taping treatments in posteromedial direction [F (3,81) = 7.099, $p < 0.001$, $\eta^2 = 0.208$]. The post-hoc analysis also showed that the mean of normalised reach distance of NT was significantly lower than that of FKT ($p = 0.003$, d = −7.1123, 95% CI = −12.242, −2.005%) and ABT ($p < 0.001$, d = −6.258, 95% CI = −10.138, −2.378%, Figure 3). For the anterior direction, no significant differences were observed in the four treatments ($p = 0.751$).

Regarding COP data, a significant difference was found amongst the four taping treatments for mediolateral COP sway range when eyes were closed. The post-hoc analysis showed that the mediolateral COP sway range of NT was significantly larger than that of FKT (p = 0.003, d = 3.750, 95% CI = 1.093–6.406 mm) and ST ($p < 0.001$, d = 3.551, 95% CI = 1.472–5.630 mm, Table 2).

Discussion

This study aimed to understand the effects of different KT methods on postural control after ankle muscle fatigue in individuals with FAI. The findings showed that KT caused a significant increase in the posterolateral and posteromedial reached distances of Y-balance test. In static postural control, proprioception and muscle strength findings demonstrated no differences amongst the four taping conditions.

Isokinetic fatigue protocols have been widely used to induce ankle muscle fatigue. Castillo et al. (2022) demonstrated that the fatigue of ankle muscle using isokinetic dynamometer was associated with deficits in postural control and reduced the functional performance. Similarly, Jahjah et al. (2018) used a similar protocol to cause fatigue in ankle muscles and observed worse joint position sense in the ankle. Impairment of neuromuscular control caused by fatigue severely affects dynamic joint stability and the body's intrinsic protection from injury, particularly in participants with FAI. In addition, Yaggie and McGregor (2002) found that the changes in postural control were transient and recovered within 20 min. Therefore, the post-fatigue test in the current study was completed within 15 min after fatigue exercise.

To the authors' knowledge, limited studies regarding the effect of KT in participants with FAI following ankle muscle fatigue are available. The current study found that KT has no effects on ankle proprioception or muscle strength in individuals with FAI after ankle muscle fatigue. In line with these results, Zanca et al. (2015). found no effect of KT application for shoulder proprioception following muscle fatigue in healthy individuals. Strutzenberger et al. (2016). also reported that KT did not influence lower limb strength in young adults compared with that in groups with no taping. The possible reason behind the ineffectiveness of KT may be that it could mediate the influence of fatigue on the ankle. However, the efficacy provided by KT may not be sufficiently strong to improve the performance in proprioception or muscle power.

The significant findings in Y-balance test are consistent with those in previous studies. Choi and Lee (2020) found that ABT could improve dynamic balance with eyes open and closed after ankle muscle fatigue in healthy individuals. Lin et al. (2020) found that KT provides a better postural control during landing following muscle fatigue than ankle brace in athletes with FAI. The significantly improved dynamic balance could be attributed to tactile stimulus and the mechanoreceptor stimulation supported by KT, compensating for the loss of the afferent feedback caused by fatigue. The current study also found that KT application significantly improved the dynamic balance but only in posterolateral and posteromedial directions. The reason may be that the different directions in the Y-balance require activation and contribution of different muscles. In the anterior direction, knee extensor and hip abductor are the most active muscles (Nelson et al., 2021) and the effects of KT are more localised to the area of its usage (Boozari et al., 2018), which may explain the significant results not present in the anterior direction. By contrast, Kodesh and Dar (2015) found that KT application did not contribute to Y-balance performance following ankle muscle fatigue in participants with CAI. And Esfandiari et al. (2020) demonstrated that KT did not affect the dynamic balance of young healthy women after local fatigue. The possible causes of the inconsistency may be the differences in KT application techniques.

In addition, according to the results of COP data, the mediolateral COP sway range of FKT and ST conditions improved compared with that of NT condition after ankle muscle fatigue. This finding may be due to the placebo effect of KT. de-la-Torre-Domingo et al. (2015) evaluated the immediate and prolonged effects of KT on balance in participants with CAI and found that the balance of the KT and control groups improved and that no difference was found between them. The authors concluded that the finding may be related to the increase in confidence after taping application. Mak et al. (2019) also found that the function of KT on muscle strength increase could be attributed to a placebo effect. Although the mechanism of the placebo effect of KT is unclear, it may be beneficial for preventing injury by contributing to stronger expectations and confidence.

Furthermore, no differences were found between the methods of KT application in regard to tests. These results are similar to those of previous studies investigating different KT applications. Fereydounnia et al. (2019) compared the effect of two methods of KT on muscle strength, balance and functional performance in participants with or without FAI and found no differences between the methods of application. Previous studies also concluded that the effect of KT is independent of the application direction (Choi and Lee, 2019). These results suggested that the effect of KT may not be related to the methods of application. However, Yu et al. (2021) argued that only long length of KT improved ankle inversion proprioception for healthy individuals. One explanation for these conflicting findings is that the long length of KT was across both the ankle and knee joints, it is possible that participants may have acquired more proprioceptive information.

Some limitations should be acknowledged in this study. Firstly, the participants could not be blinded to the methods of taping. Thus, the psychological effects of KT could not be ruled out. Secondly, some of the recruited participants were specialised in one sport and their performance in the tests may be inevitably affected to some degree by their skills. Thirdly, this study only indicated the acute effect of KT. Future studies should investigate the long-term effects of KT.

Conclusion

The current study demonstrated that KT increased dynamic postural control in individuals with FAI after ankle muscle fatigue, and this effect is not strongly related to the taping methods. By preventing fatigue-related impairments of postural control, KT may help reduce the risk of injury in individuals with FAI.

Data availability statement

The original contributions presented in the study are included in the article/supplementary material, further inquiries can be directed to the corresponding author.

Ethics statement

The studies involving human participants were reviewed and approved by Ethics Committee of Shanghai University of Sport. The patients/participants provided their written informed consent to participate in this study.

Author contributions

PL and ZW contributed to recruiting the subjects, collecting the data, and writing the manuscript. ZZ undertook the statistical analysis. LW conceived of the study and interpreted the results.

Funding

This study was supported by research project of Shanghai University of Sport (No. 2022XJ003).

Acknowledgments

The authors express their gratitude to all the volunteers who took part.

Conflict of interest

The authors declare that the research was conducted in the absence of any commercial or financial relationships that could be construed as a potential conflict of interest.

Publisher's note

All claims expressed in this article are solely those of the authors and do not necessarily represent those of their affiliated organizations, or those of the publisher, the editors and the reviewers. Any product that may be evaluated in this article, or claim that may be made by its manufacturer, is not guaranteed or endorsed by the publisher.

References

Binaei, F., Hedayati, R., Mirmohammadkhani, M., Taghizadeh Delkhoush, C., and Bagheri, R. (2021). Examining the use of Kinesiology tape during weight bearing exercises on proprioception in participants with functional ankle instability. *Percept. Mot. Ski.* 128 (6), 2654–2668. doi:10.1177/00315125211036425

Biz, C., Nicoletti, P., Tomasin, M., Bragazzi, N. L., Di Rubbo, G., and Ruggieri, P. (2022). Is kinesio taping effective for sport performance and ankle function of athletes with chronic ankle instability (CAI)? A systematic review and meta-analysis. *Medicina* 58 (5), 620. doi:10.3390/medicina58050620

Boozari, S., Sanjari, M. A., Amiri, A., and Ebrahimi Takamjani, I. (2018). Effect of gastrocnemius kinesio taping on countermovement jump performance and vertical stiffness following muscle fatigue. *J. Sport Rehabil.* 27 (4), 306–311. doi:10.1123/jsr.2017-0009

Castillo, G. B., Brech, G. C., Luna, N. M. S., Tarallo, F. B., Soares-Junior, J. M., Baracat, E. C., et al. (2022). Influence of invertor and evertor muscle fatigue on functional jump tests and postural control: A prospective cross-sectional study. *Clinics* 77, 100011. doi:10.1016/j.clinsp.2022.100011

Choi, H. S., and Lee, J. H. (2020). Immediate effect of balance taping using kinesiology tape on dynamic and static balance after ankle muscle fatigue. *Healthc. (Basel)* 8 (2), E162. doi:10.3390/healthcare8020162

Choi, I. R., and Lee, J. H. (2019). The effect of the application direction of the kinesiology tape on the strength of fatigued quadriceps muscles in athletes. *Res. Sports Med.* 27 (1), 1–10. doi:10.1080/15438627.2018.1502187

Cohen, E. J. (1988). *Statistical power analysis for the behavioral sciences*. 2nd ed.

de-la-Torre-Domingo, C., Alguacil-Diego, I. M., Molina-Rueda, F., López-Román, A., and Fernández-Carnero, J. (2015). Effect of kinesiology tape on measurements of balance in subjects with chronic ankle instability: A randomized controlled trial. *Arch. Phys. Med. Rehabil.* 96 (12), 2169–2175. doi:10.1016/j.apmr.2015.06.022

Edwards, R. H. (1981). Human muscle function and fatigue. *Ciba Found. Symp.* 82, 1–18. doi:10.1002/9780470715420.ch1

Esfandiari, A., Mostamand, J., and Baharlouei, H. (2020). The effect of quadriceps kinesiotaping on the dynamic balance of young healthy women after fatigue: A randomized controlled trial. *J. Bodyw. Mov. Ther.* 24 (4), 462–467. doi:10.1016/j.jbmt.2020.06.036

Feger, M. A., Glaviano, N. R., Donovan, L., Hart, J. M., Saliba, S. A., Park, J. S., et al. (2017). Current trends in the management of lateral ankle sprain in the United States. *Clin. J. Sport Med.* 27 (2), 145–152. doi:10.1097/jsm.0000000000000321

Fereydounnia, S., Shadmehr, A., Attarbashi Moghadam, B., Talebian Moghadam, S., Mir, S. M., Salemi, S., et al. (2019). Improvements in strength and functional performance after kinesio taping in semi-professional male soccer players with and without functional ankle instability. *Foot (Edinb)* 41, 12–18. doi:10.1016/j.foot.2019.06.006

Flevas, D. A., Bernard, M., Ristanis, S., Moraiti, C., Georgoulis, A. D., and Pappas, E. (2017). Peroneal electromechanical delay and fatigue in patients with chronic ankle instability. *Knee Surg. Sports Traumatol. Arthrosc.* 25 (6), 1903–1907. doi:10.1007/s00167-016-4243-6

Gribble, P. A., Bleakley, C. M., Caulfield, B. M., Docherty, C. L., Fourchet, F., Fong, D. T., et al. (2016). Evidence review for the 2016 International Ankle Consortium consensus statement on the prevalence, impact and long-term consequences of lateral ankle sprains. *Br. J. Sports Med.* 50 (24), 1496–1505. doi:10.1136/bjsports-2016-096189

Gribble, P. A., Delahunt, E., Bleakley, C. M., Caulfield, B., Docherty, C. L., Fong, D. T., et al. (2014). Selection criteria for patients with chronic ankle instability in controlled research: A position statement of the international ankle consortium. *J. Athl. Train.* 49 (1), 121–127. doi:10.4085/1062-6050-49.1.14

Gribble, P. A., Hertel, J., and Denegar, C. R. (2007). Chronic ankle instability and fatigue create proximal joint alterations during performance of the Star Excursion Balance Test. *Int. J. Sports Med.* 28 (3), 236–242. doi:10.1055/s-2006-924289

Halseth, T., McChesney, J. W., Debeliso, M., Vaughn, R., and Lien, J. (2004). The effects of kinesio™ taping on proprioception at the ankle. *J. Sports Sci. Med.* 3 (1), 1–7.

Han, J., Anson, J., Waddington, G., Adams, R., and Liu, Y. (2015). The role of ankle proprioception for balance control in relation to sports performance and injury. *Biomed. Res. Int.* 2015, 842804. doi:10.1155/2015/842804

Hertel, J. (2002). Functional anatomy, pathomechanics, and pathophysiology of lateral ankle instability. *J. Athl. Train.* 37 (4), 364–375.

Hiller, C. E., Kilbreath, S. L., and Refshauge, K. M. (2011). Chronic ankle instability: Evolution of the model. *J. Athl. Train.* 46 (2), 133–141. doi:10.4085/1062-6050-46.2.133

Jahjah, A., Seidenspinner, D., Schüttler, K., Klasan, A., Heyse, T. J., Malcherczyk, D., et al. (2018). The effect of ankle tape on joint position sense after local muscle fatigue: A randomized controlled trial. *BMC Musculoskelet. Disord.* 19 (1), 8. doi:10.1186/s12891-017-1909-2

Kodesh, E., and Dar, G. (2015). The effect of kinesiotape on dynamic balance following muscle fatigue in individuals with chronic ankle instability. *Res. Sports Med.* 23 (4), 367–378. doi:10.1080/15438627.2015.1076417

Lee, B. G., and Lee, J. H. (2015). Immediate effects of ankle balance taping with kinesiology tape on the dynamic balance of young players with functional ankle instability. *Technol. Health Care* 23 (3), 333–341. doi:10.3233/thc-150902

Lim, E. C., and Tay, M. G. (2015). Kinesio taping in musculoskeletal pain and disability that lasts for more than 4 weeks: Is it time to peel off the tape and throw it out with the sweat? A systematic review with meta-analysis focused on pain and also methods of tape application. *Br. J. Sports Med.* 49 (24), 1558–1566. doi:10.1136/bjsports-2014-094151

Lin, C. C., Chen, S. J., Lee, W. C., and Lin, C. F. (2020). Effects of different ankle supports on the single-leg lateral drop landing following muscle fatigue in athletes with functional ankle instability. *Int. J. Environ. Res. Public Health* 17 (10), E3438. doi:10.3390/ijerph17103438

Mak, D. N., Au, I. P., Chan, M., Chan, Z. Y., An, W. W., Zhang, J. H., et al. (2019). Placebo effect of facilitatory Kinesio tape on muscle activity and muscle strength. *Physiother. Theory Pract.* 35 (2), 157–162. doi:10.1080/09593985.2018.1441936

Nelson, S., Wilson, C. S., and Becker, J. (2021). Kinematic and kinetic predictors of y-balance test performance. *Int. J. Sports Phys. Ther.* 16 (2), 371–380. doi:10.26603/001c.21492

Nunes, G. S., Feldkircher, J. M., Tessarin, B. M., Bender, P. U., da Luz, C. M., and de Noronha, M. (2021). Kinesio taping does not improve ankle functional or performance in people with or without ankle injuries: Systematic review and meta-analysis. *Clin. Rehabil.* 35 (2), 182–199. doi:10.1177/0269215520963846

Overmoyer, G. V., and Reiser, R. F., 2nd. (2015). Relationships between lower-extremity flexibility, asymmetries, and the Y balance test. *J. Strength Cond. Res.* 29 (5), 1240–1247. doi:10.1519/jsc.0000000000000693

Paquette, M. R., Peel, S. A., Schilling, B. K., Melcher, D. A., and Bloomer, R. J. (2017). Soreness-related changes in three-dimensional running biomechanics following eccentric knee extensor exercise. *Eur. J. Sport Sci.* 17 (5), 546–554. doi:10.1080/17461391.2017.1290140

Saltan, A., Baltaci, G., and Ankarali, H. (2019). Does Kinesio® taping improve balance and functional performance in older adults? A pilot study. *J. Sports Med. Phys. Fit.* 59, 1346–1352. doi:10.23736/S0022-4707.18.09207-1

Sarvestan, J., Ataabadi, P. A., Svoboda, Z., Kovačikova, Z., and Needle, A. R. (2020). The effect of ankle Kinesio™ taping on ankle joint biomechanics during unilateral balance status among collegiate athletes with chronic ankle sprain. *Phys. Ther. Sport* 45, 161–167. doi:10.1016/j.ptsp.2020.06.007

Simon, J., Donahue, M., and Docherty, C. (2012). Development of the identification of functional ankle instability (IdFAI). *Foot Ankle Int.* 33, 755–763. doi:10.3113/fai.2012.0755

Strutzenberger, G., Moore, J., Griffiths, H., Schwameder, H., and Irwin, G. (2016). Effects of gluteal kinesio-taping on performance with respect to fatigue in rugby players. *Eur. J. Sport Sci.* 16 (2), 165–171. doi:10.1080/17461391.2015.1004372

Verschueren, J., Tassignon, B., De Pauw, K., Proost, M., Teugels, A., Van Cutsem, J., et al. (2020). Does acute fatigue negatively affect intrinsic risk factors of the lower extremity injury risk profile? A systematic and critical review. *Sports Med.* 50 (4), 767–784. doi:10.1007/s40279-019-01235-1

Wang, Y., Gu, Y., Chen, J., Luo, W., He, W., Han, Z., et al. (2018). Kinesio taping is superior to other taping methods in ankle functional performance improvement: A systematic review and meta-analysis. *Clin. Rehabil.* 32 (11), 1472–1481. doi:10.1177/0269215518780443

Wei, Z., Wang, X. X., and Wang, L. (2020). Effect of short-term kinesiology taping on knee proprioception and quadriceps performance in healthy individuals. *Front. Physiol.* 11, 603193. doi:10.3389/fphys.2020.603193

Woods, C., Hawkins, R., Hulse, M., and Hodson, A. (2003). The football association medical research programme: An audit of injuries in professional football: An analysis of ankle sprains. *Br. J. Sports Med.* 37 (3), 233–238. doi:10.1136/bjsm.37.3.233

Wu, H. W., Chang, Y. S., Arefin, M. S., You, Y. L., Su, F. C., and Lin, C. F. (2022). Six-Week remodeled bike pedal training improves dynamic control of lateral shuffling in athletes with functional ankle instability. *Sports Health* 14 (3), 348–357. doi:10.1177/19417381211035781

Yaggie, J. A., and McGregor, S. J. (2002). Effects of isokinetic ankle fatigue on the maintenance of balance and postural limits. *Arch. Phys. Med. Rehabil.* 83 (2), 224–228. doi:10.1053/apmr.2002.28032

Yin, L., Liu, K., Liu, C., Feng, X., and Wang, L. (2021). Effect of kinesiology tape on muscle activation of lower extremity and ankle kinesthesia in individuals with unilateral chronic ankle instability. *Front. Physiol.* 12, 786584. doi:10.3389/fphys.2021.786584

Yu, R., Yang, Z., Witchalls, J., Adams, R., Waddington, G., and Han, J. (2021). Kinesiology tape length and ankle inversion proprioception at step-down landing in individuals with chronic ankle instability. *J. Sci. Med. Sport* 24 (9), 894–899. doi:10.1016/j.jsams.2021.04.009

Zanca, G. G., Mattiello, S. M., and Karduna, A. R. (2015). Kinesio taping of the deltoid does not reduce fatigue induced deficits in shoulder joint position sense. *Clin. Biomech.* 30 (9), 903–907. doi:10.1016/j.clinbiomech.2015.07.011

TYPE Systematic Review
PUBLISHED 02 September 2022
DOI 10.3389/fphys.2022.973304

Check for updates

OPEN ACCESS

EDITED BY
Kwong Ming Tse,
Swinburne University of Technology, Australia

REVIEWED BY
Aleksandra Truszczyńska-Baszak,
Józef Piłsudski University of Physical Education in Warsaw, Poland
Haiyang Wu,
Tianjin Medical University, China
Yujie Liu,
Shanghai Changzheng Hospital, China

*CORRESPONDENCE
Chengpei Zhou,
zhoucpei@126.com
Jixian Qian,
pasmiss2012@163.com

†These authors have contributed equally to this work

SPECIALTY SECTION
This article was submitted to Exercise Physiology,
a section of the journal
Frontiers in Physiology

RECEIVED 20 June 2022
ACCEPTED 08 August 2022
PUBLISHED 02 September 2022

CITATION
Heng W, Wei F, Liu Z, Yan X, Zhu K, Yang F, Du M, Zhou C and Qian J (2022), Physical exercise improved muscle strength and pain on neck and shoulder in military pilots.
Front. Physiol. 13:973304.
doi: 10.3389/fphys.2022.973304

Physical exercise improved muscle strength and pain on neck and shoulder in military pilots

Wei Heng[1†], Feilong Wei[1†], Zhisheng Liu[1,2†], Xiaodong Yan[1], Kailong Zhu[1], Fan Yang[1], Mingrui Du[1], Chengpei Zhou[1]* and Jixian Qian[1]*

[1]Department of Orthopedics, Tangdu Hospital, Fourth Military Medical University, Xi'an, China, [2]94333 Military Hospital, Shandong, China

Purpose: To evaluate the effects of physical exercise on neck and shoulder muscle strength and pain in military pilots.

Method: Embase, PubMed, and Cochrane Library databases were searched studies published up to April 1, 2022. Studies that met the screening criteria were included in the final meta-analysis. We calculated neck and shoulder maximal voluntary isometric contractions (MVICs), prevalence of pain, and pain intensity. Heterogeneity was explored by subgroup and sensitivity analyses.

Result: A total of 15 studies with 907 participants were included. In the exercise group, muscle strength was significantly increased in four directions of neck motion: flexion (standardized mean difference (SMD) = 0.45; 95% CI, 0.08–0.82), extension (SMD = 0.63; 95% CI, 0.27–1.00), right lateral flexion (Rtflx) (SMD = 0.53; 95% CI, 0.12–0.94), and left lateral flexion (Ltflx) (SMD = 0.50; 95% CI, 0.09–0.91). Subgroup analysis showed that fighter pilots, strength plus endurance training, and a follow-up period <20 weeks exhibited more significant muscle strength improvements than helicopter pilots, simple strength training, and a follow-up period ≥20 weeks. Overall, the pooled odds ratio (OR) for the effect of physical exercise on the prevalence of neck pain was not statistically significant (I^2 = 60%). Sensitivity analysis revealed that the heterogeneity was restored after removing each of two studies (I^2 = 47%), and the pooled OR was statistically significant (OR = 0.46; 95% CI, 0.23 to 0.94, or OR = 0.47; 95% CI, 0.24–0.91). Furthermore, compared with observational studies (OS), the reduction in the prevalence of neck pain was more significant in randomized controlled trials (RCTs) (OR = 0.37; 95% CI, 0.18–0.78). No significant differences in the effects of exercise on shoulder muscle strength and neck and shoulder pain intensity were observed.

Conclusion: Physical exercise can improve neck muscle strength in military pilots. After removing studies that may be the source of heterogeneity, exercise showed a protective effect on neck pain, especially in RCTs. The conclusion that exercise had no effects on shoulder muscle strength and pain intensity should be taken with caution.

KEYWORDS

physical exercise, musculoskeletal disorders, neck pain, muscle strength, military pilots, meta-analysis

1 Introduction

Flight-related neck and shoulder pain is a common symptoms in military pilots (Espejo-Antunez et al., 2022). Neck disorders caused by flight have been afflicting pilots for a long time. Severe pain even leads to interruption or grounding of tasks, causing great harm to the physical and mental health of pilots (Nagai et al., 2014; Bahat et al., 2020).

Previous studies have shown that pain is affected by a variety of factors. In-flight effects, such as acceleration, sedentary behavior, head-worn equipment, and seatback, are all risk factors for neck pain and cervical spondylosis in pilots (Rintala et al., 2015; Verde et al., 2015; Posch et al., 2019). In particular, sudden movements of the pilot's head upon exposure to high Gz accelerations increase the risk of acute cervical spine injury (Honkanen et al., 2018). Studies have shown that the neck muscles in pilots are significantly activated during flight, suggesting that the neck muscle is subjected to a high load (Sovelius et al., 2019). When the load is applied for a long period, the muscle becomes fatigued, which increases the risk of neck muscle strains (O'Conor et al., 2020). With the continuous improvement of aircraft performance, the load borne by pilots is also increasing. The acceleration of high-performance fighters can reach more than +9 Gz at present, which undoubtedly poses a greater challenge to pilot cervical spine health (Wallace et al., 2021).

Currently, measures to prevent flight-related neck and shoulder pain include warm-up and stretching before and after flight, head prepositioning, and exercise etc., all of which have been reported to provide protective effects (De Loose et al., 2008; Thoolen and van den Oord, 2015; O'Conor et al., 2020; Wallace et al., 2021). However, even so, the reporting rate of neck pain among pilots has remained high in recent years (Chumbley et al., 2017; Omholt et al., 2017; Posch et al., 2019). This increase rate is undoubtedly related to the improvement of aircraft performance. In addition, pain relief through special head positions in a confined cabin is not satisfactory (Rausch et al., 2021). The method of changing the design of seat backrest or cabin environment is not only time-consuming but also requires considerable economic investment. Under such a premise, the prevention and relief of neck and shoulder pain through one's own exercise seems to be a relatively quick and effective method.

In many RCTs, strong evidence supports the effectiveness of physical exercise for neck pain (Sjøgaard et al., 2014; Saeterbakken et al., 2017; Park and Lee, 2020). The main purpose of exercise for pilots is to improve the ability to resist high Gz acceleration by improving the strength of the neck muscles and strengthening the control of the muscles (Rausch et al., 2021). In this study, we investigated the effects of physical exercise in military pilots on neck and shoulder muscle strength and pain base on a meta-analysis of previous studies, to provide more scientific and appropriate guidance for future training protocols.

2 Materials and methods

We followed the standards of PRISMA (Preferred Reporting Items for Systematic Reviews and Meta-Analyses) (Liberati et al., 2009; Zhang et al., 2021) and MOOSE (Meta-Analysis of Observational Studies in Epidemiology) (Stroup et al., 2000) guidelines during our research. The study protocol was registered with PROSPERO (International Prospective Register of Systematic Reviews: CRD42022336463).

2.1 Data sources and search strategy

The Embase, PubMed, and Cochrane Library databases were searched by three reviewers from inception to April 1st, 2022. Search items included medical subject headings (MeSH) and their following keywords: "pilot", "exercise", "training", "neck", and "shoulder". The search strategy is provided in detail in Supplementary Table S1. Outcome measures were not used as search terms because reviewers wanted to comprehensively query relevant measures of exercising intervention in pilots to avoid omissions of important information. No language restrictions were employed during the search. Duplicate studies were removed by means of Endnote and manual secondary examination. During the whole process of literature retrieval, screening, assessment and data extraction, disagreements between the two reviewers were resolved by discussion with a third reviewer.

2.2 Selection criteria and data extraction

The literature screening process followed the PICOS principles, i.e., "population", "intervention", "comparison", "outcome", and "study". The inclusion and exclusion criteria of the literature are provided in detail in Supplementary Table S2.

We extracted the following data from each included study: type of aircraft, total number of participants, age, height, weight, type of study, training site, training protocol, equipment, follow-up period, and outcomes. The primary outcomes were neck maximal voluntary isometric contractions (MVICs) (Lacio et al., 2021), including flexion, extension, left (Ltflx) and right (Rtflx) lateral flexion and the prevalence of neck pain (Ben Ayed et al., 2019). When included in our analysis, the units of the MVIC are unified and are typically reported as N or Nm. Given the paucity of studies, MVIC of shoulder elevation and pain intensity of neck and shoulder expressed by visual analog scale (VAS) (Kopsky et al., 2022) were used as secondary outcomes. The relative outcomes in the figures were analyzed with the aid of GetData Graph Digitizer 2.26.

2.3 Quality and risk-of-bias assessment

We used the Newcastle-Ottawa Quality Assessment Scale (NOS) to evaluate the risk of bias of the included observational studies (Stang, 2010). Of these, the NOS form has different terms for the case-control studies (CCS) and cohort studies. NOS scores ranged from 0 to 9, with a score of greater than 6 including a high-quality study. For randomized controlled trials (RCTs), we used the Cochrane Collaboration's tool to assess the risk of bias in six domains: sequence generation, allocation concealment, blinding, incomplete outcome data, selective outcome reporting, and other issues (Page et al., 2018). Cross-sectional studies used an 11-item checklist with a full scale of 11 scores as recommended by the Agency for Healthcare Research and Quality (AHRQ) (Song et al., 2021) as follows: low quality = 0–3; moderate quality = 4–7; high quality = 8–11.

2.4 Data synthesis and statistical analysis

We used Review Manager (Revman) software (version 5.4) for quantitative analysis of the following variables between the exercise group (EG) and the control group (CG) or between the exposure group (EG) and nonexposure group (NEG): MVIC, prevalence of pain, and VAS. As a result of the unit difference (N or Nm), we calculated pooled estimates of the standard mean differences (SMDs) with 95% confidence intervals (CIs) for MVIC. Pooled outcomes of the same unit and VAS were calculated using the MD. We calculated pooled odds ratios (ORs) and 95% confidence intervals (CIs) for the prevalence of pain, which served as a categorical variable. Random-effects models were used for the analysis of all outcomes, and the I^2 statistic was used to test for heterogeneity (Wei et al., 2022). Sensitivity analysis and subgroup analysis were performed on the results with $I^2 > 50\%$ to identify the source of heterogeneity. Leave-one-out sensitivity analysis and subgroup analysis were performed to address heterogeneity as much as possible. Subgroups were classified according to the type of study, aircraft, equipment, training protocol, and follow-up period. p values <0.05 were considered statistically significant. Due to the small number of included studies in each outcome, we did not perform a test for publication bias (Sterne et al., 2011).

3 Results

3.1 Literature search and study selection

Our search strategy identified a total of 1855 studies (PubMed = 505, Cochrane = 511, Embase = 839). After removing duplicates (n = 1186), 668 studies remained. After reading the titles and abstracts, 646 studies were excluded. Next, the full texts of 22 selected studies were reviewed. Seven studies were eliminated at this stage, and 15 studies were eligible for quantitative synthesis (Hämäläinen et al., 1993; Newman, 1997; Albano and Stanford, 1998; Jones et al., 2000; Alricsson et al., 2004; Burnett et al., 2005; De Loose et al., 2008; Ang et al., 2009; Lange et al., 2013; Salmon et al., 2013; Lange et al., 2014; Murray et al., 2017; Bahat et al., 2020; Murray et al., 2020; Rausch et al., 2021). The PRISMA flow chart for study selection is presented in Figure 1.

3.2 Quality assessment of the included studies

Supplementary Figure S1 shows a summary of the risk of bias assessment for RCTs (Alricsson et al., 2004; Burnett et al., 2005; Ang et al., 2009; Lange et al., 2013; Salmon et al., 2013; Lange et al., 2014; Murray et al., 2017; Bahat et al., 2020; Murray et al., 2020; Rausch et al., 2021). All studies were rated as high risk for the term "blinding of participants and personnel" due to the inability to conceal the intervention from the pilots who participated in the training program. We evaluated two case-control studies (Hämäläinen et al., 1993; De Loose et al., 2008) and two cohort studies (Newman, 1997; Albano and Stanford, 1998) using NOS. As a result, only one study was evaluated as high quality (total score = 6), two studies had a score of 5, and one study had a score of 4 (Supplementary Table S3). One cross-sectional study was evaluated using the 11-item checklist recommended by the AHRQ (Jones et al., 2000), and its quality was evaluated as moderate (total score = 4).

3.3 Study characteristics

The characteristics of the studies included in the meta-analysis are reported in Supplementary Table S4**.** The study region included Denmark (n = 4) (Lange et al., 2013; Lange et al., 2014; Murray et al., 2017; Murray et al., 2020); United States (n = 2) (Albano and Stanford, 1998; Jones et al., 2000); Australia (n = 2) (Newman, 1997; Burnett et al., 2005); Sweden (n = 2)

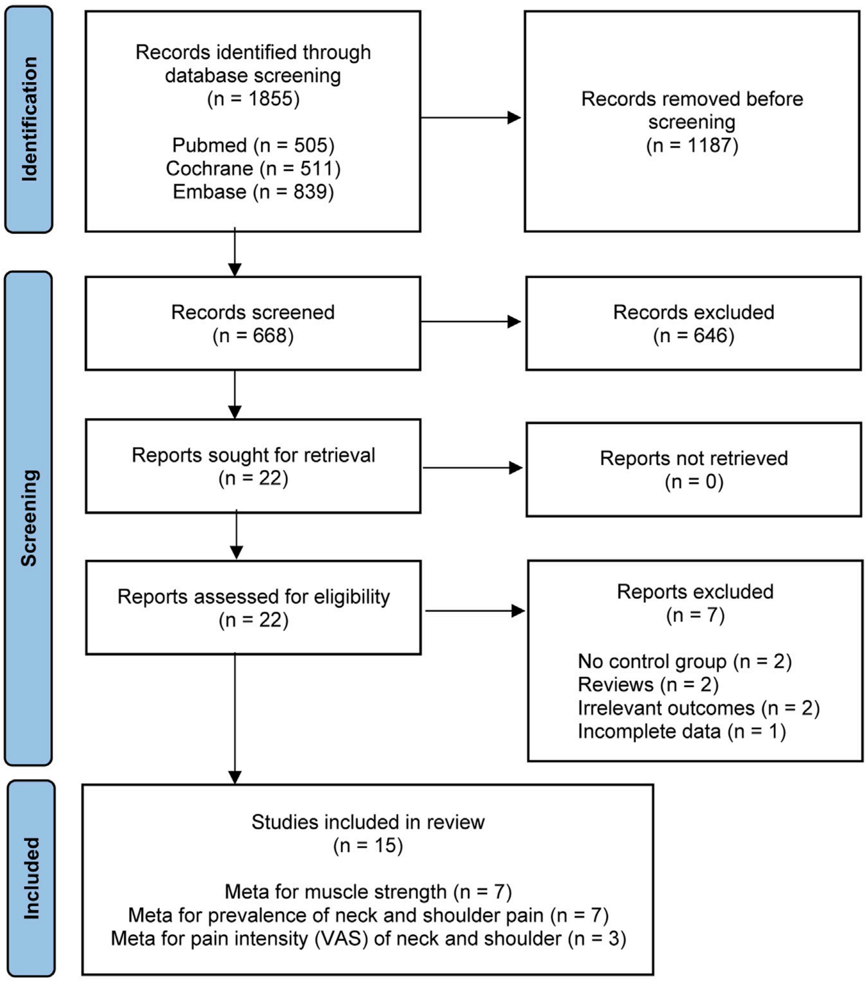

FIGURE 1
PRISMA flowchart of the study selection process for the meta-analysis.

(Alricsson et al., 2004; Ang et al., 2009); Finland (*n* = 1) (Hämäläinen et al., 1993); Belgium (*n* = 1) (De Loose et al., 2008), Canada (*n* = 1) (Salmon et al., 2013); Israel (n = 1) (Bahat et al., 2020), and Germany (*n* = 1) (Rausch et al., 2021). A total of 907 pilots, including 675 (74.4%) fighter crew members and 232 (25.6%) helicopter pilots, were analyzed. The training protocol included muscle strength training alone (*n* = 5) (Albano and Stanford, 1998; Jones et al., 2000; De Loose et al., 2008; Bahat et al., 2020; Rausch et al., 2021), strength and endurance training (*n* = 5) (Hämäläinen et al., 1993; Alricsson et al., 2004; Burnett et al., 2005; Ang et al., 2009; Salmon et al., 2013), and a combination of strength, endurance, and coordination training (*n* = 5) (Lange et al., 2013; Salmon et al., 2013; Lange et al., 2014; Murray et al., 2017; Murray et al., 2020). The equipment used included hands-free devices, small devices (elastic rubber bands, dumbbells, or body blades), and complex devices (multi-cervical units (MCUs). Given that two training groups were included in each of two studies (Burnett et al., 2005; Salmon et al., 2013) using different training protocols or equipment, the studies were split into Group A and Group B for meta-analysis (Zhao et al., 2022).

3.4 Strength of neck muscles

Figure 2 shows the forest plot of the relationship between physical exercise and muscle strength. The results showed that the increase in muscle strength was more significant in the exercise group in the four directions of neck movement: flexion (SMD, 0.45; 95% CI, 0.08 to 0.82; I^2 = 47%) (Figure 2A), extension (SMD, 0.63; 95% CI, 0.27 to 1.00; I^2 = 44%) (Figure 2B), Rtflx (SMD, 0.53; 95% CI, 0.12 to 0.94; I2 = 0%) (Figure 2C), and Ltflx (SMD, 0.50; 95% CI, 0.09 to 0.91; I^2 = 0%) (Figure 2D). The results of the unified unit of

10.3389/fphys.2022.973304

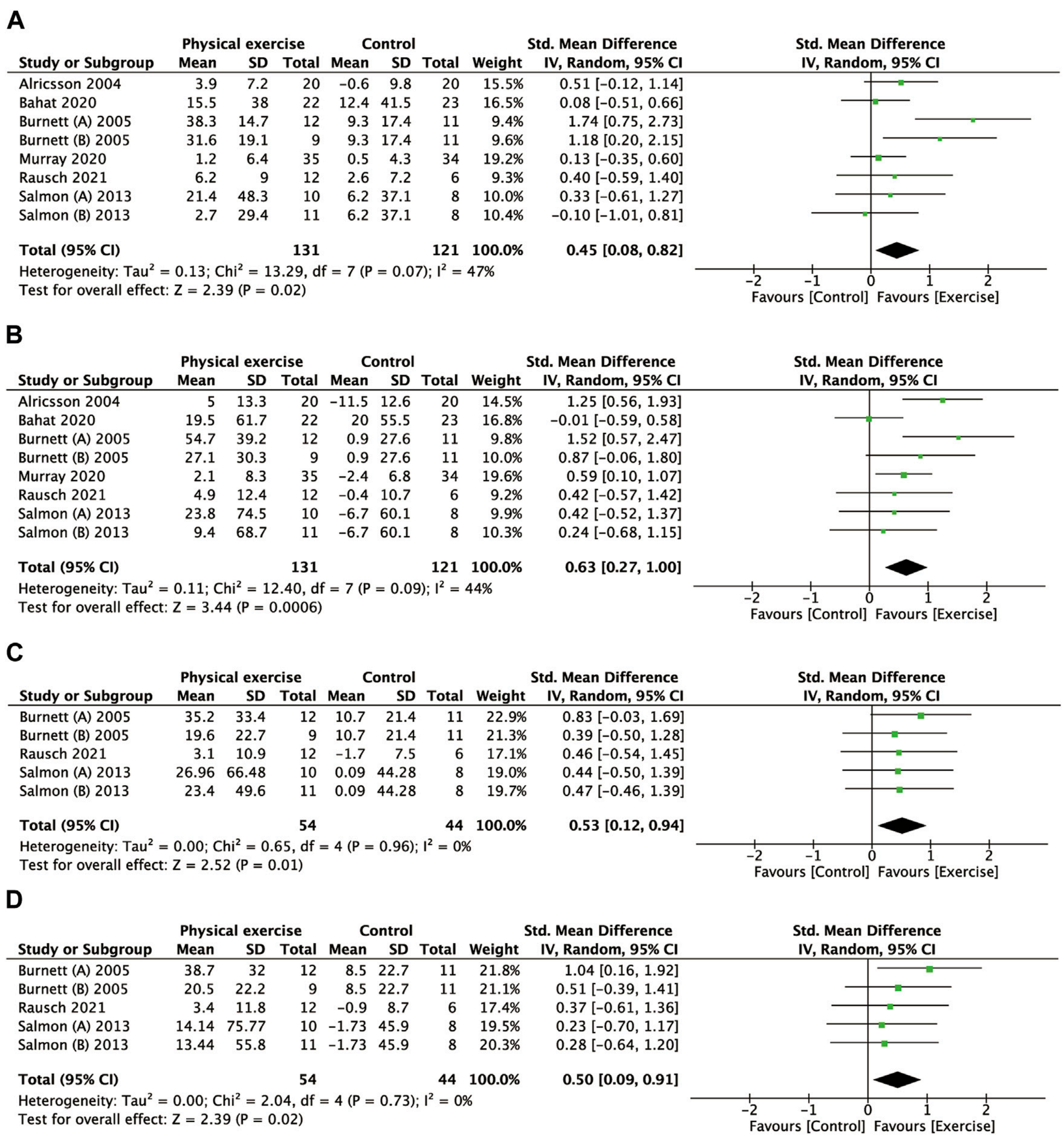

FIGURE 2
Forest plot comparing the MVIC of the neck in the physical exercise and control groups. **(A)** Flexion. **(B)** Extension. **(C)** Right lateral flexion. **(D)** Left lateral flexion. MVIC, maximal voluntary isometric contractions.

the muscle strength showed a higher change in the exercise group than the control group: 17.53 N (95% CI, 5.68 to 29.39; I^2 = 35%) in flexion (Supplementary Figure S2A); 27.55 N (95% CI, 7.11 to 47.99; I^2 = 35%) and 8.54 Nm (95% CI, 0.57 to 16.50; I^2 = 72%) in extension (Supplementary Figure S3); 17.08 N (95% CI, 3.59 to 30.56; I^2 = 0%) in Rtfix (Supplementary Figure S4); 19.25 N (95% CI, 5.54 to 32.96; I^2 = 0%) in Ltflx (Supplementary Figure S5), except for the flexion in Nm (MD, 1.60; 95% CI, -0.62, 3.81; I^2 = 0%) (Supplementary Figure S2B).

The subgroup analysis showed that muscle strength increases in neck flexion (SMD, 1.06; 95% CI, 0.32 to 1.80; I^2 = 56%) (Supplementary Figure S6), neck extension (SMD, 1.22; 95% CI, 0.74 to 1.69; I^2 = 0%) (Supplementary Figure S10), and Ltflx (SMD, 0.78; 95% CI, 0.15 to 1.41; I^2 = 0%) (Supplementary Figure S17) were significantly greater than those noted in the control group, and Rtflx (SMD, 0.62; 95% CI, 0.00 to 1.24; I^2 = 0%) (Supplementary Figure S14) approached a significant higher value. In contrast, the helicopter group exhibited no significant difference except for extension (SMD, 0.49; 95%

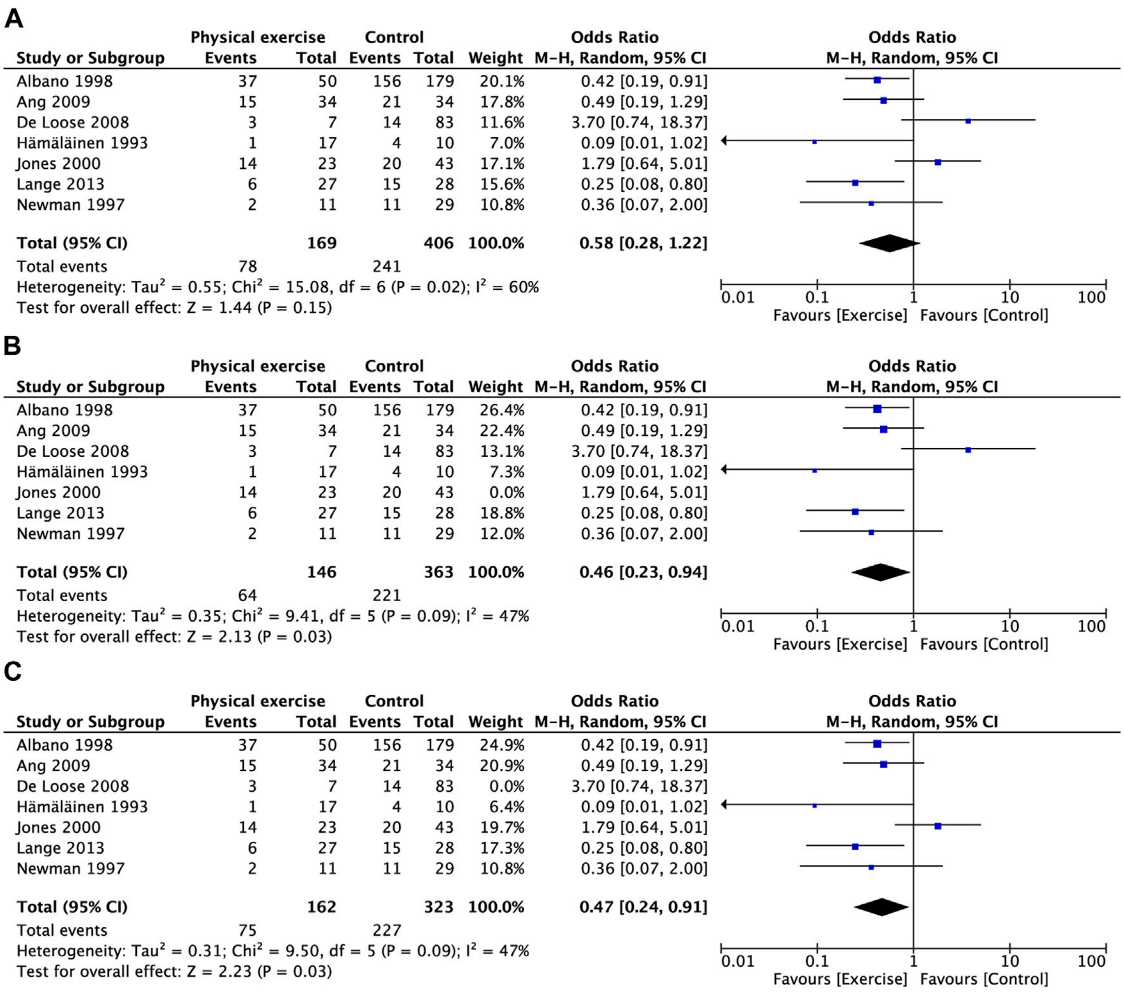

FIGURE 3
Forest plot comparing the prevalence of neck pain in the physical exercise and control groups. **(A)** Before leave-one-out sensitivity analysis **(B)** After leave-one-out sensitivity analysis (Jones et al., 2000). **(C)** After leave-one-out sensitivity analysis (De Loose et al., 2008).

CI, 0.12 to 0.85; I^2 = 0%) (Supplementary Figure S10). In addition, except for the significant heterogeneity of the aircraft type in neck extension (p = 0.004) (Supplementary Figure S10), no significant heterogeneity in other directions was noted.

The subgroup analysis of training equipment showed that the strength increase in neck flexion (SMD, 0.33; 95% CI, 0.33 to 0.63; I^2 = 0%) and extension (SMD, 0.68; 95% CI, 0.37 to 0.98; I^2 = 0%) in the exercise group using a small device was significantly greater than that in the control group (Supplementary Figures S7, S11). However, the strength increase in Ltflx and Rtflx was not significantly different (Supplementary Figures S15, S18). In addition, the strength increase using the complex device was also significant in the neck flexion (SMD, 1.74; 95% CI, 0.75–2.73) (Supplementary Figure S7), extension (SMD, 1.52; 95% CI, 0.47–2.47) (Supplementary Figure S11), and Ltflx (SMD, 1.04; 95% CI, 0.16–1.92) (Supplementary Figure S18) with near significance in Rtflx (SMD, 0.83; 95% CI, -0.03–1.69) (Supplementary Figure S15). Training equipment had significant heterogeneity in neck flexion (p = 0.01) and extension (p = 0.02) (Supplementary Figures S7, S11).

The subgroup analysis of the training protocol showed that muscle strength in the strength plus endurance training group was significantly greater than simply strength training and comprehensive (strength+endurance+coordination) training in neck flexion (SMD, 0.80; 95% CI, 0.07 to 1.52; I^2 = 65%) (Supplementary Figure S8), extension (SMD, 0.70; 95% CI, 0.47 to 1.51; I^2 = 32%) (Supplementary Figure S12), Rtflx (SMD, 0.57; 95% CI, 0.06 to 1.09; I^2 = 0%) (Supplementary Figure S16), and Ltflx (SMD, 0.62; 95% CI, 0.10 to 1.14; I^2 = 0%) (Supplementary Figure S19). The comprehensive training protocol was significant only in extension strength (SMD, 0.55; 95% CI, 0.12 to 0.98; I^2 = 0%) (Supplementary Figure

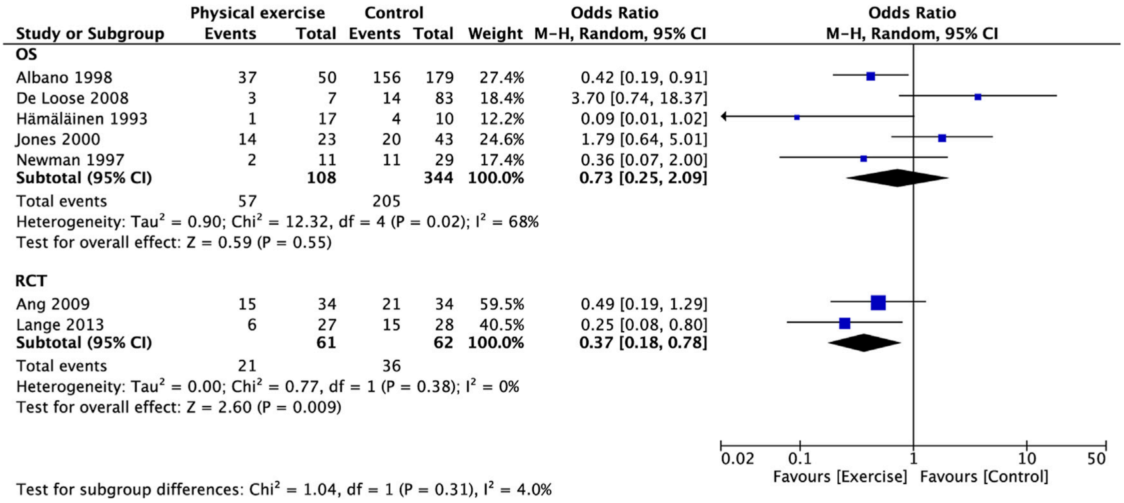

FIGURE 4
Subgroup analysis for prevalence of neck pain (type of study).

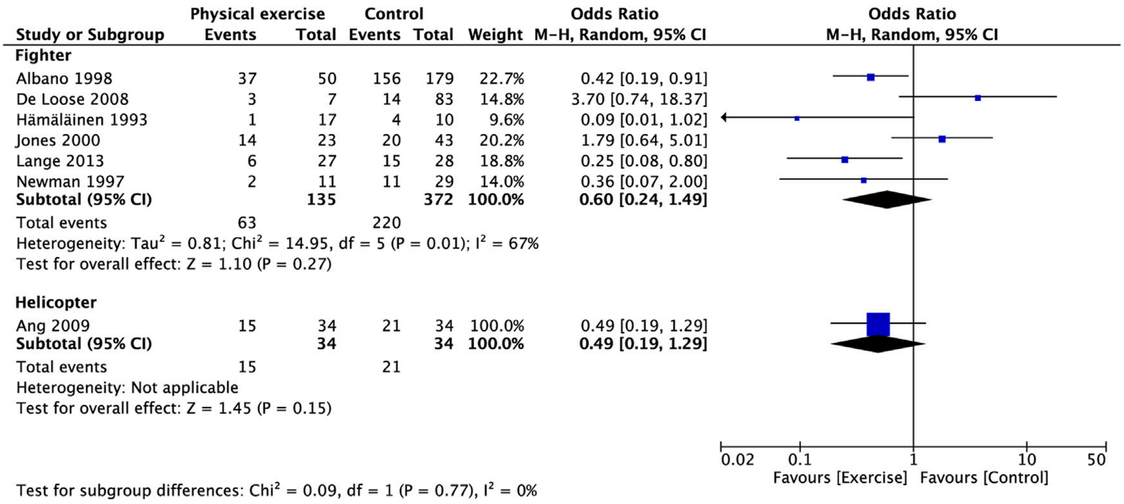

FIGURE 5
Subgroup analysis for prevalence of neck pain (type of aircraft).

S12), and the other protocols were not significantly different. The heterogeneity of the training protocol was not statistically significant.

The subgroup analysis of the follow-up period showed that there were statistically significant muscle strength increases in neck flexion (SMD, 0.55; 95% CI, 0.01 to 1.10; I^2 = 59%) (Supplementary Figure S9) and neck extension (SMD, 0.52; 95% CI, 0.06 to 0.97; I^2 = 39%) (Supplementary Figure S13) at a follow-up period of less than 20 weeks. Only the strength increase in extension (SMD, 0.87; 95% CI, 0.23 to 1.51; I^2 = 59%) at a follow-up period of no less than 20 weeks was statistically significant (Supplementary Figure S13). The heterogeneity of the follow-up period was not statistically significant.

3.5 Prevalence of neck pain

Figure 3A presents the relationship between physical exercise and the prevalence of neck pain. The results showed that the

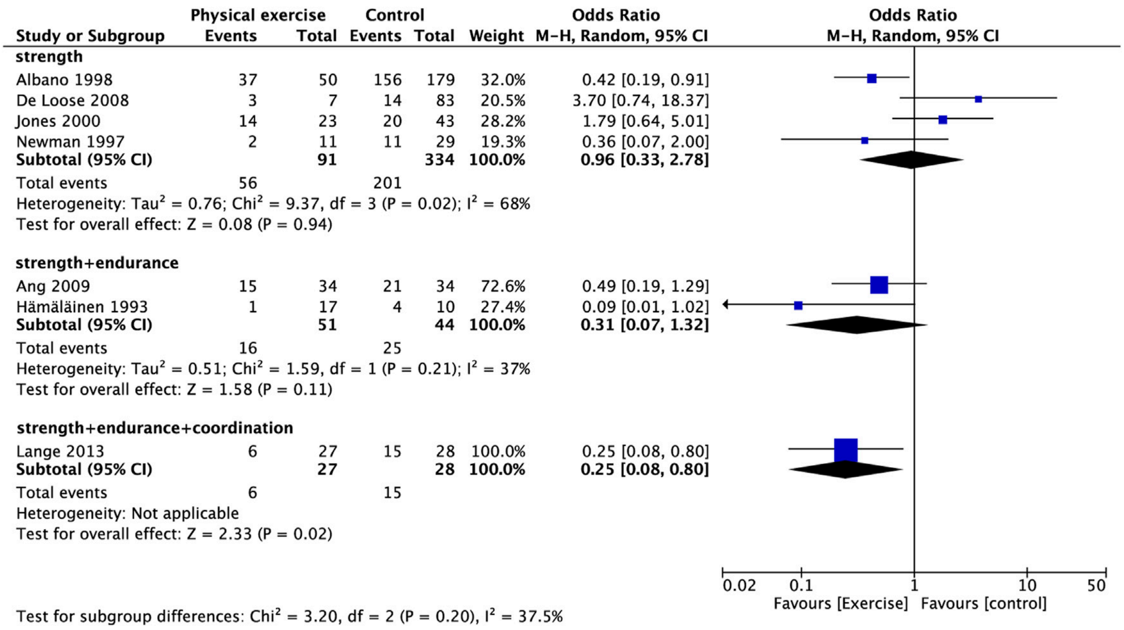

FIGURE 6
Subgroup analysis for prevalence of neck pain (training protocol).

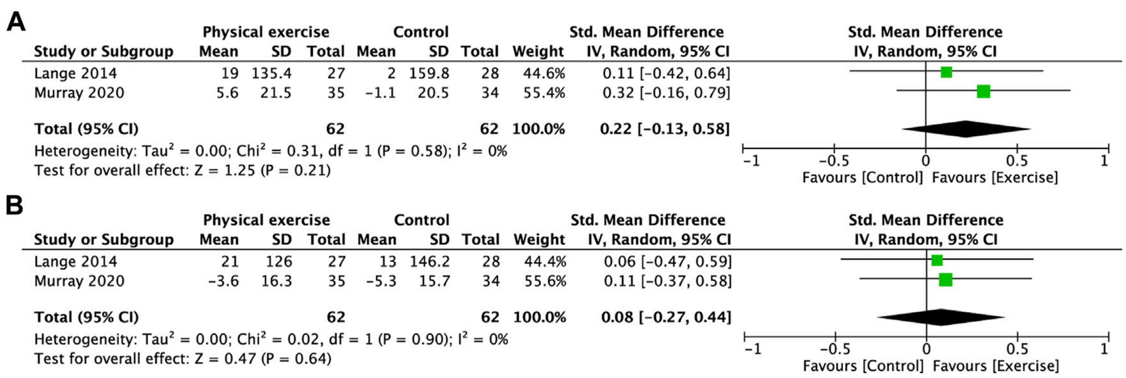

FIGURE 7
Forest plot comparing MVIC of the shoulder in the physical exercise and control groups. **(A)** Right elevation. **(B)** Left elevation. MVIC, maximal voluntary isometric contractions.

prevalence of neck pain in the exercise group was not statistically significant compared with that in the control group (OR, 0.58; 95% CI, 0.28 to 1.22; I^2 = 60%). Sensitivity analysis showed that heterogeneity was restored (I^2 = 47%) after the exclusion of two studies (Jones et al., 2000; De Loose et al., 2008), and the pooled OR showed a significant association between physical exercise and the prevalence of neck pain (OR, 0.46; 95% CI, 0.23–0.94) (Figure 3B) (OR, 0.47; 95% CI, 0.24–0.91) (Figure 3C). The subgroup analysis of study type showed that the reduction in the prevalence of neck pain with the RCT compared with OS was statistically significant (OR, 0.37; 95% CI, 0.18 to 0.78; I^2 = 0%) (Figure 4). The prevalence of neck pain was not significant based on the type of aircraft (Figure 5). In the training protocol subgroup, although comprehensive training (strength + endurance + coordination) was significant (OR, 0.25; 95% CI, 0.08–0.80) (Figure 6), the result was relatively conservative due to the small number of studies (n = 1). In addition, the prevalence of neck pain was not significant for the heterogeneity of all subgroups.

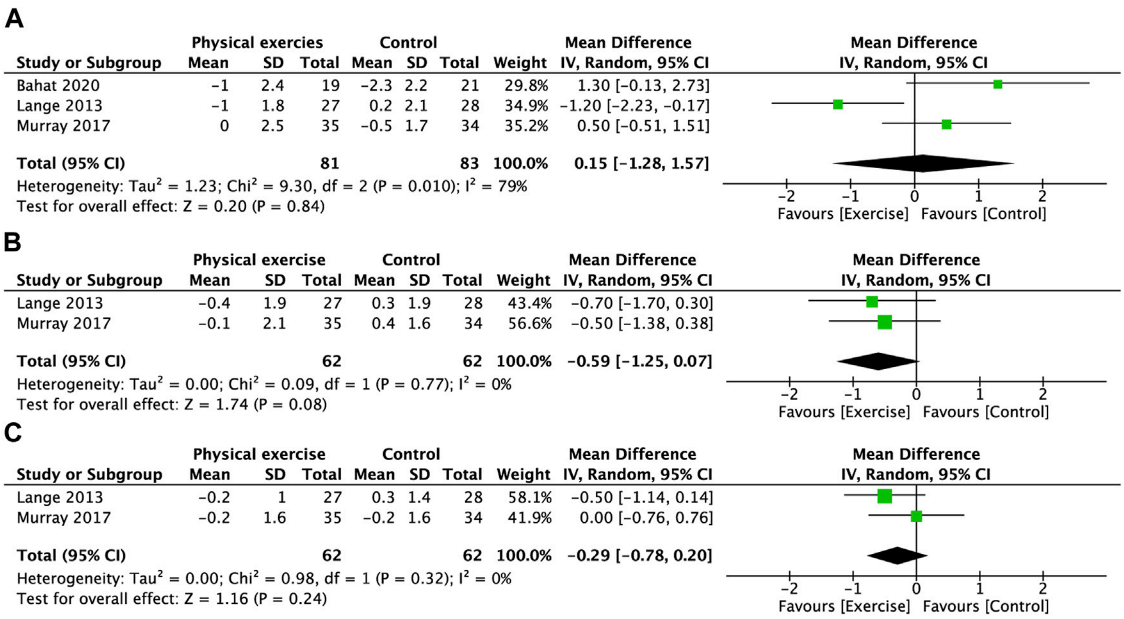

FIGURE 8
Forest plot comparing the VAS scores of the neck and shoulder in the physical exercise and control groups. **(A)** Neck. **(B)** Right shoulder. **(C)** Left shoulder. VAS, visual analog scale.

3.6 Strength of shoulder muscles

Figure 7 shows that physical exercise did not significantly improve right shoulder (Figure 7A) or left shoulder muscle strength (Figure 7B) compared with the control group.

3.7 Pain intensity of the neck and shoulder

Figure 8 shows that physical exercise did not significantly reduce pain intensity in the neck (Figure 8A), right shoulder (Figure 8B), or left shoulder (Figure 8C) compared with the control group.

4 Discussion

4.1 Association between exercise and neck and shoulder strength in pilots

Methods to improve neck muscle strength through exercise have become a consensus in the general working population. However, due to the particularity of a pilot's profession, daily flights and routine training occupy most of his/her day. Can additional training programs significantly improve neck and shoulder muscle strength, and does training have the same effect on muscle strength in different parts of the neck? These issues need to be clarified urgently because they will help us to further develop more scientific training programs. Currently, there is no evidence-based exercise program that can specifically improve the strength of muscles around the spine to reduce physiological and perceived stress during high Gz flight (Rausch et al., 2021). Fortunately, our meta-analysis yielded positive results showed that physical exercise significantly improved MVIC in the four directions of neck motion in flexion, extension, Rtflx, and Ltflx (Figure 2), indicating that exercise had a significant effect on neck muscle strengthening in pilots. In particular, the pooled estimates of the MD in unified unit showed that the muscle strength change in neck flexion increased by 17.53 N in the exercise group compared to the non-exercise group; the neck extension increased by 27.55 N, and the exercise group could do more work by 8.54 Nm with the same torque; the muscle strength in right and left flexion increased by 17.08 N and 19.25 N respectively. Although no significant result was obtained for muscle strength change in neck flexion in Nm, in general, exercise did increase the pilots' neck muscle strength to some extent (Supplementary Figure S2-5).

However, the difference in shoulder elevation was not significant (Figure 7). Murray et al. (Murray et al., 2020) found that the shoulder musculature was stronger in pilots and crew than in general working staff, whereas neck strength was not correspondingly higher. Our results also seem to corroborate his study in that the benefits obtained by neck muscles through exercise may be more pronounced than those of the shoulders. It has been demonstrated that the trapezius muscle is activated during air combat maneuvers, especially when fighter pilots adopt a specific head position (Netto and Burnett, 2006). This finding also suggests that our training protocol needs to strengthen the intensity on the shoulder to obtain significant muscle strength improvement. However, because the number of studies was too small, we remain cautious about this conclusion.

4.2 Association between exercise and neck and shoulder pain in pilots

Although many studies have demonstrated that physical exercise can relieve work-related neck pain (Blangsted et al., 2008; Sjøgaard et al., 2014; Saeterbakken et al., 2017; Chen et al., 2018; Park and Lee, 2020), there is no strong evidence that physical exercise reduces the prevalence or intensity of flight-related neck and shoulder pain because the different mechanisms contrast with the occupational pain in general high Gz and special aviation environments are the root causes. It is worth affirming that there are still many OS and RCTs with positive conclusions. Albano et al. (Albano and Stanford, 1998) investigated 268 American F-16 pilots and found that the probability of neck injury was reduced in the early exercise intervention (p = 0.024). Ang et al. (Ang et al., 2009) performed 1-year neck training in 68 helicopter pilots and found that the incidence of neck pain was reduced in the past week (OR, 3.2; 95% CI, 1.3–7.8) and the past 3 months (OR, 1.9; 95% CI, 1.2–3.2) after follow-up. Lange et al. (Lange et al., 2013) also showed that targeted neck exercises for fighter pilots can reduce their neck pain intensity. However, there are also studies that report the opposite conclusions. De Loosede et al. (De Loose et al., 2008), Newman et al. (Newman, 1997), and Jones et al. (Jones et al., 2000) showed no difference in the incidence of neck pain between the exercise and no exercise groups. In-flight acceleration loading increases the pull to the spine through the muscles and ligaments of the neck, accelerating disc degeneration and the development of neck pain (Iatridis et al., 2013). In contrast, pilots with neck pain had significantly lower muscle strength (Ang et al., 2005). More studies have shown that increasing the strength of neck muscles can yield more sustained muscle support and protect the spine from high Gz-induced injury (Green and Brown, 2004; Stergiou et al., 2017; Sovelius et al., 2019). Second, a stronger muscle reduces the transmission of force, enhances the stability of the spine, and reduces the risk of load-induced premature disc degeneration (Harrison et al., 2015; Sovelius et al., 2020).

Our pooled OR showed no significant effect of physical exercise in reducing the prevalence of neck pain (Figure 3A). However, we noted high heterogeneity in this result (I^2 = 63%). Fortunately, we found possible sources of heterogeneity through sensitivity analysis. After excluding the studies by Jones et al. (Jones et al., 2000) and De Loose et al. (De Loose et al., 2008), heterogeneity was restored (I^2 = 47%), and the pooled OR showed a significant association between physical exercise and the prevalence of neck pain (Figures 3B,C). The study by Jones et al. (Jones et al., 2000) was a cross-sectional study and was lower in level of evidence than RCTs, cohort studies, and case-control studies according to Oxford Centre for Evidence-Based Medicine (Howick and Glasziou, 2011). De Loose et al. (De Loose et al., 2008) had a smaller sample size, especially in the exposure group. Only seven people participated in exercise. Although only three people in the exposure group had neck pain, which may seem like a small number, the smaller denominator resulted in a seemingly increased prevalence. In addition, the study was a case-control study with no a high-level of evidence (Howick and Glasziou, 2011). Our subgroup analysis of study types revealed that RCTs had a significantly lower prevalence of neck pain, but not for the OS (Figure 4). Given that OS are retrospective, the exercises were unsupervised, and a large recall bias was noted in the respondents. Second, we noted a large difference in reporting pain rates at baseline across studies, which was attributed to the different definitions of neck pain, which also contributed to heterogeneity to some extent.

Our analysis for pain intensity showed no difference in pain scores between the exercise and control groups, either in the neck or shoulder (Figure 8). However, the findings are cautious due to the small number of studies. The investigation by Lange et al. (Lange et al., 2013) showed that although a significant majority (82%) of pilots experienced neck pain in the year, none experienced symptoms on a daily basis. Seventy-three percent of the pilots had a pain frequency of <31 days in a year. Bahat et al. (Bahat et al., 2020) also expressed a consistent view that flight-related neck pain usually occurs acutely after a flight and recovers over several days. This also suggests that pilot neck pain is not chronic, but periodically occurs with exposure. This cyclical pain would result in lower mean scores because the odds of experiencing pain in such a short duration are low. Murray et al. (Murray et al., 2016) suggested that the "dilution" effect of participants without pain results in lower pain scores at baseline and a lower likelihood of reducing pain intensity through exercise. Some studies have used the percentage of individuals with a 50% reduction in VAS (Salmon et al., 2013) as an outcome indicator to evaluate the effect of exercise, which seems to be an option. In addition, we believe that the reporting of pain frequency may be more representative of the characteristics of cyclical pain than intensity and prevalence.

4.3 Association between subgroups and outcome

4.3.1 Type of aircraft

Our subgroup analysis found that the muscle strength changes in fighter pilots after exercise were more significant than those of helicopter pilots (Supplementary Figures S6, S10, S14, S17). Studies on the differences in muscle strength of pilots of different aircraft types are limited. Ang et al. (Ang et al., 2005) measured the MVC of the neck muscle in pilots with neck pain and found that muscle strength was decreased in fighter pilots with neck pain, but not in helicopter pilots. The source of the difference may be that fighter pilots are frequently exposed to high Gz loads, resulting in decreased skeletal muscle stress. Helicopter pilots have a long driving time, and long fixed postures more often manifest as muscle fatigue. Fighter pilots may have generally lower neck strength than helicopter pilots, which may explain our results. Specially, fighter pilots may have more room to improve their neck strength due to reduced muscle strength caused by a high prevalence of neck pain. Because pilots in different types of aircraft have different types of exposure and pain, the training will also have a different focus (Ang et al., 2005; Murray et al., 2015). Helicopter pilots are more suitable for endurance exercise due to frequent neck muscle fatigue.

The prevalence of neck pain varies among different types of aircraft. Grossman et al. (Grossman et al., 2012) found that neck pain is more common in fighter pilots compared with attack helicopter and transport aircraft pilots possibly because the necks of fighter pilots are more susceptible to a combination of factors, such as helmets, acceleration, and sitting posture. De Loose et al. (De Loose et al., 2008) stated that "check six" is a routine flight maneuver for fighter pilots and the most common cause of neck pain in investigated pilots. This action requires the combination of lateral neck flexion and extension muscles to achieve maximal rotation of the neck. Therefore, the neck muscles of fighter pilots are affected by greater flight stress than other types of pilots. In summary, the incidence of neck pain was greater in fighter pilots compared with helicopter pilots. We included seven studies in our analysis on the prevalence of neck pain, six of which focused on fighter pilots and only one study focused on helicopter pilots, which resulted in a high baseline in the prevalence of neck pain. Due to the paucity of studies on helicopter pilots, we did not observe a difference in the effect of exercise on the prevalence of neck pain in pilots of different aircraft types (Figure 5).

4.3.2 Equipment

A commonly used device for neck training is an elastic band named the Thera-band (THER) (Burnett et al., 2005; Ang et al., 2009) (2009, Ang)(Salmon et al., 2013; Murray et al., 2020), which is also referred to as a headband (Lange et al., 2013) or rubber tube in some literature (Alricsson et al., 2004). In general, one end of the elastic band is fixed to a helmet or a harness over the head, and the other end is fixed or attached to a weight. The trainer then performs muscle contractions in different directions of neck movement. This equipment is also suitable for shoulder training (Murray et al., 2020) or is replaced with other weights, such as dumbbells (Lange et al., 2013). In most studies, muscle strength increased and pain improved in pilots who applied elastic bands (Alricsson et al., 2004; Lange et al., 2013; Salmon et al., 2013; Murray et al., 2020), but some studies also yielded negative results (2017, Murray). Our subgroup analysis is consistent with most studies, where the muscle strength increase in neck flexion and extension with small devices (including THER, rubber tube, headband, band) was significant (Supplementary Figures S7, S11) with the exception of lateral flexion (Supplementary Figures S15, S18). In addition, a larger neck training device called the multi-cervical unit (MCU) has also been used in pilot neck training (Chiu and Sing, 2002; Burnett et al., 2005). Burnett et al. (Burnett et al., 2005) compared the effectiveness of muscle strength training in pilots using MCU or THER. The researchers found that MCU was superior to elastic bands. Although our analysis included this study as a separate subgroup, we cannot conclude that MCU was more effective than elastic bands for neck muscle training due to the lack of additional literature support. Netto et al. (Netto et al., 2007) performed neck exercises in pilots using elastic bands and resistance machines to simulate different intensities of muscle activation during air combat maneuver. They concluded that neck training using the elastic band might be most practical for pilots who were exposed to low gravity flight and maintained a neutral neck position, such as transport, bomber, or helicopter pilots. In addition, elastic band training is more suitable for rehabilitation after + Gz injury. On the other hand, resistance machines were recommended for overload intensity training of fighter pilots to obtain maximal muscle strength (TAN, 1999; Coutts et al., 2007; Cheng et al., 2011).

Some studies applied virtual reality (VR) systems for training assistance and instruction (Bahat et al., 2020), but did not report differences in terms of muscle strength improvement and pain relief. Given that we do not know what devices their subjects used during training, it is not possible to categorize it into any of the subgroups. The frequent deployments and relocations of pilots prevent them from regularly accessing the gym for training and make it difficult to obtain training equipment suitable for counterweight (Rausch et al., 2021). Therefore, we need to seek forms of strength exercise that do not require special equipment, and the training equipment is portable (O'Conor et al., 2020). More studies suggested the use of an elastic band for training (Netto et al., 2007; Salmon et al., 2011) given its convenience compared to large equipment. One study reported a wearable cervical resistance exercise device that has been shown to be effective in improving strength and endurance in the cervical muscle. Targeted at implementing portable countermeasures, this device may represent a good alternative to elastic bands (O'Conor et al., 2020).

4.3.3 Training protocol

In general occupational groups, work-related neck pain is reduced by various physical exercises (Blangsted et al., 2008), proprioceptive muscle coordination training (Waling et al., 2000; Blomgren et al., 2018), and strength training (Lange et al., 2013; Price et al., 2020). Currently, there is no recognized form of exercise that can prevent neck pain in pilots. The most common form of training that target the neck and shoulder muscle include strength, endurance, and coordination training (Lange et al., 2013; Murray et al., 2017; Rausch et al., 2021). It has been reported that muscle strength training for more than 1 hour per week may represent a protective factor for neck pain in helicopter pilots (Ang et al., 2009). Many investigators have used electromyographic measures based on flight exposure to assess neck and shoulder fatigue and found prolonged muscle activation, indicating that muscle fatigue may be a risk factor for the development of neck and shoulder pain (Ang et al., 2005; Harrison et al., 2009; Salmon et al., 2011). In the general population, the strength and endurance of cervical muscles are decreased in patients with neck pain (Falla et al., 2004; Selistre et al., 2021). Hämäläinen et al, (1998) investigated the effects of a training program on pilots and found that dynamic endurance trainers had less sick leave and +Gz limitation due to neck complaints than resistance training. This finding suggests that pilots with neck and shoulder pain may also benefit from endurance training rather than just strength training. Generally, in muscle fibers, type I fibers are activated superior to type II fibers to provide sustained low-intensity muscle pull (Visser and van Dieën, 2006). Increasing the number of type I fibers can increase the ability of muscles to aerobically breathe, maintaining muscle contraction against fatigue for extended periods of time (Harrison et al., 2009). A longer duration of pain is associated with significantly reduced number of type I fibers and higher proportion type II fibers (Purushotham et al., 2022). Endurance training programs that provide low loads have the potential to slow or reverse this change.

In addition to endurance training, an increasing number of studies emphasize the importance of pilot coordination training (Salmon et al., 2013; Lange et al., 2014; Murray et al., 2020; Rausch et al., 2021). Superficial musculature is used for segmental control during neck movements, which requires deep stability to support the anterior convex curve of the cervical spine (Salmon et al., 2011). When the deep muscles are weakened, the superficial muscles overcompensate, leading to dysfunction of the neck muscles (Falla, 2004). Falla, (2004) proposed the use of low-load exercise to re-establish coordination between the deep and superficial layers of the neck muscles. Salmon et al, (2013) performed neck coordination and endurance training on pilots and showed that the participants in both groups exhibited significant increases in maximum neck strength and endurance compared to the control group, and the effect of the coordination training group showed a greater increase than the endurance training group. In another study, pilots used trampoline training to improve neck muscle function, and the results showed that it was as effective as strength training in increasing maximal muscle strength and reducing neck strain in flight. Trampoline training may increase neuromuscular performance and intermuscular coordination, which may improve the mechanical efficiency of maintaining cervical spine stability and thus have beneficial effects in reducing flight muscle strain (Sovelius et al., 2006). Our subgroup analysis showed that strength training alone did not improve the neck muscle strength of pilots (Supplementary Figures S8, S12, S16, S19) or reduce the prevalence of neck pain (Figure 6), In contrast, strength with endurance training significantly improved neck muscle strength (Supplementary Figures S8, S12, S16, S19) but also did not show a significant reduction in the prevalence of neck pain. In contrast, a combination of strength, endurance and coordination training appeared to achieve significant neck pain relief. However, due to the small pooled number, we need to include more studies to verify this finding.

4.3.4 Follow-up period

In the subgroup analysis of follow-up time, muscle strength was improved in the follow-up less than 20 weeks, while the follow-up group with no less than 20 weeks had a significant improvement in the extension but not in the flexion muscle. (Supplementary Figures S9, S13). However, we generally believe that the exercise period can accumulate higher changes in outcomes. However, the length of the training period greatly affects compliance. Ang et al. (Ang et al., 2009) reported 77% compliance at a follow-up time of 6 weeks, which was acceptable. Another study conducted a 12-weeks training follow-up and reported 52.8% and 76.1% adherence in the two groups (Salmon et al., 2013). The study by Murray et al. (Murray et al., 2017; Murray et al., 2020) included a long follow-up time (20 weeks), whereas only 28.6% of participants adhered to regular training. In the study by Lange et al. (Lange et al., 2014) with a follow-up of 24 weeks, only 58% of the participants regularly trained three times a week. Overall, the compliance of pilots is reduced with a longer follow-up period.

Therefore, we need to identify the optimal training period to achieve the maximum payoff. Bahat et al, (2020) reported self-supervised 4-weeks short-period training in pilots, but the results showed no significant improvement in muscle strength. Other groups reported that 6 weeks of training increased muscle strength (Stasinaki et al., 2015) and reduced in-flight neck strain or pain under + Gz loading (Sovelius et al., 2006). For office workers, their neck pain was reduced when they performed specific strength training for 10 weeks (Saeterbakken et al., 2017). Similarly, Burnett et al. (Burnett et al., 2005) suggested neck training 10 weeks before pilots start flying high-performance aircraft to be completely prepared for the load of high-performance. In addition, a neck strengthening program should be developed for those who return to service after a flight break to increase neck strength. Based on previous research experience, the research and development of exercise programs for future combat pilots should include exercise schedules and supervised programs to ensure compliance (Bahat et al., 2020). Based on this notion, we believe that a short period of adequate stimulation is more suitable than a longer exercise program for the professional needs of pilots, and this time can be roughly limited to approximately 6–12 weeks. Moreover, training must be highly specific and supervised because general whole-body reinforcement is not thought to produce similar improvements in neck strength (Conley et al., 1997). In the future, an informatization management means that breaks geographical restrictions are indispensable.

4.4 Limitations

This study has some limitations. First, we included observational studies (cohort studies, case-control studies, and cross-sectional studies), when investigating the effects of exercise on neck pain. This design will cause an unavoidable bias due to the presence of potential confounding factors. Second, the number of studies included in each outcome was small, and the quality was uneven. The small sample size of each study leads to a wide confidence interval for the pooled effect value, which reduces the power of the results. Third, differences in the definition of outcomes and measurement criteria were noted. There were differences in the criteria for the pain and pain-free groups between studies. Fourth, differences in exercise programs were noted. To address the above limitations, we will continuously follow up the relevant research progress and try to identify more high-quality studies to expand the sample size. The mesh meta-analysis will be performed to compare the differences between types of exercise intervention.

5 Conclusion

Physical exercise can improve the neck muscle strength of military pilots and is significantly effective in flexion, extension, and left and right lateral flexion. Moreover, fighter pilots, complex devices, comprehensive training (strength plus endurance), and a follow-up period less than 20 weeks seemed to obtain more significant muscle strength improvement than helicopter pilots, small devices, simple strength training, and a follow-up period greater than 20 weeks. Overall, the pooled results did not show a significant effect of exercise on neck pain. However, sensitivity analysis revealed that the lack of a significant effect was due to heterogeneity. The sources of heterogeneity may include observational studies and studies with small samples. After removing the above studies, exercise showed a significant protective effect on neck pain. No significant differences in shoulder muscle strength or neck and shoulder pain intensity were noted between exercises. However, this conclusion should be taken with caution, and more studies need to be included to improve the persuasiveness of these findings. There are great challenges in the development of training programs for military pilots due to the differences in aircraft types and the uncertainty of working hours and locations. In the future, training protocols, equipment, periods and methods of supervision should be fully considered.

Data availability statement

The raw data supporting the conclusion of this article will be made available by the authors, without undue reservation.

Author contributions

JQ, CZ, and WH designed the study. WH, FW, and ZL performed the literature search. WH, FW, and ZL conducted the literature retrieval, screening, and assessment. XY, KZ and FY extracted data. WH, FW, ZL, XY and MD did the statistical analyses. WH, FW, and ZL drafted the manuscript. All authors reviewed and edited the manuscript. CZ and JQ supervised the study. All authors read and approved the submitted version.

Funding

This work was supported by grants from the National Natural Science Foundation of China (No. 81871818) and Natural Science Basic Research Plan in Shaanxi Province of China (No.2019JM-265).

Conflict of interest

The authors declare that the research was conducted in the absence of any commercial or financial relationships that could be construed as a potential conflict of interest.

Supplementary material

The Supplementary Material for this article can be found online at: https://www.frontiersin.org/articles/10.3389/fphys.2022.973304/full#supplementary-material

References

Abe, T., Dehoyos, D. V., Pollock, M. L., and Garzarella, L. (2000). Time course for strength and muscle thickness changes following upper and lower body resistance training in men and women. *Eur. J. Appl. Physiol.* 81, 174–180. doi:10.1007/s004210050027

Albano, J. J., and Stanford, J. B. (1998). Prevention of minor neck injuries in F-16 pilots. *Aviat. Space Environ. Med.* 69, 1193–1199.

Alricsson, M., Harms-Ringdahl, K., Larsson, B., Linder, J., and Werner, S. (2004). Neck muscle strength and endurance in fighter pilots: Effects of a supervised training program. *Aviat. Space Environ. Med.* 75, 23–28.

Ang, B., Linder, J., and Harms-Ringdahl, K. (2005). Neck strength and myoelectric fatigue in fighter and helicopter pilots with a history of neck pain. *Aviat. Space Environ. Med.* 76, 375–380.

Ang, B. O., Monnier, A., and Harms-Ringdahl, K. (2009). Neck/shoulder exercise for neck pain in air force helicopter pilots: A randomized controlled trial. *Spine (Phila Pa 1976)* 34, E544–E551. doi:10.1097/BRS.0b013e3181aa6870

Bahat, H. S., German, D., Palomo, G., Gold, H., and Nir, Y. F. (2020). Self-kinematic training for flight-associated neck pain: A randomized controlled trial. *Aerosp. Med. Hum. Perform.* 91, 790–797. doi:10.3357/AMHP.5546.2020

Ben Ayed, H., Yaich, S., Trigui, M., Ben Hmida, M., Ben Jemaa, M., Ammar, A., et al. (2019). Prevalence, risk factors and outcomes of neck, shoulders and low-back pain in secondary-school children. *J. Res. Health Sci.* 19, e00440.

Blangsted, A. K., Søgaard, K., Hansen, E. A., Hannerz, H., and Sjøgaard, G. (2008). One-year randomized controlled trial with different physical-activity programs to reduce musculoskeletal symptoms in the neck and shoulders among office workers. *Scand. J. Work Environ. Health* 34, 55–65. doi:10.5271/sjweh.1192

Blomgren, J., Strandell, E., Jull, G., Vikman, I., and Röijezon, U. (2018). Effects of deep cervical flexor training on impaired physiological functions associated with chronic neck pain: A systematic review. *BMC Musculoskelet. Disord.* 19, 415. doi:10.1186/s12891-018-2324-z

Burnett, A. F., Naumann, F. L., Price, R. S., and Sanders, R. H. (2005). A comparison of training methods to increase neck muscle strength. *Work* 25, 205–210.

Chen, X., Coombes, B. K., Sjøgaard, G., Jun, D., O'Leary, S., and Johnston, V. (2018). Workplace-based interventions for neck pain in office workers: Systematic review and meta-analysis. *Phys. Ther.* 98, 40–62. doi:10.1093/ptj/pzx101

Cheng, H., Wang, Z., Liu, S., Yang, Y., Zhao, G., Cong, H., et al. (2011). Research, design and application of model NSE-1 neck muscle training machine for pilots. *Sheng Wu Yi Xue Gong Cheng Xue Za Zhi* 28, 387–391.

Chiu, T. T., and Sing, K. L. (2002). Evaluation of cervical range of motion and isometric neck muscle strength: Reliability and validity. *Clin. Rehabil.* 16, 851–858. doi:10.1191/0269215502cr550oa

Chumbley, E. M., Stolfi, A., and Mceachen, J. C. (2017). Risk factors for cervical pain in F-15C pilots. *Aerosp. Med. Hum. Perform.* 88, 1000–1007. doi:10.3357/AMHP.4848.2017

Coakwell, M. R., Bloswick, D. S., and Moser, R. (2004). High-risk head and neck movements at high G and interventions to reduce associated neck injury. *Aviat. Space Environ. Med.* 75, 68–80.

Conley, M. S., Stone, M. H., Nimmons, M., and Dudley, G. A. (1997). Resistance training and human cervical muscle recruitment plasticity. *J. Appl. Physiol.* 83, 2105–2111. doi:10.1152/jappl.1997.83.6.2105

Coury, H., Moreira, R., and Dias, N. B. (2009). Efetividade do exercício físico em ambiente ocupacional para controle da dor cervical, lombar e do ombro: uma revisão sistemática. *Rev. Bras. Fisioter.* 13, 461–479. doi:10.1590/s1413-35552009000600002

Coutts, A., Reaburn, P., Piva, T. J., and Murphy, A. (2007). Changes in selected biochemical, muscular strength, power, and endurance measures during deliberate overreaching and tapering in rugby league players. *Int. J. Sports Med.* 28, 116–124. doi:10.1055/s-2006-924145

De Loose, V., van Den Oord, M., Burnotte, F., van Tiggelen, D., Stevens, V., Cagnie, B., et al. (2008). Individual, work-and flight-related issues in F-16 pilots reporting neck pain. *Aviat. Space Environ. Med.* 79, 779–783. doi:10.3357/asem.2285.2008

Espejo-Antunez, L., Fernandez-Morales, C., Moreno-Vazquez, J. M., Tabla-Hinojosa, F. B., Cardero-Duran, M. L. A., and Albornoz-Cabello, M. (2022). *An Observational Study*, 12. Diagnostics (Basel).Assessment from a biopsychosocial approach of flight-related neck pain in fighter pilots of Spanish air force

Falla, D. (2004). Unravelling the complexity of muscle impairment in chronic neck pain. *Man. Ther.* 9, 125–133. doi:10.1016/j.math.2004.05.003

Falla, D. L., Jull, G. A., and Hodges, P. W. (2004). Patients with neck pain demonstrate reduced electromyographic activity of the deep cervical flexor muscles during performance of the craniocervical flexion test. *Spine (Phila Pa 1976)* 29, 2108–2114. doi:10.1097/01.brs.0000141170.89317.0e

Green, N. D., and Brown, L. (2004). Head positioning and neck muscle activation during air combat. *Aviat. Space Environ. Med.* 75, 676–680.

Grossman, A., Nakdimon, I., Chapnik, L., and Levy, Y. (2012). Back symptoms in aviators flying different aircraft. *Aviat. Space Environ. Med.* 83, 702–705. doi:10.3357/asem.3225.2012

Hämäläinen, O., Heinijoki, H., and Vanharanta, H. (1998). Neck training and +Gz-related neck pain: A preliminary study. *Mil. Med.* 163, 707–708. doi:10.1093/milmed/163.10.707

Hämäläinen, O., Vanharanta, H., and Bloigu, R. (1993). Determinants of +Gz-related neck pain: A preliminary survey. *Aviat. Space Environ. Med.* 64, 651–652.

Harrison, M. F., Coffey, B., Albert, W. J., and Fischer, S. L. (2015). Night vision goggle-induced neck pain in military helicopter aircrew: A literature review. *Aerosp. Med. Hum. Perform.* 86, 46–55. doi:10.3357/AMHP.4027.2015

Harrison, M. F., Neary, J. P., Albert, W. J., Kuruganti, U., Croll, J. C., Chancey, V. C., et al. (2009). Measuring neuromuscular fatigue in cervical spinal musculature of military helicopter aircrew. *Mil. Med.* 174, 1183–1189. doi:10.7205/milmed-d-00-7409

Higgins, J. P., Thompson, S. G., Deeks, J. J., and Altman, D. G. (2003). Measuring inconsistency in meta-analyses. *Bmj* 327, 557–560. doi:10.1136/bmj.327.7414.557

Honkanen, T., Sovelius, R., Mantysaari, M., Kyrolainen, H., Avela, J., and Leino, T. K. (2018). +Gz exposure and spinal injury-induced flight duty limitations. *Aerosp. Med. Hum. Perform.* 89, 552–556. doi:10.3357/AMHP.4999.2018

Howick, J, C. I., and Glasziou, P. (2011). *Oxford Centre for evidence-based medicine - level of evidence*. [Online]. Available: http://www.cebm.net/index.aspx?o51025 (Accessed March 10, 2022).

Hurwitz, E. L., Carragee, E. J., van der Velde, G., Carroll, L. J., Nordin, M., Guzman, J., et al. (2009). Treatment of neck pain: Noninvasive interventions: Results of the bone and joint decade 2000-2010 task force on neck pain and its associated disorders. *J. Manip. Physiol. Ther.* 32, S141–S175. doi:10.1016/j.jmpt.2008.11.017

Iatridis, J. C., Nicoll, S. B., Michalek, A. J., Walter, B. A., and Gupta, M. S. (2013). Role of biomechanics in intervertebral disc degeneration and regenerative therapies: What needs repairing in the disc and what are promising biomaterials for its repair? *Spine J.* 13, 243–262. doi:10.1016/j.spinee.2012.12.002

Jones, J. A., Hart, S. F., Baskin, D. S., Effenhauser, R., Johnson, S. L., Novas, M. A., et al. (2000). Human and behavioral factors contributing to spine-based neurological cockpit injuries in pilots of high-performance aircraft: Recommendations for management and prevention. *Mil. Med.* 165, 6–12. doi:10.1093/milmed/165.1.6

Kay, T. M., Gross, A., Goldsmith, C. H., Rutherford, S., Voth, S., Hoving, J. L., et al. (2012). *Exercises for mechanical neck disorders*. New York, United States: The Cochrane Collaboration by John Wiley & Sons, Ltd., CD004250.

Kopsky, D. J., Szadek, K. M., Schober, P., Vrancken, A., and Steegers, M. A. H. (2022). Study design characteristics and endpoints for enriched enrollment randomized withdrawal trials for chronic pain patients: A systematic review. *J. Pain Res.* 15, 479–496. doi:10.2147/JPR.S334840

Lacio, M., Vieira, J. G., Trybulski, R., Campos, Y., Santana, D., Filho, J. E., et al. (2021). Effects of resistance training performed with different loads in untrained and trained male adult individuals on maximal strength and muscle hypertrophy: A systematic review. *Int. J. Environ. Res. Public Health* 18, 11237. doi:10.3390/ijerph182111237

Lange, B., Murray, M., Chreiteh, S. S., Toft, P., Jorgensen, M. B., Sogaard, K., et al. (2014). Postural control and shoulder steadiness in F-16 pilots: A randomized controlled study. *Aviat. Space Environ. Med.* 85, 420–425. doi:10.3357/asem.3783.2014

Lange, B., Toft, P., Myburgh, C., and Sjøgaard, G. (2013). Effect of targeted strength, endurance, and coordination exercise on neck and shoulder pain among fighter pilots: A randomized-controlled trial. *Clin. J. Pain* 29, 50–59. doi:10.1097/AJP.0b013e3182478678

Liberati, A., Altman, D. G., Tetzlaff, J., Mulrow, C., Gotzsche, P. C., Ioannidis, J. P., et al. (2009). The PRISMA statement for reporting systematic reviews and meta-analyses of studies that evaluate healthcare interventions: Explanation and elaboration. *BMJ* 339, b2700. doi:10.1136/bmj.b2700

Misailidou, V., Malliou, P., Beneka, A., Karagiannidis, A., and Godolias, G. (2010). Assessment of patients with neck pain: A review of definitions, selection criteria, and measurement tools. *J. Chiropr. Med.* 9, 49–59. doi:10.1016/j.jcm.2010.03.002

Murray, M., Lange, B., Chreiteh, S. S., Olsen, H. B., Nornberg, B. R., Boyle, E., et al. (2016). Neck and shoulder muscle activity and posture among helicopter pilots and crew-members during military helicopter flight. *J. Electromyogr. Kinesiol.* 27, 10–17. doi:10.1016/j.jelekin.2015.12.009

Murray, M., Lange, B., Nornberg, B. R., Sogaard, K., and Sjogaard, G. (2017). Self-administered physical exercise training as treatment of neck and shoulder pain among military helicopter pilots and crew: A randomized controlled trial. *BMC Musculoskelet. Disord.* 18, 147. doi:10.1186/s12891-017-1507-3

Murray, M., Lange, B., Nornberg, B. R., Sogaard, K., and Sjogaard, G. (2015). Specific exercise training for reducing neck and shoulder pain among military helicopter pilots and crew members: A randomized controlled trial protocol. *BMC Musculoskelet. Disord.* 16, 198. doi:10.1186/s12891-015-0655-6

Murray, M., Lange, B., Sogaard, K., and Sjogaard, G. (2020). The effect of physical exercise training on neck and shoulder muscle function among military helicopter pilots and crew: A secondary analysis of a randomized controlled trial. *Front. Public Health* 8, 546286. doi:10.3389/fpubh.2020.546286

Nagai, T., Abt, J. P., Sell, T. C., Clark, N. C., Smalley, B. W., Wirt, M. D., et al. (2014). Neck proprioception, strength, flexibility, and posture in pilots with and without neck pain history. *Aviat. Space Environ. Med.* 85, 529–535. doi:10.3357/asem.3874.2014

Netto, K. J., Burnett, A. F., and Coleman, J. L. (2007). Neck exercises compared to muscle activation during aerial combat maneuvers. *Aviat. Space Environ. Med.* 78, 478–484.

Netto, K. J., and Burnett, A. F. (2006). Neck muscle activation and head postures in common high performance aerial combat maneuvers. *Aviat. Space Environ. Med.* 77, 1049–1055.

Newman, D. G. (1997). +GZ-induced neck injuries in Royal Australian Air Force fighter pilots. *Aviat. Space Environ. Med.* 68, 520–524.

O'conor, D. K., Dalal, S., Ramachandran, V., Shivers, B., Shender, B. S., and Jones, J. A. (2020). Crew-friendly countermeasures against musculoskeletal injuries in aviation and spaceflight. *Front. Physiol.* 11, 837. doi:10.3389/fphys.2020.00837

Omholt, M. L., Tveito, T. H., and Ihlebaek, C. (2017). Subjective health complaints, work-related stress and self-efficacy in Norwegian aircrew. *Occup. Med.* 67, 135–142. doi:10.1093/occmed/kqw127

Page, M. J., Mckenzie, J. E., and Higgins, J. P. T. (2018). Tools for assessing risk of reporting biases in studies and syntheses of studies: A systematic review. *BMJ Open* 8, e019703. doi:10.1136/bmjopen-2017-019703

Park, S. H., and Lee, M. M. (2020). Effects of lower trapezius strengthening exercises on pain, dysfunction, posture alignment, muscle thickness and contraction rate in patients with neck pain; randomized controlled trial. *Med. Sci. Monit.* 26, e920208. doi:10.12659/MSM.920208

Posch, M., Schranz, A., Lener, M., Senn, W., Ang, B. O., Burtscher, M., et al. (2019). Prevalence and potential risk factors of flight-related neck, shoulder and low back pain among helicopter pilots and crewmembers: A questionnaire-based study. *BMC Musculoskelet. Disord.* 20, 44. doi:10.1186/s12891-019-2421-7

Price, J., Rushton, A., Tyros, I., Tyros, V., and Heneghan, N. R. (2020). Effectiveness and optimal dosage of exercise training for chronic non-specific neck pain: A systematic review with a narrative synthesis. *PLoS One* 15, e0234511. doi:10.1371/journal.pone.0234511

Purushotham, S., Stephenson, R. S., Sanderson, A., Abichandani, D., Greig, C., Gardner, A., et al. (2022). Microscopic changes in the spinal extensor musculature in people with chronic spinal pain: A systematic review. *Spine J.* 22, 1205–1221. doi:10.1016/j.spinee.2022.01.023

Rausch, M., Weber, F., Kuhn, S., Ledderhos, C., Zinner, C., and Sperlich, B. (2021). The effects of 12 weeks of functional strength training on muscle strength, volume and activity upon exposure to elevated Gz forces in high-performance aircraft personnel. *Mil. Med. Res.* 8, 15. doi:10.1186/s40779-021-00305-8

Rintala, H., Hakkinen, A., Siitonen, S., and Kyrolainen, H. (2015). Relationships between physical fitness, demands of flight duty, and musculoskeletal symptoms among military pilots. *Mil. Med.* 180, 1233–1238. doi:10.7205/MILMED-D-14-00467

Saeterbakken, A. H., Nordengen, S., Andersen, V., and Fimland, M. S. (2017). Nordic walking and specific strength training for neck- and shoulder pain in office workers: A pilot-study. *Eur. J. Phys. Rehabil. Med.* 53, 928–935. doi:10.23736/S1973-9087.17.04623-8

Salmon, D. M., Harrison, M. F., and Neary, J. P. (2011). Neck pain in military helicopter aircrew and the role of exercise therapy. *Aviat. Space Environ. Med.* 82, 978–987. doi:10.3357/asem.2841.2011

Salmon, D. M., Harrison, M. F., Sharpe, D., Candow, D., Albert, W. J., and Neary, J. P. (2013). Exercise therapy for improved neck muscle function in helicopter aircrew. *Aviat. Space Environ. Med.* 84, 1046–1054. doi:10.3357/asem.3593.2013

Selistre, L. F. A., Melo, C. S., and Noronha, M. A. (2021). Reliability and validity of clinical tests for measuring strength or endurance of cervical muscles: A systematic review and meta-analysis. *Arch. Phys. Med. Rehabil.* 102, 1210–1227. doi:10.1016/j.apmr.2020.11.018

Sjøgaard, G., Justesen, J. B., Murray, M., Dalager, T., and Søgaard, K. (2014). A conceptual model for worksite intelligent physical exercise training--IPET--intervention for decreasing life style health risk indicators among employees: A randomized controlled trial. *BMC Public Health* 14, 652. doi:10.1186/1471-2458-14-652

Song, R., Zhao, X., Zhang, D. Q., Wang, R., and Feng, Y. (2021). Lower levels of irisin in patients with type 2 diabetes mellitus: A meta-analysis. *Diabetes Res. Clin. Pract.* 175, 108788. doi:10.1016/j.diabres.2021.108788

Sovelius, R., Mantyla, M., Heini, H., Oksa, J., Valtonen, R., Tiitola, L., et al. (2019). Joint helmet-mounted cueing system and neck muscle activity during air combat maneuvering. *Aerosp. Med. Hum. Perform.* 90, 834–840. doi:10.3357/AMHP.5281.2019

Sovelius, R., Mantyla, M., Huhtala, H., Oksa, J., Valtonen, R., Tiitola, L., et al. (2020). Head movements and neck muscle activity during air combat maneuvering. *Aerosp. Med. Hum. Perform.* 91, 26–31. doi:10.3357/AMHP.5425.2020

Sovelius, R., Oksa, J., Rintala, H., Huhtala, H., Ylinen, J., and Siitonen, S. (2006). Trampoline exercise vs. strength training to reduce neck strain in fighter pilots. *Aviat. Space Environ. Med.* 77, 20–25.

Stang, A. (2010). Critical evaluation of the Newcastle-Ottawa scale for the assessment of the quality of nonrandomized studies in meta-analyses. *Eur. J. Epidemiol.* 25, 603–605. doi:10.1007/s10654-010-9491-z

Stasinaki, A. N., Gloumis, G., Spengos, K., Blazevich, A. J., Zaras, N., Georgiadis, G., et al. (2015). Muscle strength, power, and morphologic adaptations after 6 Weeks of compound vs. Complex training in healthy men. *J. Strength Cond. Res.* 29, 2559–2569. doi:10.1519/JSC.0000000000000917

Stergiou, A., Tzoufi, M., Ntzani, E., Varvarousis, D., Beris, A., and Ploumis, A. (2017). Therapeutic effects of horseback riding interventions: A systematic review and meta-analysis. *Am. J. Phys. Med. Rehabil.* 96, 717–725. doi:10.1097/PHM.0000000000000726

Sterne, J. A., Sutton, A. J., Ioannidis, J. P., Terrin, N., Jones, D. R., Lau, J., et al. (2011). Recommendations for examining and interpreting funnel plot asymmetry in meta-analyses of randomised controlled trials. *BMJ* 343, d4002. doi:10.1136/bmj.d4002

Stroup, D. F., Berlin, J. A., Morton, S. C., Olkin, I., Williamson, G. D., Rennie, D., et al. (2000). Meta-analysis of observational studies in epidemiology: A proposal for reporting. Meta-Analysis of observational studies in Epidemiology (MOOSE) group. *Jama* 283, 2008–2012. doi:10.1001/jama.283.15.2008

Tan, B. (1999). Manipulating resistance training program variables to optimize maximum strength in men: A review. *J. Strength Cond. Res.* 13, 289–304. doi:10.1519/1533-4287(1999)013<0289:mrtpvt>2.0.co;2

Thoolen, S. J., and van Den Oord, M. H. (2015). Modern air combat developments and their influence on neck and back pain in F-16 pilots. *Aerosp. Med. Hum. Perform.* 86, 936–941. doi:10.3357/AMHP.4303.2015

Treleaven, J., Jull, G., and Atkinson, L. (1994). Cervical musculoskeletal dysfunction in post-concussional headache. *Cephalalgia* 14, 273–279. doi:10.1046/j.1468-2982.1994.1404273.x

Uhlig, Y., Weber, B. R., Grob, D., and Müntener, M. (1995). Fiber composition and fiber transformations in neck muscles of patients with dysfunction of the cervical spine. *J. Orthop. Res.* 13, 240–249. doi:10.1002/jor.1100130212

Verde, P., Trivelloni, P., Angelino, G., Morgagni, F., and Tomao, E. (2015). Neck pain in F-16 vs. Typhoon fighter pilots. *Aerosp. Med. Hum. Perform.* 86, 402–406. doi:10.3357/AMHP.4063.2015

Visser, B., and Van Dieën, J. H. (2006). Pathophysiology of upper extremity muscle disorders. *J. Electromyogr. Kinesiol.* 16, 1–16. doi:10.1016/j.jelekin.2005.06.005

Waling, K., Sundelin, G., Ahlgren, C., and Järvholm, B. (2000). Perceived pain before and after three exercise programs--a controlled clinical trial of women with work-related trapezius myalgia. *Pain* 85, 201–207. doi:10.1016/s0304-3959(99)00265-1

Wallace, J. B., Newman, P. M., Mcgarvey, A., Osmotherly, P. G., Spratford, W., and Gabbett, T. J. (2021). Factors associated with neck pain in fighter aircrew: A systematic review and meta-analysis. *Occup. Environ. Med.* 78, 900–912. doi:10.1136/oemed-2020-107103

Wei, F. L., Gao, Q. Y., Heng, W., Zhu, K. L., Yang, F., du, R. M., et al. (2022). Association of robot-assisted techniques with the accuracy rates of pedicle screw placement: A network pooling analysis. *EClinicalMedicine* 48, 101421. doi:10.1016/j.eclinm.2022.101421

Zebis, M. K., Andersen, L. L., Pedersen, M. T., Mortensen, P., Andersen, C. H., Pedersen, M. M., et al. (2011). Implementation of neck/shoulder exercises for pain relief among industrial workers: A randomized controlled trial. *BMC Musculoskelet. Disord.* 12, 205. doi:10.1186/1471-2474-12-205

Zhang, F., Wang, K., du, P., Yang, W., He, Y., Li, T., et al. (2021). Risk of stroke in cancer survivors: A meta-analysis of population-based cohort studies. *Neurology* 96, e513–e526. doi:10.1212/WNL.0000000000011264

Zhao, J., Dong, X., Zhang, Z., Gao, Q., Zhang, Y., Song, J., et al. (2022). Association of use of tourniquets during total knee arthroplasty in the elderly patients with post-operative pain and return to function. *Front. Public Health* 10, 825408. doi:10.3389/fpubh.2022.825408

TYPE Original Research
PUBLISHED 02 September 2022
DOI 10.3389/fbioe.2022.978554

OPEN ACCESS

EDITED BY
Qichang Mei,
Ningbo University, China

REVIEWED BY
Qiaolin Zhang,
Ningbo University, China
Junlin Yang,
Xinhua Hospital Affiliated to Shanghai Jiao Tong University School of Medicine, China

*CORRESPONDENCE
Yong Hai,
yong.hai@ccmu.edu.cn
Yuzeng Liu,
beijingspine2010@163.com

†These authors have contributed equally to this work and share first authorship

SPECIALTY SECTION
This article was submitted to Biomechanics, a section of the journal Frontiers in Bioengineering and Biotechnology

RECEIVED 26 June 2022
ACCEPTED 08 August 2022
PUBLISHED 02 September 2022

CITATION
Pan A, Ding H, Wang J, Zhang Z, Zhang H, Liu Y and Hai Y (2022), The application of finite element analysis to determine the optimal UIV of growing-rod treatment in early-onset scoliosis. *Front. Bioeng. Biotechnol.* 10:978554. doi: 10.3389/fbioe.2022.978554

The application of finite element analysis to determine the optimal UIV of growing-rod treatment in early-onset scoliosis

Aixing Pan[1†], Hongtao Ding[1†], Junjie Wang[2], Zhuo Zhang[2], Hongbo Zhang[2], Yuzeng Liu[1*] and Yong Hai[1*]

[1]Beijing Chaoyang Hospital, Capital Medical University, Beijing, China, [2]School of Mechanical and Power Engineering, East China University of Science and Technology, Shanghai, China

Objectives: To analyze the stress distribution in the proximal vertebral body and soft tissue of dual growing-rod (GR) with different upper instrumented vertebra (UIV) to determine the optimal UIV.

Methods: A ten-year-old male EOS case treated with GR was selected. Based on spiral computed tomography (CT) scanning performed in 0.6 mm thick slices, a finite element model (FEM) of the preoperative state (M0, the original spine state) of the patient was created. Subsequently, four models with different UIV fixations were numerically analyzed by FEM, including M1 (UIV = T1, i.e., the upper-end vertebrae (UEV) of the upper thoracic curve), M2 (UIV = T2), M3 (UIV = T3) and M4 (UIV = T4, i.e., the lower end vertebrae (LEV) of the upper thoracic curve). Displacement and maximum stress in the proximal vertebral body and soft tissue were measured and compared among the five models.

Results: The spine model was fixed with the sacrum, and the gravity conditions were imposed on each vertebral body according to the research of Clin and Pearsall. The results are as follows:M4 model has the largest overall displacement, while M1 has the least displacement among the four models. Except M2, the maximum normalized stress of UIV increases with the downward movement of UIV. M1 has the lowest annulus fibrosus stress and highest joint capsule stress, which is characterized by the vertebrae backward leaning, while M4 is the opposite. The supraspinous ligament stress of M3 and M4 is significantly higher than that of M1 and M2. This suggests that UIV downshift increases the tendency of the proximal vertebral bodies to bend forward, thereby increasing the tension of the posterior ligaments (PL).

Conclusion: The UIV of the GR is recommended to be close to the UEV of the upper thoracic curve, which can reduce the stress of the proximal PL, thereby reducing the occurrence of proximal junctional kyphosis (PJK).

KEYWORDS

early-onset scoliosis, growing-rod, proximal junctional kyphosis, finite element analysis, upper instrumented vertebra

Introduction

Early-onset scoliosis (EOS) referred to as the spinal deformities in patients under 10 years of age is a complex spinal diseases difficult to solve (Hasler, 2018; Zhang and Zhang, 2020). During the period of rapid bone growth, EOS will seriously compromise the development of the spine, throacic and lungs, and even endangers life if not received optimal management in time (Senkoylu et al., 2020). There are great differences among patients with EOS in terms of the locations and types of deformation. Hence, the treatment of EOS required personalized plan due to the complexity of deformity feature.

Among the current treatment methods of EOS, the growing-rod (GR) technique, which can maximize the potential growth of the spine and deformity correction has gained great success (Cengiz et al., 2021). However, there are still complications during the process of GR treatment according to current studies, which mainly include wound infection, proximal junctional kyphosis (PJK), instrument failure, and autologous fusion (Hardesty et al., 2018; Karol, 2019). PJK refers to the progress of proximal junction angle greater than 10° after the operation, leading to severe pain, instrument-realated complication and even neurological deficits (Watanabe et al., 2016). The independent studies showed that the incidence of PJK ranged from 7% to 56% after dual growing-rods surgery (Hardesty et al., 2018).

The risk factors of PJK are mainly obtained from the retrospective study of clinical cohorts, making it difficult to directly use cadavers for experiments since the samples will gradually produce operating errors during repeated percedure (Cahill et al., 2012; Zhu et al., 2019). Although there have been many finite element models to investigate the risk factors of PJK, there is still little research on the fixed position of the growing rod, and most of which only carry out short segment modeling, without considering the stress situation in the environment of intact spine.

Thus, the C1-S1 full-spinal models of EOS patients with dual growing rod were established in the present study. The stress distribution of the proximal vertebral body and soft tissue at different levels of dual growing rods fixation was simulated by the finite element method, and the risk of PJK was analyzed, ultimately to explore the optimal upper instrumented vertebrae (UIV) of the growing rod.

Materials and methods

Case evaluation

A 10-year-old patient with early-onset scoliosis (male, height 109 cm, weight 14 Kg) was selected. The patient underwent single growing rods surgery with T3 as the UIV and L4 as the lower instrumented vertebra (LIV) (Figure 1). The scoliosis was well corrected, but the PJK occurred in the patient during the follow-up (Figure 1F). The data were provided by Beijing Chao-yang Hospital, Capital Medical University, which included posteroanterior and lateral radiographs of patients before and after correction. The preoperative CT scan tomographic images were also provided.

Image data acquisition

The geometry was reconstructed by 3D CT-scan images (slice thickness: 0.6 mm) from the patient, ranging from C1 to S1 segments. The CT tomographic data were stored in standard Dicom format.

Establishment of spine 3D model

The extracted Dicom file was imported into Mimics Research 21.0 (Materialise Inc., Belgium), and the bone

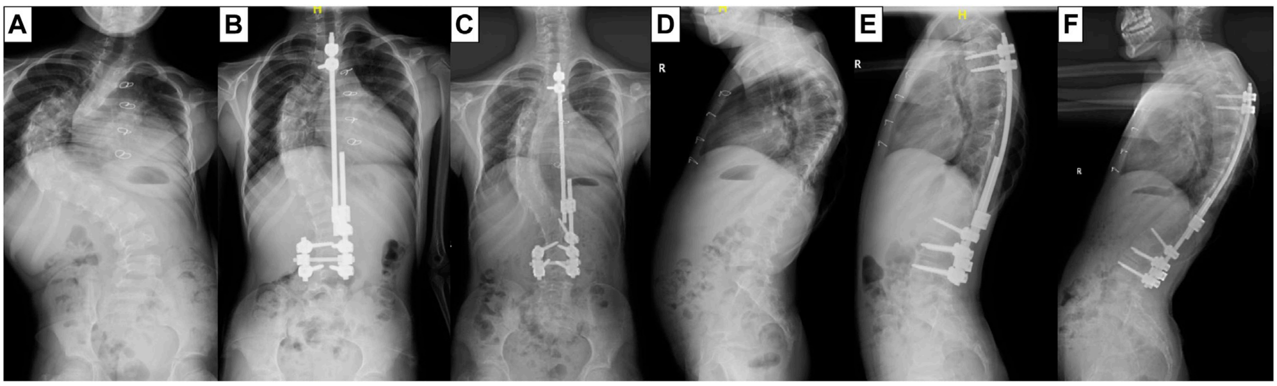

FIGURE 1
X-ray film of the patient before GR surgery **(A,D)**, after surgery **(B,E)** and at the follow-up **(C,F)**.

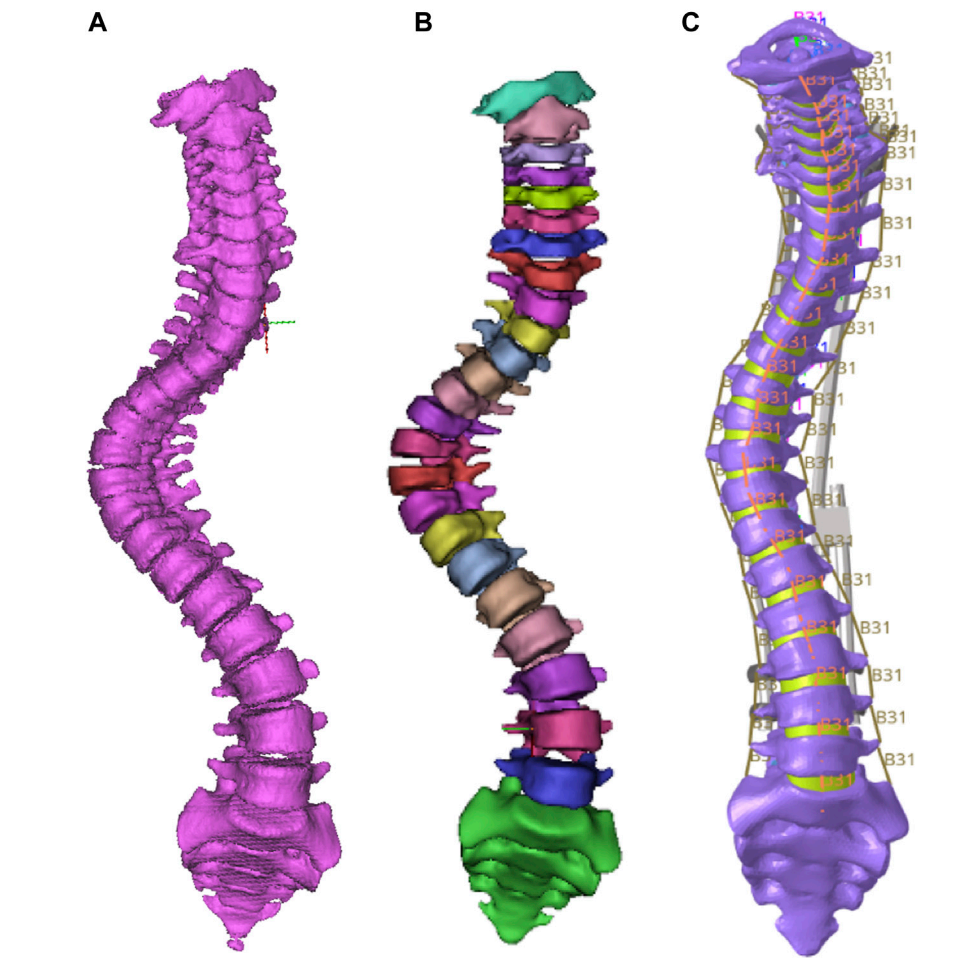

FIGURE 2
The original spine model **(A)** and FEM before **(B)** and after **(C)** meshing.

boundary was extracted through threshold segmentation. Each segment of the vertebra was acquired with filling and splitting and saved as a different Mask. The reconstructed vertebras were saved in STL format. The model surface was smoothed, meshed, and converted to a STEP solid model with Geomagic Studio (3D Systems Corporation, Rock Hill, South Carolina, United States). The C1-S1 segment model in STEP format was imported into Solidworks 2019 (Dassault Systèmes SolidWorks Corporation, Vélizy-Villacoublay, France) to simulate surgical correction according to the patient's postoperative radiographs. Subsequently, cortical and cancellous bone were divided, and the intervertebral disc and facet joint capsule were established, where the intervertebral disc contained the annulus fibrosus and nucleus pulposus. The proportion of nucleus pulposus was between 30% and 50%. The thickness of cortical bone was 1 mm.

Establishment of spine finite element model

The established C1-S1 segment geometric model of the spine was imported into HyperMesh 2019 (Altair Engineering, Inc., United States) for FEM establishment. Vertebrae, intervertebral discs, and joint capsules were defined as elastic, with material properties defined in terms of elastic modulus and Poisson's ratio (Schmidt et al., 2012; Erbulut et al., 2015; Shen et al., 2019; Kahaer et al., 2022; Liang et al., 2022). The model was meshed into tetrahedral elements (as shown in Figure 2) with 118,820 nodes and 561,469 elements. The ligaments included anterior longitudinal ligament, posterior longitudinal ligament, ligamentum flavum, interspinous ligament, supraspinous ligament, and intertransverse ligament, using a one-dimensional unit with a circular cross-section. These ligaments were subjected to tension only, and no compression

TABLE 1 Material properties of each part of the models.

Part	Modulus (MPa)	Poisson's ratio μ	Area (mm^2)
Cortical bone	12,000	0.30	—
Cancellous bone	500	0.20	—
Annulus fibrosus	4.20	0.30	—
Nucleus pulposus	2	0.49	—
Joint capsule	20	0.30	—
Growing rod	110,000	0.28	—
Anterior longitudinal ligament	20	0.30	38
Posterior longitudinal ligament	70	0.30	20
Ligamentum flavum	50	0.30	60
Interspinous ligament	28	0.30	35.5
Supraspinous ligament	28	0.30	35.5
intertransverse ligament	50	0.30	10

TABLE 2 Gravity value and percentage of body weight borne by the vertebral body.

Vertebral body	Percentage (%)	Gravity value(N)
C1	1.14	1.60
C2	1.14	1.60
C3	1.14	1.60
C4	1.14	1.60
C5	1.14	1.60
C6	1.14	1.60
C7	1.14	1.60
T1	1.10	1.54
T2	1.10	1.54
T3	5.30	7.42
T4	5.30	7.42
T5	5.30	7.42
T6	1.30	1.82
T7	1.40	1.96
T8	1.50	2.10
T9	1.60	2.24
T10	3.00	2.80
T11	2.10	2.94
T12	2.50	3.50
L1	2.40	3.36
L2	2.40	3.36
L3	2.30	3.22
L4	2.60	3.64
L5	2.60	3.64

(Wang et al., 2019). The material properties of each part in the spine model were shown in Table 1. Tying constraints were defined between parts of the spine. The lower part of the sacrum was fixed, and gravity was applied to the upper surface of each vertebral body to simulate the force of the spine in a standing state. Gravity value and percentage of body weight borne by the vertebral body were shown in Table 2 (Pearsall et al., 1996; Clin et al., 2011). The gravitational acceleration was 9.8 m/s^2.

Analysis of different fixations

Dual growing rod fixation was adopted with four screws at the upper and lower end. The lower four screws are located at L3 and L4. Four post-orthopedic models, M1 (UIV = 1), M2 (UIV = 2), M3 (UIV = 3), M4 (UIV = 4), and one pre-orthopedic model M0 were established according to the different positions of the upper screws (Figure 3). In addition, the stress cannot be compared due to the different spatial positions of the different vertebral bodies. Therefore, according to the normalization principle, a model MC with the same spine curve after correction without using growing rods was established, to compare the stress changes before and after fusion at the same position. The finished model was solved in Abaqus.

Results

Model validation

To validation the numerical simulation procedure, the average stiffness of spine segments without growth rods under the same load were compared with the literature (Busscher et al., 2009). The average stiffness refers to the ratio of the moment loaded on the spine to its angular offset, in Nm/°. The specific method was intercepting the T1-T4 segments of the complete spine model, and applying a moment of 4 N m on the upper surface of T1 to simulate six motion states of the forward bend and backward extension, the left and right lateral flexion, and the

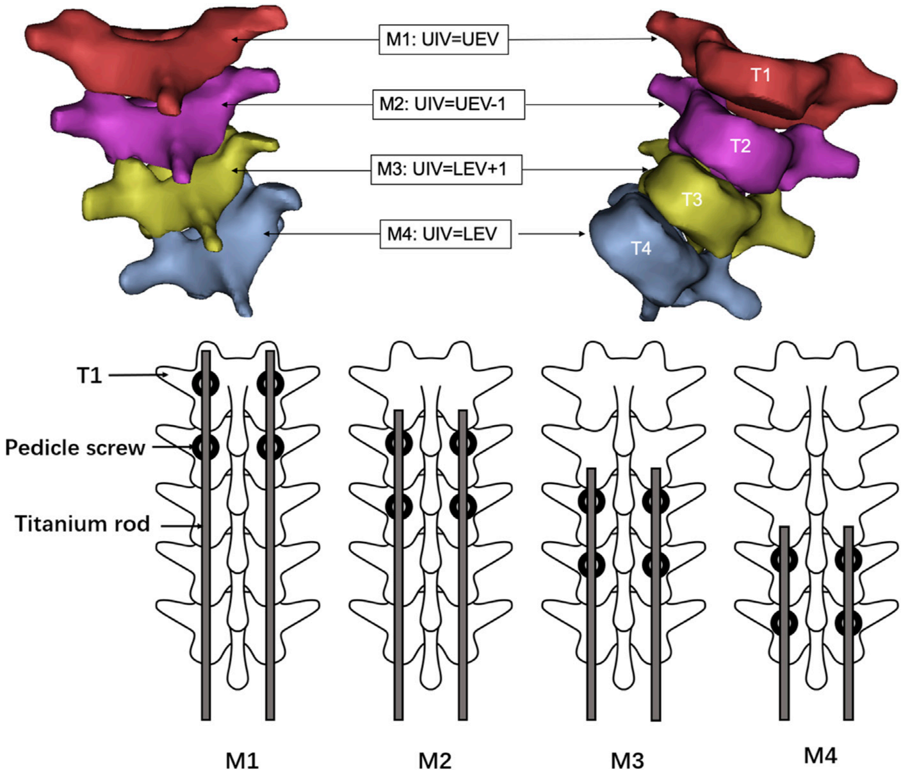

FIGURE 3
Schematic diagram of internal fixation scheme of M1–M4 model. M1:UIV = T1, i.e., the UEV of the upper thoracic curve; M2: UIV = T2, i.e., UEV-1; M3: UIV = T3, i.e., LEV+1; M4: UIV = T4, i.e., the LEV of the upper thoracic curve.

left and right handed twist. The displacement nephograms of the spine model under six motion states were shown in Figure 4. Now take the left handed twist as an example to introduce the solution of the average stiffness. The foremost point and the last point on the upper surface of the T1 were selected in Abaqus, and the coordinate values of the nodes before and after the deformation were recorded. With two straight lines before and after the deformation draw in Solidworks according to the coordinate values, the angle can be calculate. Since the offset before and after twist of the upper surface of T1 mainly occured in the parallel plane of the surface, the displacement component in the vertical plane was very small and can be ignored. Therefore, the straight lines were projected into the parallel plane of the upper surface of T1, and the angle was measured to be 7.53°.The average stiffness was the ratio of the moment value to the angle. The average stiffness values of T1–T4 segments under the six motion states were shown in Table 3.

It can be seen from the table that the biomechanical properties of the T1–T4 segments of the spine model established in this study are not significantly different from those of the spine model in the previously recognized literature. Because the whole spine segments and the T1–T4 segments use the same modeling method and material properties, the model of the full-segment spine can be considered valid and can be used for further analysis.

Displacement

The overall displacements of the M0–M4 model are shown in Figure 5. The M1–M4 model was unified with the scale of the M4 model with the largest deformation. Due to the fixation of the lower surface of the sacrum, all models showed an increase in displacement from bottom to top, and the maximum displacement was located at C1. As the UIV position of the dual growing rods was shifted inferiorly, the maximum displacement of the models gradually increases, from 1.37 mm in the M1 model to 1.73 mm in the M4 model, while the M0 model without the growing rod fixation has the maximum displacement of 19.31 mm. It can be seen that the growing rod has a significant function of stabilizing the spine that can avoid a lot of displacement of the spine.

Figure 6A shows that the longitudinal displacement of growing rods in the M1-M4 model generally decreases with the UIV shifting inferiorly. The reason may be that the length of the growing rods decreased, and the difference in the stress

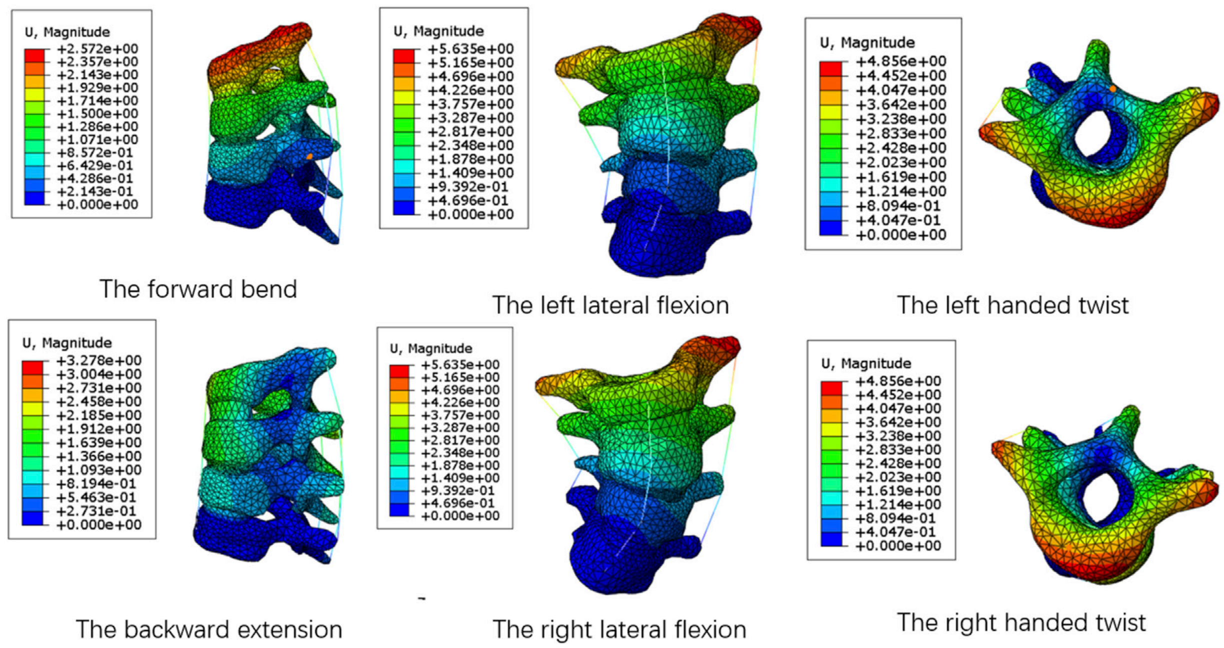

FIGURE 4
The displacement nephograms of T1–T4 segments under six motion states.

TABLE 3 The average stiffness values of T1–T4 segments under the six motion states.

	Forward bend	Backward extension	Left lateral flexion	Right lateral flexion	Left handed twist	Right handed twist
Literature 1 (Busscher et al. (2009)	0.667	0.667	0.656	0.656	0.548	0.548
Our study	0.728	0.723	0.655	0.672	0.531	0.508

level was not obvious. The maximum longitudinal displacements of the five models are presented in Figure 6B, showing the same trend as the overall displacement. The fixation of longer segments can reduce the overall displacement of the spine.

Figure 7 shows the displacement of the posterior end of the M1–M4 spine. The displacement of the three to six vertebral bodies below UIV was smaller than that of other vertebral bodies. This small-displacement area changed with the UIV shifting inferiorly. This separation of displacement around UIV and UIV+1 may be related to the occurrence of PJK due to the mismatch between the stiffness of the growing rods and the spine.

Von Mises stress

The stress nephogram of the M1 model is shown in Figure 8. The stress levels in the spinal column were low, and the maximum Von Mises stress was observed on pedicle screws in all models, ranging from 96.5 to 162.8 MPa (139.15 ± 25.84 MPa). The comparison of the maximum stress of growing rods in the M1–M4 model is shown in Figure 9. The maximum Von Mises stress on UIV ranged from 10.71 to 14.01 MPa (12.36 ± 1.33 MPa), which was significantly higher than that on other vertebral bodies. The maximum Von Mises stress range on UIV+1 was 0.50–1.04 MPa (0.77 ± 0.19 MPa).

The GR fixation system had maximum stress of 162.8 MPa occurring on the pedicle screw. However, the stress was far from causing fracture to the fixation system. As the UIV position was shifted inferiorly, the maximum Von Mises stress of the pedicle screw did not show the same trend as that of UIV and UIV+1. The maximum fixation stress of the M3 model was larger than that of other models. While the maximum value of UIV stress of M2 and UIV+1 stress of M4 are the largest.

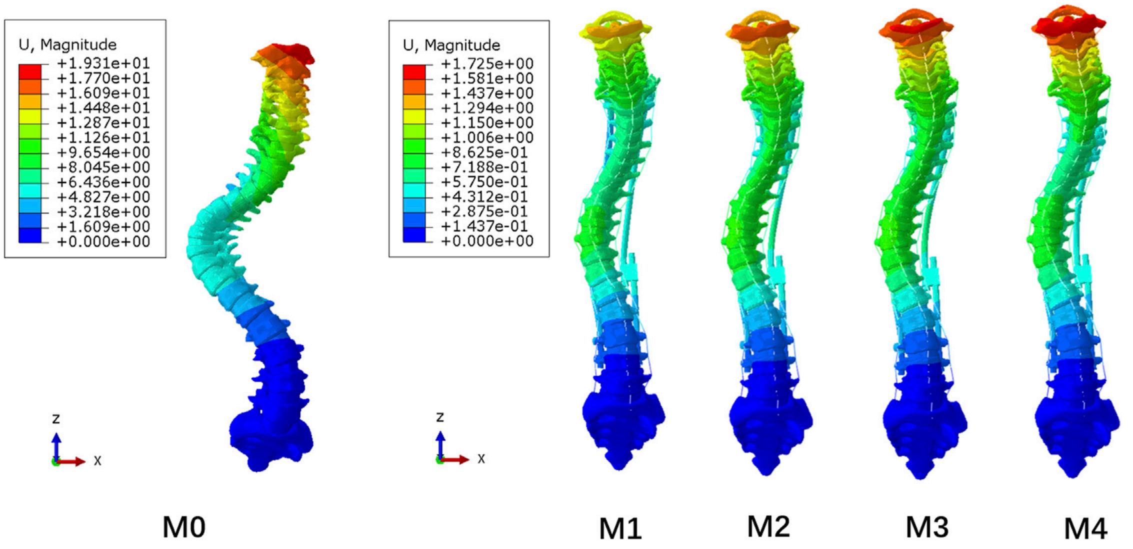

FIGURE 5
Displacement nephogram of M0–M4 model.

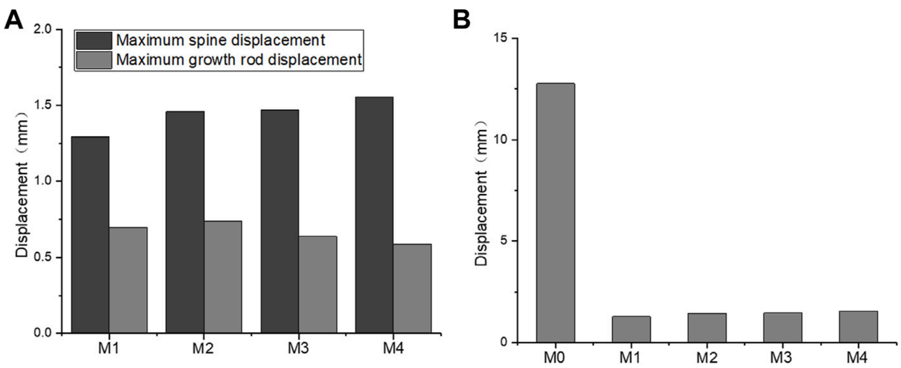

FIGURE 6
Maximum longitudinal displacement. **(A)** M1–M4 maximum longitudinal displacement of the spine and growing rods; **(B)** M0–M4 maximum longitudinal displacement of the spine.

Normalized von mises stress

The spatial position and stress concentration area of different vertebrae were completely different. UIV and UIV+1 in M1–M4 were not in the same position, which made it difficult to compare with each other. Therefore, normalization was necessary to be performed before comparison. The normalized method was to reconstruct an orthopedic spinal model (MC) without any fixation and simulate it in the light of the same pre-processing. The maximum Von Mises stress of UIV and UIV+1 of M1–M4 was divided by the maximum stress of the corresponding vertebral body of MC to obtain the normalized results of stress.

The normalized maximum value of UIV and UIV+1 stress are shown in Figure 10. Except for M1, the maximum stress of UIV increased significantly, while the maximum stress of UIV+1 decreased significantly comparing with the normalized model MC. In models with the absence of growing rods, the stress distribution of C7–T5 ranged from 4.73 to 11.05 MPa (7.88 ± 2.34 MPa), and the stress difference between UIV and UIV+1 increased significantly after fixation with growing rods.

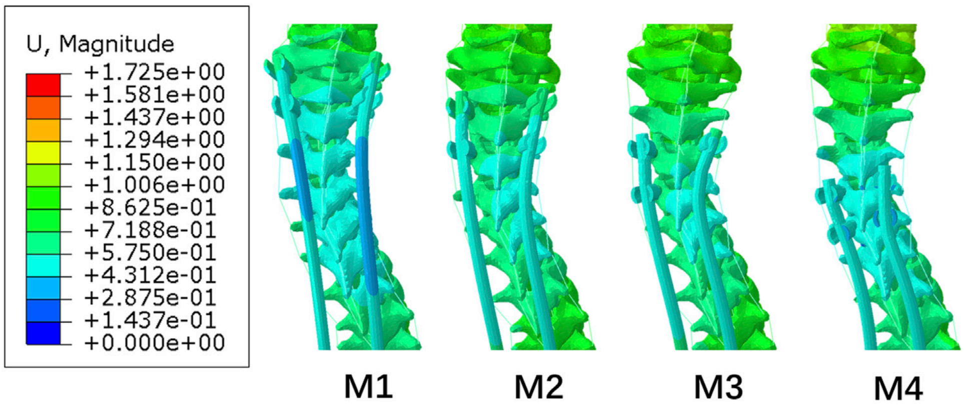

FIGURE 7
Displacement nephogram of posterior proximal of M1–M4.

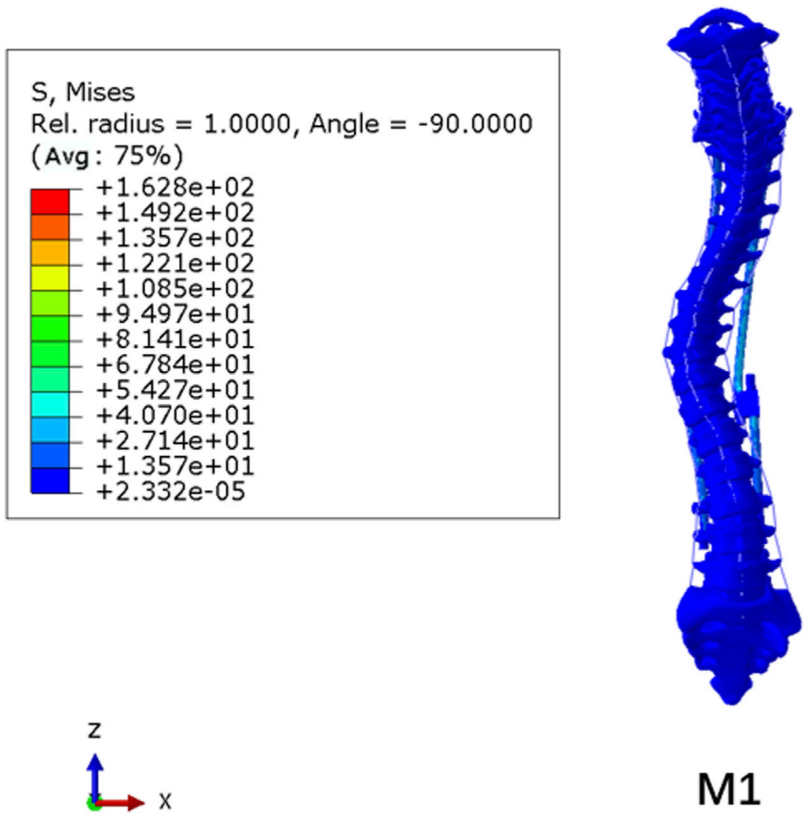

FIGURE 8
Stress nephogram of M1 model.

The stress differencebetween UIV and UIV+1 in M2 (T1, T2) was the largest, followed by M4 (T3, T4), and the smallest is M1 (C7, T1). Even before normalization, the Von Mises stress of UIV in M2 was the largest among the four groups.

According to the stress changes of the vertebral body, the dual growing rods and pedicle screw fixation system can increase the stress of UIV and reduce the stress of UIV+1. The stress distribution of the vertebral body is shown in Figure 11. The

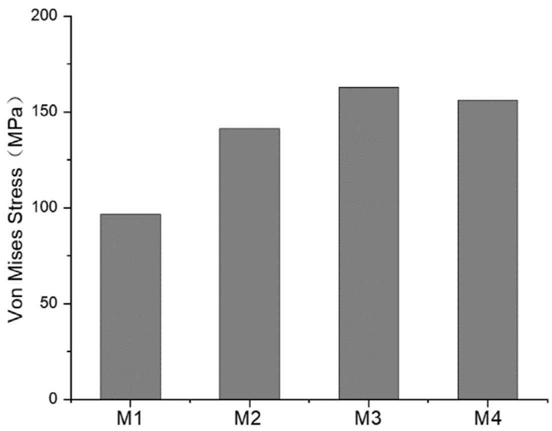

FIGURE 9
The maximum stress of M1–M4 growing rods.

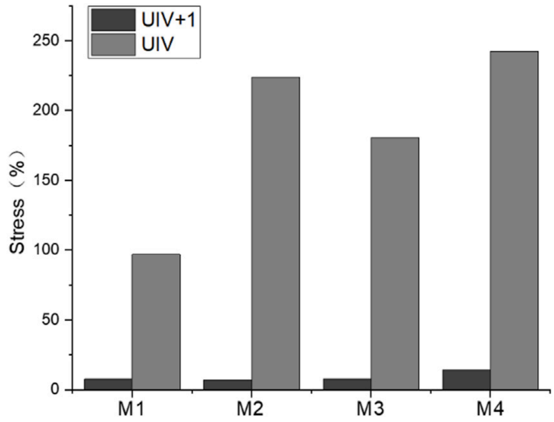

FIGURE 11
UIV and UIV+1 stress nephogram of M1–M4 model.

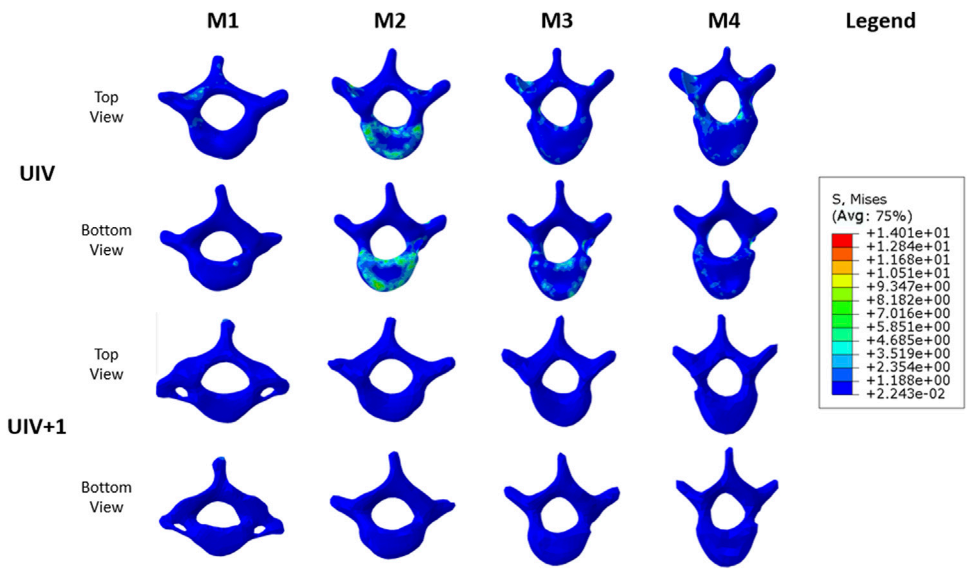

FIGURE 10
M1–M4 UIV and UIV+1 stress nephogram.

stress distribution maps of UIV and UIV+1 were compared under the same scale. The stress of UIV+1 was all below 1.19 MPa, and the stress in most areas of UIV was low, while a few stress concentrated areas were mainly in the contact part of the vertebral body and annulus fibrosus, joint capsule connection, and the connection part of vertebral body and screw. There were large areas of stress concentration in both the upper and lower vertebral bodies of the UIV in M2, and the stress level was significantly higher than that of the other three groups (Figure 11). The stress in the M1 model was significantly lower overall, with only a small stress concentration at the pedicle and pedicle screw fixation sites. The stress on the lower surface of the UIV vertebral body in M3 was more concentrated than that on the upper surface, while that on M4 was the opposite.

The stress distribution results were better than other groups when UIV was T1. M1 was a better solution because not only was the maximum stress of UIV almost unchanged before and after fixation but there was no stress concentration on the upper and lower surface of the vertebral body. Excluding M2, the maximum normalized stress value of UIV increased with the downward movement of UIV, while the value of M2 was close to that of M4, which may be related to the spinal curve of the case.

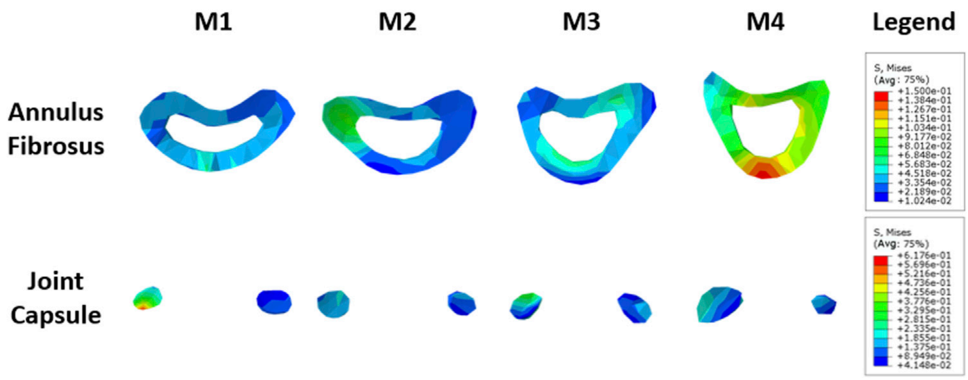

FIGURE 12
Stress nephogram of annulus fibrosus and joint capsule.

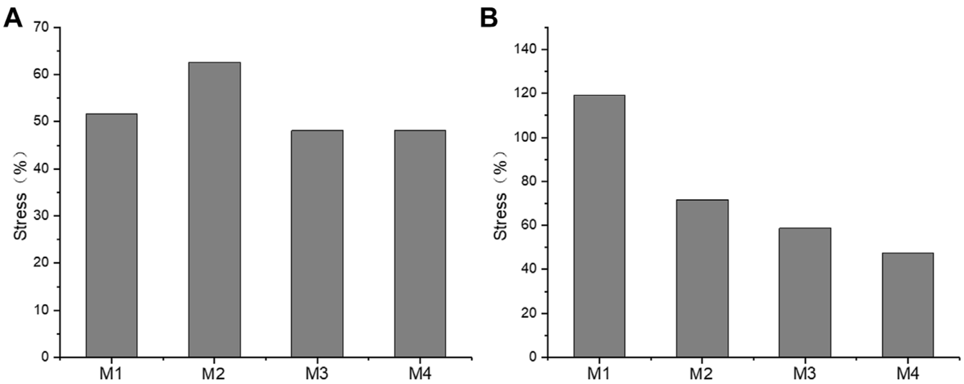

FIGURE 13
The maximum stress of fiber ring **(A)** and joint capsule **(B)** of the M1–M4 model.

Annulus fibrosus and joint capsule

The annulus fibrosus and joint capsule stresses associated with UIV and UIV+1 were also compared. Figure 12 shows the stress distribution of the annulus fibrosus and joint capsule proximal to the device. Figure 13 exhibits the comparasion results of the normalized Von Mises stress maxima of the annulus fibrosus and joint capsule. The fixation with growing rods reduced the maximum stress in M1, M3, and M4 by about half, and in M2 by about 40%. The Von Mises stress of M2–M4 decreased to 72%, 59%, and 48%, respectively, while the Von Mises stress of M1 increased to 119%. The joint capsule stress of M1–M4 showed a downward trend after normalization. The comparison of the fiber ring stress cloud showed that the stress level of M2 and M3 was higher than that of M1, while the stress of the four models was almost greater than that of M1 overall, and the maximum stress appeared in the front end. The stress peak of the joint capsule appeared at UIV = T1, but there was no significant difference among the other groups.

Interspinous ligament and supraspinous ligament

The normalized stress of the interspinous ligament (ISL) and supraspinous ligament (SSL) is shown in Figure 14**.** The stress of ISL after normalization was significantly lower than that of SSL before fixation with growing rods, with ISL stress of 5.4%–7.7% and SSL stress of 4.6%–16.9%. The difference between groups was significant. The ISL stress variation of M1–M3 was similar, while the stress of M4 was lower. The SSL of M1 and M2 were almost free from stress with the influence of growing rods, but the SSL stress of M4 was the largest.

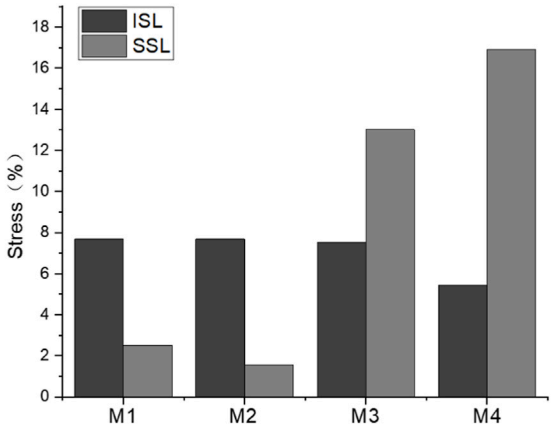

FIGURE 14
Maximum ISL and SSL stress of M1–M4 model.

Discussion

EOS is a spinal deformity with the characteristic of early occurance, rapid progression, and continuous growth of the spine, with a significant risk of cardiopulmonary insufficiency (Chang et al., 2021; Zhang et al., 2022). Patients with severe spinal curvature usually require spinal correction with growing rods after the failed attempts at conservative treatment (Akbarnia et al., 2022; Heffernan et al., 2022). Compared with single growing rods, dual growing rods system contributes to a more stable constrution for spine (Urbanski et al., 2020; Cengiz et al., 2021). It can provide a stronger control force and reduce the mechanical stress of the instrumentation. However, dual growing rods and pedicle screw fixation, the most stable and effective option, may be more likely to lead to PJK (Pan et al., 2018; Ogura et al., 2021). Clinical studies have shown that there are many factors associated with PJK, but the relationship between the position of pedicle screw fixation and PJK is still a controversial topic (Homans et al., 2020). PJK occurs at the proximal end of orthopedic instruments and is closely related to local stress concentration after surgery (Erkilinc et al., 2022). Therefore, the stress quantity of the functional spine unit (FSU) composed of UIV and UIV+1 is mainly concerned, including the stress of UIV and UIV+1, annular fiber, joint capsule, interspinous and supraspinal ligaments. In addition, the morphological variables of the spine were compared.

Finite element models have been introduced to investigate the biomechanical behavior of the spine and provide information cannot be easily obtained through *in vivo* and *in vitro* experimental studies, such as stress distribution and displacement under static conditions (Rohlmann et al., 2006; Zhu et al., 2019). Despite these successful outcomes, that segmental spinal model has natural shortcomings. An intact spine model used in finite element analysis could provide a more comprehensive and close-to-real simalution in the dynamical investigation of the biomechanical behavior of the spine. The biomechanical modeling and simulations of an intact scoliotic spine can effectively help surgeons assess and evaluate the appropriateness of various instrumentation scenarios, and accordingly find an optimal solution to maximally correct the scoliotic spine and avoid complications (Robitaille et al., 2009; Majdouline et al., 2012; Jalalian et al., 2013). Thus, an intact spinal was applied in the finite element modeling to determine an optimal UIV of growing-rod to minimalize the risk of PJK in the present study.

The surgically induced changes in the UIV are an important parameter associated with the development of PJK (Homans et al., 2020). Our study shows that as the UIV position of the dual growing rods is shifted inferiorly, the maximum displacement of the models gradually increases, therefore the fixation of longer segments reduces the overall displacement of the spine. Simultaneously comparing the UIV and UIV+1 stress nephogram of the four models, it is found that the dual growing rods and pedicle screw fixation system can increase the stress of UIV and reduce the stress of UIV+1. By analyzing the UIV stress nephogram, it seems that the stress concentration areas of the vertebral body are mainly in the contact part of the vertebral body and annulus fibrosus, joint capsule connection, and the connection part of the vertebral body and screw. The stress results of the vertebral body show that the stress in the M1 model is significantly lower overall, with only a small stress concentration at the pedicle and pedicle screw fixation sites. Therefore the stress distribution results are better than other groups when UIV is T1, which is the UEV of the upper thoracic curve.

Intervertebral disc injury and degeneration is a risk factor for PJK (Yagi et al., 2011), and the pressure on the annulus fibrosus may lead to annulus fibrosus injury or failure (Iatridis and ap Gwynn, 2004). Combined with the stress distribution of the annulus fibrosus and the joint capsule, it can be seen that M1 has lower annulus fibrosus stress and higher joint capsule stress, while M4 has the opposite result. The tendency of the former was vertebrae backward leaning, while the latter was vertebrae forward-leaning. The deformation trend of UIV and UIV+1 of the M4 model is consistent with the development of PJK (Pan et al., 2018). The result suggests that UIV downshift may be more likely to lead to PJK.

Posterior Ligament Complex (PLC) consists of ISL, SSL, and facet capsular ligaments, which play an important role in maintaining spinal stability and limiting the normal range of movement of the spine (Radcliff et al., 2012). Some researchers believe that the ligamentum flavum should be part of PLC, the damage of which during surgery is also recognized as a risk factor for PJK (Hostin et al., 2013). Therefore, the stress levels of SSL and ISL are of great significance to analyze the stress of the spine. The results showed that the growing rods significantly reduced the stress of each ligament, but this may stem from that the model used in the study was not a normal healthy spine, and the stress of the PL in the MC model was already higher than normal.

However, the comparison between each group of models shows that the SSL stress of M3 and M4 is significantly higher than that of M1 and M2. This indicated that the deformation trend of UIV and UIV+1 vertebrae was bending forward in M3 and M4, which was consistent with the analysis results of the annulus fibrosus and joint capsule.

Our study has several limitations. First, the EOS spine FE model was developed based on the geometric information of the spine from a single EOS patient, which cannot calculate the statistical significance. Then, the paraspinal muscles were not constructed in this model, although a widely recognized physiological follower load was applied to simulate the effect of muscle force (Yu et al., 2016; Wong et al., 2020). Nevertheless, the follower load could not entirely replace the muscle functions, which might have more complex contributions to spinal stability. Besides, the FE models were constructed without considering the degenerative and deformity changes such as facet hyperplasia, annular tearing, endplate sclerosis, or vertebral osteoporosis, which may make the conclusion less persuasive.

Conclusion

In the current study, the stress distribution in the proximal vertebral body and soft tissues of dual growing rods with different proximal fixation segments were analyzed using FEM to explore the optimal UIV. The results showed that the stress of the vertebra and soft tissue at M1 was the lowerest, and the fixed condition could conquer the PJK formation and progression. M4 model, on the contrary, is more likely to cause PJK occurrence. Therefore, PJK is less likely to occur when the upper end of the dual growing rods is fixed close to the UEV of the upper thoracic curve.

Data availability statement

The raw data supporting the conclusion of this article will be made available by the authors, without undue reservation.

Ethics statement

The studies involving human participants were reviewed and approved by the ethics committee of Beijing Chaoyang Hospital. Written informed consent to participate in this study was provided by the participants' legal guardian/next of kin. Written informed consent was obtained from the individual(s), and minor(s)' legal guardian/next of kin, for the publication of any potentially identifiable images or data included in this article.

Author contributions

All authors contributed to the research conception and design. The first draft of the paper was written by HTD. FE model was established by JW and ZZ. Data calculation and analysis were performed by HD and AP. The work was critically revised by YH and YL. All authors commented on previous versions of the paper, as well as, read and approved the final version.

Conflicts of interest

The authors declare that the research was conducted in the absence of any commercial or financial relationships that could be construed as a potential conflict of interest.

Publisher's note

All claims expressed in this article are solely those of the authors and do not necessarily represent those of their affiliated organizations, or those of the publisher, the editors and the reviewers. Any product that may be evaluated in this article, or claim that may be made by its manufacturer, is not guaranteed or endorsed by the publisher.

References

Akbarnia, B. A., Pawelek, J. B., Hosseini, P., Salari, P., Kabirian, N., Marks, D., et al. (2022). Treatment of early-onset scoliosis: Similar outcomes despite different etiologic subtypes in traditional growing rod graduates. *J. Pediatr. Orthop.* 42, 10–16. doi:10.1097/bpo.0000000000001985

Busscher, I., Van Dieen, J. H., Kingma, I., Van Der Veen, A. J., Verkerke, G. J., and Veldhuizen, A. G. (2009). Biomechanical characteristics of different regions of the human spine: An *in vitro* study on multilevel spinal segments. *Spine (Phila Pa 1976)* 34, 2858–2864. doi:10.1097/brs.0b013e3181b4c75d

Cahill, P. J., Wang, W., Asghar, J., Booker, R., Betz, R. R., Ramsey, C., et al. (2012). The use of A transition rod may prevent proximal junctional kyphosis in the thoracic spine after scoliosis surgery: A finite element analysis. *Spine (Phila Pa 1976)* 37, E687–E695. doi:10.1097/brs.0b013e318246d4f2

Cengiz, B., Ozdemir, H. M., Sakaogullari, A., Isik, M., and Aydogan, N. H. (2021). Traditional dual growing rod technique in the management of early onset scoliosis and its effects on spinal growth and lung development: The mid-term prospective results. *Cureus* 13, E14422. doi:10.7759/cureus.14422

Chang, W. C., Hsu, K. H., and Feng, C. K. (2021). Pulmonary function and health-related quality of life in patients with early onset scoliosis after repeated traditional growing rod procedures. *J. Children's. Orthop.* 15, 451–457. doi:10.1302/1863-2548.15.210021

Clin, J., Aubin, C. E., Lalonde, N., Parent, S., and Labelle, H. (2011). A new method to include the gravitational forces in A finite element model of the scoliotic spine. *Med. Biol. Eng. Comput.* 49, 967–977. doi:10.1007/s11517-011-0793-4

Erbulut, D. U., Zafarparandeh, I., Hassan, C. R., Lazoglu, I., and Ozer, A. F. (2015). Determination of the biomechanical effect of an interspinous process device on implanted and adjacent lumbar spinal segments using A hybrid testing protocol: A finite-element study. *J. Neurosurg. Spine* 23, 200–208. doi:10.3171/2014.12.spine14419

Erkilinc, M., Baldwin, K. D., Pasha, S., and Mistovich, R. J. (2022). Proximal junctional kyphosis in pediatric spinal deformity surgery: A systematic review and critical analysis. *Spine Deform.* 10, 257–266. doi:10.1007/s43390-021-00429-w

Hardesty, C. K., Huang, R. P., El-Hawary, R., Samdani, A., Hermida, P. B., Bas, T., et al. (2018). Early-onset scoliosis: Updated treatment techniques and results. *Spine Deform.* 6, 467–472. doi:10.1016/j.jspd.2017.12.012

Hasler, C. C. (2018). Early-onset scoliosis: Contemporary decision-making and treatment options. *J. Pediatr. Orthop.* 38 (1), S13–S20. doi:10.1097/bpo.0000000000001184

Heffernan, M. J., Younis, M., Glotzbecker, M. P., Garg, S., Leonardi, C., Poon, S. C., et al. (2022). The effect of surgeon experience on outcomes following growth friendly instrumentation for early onset scoliosis. *J. Pediatr. Orthop.* 42, E132–E137. doi:10.1097/bpo.0000000000002000

Homans, J. F., Kruyt, M. C., Schlosser, T. P. C., Colo, D., Rogers, K., Shah, S. A., et al. (2020). Changes in the position of the junctional vertebrae after posterior spinal fusion in adolescent idiopathic scoliosis: Implication in risk assessment of proximal junctional kyphosis development. *J. Pediatr. Orthop.* 40, E84–E90. doi:10.1097/bpo.0000000000001400

Hostin, R., Mccarthy, I., O'brien, M., Bess, S., Line, B., Boachie-Adjei, O., et al. (2013). Incidence, mode, and location of acute proximal junctional failures after surgical treatment of adult spinal deformity. *Spine (Phila Pa 1976)* 38, 1008–1015. doi:10.1097/brs.0b013e318271319c

Iatridis, J. C., and Ap Gwynn, I. (2004). Mechanisms for mechanical damage in the intervertebral disc annulus fibrosus. *J. Biomech.* 37, 1165–1175. doi:10.1016/j.jbiomech.2003.12.026

Jalalian, A., Gibson, I., and Tay, E. H. (2013). Computational biomechanical modeling of scoliotic spine: Challenges and opportunities. *Spine Deform.* 1, 401–411. doi:10.1016/j.jspd.2013.07.009

Kahaer, A., Zhou, Z., Maitirouzi, J., Wang, S., Shi, W., Abuduwaili, N., et al. (2022). Biomechanical investigation of the posterior pedicle screw fixation system At level L4-L5 lumbar segment with traditional and cortical trajectories: A finite element study. *J. Healthc. Eng.* 2022, 1–11. doi:10.1155/2022/4826507

Karol, L. A. (2019). The natural history of early-onset scoliosis. *J. Pediatr. Orthop.* 39, S38–S43. doi:10.1097/bpo.0000000000001351

Liang, W., Han, B., Hai, Y., Yang, J., and Yin, P. (2022). Biomechanical analysis of the reasonable cervical range of motion to prevent non-fusion segmental degeneration after single-level acdf. *Front. Bioeng. Biotechnol.* 10, 918032. doi:10.3389/fbioe.2022.918032

Majdouline, Y., Aubin, C. E., Wang, X., Sangole, A., and Labelle, H. (2012). Preoperative assessment and evaluation of instrumentation strategies for the treatment of adolescent idiopathic scoliosis: Computer simulation and optimization. *Scoliosis* 7, 21. doi:10.1186/1748-7161-7-21

Ogura, Y., Glassman, S. D., Sucato, D., Hresko, M. T., and Carreon, L. Y. (2021). Incidence of proximal junctional kyphosis with pedicle screws at upper instrumented vertebrae in posterior spinal fusion for adolescent idiopathic scoliosis. *Glob. Spine J.* 11, 1019–1024. doi:10.1177/2192568220935107

Pan, A., Hai, Y., Yang, J., Zhang, Y., and Zhang, Y. (2018). Upper instrumented vertebrae distal to T2 leads to A higher incidence of proximal junctional kyphosis during growing-rod treatment for early onset scoliosis. *Clin. Spine Surg. A Spine Publ.* 31, E337–E341. doi:10.1097/bsd.0000000000000661

Pearsall, D. J., Reid, J. G., and Livingston, L. A. (1996). Segmental inertial parameters of the human trunk as determined from computed tomography. *Ann. Biomed. Eng.* 24, 198–210. doi:10.1007/bf02667349

Radcliff, K., Su, B. W., Kepler, C. K., Rubin, T., Shimer, A. L., Rihn, J. A., et al. (2012). Correlation of posterior ligamentous complex injury and neurological injury to loss of vertebral body height, kyphosis, and canal compromise. *Spine (Phila Pa 1976)* 37, 1142–1150. doi:10.1097/brs.0b013e318240fcd3

Robitaille, M., Aubin, C. E., and Labelle, H. (2009). Effects of alternative instrumentation strategies in adolescent idiopathic scoliosis: A biomechanical analysis. *J. Orthop. Res.* 27, 104–113. doi:10.1002/jor.20654

Rohlmann, A., Bauer, L., Zander, T., Bergmann, G., and Wilke, H. J. (2006). Determination of trunk muscle forces for flexion and extension by using A validated finite element model of the lumbar spine and measured *in vivo* data. *J. Biomech.* 39, 981–989. doi:10.1016/j.jbiomech.2005.02.019

Schmidt, H., Galbusera, F., Rohlmann, A., Zander, T., and Wilke, H. J. (2012). Effect of multilevel lumbar disc arthroplasty on spine kinematics and facet joint loads in flexion and extension: A finite element analysis. *Eur. Spine J.* 21 (5), S663–S674. doi:10.1007/s00586-010-1382-1

Senkoylu, A., Riise, R. B., Acaroglu, E., and Helenius, I. (2020). Diverse approaches to scoliosis in young children. *EFORT Open Rev.* 5, 753–762. doi:10.1302/2058-5241.5.190087

Shen, H., Fogel, G. R., Zhu, J., Liao, Z., and Liu, W. (2019). Biomechanical analysis of different lumbar interspinous process devices: A finite element study. *World Neurosurg. x.* 127, E1112–E1119. doi:10.1016/j.wneu.2019.04.051

Urbanski, W., Tucker, S., Ember, T., and Nadarajah, R. (2020). Single vs dual rod constructs in early onset scoliosis treated with magnetically controlled growing rods. *Adv. Clin. Exp. Med.* 29, 1169–1174. doi:10.17219/acem/126289

Wang, W., Pei, B., Pei, Y., Shi, Z., Kong, C., Wu, X., et al. (2019). Biomechanical effects of posterior pedicle fixation techniques on the adjacent segment for the treatment of thoracolumbar burst fractures: A biomechanical analysis. *Comput. Methods Biomech. Biomed. Engin.* 22, 1083–1092. doi:10.1080/10255842.2019.1631286

Watanabe, K., Uno, K., Suzuki, T., Kawakami, N., Tsuji, T., Yanagida, H., et al. (2016). Risk factors for proximal junctional kyphosis associated with dual-rod growing-rod surgery for early-onset scoliosis. *Clin. Spine Surg.* 29, E428–E433. doi:10.1097/bsd.0000000000000127

Wong, C. E., Hu, H. T., Hsieh, M. P., and Huang, K. Y. (2020). Optimization of three-level cervical hybrid surgery to prevent adjacent segment disease: A finite element study. *Front. Bioeng. Biotechnol.* 8, 154. doi:10.3389/fbioe.2020.00154

Yagi, M., Akilah, K. B., and Boachie-Adjei, O. (2011). Incidence, risk factors and classification of proximal junctional kyphosis: Surgical outcomes review of adult idiopathic scoliosis. *Spine (Phila Pa 1976)* 36, E60–E68. doi:10.1097/brs.0b013e3181eeaee2

Yu, C. C., Liu, P., Huang, D. G., Jiang, Y. H., Feng, H., and Hao, D. J. (2016). A new cervical artificial disc prosthesis based on physiological curvature of end plate: A finite element analysis. *Spine J.* 16, 1384–1391. doi:10.1016/j.spinee.2016.06.019

Zhang, Y. B., and Zhang, J. G. (2020). Treatment of early-onset scoliosis: Techniques, indications, and complications. *Chin. Med. J.* 133, 351–357. doi:10.1097/cm9.0000000000000614

Zhang, Y., Wang, Y., Xie, J., Bi, N., Zhao, Z., Li, T., et al. (2022). Factors associated with postoperative respiratory complications following posterior spinal instrumentation in children with early-onset scoliosis. *Orthop. Surg.* 14 (7), 1489–1497. doi:10.1111/os.13351

Zhu, W. Y., Zang, L., Li, J., Guan, L., and Hai, Y. (2019). A biomechanical study on proximal junctional kyphosis following long-segment posterior spinal fusion. *Braz. J. Med. Biol. Res.* 52, E7748. doi:10.1590/1414-431x20197748

frontiers | Frontiers in Bioengineering and Biotechnology

TYPE Original Research
PUBLISHED 09 September 2022
DOI 10.3389/fbioe.2022.918315

Check for updates

OPEN ACCESS

EDITED BY
Qichang Mei,
Ningbo University, China

REVIEWED BY
Tianyun Jiang,
China Academy of Chinese Medical Sciences, China
Zixiang Gao,
Ningbo University, China

*CORRESPONDENCE
Pui Wah Kong,
puiwah.kong@nie.edu.sg

SPECIALTY SECTION
This article was submitted to Biomechanics, a section of the journal Frontiers in Bioengineering and Biotechnology

RECEIVED 12 April 2022
ACCEPTED 23 August 2022
PUBLISHED 09 September 2022

CITATION
Kong PW, Kan TYW, Mohamed Jamil RAGB, Teo WP, Pan JW, Hafiz Abd Halim MN, Abu Bakar Maricar HK and Hostler D (2022), Functional versus conventional strength and conditioning programs for back injury prevention in emergency responders. *Front. Bioeng. Biotechnol.* 10:918315. doi: 10.3389/fbioe.2022.918315

Functional versus conventional strength and conditioning programs for back injury prevention in emergency responders

Pui Wah Kong[1]*, Tommy Yew Weng Kan[1], Roslan Abdul Ghani Bin Mohamed Jamil[1], Wei Peng Teo[1], Jing Wen Pan[1], Md Noor Hafiz Abd Halim[2], Hasan Kuddoos Abu Bakar Maricar[2] and David Hostler[3]

[1]Physical Education and Sports Science Academic Group, National Institute of Education, Nanyang Technological University, Singapore, Singapore, [2]Responder Performance Centre, Civil Defence Academy, Singapore Civil Defence Force, Singapore, Singapore, [3]Center for Research and Education in Special Environments, University at Buffalo, Buffalo, CA, United States

Back pain and back-related injuries are common complaints among emergency responders. The purpose of this study was to compare the effectiveness of two strength and conditioning programs in improving back muscle characteristics and disabilities in emergency responders (firefighters/paramedics). Participants (n = 24) were randomized into two groups to complete 16 weeks of supervised exercise intervention: 1) Functional training used unilateral movements that mimicked the asymmetrical nature of emergency operations, 2) Conventional training performed bilaterally loaded exercises. Outcome measures were maximum isometric back extension strength, passive muscle stiffness, lumbar extensor fatigability, and revised Oswestry Low Back Pain Questionnaire. A mixed model Analysis of Variance with repeated measures was performed to compare the difference over time and between groups. While the training effects were similar between groups, both programs improved isometric back extension strength (+21.3% functional, +20.3% conventional, $p <$ 0.001, $\eta_p^2 = 0.625$) and lumbar extensor muscle fatigability (+17.4% functional, +9.5% conventional, $p = 0.009$, $\eta_p^2 = 0.191$). Bilateral symmetry in muscle stiffness was improved as indicated by reduction in symmetry index (-7.1% functional, -11.8% conventional, $p = 0.027$, $\eta_p^2 = 0.151$). All self-reported pain and disability scores fell within the category of "*minimum functional limitation*" throughout the intervention and 6-month follow-up periods. For frontline firefighters and paramedics, both functional and conventional strength training are effective for improving back muscle characteristics.

KEYWORDS

firefighters, paramedics, stiffness, EMG, fatigability, low back pain, Oswestry Disability Index, isometric strength

1 Introduction

Emergency response plays a critical role in ensuring public safety, but it is an inherently dangerous occupation. Emergency situations warranting a response can range from natural disasters to home fire and transportation incidents. Emergency responders such as firefighters and paramedics must be physically fit in order to with the challenges during emergency situations (Beach et al., 2014). Considering the exposures to strenuous and physically demanding tasks (Nazari et al., 2020b; Stassin et al., 2021), it is not surprising to note frequent complaints of low back pain (LBP) and back injuries among emergency responders. For instance, the prevalence of LBP in firefighters has been reported to be approximately 30% across many countries (Katsavouni et al., 2014; Negm et al., 2017; Damrongsak et al., 2018; Nazari et al., 2020a; Pelozato de Oliveira et al., 2021) and up to 71.1% in South Korea (Kim and Ahn, 2021). A similar range from 31.8 to 85.1% of LBP prevalence was also observed in emergency medical services (EMS) personnel (Ham and Ahn, 2008; Kim et al., 2017; Aljerian et al., 2018; Imani et al., 2018). In additional to the dangerous nature of emergency work, inadequate level of physical fitness may also increase the risk of work-related injuries (Griffin et al., 2016). One possible strategy to reduce back pain and injuries in emergency responders is to design and implement an effective strength and conditioning program to improve back muscle strength and overall fitness (Abel et al., 2015).

Resistance training is a key element in all well-rounded strength and conditioning programs. Traditionally, conventional resistance training emphasizes symmetrical exercises whereby the left and right limbs are loaded together and perform the same range of motion simultaneously (bench press, back squat, deadlift, strict press) (Beach et al., 2014; Moon et al., 2015). These conventional exercises, when performed at appropriate intensity and volume, may provide sufficient back and core strength to protect the emergency responders from back injuries. In emergency work, however, the operational tasks such as swinging an axe, advancing hose, and handling casualties are not symmetrically loaded. Thus, functional exercises, defined here as loading of a single limb and activating the core from shoulder to opposite hip, better simulate the asymmetrical nature of the emergency response tasks. High-intensity functional training programs have been shown to be safe and effective for the military and general population (Poston et al., 2016; Feito et al., 2018). While both conventional and functional fitness programs should target all major muscle groups, a functional program that takes firefighting and paramedic related tasks into consideration may be superior to improve back muscle characteristics and thereby reducing back pain and injuries.

The purpose of study was to compare the effectiveness of two strength and conditioning programs on back muscle characteristics and disabilities in emergency responders in Singapore. It was hypothesized that functional training would be more effective than conventional training in improving back muscle strength, stiffness, fatigability, and self-report disability outcomes. This study will pioneer the implementation of customized strength and conditioning programs among frontline emergency responders at their workplace. Findings from this study can provide empirical evidence on whether such physical training programs can improve back muscle function and disabilities. Such information can guide future practice and policy pertaining to workplace safety and well-being of emergency responders.

2 Materials and methods

2.1 Study design

This was a longitudinal training study with two arms (Figure 1). Participants were randomly allocated into one of the two exercise groups undergoing different types of strength and conditioning programs for 16 weeks. The Functional Group performed exercises that simulated the asymmetrical and/or diagonal loading nature of the movements which emergency responders would encounter in their regular work routine. The Conventional Group was prescribed traditional strength training that comprised bilaterally symmetrical multi-muscle group exercises. Back muscle characteristics were assessed at pre-intervention (baseline), mid-intervention, and post-intervention. Self-report pain and disability surveys were administered as pre-intervention, mid-intervention, post-intervention, and follow-ups at 2, 4, and 6 months after the intervention.

2.2 Participants

This study was approved by the Nanyang Technological University Institutional Review Board (Protocol Number: IRB-2020-06-85). All participants provided written informed consent to enroll in the study. The inclusion criteria were that participants were 1) males or females, 2) between the age of 21 and 45 years old, 3) a full-time emergency responder at the Singapore Civil Defence Force (SCDF), and 4) healthy to perform work duties at the time of the recruitment. Participants were excluded if they had any histories of back surgery or self-reported to be pregnant (females only).

At the start of the study, a total of SCDF 58 emergency responders who met the inclusion criteria have enrolled. Due to the unforeseeable circumstances associated with COVID-19, we encountered a high drop-out rate in the early phase of the study, shortly after the pre-intervention test. Since the early drop-outs did not engage in sufficient exercise training to allow meaningful data analysis, we adopted the modified intention-to-treat approach (Gupta, 2011; Montedori et al., 2011). Only

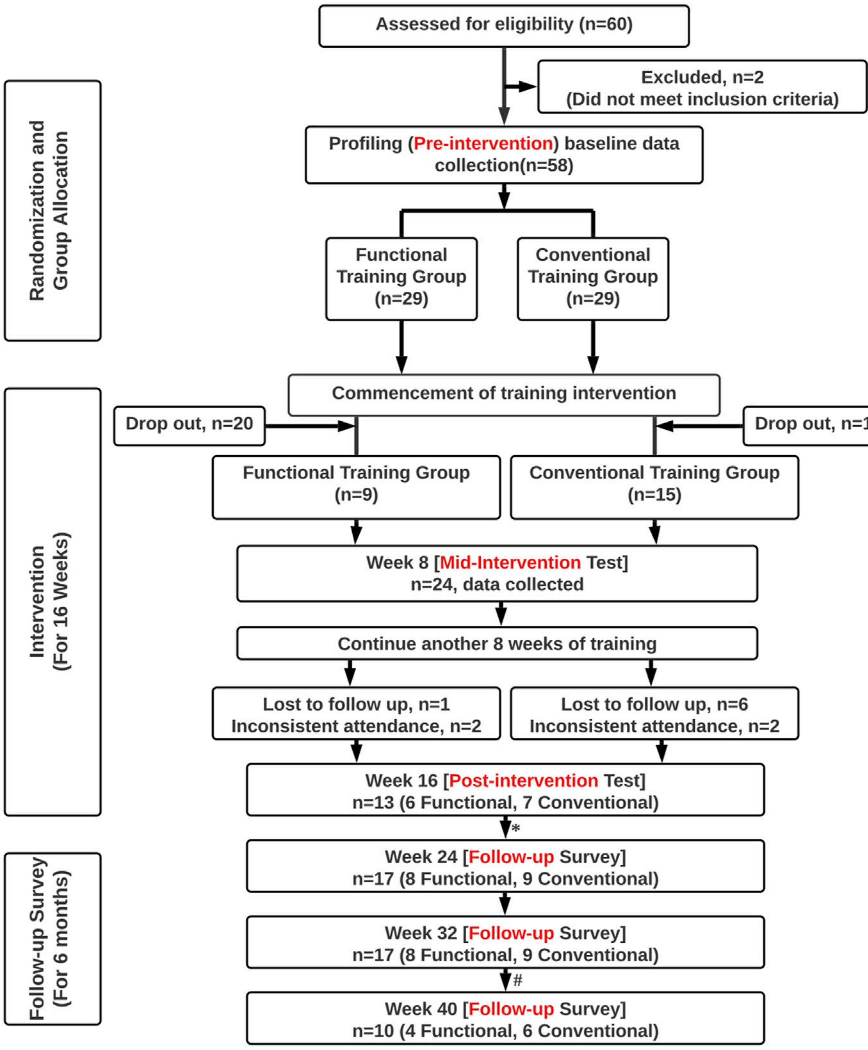

FIGURE 1
Study overview. [Note. *4 participants (2 Functional, 2 Conventional) who did not attend the physical post-intervention test at Week 16 were able to complete the online follow-up survey at Week 24. # 7 participants (4 Functional, 3 Conventional) were lost to contact at Week 40.].

participants who had completed at least 8 weeks of training and the mid-intervention test were included in the data analysis. The physical characteristics of these 24 male emergency responders (23 firefighters, 1 administration officer) are shown in Table 1.

2.3 Strength and conditioning exercise intervention

Participants were randomized into either the Functional Group or Conventional Group for exercise interventions. They were required to attend the exercise training on their duty days at their respective fire stations, two sessions per week for 16 weeks. All training was conducted in the gym at the assigned fire stations under the supervision of the same researcher (TYWK) who was trained and experienced in strength and conditioning.

A typical training session consisted about 8 different types of exercises and lasted for 45–60 min (Table 2). In the beginning of each training session, participants from both groups went through the same sequence of warm-up exercises before the commencement of their specific training. Examples of warm-up exercises included 6 to 10 repetitions of forward lunges (with and without twist), dynamic chest stretch, single-leg hamstring stretch, walk-ins and T-spine rotation. All participants would execute four types of exercises: Exercises A, B, and C were designed to focus on different muscle groups while exercise D was largely cardiovascular-intensive. The Functional Group

TABLE 1 Physical characteristics and demographic background of emergency responders (n = 24).

Characteristics	All 24	Functional Group (8 firefighters, 1 officer)	Conventional Group (15 firefighters)	*P*
Ethnicity	Malay (n = 18)	Malay (n = 7)	Malay (n = 12)	--
	Chinese (n = 3)	Chinese (n = 2)	Chinese (n = 1)	
	Others (n = 3)	Others (n = 1)	Others (n = 2)	
Age (years)	32.4 (5.2)	31.9 (5.0)	32.7 (5.4)	0.729
Body mass (kg)	73.4 (10.0)	70.1 (9.6)	75.6 (10.0)	0.193
Height (cm)	172.0 (7.5)	169.2 (8.4)	173.6 (6.8)	0.168
BMI (kg/m^2)	24.8 (2.5)	24.5 (3.0)	25.0 (2.3)	0.618
LBP history	Yes (n = 13)	Yes (n = 7)	Yes (n = 6)	--
	No (n = 11)	No (n = 2)	No (n = 9)	
Pain disability	Minimum (n = 22)	Minimum (n = 7)	Minimum (n = 15)	--
	Moderate (n = 2)	Moderate (n = 2)	Moderate (n = 0)	
Regular smoker	Yes (n = 6)	Yes (n = 1)	Yes (n = 5)	--
	No (n = 18)	No (n = 8)	No (n = 10)	
Alcohol consumer	Yes (n = 1)	Yes (n = 1)	Yes (n = 0)	--
	No (n = 23)	No (n = 8)	No (n = 15)	

All 24 participants were males. Data are expressed as mean (SD) unless otherwise stated. Ethnicity (Others) comprises 1 Indian, 1 Javanese, and 1 Boyanese. BMI denotes body mass index. LBP denotes low back pain. Pain disability was measured with the Oswestry Disability Index (ODI). Differences between the Functional and Conventional groups were compared using independent t-tests.

TABLE 2 Sample exercises of functional group training program.

Session	Exercise	Repetition	Set
Week 1 Day 1	A1. DB Reverse Lunges	8—9 reps	3
	A2. DB Bench Press	8—9 reps	3
	B1. SL Kettlebell Deadlift	8—9 reps per leg	3
	B2. Bent Over Kettlebell Row	8—9 reps per arm	3
	C1. Forearm Plank	30 s	3
	C2. SA DB Row	8 reps	3
	D. Tabata	4 min	
	- Burpees	30 s	
	- Air Squats	30 s	
Week 1 Day 2	A1. DB Box Step Up	8—9 reps	3
	A2. Incline DB Bench Press	8—9 reps	3
	B1. Half Kneeling SA Press	8—9 reps	3
	B2. Bent Over Kettlebell Row	8—9 reps	3
	C1. Hollow Body Hold	20 s	3
	C2. Plank Hold DB Drag	8—9 reps	3
	D. EMOM	6 min	
	- 100 m Treadmill Run	60 s	
	- Bear Crawl Hold	60 s	

DB, denotes dumbbell; SL, denotes single leg; SA, denotes single arm; EMOM, denotes every minute on the minute.

performed exercises that are bilaterally asymmetrical and/or involve diagonal loading (Figure 2). The Conventional Group was prescribed traditional strength training exercises that comprised bilaterally symmetrical multi-muscle group exercises (e.g., barbell back squat, push-up). Efforts were made to match the training load and training volume of the two groups as similar as possible. Detailed training programs for the full 16 weeks can be found in Supplementary Table S1 (Functional training) and Supplementary Table S2 (Conventional training).

Participants performed the prescribed exercises in groups with a superset training method where two exercises were done continuously with no long rest in-between. After completing one set of superset training (e.g., A1 and A2 in Table 2), the participants would rest for 2–3 min before commencing the following sets. Once the participants complete all the superset exercises (A, B and C), they would proceed to exercise D which was to perform either a Tabata training, EMOM (Every minute on the minute) training or AMRAP (As many rounds as possible) conditioning before ending the training session.

Participants were asked to indicate their rate of perceived exertion (RPE) of the exercise intensity after working out using the Borg's CR-10 scale (Borg, 1990). On the very first day of training (i.e., Week 1 Day 1), participants of both groups were advised to work out at a RPE scale of 5 or 6 in a scale of 0 (nothing at all) to 10 (extremely strong). Subsequently, they were encouraged to progressively increase the intensity of training by either increasing the repetitions, weight or reducing the rest time between supersets as part of the progressive nature of the training program.

The training intervention was conducted in 2020–2021 during which we encountered great difficulties and uncertainties associated with COVID-19. For instance, there were restrictions and frequent updates of safe measures

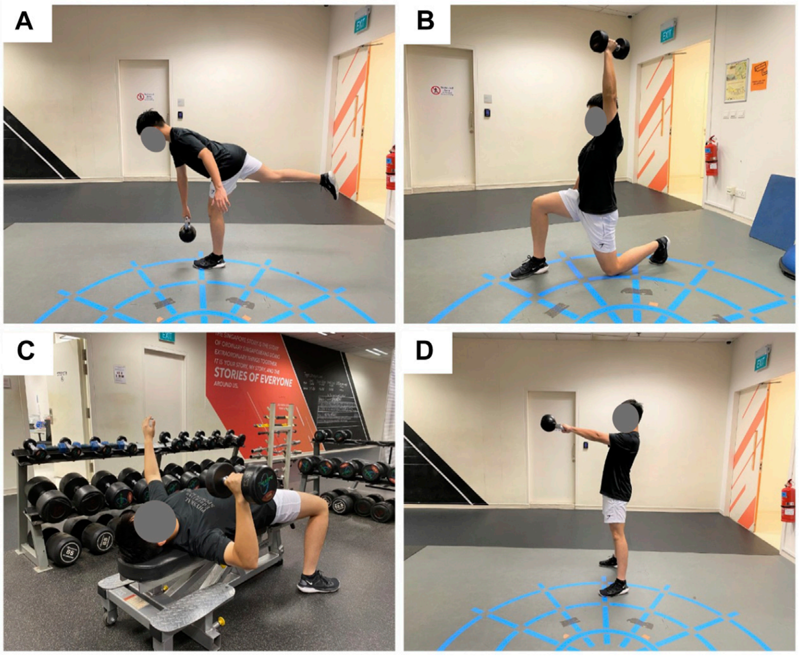

FIGURE 2
Example of Functional training exercises that are bilaterally asymmetrical and/or involve diagonal loading. **(A)** Single leg kettlebell deadlift. **(B)** Single arm dumbbell press. **(C)** Single arm chest press. **(D)** Kettlebell swing.

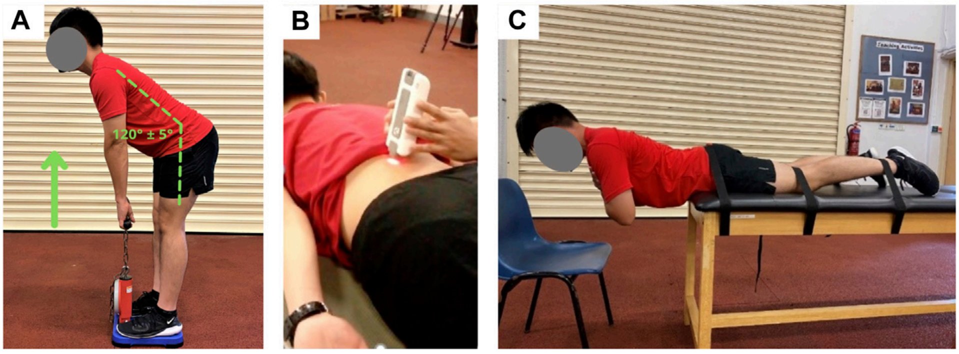

FIGURE 3
Back muscle characteristics assessment: **(A)** Maximal isometric hip extension test, **(B)** Passive stiffness of lumbar extensor muscles, **(C)** Modified Sorensen test for fatigability.

management (e.g., closure of gym facilities, limitation in group size, safe distancing measures). In addition to COVID-related measures, the work shift schedule of the emergency responders (e.g., 1 working day followed by 2 days off) also contributed to some interruptions in implementing the training intervention. Occasionally, the participants had to stop the exercise training to respond to an emergency immediately. These challenges required the research team to be flexible, adaptive, and ready for prompt action in order to execute the training study under sub-optimal conditions. For the participants' safety, some adjustments to the number of repetitions, rest time and weights used were made for individual participants to accommodate absences from training.

2.4 Outcome measures

2.4.1 Back extension strength

Maximal isometric back extension strength was measured using a dynamometer (Takei T.K.K.5402 BACK-D, Takei Scientific Instruments Co., Ltd, Tokyo, Japan) and expressed in kilograms (kg) of force produced. The hip angle was measured and standardized at 120 (±5) degrees before the commencement of the test (Figure 3A). This was to ensure that the testing postures and hence muscle lengths were similar across all participants and on different days. After a countdown "3, 2, 1, pull", participants were asked to extend their back as hard as they could while holding on to the handle of the dynamometer for a minimum of 3 s. Participants were given a total of 3 attempts and the best maximum force produced was recorded. Sufficient time was given to rest between trials. The maximum force data were normalized to each participant's body mass to facilitate comparison between groups. A normalized strength of 1.0 indicates the amount of force, that is, equivalent to one's own body weight.

2.4.2 Passive muscle stiffness

Muscle stiffness was measured in a relaxed state when the participants were lying in a prone position on an examination table (Figure 3B). The passive stiffness of the longissimus muscles was measured using a hand-held myotonometry device (MyotonPRO, Myoton AS, Tallinn, Estonia). This device has been used to monitor changes in muscle stiffness after strenuous exercise (Kong et al., 2018) and to assess the stiffness of previously-injured and uninjured muscles (Nin et al., 2021). The sites of measurement were 2 cm lateral to the L1 spinous process on both left and right sides (Criswell, 2010). The myotonometry device applies a brief mechanical impulse to elicit damped oscillations of the muscle to calculate muscle stiffness (in N/m) (Kong et al., 2018). The average of 5 consecutive measurements was taken on each side.

2.4.3 Muscle fatigability

The modified Sorensen test was used to assess the lumbar extensor muscles' fatigability using electromyography (EMG) measurements (Cai and Kong, 2015; Cai et al., 2017). In this test, participants were required to lie on an examining table in a prone position with the upper edge of the iliac crests aligned with the edge of the table and the lower body is being strapped down around the pelvis, knees, and ankles (Figure 3C). Participants were asked to maintain a horizontal position for 2 min while keeping their arms folded across the chest. The test would be terminated if participants failed to maintain the upper body in a horizontal position. During the 2-minute test duration, the lumbar extensors muscles activation (longissimus of both left and right sides) was captured using surface EMG (Biomonitor ME6000, Mega Electronics Ltd., Finland). The electrodes were placed on the same measurement sites as the muscle stiffness tests which were 2 cm lateral to the L1 spinous process of each side (Criswell, 2010). Raw EMG data were band-pass filtered at 20–450 Hz and then analyzed in the frequency domain. To examine the back muscle's resistance to fatigue, the median frequency slope (MFS) of EMG signals was calculated from the power density spectrum (Cai et al., 2017). As muscle fatigue develops over the 2-minute period, the EMG-MFS would decline over time (i.e., negative slope). A steeper slope indicates less resistance to fatigue.

2.4.4 Self-reported disability survey

Perceived back pain and disabilities were assessed using the revised Oswestry Low Back Pain Questionnaire (Fairbank and Pynsent, 2000). This survey asks participants about their back pain intensity during daily situations such as lifting heavy weights, walking, standing, sitting, sleeping, socializing, and the change in degree of pain. There are a total of 10 questions with 6 different options. For each question, the total possible score is 5 (if the first option is marked, score = 0; if the last option is marked, score = 5). The Oswestry Disability Index (ODI) was calculated as a disability score by summing up the scores of all 10 questions. The ODI was then expressed as percentage (0–100%), with higher disability scores indicating greater functional limitation. The classification of the scores was as follow: 0–20%: *minimum functional limitation*; 21–40%: *moderate functional limitation*; 41–60%: *intense functional limitation*; 61–80%: *disability*, and above 80%: *maximum functional limitation* (Fairbank and Pynsent, 2000; Marín-Jiménez et al., 2019).

2.5 Statistical analyses

There were missing data among the 24 participants at post-intervention and subsequent follow-up tests due to factors such as loss of interest, work commitment, Ramadan fasting, health, COVID-19, or lost to contact. Missing data were imputed following the last observation carried forward approach. Data were imported into JASP (version 0.14.1) statistical software for analyses, with significance level set at $p < 0.05$. Data are expressed as mean (standard deviation). The outcome variables were strength, stiffness (average of left and right sides), EMG-MFS (average of left and right sides) and ODI. In order to examine the balance between the left and right sides, a symmetry index (%) was calculated for stiffness and EMG-MFS using the formula below (Kong et al., 2010):

$$\text{Symmetry index} = \frac{|x_R - x_L|}{0.5\ (x_R + x_L)} \times 100\%$$

where x_R represents the variable of the right side and x_L represents the variable of the left side.

A mixed model Analysis of Variance (ANOVA) with repeated measures was performed to compare the difference

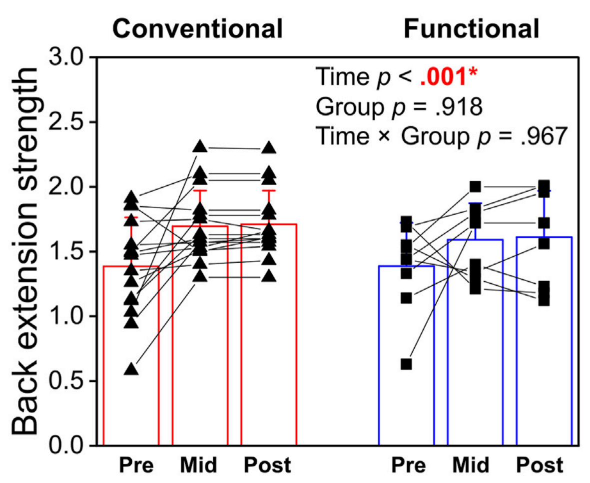

FIGURE 4
Comparison of the normalized isometric back extension strength between the conventional and functional training at pre-, mid- and post-intervention. *Statistical significance (p <0 .05) is shown in red font and indicated by an asterisk.

over time and between groups for each variable of interest (α = 0.05). Effect size was calculated as partial eta-squared (η_p^2). *Post-hoc* tests with Bonferroni adjustments were performed where appropriate.

3 Results

Compliance with exercise program was 17.4 (5.5) out of 32 prescribed training sessions over 16 weeks. There was no difference between the Functional (19.3 (7.2)) and Conventional (16.2 (4.1)) group compliance (p = 0.184, d = 0.578). There was no adverse incident or injuries happened during the supervised training sessions.

3.1 Normalized back extension strength

There was a significant main effect of Time ($p < 0.001$, η_p^2 = 0.625, Figure 4) in isometric back extension strength but no interaction effect (p = 0.967, η_p^2 = 0.002) or difference between the Functional and Conventional groups (p = 0.918, $\eta_p^2 < 0.001$). *Post-hoc* tests revealed that participants increased their back extension strength by 19.6% (+20.3% functional, +18.9% conventional) at mid-intervention ($p < 0.001$) and 20.8% (+21.3% functional, +20.3% conventional) at post-intervention ($p < 0.001$) when compared with baseline (Figure 4). No difference in normalized strength was found between the mid- and post-intervention tests.

3.2 Passive muscle stiffness

Taking the average of left and right sides, there was no significant effects of Time (p = 0.056, η_p^2 = 0.123, Figure 5A), Group (p =0 .261, η_p^2 = 0.057), or Time × Group interaction (p =0 .975, $\eta^2{}_p$ = 0.011) on back muscle stiffness. The symmetry index of stiffness decreased over time (p = 0.027, η_p^2 = 0.151), with lower stiffness at post-intervention (-7.1% functional, -11.8% conventional, p = 0.023) compared with pre-intervention (Figure 5A). No Group (p = 0.992, $\eta_p^2 < 0.001$) or interaction (p = 0.720, η_p^2 = 0.015) effects were noted in the stiffness symmetry.

To further understand the left-right balance in muscle stiffness, an additional two-way repeated measures ANOVA was run to compare the stiffness between the left and right sides over time (Figure 5B). The results revealed significant Time × Side interaction (p < 0.001 η_p^2 = 0.388). At baseline, the back muscle stiffness in the right side was lower than that of the left side ($p < 0.001$) but this left-right imbalance no longer existed in the mid- or post-intervention. No significant main effects of Time (p = 0.069, η_p^2 = 0.125) or Side (p = 0.083, η_p^2 = 0.125) were identified. These results showed that left-right symmetry in back muscle stiffness improved after 8 weeks of training, and that this improvement can be maintained with regular exercise training.

3.3 Muscle fatigability

Taking the average EMG-MFS of the left and right longissimus, there was a significant main effect of Time (p = 0.009, η_p^2 = 0.191) but not interaction effect (p = 0.566, η_p^2 = 0.026) or difference between groups (p = 0.667, η_p^2 = 0.009). A less negative slope indicates improvement in resistance to fatigue (Figure 6A). *Post-hoc* analysis revealed significant 13.6% (+17.4% functional, +9.5% conventional) improvement in fatigability at post-intervention (p = 0.009) compared with baseline (Figure 6A). When the symmetry index of EMG-MFS was analyzed, there was no significant effects of Time (p = 0.834, η_p^2 = 0.008, Figure 6B), Group (p = 0.514, η_p^2 = 0.020), or Time × Group interaction (p = 0.325, η_p^2 = 0.050).

3.4 Self-reported pain and disability

There was no adverse incident during the training period that caused low back pain or negatively impacted back function. The ODI for lower back pain and functionality are tabulated in Table 3. All disability scores throughout the study period were very low and fell well within the category of "*minimum functional limitation*" (0–20%). There were no significant changes over time (p = 0.951, η_p^2 = 0.010) or difference between groups (p = 0.785, η_p^2 = 0.03). While a significant interaction effect was found (p = 0.008, η_p^2 = 0.131), no pairwise differences could be identified from *post-hoc* analysis.

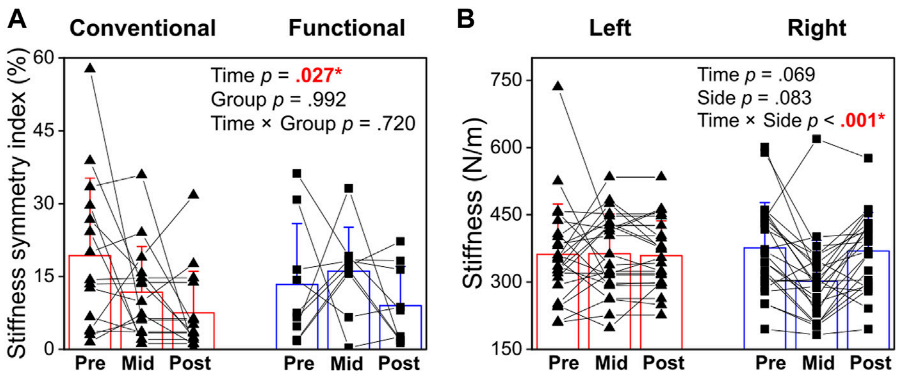

FIGURE 5
(A) Symmetry index of passive muscle stiffness at pre-, mid- and post-intervention in Conventional and Functional training groups. **(B)** Changes in back muscle stiffness over time in left and right back muscles. *Statistical significance (p <0 .05) is shown in red font and indicated by an asterisk.

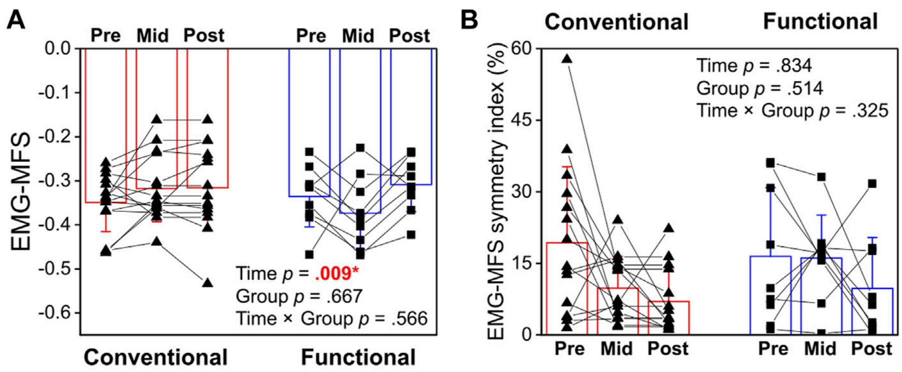

FIGURE 6
(A) Comparison of electromyography median frequency slope (EMG-MFS) between the Conventional and Functional groups at pre-, mid- and post-intervention. **(B)** Changes in symmetry index of EMG-MFS over time between conventional and functional training. *Statistical significance (p <0 .05) is shown in red font and indicated by an asterisk.

TABLE 3 Self-report Pain and Disability Scores (%) measured using the Oswestry Disability Index (ODI).

	All	Functional Group	Conventional Group
Pre-Intervention	4.8 (14.4)	1.1 (2.0)	7.1 (18.0)
Mid-Intervention	4.8 (14.4)	1.1 (2.0)	7.1 (18.0)
Post-Intervention	4.3 (4.9)	7.3 (10.8)	2.4 (5.0)
2-month Follow-up	4.3 (7.8)	6.9 (8.1)	2.8 (7.4)
4-month Follow-up	3.4 (5.4)	6.2 (5.9)	1.7 (4.5)
6-month Follow-up	2.5 (6.6)	4.9 (9.6)	1.1 (3.6)

*All ODI scores were classified in the category of "Minimal functional limitation" (0–20%). Data are expressed as mean (standard deviation).

4 Discussion

This study compared the effectiveness of two strength and conditioning programs, namely functional versus conventional training, that were implemented over 16 weeks in emergency responders. The results did not support our hypothesis that functional training would be superior to conventional training in improving back muscle characteristics and disabilities as there was no difference between groups in any outcome measures. Regardless of the type of exercises prescribed, participants showed improvement in hip extension strength and lumbar extensor fatigability after completing the intervention. Initial left-right imbalance in back muscle stiffness was observed at baseline and the symmetry improved with training. Self-reported pain and disability scores remained low throughout the intervention and 6-month follow-up periods, indicting the high functional ability of the participants.

4.1 Improvement in strength and fatigability

The present study showed that back extension strength improved sharply after 8 weeks of training, but no further gain was observed from mid- to post-intervention tests. These results are in line with the literature that 6–8 weeks of exercise training can induce substantial improvement in strength (Moon et al., 2015; Schoenfeld et al., 2015; Steele et al., 2015; Haun et al., 2019; Tay et al., 2019). Given the relatively short duration of 8 weeks, it is believed that most of the initial strength improvement are of a neurological nature rather than muscle hypertrophy (Balshaw et al., 2017). In recreationally trained males, Steele et al. (2015) reported that back extension strength improved after 6 weeks of training with no difference between single-set (8.3% improvement) and multiple-set (10.7% improvement). The current study on emergency responders showed 20.7% of improvement after 8 weeks of training and this initial gain in strength was maintained for a further 8 weeks with regular physical training. The lack of difference between the Functional and Conventional Groups indicates that both types of training can elicit significant increases back muscle extension strength. In the general population, individuals with chronic LBP demonstrated lower strength in lumbar extension and flexion compared with healthy controls (Vanhauter et al., 2021). Thus, regular resistance training is recommended for emergency responders to improve and maintain their back muscles strength.

Lumbar extensor muscle fatigability improved after 16 weeks of training with no difference between functional or conventional exercises. There are currently no data in the available literature regarding the fatigability of back muscles in emergency responders and hence no direct comparison can be made. Previous studies have reported deficit in lumbar extensor endurance among individuals with chronic LBP compared with healthy controls (Klein et al., 1991; Ashmen et al., 1996). Using isoinertial exercise intervention, researchers reported no change in muscle fatigability after a 12-week lumbar extensor training program (Mannion et al., 2001). For runners with chronic LBP, one study demonstrated improvement in longissimus fatigability after 8 weeks of rehabilitation exercise training (Cai et al., 2017). The authors cautioned that despite statistical differences in EMG-MFS were found, the improvement of 0.046 was too small to overcome the minimal detectable changes (MDC, 95% CI) ranging from 0.11 to 0.17. Similar to the study by Cai and colleagues (2017), the present study also observed statistically significant but small improvement in lumbar extensor muscles EMG-MFS after 16 weeks of training (mean change on 0.049 from pre- to post-intervention). Future studies can further investigate the practical relevance of this small improvement in back muscle fatigability and search for optimal strength and conditioning programs for back injuries prevention in emergency responders.

The lack of difference between functional and conventional training may be due to advantage of multi-joint exercises (e.g., squats, push-ups) that were included in both groups, which may have overshadowed other subtle differences (Iversen et al., 2021). In elite soccer players, Turna and Alp (2020) also found no difference between functional and traditional training in biomotor abilities and physiological characteristics. Another point to note is that the outcome assessments of back extension and fatigability were both performed in a bilaterally symmetrical manner. These tests may not fully capture the possible benefits gained via functional training. It will be of interest to explore if the Functional Group demonstrate any advantage in operational-specific movement tasks in the future. Functional outcome assessment tests can be developed to cater for the occupational needs of emergency responders.

4.2 Left-right symmetry in muscle stiffness

Stiffness of a muscle unit can influence force production (Kalkhoven and Watsford, 2018; Ando and Suzuki, 2019) and injury risk (Bradshaw and Hume, 2012; Pickering Rodriguez et al., 2017; Nin et al., 2021). At baseline, the passive stiffness of the lumbar extensor muscle of the emergency responders was higher in the left side than the right side (Figure 5B). Koppenhaver et al. (2020) reported that lumbar muscle stiffness was associated with self-reported pain and disability, with greater resting stiffness in individuals with LBP than asymptomatic control. In the literature, an optimal range of back muscle stiffness is yet to be established. An increase in muscle stiffness can contribute to more force production (Kalkhoven and Watsford, 2018; Ando and Suzuki, 2019) but previously injured muscles are found to be stiffer than the non-injured muscles (Nin et al., 2021). On the other hand, muscles with too low stiffness and are too compliant may be more prone to soft-tissue related injuries (Bradshaw and Hume, 2012; Pickering Rodriguez et al., 2017). Most participants (over 85%) in the present study were right-handed. Their limb preference (e.g., the arm operating an axe, the way carrying casualties) may be related to the lower stiffness in the right back muscles. Variations of muscle recruitment patterns could be caused by handedness or training (Merletti et al., 1994; Renkawitz et al., 2006). In a study on tennis players with and without LBP, Renkawitz et al. (2006) discovered that almost all right-handed tennis players showed substantially lower muscle activity on the left back muscles while left-handed players showed lower muscle activity on the right side. For individual with LBP, it is conceivable that they execute different movements between the left and right sides to avoid pain (Shamsi et al., 2020).

There are some evidence to suggest that asymmetry in back muscle properties may lead to back pain or disabilities. Parkhurst and Burnett (1994) found that proprioceptive asymmetries were associated with injuries in male firefighters. In older adults, asymmetrical biomechanical properties of paravertebral muscles are also linked to chronic LBP severity (Wu et al., 2022). The present study provided empirical data to illustrate bilateral asymmetry in back muscle stiffness among emergency responders. As the participants engaged in the supervised strength and conditioning intervention programs, the symmetry index of stiffness progressively decreased over time (Figure 5A). The initial left-right imbalance in muscle stiffness observed at baseline no longer existed in the mid- or post-intervention (Figure 5B). While the two programs emphasized either unilateral or bilaterally loaded exercises, both programs loaded the same muscle groups with equal sets and repetitions and therefore the total training volume was similar. The lack of difference in the programs may indicate that engaging in any well-rounded strength and conditioning program is effective for improving back strength and symmetry and superior to the lack of strength training being performed prior to enrolling in the study.

4.3 Self-reported pain and disabilities

The ODI scores were very low among the participants throughout the intervention and 6-month follow-up periods (Table 3). This is expected as our participants were mostly active, frontline firefighters who were physically fit and healthy to perform duties. Since they did not suffer from intense pain or severe functional limitation in the beginning, no improvement in disability measures would be expected. In a study on Iranian EMS personnel, the ODI has decreased from 34.1 to 27.5% (after 1 month) and 19.7% (after 3 months) with ergonomic intervention of patient transfer technique (Yahyaei et al., 2019). In another cross-sectional study on 61 Polish firefighters, the mean ODI was reported as 13.7% and this disability score was not correlated with age (Fiodorenko-Dumas et al., 2018). Compared with the ODI values of emergency responders reported in other countries (13.7–34.1%), the emergency responders in Singapore who participated in our study reported less pain and disabilities associated with their back throughout the entire study duration (mean 2.5–4.8%, Table 3).

4.4 Limitations

There are some limitations to the present study. First, the study plan was severely interrupted by COVID-19 especially during the early stage of the training. The frequent changes and strict restrictions (e.g., closure of gym, group size limitation), coupling with change in work arrangement, resulted in a high drop-out rate in the first few weeks. Given the relatively small sample size of 24 participants, future work on a larger cohort is warranted to confirm the present findings. Second, the compliance rate for supervised training was lower than expected. Out of the 32 planned training sessions, participants only attended 17 (ranging from 9 to 30) sessions on average. On-duty strength training has been promoted as one way to improve health and fitness among emergency responders, with promising positive impact on injury prevention (Griffin et al., 2016). Despite the present study conducted training of the participants' duty days, the compliance rate remained low. This highlighted the challenges of implementing physical training programs in frontline emergency responders who have different work shifts and other priorities. Third, the post-intervention test was conducted around the Ramadan fasting period during which the exercise and diet routines of our Muslim participants were affected. Some participants missed training towards the end. Others delayed the post-intervention tests until after the fasting period. As such, the training effect may not be accurately captured by the post-intervention test results.

5 Conclusion

This study showed that 16 weeks of strength and conditioning training was promising in improving back extension strength, bilateral symmetry in back muscle stiffness, and lumbar extensor muscle fatigability. The training effects were similar between functional exercises (which puts more emphasis on unilateral movements) and conventional exercises (which tends to be more bilateral symmetrical). All self-reported pain and disability scores were very low and fell well within the category of "*minimum functional limitation*" throughout the study. Therefore, we conclude that a structured strength training program targeting all major muscle groups improves back strength, stiffness symmetry and fatigability among firefighters and paramedics. Functional training does not provide superior results to conventional strength training in this interval and cohort of firefighters and paramedics. Future studies can examine if long-term compliance to strength and conditioning programs can improve occupational performance and/or to reduce the risk of injuries in emergency responders.

Data availability statement

The datasets presented in this study can be found in online repositories. The names of the repository/repositories and accession number(s) can be found below: The datasets generated for this study can be found in the NIE Data Repository [https://doi.org/10.25340/R4/CLHRWV].

Ethics statement

The studies involving human participants were reviewed and approved by the Nanyang Technological University Institutional Review Board. The patients/participants provided their written informed consent to participate in this study.

Author contributions

PK, DH and WT contributed to the study conception and design. Material preparation and data collection were performed by TK, RA, JP, HH and HK. Data analysis was performed by JP and PK. The first draft of the manuscript was written by PK and TK. All authors critically reviewed and revised the manuscript. All authors read and approved the final manuscript.

Funding

This study is supported by the Singapore Civil Defence Force (SCDF), Home Team Science and Technology Agency, Ministry of Home Affairs.

Acknowledgments

The authors would like to thank SCDF for providing facilities for exercise training.

Conflict of interest

HH and HK were full-time employees hired under the Singapore Civil Defence Force (SCDF) which funded this research study.

The remaining authors declare that the research was conducted in the absence of any commercial or financial relationships that could be construed as a potential conflict of interest.

Publisher's note

All claims expressed in this article are solely those of the authors and do not necessarily represent those of their affiliated organizations, or those of the publisher, the editors and the reviewers. Any product that may be evaluated in this article, or claim that may be made by its manufacturer, is not guaranteed or endorsed by the publisher.

Supplementary material

The Supplementary Material for this article can be found online at: https://www.frontiersin.org/articles/10.3389/fbioe.2022.918315/full#supplementary-material

References

Abel, M. G., Palmer, T. G., and Trubee, N. (2015). Exercise program design for structural firefighters. *Strength Cond. J.* 37, 8–19. doi:10.1519/SSC.0000000000000123

Aljerian, N., Alshehri, S., Masudi, E., Albawardi, A. M., Alzahrani, F., and Alanazi, R. (2018). The prevalence of musculoskeletal disorders among EMS personnel in Saudi Arabia, Riyadh. *Egypt. J. Hosp. Med.* 73, 5777–5782. doi:10.21608/ejhm.2018.11879

Ando, R., and Suzuki, Y. (2019). Positive relationship between passive muscle stiffness and rapid force production. *Hum. Mov. Sci.* 66, 285–291. doi:10.1016/j.humov.2019.05.002

Ashmen, K. J., Swanik, C. B., and Lephart, S. M. (1996). Strength and flexibility characteristics of athletes with chronic low-back pain. *J. Sport Rehabil.* 5, 275–286. doi:10.1123/jsr.5.4.275

Balshaw, T. G., Fry, A., Maden-Wilkinson, T. M., Kong, P. W., and Folland, J. P. (2017). Reliability of quadriceps surface electromyography measurements is improved by two vs. single site recordings. *Eur. J. Appl. Physiol.* 117, 1085–1094. doi:10.1007/s00421-017-3595-z

Beach, T. A. C., Frost, D. M., McGill, S. M., and Callaghan, J. P. (2014). Physical fitness improvements and occupational low-back loading - an exercise intervention study with firefighters. *Ergonomics* 57, 744–763. doi:10.1080/00140139.2014.897374

Borg, G. (1990). Psychophysical scaling with applications in physical work and the perception of exertion. *Scand. J. Work Environ. Health* 16, 55–58. doi:10.5271/sjweh.1815

Bradshaw, E. J., and Hume, P. A. (2012). Biomechanical approaches to identify and quantify injury mechanisms and risk factors in women's artistic gymnastics. *Sports Biomech.* 11, 324–341. doi:10.1080/14763141.2011.650186

Cai, C., and Kong, P. W. (2015). Low back and lower-limb muscle performance in male and female recreational runners with chronic low back pain. *J. Orthop. Sports Phys. Ther.* 45, 436–443. doi:10.2519/jospt.2015.5460

Cai, C., Yang, Y., and Kong, P. W. (2017). Comparison of lower limb and back exercises for runners with chronic low back pain. *Med. Sci. Sports Exerc.* 49, 2374–2384. doi:10.1249/MSS.0000000000001396

Criswell, E. (2010). *Cram's introduction to surface electromyography*. 2nd ed. Boston, USA: Jones & Bartlett Publishers. Available at: https://books.google.com.sg/books?hl=en&lr=&id=ADYm0TqiDo8C&oi=fnd&pg=PP1&dq=Cram%27s+introduction+ to+surface+electromyography&ots=RxrfKwMq2N&sig=x7SuSJZ-T2tTum92dJ20q FyLqGk#v=onepage&q&f=false.

Damrongsak, M., Prapanjaroensin, A., and Brown, K. C. (2018). Predictors of back pain in firefighters. *Workplace Health Saf.* 66, 61–69. doi:10.1177/2165079917709020

Fairbank, J. C., and Pynsent, P. B. (2000). The Oswestry disability index. *Spine (Phila. Pa. 1976)* 25, 2940–2953. doi:10.1097/00007632-200011150-00017

Feito, Y., Heinrich, K. M., Butcher, S. J., and Carlos Poston, W. S. (2018). High-intensity functional training (Hift): Definition and research implications for improved fitness. *Sports* 6, 76–19. doi:10.3390/sports6030076

Fiodorenko-Dumas, Ż., Kurkowska, A., and Paprocka-Borowicz, M. (2018). Spine pain in the firefighter profession. *Med. Pr.* 69, 365–373. doi:10.13075/mp.5893.00679

Griffin, S. C., Regan, T. L., Harber, P., Lutz, E. A., Hu, C., Peate, W. F., et al. (2016). Evaluation of a fitness intervention for new firefighters: Injury reduction and economic benefits. *Inj. Prev.* 22, 181–188. doi:10.1136/injuryprev-2015-041785

Gupta, S. K. (2011). Intention-to-treat concept: A review. *Perspect. Clin. Res.* 2, 109–112. doi:10.4103/2229-3485.83221

Ham, Y.-L., and Ahn, Y.-H. (2008). A study on low back pain prevalence rate and related factors among emergency medical technicians working at fire stations. *J. Muscle Jt. Heal.* 15, 175–182.

Haun, C. T., Vann, C. G., Mobley, C. B., Osburn, S. C., Mumford, P. W., Roberson, P. A., et al. (2019). Pre-training skeletal muscle fiber size and predominant fiber type best predict hypertrophic responses to 6 weeks of resistance training in previously trained young men. *Front. Physiol.* 10, 297. doi:10.3389/fphys.2019.00297

Imani, A., Borna, J., Alami, A., Khosravan, S., Hasankhani, H., and Bafandeh Zende, M. (2018). Prevalence of low back pain and its related factors among pre-hospital emergency personnel in Iran. *J. Emerg. Pract. Trauma* 5, 8–13. doi:10.15171/jept.2018.01

Iversen, V. M., Norum, M., Schoenfeld, B. J., and Fimland, M. S. (2021). No time to lift? Designing time-efficient training programs for strength and hypertrophy: A narrative review. *Sports Med.* 51, 2079–2095. doi:10.1007/s40279-021-01490-1

Kalkhoven, J. T., and Watsford, M. L. (2018). The relationship between mechanical stiffness and athletic performance markers in sub-elite footballers. *J. Sports Sci.* 36, 1022–1029. doi:10.1080/02640414.2017.1349921

Katsavouni, F., Bebetsos, E., Antoniou, P., Malliou, P., and Beneka, A. (2014). Work-related risk factors for low back pain in firefighters. Is exercise helpful? *Sport Sci. Health* 10, 17–22. doi:10.1007/s11332-013-0167-4

Kim, M. G., and Ahn, Y.-S. (2021). Associations between lower back pain and job types in South Korean male firefighters. *Int. J. Occup. Saf. Ergon.* 27, 570–577. doi:10.1080/10803548.2019.1608061

Kim, M. G., Seo, J., Kim, K., and Ahn, Y.-S. (2017). Nationwide firefighter survey: The prevalence of lower back pain and its related psychological factors among Korean firefighters. *Int. J. Occup. Saf. Ergon.* 23, 447–456. doi:10.1080/10803548.2016.1219149

Klein, A. B., Snyder-Mackler, L., Roy, S. H., and DeLuca, C. J. (1991). Comparison of spinal mobility and isometric trunk extensor forces with electromyographic spectral analysis in identifying low back pain. *Phys. Ther.* 71, 445–454. doi:10.1093/ptj/71.6.445

Kong, P. W., Beauchamp, G., Suyama, J., and Hostler, D. (2010). Effect of fatigue and hypohydration on gait characteristics during treadmill exercise in the heat while wearing firefighter thermal protective clothing. *Gait Posture* 31, 284–288. doi:10.1016/j.gaitpost.2009.11.006

Kong, P. W., Chua, Y. H., Kawabata, M., Burns, S. F., and Cai, C. (2018). Effect of post-exercise massage on passive muscle stiffness measured using myotonometry - a double-blind study. *J. Sports Sci. Med.* 17, 599–606. Available at: http://www.ncbi.nlm.nih.gov/pubmed/30479528.

Koppenhaver, S., Gaffney, E., Oates, A., Eberle, L., Young, B., Hebert, J., et al. (2020). Lumbar muscle stiffness is different in individuals with low back pain than asymptomatic controls and is associated with pain and disability, but not common physical examination findings. *Musculoskelet. Sci. Pract.* 45, 102078. doi:10.1016/j.msksp.2019.102078

Mannion, A. F., Taimela, S., Müntener, M., and Dvorak, J. (2001). Active therapy for chronic low back pain: Part 1. Effects on back muscle activation, fatigability, and strength. *Spine* 26, 897–908. doi:10.1097/00007632-200104150-00013

Marín-Jiménez, N., Acosta-Manzano, P., Borges-Cosic, M., Baena-García, L., Coll-Risco, I., Romero-Gallardo, L., et al. (2019). Association of self-reported physical fitness with pain during pregnancy: The GESTAFIT Project. *Scand. J. Med. Sci. Sports* 29, 1022–1030. doi:10.1111/sms.13426

Merletti, R., De Luca, C. J., and Sathyan, D. (1994). Electrically evoked myoelectric signals in back muscles: Effect of side dominance. *J. Appl. Physiol. (1985)* 77, 2104–2114. doi:10.1152/jappl.1994.77.5.2104

Montedori, A., Bonacini, M. I., Casazza, G., Luchetta, M. L., Duca, P., Cozzolino, F., et al. (2011). Modified versus standard intention-to-treat reporting: Are there differences in methodological quality, sponsorship, and findings in randomized trials? A cross-sectional study. *Trials* 12, 58. doi:10.1186/1745-6215-12-58

Moon, T.-Y., Kim, J.-H., Gwon, H.-J., Hwan, B.-S., Kim, G.-Y., Smith, N., et al. (2015). Effects of exercise therapy on muscular strength in firefighters with back pain. *J. Phys. Ther. Sci.* 27, 581–583. doi:10.1589/jpts.27.581

Nazari, G., MacDermid, J., and Cramm, H. (2020b). Prevalence of musculoskeletal disorders among Canadian firefighters: A systematic review and meta-analysis. *J. Mil. Veteran Fam. Health* 6, 83–97. doi:10.3138/jmvfh-2019-0024

Nazari, G., MacDermid, J. C., Sinden, K., and D'Amico, R. (2020a). Prevalence of musculoskeletal symptoms among Canadian firefighters. *Work* 67, 185–191. doi:10.3233/WOR-203264

Negm, A., MacDermid, J., Sinden, K., D'Amico, R., Lomotan, M., and MacIntyre, N. J. (2017). Prevalence and distribution of musculoskeletal disorders in firefighters are influenced by age and length of service. *J. Mil. Veteran Fam. Health* 3, 33–41. doi:10.3138/jmvfh.2017-0002

Nin, D. Z., Pain, M. T. G., Lim, Y. H., and Kong, P. W. (2021). Hamstring muscle architecture and viscoelastic properties: Reliability and retrospective comparison between previously injured and uninjured athletes. *J. Mech. Med. Biol.* 21, 2150007. doi:10.1142/S021951942150007X

Parkhurst, T. M., and Burnett, C. N. (1994). Injury and proprioception in the lower back. *J. Orthop. Sports Phys. Ther.* 19, 282–295. doi:10.2519/jospt.1994.19.5.282

Pelozato de Oliveira, D. I., de Souza Teixeira, B. M., de Macedo, O. G., dos Santos, V., Grossi Porto, L. G., and Rodrigues Martins, W. (2021). Prevalence of chronic lower back pain in Brazilian military firefighters. *Int. J. Occup. Saf. Ergon.* 28, 1699–1704. doi:10.1080/10803548.2021.1929699

Pickering Rodriguez, E. C., Watsford, M. L., Bower, R. G., and Murphy, A. J. (2017). The relationship between lower body stiffness and injury incidence in female netballers. *Sports Biomech.* 16, 361–373. doi:10.1080/14763141.2017.1319970

Poston, W. S. C., Haddock, C. K., Batchelor, C. D. B., Jahnke, S. A., Jitnarin, N., and Batchelor, D. B. (2016). Is high-intensity functional training (HIFT)/crossfit safe for military fitness training? *Mil. Med.* 181, 627–637. doi:10.7205/MILMED-D-15-00273

Renkawitz, T., Boluki, D., and Grifka, J. (2006). The association of low back pain, neuromuscular imbalance, and trunk extension strength in athletes. *Spine J.* 6, 673–683. doi:10.1016/j.spinee.2006.03.012

Schoenfeld, B. J., Peterson, M. D., Ogborn, D., Contreras, B., and Sonmez, G. T. (2015). Effects of low- vs. High-load resistance training on muscle strength and hypertrophy in well-trained men. *J. Strength Cond. Res.* 29, 2954–2963. doi:10.1519/JSC.0000000000000958

Shamsi, M., Mirzaei, M., and HamediRad, M. (2020). Comparison of muscle activation imbalance following core stability or general exercises in nonspecific low back pain: A quasi-randomized controlled trial. *BMC Sports Sci. Med. Rehabil.* 12, 24. doi:10.1186/s13102-020-00173-0

Stassin, N., Games, K. E., and Winkelmann, Z. K. (2021). The relationship between fear avoidance beliefs and low back pain in firefighters. *Athl. Train. Sports Health Care* 13, 18–24. doi:10.3928/19425864-20190724-01

Steele, J., Fitzpatrick, A., Bruce-Low, S., and Fisher, J. (2015). The effects of set volume during isolated lumbar extension resistance training in recreationally trained males. *PeerJ* 3, e878. doi:10.7717/peerj.878

Tay, Z. M., Lin, W.-H., Kee, Y. H., and Kong, P. W. (2019). Trampoline versus resistance training in young adults: Effects on knee muscles strength and balance. *Res. Q. Exerc. Sport* 90, 452–460. doi:10.1080/02701367.2019.1616045

Turna, B., and Alp, M. (2020). The effects of functional training on some biomotor abilities and physiological characteristics in elite soccer players. *J. Educ. Learn.* 9, 164. doi:10.5539/jel.v9n1p164

Vanhauter, N., Van Erck, A., Anciaux, M., Pollefliet, A., and Joos, E. (2021). Isometric and isokinetic muscle strength measurements of the lumbar flexors and extensors with BioniX Sim3 pro in patients with chronic low back pain: A pilot study. *J. Back Musculoskelet. Rehabil.* 34, 381–388. doi:10.3233/BMR-200225

Wu, Z., Ye, X., Ye, Z., Hong, K., Chen, Z., Wang, Y., et al. (2022). Asymmetric biomechanical properties of the paravertebral muscle in elderly patients with unilateral chronic low back pain: A preliminary study. *Front. Bioeng. Biotechnol.* 10, 814099–814111. doi:10.3389/fbioe.2022.814099

Yahyaei, K., Yazdi, K., Kolagari, S., and Rahmani, H. (2019). Effect of patient transfer training on low back pain in pre-hospital emergency medical services personnel. *jcbr.* 3, 31–36. doi:10.29252/jcbr.3.4.31

TYPE Original Research
PUBLISHED 16 September 2022
DOI 10.3389/fbioe.2022.974724

Check for updates

OPEN ACCESS

EDITED BY
Qichang Mei,
Ningbo University, China

REVIEWED BY
Feza Korkusuz,
Hacettepe University, Turkey
Bård Bogen,
Western Norway University of Applied Sciences, Norway

*CORRESPONDENCE
Shaobai Wang,
wangs@innomotion.biz
Weidong Xu,
xuwdshanghai@126.com

†These authors contributed equally to this work and share first authorship

SPECIALTY SECTION
This article was submitted to Biomechanics, a section of the journal Frontiers in Bioengineering and Biotechnology

RECEIVED 21 June 2022
ACCEPTED 01 September 2022
PUBLISHED 16 September 2022

CITATION
Zhou L, Xu Y, Zhang J, Guo L, Zhou T, Wang S and Xu W (2022), Multiplanar knee kinematics-based test battery helpfully guide return-to-sports decision-making after anterior cruciate ligament reconstruction.
Front. Bioeng. Biotechnol. 10:974724.
doi: 10.3389/fbioe.2022.974724

Multiplanar knee kinematics-based test battery helpfully guide return-to-sports decision-making after anterior cruciate ligament reconstruction

Lan Zhou[1†], Yihong Xu[2†], Jing Zhang[1], Luqi Guo[1], Tianping Zhou[2], Shaobai Wang[1*] and Weidong Xu[2*]

[1]Key Laboratory of Exercise and Health Sciences of Ministry of Education, Shanghai University of Sport, Shanghai, China, [2]Department of Orthopedics, Changhai Hospital, The Navy Medical University, Shanghai, China

Background: There are currently no well-established criteria to guide return to sports (RTS) after anterior cruciate ligament reconstruction (ACLR). In this study, a new test battery consisting of subjective and objective tests, especially multiplanar knee kinematics assessment, was developed to aid RTS decision making after ACLR.

Methods: This study was conducted with 30 patients who were assessed a mean of 9.2 $\pm$ 0.5 months after ACLR. All patients underwent complete evaluations of both lower limbs with four objective assessments [isokinetic, hop, knee laxity, and 6−degree of freedom (6DOF, angle: flexion-extension, varus-valgus, internal-external rotation; translation: anteroposterior, proximodistal, mediolateral) knee kinematics tests] and two subjective assessments [International Knee Documentation Committee (IKDC) and Anterior Cruciate Ligament Return to Sport after Injury (ACL-RSI) questionnaires]. Limb symmetry indices (LSIs) of knee strength, hop distance, and range of motion (ROM) of knee kinematics were calculated. LSI ≥90%, IKDC scale score within the 15th percentile for healthy adults, and ACL-RSI score >56 were defined as RTS criteria.

Results: Significant differences between affected and contralateral knees were observed in the quadriceps strength ($p < 0.001$), hamstring strength ($p = 0.001$), single hop distance ($p < 0.001$), triple hop distance ($p < 0.001$), and rotational ROM ($p = 0.01$). Only four patients fulfilled the overall RTS criteria. The percentages of patients fulfilling individual criteria were: quadriceps strength, 40%; hamstring strength, 40%; single hop distance, 30%; triple hop distance, 36.7%; knee ligament laxity, 80%; flexion-extension, 23.3%; varus-valgus rotation, 20%; internal-external rotation, 66.7%; anteroposterior translation, 20%; proximodistal translation, 33.3%; mediolateral translation, 26.7%; IKDC scale score, 53.3%; and ACL-RSI score, 33.3%.

Conclusion: At an average of 9 months after ACLR, objectively and subjectively measured knee functional performance was generally unsatisfactory especially the recovery of knee kinematics, which is an important prerequisite for RTS.

KEYWORDS

return to sport, anterior cruciate ligament reconstruction, kinematics, hop test, isokinetic test

Introduction

The return to sports (RTS) after anterior cruciate ligament reconstruction (ACLR) has been focus of recent research. However, the timing of safe RTS after ACLR remains unclear. Inappropriate RTS may result in delayed recovery, reinjury and accelerated joint degeneration. A systematic review showed that only 63% of individuals returned to sports at pre-injury levels after ACLR (Webster and Feller, 2019). Among young people, the reinjury rate following postoperative RTS is as high as 35% (Webster and Feller, 2016). Thus, the development of criteria to guide RTS decision making is essential. Consensus has been reached that an extensive test battery including objective physical evaluation is needed for this purpose (Meredith et al., 2020).

Factors influenced RTS after ACLR include, deficits in knee strength and lower-limb neuromuscular control (Barber-Westin and Noyes, 2011; Thomee et al., 2011), psychological factors such as fear of reinjury (Sonesson et al., 2017), and patient-reported outcomes (PROs) (Logerstedt et al., 2014). Based on these risk factors, series of tests and criteria to determine the RTS have been used in recent studies. They include hop tests (Hildebrandt et al., 2015), strength tests (Thomee et al., 2011), use of the jump landing and landing error scoring systems (Gokeler et al., 2017), and psychological readiness assessments (McPherson et al., 2019). At present, the test battery used to evaluate patient RTS after ACLR is still under continuous improvement and on the way to satisfaction.

Recently, in addition to the quantity of movements after ACLR, the quality of movements is of increasing concern when it comes to RTS after ACLR. Several studies have reported persistent kinematic deficits after ACLR, which may cause many adverse effects on patients (Di Stasi et al., 2013; Meredith et al., 2020). A systematic review of 90 studies showed that such knee kinematic asymmetry (e.g., of knee flexion) was a risk factor for post-ACLR reinjury and may contribute to the failure of RTS (van Melick et al., 2016). In addition, biomechanical gait asymmetry after RTS is implicated in the development of osteoarthritis, which has been identified in more than half of patients at 20 years after ACLR (Andriacchi et al., 2004; Cinque et al., 2018). To our knowledge, only a few studies focused on the kinematics of a single plane and no study conducted the assessment of multiplanar knee kinematics when considering the RTS after ACLR currently.

Thus, we developed a new test battery consisted of four objective assessments [isokinetic, hop, knee ligament laxity, and 6–degree of freedom (6DOF, angle: flexion-extension, varus-valgus, internal-external rotation; translation: anteroposterior, proximodistal, mediolateral) kinematics tests] and two subjective assessments [the International Knee Documentation Committee (IKDC) and Anterior Cruciate Ligament Return to Sport after Injury (ACL-RSI) PRO questionnaires]. The limb symmetry index (LSI), by which muscle strength, hop distance, and affected knee kinematics are expressed as percentages of contralateral limb values, is usually used to evaluate knee function recovery after ACLR (Teichtahl et al., 2009; Arhos et al., 2021). In current study, we aimed to use this test battery to identify post-ACLR knee functional deficits after ACLR and explore the importance of multiplanar knee kinematics on RTS decision-making.

Materials and methods

Participants

Patients who underwent ACLR in the XXXX hospital and met the inclusion criteria were enrolled in this study. The inclusion criteria were: 1) age 18–40 years; 2) regular participation in sports involving jumping, contact, or pivoting (>50 h/year) (Zarzycki et al., 2018); 3) completeness of required data and voluntary participation; and 4) no previous history of

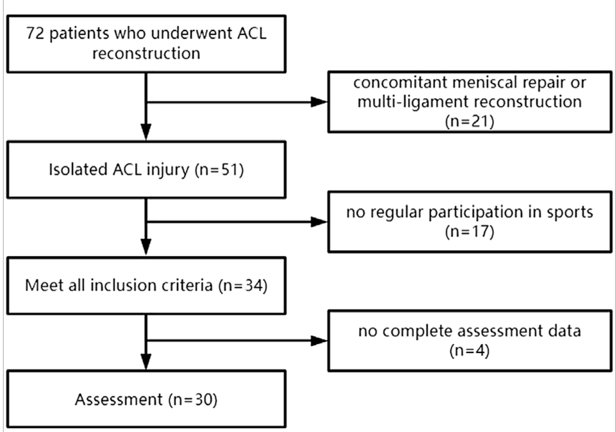

FIGURE 1
Flow charm of the participants enrollment.

knee injury. The exclusion criteria were: 1) with meniscus repair or multi-ligament reconstruction and 2) development of postoperative complications, including joint fibrosis, pain, effusion, and infection.

From May 2020 to June 2021, of the 72 patients who underwent ACLR, 21 were excluded due to concomitant meniscal repair or multi-ligament reconstruction, and 17 were excluded because of age or having no regular participation in sports. Of the remaining 34 patients, four were excluded because they did not have complete assessment data. Hence, eventually 30 patients were included in the study (Figure 1). All patients will be clinically examined by our physicians prior to testing. The Institutional Review Board approved the study (NO.102772021RT134) and all patients provided written informed consent.

Surgical procedure and rehabilitation

An experienced orthopedic surgeon performed all surgeries. During the surgery, the hamstring tendons or synthetic grafts were chosen which were up to the patients to decide. Tunnels were drilled at the tibial and femoral footprints of the ACL using an anteromedial approach. The residual tissues on both sides were preserved. The femoral and tibial ends of the hamstring tendons autografts were fixed with endobuton and intrafix screws, respectively. The range of motion (ROM), graft tension, and possible graft impact were examined under arthroscopy. After surgery, all patients completed a standard postoperative rehabilitation protocol, which focused on the achievement of full knee-extension ROM immediately and knee flexion as tolerated, progression of functional activities, and quadriceps strengthening. Specifically, in the first 2 weeks, patients were encouraged to reduce pain and swelling with ice, elevation, compression and proper rest and passive/active knee flexion and extension to restore knee ROM. In the 3–5 weeks, stairs up and down and neuromuscular training were added. At 12 weeks, patients were allowed to perform running activities and focused on muscle strengthening. All patients were followed up in outpatient clinic 2 weeks, 1 month, 3 months and 6 months after surgery to provide rehabilitation guideline and the test battery was performed 9 months postoperatively. The decision of returning to specific sport was made by the treating surgeon and the physical therapist.

Subjective RTS assessments

Nine months postoperatively, patients were asked to completed all the assessments. The IKDC scale, considered to be an important measure of successful outcomes after ACLR (Logerstedt et al., 2014), and the ACL-RSI scale were administered to the study participants. The 12-item ACL-RSI scale is used to evaluate the psychological influence (patients' emotions, confidence in performance, and risk appraisal) of the RTS after ACL (Webster et al., 2008; Sonesson et al., 2017) and has been proven to be a reliable and effective tool for this purpose (Jia et al., 2018). As an RTS criterion, IKDC scale scores within the 15th percentile for normal age- and sex-matched individuals were chosen (Logerstedt et al., 2014). A critical score of 56 points of ACL-RSI scale was used, which could distinguish the difference in psychological readiness between athletes who return to sport after ACLR and those who did not (Ardern et al., 2013).

Objective RTS assessments

Two experienced rehabilitation therapists conducted the objective assessments (isokinetic, hop, knee laxity, and 6-DOF kinematics tests) in the same laboratory. Quadricep and hamstring strength was measured using an isokinetic dynamometer (Con-Trex® MJ; CMV AG, Dubendorf, Switzerland) and a standard protocol that has been proven to be highly reliable [intraclass correlation coefficient (ICC) > 0.96] (Maffiuletti et al., 2007). All subjects performed three exercises to familiarize them with this task. One set of five isokinetic muscle strength tests was performed at 60°/s. The contralateral knee was assessed first, followed by the affected knee. The mean isokinetic peak torque (Nm) was calculated and normalized to the body weight (Nm/kg). The LSI was calculated as (affected limb value/contralateral limb value) × 100% (Arhos et al., 2021).

Knee laxity was evaluated using a Ligs Digital Arthrometer (Innomotion Inc, Shanghai, China), which was proved with excellent reliability (Chen et al., 2022). The patients placed the knee joint under the direction of the tester. The instrument was then adjusted to increase the forward force slowly from 10 to 133 N. The system recorded the loading force and displacement in real time. ACL injury was suspected when the difference in joint displacement between knees exceeded 3 mm (Arneja and Leith, 2009).

The single-hop (SH) and triple-hop (TH) tests for distance (cm) were performed, in that order, according to the method described by Alexandre et al. (Rambaud et al., 2017). The best distance for each leg from three trials was recorded. The difference between the affected and contralateral limbs was calculated and presented as a percentage (Rambaud et al., 2017). With reference to previous findings (ICC, 0.84–0.92), we considered LSIs >90% for these tests to reliably reflect good recovery (Reid et al., 2007).

The 6DOF knee kinematics test was performed using a marker-based motion analysis system (Opti-Knee®, Innomotion Inc, Shanghai, China). The system is based on

TABLE 1 Participant characteristics.

	Patients
Sex: male/female, n	26/4
Injured knee: left/right, n	12/18
Graft type: HT/SG, n	27/3
Age, y	27.8 ± 5.9
Height, cm	178.7 ± 7.4
Weight, kg	78.2 ± 13.9
BMI, kg/m^2	24.3 ± 3.4
Time post-surgery, m	9.2 ± 0.5
IKDC score	81.4 ± 10.6
ACL-RSI score	50.5 ± 9.8

HT, hamstring tendon graft; SG, synthetic graft; BMI, body mass index; IKDC, international.
Knee Documentation Committee Subjective Knee Evaluation Form; ACL-RSI, Anterior Cruciate Ligament-Return to Sport After Injury Scale.

surgical navigation technology, with an integrated two-head stereo-infrared camera at a frequency of 60 Hz. The total space requirement of the system and test area is about 10 m^2. During the test, two rigid bodies, each composed of four infrared light reflection markers (OK_Marquer, Innomotion) were connected to each participant's thigh and shin with bandages. This system was used to obtain a 6-DOF kinematic curve of the tibia relative to the femur in real time during treadmill walking (5 km/h) (Tian et al., 2020), reflecting rotation in three directions [flexion (+)-extension (-), valgus (+)-varus (-), and external (+)-external (-) rotation] around the *x*, *y*, and *z* axes of the knee's local coordinate system and displacement [(anterior (+)-posterior (-), lateral (+)-medial (-), and proximal (+)-distal (-)] along these axes. The repeatability of measures obtained with this system has been demonstrated, with tolerances within 1.3 mm translation and 0.9° rotation (Zhang et al., 2015). To assess the symmetry of kinematics between limbs, maximum and minimum values were calculated, and eventually obtained the ROM. To better reflect the knee stability and symmetry, we took the ratio of the smaller value and larger value between two sides of limbs as the LSI. Asymmetry values ≤10% were considered to reflect satisfactory recovery after ACLR (Teichtahl et al., 2009; Arhos et al., 2021).

The RTS test battery is thus used to evaluate fulfillment of the following criteria:

1. IKDC score within the 15th percentile for normal age- and sex-matched subjects (Logerstedt et al., 2014).
2. ACL-RSI score >56 (Ardern et al., 2013).
3. LSI ≥90% peak torque for quadriceps and hamstring strength at 60°/s (Thomee et al., 2011).
4. LSI ≥90% for SH and TH tests (Thomee et al., 2011).
5. Bilateral displacement difference <3 mm (Arneja and Leith, 2009).
6. Difference in ROM between limbs ≤10% in the 6-DOF knee kinematics test (Teichtahl et al., 2009; Arhos et al., 2021)

Statistical analysis

Continuous and quantitative data are expressed as means ± standard deviations. The Shapiro–Wilk test was used to assess the normality of data distribution. Differences in function between affected and contralateral limbs were analyzed using the paired *t* test or Wilcoxon test, depending on the data distribution. All statistical analyses were conducted using SPSS version 20 (IBM Corporation, Armonk, NY, United States). p values <0.05 were considered to be significant.

Results

Sample characteristics and subjective assessment outcomes

30 patients (26 men, four women) with a mean age of 27.7 ± 5.9 years were included in the study. The mean postoperative time was 9.2 ± 0.5 months. Detailed information, including the body mass index and graft type, are provided in Table 1. The average IKDC and ACL-RSI scale scores were 81.4 ± 10.6 and 50.5 ± 9.8, respectively.

Objective assessment outcomes

Significant differences between affected and contralateral limbs were observed in the quadriceps strength ($p < 0.001$), hamstring strength ($p = 0.001$), SH distance ($p < 0.001$), and TH distance ($p < 0.001$) at 9 months after ACLR. Affected limbs had smaller rotational angles than did contralateral limbs ($p = 0.01$; Table 2); no significant difference in other kinematic parameters was observed. The mean kinematics LSIs did not exceed 80%, except for that for the flexion angle ROM (Table 3).

Rates of criterion fulfillment

Four (13.33%) patients fulfilled the criteria of the test protocol. Twelve patients fulfilled the quadriceps and hamstring strength criteria, nine patients fulfilled the SH criterion, 11 patients fulfilled the TH criterion, and 24 patients fulfilled the knee laxity criterion. Twenty, 7, six patients fulfilled the flexion-extension, varus-valgus, and internal-external rotation ROM criterion. Six, 10, and eight patients, respectively, fulfilled the anterior-posterior, proximal-distal, medial-lateral translation ROM criterion. Sixteen patients fulfilled the IKDC scale score criterion and 10 patients fulfilled

TABLE 2 Functional parameters outcomes[a].

	Affected limb	Contralateral limb	LSI	*p* Value
Functional tests				
Extensor strength, Nm/kg	1.5 ± 0.5	1.8 ± 0.6	82.9 ± 20.9	<0.001*
Flexor strength, Nm/kg	0.9 ± 0.3	1.1 ± 0.3	85.9 ± 24.1	0.001*
SH, cm	126.2 ± 15.8	145.2 ± 12.7	86.8 ± 6.7	<0.001*
TH, cm	397.3 ± 63.7	460.5 ± 48.2	86.1 ± 8.3	<0.001*
Laxity, mm	16.5 ± 3.0	15.8 ± 3.1	—	0.184

[a]Data are expressed as mean ± standard deviation; LSI: limb symmetry index; SH: single-hop test; TH: triple-hop test; *Statistically significant difference ($p < 0.05$).

TABLE 3 Knee kinematics outcomes.

Knee kinematics	LSI
F-E, °	91.7 ± 6.5
IR-ER, °	77.6 ± 12.4
VR-VL, °	73.2 ± 16.4
A-P, mm	69.7 ± 15.5
P-D, mm	76.0 ± 22.3
M-L, mm	73.8 ± 16.9

LSI, limb symmetry index; F-E, flexion-extension; IR-ER, internal-external rotation. VR-VL, varus-valgus; A-P, anterior-posterior translation; M-L, medial-lateral translation; P-D, proximal-distal translation.

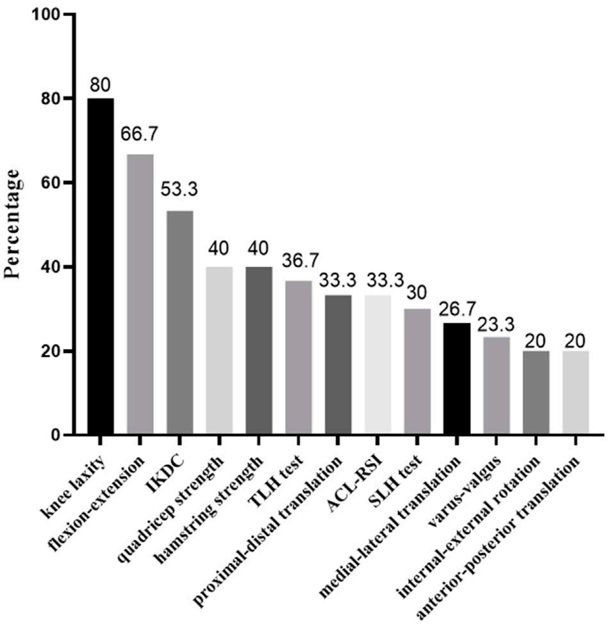

FIGURE 2
Percentages of participants fulfilling the tests criteria, ranked from high to low.

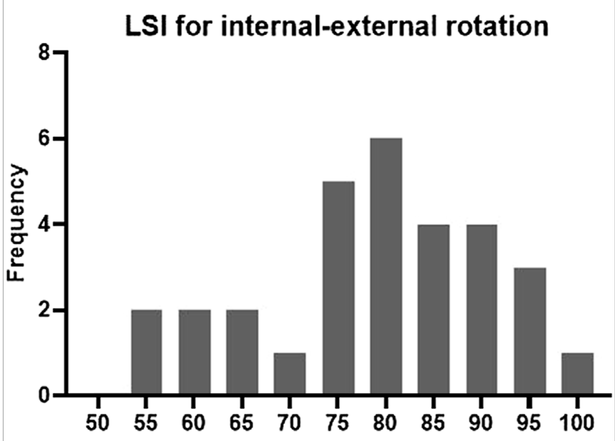

FIGURE 3
Frequency distribution of internal-external rotation LSIs.

the ACL-RSI scale score criterion (Figure 2). Representative examples of the frequency distributions of the LSIs for the internal-external rotation and flexion-extension angle are presented in Figure 3 and Figure 4, respectively.

Discussion

This study found that only 4 (13.3%) of 30 patients fulfilled RTS criteria of the new test battery at approximately 9 months after ACLR, which means further targeted rehabilitation is needed in the future. Notably, only 6 (20%) patients had 6-DOF knee kinematics deficits ≤10%, which implied that knee kinematics may play an important role in indicating the recovery of knee function and RTS.

The low pass rate for the new test battery is similar with previously reported rates for the meeting of strict RTS standards (Thomeé et al., 2012; Gokeler et al., 2017; Raoul et al., 2019). Gokeler et al. (2017) reported that 2 (7.1%) of 28 patients 8 months postoperatively fulfilled all criteria of a test battery consisting of three strength tests, three hop tests, and the Landing

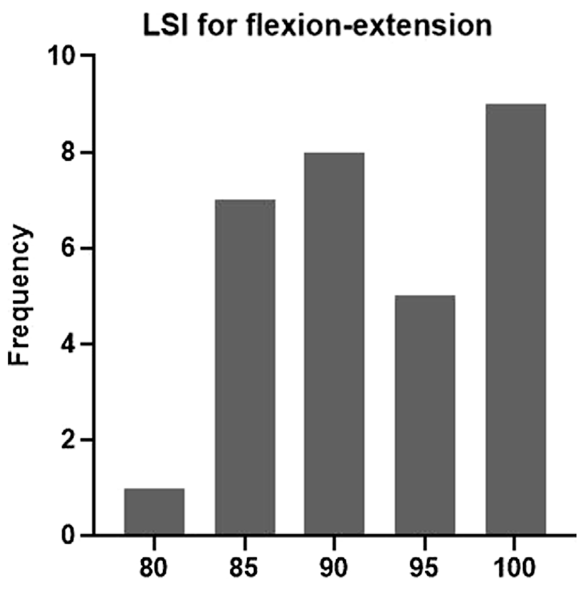

FIGURE 4
Frequency distribution of flexion-extension angle LSIs.

Error Scoring System test. Raoul et al. (2019) used a test battery consisting of isokinetic, hop tests and ACL-RSI scale to evaluate the function recovery of patients after ACLR. As a result, only 44 (18.5%) of 234 patients had satisfactory function. The battery developed in this study features the addition of multiplanar kinematic tests. The mean LSI for 6-DOF knee kinematics during running was low, despite good knee laxity and muscle strength symmetry, in our sample, consistent with previous authors' statements that RTS evaluations after ACLR should focus not only on the quantity, but also the quality, of movement (Kaplan and Witvrouw, 2019; Meredith et al., 2020).

Multiplanar kinematics testing has attracted increasing attention. Asymmetrical kinematics during dynamic movement after ACLR have been observed in several studies. Persistent kinematic abnormalities have been found to be related closely to short-term ACL reinjury after the RTS and long-term osteoarthritis development (Andriacchi et al., 2004; Hewett et al., 2005). Few studies, however, have involved multiplanar kinematics evaluations as part of RTS test batteries. Di Stasi et al. (2013) reported that patients with superior functional outcomes 6 months after ACLR had less asymmetrical gait patterns in the sagittal plane. Similarly, Palmieri-Smith et al. (Palmieri-Smith and Lepley, 2015) observed that patients with less quadriceps strength had greater movement asymmetries in the sagittal plane. In the transverse plane, increased external tibial rotation is related directly to the alteration of the peak contact pressure in the patellofemoral joint (Li et al., 2004). The restoration of knee kinematics after ligament reconstruction may be necessary to protect the knee from abnormal loading (Yoo et al., 2005). In the frontal plane, Mark et al. (Paterno et al., 2010) found that increased valgus deformity during dynamic movement after ACLR is predictor of ACL reinjury after the RTS in athletes. However, kinematic tests have not been successfully implemented routinely in daily clinical practice currently. The test battery used in this study for RTS decision making is clinically practical because it requires little space and takes little time (about 45 min), and is a convenient means of quantifying performance.

RTS decision making based only on the postoperative time is not recommended; and objective measures are considered to be essential (Meredith et al., 2020). Grindem et al. (2016) reported that the post-RTS reinjury rate was 20% higher among patients with quadriceps symmetry indices <90% than among those with indices >90%. Undheim et al. (2015) suggested that isokinetic strength evaluation following ACLR was an important factor when considering an athlete's readiness for the RTS. Müller et al. (2014) showed that the SH test is one of the strongest predictors of the return to recreational sports activities at 6 months after ACLR. The hop test is generally used to determine the neuromuscular control ability in the knee joint. Abundant evidence shows that such control during sports is poor after ACLR (Hewett et al., 2005). Neuromuscular control is essential to keep the knee joint stable during dynamic activities, and deficiencies may lead to the exertion of greater stress on the passive joint structures (e.g., ligaments and joint capsule), eventually increasing the risk of ACL reinjury. In this study, the mean LSIs for quadriceps strength and SH distance were 82.9 and 86.8%, respectively, but only 40% of patients reached the 90% thresholds for these criteria, reinforcing the importance of LSI thresholds. Ardern et al. (2011) reported patients with SH distance LSIs >85% were more likely to return to pre-injury sports levels. The reason for using 90% LSI in this study was that the participants participated in sports involving jumping, contact, or pivoting regularly before injury and they expected to return to the same type of preinjury sport. It is recommended at least 90% LSI for the affected limb knee when considering RTS (Thomee et al., 2011).

The average IKDC scale score in this study was 81.4, and 15 (50%) patients did not fulfill the criteria recommended for this score by previous researchers (Logerstedt et al., 2014). Low IKDC scale scores can indicate the failure of a series of functional performance RTS tests, including the quadriceps strength and SH tests (Logerstedt et al., 2014). In addition, 20 of 30 patients in this study did not achieve the threshold ACL-RSI scale score of 56 (mean, 50.5). Ardern et al. (2013) found that ACL-RSI scale scores <56 were associated with the failure of RTS. Psychological factors have been shown to influence the RTS after ACLR significantly (Müller et al., 2014; Sonesson et al., 2017; McPherson et al., 2019). Various ACL-RSI scale score cut-offs have been used in different studies, which may be related to differences in subjects' ages, activity levels, and occupations.

Based on the multiplanar knee kinematics test and other subjective and objective tests results obtained at 9 months after ACLR in this study, suggestions for future rehabilitation and training programs can be offered. For patients, objective test results provide motivation for further rehabilitation, which is very important to reduce the risk of premature RTS. Objective test results may also help enhance patients' psychological readiness for the RTS.

Functional test remains an important part of RTS consideration after ACLR, and should include the subjective and objective measurement of a series of specific skill. Inadequate RTS tests may not identify residual biological, functional and psychological deficits, which may result in an increased risk of secondary ACL injury when allowing athletes to RTS after ACLR. The ideal test battery content and which tests should be prioritized over others also need to be determined.

Some limitations of the current study should be noted. Firstly, the accuracy of the test battery in the current study in predicting RTS or re-injury after RTS has not been validated. But the primary purpose of this paper was to initiate a new test battery especially adding the multiplanar knee kinematics and highlight the important role of multiplanar knee kinematics in decision-making for RTS after ACLR. Secondly, the participants in this study involved both males and females, and the ligament types included hamstring tendon autograft and synthetic graft, these variables may affect the study results. However, we additionally analyzed the male group and the hamstring tendon autograft group, the trend of the results and the conclusion were consistent with the overall group. In following study, we will continue to include more patients to allow us to perform subgroup analyses. Thirdly, the test battery may be not multifactorial enough to assess safe RTS as it is not clear which components of movement, such as strength, endurance, balance, proprioception are needed individually and in combination to achieve the best effectiveness of safe RTS currently.

Conclusion

At an average of 9 months after ACLR, only four of 30 patients fulfilled all criteria of the new test battery and only 6 (20%) patients had 6-DOF knee kinematics deficits ≤10%. The knee functional performance especially multiplanar knee kinematics were generally unsatisfactory. Further targeted rehabilitation is needed to release patients to RTS, and knee kinematics may play an important role in indicating the recovery of knee function and RTS.

Data availability statement

The original contributions presented in the study are included in the article/Supplementary Material, further inquiries can be directed to the corresponding authors.

Ethics statement

The studies involving human participants were reviewed and approved by the Institutional Review Board of Shanghai University of Sports (NO. 102772021RT134). The patients/participants provided their written informed consent to participate in this study.

Author contributions

Conceptualization: WX, LZ, and SW; Methodology: LZ, LG, JZ, TZ, and YX; Formal analysis and investigation: LZ, LG, JZ, TZ, and YX; Writing—original draft preparation: LZ and YX; Writing—review and editing: LZ, SW, and WX; Funding acquisition: YX and WX; Resources: SW and WX; Supervision: SW and WX.

Funding

The research was funded by "234 discipline peak climbing plan" Program of Changhai Hospital (2020YXK002) and Shanghai Sports Science and Technology "preparation for tackling key problems" Program of Shanghai Sports Bureau (20J017).

Conflict of interest

The authors declare that the research was conducted in the absence of any commercial or financial relationships that could be construed as a potential conflict of interest.

Supplementary material

The Supplementary Material for this article can be found online at: https://www.frontiersin.org/articles/10.3389/fbioe.2022.974724/full#supplementary-material

References

Andriacchi, T. P., Mündermann, A., Smith, R. L., Alexander, E. J., Dyrby, C. O., and Koo, S. (2004). A framework for the *in vivo* pathomechanics of osteoarthritis at the knee. *Ann. Biomed. Eng.* 32 (3), 447–457. doi:10.1023/b:abme.0000017541.82498.37

Ardern, C. L., Taylor, N. F., Feller, J. A., Whitehead, T. S., and Webster, K. E. (2013). Psychological responses matter in returning to preinjury level of sport after anterior cruciate ligament reconstruction surgery. *Am. J. Sports Med.* 41 (7), 1549–1558. doi:10.1177/0363546513489284

Ardern, C. L., Webster, K. E., Taylor, N. F., and Feller, J. A. (2011). Return to the preinjury level of competitive sport after anterior cruciate ligament reconstruction surgery: Two-thirds of patients have not returned by 12 months after surgery. *Am. J. Sports Med.* 39 (3), 538–543. doi:10.1177/0363546510384798

Arhos, E. K., Capin, J. J., Buchanan, T. S., and Snyder-Mackler, L. (2021). Quadriceps strength symmetry does not modify gait mechanics after anterior cruciate ligament reconstruction, rehabilitation, and return-to-sport training. *Am. J. Sports Med.* 49 (2), 417–425. doi:10.1177/0363546520980079

Arneja, S., and Leith, J. (2009). Review article: Validity of the KT-1000 knee ligament arthrometer. *J. Orthop. Surg. Hong. Kong.* 17 (1), 77–79. doi:10.1177/230949900901700117

Barber-Westin, S. D., and Noyes, F. R. (2011). Factors used to determine return to unrestricted sports activities after anterior cruciate ligament reconstruction. *Arthrosc. J. Arthrosc. Relat. Surg.* 27 (12), 1697–1705. doi:10.1016/j.arthro.2011.09.009

Chen, Y., Cao, S., Wang, C., Ma, X., and Wang, X. (2022). Quantitative analysis with load-displacement ratio measured via digital arthrometer in the diagnostic evaluation of chronic ankle instability: A cross-sectional study. *J. Orthop. Surg. Res.* 17 (1), 287. doi:10.1186/s13018-022-03177-3

Cinque, M. E., Dornan, G. J., Chahla, J., Moatshe, G., and LaPrade, R. F. (2018). High rates of osteoarthritis develop after anterior cruciate ligament surgery: An analysis of 4108 patients. *Am. J. Sports Med.* 46 (8), 2011–2019. doi:10.1177/0363546517730072

Di Stasi, S. L., Logerstedt, D., Gardinier, E. S., and Snyder-Mackler, L. (2013). Gait patterns differ between ACL-reconstructed athletes who pass return-to-sport criteria and those who fail. *Am. J. Sports Med.* 41 (6), 1310–1318. doi:10.1177/0363546513482718

Gokeler, A., Welling, W., Zaffagnini, S., Seil, R., and Padua, D. (2017). Development of a test battery to enhance safe return to sports after anterior cruciate ligament reconstruction. *Knee Surg. Sports Traumatol. Arthrosc.* 25 (1), 192–199. doi:10.1007/s00167-016-4246-3

Grindem, H., Snyder-Mackler, L., Moksnes, H., Engebretsen, L., and Risberg, M. A. (2016). Simple decision rules can reduce reinjury risk by 84% after ACL reconstruction: The Delaware-oslo ACL cohort study. *Br. J. Sports Med.* 50 (13), 804–808. doi:10.1136/bjsports-2016-096031

Hewett, T. E., Myer, G. D., Ford, K. R., Heidt, R. S., Jr., Colosimo, A. J., McLean, S. G., et al. (2005). Biomechanical measures of neuromuscular control and valgus loading of the knee predict anterior cruciate ligament injury risk in female athletes: A prospective study. *Am. J. Sports Med.* 33 (4), 492–501. doi:10.1177/0363546504269591

Hildebrandt, C., Müller, L., Zisch, B., Huber, R., Fink, C., and Raschner, C. (2015). Functional assessments for decision-making regarding return to sports following ACL reconstruction. Part I: Development of a new test battery. *Knee Surg. Sports Traumatol. Arthrosc.* 23 (5), 1273–1281. doi:10.1007/s00167-015-3529-4

Jia, Z. Y., Cui, J., Wang, W., Xue, C. C., Liu, T. Z., Huang, X., et al. (2018). Translation and validation of the simplified Chinese version of the anterior cruciate ligament-return to sport after injury (ACL-RSI). *Knee Surg. Sports Traumatol. Arthrosc.* 26 (10), 2997–3003. doi:10.1007/s00167-018-4850-5

Kaplan, Y., and Witvrouw, E. (2019). When is it safe to return to sport after ACL reconstruction? Reviewing the criteria. *Sports Health.* 11 (4), 301–305. doi:10.1177/1941738119846502

Li, G., DeFrate, L. E., Zayontz, S., Park, S. E., and Gill, T. J. (2004). The effect of tibiofemoral joint kinematics on patellofemoral contact pressures under simulated muscle loads. *J. Orthop. Res.* 22 (4), 801–806. doi:10.1016/j.orthres.2003.11.011

Logerstedt, D., Di Stasi, S., Grindem, H., Lynch, A., Eitzen, I., Engebretsen, L., et al. (2014). Self-reported knee function can identify athletes who fail return-to-activity criteria up to 1 year after anterior cruciate ligament reconstruction: A Delaware-oslo ACL cohort study. *J. Orthop. Sports Phys. Ther.* 44 (12), 914–923. doi:10.2519/jospt.2014.4852

Maffiuletti, N. A., Bizzini, M., Desbrosses, K., Babault, N., and Munzinger, U. (2007). Reliability of knee extension and flexion measurements using the Con-Trex isokinetic dynamometer. *Clin. Physiol. Funct. Imaging* 27 (6), 346–353. doi:10.1111/j.1475-097X.2007.00758.x

McPherson, A. L., Feller, J. A., Hewett, T. E., and Webster, K. E. (2019). Psychological readiness to return to sport is associated with second anterior cruciate ligament injuries. *Am. J. Sports Med.* 47 (4), 857–862. doi:10.1177/0363546518825258

Meredith, S. J., Rauer, T., Chmielewski, T. L., Fink, C., Diermeier, T., Rothrauff, B. B., et al. (2020). Return to sport after anterior cruciate ligament injury: Panther symposium ACL injury return to sport consensus group. *Knee Surg. Sports Traumatol. Arthrosc.* 28 (8), 2403–2414. doi:10.1007/s00167-020-06009-1

Müller, U., Krüger-Franke, M., Schmidt, M., and Rosemeyer, B. (2014). Predictive parameters for return to pre-injury level of sport 6 months following anterior cruciate ligament reconstruction surgery. *Knee Surg. Sports Traumatol. Arthrosc.* 23 (12), 3623–3631. doi:10.1007/s00167-014-3261-5

Palmieri-Smith, R. M., and Lepley, L. K. (2015). Quadriceps strength asymmetry after anterior cruciate ligament reconstruction alters knee joint Biomechanics and functional performance at time of return to activity. *Am. J. Sports Med.* 43 (7), 1662–1669. doi:10.1177/0363546515578252

Paterno, M. V., Schmitt, L. C., Ford, K. R., Rauh, M. J., Myer, G. D., Huang, B., et al. (2010). Biomechanical measures during landing and postural stability predict second anterior cruciate ligament injury after anterior cruciate ligament reconstruction and return to sport. *Am. J. Sports Med.* 38 (10), 1968–1978. doi:10.1177/0363546510376053

Rambaud, A. J. M., Semay, B., Samozino, P., Morin, J. B., Testa, R., Philippot, R., et al. (2017). Criteria for return to sport after anterior cruciate ligament reconstruction with lower reinjury risk (CR'STAL study): Protocol for a prospective observational study in France. *BMJ Open* 7 (6), e015087. doi:10.1136/bmjopen-2016-015087

Raoul, T., Klouche, S., Guerrier, B., El-Hariri, B., Herman, S., Gerometta, A., et al. (2019). Are athletes able to resume sport at six-month mean follow-up after anterior cruciate ligament reconstruction? Prospective functional and psychological assessment from the French anterior cruciate ligament study (FAST) cohort. *Knee* 26 (1), 155–164. doi:10.1016/j.knee.2018.11.006

Reid, A., Birmingham, T. B., Stratford, P. W., Alcock, G. K., and Giffin, J. R. (2007). Hop testing provides a reliable and valid outcome measure during rehabilitation after anterior cruciate ligament reconstruction. *Phys. Ther.* 87 (3), 337–349. doi:10.2522/ptj.20060143

Sonesson, S., Kvist, J., Ardern, C., Osterberg, A., and Silbernagel, K. G. (2017). Psychological factors are important to return to pre-injury sport activity after anterior cruciate ligament reconstruction: Expect and motivate to satisfy. *Knee Surg. Sports Traumatol. Arthrosc.* 25 (5), 1375–1384. doi:10.1007/s00167-016-4294-8

Teichtahl, A. J., Wluka, A. E., Morris, M. E., Davis, S. R., and Cicuttini, F. M. (2009). The associations between the dominant and nondominant peak external knee adductor moments during gait in healthy subjects: Evidence for symmetry. *Arch. Phys. Med. Rehabil.* 90 (2), 320–324. doi:10.1016/j.apmr.2008.07.030

Thomee, R., Kaplan, Y., Kvist, J., Myklebust, G., Risberg, M. A., Theisen, D., et al. (2011). Muscle strength and hop performance criteria prior to return to sports after ACL reconstruction. *Knee Surg. Sports Traumatol. Arthrosc.* 19 (11), 1798–1805. doi:10.1007/s00167-011-1669-8

Thomeé, R., Neeter, C., Gustavsson, A., Thomeé, P., Augustsson, J., Eriksson, B., et al. (2012). Variability in leg muscle power and hop performance after anterior cruciate ligament reconstruction. *Knee Surg. Sports Traumatol. Arthrosc.* 20 (6), 1143–1151. doi:10.1007/s00167-012-1912-y

Tian, F., Li, N., Zheng, Z., Huang, Q., Zhu, T., Li, Q., et al. (2020). The effects of marathon running on three-dimensional knee kinematics during walking and running in recreational runners. *Gait Posture* 75, 72–77. doi:10.1016/j.gaitpost.2019.08.009

Undheim, M. B., Cosgrave, C., King, E., Strike, S., Marshall, B., Falvey, E., et al. (2015). Isokinetic muscle strength and readiness to return to sport following anterior cruciate ligament reconstruction: Is there an association? A systematic review and a protocol recommendation. *Br. J. Sports Med.* 49 (20), 1305–1310. doi:10.1136/bjsports-2014-093962

van Melick, N., van Cingel, R. E., Brooijmans, F., Neeter, C., van Tienen, T., Hullegie, W., et al. (2016). Evidence-based clinical practice update: Practice guidelines for anterior cruciate ligament rehabilitation based on a systematic review and multidisciplinary consensus. *Br. J. Sports Med.* 50 (24), 1506–1515. doi:10.1136/bjsports-2015-095898

Webster, K. E., and Feller, J. A. (2019). A research update on the state of play for return to sport after anterior cruciate ligament reconstruction. *J. Orthop. Traumatol.* 20 (1), 10. doi:10.1186/s10195-018-0516-9

Webster, K. E., and Feller, J. A. (2016). Exploring the high reinjury rate in younger patients undergoing anterior cruciate ligament reconstruction. *Am. J. Sports Med.* 44 (11), 2827–2832. doi:10.1177/0363546516651845

Webster, K. E., Feller, J. A., and Lambros, C. (2008). Development and preliminary validation of a scale to measure the psychological impact of returning to sport following anterior cruciate ligament reconstruction surgery. *Phys. Ther. Sport* 9 (1), 9–15. doi:10.1016/j.ptsp.2007.09.003

Yoo, J. D., Papannagari, R., Park, S. E., DeFrate, L. E., Gill, T. J., and Li, G. (2005). The effect of anterior cruciate ligament reconstruction on knee joint kinematics under simulated muscle loads. *Am. J. Sports Med.* 33 (2), 240–246. doi:10.1177/0363546504267806

Zarzycki, R., Failla, M., Capin, J. J., and Snyder-Mackler, L. (2018). Psychological readiness to return to sport is associated with knee kinematic asymmetry during gait following anterior cruciate ligament reconstruction. *J. Orthop. Sports Phys. Ther.* 48 (12), 968–973. doi:10.2519/jospt.2018.8084

Zhang, Y., Yao, Z., Wang, S., Huang, W., Ma, L., Huang, H., et al. (2015). Motion analysis of Chinese normal knees during gait based on a novel portable system. *Gait Posture* 41 (3), 763–768. doi:10.1016/j.gaitpost.2015.01.020

frontiers | Frontiers in Bioengineering and Biotechnology

TYPE Original Research
PUBLISHED 05 October 2022
DOI 10.3389/fbioe.2022.1022910

OPEN ACCESS

EDITED BY
Qichang Mei,
Ningbo University, China

REVIEWED BY
Alessandra Bento Matias,
Faculty of Medicine, University of São Paulo, Brazil
Duo Wai-Chi Wong,
Hong Kong Polytechnic University,
Hong Kong SAR, China

*CORRESPONDENCE
Shen Zhang,
zhangshen0708@163.com

SPECIALTY SECTION
This article was submitted to Biomechanics,
a section of the journal
Frontiers in Bioengineering and Biotechnology

RECEIVED 19 August 2022
ACCEPTED 20 September 2022
PUBLISHED 05 October 2022

CITATION
Shen B, Zhang S, Cui K, Zhang X and Fu W (2022), Effects of a 12-week gait retraining program combined with foot core exercise on morphology, muscle strength, and kinematics of the arch: A randomized controlled trial.
Front. Bioeng. Biotechnol. 10:1022910.
doi: 10.3389/fbioe.2022.1022910

Effects of a 12-week gait retraining program combined with foot core exercise on morphology, muscle strength, and kinematics of the arch: A randomized controlled trial

Bin Shen[1], Shen Zhang[2,3,4]*, Kedong Cui[1], Xini Zhang[1] and Weijie Fu[1,3,4]

[1]School of Exercise and Health, Shanghai University of Sport, Shanghai, China, [2]School of Athletic Performance, Shanghai University of Sport, Shanghai, China, [3]Key Laboratory of Exercise and Health Sciences of Ministry of Education, Shanghai University of Sport, Shanghai, China, [4]Shanghai Frontiers Science Research Base of Exercise and Metabolic Health, Shanghai University of Sport, Shanghai, China

Objective: This study aims to explore the effects of a 12-week gait retraining program combined with foot core exercise on arch morphology, arch muscles strength, and arch kinematics.

Methods: A total of 26 male recreational runners with normal arch structure who used rear-foot running strike (RFS) were divided into the intervention group (INT group) and control group (CON group) (n = 13 in each group). The INT group performed a 12-week forefoot strike (FFS) training combined with foot core exercises. The CON group did not change the original exercise habit. Before and after the intervention, the arch morphology, as well as the strength of hallux flexion, lesser toe flexion, and the metatarsophalangeal joint (MPJ) flexors were measured in a static position, and changes in the arch kinematics during RFS and FFS running were explored.

Results: After a 12-week intervention, 1) the normalized navicular height increased significantly in the INT group by 5.1% (p = 0.027, Cohen's d = 0.55); 2) the hallux absolute flexion and relative flexion of the INT group increased significantly by 20.5% and 21.7%, respectively (p = 0.001, Cohen's d = 0.59; p = 0.001, Cohen's d = 0.73), the absolute and relative strength of the MPJ flexors of the INT group were significantly improved by 30.7% and 32.5%, respectively (p = 0.006, Cohen's d = 0.94; p = 0.006, Cohen's d = 0.96); 3) and during RFS, the maximum arch angle of the INT group declined significantly by 5.1% (p < 0.001, Cohen's d = 1.49), the arch height at touchdown increased significantly in the INT group by 32.1% (p < 0.001, Cohen's d = 1.98).

Conclusion: The 12-week gait retraining program combined with foot core exercise improved the arch in both static and dynamic positions with a moderate to large effect size, demonstrating the superiority of this combined intervention over the standalone interventions. Thus, runners with weak arch muscles are encouraged to use this combined intervention as an approach to enhance the arch.

KEYWORDS

gait retraining, foot core exercises, arch morphology, arch muscles strength, arch kinematics

1 Introduction

Running is one of the most popular fitness activities today as it offers easy accessibility and obvious health gains (De Wit et al., 2000). Many researchers have investigated extrinsic and intrinsic risk factors to reduce the risk of running-related injuries (Hespanhol Junior et al., 2016; Kelly et al., 2016; Krabak et al., 2017; Yang et al., 2020). However, in the past 50 years, the rate of various lower limb injuries caused by running has remained at a relatively high level (Kakouris et al., 2021), of which the incidence of foot injuries, such as plantar fascia injury, accounted for about 20% (Taunton et al., 2002). The fascia and ligaments of the plantar are important structures that maintain the dome structure of the foot. However, maintaining the stability of the medial longitudinal arch (MLA) during gait and controlling the movement of the foot rely on the intrinsic and extrinsic foot muscles (McKeon et al., 2015). Weak foot muscles cannot provide sufficient support to MLA during dynamic movement, resulting in repeated strains of the plantar fascia, which in turn, increase the risk of plantar injuries (Cheung et al., 2016).

The anatomical structure of the longitudinal arch gives it spring-like compression and rebound characteristics, which are affected by different running postures and modern running shoes (Lieberman, 2012; Perl et al., 2012). For rearfoot strike (RFS) running, MLA rarely compresses from the foot touch down to mid-stance. In addition, impact transients associated with RFS running are sudden forces with high rates and magnitudes of loading that travel rapidly up to the musculoskeletal system, thus resulting in a high incidence of running-related injuries, especially tibial stress fractures and plantar fasciitis (Kakouris et al., 2021; Milner et al., 2006; Lieberman et al., 2010). As a result, RFS runners prefer to wear cushioned running shoes with an elastic material in the heel to reduce the transient impact forces and disperse them over time (Lieberman et al., 2010; Zhang et al., 2019). Although modern cushioned running shoes have certain shock absorption advantages, some scholars believe that the thick cushioning medium between the foot and the ground surface may damage the feedback effect of plantar mechanoreceptors (Lieberman, 2012), thus limiting arch compression and rebound, resulting in the loss of elastic work and increased metabolic energy costs (Perl et al., 2012; Stearne et al., 2016). In contrast, the arch undergoes a three-point bending during the touchdown phase of the forefoot strike (FFS) running (Perl et al., 2012). To better control arch deformation, the foot muscles will have adaptive muscle strength enhancement (Jenkins and Cauthon, 2011; Perl et al., 2012; Kelly et al., 2018). Meanwhile, the longitudinal and transverse arches include many elastic tissues that recover an estimated 17% of the mechanical energy generated per step (Ker et al., 1987). Hence, FFS can be regarded as good training to enhance the performance of the arch (Kelly et al., 2018).

Foot core exercise includes foot doming, towel curls, toe spread, and more (Lynn et al., 2012; Goo et al., 2014; Kamonseki et al., 2016). In addition, the FFS has also been proven to effectively stimulate the foot muscles and strengthen the muscle function of the foot (Kelly et al., 2018). Numerous studies have investigated the separate effects of two interventions, namely, the effect of minimal shoes or FFS on foot muscles strength or size (Miller et al., 2014; Ridge et al., 2019), and the effects of foot core exercise on the balance and postural control (Rothermel et al., 2004; Lynn et al., 2012; Mulligan and Cook, 2013). However, foot core exercise alone may fail to meet the functional requirements of the arch under dynamic conditions (e.g., running, jumping.), while FFS training alone may increase the risk of running-related injury because the foot structure cannot support the rapid increase in load caused by the sudden change in strike pattern (Ridge et al., 2013). A more appropriate training program would be a combined intervention to enhance both the intrinsic and extrinsic foot muscles (i.e., active subsystem) of the foot core system, which can simultaneously improve foot function in static posture and dynamic activities (McKeon et al., 2015). Accordingly, previous gait retraining studies have begun to incorporate foot core exercise to reduce the risk of injury in participants when the strike pattern suddenly changes (Warne et al., 2014; Deng et al., 2020; Zhang et al., 2021). Nevertheless, few studies have investigated the effect of this combined intervention on the MLA at a static position and during running. Furthermore, as the conversion of RFS to FFS is a gradual process (McCarthy et al., 2014; Zhang et al., 2020), the effects of intervention training on arch kinematics reflected in both RFS and FFS remain unclear and require further exploration.

Therefore, this study aims to investigate the effects of a 12-week gait retraining program combined with foot core exercise on arch morphology in static postures, arch muscles strength (i.e., separated toe flexion strength and the metatarsophalangeal joints (MPJ) flexor strength), and arch kinematics changes during RFS and FFS running among RFS runners. We hypothesized that the intervention would benefit arch shape maintenance, enhance arch muscle strength, and produce favorable changes in arch kinematics during running.

2 Methods

2.1 Participants

Based on the previous data (a significant group*time interaction effect on toe-flexor strength, effect size $f = 0.6$) published by Day and Hahn (2019), *a priori* power analysis (G*Power, Version 3.1.9.6, Kiel University, Germany) was conducted for expected outcomes with a type I error probability of 0.05 and an effect size f of 0.6 (Cohen defines effect size f of 0.1, 0.25, and 0.4 as small, medium, and large effects, respectively). This analysis indicated that $n = 26$ would provide a statistical power of ~95% (Faul et al., 2007). Considering a drop-out rate of 15–20%, 32 male recreational runners were recruited through online social media, running clubs, and flyers (Wang J et al., 2020). They were all habitual runners who run at least 20 km/week in the RFS pattern while running on the ground with cushioned shoes were recruited (Lieberman et al., 2010). The inclusion criteria included the following: 1) normal arch height index (AHI, the height of the dorsum of the foot at 50% of the foot length divided by the truncated foot length) ranging from 0.31 to 0.37 (Butler et al., 2008), 2) no musculoskeletal injuries over the past 1 year and good exercise ability, 3) running distance that did not change in 3 months, and 4) never attempted foot core exercises, such as those included in this study or FFS pattern. All the participants signed an informed consent form provided by the Human Ethics Committee of Shanghai University of Sport prior to the study (IRB no. 2017007). After the baseline measurement, the participants were divided randomly into the intervention group (INT) or control group (CON). A research assistant generated the randomization schedule using a computer program and handed the results of allocation to the participants in a sealed envelope, ensuring that the researchers involved in outcome measurement and data analysis were unaware of the allocation.

2.2 Intervention

The INT group performed FFS training combined with foot core exercise (Tam et al., 2015; Krabak et al., 2017) to enhance intrinsic and extrinsic foot muscle strength during static and dynamic tasks. To ensure that the INT group can master the intervention method, we gathered the INT group and our running coach explained and demonstrated the FFS and foot core exercises in the first week. For the subsequent 11 weeks, the INT group underwent centralized training on an indoor track on our campus once a week. The foot core exercise protocol was based on previous literature and previous results of our team, and it had shown to be effective in enhancing foot muscles and potentially reducing the risk of injury (Warne et al., 2014; Ridge et al., 2019; Wang B et al., 2020; Zhang et al., 2021). It included heel raises, towel curls, foot doming, toe spread, balance board, and foot relaxation exercises by stepping on a tennis ball with progressive intensity (Table 1).

During the FFS training, each participant was required to run in an FFS pattern and was given an appropriately fitted pair of Vibram Five Fingers shoes, which aimed to protect the foot soles from the rough ground and simulate barefoot running to give the participant a habituation process for the strike pattern transition (Paquette et al., 2013; McCarthy et al., 2014). The duration of FFS running was increased every week based on protocols from previous literature (Tam et al., 2015; Zhang et al., 2021) (Table 2). The INT group was allowed to do rear-foot strike running with cushioning running shoes when out of training to maintain a running distance of a total of at least 20 km/week.

Participants in the CON group were required to continue their regular running routines in an RFS pattern using cushioned running shoes and running at their habitual pace in places where they were accustomed to running (e.g., parks, roads, tracks.) for 12 weeks. All participants in the INT and CON groups were required to provide us feedback after each training, including running location, duration, and mileage, as well as photos while doing foot core exercises. During the entire experiment and intervention, no participants suffered injuries.

The criteria for successful intervention were as follows: 1) completion of all the tests, 2) no more than three times of absences, and 3) completion of the last three-week training. During the intervention period, the participants were allowed to postpone or quit due to injuries or personal reasons (Zhang et al., 2020).

2.3 Arch morphology

Initially, a participant was in a standing posture, and the most prominent aspect of the navicular tuberosity was palpated by a certified rehabilitation therapist who performed all of the palpation, manual measurements, and marker sticking throughout the whole experiment (Langley et al., 2016). If the navicular tuberosity was not sufficiently prominent, we instructed the subject to maintain the foot adducted and identified the navicular tuberosity by palpation along the clearly visible tendon of the posterior tibialis (Golano et al., 2004). The position of navicular tuberosity was marked with a washable pen for subsequent measurements. Then, a digital caliper was used to test the arch morphology in the standing and sitting positions in this study. In the standing position, participants were required to keep upright and maintain a bilateral standing posture with their bare feet pelvis-width apart as they tried to make their legs as parallel as possible to avoid foot inversion or eversion. When switching to a sitting position, the participants sat back in the seat without moving their feet and kept their hip, knee, and ankle joints in 90° flexion, as well as the hands hanging at

TABLE 1 Foot core exercise schedule.

	1 ~ 2 weeks	3 ~ 4 weeks	5 ~ 6 weeks	7 ~ 8 weeks	9 ~ 10 weeks	11 ~ 12 weeks
Heel raises (double in a flat)	1 × 10 times	2 × 10 times	2 × 15 times	—	—	—
Heel raises (double on a step)	—	—	—	2 × 20 times	2 × 25 times	3 × 30 times
Heel raises (single on a step)	—	—	—	1 × 10 times	2 × 10 times	3 × 15 times
Towel curls	3 × 10 times	3 × 20 times	3 × 10 times (+0.25 kg)	3 × 15 times (+0.25 kg)	3 × 10 times (+0.5 kg)	3 × 15 times (+0.5 kg)
Foot doming	2 × 10 times	2 × 15 times	2 × 20 times	3 × 20 times	3 × 25 times	4 × 25 times
Toe spread	2 × 10 times	2 × 15 times	2 × 20 times	3 × 20 times	3 × 25 times	4 × 25 times
Balance board	2 × 20 s	2 × 25 s	2 × 30 s	3 × 30 s	3 × 35 s	3 × 40 s
Foot relaxes	1 × 30 s	1 × 30 s	1 × 30 s	1 × 30 s	1 × 30 s	1 × 30 s

TABLE 2 FFS training schedule.

Week	1	2	3	4	5	6	7	8	9	10	11	12
Duration (min)	5	10	15	20	25	30	35	40	42	44	46	48
Times per week	3	3	3	3	3	3	3	3	3	3	3	3

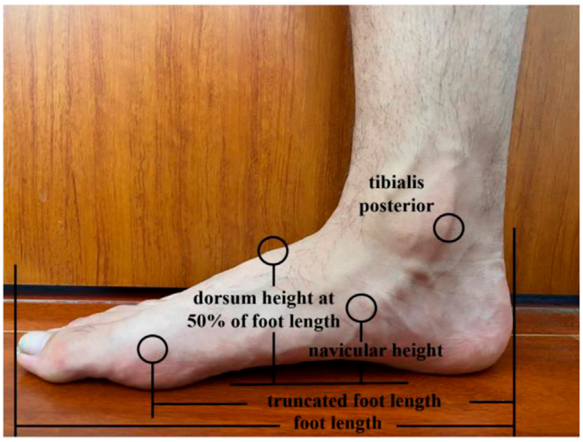

FIGURE 1
Arch morphology variables.

the sides of the body. Then, both forefeet were raised and lowered on the ground with subtalar joint in a natural position. The arch morphological variables (Williams and Mcclay, 2000; Fiolkowski et al., 2003) included the following: 1) standing/sitting arch height: distance from navicular center to the ground; 2) normalized arch height: navicular height divided by foot length; and 3) navicular drop: the difference between standing arch height and sitting arch height (Figure 1).

2.4 Arch muscles strength

2.4.1 Separated toe flexion strength

A modified dynamometer (Ailitech ADF 500, China) attached to a wooden frame (Figure 2) was used to measure the hallux flexion initially, and then simultaneously with the lesser toe flexion (from 2nd to 5th toes). The board under the foot can provide support from the heel to the head of the first metatarsal, thereby allowing toe flexion. To avoid missing the force values, metal hooks and rings were used to connect the toes and the dynamometer. During the test, participants were required to maintain a sitting position with the hip, knee, and ankle joints flexed at 90°.

To test hallux flexion, the hallux was aligned with the dynamometer and then a metal ring was set to the hallux. When the hallux relaxed, the force value was 0 N. The participants were required to flex their big toe and pull the ring back as hard as possible. The tests were repeated if the participants' heel and/or ball of the foot left the board. The combined strength of the 2nd to 5th toes was assessed in a similar manner. This method has been associated with excellent repeatability and reliability for all tests between days, raters, and sessions (Ridge et al., 2017; Zhang et al., 2019).

2.4.2 Metatarsophalangeal joint flexors strength

A customized strength tester (CN103278278B, China) was used to measure the MPJ flexors strength with the sampling rate of 120 Hz. The strength tester consisted of a chassis, a seat, force sensors, a computer, a foot platform, and a 30° raised toe platform,

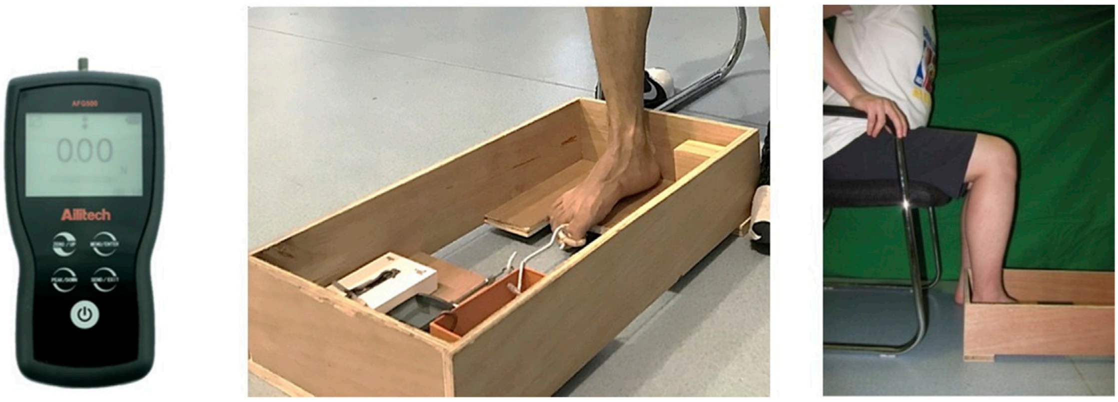

FIGURE 2
The digital calliper and separated toes flexion test (Zhang et al., 2019).

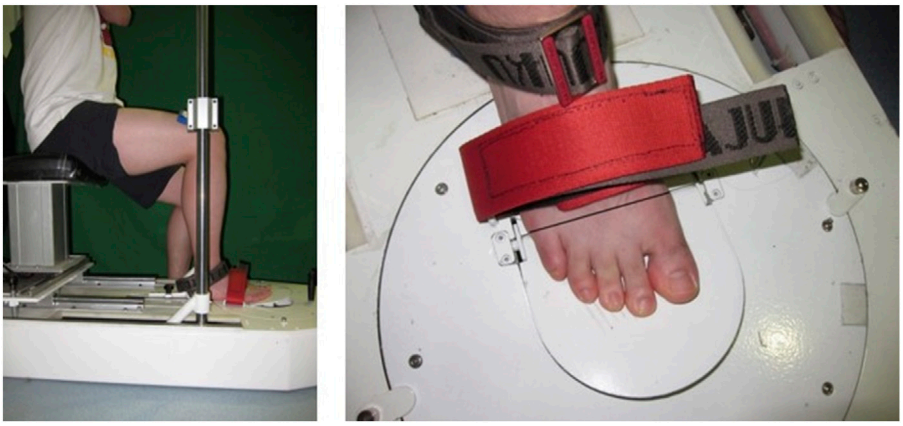

FIGURE 3
A self-developed strength tester for the metatarsophalangeal joint flexors (Zhang et al., 2019).

and was similar to the device used in the study of Man et al. (2016). The participants were required to sit on a chair with their knees and feet fixed by a stopper plate to avoid the data being interfered with by other joints. During the tests, they were asked to keep the toes as close to the surface of the toe platform as possible and then try their best to flex all their MPJs together for 10 s to press the toe platform. If there was an elevation of the interphalangeal joints, the test was considered a failure and then repeated after a short rest. The tester used the pedal movement is transmitted the metatarsophalangeal by the tension sensor (Figure 3). The MPJ flexor strength data were measured and processed using a computer. The interclass correlation coefficients (ICC = 0.874) of this measurement were calculated in SPSS to test the reliability between sessions of the same rater on the same day (Ridge et al., 2017; Zhang et al., 2019).

2.5 Arch kinematics and arch stiffness

A 12-camera motion analysis system (100Hz, Vicon Motion Analysis Inc., Oxford, United Kingdom) was used to obtain the three-dimensional (3D) kinematic data of the foot. Given the methodological design described in the previous study, more accurate data on the arch kinematics of participants were obtained by placing infrared reflective markers onto the dominant leg at the following landmarks in the barefoot condition (Perl et al., 2012): 1) the first toe, 2) the medial side of the first metatarsal joint, 3) the lateral side of the 5th metatarsal head, 4) the navicular tuberosity, 5) the highest point on the dorsum, 6) the medial calcaneus process, 7) the lateral calcaneus process, and 8) the location of Achilles tendon insertion on the calcaneus (Figure 4). Two 90 × 60 × 10 cm force platforms

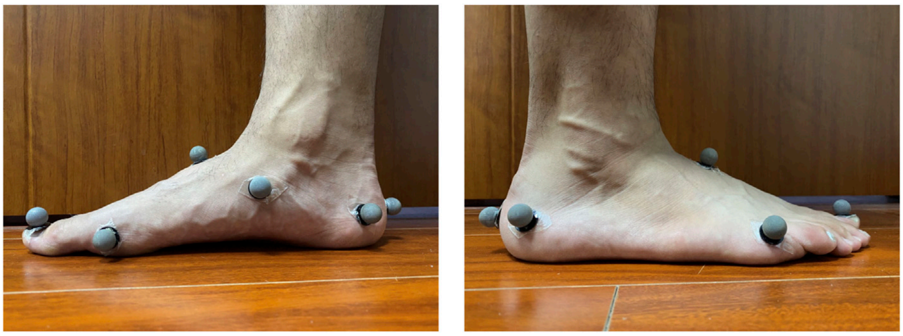

FIGURE 4
Marker position.

(1000 Hz, 9287 B, Kistler Corporation, Winterthur, Switzerland) were used to collect ground reaction force (GRF) simultaneously with 3D kinematic data using the Vicon workstation during running.

The INT and CON groups were assessed using RFS and FFS barefoot running tests pre- and post-intervention. We introduced the RFS pattern to the participants, which was defined as initial heel contact, and the FFS pattern as initial forefoot contact much like "running on one's toes" (Williams et al., 2012; Rice and Patel, 2017). Before the running tests, the participants performed a warm-up protocol consisting of 5 min on the treadmill at a self-selected speed running followed by a set of static stretching exercises. At the start of the recording sessions, the participants were instructed to practice running barefoot across the running path until they could touchdown naturally. Three successful trials were recorded while their right foot comes into contact with the force plate at a speed of 3.33 m/s (±5%) (McCarthy et al., 2014).

Kinematic data and GRF were analyzed *via* the Visual 3D (V5, C-Motion, Inc., Germantown, MD, United States). All marker trajectories were filtered using a fourth-order Butterworth low-pass filter with a cut-off frequency of 7 Hz. The GRF was filtered with a cut-off frequency of 50 Hz (Kelly et al., 2018). The ankle joint rotation was calculated *via* Cardan sequencing where motion about the X-axis was defined as plantarflexion/dorsiflexion (Williams et al., 2012).

Arch kinematic variables included the following (Holowka et al., 2018): 1) Δarch angle, which is the angle variation of the metatarsal bone relative to the calcaneus from touchdown to the maximum angle; 2) maximum arch angle, which is the arch angle compressed to maximum value during the stance phase; 3) arch height at touchdown, which is the perpendicular distance at touchdown between the navicular tuberosity and a line bisecting the medial side of the first metatarsal head and the medial calcaneus process; and 4) Δarch height, which is the difference between arch height at touchdown and arch height at 50% of stance phase 5) arch stiffness, the change in arch height

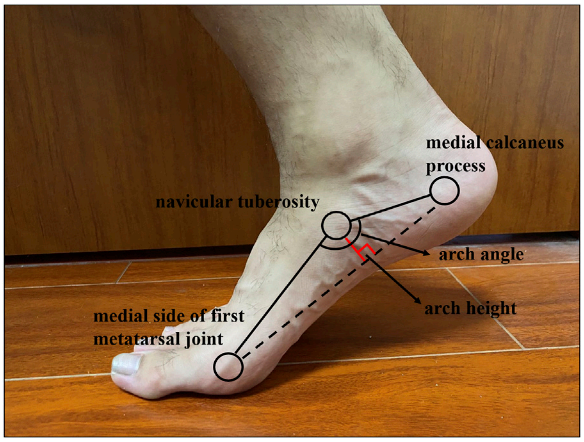

FIGURE 5
Arch kinematic variables.

dividing the vertical GRF at mid-stance normalized by (body mass)$^{0.67}$ (Figure5).

2.6 Statistics

The results are shown with mean and standard deviation for each variable. All variables were inspected for normality and for homogeneity of variance between the two groups. Arch stiffness was log-transformed to achieve normality (Holowka et al., 2018). A 2 × 2 mixed factor ANOVA with baseline data as a covariate was used to examine the interaction effects of groups (INT vs. CON) and time (before vs. after intervention) on the arch morphology, arch muscle strength, and arch kinematics variables (Wang et al., 2021). When a significant interaction effect or main effect was detected, independent *t*-tests and paired *t*-tests were

TABLE 3 The basic information of participants.

Group	Age (yrs)	Height (cm)	Weight (kg)	AHI	Running distance (km/w)	Training frequency (d/w)
INT (n = 13)	25.2 ± 4.8	175.5 ± 8.2	72.8 ± 14.9	0.34 ± 0.02	29.4 ± 4.3	2.8 ± 0.4
CON (n = 13)	23.8 ± 1.7	176.6 ± 4.9	72.0 ± 7.1	0.35 ± 0.01	28.8 ± 3.0	2.8 ± 0.4

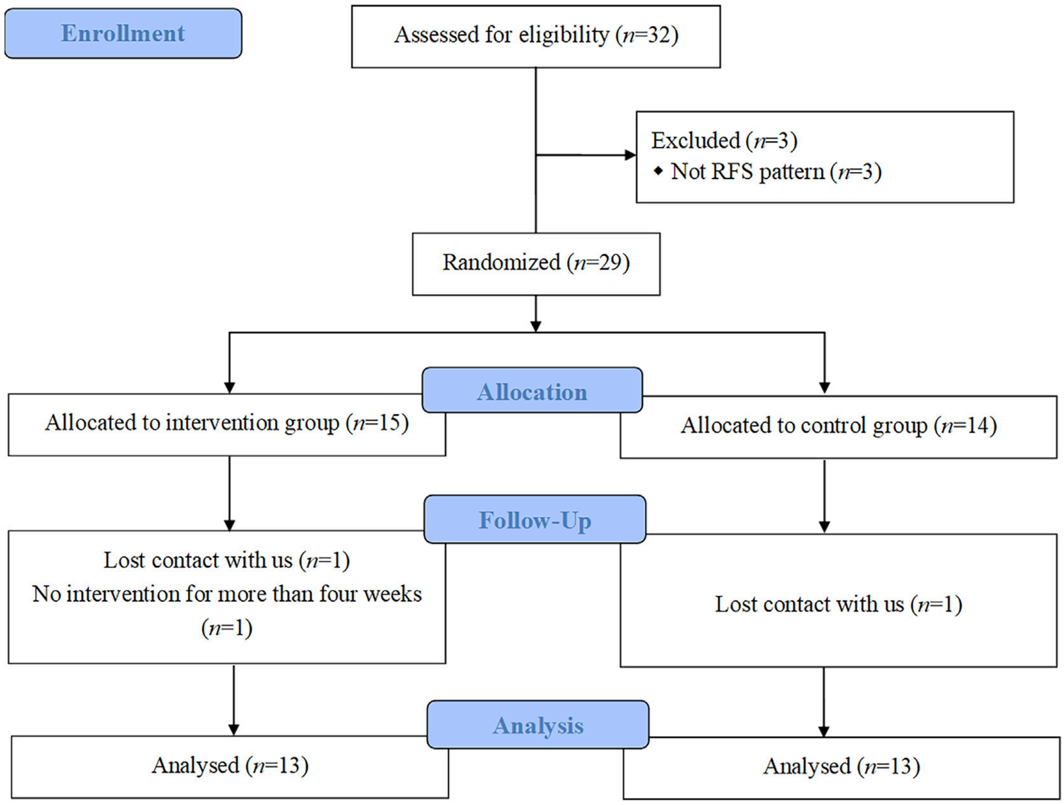

FIGURE 6
CONSORT flow chart.

used as a post-hoc test to compare differences between-groups and within-subjects, respectively. When a significant main effect of time was detected, independent t-tests were used to compare the differences in percentage changes between the two groups. Effect sizes were calculated for ANOVA and t-test comparisons using η_p^2 and Cohen's d respectively. η_p^2 of 0.01, 0.09, and 0.25 were respectively interpreted as small, medium and large effects, while Cohen's d of 0.2–0.5, 0.5–0.8 and >0.8 were respectively interpreted as small, moderate and large effects (Miller et al., 2014; Wang et al., 2021). The level of significance was set at α = 0.05. If no significant changes were found, the Cohen's d was calculated and reported. All statistical analyses were performed in SPSS (19.0, SPSS Inc., Chicago, IL, U.S.A.).

3 Results

3.1 Dropout rate

Six participants dropped out. Among them, three FFS participants were excluded from the test before training due to their inability to meet the inclusion criteria, one participant did not train for more than 4 weeks due to a

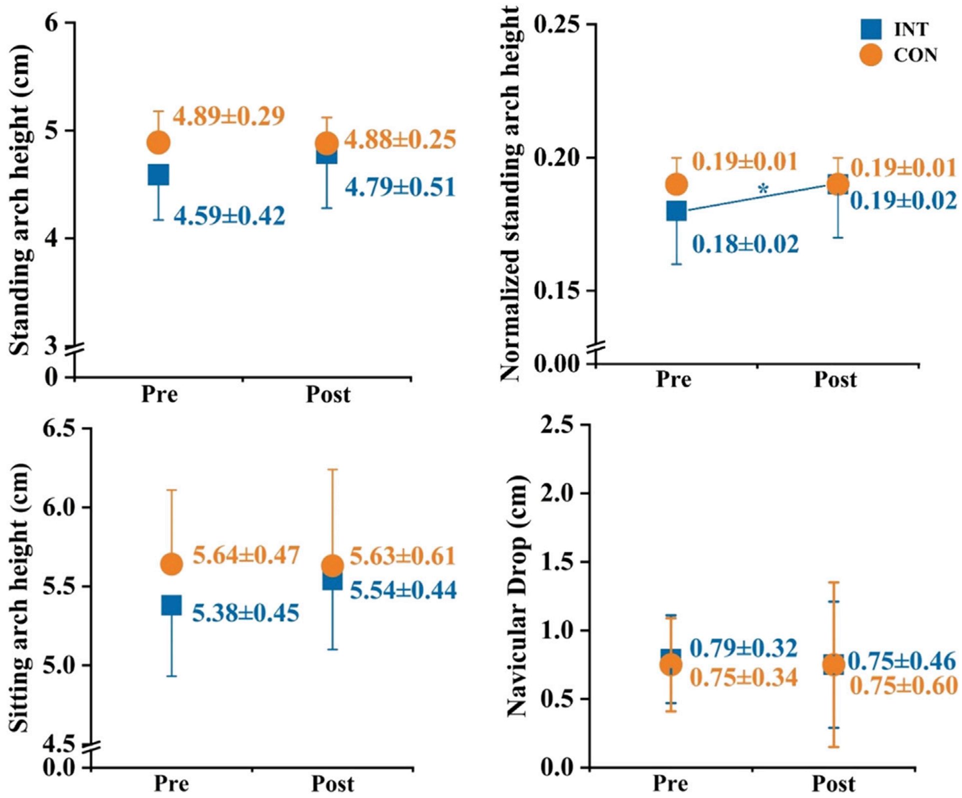

FIGURE 7
Effects of a 12-week gait retraining program combined with foot core exercise on the arch morphology. Notes: * significant difference from pre- to post-tests.

business trip, and two participants lost contact with us. Given that the per-protocol approach has been widely used in previous studies on gait retraining or foot muscle training (Miller et al., 2014; Ridge et al., 2019), which could be because including participants who did not complete the intervention program in the final analysis would underestimate the potential benefits of the intervention (Moher et al., 2010). Based on the above consideration, we also used a per-protocol approach to analyse all outcomes. Thus, 26 participants who completed the intervention and met the inclusion criteria (13 in the INT, 13 in the CON) were included in the final analysis and statistics (Table 3; Figure 6).

3.2 Arch morphology

A significant main effect of time on the normalized standing arch height was observed ($F_{1,23} = 6.430$, $p = 0.018$, $\eta_p^2 = 0.218$). Paired t-tests indicated that after the intervention, the normalized standing arch height increased significantly in the INT group by 5.1% ($p = 0.027$, Cohen's $d = 0.55$) while decreased in the CON group by 1.6% ($p = 0.427$, Cohen's $d = 0.18$), and independent t-tests showed a significant difference in percentage changes between the INT group and the CON group ($p = 0.025$, Cohen's $d = 0.94$). There was no significant interaction effect or main effect on standing/sitting arch height and navicular drop (Figure 7).

3.3 Arch muscles strength

3.3.1 Separated toe flexion strength

Significant interaction effects between time and group on the hallux absolute flexion ($F_{1,23} = 5.840$, $p = 0.024$, $\eta_p^2 = 0.202$) and the hallux relative flexion ($F_{1,23} = 4.974$, $p = 0.036$, $\eta_p^2 = 0.178$) were observed. Paired t-tests revealed that after the intervention, the hallux absolute flexion and relative flexion of the INT group increased significantly by 20.5% and 21.7%, respectively ($p = 0.001$, Cohen's $d = 0.59$; $p = 0.001$, Cohen's $d = 0.73$), while the CON group showed no significant changes ($p = 0.842$, Cohen's $d = 0.04$; $p = 0.762$, Cohen's $d = 0.06$). There was no significant interaction effect or main effect on lesser toe absolute flexion and lesser toe relative flexion.

TABLE 4 Effects of a 12-week gait retraining program combined with foot core exercise on the arch muscles strength.

Variables	INT		CON	
	Pre	Post	Pre	Post
Hallux absolute flexion (N)	103.31 ± 34.38	124.55 ± 37.25*	118.65 ± 25.97	119.86 ± 31.00
Hallux relative flexion (N/kg)	1.43 ± 0.39	1.74 ± 0.44*	1.67 ± 0.44	1.70 ± 0.50
Lesser toe absolute flexion (N)	67.52 ± 17.58	90.79 ± 27.39	69.24 ± 22.95	73.77 ± 30.04
Lesser toe relative flexion (N/kg)	0.94 ± 0.21	1.29 ± 0.43	0.98 ± 0.34	1.05 ± 0.46
Metatarsophalangeal joint flexors absolute strength (N)	83.47 ± 24.54	109.08 ± 29.71*	112.44 ± 41.57	108.36 ± 41.89
Metatarsophalangeal joint flexors relative strength (N/kg)	1.17 ± 0.39	1.55 ± 0.40*	1.58 ± 0.60	1.54 ± 0.60

* significant difference from pre- to post-tests.

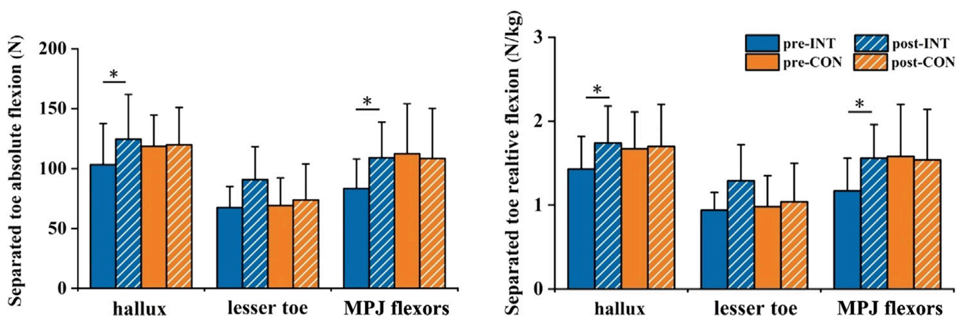

FIGURE 8
Effects of a 12-week gait retraining program combined with foot core exercise on arch muscles strength. Notes: * significant difference from pre- to post-tests.

3.3.2 Metatarsophalangeal joint flexors strength

There were significant main effects of time on the absolute ($F_{1,23}$ = 9.399, p = 0.005, η_p^2 = 0.290) and relative strength ($F_{1,23}$ = 11.785, p = 0.002, η_p^2 = 0.339) of the MPJ flexors. Paired t-tests revealed that after the intervention, the absolute and relative strength of the MPJ flexors increased significantly in the INT group by 30.7% and 32.5%, respectively (p = 0.006, Cohen's d = 0.94; p = 0.006, Cohen's d = 0.96), while no significant changes in the CON group (p = 0.749, Cohen's d = 0.10; p = 0.813, Cohen's d = 0.07). (Table 4; Figure 8).

3.4 Arch kinematics and arch stiffness

All participants exhibited consistent ankle dorsiflexion at touchdown in RFS (INT vs. CON in the pre-test: 6.74 ± 4.29 vs. 5.05 ± 4.38; INT vs. CON in the post-test: 7.46 ± 4.10 vs. 6.52 ± 4.59), and ankle plantarflexion at touchdown in FFS (INT vs. CON in the pre-test: −14.65 ± 5.81 vs. −15.48 ± 4.31; INT vs. CON in the post-test: −12.70 ± 6.54 vs. −14.59 ± 3.83).

During RFS, there was a significant interaction effect between time and group on the maximum arch angle ($F_{1,23}$ = 5.296, p = 0.031, η_p^2 = 0.187), paired t-tests revealed that after the intervention, the maximum arch angle of the INT group declined significantly by 5.1% (p < 0.001, Cohen's d = 1.49), while the CON group showed no significant change (p = 0.733, Cohen's d = 0.08). The significant main effects of time were observed on Δarch angle ($F_{1,23}$ = 6.885, p = 0.015, η_p^2 = 0.230), the arch height at touchdown ($F_{1,23}$ = 41.658, p < 0.001, η_p^2 = 0.644), Δarch height ($F_{1,23}$ = 13.949, p = 0.001, η_p^2 = 0.378), and arch stiffness ($F_{1,23}$ = 31.030, p < 0.001, η_p^2 = 0.574). Paired t-tests indicated that after the intervention, the arch height at touchdown and the Δarch height increased significantly in the INT group by 32.1% and 29.5%, respectively (p < 0.001, Cohen's d = 1.98; p = 0.023, Cohen's d = 0.71), and the arch stiffness decreased significantly in the INT group by 33.3% (p = 0.021, Cohen's d = 0.80), while no significant changes in the CON group (p = 0.811, Cohen's d = 0.08; p = 0.620, Cohen's d = 0.09; p = 0.210, Cohen's d = 0.42). Independent t-tests showed a significant difference in percentage changes between the INT group and the CON group on the arch height at touchdown (p < 0.001, Cohen's d = 1.80).

During FFS, the significant main effects of time were observed on Δarch angle ($F_{1,23}$ = 15.411, p = 0.001, η_p^2 =

TABLE 5 Effects of a 12-week gait retraining program combined with foot core exercise on the arch kinematics.

Variables	INT		CON	
	Pre	Post	Pre	Post
RFS				
ΔArch angle (°)	11.29 ± 1.47	11.22 ± 2.26	9.69 ± 3.74	9.60 ± 2.79
Maximum arch angle (°)	170.07 ± 6.51	161.45 ± 5.00*	160.58 ± 5.47	160.20 ± 4.63
Arch height at touchdown (cm)(cm)	1.84 ± 0.30*#	2.43 ± 0.30*	2.44 ± 0.44	2.41 ± 0.24
ΔArch height (cm)	0.44 ± 0.19	0.57 ± 0.17*	0.52 ± 0.21	0.54 ± 0.18
Arch stiffness (N/cm·kg$^{2/3}$)	266.47 ± 142.63	177.68 ± 64.47*	269.20 ± 210.21	203.77 ± 71.77
FFS				
Δ Arch angle (°)	15.47 ± 2.22	15.59 ± 2.05	12.14 ± 3.04	13.59 ± 2.73
Maximum arch angle (°)	169.48 ± 18.27	161.02 ± 4.72	158.40 ± 7.41	159.92 ± 4.00
Arch height at touchdown (cm)(cm)	2.47 ± 0.33	2.72 ± 0.30*	2.71 ± 0.56	2.68 ± 0.20
Δ Arch height (cm)	0.81 ± 0.19	0.87 ± 0.19	0.76 ± 0.21	0.84 ± 0.19
Arch stiffness (N/cm·kg$^{2/3}$)	127.51 ± 30.25	119.15 ± 30.10	161.74 ± 76.30	132.75 ± 30.47

* significant difference from pre- to post-tests.

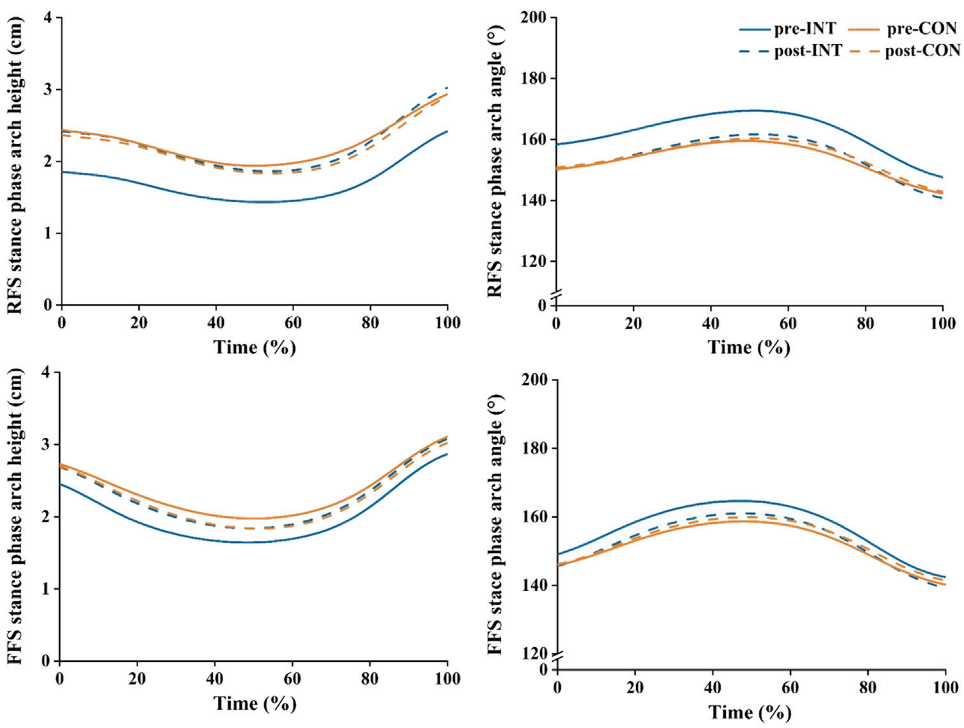

FIGURE 9
Effects of a 12-week gait retraining program combined with foot core exercise on the arch height and angle.

0.401), the maximum arch angle ($F_{1,23} = 221.248$, $p < 0.001$, $\eta_p^2 = 0.906$), the arch height at touchdown ($F_{1,23} = 77.381$, $p < 0.001$, $\eta_p^2 = 0.771$), Δarch height ($F_{1,23} = 13.565$, $p = 0.001$, $\eta_p^2 = 0.371$), and arch stiffness ($F_{1,23} = 20.507$, $p < 0.001$, $\eta_p^2 = 0.471$). Paired *t*-tests indicated that after the intervention, the arch height at touchdown increased significantly in the INT group ($p = 0.040$, Cohen's $d = 0.81$), while no significant changes in the CON group ($p = 0.845$, Cohen's $d = 0.08$) (Table 5; Figure 9).

4 Discussion

The purpose of this study was to investigate the effect of a 12-week gait retraining program combined with foot core exercise on arch morphology and arch muscle strength, and to further explore changes in arch kinematics in the RFS and FFS patterns. Overall, 12-week gait retraining combined with foot core exercise improved the arch height when standing, strengthen the toe flexors, decrease the maximum arch angle, and increase the arch height at touchdown during RFS running. Furthermore, the proposed intervention caused adaptive changes in the arch and surrounding muscles, which were also reflected in the arch kinematic of the running gait.

4.1 Arch morphology

The 12-week gait retraining combined with foot core exercise significantly increased the normalized standing arch height in the INT group, thus corroborating the finding of McKeon et al. (McKeon et al., 2015). Moreover, the improvement reached a moderate effect size (Cohen's d = 0.55), which was superior to previous studies with no significant changes in arch height after standalone interventions (Lynn et al., 2012; Miller et al., 2014). Some researchers pointed out that the function of the foot intrinsic muscles is directly related to the structure of the longitudinal arch (Fiolkowski et al., 2003; Soysa et al., 2012; Kelly et al., 2014; Xiao et al., 2020). For example, to prevent the occurrence of excessive arch deformation, the recruitment of foot muscles increases with external increasing load when a decrease in electromyographic activity of these muscles leads to an increase in the navicular drop, thus revealing the relationship between the lower extremity loading and the foot muscles activation levels (Fiolkowski et al., 2003; Kelly et al., 2014). Accordingly, the shape of the arch could be stabilized by strengthening the foot muscles using the rowel curls, foot doming, and toe spread, which were proven to be effective interventions to strengthen the arch muscles (Jung et al., 2011; Yoo, 2014; McKeon et al., 2015). In addition, forefoot strike running with minimal shoes can stimulate the arch muscle function development in the activity due to the lack of plantar support, which will increase the work requirements of the foot and ankle muscles (Altman and Davis, 2012). For example, an intervention comprising 12-week forefoot running in minimal shoes increased the anatomical cross-sectional area and muscle volume of flexor digitorum brevis and abductor digiti minimi (Miller et al., 2014). Studies have also shown that the cross-sectional area is proportional to the maximum strength of the muscle (An et al., 1991). Given a number of studies that the foot intrinsic and extrinsic muscles are effective in maintaining the arch shape, the 12-week intervention method in this research can strengthen the function of the foot muscles and improve the arch shape under the condition of weight-bearing.

4.2 Arch muscles strength

After the 12-week gait retraining combined with foot core exercise, the strength of hallux flexion and the MPJ flexors improved effectively. It is worth noting that the improvements in arch muscles strength all had a moderate to large effect size, with the percentage change in relative strength of the MPJ flexors reaching 32.5%, which was higher than that achieved by Day and Hahn (2019) who used foot muscle training alone (27%). The plantar intrinsic muscles include abductor hallucis, flexor digitorum brevis and quadratus plantae as accessory toe flexors (Kelly et al., 2014), which produce force at the MPJ (Koyama et al., 2019). In the single-support phase and early stage of double support phase in the gait, the metatarsophalangeal moment plays a role in controlling the angular momentum of the whole body, with the maximum metatarsophalangeal moment being as large as one-fifth to one-third of the maximum ankle joint plantarflexion moment (Miyazaki and Yamamoto, 1993). Accordingly, the toe flexion and extension activities are particularly important in running and jumping, which need the action to push off. Therefore, many coaches of sprint and jumping events believe that increasing the output power of the MPJ can improve athletes' sports performance (Goldmann et al., 2013).

These muscles that affect the strength of the MPJ are also necessary structures to support the longitudinal arch. A previous study has provided evidence that strengthening these muscles can attenuate the mechanical load directly related to running-related injuries, with the result that participants in the foot core training group had a 2.42-fold lower rate of running-related injuries compared with the control group (Taddei et al., 2020). In our research, an intervention method combining FFS training and foot core exercise was used to try to strengthen the arch muscles' ability to exert force in a relatively static and running gait. Some of our findings confirm the hypothesis of this research, therefore, our methods can be referenced by athletes in running and jumping events to obtain stronger foot muscle function.

4.3 Arch kinematics and arch stiffness

During RFS, the 12-week gait retraining combined with foot core exercise reduced the maximal arch angle by 5.1% while increasing the arch height at touchdown by 32.1%. However, Day and Hahn (2019) showed that foot muscle training alone had no effect on the mechanics of the MPJ and ankle during running, suggesting that kinematic changes in this study may benefit from additional effects of the combined intervention. When a certain type of exercise forms a repetitive load on the body, special neuromuscular adaptability will appear, such as the sport-specific adaptability of foot muscle function and foot structure (Häkkinen and Keskinen, 1989; Koyama et al., 2019). In the late swing of FFS, the abductor hallucis activation is increased, resulting in a higher arch at touchdown to allow the midfoot to compress a larger range of motion during the stance phase without altering arch peak deformation (McDonald et al., 2016; Kelly et al., 2018). Considering the abovementioned results of arch muscle strength, the foot training methods in this research effectively enhanced the arch muscles, and the arch kinematic performance in running was improved to a certain extent. Furthermore, when considering how to increase the foot-spring function during the gait, Perl et al. (Perl et al., 2012) found that at the same running speed, the FFS pattern has higher arch compliance compared to RFS, which means a greater range of midfoot motion. As the foot intrinsic muscles and tendons have relatively long tendons, they can be stretched and shortened during the running stance phase, thus allowing the storage of energy in the tendons. The resulting higher compliance may be very conducive to elastic energy storage and release, thus reducing the elastic potential energy loss in this process (Kelly et al., 2018). This research found that after intervention training, RFS showed similarities in arch movement characteristics with the FFS, namely, the arch height increased at touchdown, and the motion of the midfoot increased. However, whether the increase in the motion of the midfoot during the RFS stance phase is conducive to the advancement of the body may require further analysis.

The arch stiffness decreased in the post condition during RFS, it may be that the participants gradually mastered a more comfortable running gait during multiple familiarization sessions prior to the test to reduce the peak impact in the RFS (Altman and Davis, 2012; Thompson et al., 2015). Furthermore, the greater decrease in stiffness in the INT group (33.3%) than in the CON group (24.3%) may benefit from the increased compliance of the arch due to the 12-week gait retraining program combined with foot core exercise (Kelly et al., 2018).

In summary, the 12-week gait retraining combined with foot core exercise in this study had certain effects on the arch morphology, arch muscle strength, and arch kinematics characteristics of RFS. As an important part of the lower limb system, whether the changes in the arch kinematics during the RFS are beneficial to the health of the foot may need further exploration.

There are several limitations to this study: 1) we did not continue to observe the adaptive changes of arch function in different running postures to judge the durability of the intervention; 2) arch dynamics were not analyzed in this study, which may further explore the arch work in different running strike patterns; and 3) only male habitual runners were recruited in this study.

5 Conclusion

The 12-week gait retraining program combined with foot core exercise significantly increased the normalized navicular height during standing and the strength of arch muscles. During RFS running, such intervention decreased the maximum arch angle and increase arch height at touchdown, which indicated that the arch was improved in both static and dynamic positions. Furthermore, all of these significant changes had a moderate to large effect size, demonstrating the superiority of the combined intervention over the standalone interventions. Therefore, it is recommended that runners with weak arch muscles use this combined intervention as an approach to strengthen the arch muscles.

Data availability statement

The original contributions presented in the study are included in the article/supplementary material, further inquiries can be directed to the corresponding author.

Ethics statement

The studies involving human participants were reviewed and approved by the Human Ethics Committee of Shanghai University of Sport. The patients/participants provided their written informed consent to participate in this study.

Author contributions

BS and SZ contributed to study design, data collection, drafting and revising the manuscript; KC and WF, contributed to supervising study design, completing data analysis and interpretation, and revising the manuscript; XZ revised the manuscript. All authors have read and approved the final version of the manuscript and agree with the order of the presentation of the authors.

Funding

This research was funded by the National Key Technology Research and Development Program of the Ministry of Science and Technology of China (2021YFC2009201), the National Natural Science Foundation of China (12272238, 11772201), the "Outstanding Young Scholar" Program of Shanghai Municipal and the "Dawn" Program of Shanghai Education Commission, China (19SG47).

Conflict of interest

The authors declare that the research was conducted in the absence of any commercial or financial relationships that could be construed as a potential conflict of interest.

Publisher's note

References

Altman, A. R., and Davis, I. S. (2012). Barefoot running: biomechanics and implications for running injuries. *Curr. Sports Med. Rep.* 11 (5), 244–250. doi:10.1249/JSR.0b013e31826c9bb9

An, K. N., Linscheid, R. L., and Brand, P. W. (1991). Correlation of physiological cross-sectional areas of muscle and tendon. *J. hand Surg. Edinb. Scotl.* 16 (1), 66–67. doi:10.1016/0266-7681(91)90130-g

Butler, R. J., Hillstrom, H., Song, J., Richards, C. J., and Davis, I. S. (2008). Arch height index measurement system: establishment of reliability and normative values. *J. Am. Podiatr. Med. Assoc.* 98 (2), 102–106. doi:10.7547/0980102

Cheung, R. T. H., Sze, L. K. Y., Mok, N. W., and Ng, G. Y. F. (2016). Intrinsic foot muscle volume in experienced runners with and without chronic plantar fasciitis. *J. Sci. Med. Sport* 19 (9), 713–715. doi:10.1016/j.jsams.2015.11.004

Day, E. M., and Hahn, M. E. (2019). Increased toe-flexor muscle strength does not alter metatarsophalangeal and ankle joint mechanics or running economy. *J. Sports Sci.* 37 (23), 2702–2710. doi:10.1080/02640414.2019.1661562

De Wit, B., De Clercq, D., and Aerts, P. (2000). Biomechanical analysis of the stance phase during barefoot and shod running. *J. Biomechanics* 33 (3), 269–278. doi:10.1016/s0021-9290(99)00192-x

Deng, L., Zhang, X., Xiao, S., Yang, Y., Li, L., and Fu, W. (2020). Changes in the plantar flexion torque of the ankle and in the morphological characteristics and mechanical properties of the Achilles tendon after 12-week gait retraining. *Life (Basel)* 10 (9), 159. doi:10.3390/life10090159

Faul, F., Erdfelder, E., Lang, A. G., and Buchner, A. (2007). G*Power 3: a flexible statistical power analysis program for the social, behavioral, and biomedical sciences. *Behav. Res. Methods* 39 (2), 175–191. doi:10.3758/bf03193146

Fiolkowski, P., Brunt, D., Bishop, M., Woo, R., and Horodyski, M. (2003). Intrinsic pedal musculature support of the medial longitudinal arch: an electromyography study. *J. Foot Ankle Surg.* 42 (6), 327–333. doi:10.1053/j.jfas.2003.10.003

Golano, P., Fariñas, O., and Sáenz, I. (2004). The anatomy of the navicular and periarticular structures. *Foot ankle Clin.* 9 (1), 1–23. doi:10.1016/S1083-7515(03)00155-4

Goldmann, J. P., Sanno, M., Willwacher, S., Kai, H., and Brüggemann, G. P. (2013). The potential of toe flexor muscles to enhance performance. *J. Sports Sci.* 31 (4), 424–433. doi:10.1080/02640414.2012.736627

Goo, Y. M., Heo, H. J., and An, D. H. (2014). EMG activity of the abductor hallucis muscle during foot arch exercises using different weight bearing postures. *J. Phys. Ther. Sci.* 26 (10), 1635–1636. doi:10.1589/jpts.26.1635

Häkkinen, K., and Keskinen, K. L. (1989). Muscle cross-sectional area and voluntary force production characteristics in elite strength- and endurance-trained athletes and sprinters. *Eur. J. Appl. Physiol. Occup. Physiol.* 59 (3), 215–220. doi:10.1007/bf02386190

Hespanhol Junior, L. C., de Carvalho, A. C., Costa, L. O., and Lopes, A. D. (2016). Lower limb alignment characteristics are not associated with running injuries in runners: Prospective cohort study. *Eur. J. Sport Sci.* 16 (8), 1137–1144. doi:10.1080/17461391.2016.1195878

Holowka, N. B., Wallace, I. J., and Lieberman, D. E. (2018). Foot strength and stiffness are related to footwear use in a comparison of minimally- vs. conventionally-shod populations. *Sci. Rep.* 8 (1), 3679. doi:10.1038/s41598-018-21916-7

Jenkins, D. W., and Cauthon, D. J. (2011). Barefoot running claims and controversies: a review of the literature. *J. Am. Podiatr. Med. Assoc.* 101 (3), 231–246. doi:10.7547/1010231

Jung, D. Y., Kim, M. H., Koh, E. K., Kwon, O. Y., Cynn, H. S., and Lee, W. H. (2011). A comparison in the muscle activity of the abductor hallucis and the medial longitudinal arch angle during toe curl and short foot exercises. *Phys. Ther. Sport* 12 (1), 30–35. doi:10.1016/j.ptsp.2010.08.001

Kakouris, N., Yener, N., and Fong, D. T. P. (2021). A systematic review of running-related musculoskeletal injuries in runners. *J. Sport Health Sci.* 10 (5), 513–522. doi:10.1016/j.jshs.2021.04.001

Kamonseki, D. H., Goncalves, G. A., Yi, L. C., and Junior, I. L. (2016). Effect of stretching with and without muscle strengthening exercises for the foot and hip in patients with plantar fasciitis: A randomized controlled single-blind clinical trial. *Man. Ther.* 23, 76–82. doi:10.1016/j.math.2015.10.006

Kelly, L. A., Cresswell, A. G., Racinais, S., Whiteley, R., and Lichtwark, G. (2014). Intrinsic foot muscles have the capacity to control deformation of the longitudinal arch. *J. R. Soc. Interface* 11 (93), 20131188. doi:10.1098/rsif.2013.1188

Kelly, L. A., Farris, D. J., Lichtwark, G. A., and Cresswell, A. G. (2018). The influence of foot-strike technique on the neuromechanical function of the foot. *Med. Sci. Sports Exerc.* 50 (1), 98–108. doi:10.1249/mss.0000000000001420

Kelly, L. A., Lichtwark, G. A., Farris, D. J., and Cresswell, A. (2016). Shoes alter the spring-like function of the human foot during running. *J. R. Soc. Interface* 13 (119), 20160174. doi:10.1098/rsif.2016.0174

Ker, R. F., Bennett, M. B., Bibby, S. R., Kester, R. C., and Alexander, R. M. (1987). The spring in the arch of the human foot. *Nature* 325 (7000), 147–149. doi:10.1038/325147a0

Koyama, K., Hirokawa, M., Yoshitaka, Y., and Yamauchi, J. (2019). Toe flexor muscle strength and morphological characteristics of the foot in judo athletes. *Int. J. Sports Med.* 40 (4), 263–268. doi:10.1055/a-0796-6679

Krabak, B., Lipman, G., and Waite, B. (2017). *The long distance runner's guide to injury prevention and treatment: How to avoid common problems and deal with them when they happen*. New York: Simon & Schuster.

Langley, B., Cramp, M., and Morrison, S. C. (2016). Clinical measures of static foot posture do not agree. *J. Foot Ankle Res.* 9, 45–46. doi:10.1186/s13047-016-0180-3

Lieberman, D. E., Venkadesan, M., Werbel, W. A., Daoud, A. I., D'Andrea, S., Davis, I. S., et al. (2010). Foot strike patterns and collision forces in habitually barefoot versus shod runners. *Nature* 463 (7280), 531–535. doi:10.1038/nature08723

Lieberman, D. E. (2012). What we can learn about running from barefoot running: an evolutionary medical perspective. *Exerc. Sport Sci. Rev.* 40 (2), 63–72. doi:10.1097/JES.0b013e31824ab210

Lynn, S. K., Padilla, R. A., and Tsang, K. K. (2012). Differences in static- and dynamic-balance task performance after 4 weeks of intrinsic-foot-muscle training: the short-foot exercise versus the towel-curl exercise. *J. Sport Rehabilitation* 21 (4), 327–333. doi:10.1123/jsr.21.4.327

Man, H. S., Leung, A. K., Cheung, J. T., and Sterzing, T. (2016). Reliability of metatarsophalangeal and ankle joint torque measurements by an innovative device. *Gait Posture* 48, 189–193. doi:10.1016/j.gaitpost.2016.05.016

McCarthy, C., Fleming, N., Donne, B., and Blanksby, B. (2014). 12 weeks of simulated barefoot running changes foot-strike patterns in female runners. *Int. J. Sports Med.* 35 (5), 443–450. doi:10.1055/s-0033-1353215

McDonald, K. A., Stearne, S. M., Alderson, J. A., North, I., Pires, N. J., and Rubenson, J. (2016). The role of arch compression and metatarsophalangeal joint dynamics in modulating plantar fascia strain in running. *PLoS One* 11 (4), e0152602. doi:10.1371/journal.pone.0152602

McKeon, P. O., Hertel, J., Bramble, D., and Davis, I. (2015). The foot core system: a new paradigm for understanding intrinsic foot muscle function. *Br. J. Sports Med.* 49 (5), 290. doi:10.1136/bjsports-2013-092690

Miller, E. E., Whitcome, K. K., Lieberman, D. E., Norton, H. L., and Dyer, R. E. (2014). The effect of minimal shoes on arch structure and intrinsic foot muscle strength. *J. Sport Health Sci.* 3 (2), 74–85. doi:10.1016/j.jshs.2014.03.011

Milner, C. E., Ferber, R., Pollard, C. D., Hamill, J., and Davis, I. S. (2006). Biomechanical factors associated with tibial stress fracture in female runners. *Med. Sci. Sports Exerc.* 38 (2), 323–328. doi:10.1249/01.mss.0000183477.75808.92

Miyazaki, S., and Yamamoto, S. (1993). Moment acting at the metatarsophalangeal joints during normal barefoot level walking. *Gait Posture* 1 (3), 133–140. doi:10.1016/0966-6362(93)90054-5

Moher, D., Hopewell, S., Schulz, K. F., Montori, V., Gøtzsche, P. C., Devereaux, P. J., et al. (2010). CONSORT 2010 explanation and elaboration: updated guidelines for reporting parallel group randomised trials. *BMJ* 340, c869. doi:10.1136/bmj.c869

Mulligan, E. P., and Cook, P. G. (2013). Effect of plantar intrinsic muscle training on medial longitudinal arch morphology and dynamic function. *Man. Ther.* 18 (5), 425–430. doi:10.1016/j.math.2013.02.007

Paquette, M. R., Zhang, S., and Baumgartner, L. D. (2013). Acute effects of barefoot, minimal shoes and running shoes on lower limb mechanics in rear and forefoot strike runners. *Footwear Sci.* 7 (3), 9–18. doi:10.1080/19424280.2012.692724

Perl, D. P., Daoud, A. I., and Lieberman, D. E. (2012). Effects of footwear and strike type on running economy. *Med. Sci. Sports Exerc.* 44 (7), 1335–1343. doi:10.1249/MSS.0b013e318247989e

Rice, H., and Patel, M. (2017). Manipulation of foot strike and footwear increases Achilles tendon loading during running. *Am. J. Sports Med.* 45 (10), 2411–2417. doi:10.1177/0363546517704429

Ridge, S. T., Johnson, A. W., Mitchell, U. H., Hunter, I., Robinson, E., Rich, B. S., et al. (2013). Foot bone marrow edema after a 10-wk transition to minimalist running shoes. *Med. Sci. Sports Exerc.* 45 (7), 1363–1368. doi:10.1249/MSS.0b013e3182874769

Ridge, S. T., Myrer, J. W., Olsen, M. T., Jurgensmeier, K., and Johnson, A. W. (2017). Reliability of doming and toe flexion testing to quantify foot muscle strength. *J. Foot Ankle Res.* 10, 55. doi:10.1186/s13047-017-0237-y

Ridge, S. T., Olsen, M. T., Bruening, D. A., Jurgensmeier, K., Griffin, D., Davis, I. S., et al. (2019). Walking in minimalist shoes is effective for strengthening foot muscles. *Med. Sci. Sports Exerc.* 51 (1), 104–113. doi:10.1249/mss.0000000000001751

Rothermel, S. A., Hale, S. A., Hertel, J., and Denegar, C. R. (2004). Effect of active foot positioning on the outcome of a balance training program. *Phys. Ther. Sport* 5 (2), 98–103. doi:10.1016/s1466-853x(04)00027-6

Soysa, A., Hiller, C., Refshauge, K., and Burns, J. (2012). Importance and challenges of measuring intrinsic foot muscle strength. *J. Foot Ankle Res.* 5 (1), 29. doi:10.1186/1757-1146-5-29

Stearne, S. M., McDonald, K. A., Alderson, J. A., North, I., Oxnard, C. E., and Rubenson, J. (2016). The foot's arch and the energetics of human locomotion. *Sci. Rep.* 6, 19403. doi:10.1038/srep19403

Taddei, U. T., Matias, A. B., Duarte, M., and Sacco, I. C. N. (2020). Foot core training to prevent running-related injuries: A survival analysis of a single-blind, randomized controlled trial. *Am. J. Sports Med.* 48 (14), 3610–3619. doi:10.1177/0363546520969205

Tam, N., Tucker, R., Astephen Wilson, J. L., and Santos-Concejero, J. (2015). Effect on oxygen cost of transport from 8-weeks of progressive training with barefoot running. *Int. J. Sports Med.* 36 (13), 1100–1105. doi:10.1055/s-0035-1548888

Taunton, J. E., Ryan, M. B., Clement, D. B., Mckenzie, D. C., and Lloyd-Smith, D. R. (2002). Plantar fasciitis: a retrospective analysis of 267 cases. *Phys. Ther. Sport* 3 (2), 57–65. doi:10.1054/ptsp.2001.0082

Thompson, M. A., Lee, S. S., Seegmiller, J., and McGowan, C. P. (2015). Kinematic and kinetic comparison of barefoot and shod running in mid/forefoot and rearfoot strike runners. *Gait Posture* 41 (4), 957–959. doi:10.1016/j.gaitpost.2015.03.002

van Gent, R. N., Siem, D., van Middelkoop, M., van Os, A. G., Bierma-Zeinstra, S. M., Koes, B. W., et al. (2007). Incidence and determinants of lower extremity running injuries in long distance runners: a systematic review * COMMENTARY. *Br. J. Sports Med.* 41 (8), 469–480. doi:10.1136/bjsm.2006.033548

Wang, B., Yang, Y., Zhang, X., Wang, J., Deng, L., and Fu, W. (2020). Twelve-week gait retraining reduced patellofemoral joint stress during running in male recreational runners. *BioMed Res. Int.* 2020, 1–9. doi:10.1155/2020/9723563

Wang, J., Luo, Z., Dai, B., and Fu, W. (2020). Effects of 12-week cadence retraining on impact peak, load rates and lower extremity biomechanics in running. *PeerJ* 8, e9813. doi:10.7717/peerj.9813

Wang, S., Chan, P. P. K., Lam, B. M. F., Chan, Z. Y. S., Zhang, J. H. W., Wang, C., et al. (2021). Sensor-based gait retraining lowers knee adduction moment and improves symptoms in patients with knee osteoarthritis: A randomized controlled trial. *Sensors (Basel)* 21 (16), 5596. doi:10.3390/s21165596

Warne, J. P., Kilduff, S. M., Gregan, B. C., Nevill, A. M., Moran, K. A., and Warrington, G. D. (2014). A 4-week instructed minimalist running transition and gait-retraining changes plantar pressure and force. *Scand. J. Med. Sci. Sports* 24 (6), 964–973. doi:10.1111/sms.12121

Williams, D. S., 3rd, Green, D. H., and Wurzinger, B. (2012). Changes in lower extremity movement and power absorption during forefoot striking and barefoot running. *Int. J. Sports Phys. Ther.* 7 (5), 525–532.

Williams, D. S., and Mcclay, I. S. (2000). Measurements used to characterize the foot and the medial longitudinal arch: reliability and validity. *Phys. Ther.* 80 (9), 864–871. doi:10.1093/ptj/80.9.864

Xiao, S., Zhang, X., Deng, L., Zhang, S., Cui, K., and Fu, W. (2020). Relationships between foot morphology and foot muscle strength in healthy adults. *Int. J. Environ. Res. Public Health* 17 (4), 1274. doi:10.3390/ijerph17041274

Yang, Y., Zhang, X., Luo, Z., Wang, X., Ye, D., and Fu, W. (2020). Alterations in running biomechanics after 12 Week gait retraining with minimalist shoes. *Int. J. Environ. Res. Public Health* 17 (3), 818. doi:10.3390/ijerph17030818

Yoo, W. G. (2014). Effect of the intrinsic foot muscle exercise combined with interphalangeal flexion exercise on metatarsalgia with morton's toe. *J. Phys. Ther. Sci.* 26 (12), 1997–1998. doi:10.1589/jpts.26.1997

Zhang, S., Fu, W., and Liu, Y. (2019). Does habitual rear-foot strike pattern with modern running shoes affect the muscle strength of the longitudinal arch? *Isokinet. Exerc. Sci.* 27 (3), 213–218. doi:10.3233/ies-192139

Zhang, X., Deng, L., Yang, Y., Xiao, S., Li, L., and Fu, W. (2021). Effects of 12-week transition training with minimalist shoes on Achilles tendon loading in habitual rearfoot strike runners. *J. Biomechanics* 128, 110807. doi:10.1016/j.jbiomech.2021.110807

Zhang, X., Luo, Z., Wang, J., Yang, Y., and Fu, W. (2020). Ultrasound-based mechanical adaptation of Achilles tendon after 12-week running with minimalist shoes. *J. Med. Imaging Health Inf.* 10 (5), 1205–1209. doi:10.1166/jmihi.2020.2997

frontiers | Frontiers in Physiology

TYPE Original Research
PUBLISHED 11 October 2022
DOI 10.3389/fphys.2022.1006179

OPEN ACCESS

EDITED BY
Qichang Mei,
Ningbo University, China

REVIEWED BY
Tianyun Jiang,
China Academy of Chinese Medical Sciences, China
Fei-Long Wei,
Fourth Military Medical University (Air Force Medical University), China

*CORRESPONDENCE
Baoge Liu,
baogeliu@hotmail.com

SPECIALTY SECTION
This article was submitted to Exercise Physiology,
a section of the journal
Frontiers in Physiology

RECEIVED 29 July 2022
ACCEPTED 20 September 2022
PUBLISHED 11 October 2022

CITATION
Wang D and Liu B (2022), Effects of hanger reflex on the cervical muscular activation and function: A surface electromyography assessment.
Front. Physiol. 13:1006179.
doi: 10.3389/fphys.2022.1006179

Effects of hanger reflex on the cervical muscular activation and function: A surface electromyography assessment

Dian Wang and Baoge Liu*

Department of Orthopaedic Surgery, Beijing Tiantan Hospital, Capital Medical University, Beijing, China

Introduction: Cervical muscular dysfunction is closely associated with disorders and neuromuscular diseases of the cervical spine, and the hanger reflex (HR) has the potential to become a rehabilitation method. The muscular electrophysiology mechanism of HR is unclear. This study aims to identify the impacts of HR on cervical rotators' myoelectrical activity and function.

Methods: We designed a self-control clinical trial, and asymptomatic volunteers were continuously included from 1 September 2021 to 30 April 2022 in our department. Rotation tasks were performed on both sides under each of the situations: no HR, unilateral HR, and bilateral HR. Surface electromyography (SEMG) was used to detect the myoelectrical activity of agonistic splenius capitis (SPL), upper trapezius (UTr), and sternocleidomastoid (SCM). The co-contraction ratio (CCR) during rotation tasks was calculated. Correlation analyses and multiple linear regression were performed.

Results: Finally, 90 subjects were enrolled (power >90%). The adjusted EMG value (aEMG) of SPL UTr, SCM, and rotating CCR under the unilateral HR and bilateral HR were higher than no HR; the aEMG of SPL and rotating CCR under the bilateral HR were higher than the unilateral HR. Multiple linear regression showed that HR pattern and age were the independent affecting factors for the aEMG of SPL ($p < 0.001$, $p < 0.001$), UTr ($p < 0.001$, $p < 0.001$), and SCM ($p < 0.001$, $p < 0.001$); BMI was an independent affecting factor for the aEMG of SPL ($p < 0.001$) and SCM ($p < 0.001$); HR pattern was the only affecting factor for CCR ($p < 0.001$).

Conclusion: HR can increase the cervical rotators' myoelectrical activities and rotating CCR, and the effects of bilateral HR are greater than unilateral HR, suggesting that bilateral HR has a greater clinical potential to become a rehabilitation method for treating cervical neuromuscular disorders.

KEYWORDS

muscular function, hanger reflex, electrophysiology, surface electromyography, co-contraction ratio, cervical stability, neuromuscular disorder

Introduction

Cervical muscular function is of great significance to the cervical stability, alignment, head posture, and motion (Cheng et al., 2011; Thakar et al., 2014; Ding et al., 2020). Cervical muscular dysfunction can contribute to a series of disorders and neuromuscular diseases, such as neck pain (NP) (Cheng et al., 2011), cervical dystonia, and cervical bending and rotation deformities (Hussein et al., 2017), as well as abnormal postures, such as wryneck posture. Rehabilitation and non-invasive treatments are always needed for treating the cervical disorders related to muscular dysfunction.

The hanger reflex (HR) is an involuntary head rotation that occurs in response to a clothes hanger encircling the head, which compresses the unilateral frontal-temporal area (Asahi et al., 2018). In this situation, the head will rotate towards the compressed side spontaneously, which is termed as the HR (Asahi et al., 2018; Agyei et al., 2019; Asahi et al., 2020). HR is a general phenomenon in populations, and it can be observed in 92.1% of the healthy subjects (Asahi et al., 2015). The mechanism of HR is closely related to the deep sensation-associated cervical muscular activation. It has been reported that HR can correct the abnormal head position in patients with cervical dystonia (Asahi et al., 2018), and HR can be used as a potential rehabilitation method for cervical muscular dysfunction and disorders (Asahi et al., 2018; Asahi et al., 2020).

To our knowledge, the potential mechanism of HR on the cervical rotators is still unclear. Although previous studies have proved the HR phenomenon and estimated the efficacy on several kinds of muscular diseases, the muscular electrophysiology mechanism of HR is still unclear. The superficial and deep cervical rotators synergistically contribute to the posture control and rotation movement (Panjabi et al., 1998; Cheng et al., 2011; Agyei et al., 2019). This study aims to identify the impacts of HR on myoelectrical activity of cervical rotators and neuromuscular function, as well as the affecting factors. We hypothesized that: 1) the subject's general characteristics may have impacts on the cervical rotators' myoelectrical activity; 2) the different HR patterns may be an independent affecting factor of the cervical rotators' electrophysiology function.

Materials and methods

Subjects and enrollment

This was a self-control clinical trial, and asymptomatic volunteers were continuously included from 1 September 2021 to 30 April 2022 in our department.

The inclusion criteria were as follows: 1) asymptomatic volunteer; 2) 20–65 years, BMI < 28. The exclusion criteria were as follows: 1) Parkinson's disease, amyotrophic lateral sclerosis, and the other neuromuscular diseases (Ding et al., 2020); 2) history of spinal deformity, spinal tumor, or compression fracture; 3) surgery history of spine; 4) moderate neck pain with a visual analogue scale (VAS) > 3 (Falla et al., 2007); 5) can not cooperate to the surface electromyography (SEMG) test.

The Institutional Review Board of our hospital has approved human subject protection programs and procedures (Ethic number, KY 2020–073-02). Informed consent was acquired from all participants. The general characteristics included sex, age, height, weight, and BMI.

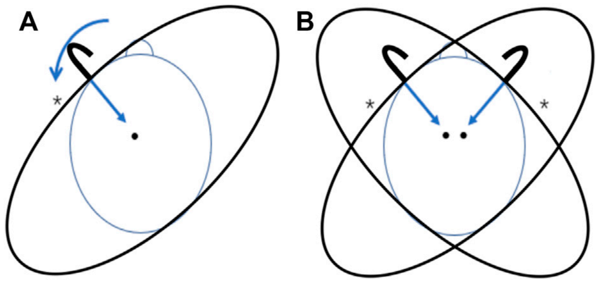

FIGURE 1
The unilateral and bilateral HR. **(A)** Unilateral HR on the left side, the hanger was placed on the left frontal-temporal area; **(B)** Bilateral HR, two hangers were placed on both sides of the frontal-temporal areas; *, the compressed side of HR.

Unilateral and bilateral hanger reflex

An ordinary wire clothes hanger was used for the HR, which was flexible and large enough to encircle the subject's head. The HR of present study consisted of a unilateral HR and a bilateral HR.

In the unilateral HR, the hanger was placed on a unilateral frontal-temporal area, and the subject's head would rotate to the compressed side spontaneously due to the compression (Figure 1A). In the bilateral HR, two hangers were placed on both sides of the frontal-temporal areas (Figure 1B).

Rotation task

The rotation task comprised 3 phases of movement: the resting phase (phase I), axial rotation to one side (phase II, rotating phase, subject was asked to rotate to the compressed side), and rotation to the neutral position (phase III, returning phase, subject was asked to rotate to the neutral position), and each movement phase lasted 4 s at a constant speed process (Cheng et al., 2008).

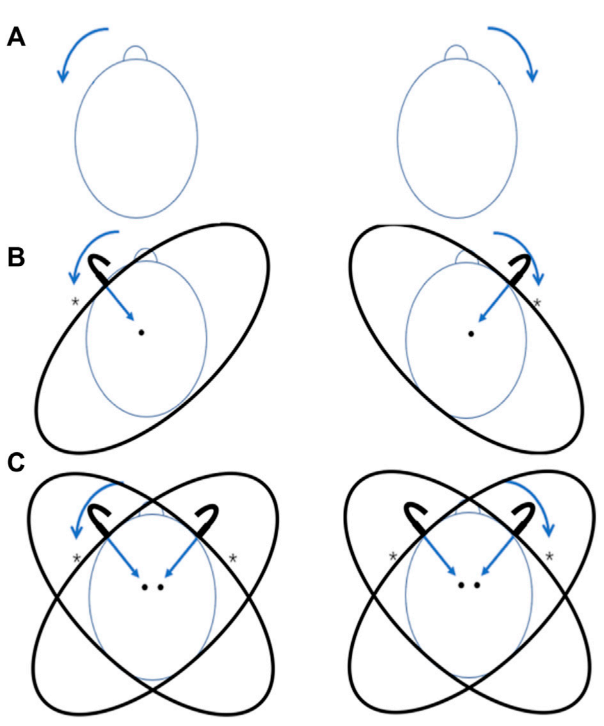

FIGURE 2
The rotation tasks at on no HR, unilateral and bilateral HR. **(A)** Subjects were asked to start the rotation tasks firstly on the left then the right; **(B)** The compressed sides of unilateral HR were set firstly on the left then the right, and subjects were asked to rotate their heads to the compressed side respectively (first the left then the right); **(C)** In bilateral HR, subjects were asked to start the rotation tasks firstly on the left then the right; *, the compressed side of HR; brow peak, the rotation direction.

Rotation tasks were performed on both sides (first the left then the right) under each of the situations: no HR (Figure 2A), unilateral HR (Figure 2B), and bilateral HR (Figure 2C). The unilateral HR was started on the left side (the compressed side was set on the left side firstly) and then transferred to the right side (Figure 2B). The bilateral HR was also started on the left side, followed by the right side with bilateral compression (Figure 2C). 1 subject provided 2 data (left and right), and both were from the compressed sides (first the left then the right).

SEMG-based muscle electrical activities and co-contraction ratio

SEMG is an objective and non-invasive tool for detecting myoelectrical activities and assessing muscular function (Colloca and Hinrichs, 2005; Marshall and Murphy, 2006). The myoelectrical activity of splenius capitis (SPL), upper trapezius (UTr), and sternocleidomastoid (SCM) were recorded with a SEMG device (FlexComp Infiniti System, T7550, Thought Technology Ltd, Canada) during the rotation tasks. The electrodes (Ag–AgCl electrode, diameter 2 cm, CH55RD, Cathay manufacturing group, Shanghai, China) for SPL were located 2 cm from the spinous process at the C4 level (Joines et al., 2006; Ding et al., 2020), and the electrodes for UTR were located at the midpoint of a line between the C7 spinous process and the middle of the acromion (Ding et al., 2020), the electrodes for SCM were located at the lower one-third of the mastoid process and sternal notch (Falla et al., 2002) (Figure 3).

All subjects were asked to perform the rotation task (rotated to left/right sides) for 6 times: with no HR, with unilateral HR (compressed side: left/right), and with bilateral HR. There was a 2-min break between each task to minimize the effects of fatigue (Cheng et al., 2008). To familiarize the subjects with the movement phases and speeds, sufficient practice was needed. The SEMG signal was 1000 Hz and was band-pass filtered between 20 and 450 Hz. The electromyogram (EMG) of SPL, UTr, and SCM (agonists) on the ipsilateral side of the rotating orientation were recorded during the tasks, and the root mean square (RMS) values of EMG were calculated automatically by the system. Finally, the adjusted EMG value (aEMG) of SPL, UTr, and SCM under no HR, unilateral HR, and bilateral HR were calculated. The aEMG = the maximal activity during the rotating phase - mean activity during the returning phase.

The sEMG-based CCR is an objective and quantified method for assessing the co-contraction pattern of the muscular system of cervical spine (Cheng et al., 2008; Chih-hsiu et al., 2014). CCR is the reference for the coordination of agonists and antagonists in a balanced muscular system. The maximal voluntary isometric contraction (MVIC) of SPL, UTr, and SCM was recorded for 3-s. The normalized average integration EMG (NAIEMG) during the rotating phase was calculated, using the central 1-s MVIC as reference (Chih-hsiu et al., 2014). The rotating CCR under no HR, unilateral HR, and bilateral HR were calculated. CCR = NAIEMG of the agonists (ipsilateral SPL+UTr+SC)/ NAIEMG of total muscle (ipsilateral and contralateral SPL+UTr+SC).

Statistical analysis

The sample size was calculated with a formula: $n=(\mu\alpha+ \mu\beta)^2 \sigma^2/ \delta^2$ (for paired sample *t*-test), α was set as 0.05, and β was set as 0.01. According to the μ Table, values of μα and μβ were 1.96 and 1.2816 respectively. Values of σ (25.83) and δ (10.77) came from the preliminary experiment (n = 26, aEMG of SPL without HR and with unilateral HR). The calculated sample size was 60.4, which was further amplified by 20%–72.5.

All of the statistical analyses were performed using IBM SPSS 20.0.0 (SPSS Inc. 2009; Chicago, IL, United States). Measurement data were checked for normal distribution by Kolmogorov-Smirnov test. Comparisons between groups (no HR, unilateral HR, bilateral

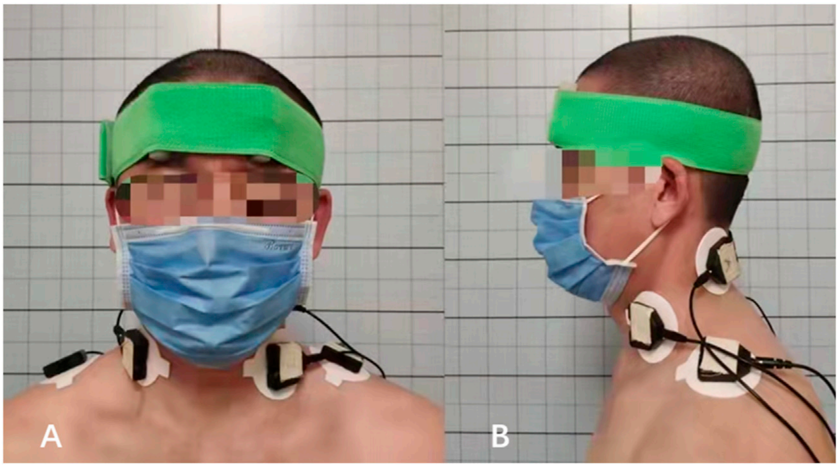

FIGURE 3
SEMG test of the cervical rotators. **(A)** The anterior view on the surface location of the electrodes, the electrode for SCM was located at the midpoint of the muscle; **(B)** The lateral view on the surface location of the electrodes, the electrode for SPL was located 2 cm from the spinous process at the C4 level, and electrode for UTR was located at the midpoint of a line between the C7 spinous process and the middle of the acromion.

TABLE 1 The basic characteristics of the subjects.

Basic characteristic	Asymptomatic subjects
Number (case)	90
Sex (male/female)	36/54
Age (years)	40.35±16.45 (range: 20–65)
Height (m)	1.66±0.11 (range: 1.44–1.91)
Weight (kg)	64.46±6.91 (range: 50.19–84.63)
BMI (kg/ cm^2)	23.38±1.6 (range: 19.05–26.89)

HR) were processed by paired sample *t*-tests and Levene variance homogeneity tests. Correlations between parameters were performed by Spearman analysis. Multiple linear regression analysis was performed to determine the independent factors of aEMG and CCR. ROC (receiver operating characteristic) curves were performed in order to determine the cut-off values of indicators. The level of significance was set at 0.05.

Results

General characteristics

The calculated sample size was further amplified by 20%–72.5. Finally, we enrolled 90 subjects (power >90%), and all of those subjects had accomplished the whole study. The basic characteristics of the subjects were listed below, and all of them obeyed the normal distribution (Table 1).

The aEMG of cervical rotators

EMG test showed that the RMS of SPL, UTr, and SCM were increased notably under the unilateral HR and bilateral HR, comparing to the no HR (Figure 4). The aEMG of those rotating agonists were calculated by using the maximal EMG during the rotating phase (Figure 4D) minus the mean EMG during the returning phase (Figure 4D). The aEMG of SPL, UTr, SCM, as well as the CCR under the unilateral HR were higher than the no HR situation (Table 2). The aEMG of SPL and CCR under the bilateral HR were higher than the unilateral HR (Table 2).

Correlation analyses

Correlation analyses were performed between the HR pattern (no HR = 0, unilateral HR = 1, bilateral HR = 2), aEMG of the agonists rotators, CCR, and the general characteristics (Table 3). The HR pattern had mild correlations with the aEMG of SPL, UTr, and SCM, and it had a moderate correlation with the CCR. Mild correlations existed commonly between the general characteristics including sex, age, height, weight, BMI, and the aEMG of rotating agonists (Table 3).

Multiple linear regression analysis

The multiple linear regression of aEMG showed that the HR pattern and age were the independent affecting

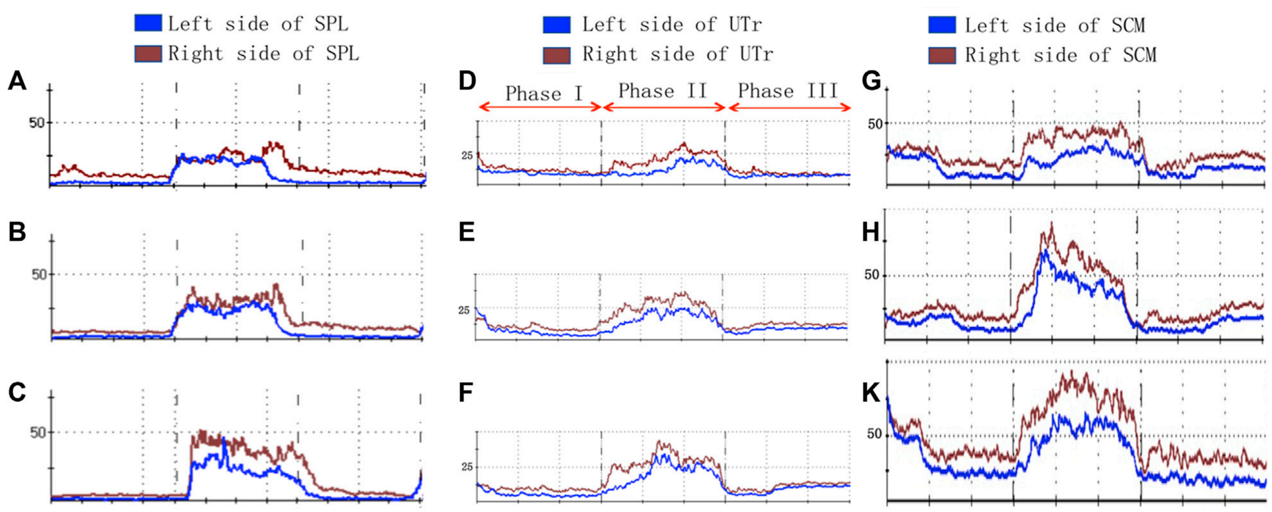

FIGURE 4
SEMG-based myoelectrical activities of the cervical rotators under the different HR patterns. **(A–C)**, no HR; **(D–E)**, unilateral HR; **(G–K)**, bilateral HR; Phase I, resting phase; Phase II, rotating phase; Phase III, returning phase.

TABLE 2 The aEMG and CCR under no HR, unilateral HR and bilateral HR.

Parameters	No HR (A)	Unilateral HR (B)	Bilateral HR (C)	A vs. B	B vs. C
aEMG of SPL	29.11±13.72	33.48±18.14	40.58±22.91	t = -2.595 p = 0.010*	t = -3.278 p = 0.001**
aEMG of UTr	12.69±6.90	14.74±8.75	16.35±9.91	t = -2.491 p = 0.013*	t = -1.639 p = 0.102
aEMG of SCM	41.97±20.12	54.57±36.18	58.84±35.28	t = -4.102 p < 0.001**	t = -1.140 p = 0.225
CCR	0.50 ±0.01	0.51±0.02	0.53±0.02	t = -7.271 p < 0.001**	t = -7.125 p < 0.001**

aEMG, adjust electromyogram; CCR, co-contraction ratio; SPL, splenius capitis; UTr, upper trapezius; SCM, sternocleidomastoid; *, $p < 0.05$ **, $p < 0.01$.

factors for the aEMG of SPL, UTr, and SCM, and the subject's BMI was also an independent affecting factor for the aEMG of SPL and SCM (Table 4). The multiple linear regression of CCR showed that the HR pattern was the only affecting factor for the rotating CCR of the cervical spine (Table 5).

ROC curve analysis and the cut-off values

The ROC analysis showed that the cut-off value of BMI for the aEMG of SPL was 24.37 ($p < 0.05$) (Figure 5A), and the cut-off value of BMI for the aEMG of SCM was 23.99 ($p < 0.05$) (Figure 5B).

Discussion

SPL, UTr, and SCM are the main rotators of the cervical spine, which play a critical role in maintaining normal posture, alignment, and spinal stability (Vasavada et al., 1998). SPL is a deep layer rotator, and UTr and SCM are superficial rotators. The superficial and deep rotators synergistically contribute to the posture control and rotating motion (Panjabi et al., 1998; Cheng et al., 2011; Agyei et al., 2019). HR is a general phenomenon in populations. It first came to light publicly in 1995 in Japan when a television program reported that a man who wore a wire hanger around his head subsequently rotated his head (Agyei et al., 2019), and this phenomenon was formally termed as the "HR" by Kajimoto et al. at the University of Electro-

TABLE 3 Correlation analysis of the aEMG, CCR and general characteristics.

Group		Sex	Age	Height	Weight	BMI	SPL aEMS	UTr aEMS	SCM aEMS	CCR
Group	1	0	0	0	0	0	0.222** $p < 0.001$	0.137** $p = 0.001$	0.201** $p < 0.001$	0.582** $p < 0.001$
Sex		1	−0.009 $p = 0.834$	0.468** $p < 0.001$	0.360** $p < 0.001$	−0.362** $p < 0.001$	0.092* $p = 0.031$	0.081 $p = 0.060$	0.139** $p = 0.001$	−0.002 $p = 0.958$
Age			1	0.006 $p = 0.889$	0.328** $p < 0.001$	0.540** $p < 0.001$	0.045 $p = 0.294$	0.370** $p < 0.001$	0.151** $p < 0.001$	0
Height				1	0.865** $p < 0.001$	−0.575** $p < 0.001$	0.180** $p < 0.001$	0.140** $p = 0.001$	0.229** $p < 0.001$	−0.014 $p = 0.741$
Weight					1	−0.122** $p = 0.004$	0.155** $p < 0.001$	0.265** $p < 0.001$	0.258** $p < 0.001$	−0.030 $p = 0.477$
BMI						1	−0.102* $p = 0.017$	0.168** $p < 0.001$	−0.196** $p < 0.001$	−0.013 $p = 0.754$
SPL aEMS							1	0.079 $p = 0.066$	0.146** $p = 0.001$	0.078 $p = 0.067$
UTr aEMS								1	0.151** $p < 0.001$	0.083 $p = 0.052$
SCM aEMS									1	0.169** $p < 0.001$
CCR										1

aEMG, adjust electromyogram; CCR, co-contraction ratio; SPL, splenius capitis; UTr, upper trapezius; SCM, sternocleidomastoid; HR pattern, no HR = 0, unilateral HR = 1, bilateral HR = 2; Sex, male = 1, female = 0; *, $p < 0.05$ **, $p < 0.01$.

TABLE 4 Multiple linear regression analysis for aEMG of the cervical rotators.

Factors	SPL aEMG (R = 0.345)				UTr aEMG (R = 0.428)				SCM aEMG (R = 0.416)			
	B	SEM	P	VIF	B	SEM	p	VIF	B	SEM	p	VIF
HR pattern	5.738	0.948	<0.001**	1.000	1.831	0.415	<0.001**	1.000	8.431	1.538	<0.001**	1.000
Sex	0.535	1.753	0.761	1.260	1.347	0.767	0.080	1.260	1.273	2.845	0.655	1.260
Age	0.249	0.063	<0.001**	1.782	0.227	0.027	<0.001**	1.782	0.672	0.102	<0.001**	1.782
BMI	−3.604	0.694	<0.001**	2.057	−0.485	0.303	0.110	2.057	−8.727	1.126	<0.001**	2.057

aEMG, adjust electromyogram; SPL, splenius capitis; UTr, upper trapezius; SCM, sternocleidomastoid; SEM, standard error of mean; VIF, variance inflation factor; **, $p < 0.01$.

TABLE 5 Multiple linear regression analysis for the cervical rotating CCR.

Factors	B	CCR (R = 0.345)		
		SEM	P	VIF
HR pattern	0.015	0.001	<0.001**	1.160
Sex	$8.18*10^{-5}$	0.002	0.962	1.268
Age	$1.22*10^{-5}$	0.000	0.859	2.201
BMI	0.000	0.001	0.632	2.399
SPL aEMG	$-4.78*10^{-5}$	0.000	0.261	1.135
UTr aEMG	$-2.00*10^{-5}$	0.000	0.837	1.225
SCM aEMG	$2.15*10^{-5}$	0.000	0.412	1.210

CCR, co-contraction ratio; aEMG, adjust electromyogram; SPL, splenius capitis; UTr, upper trapezius; SCM, sternocleidomastoid; SEM, standard error of mean; VIF, variance inflation factor; **, $p < 0.01$.

Communications in 2008 (Matsue et al., 2008). An epidemiological investigation by Asahi T et al. found that HR is a general phenomenon in populations (120 healthy Japanese adults, 60 men and 60 women, aged 19–65 years), and it can be observed in 92.1% of the healthy subjects (Asahi et al., 2015). Till now, the potential mechanism of HR remains unknown. Previous study explained the HR phenomenon as the unilateral muscular activation of cervical rotators caused by imbalance stress (deep sensation) in the frontal-temporal area, and the subject feels an urge to rotate the head to the compressed side, in order to maintain an original position and a balanced posture (Asahi et al., 2020). However, none of them have explored the effects of HR on the muscular system, such as SEMG or kinematic study.

In this study, we observed the immediate electromyography activations of the cervical rotators in two patterns of HR. To our knowledge, it was the first study focusing on the

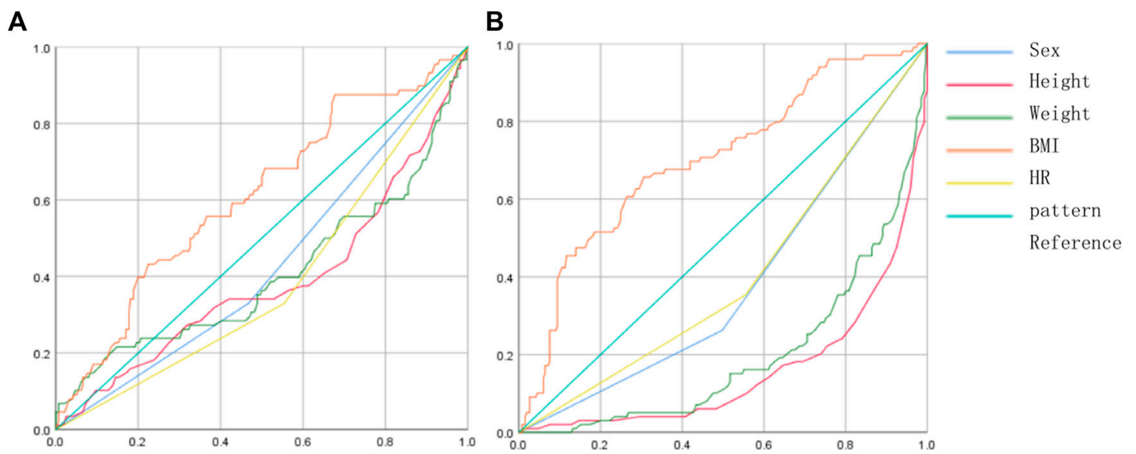

FIGURE 5
ROC curves of BMI and aEMG of the SPL and SCM. **(A)** ROC curves of the factors and SPL aEMG, the orange color represented the BMI; **(B)** ROC curves of the factors and SCM aEMG, the orange color represented the BMI.

electromyography mechanism of HR and the cervical rotator function. Our results found that the aEMG of SPL, UTr, and SCM were significantly increased, both under the unilateral and bilateral HR, however, the aEMG of SPL was further increased under the bilateral HR, compared with the unilateral HR. It indicated that HR can activate the cervical rotators by increasing their myoelectrical activities during the active rotation, and the effects of bilateral HR were stronger than unilateral HR. It has been reported that HR-associated muscular activation can be used as a non-invasive treatment for some neuromuscular disorders with imbalanced muscular strength and posture, such as cervical dystonia, NP, and adhesive capsulitis (Agyei et al., 2019). It has been reported that unilateral HR can immediately correct the abnormal posture and improve the symptoms in cervical dystonia patients (Asahi et al., 2010). A pilot clinical study also found that an HR-simulated device (30 min/day, 3 months) can significantly improve the symptoms and subjective severity scale in 19 patients with cervical dystonia, both at the baseline and after the 3-month trial, suggesting that HR can improve abnormal head rotation in patients with cervical dystonia (Asahi et al., 2018). However, all of those studies were based on unilateral HR, and did not investigate the potential mechanism about HR. In the present study, the SEMG test found that the effects of bilateral HR on the myoelectrical activities (aEMG) of SPL was much higher than unilateral HR (Table 2), and further multiple linear regression analysis also showed the HR pattern (no HR = 0, unilateral HR = 1, bilateral HR = 2) was an independent affecting factor for the rotators' myoelectrical activities (Table 4), which means the bigger the HR pattern (bilateral HR = 2 > unilateral HR = 1), the higher the aEMG. SPL is a deep layer rotator, which is also one of the most powerful rotators of the cervical spine. Our results indicate that the bilateral HR can induce a much stronger muscle contraction of SPL (higher aEMG value) than the unilateral HR, suggesting that bilateral HR has greater clinical potential to be used as a new rehabilitation therapy for cervical neuromuscular disorders than unilateral HR.

The present study also found that the subject's general characteristics were independent affecting factors for the rotators' myoelectrical activities. The multiple linear regression analysis showed that age and BMI were independent affecting factors for the aEMG of SPL and SCM, and age was an independent affecting factor for the aEMG of UTr. It suggests that subjects with older age can achieve the higher myoelectrical activities of SPL, UTr, and SCM, and subjects with smaller BMI can achieve the higher myoelectrical activities of SPL and SCM. Similar to our results, many studies have proved that aging factors can affect spinal muscular activity and neuromuscular function (Aubertin-Leheudre et al., 2020). Many cervical disorders are related to aging, for example, NP has a lifetime prevalence rate of 48.5% and is very common in elder people (Cohen and Hooten, 2017), and Shuang et al. (Ao et al., 2019) have pointed out that the subject's age was the independent risk factor of cervical kyphosis. Hence, the clinical application of HR has a particular significance for elder patients. High BMI is associated with muscular degeneration, for example, the musculature fatty infiltration is a classic indicator of muscular degeneration (Koji et al., 2019), which leads to muscular dysfunction and disorders. Hence, subjects with lower BMI are prone to have more functional cervical rotators. Besides, the present study also calculated the BMI cut-off values. The cut-off value is also called as the "critical value", which is the critical point obtained from the ROC curve of the subject. We found that the cut-off value of BMI for the aEMG of SPL was 24.37 (Figure 5A), and the cut-off value of BMI for the aEMG of SCM was 23.99 (Figure 5B). It indicates that subjects with BMI more than 24.37 and less than 24.37 can obtain a significantly different efficacy on SPL aEMG during the HR, and subjects with BMI<24.37 are prone to have more functional SPL; subjects with BMI more than 23.99 and less than 23.99 can obtain a significantly different efficacy on SCM aEMG during the HR, and subjects with BMI<23.99 are prone to have more functional SCM. In all, our results indicate that patients with lower BMI and older age can achieve the higher cervical rotators' myoelectrical activities during HR, which may result in better efficacy and outcome.

CCR is a functional parameter representing muscular coordination and balance. Muscular co-contraction refers to the simultaneous activation of agonists and antagonists in static or dynamic state (Chih-hsiu et al., 2014), and it is an important mechanism for spinal stabilization (Le et al., 2017). In fact, the cervical muscular function is of great significance to spinal stability, it even plays a more important role than the osseous-ligamentous system (Panjabi et al., 1998; Cheng et al., 2011). The rotating CCR is the reference for the coordination of rotators and antagonists in a balanced muscular system. Our result showed the rotating CCR was significantly increased under the unilateral HR comparing to no HR, and it was further increased under the bilateral HR. The increased CCR is considered as a protective mechanism for maintaining the spinal stability during motion (Ford et al., 2008). HR benefits both the rotators' electrophysiology function and cervical stability. When HR increased the rotators' myoelectrical activities during active cervical rotation, it can also increase the antagonists' muscular tension, resulting in a higher CCR and cervical stability. What's more, the increased CCR also indicated the antagonists' stretching, which has a great clinical application value for patients with unbalanced musculature and posture, such as cervical dystonia. Higher CCR indicates that the muscular system is in a higher energy consumption model, as the antagonists' muscular tension is also increased simultaneously with the agonists' during the rotation, which applies to the systematic muscular exercise. The multiple linear regression analysis showed the HR pattern (no HR = 0, unilateral HR = 1, bilateral HR = 2) was the only independent affecting factor for CCR, which means only the HR pattern can change the CCR, and the bilateral HR can achieve a higher CCR than unilateral HR (bilateral HR = 2 > unilateral HR = 1). Our results indicated that the cervical muscular system (both the agonists and antagonists) contracted much more strongly during the rotation motion under the bilateral HR than the unilateral HR, suggesting that bilateral HR has the greater clinical potential to be used as a non-invasive treatment for cervical neuromuscular disorders related to unbalanced musculature and instability.

There were some limitations of this pilot study. Firstly, the present study only explored the impacts of HR on cervical rotators' electromyography and neuromuscular function in asymptomatic subjects. Although the pilot study included asymptomatic volunteers as the subjects, it found out the muscular electromyography mechanism of HR, which can be a rationale for the clinical application as a new rehabilitation method for treating cervical neuromuscular disorders. However, in order to identify the effects of HR on the patients, further clinical trials need to be carried out in patients with neuromuscular disorders. Secondly, we only detect the instant impacts of HR on cervical rotators' EMG, and this pilot study suggests that HR has a greater clinical potential to become a rehabilitation method for treating cervical neuromuscular disorders. However, in order to identify the long-term effects of HR on cervical musculature, further clinical trials with continuous rehabilitation of different HR patterns need to be carried out.

Conclusion

The present study was a pilot clinical study, which has explored the impacts of HR on cervical rotators' electromyography and neuromuscular function in asymptomatic subjects. To our knowledge, it was the first study focusing on the electromyography mechanism of HR and its effects on cervical rotators' function. The present study found that: 1) HR can increase the rotators' myoelectrical activities of cervical spine, as well as the rotating CCR of cervical muscular system; 2) the effects of bilateral HR pattern on the myoelectrical activity and CCR are greater than unilateral HR pattern; 3) HR pattern, age, and BMI are independent affecting factors for the rotators' EMG values, and HR pattern is the only independent factor for the rotating CCR. Our study suggests that HR has a greater clinical potential to become a rehabilitation method for treating cervical neuromuscular disorders, and the efficacy of the bilateral HR on cervical neuromuscular disorders maybe stronger than the unilateral HR.

Data availability statement

The raw data supporting the conclusion of this article will be made available by the authors, without undue reservation.

Ethics statement

The studies involving human participants were reviewed and approved by Tiantan hospital human subject protection programs and procedures (Ethic number, KY 2020–073-02). The patients/participants provided their written informed consent to participate in this study. Written informed consent was obtained from the individual(s) for the publication of any potentially identifiable images or data included in this article.

Author contributions

Conception and design of study: DW acquisition of data: DW analysis and/or interpretation of data: DW Drafting the manuscript: DW revising the manuscript critically for important intellectual content: BL Approval of the version of the manuscript to be published: DW, BL.

Funding

This work was supported by the National Key Research and Development Program of China (grant number 2018YFF0301103), the funding from National Natural Science Foundation of China (grant numbers 81772370, 81972084).

Conflict of interest

The authors declare that the research was conducted in the absence of any commercial or financial relationships that could be construed as a potential conflict of interest.

Publisher's note

All claims expressed in this article are solely those of the authors and do not necessarily represent those of their affiliated organizations, or those of the publisher, the editors and the reviewers. Any product that may be evaluated in this article, or claim that may be made by its manufacturer, is not guaranteed or endorsed by the publisher.

References

Agyei, J. O., Smolar, D. E., Hartke, J., Fanous, A. A., and Gibbons, K. J. (2019). Cervical kyphotic deformity worsening after extensor cervical muscle paralysis from botulinum toxin injection. *World Neurosurg.* 125, 409–413. doi:10.1016/j.wneu.2019.02.057

Ao, S., Liu, Y., Wang, Y., Zhang, H., and Leng, H. (2019). Cervical kyphosis in asymptomatic populations: Incidence, risk factors, and its relationship with health-related quality of life. *J. Orthop. Surg. Res.* 14, 322. doi:10.1186/s13018-019-1351-2

Asahi, T., Hayashi, N., and Hamada, H. (2010). "Application of the Hanger Reflex to the treatment of cervical dystonia," in *Functional neurosurgery: Meeting of the Japan society for stereotactic & functional neurosurgery*.

Asahi, T., Nakamura, T., Sato, M., Kon, Y., Kajimoto, H., and Sato, S. (2020). The hanger reflex: An inexpensive and non-invasive therapeutic modality for dystonia and neurological disorders. *Neurol. Med. Chir.* 60, 525–530. doi:10.2176/nmc.ra.2020-0156

Asahi, T., Sato, M., Kajimoto, H., Koh, M., Kashiwazaki, D., and Kuroda, S. (2015). Rate of hanger reflex occurrence: Unexpected head rotation on fronto-temporal head compression. *Neurol. Med. Chir.* 55, 587–591. doi:10.2176/nmc.oa.2014-0324

Asahi, T., Sato, M., Nakamura, T., Kon, Y., Kajimoto, H., Oyama, G., et al. (2018). Pilot study of a device to induce the hanger reflex in patients with cervical dystonia. *Neurol. Med. Chir.* 58, 206–211. doi:10.2176/nmc.oa.2017-0111

Aubertin-Leheudre, M., Pion, C. H., Vallée, J., Marchand, S., Morais, J. A., Belanger, M., et al. (2020). Improved human muscle biopsy method to study neuromuscular junction structure and functions with aging. *J. Gerontol. A Biol. Sci. Med. Sci.* 75, 2098–2102. doi:10.1093/gerona/glz292

Cheng, C. H., Chen, P. J., Kuo, Y. W., and Wang, J. L. (2011). The effects of disc degeneration and muscle dysfunction on cervical spine stability from a biomechanical study. *Proc. Inst. Mech. Eng. H.* 225, 149–157. doi:10.1243/09544119JEIM805

Cheng, C. H., Lin, K. H., and Wang, J. L. (2008). Co-contraction of cervical muscles during sagittal and coronal neck motions at different movement speeds. *Eur. J. Appl. Physiol.* 103, 647–654. doi:10.1007/s00421-008-0760-4

Chih-hsiu, C., Pai-Chu Chen, C., Kwan-hwa, L., Liu, W-Y., Wang, S-F., Hsu, W-L., et al. (2014). Altered Co-contraction of cervical muscles in young adults with chronic neck pain during voluntary neck motions. *J. Phys. Ther. Sci.* 26, 587–590. doi:10.1589/jpts.26.587

Cohen, S. P., and Hooten, W. M. (2017). Advances in the diagnosis and management of neck pain. *BMJ* 358, j3221. doi:10.1136/bmj.j3221

Colloca, C. J., and Hinrichs, R. N. (2005). The biomechanical and clinical significance of the lumbar erector spinae flexion-relaxation phenomenon: A review of literature. *J. Manip. Physiol. Ther.* 28, 623–631. doi:10.1016/j.jmpt.2005.08.005

Ding, Y., Liu, B., Qiao, H., Yin, L., He, W., Si, F., et al. (2020). Can knee flexion contracture affect cervical alignment and neck tension? A prospective self-controlled pilot study. *Spine J.* 20 (2), 251–260. doi:10.1016/j.spinee.2019.09.008

Falla, D., Dall'Alba, P., Rainoldi, A., Merletti, R., and Jull, G. (2002). Location of innervation zones of sternocleidomastoid and scalene muscles--a basis for clinical and research electromyography applications. *Clin. Neurophysiol.* 113 (1), 57–63. doi:10.1016/s1388-2457(01)00708-8

Falla, D., Farina, D., Dahl, M. K., and Graven-Nielsen, T. (2007). Muscle pain induces task-dependent changes in cervical agonist/antagonist activity. *J. Appl. Physiol. (1985)* 102, 601.

Ford, K. R., Bogert, J., Myer, G. D., Shapiro, R., and Hewett, T. E. (2008). The effects of age and skill level on knee musculature co-contraction during functional activities: A systematic review. *Br. J. Sports Med.* 42, 561–566. doi:10.1136/bjsm.2007.044883

Hussein, M. A., Yun, I. S., Park, H., and Kim, Y. O. (2017). Cervical spine deformity in long-standing, untreated congenital muscular torticollis. *J. Craniofac. Surg.* 28, 46–50. doi:10.1097/SCS.0000000000003182

Joines, S. M. B., Sommerich, C. M., Mirka, G. A., Wilson, J. R., and Moon, S. D. (2006). Low-level exertions of the neck musculature: A study of research methods. *J. Electromyogr. Kinesiol.* 16, 485–497. doi:10.1016/j.jelekin.2005.09.007

Koji, T., Phillip, G., Romanu, J., Paholpak, P., Nakamura, H., Wang, J. C., et al. (2019). The impact of cervical spinal muscle degeneration on cervical sagittal balance and spinal degenerative disorders. *Clin. Spine Surg.* 32, E206–E213. doi:10.1097/BSD.0000000000000789

Le, P., Best, T. M., Khan, S. N., Mendel, E., and Marras, W. S. (2017). A review of methods to assess coactivation in the spine. *J. Electromyogr. Kinesiol.* 32, 51–60. doi:10.1016/j.jelekin.2016.12.004

Marshall, P. W., and Murphy, B. A. (2006). Evaluation of functional and neuromuscular changes after exercise rehabilitation for low back pain using a Swiss ball: A pilot study. *J. Manip. Physiol. Ther.* 29, 550–560. doi:10.1016/j.jmpt.2006.06.025

Matsue, R., Sato, M., Hashimoto, Y., and Kajimoto, H. (2008). Hanger reflex":A reflex motion of a head by temporal pressure for wearable interface. *SICE Annu. Conf.* 2008.

Panjabi, M. M., Cholewicki, J., Nibu, K., Grauer, J., Babat, L. B., and Dvorak, J. (1998). Critical load of the human cervical spine: An *in vitro* experimental study. *Clin. Biomech.* 13, 11–17. doi:10.1016/s0268-0033(97)00057-0

Thakar, S., Mohan, D., Furtado, S. V., Sai Kiran, N. A., Dadlani, R., Aryan, S., et al. (2014). Paraspinal muscle morphometry in cervical spondylotic myelopathy and its implications in clinicoradiological outcomes following central corpectomy: Clinical article. *J. Neurosurg. Spine* 21, 223–230. doi:10.3171/2014.4.SPINE13627

frontiers | Frontiers in Bioengineering and Biotechnology

TYPE Original Research
PUBLISHED 03 November 2022
DOI 10.3389/fbioe.2022.976242

Check for updates

OPEN ACCESS

EDITED BY
Kwong Ming Tse,
Swinburne University of Technology,
Australia

REVIEWED BY
Daihua Yu,
University of Pittsburgh, United States
Ghorban Taghizadeh,
Iran University of Medical Sciences, Iran

*CORRESPONDENCE
Fong-Chin Su,
fcsu@ncku.edu.tw

SPECIALTY SECTION
This article was submitted to Biomechanics,
a section of the journal
Frontiers in Bioengineering and Biotechnology

RECEIVED 23 June 2022
ACCEPTED 19 October 2022
PUBLISHED 03 November 2022

CITATION
Ma CC, Mo PC, Hsc HY and Su FC (2022), A novel sensor-embedded holding device for monitoring upper extremity functions.
Front. Bioeng. Biotechnol. 10:976242.
doi: 10.3389/fbioe.2022.976242

A novel sensor-embedded holding device for monitoring upper extremity functions

Charlie Chen Ma[1], Pu-Chun Mo[1], Hsiu-Yun Hsu[2] and Fong-Chin Su[1,3]*

[1]Department of Biomedical Engineering, National Cheng Kung University, Tainan, Taiwan, [2]Department of Physical Medicine Rehabilitation, National Cheng Kung University Hospital, Tainan, Taiwan, [3]Medical Device Innovation Center, National Cheng Kung University, Tainan, Taiwan

There are several causes that can lead to functional weakness in the hands or upper extremities (UE), such as stroke, trauma, or aging. Therefore, evaluation and monitoring of UE rehabilitation have become essential. However, most traditional evaluation tools (TETs) and assessments require clinicians to assist or are limited to specific clinical settings. Several novel assessments might apply to wearable devices, yet those devices will still need clinicians or caretakers to help with further tests. Thus, a novel UE assessment device that is user-friendly and requires minimal assistance would be needed. The cylindrical grasp is one of the common UE movements performed in daily life. Therefore, a cylindrical sensor-embedded holding device (SEHD) for training and monitoring was developed for a usability test within this research. The SEHD has 14 force sensors with an array designed to fit holding positions and a six-axis inertial measurement unit (IMU) to monitor grip strength, hand dexterity, acceleration, and angular velocity. Six young adults, six healthy elderly participants, and three stroke survivors had participated in this study to see if the SEHD could be used as a reference to TETs. During result analyses, where the correlation coefficient analyses were applied, forearm rotation smoothness and the Purdue Pegboard Test (PPT) showed a moderate negative correlation [r (16) = −0.724, $p < 0.01$], and the finger independence showed a moderate negative correlation with the PPT [r (10) = −0.615, $p < 0.05$]. There was also a highly positive correlation between the maximum pressing task and Jamar dynamometer in maximum grip strength [r (16) = 0.821, $p < 0.01$]. These outcomes suggest that the SEHD with simple movements could be applied as a reference for users to monitor their UE ability.

KEYWORDS

biomechanics, rehabilitation, aging, upper extremities, robotic

Introduction

The elderly population is rapidly increasing thanks to better medical support globally (Nation, 2019). Several studies have suggested that normal aging might alter physical, mental, and social health (Onder et al., 2002). Physical changes include decreased strength and mobility (Chodock et al., 2020). In particular, upper extremity (UE) functions and strategies may affect activities of daily living (ADL) due to physical changes in normal aging (Reissner et al., 2019). However, aging is not the only cause of UE dysfunction; these physical problems are also seen in patients who have suffered stroke (Shi et al., 2011), trauma (Dowrick et al., 2005; Crowe et al., 2020), Parkinson's disease (Quinn et al., 2013), and other UE musculoskeletal disorders (Huisstede et al., 2006) such as carpal tunnel syndrome (Yoshida et al., 2019). In addition, UE functions are important components of ADL capability and may impact the quality of life (QoL) (Kanti Majumdar, 2014). Therefore, assessing and monitoring UE function is critical for people with varying degrees of dysfunction.

Several clinical evaluation methods could be applied to evaluate one's UE functions (Kim et al., 2016). However, most of them are not digitized and based on clinical observations. For example, the common assessment tool for UE are the Upper Extremity Functional Index (UEFI-20 and UEFI-15), which is a self-administered questionnaire consisting of activity lists. Users give a score to each activity based on its difficulty of completion. Healthy individuals can score 80 out of 80 in UEFI-20 or 100 out of 100 in UEFI-15 (13). Aside from the self-administered questionnaires, the Purdue Pegboard Test (PPT) is one of the most commonly used clinical evaluation tools for fine and gross motor dexterity and coordination. The participants perform tasks within the designed period and clinicians calculate their performances based on how many pieces (pegs) are placed in the desired locations (holes) during the tasks. It is a performance-based outcome measure (Sigirtmac and Oksuz, 2022). The normal range of the score can vary due to the different age groups and genders. For example, in the healthy male group aged 21 to 25 years, the average PPT is 15.44 ± 1.71 in the preferred hand task (Yeudall et al., 1986; Marvin, 2012). The PPT could evaluate one's hand dexterity and UE gross movements. However, the outcome measure of the PPT presents the number of pieces that might not present one's UE abilities on a different scale. It could be considered an overall evaluation tool instead of a segmented ability evaluation. Besides PPT, the Jamar dynamometer is a common clinical assessment instrument for upper extremities; it evaluates one's grip-force. It is considered a gold standard tool with excellent validity and reliability in research and the clinic (Mathiowetz, 2002; Bohannon et al., 2006). However, similar to the PPT, the Jamar dynamometer requires at least one clinician to be on-site, which calls for additional human labor. Clinicians must be trained before collecting or grading subjects' functions. An experienced clinician might grade differently from an inexperienced one when operating the same evaluation tool on the same patient. Therefore, some current clinical assessments might end up with more subjective results based on the clinician's experience (Kim et al., 2013). Aside from that, several tests have ceiling effects, meaning healthy individuals might get total scores even though their hand functions may differ. Moreover, many people do not realize or deny functional changes in their UE with age, so they do not visit the clinic or hospital for further evaluations (Kim et al., 2016). Therefore, there is a need for an easily accessible device that can digitize the assessment results to provide a reference for clinicians, which will, in turn, also help the users.

Several wearable smart gloves have been invented to help people with UE functional impairments perform training or rehabilitation (Wang et al., 2014; Shin et al., 2016). However, such wearable smart gloves might not be suitable for all users. Researchers have developed data gloves embedded with different sensors, such as inertia measurement unit (IMU) sensor-embedded gloves (Hsiao et al., 2015; Lin et al., 2017; Lin et al., 2018), data gloves with force sensors (Tarchanidis and Lygouras, 2003; Hsiao et al., 2015), data gloves with flexible sensors (Tognetti et al., 2006), and gloves with flexible optic fiber bending transducers (Fujiwara et al., 2014). However, studies have shown that the elderly resist the adoption of assistive technology for reasons such as (A) the devices not being easy to set up; (B) the devices being so expensive that they are afraid of breaking or losing them; (C) or the caretakers not bothering to help them put these on (Yusif et al., 2016; Golant, 2017). Aside from that, although some of the data gloves use force sensors, many of the force sensors in the gloves do not provide actual force acquisition due to erroneous placement of the sensors. Most wearable devices use pseudo-augmented reality environments (screen projections) or virtual reality environments to integrate with the hardware. However, the lack of tactile feedback of the actual object might lead to inappropriate force application during training or rehabilitation. Although smart gloves are considered a potential developing technology and many companies and research groups are devoted to these in this field, most wearable smart gloves are still not widely used (Caeiro-Rodríguez et al., 2021).

Grabbing is one of the earliest reflexes in human development (Halverson, 1937), while gripping and grasping are intuitive movements in daily living (Yang et al., 2015). The three holding-related verbs might be confusing. The movements of gripping, grasping, and grabbing are all similar since they use the hands to hold and apply appropriate force to keep and move the object. These movements are also different in that they require different reaction times to make contact with the object, e.g., grabbing represents a quicker action than gripping. In other words, the grasping movement tends to be more planned, while gripping is more intuitive. In this article, we will use "grasping" to present the planned holding movement. Generally, there are two major types of grasping: power grasp and precision grasp. Power grasp, which means force application, is the key element in movements such as the large wrap, cylindrical grasp, and power sphere grasp. Precision grasp, which means the stability of the object or trajectory of the following movement, is more important than the force application of the movement, such as the writing tripod and precision sphere. In these two types of grasping, several subtypes are categorized by the involvement of the digits, grasping shapes, and purposes (Yang et al., 2015; Cai et al., 2016).

Grasping is a complex movement that involves motor planning and the proper use of force application. Many muscles and the nervous system are involved in grasping (Castiello, 2005; Koester et al., 2016; Chen et al., 2022). Different people can employ different strategies when performing the same task and respond differently to different outcomes. Studies have shown that motor learning and motor control improve with more sensory inputs during movements (Chiu et al., 2009; Cano-De-La-Cuerda et al., 2015; Sani and Shanechi, 2021). The complexity of grasping can enhance brain activation by observing the environment (occipital cortex), understanding and planning movements (prefrontal cortex), and performing responsive movements (premotor cortex, primary motor cortex, and complementary motor cortex).

Overall, sensory feedback collected during grasping may help improve force application and motor performance. Therefore, the idea of innovating a grasping device for evaluation, monitoring, and rehabilitation was initiated and developed.

The purposes of this study are to (A) develop the novel sensor-embedded holding device (SEHD) for functional evaluation of grip-force and movements and (B) apply the SEHD to collect useful data that could further be used as references for clinicians to monitor UE functions.

The hypothesis of this study is that the SEHD could offer data, which after being processed, could provide results that can be considered as references to traditional evaluation tools (TETs) for users and clinicians to monitor the conditions of the users' UE functions.

Design of upper extremities evaluation device

Design of hardware and its purposes

According to previous studies related to handgrips, holding devices could provide higher degrees of freedom to perform various movements, such as lifting, rotation, and horizontal position modification (Harwin and Barrow, 2013; Turella and Lingnau, 2014; Yang et al., 2015). In addition, studies related to grip force during movements suggest that data recorded from surface pressure or force sensors appear to facilitate further analysis to understand patterns of hand movement and hand function (Hsu et al., 2021a; Chen et al., 2022). Therefore, the design of the SEHD includes an inertial motor unit (IMU) that could provide speed and angular profiles. Based on this, we also encouraged the development of SEHD to collect sensory feedback.

Overall, the SEHD was designed and developed around several goals: 1) the SEHD should be capable of acquiring digitized data from different hand movements and UE movements; 2) it should be used and accepted by different users, such as the elderly, people with hand/UE disabilities, those who had survived a stroke, and children with developmental delays; 3) it should be affordable for the public and provide valuable analysis for monitoring, assessment, and even auxiliary training in the future. Therefore, designing and developing a proper SEHD appearance with useful functional details was very important and challenging.

Development of hardware and data collection

The cylindrical grasp is considered one of the common UE movements in daily living (Vergara et al., 2014). The cylindrical design of the SHED comes from a widely accepted everyday item—the soda can (diameter: 65 mm and height: 140 mm), which is a widely accepted daily object. Relative research supports the idea that the cylindrical shape for grasping was easy to use and could offer a nice grip feeling (Harih and Dolšak, 2014). A diameter of 65 mm was decided in accordance with the study on grip strength (Domalain et al., 2008) and the average hand length (Guerra et al., 2014) such that the SEHD could be wrapped comfortably by the participants. The initial design focused on the functionality of the device. The commercial circuit board and sensors were adapted for the SEHD.

We used 3D printing to build the shell, which consisted of two materials: polylactic acid (PLA) and thermoplastic elastomer (TPE). PLA was used for the hard shell of the case, while TPE was used for the elastic, flexible cover of the force sensors. Red and white were used for different materials because people tend to stick their palms to the colored areas intuitively. The weight of the object was 200 g, and the weight of the device linked to the IC board was 500 g.

A six-axis inertia measurement unit (IMU) and 14 force sensors were embedded in the SEHD (Figure 1). The IMU has been widely applied in many devices to evaluate or monitor different movement tasks (Hsu et al., 2021b; Nikkhoo et al., 2021). The embedded IMU was an MPU-6050 sensor (GY-521) from InvenSense, which has been applied in many studies related to motion control, wearable device innovation, and movement sensation inputs (Ngui and Lee, 2019; Karnik et al., 2020; Ares et al., 2022). The validity and reliability of this model of IMU have been demonstrated in many of the previous studies that have been accepted for clinical applications. The IMU was placed at the center of the device so as to measure movement parameters, and the force sensors were placed under the TPE

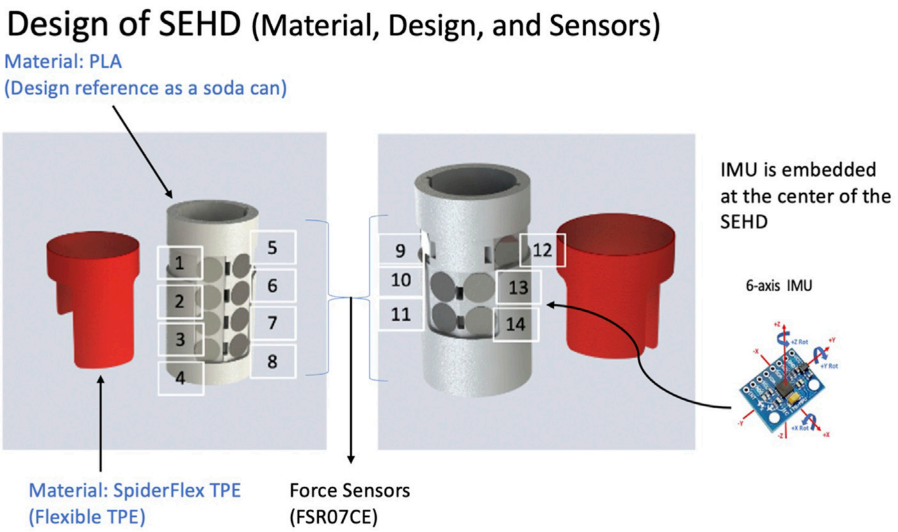

FIGURE 1
Design of the sensor-embedded holding device. Fourteen pressure sensors (FSR07CE, Ohmite) and the placement of the pressure sensors. Six-axis inertial measurement unit placed at the center of device. Inner part of structure made of PLA and outer part of the holding piece made of TPE material, and a 3D printer made both parts.

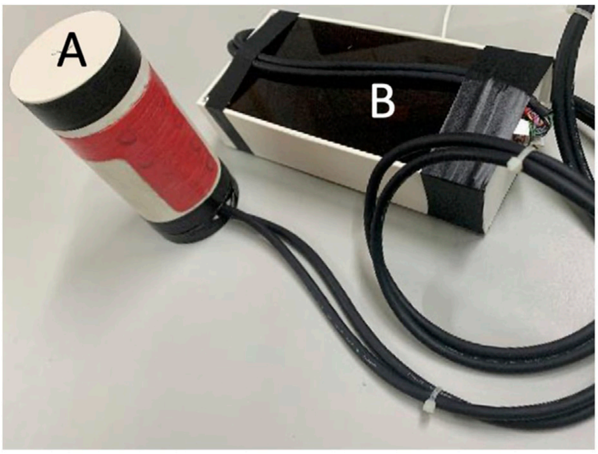

FIGURE 2
Actual product of SEHD. **(A)** Actual product of SEHD. **(B)** Process board of SEHD.

cover. Wires linked the processing board with the device. The output of the processing board provides data transfer and power to a PC or laptop *via* micro USB (Figure 2, Figure 3).

Development of software

During initial design, the core functionality of the SHED software was to monitor device connectivity, monitor IMU and force sensor data in real time, and acquire data from the device. As shown in Figure 4, the interface design is dominated by simplicity and focuses on providing appropriate information. In particular, the data acquisition frequency was 100 Hz, and the IMU and force sensors were calibrated. The data were processed through the software, and the unit of each axis of the accelerometers is "G," while that of each axis of the gyroscope is "degree/second."

In addition, we had added some function buttons to improve user experience for the researchers. The a "calibration" button was used to zero the pressure from the elastic cover to the force sensors. A "Tag" button was designed for researchers to provide voice prompts to the participants during the experiment while also providing a "Tag" time point in the final output data. The adjustable duration could offer a fixed time for the researcher to conduct the tasks. After pressing the "record" button, the participants started performing the designed task. After the task was completed according to the preset duration, a pop-up window prompted that the data had been recorded and the storage path of the data.

Methods

Participants

Three groups of participants were recruited for this study: healthy young adults, healthy elderly, and stroke survivors. Fifteen participants (six healthy young adults, six healthy

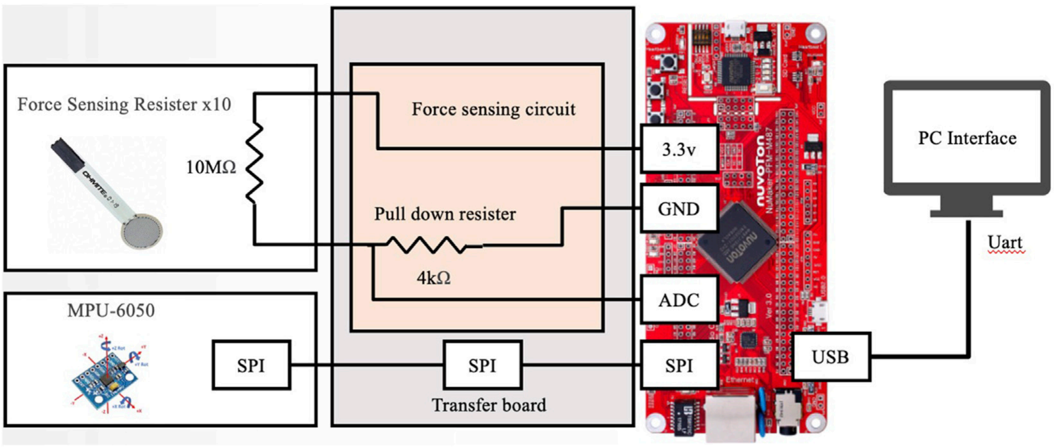

FIGURE 3
Circuit layout of SEHD: 14 force sensors linked to processing board (NuMaker-PFM-M487, Nuvoton, Taiwan) and IMU (MPU-6050, GY-521, InvenSense Inc., Taiwan) linked to SPI transfer board to transfer data to processing board. Processing board transfers data into digital output using micro-USB to the computer.

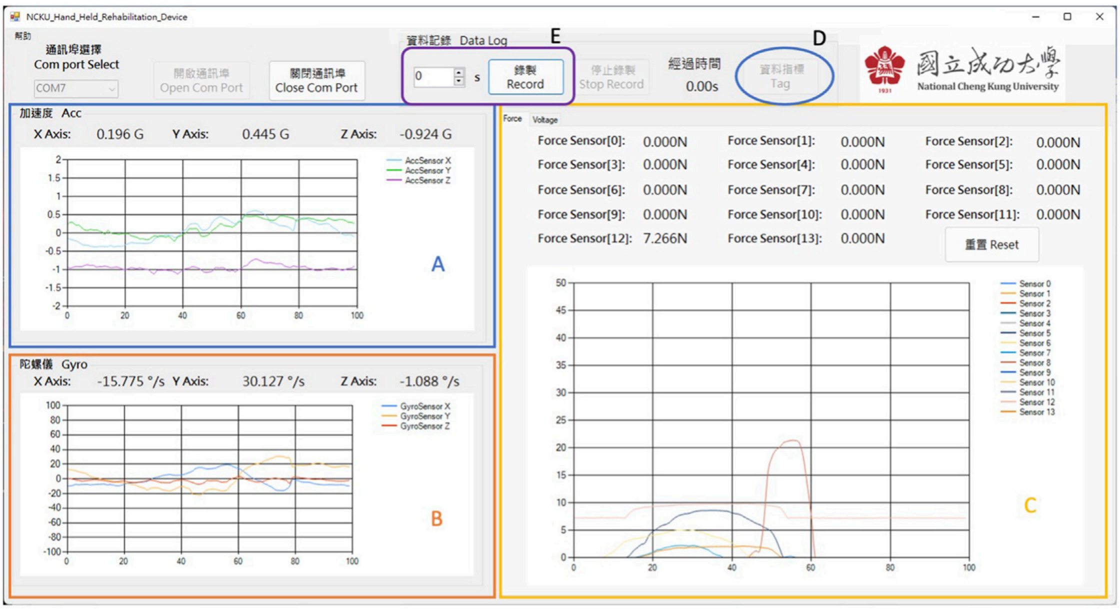

FIGURE 4
Software of SEHD: offers real-time monitoring during experiments. **(A)** Acceleration data; **(B)** angular velocity; **(C)** force sensor data: the reset button is for calibration; **(D)** "tag" button used as cues for different movement segments; **(E)** "record" button to preset the duration of each movement.

elderly, and three stroke survivors) were recruited based on the calculation of the sample size.

The calculation of the sample size was based on the textbook "Designing Clinical Research" by Hulley (2007). The α of the two-tailed test was set as 0.05, β was set as 0.20, and $r = 0.6$ or 0.7. The results of the sample size would be N = 19 when $r = 0.6$ and N = 13 when $r = 0.7$. Therefore, 15 participants were recruited.

The inclusion criteria for healthy young adults were

1) aged between 20 and 30 years;

2) having no neurological or musculoskeletal disorders;
3) having had no UE surgery within past 6 months.

The inclusion criteria for the healthy elderly were

1) aged above 65 years;
2) having no neurological or musculoskeletal disorders;
3) having had no UE surgery within past 6 months;
4) being able to understand and follow instructions.

The inclusion criteria for the participants who had survived a stroke in the chronic stage were

1) survived more than 6 months after a stroke;
2) experienced only one stroke;
3) having no other neurological or musculoskeletal disorders;
4) having had no UE surgery within past 6 months;
5) capable of performing the Purdue Pegboard Test;
6) having no other cognitive impairment and being able to follow verbal instructions.

All participants were fully informed about the study and had signed the IRB-approved consent form of the National Cheng Kung University, Taiwan.

Procedure of study

The procedure was separated into two parts: 1) clinical traditional evaluation methods and 2) novel SEHD simple tasks. The traditional evaluation tools included 1) the Jamar dynamometer to evaluate maximum grip strength and 2) the Purdue Pegboard Test (PPT) to assess fine movement and hand dexterity.

The background information on each participant was collected before the traditional evaluation. This background information included name, gender, date of birth, and upper extremity dominance side. Three groups of participants were included in this study to increase the diversity of the users.

The Purdue Pegboard Test (PPT) was conducted according to the guidelines of the clinical tutorial. The PPT is a common clinical evaluation tool for UE and hand movement. The participants were asked to start the PPT assessment from the dominant side, the nondominant side, and with both hands and to do the assembly task. The first three parts of the PPT made the participants place pegs in the holes from the top to bottom. The researcher would offer verbal cues like "Start" and "Time is up" to the participants. Thirty seconds were given to the participants, and the researcher would count how many pegs had been placed within the 30-s period. The assembly task required the participants to assemble a set of pieces, which included a peg, washers, and a nut. The participants were asked to assemble the set by alternating their hands and placing the set from the top to bottom. The given time was 1 minute, and the researcher would count how many pieces had been placed and assembled correctly within this period. Three trials were given for each task. The participants could ask for rest during the PPT.

After the PPT assessments had been completed, the participants were asked to use the Jamar dynamometer to assess their grip-force, which is considered a clinical gold standard test for assessing grip-force. Three trials were collected for each participant with breaks of 1 minute between the trials. The purpose of the 1-min break was to avoid fatigue that might affect the results of the trials. The participants were asked to sit comfortably on a chair and hold the Jamar dynamometer in an upright position. When the researcher says "grasp," the participants had to grasp as hard as they could until the researcher says "rest."

Based on the task activities using the Jamar dynamometer and PPT that have been described above, we divided each activity and its characteristics into three task groups: forearm rotation, maximum grip strength, and sequential press (see Table 1).

All movement data were collected while the participants were sitting and holding the SEHD with their dominant hand. We verbally instructed and offered demo movement before collecting the data. There was no verbal instruction given during the experiments, but we provided sound cues for participants to understand and perform the related movements. The reasons for using sound cues (beep) during the experiment are that 1) sound cues are shorter and quicker for the participants to respond to, especially since the movement duration is relatively short; 2) it avoids additional cognitive burden, since sound cues are more intuitive than verbal cues that need more processing; and 3) it avoids any opportunity for researchers' mistakes when offering the wrong verbal cues. The participants were asked to place their fingers at the desired places. Five trials were conducted for each task, and the average was calculated in post-processing as the performance ability of the participants.

In the first movement task—the forearm rotation task—the participants were asked to sit comfortably in front of a desk such that their forearms could be placed on the desk at the resting position. The participants were asked to hold the SEHD restfully with their fingers placed on the red TPE area before the experiment started. They were asked to respond by raising the SEHD to an appropriate height when they heard the first sound cue (beep). When the second sound cue occurred, they had to respond by performing pronation, mimicking the action of pouring water from a cup parallel to the table. When the third sound cue occurred, they had to respond by performing supination back to the original position and wait for the last cue to complete the trial. After the trial, the participants were asked to place the SEHD back on the desk and wait for the next trial or the next task. The collection duration of each trial was 15 s. The participants could ask for a resting period between the trials.

In the second task—the maximum grip strength task—the participants were asked to sit restfully in front of the desk. The

TABLE 1 Clarification of designed tasks and clinical meanings.

Task	What do I want to see	Related body parts	Parameters	Clinical implications
Forearm rotation	Rotation smoothness/rotation stability	Wrist	Angular speed profile	Related to daily functional activities
Maximum grip strength	Grip strength	Fingers	Force	Grip strength
Sequential press	Finger independence/finger coordination/holding position	Fingers	Force	Functional ability related to grip/fine movements

participants were asked to hold the SEHD restfully with their fingers placed on the red TPE area before the experiment started. The participants were asked to apply maximum grip when they heard the first beep and relax when they heard the second beep. Because the force application of the grip is a fast and quick movement that usually lasts less than 3 s (Kamimura and Ikuta, 2001), the duration of this task was designed to be 10 s and the duration of the compressions was to be less than 4 s to avoid additional fatigue. The participants were asked to take at least 1 minute of rest between each trial.

In the third task—the sequential pressing task—the participants were asked to perform sequential independent finger compressions from the index finger to little finger and from the little finger to index finger. A complete "sequential press trial" consisted of recording eight finger presses. A metronome offering 75 beats-per-minute (bpm) (0.8 s/cue) indicated that when the participants heard the first beep, they could start performing the task. They were asked to follow 75 bpm for each digit pressing and releasing (pressing for 0.8 s and releasing for 0.8 s). Once the full round of the sequential pressing trial (the index finger to little finger and the little finger to index finger) was completed, the participants were asked to hold their positions until the last sound cue occurred. The duration of each trial was 20 s.

The participants who had survived a stroke were only asked to collect three trials for the first two tasks, while the other participants were required to collect five trials for all three tasks. Fewer trials were collected due to the lower physical abilities of the participants who had suffered a stroke. The tasks were performed on both sides (affected and less affected) in order to gain a better understanding of the SEHD performance and TETs. The stroke survivors were not asked to perform the third task due to a lack of control of each digit and the poor understanding of the task.

Data collection and statistical analysis

The designed software collected task performance data in real time, and the default collection frequency was 100 Hz. After the collection process, the system automatically transferred the data to a text file for further processing.

The results of the first task (forearm rotation) were processed in order to identify the "movement phase" and "holding phase." The "movement phase" is how we calculate the movement's smoothness. First, we had to identify the duration of the movement such that we could further calculate movement smoothness. There are several methods to calculate the moving phase from the data of the IMU, and we used one of the common ways to calculate the movement by finding the peak of acceleration and then 5% of the acceleration as the initiation of the action. Similarly, to find the termination of the movement. The time between the initiation and termination of the movement was considered the duration of the movement. Movement smoothness was calculated during the movement phase so as to understand the quality of the movement. Log dimensionless jerk (LDLJ) (Eq. (1)) was applied to represent movement smoothness (Gulde and Hermsdörfer, 2018; Melendez-Calderon et al., 2021). The results of the parameters were analyzed using the Pearson correlation coefficient with the Purdue Pegboard Test in order to understand the correlation between the SEHD and traditional evaluation tools.

Log dimensionless jerk (angular velocity)

$$\lambda_L^{\omega}(\omega) \triangleq -\ln\left(\frac{(t_2-t_1)^3}{\omega_{peak}^2}\int_{t_1}^{t_2}\left\|\frac{d^2}{dt^2}\omega(t)\right\|_2^2 dt\right),$$
$$\omega_{peak} \triangleq \max_{t\in[t_1,t_2]}\|\omega(t)\|_2. \qquad (1)$$

ω represents angular velocity, where $\omega(t)$ represents the angular velocity of a movement in the time domain, and t_1 and t_2 are the start and stop times of the movement. The parameters that were applied in the following analysis were the duration of the movements (pronation and supination) and the LDLJ of the movements. Pearson's correlation coefficient was applied to compare the correlations between the parameters and results of the PPT.

Pearson's correlation coefficient was applied to compare the maximum grip strength of the device and results of the Jamar dynamometer.

The process of the sequential press was to calculate the percentage of total digit force application to the designed digit force application during the digit-pressing interval (Eq. 2). The results of the parameters were compared with the Purdue Pegboard Test so as to understand the correlation between the

TABLE 2 Demographic information of participants.

Group	Number	Age (mean ± SD)	Gender (male:female)	Dominant side of UE (right:left)
Healthy young adults	6	21.13 ± 0.46	4:2	6:0
Healthy elderly	6	64.18 ± 4.70	3:3	6:0
Stroke survivors	3	74.9 ± 4.16	0:3	3:0

novel device and traditional tools by using Pearson's correlation coefficient.

Finger independence

$$\text{Finger Independence} = \frac{F_{\text{disired digit}}}{F_{\text{total digits}}} \times 100\% \quad (2)$$

All data were processed using MATLAB software (MathWorks, Natick, Massachusetts, United States) and analyzed by SPSS (SPSS Inc., Chicago, Illinois, United States).

Results

Participants' demographic information and traditional evaluation tools

There were three groups that participated in the study. The demographic information is listed in Table 2. The selection of the groups and the number of groups have been explained in the abovementioned Methods section. All the participants were right-side dominant.

The results from the traditional evaluation tools showed that stroke survivors performed the worst among the three groups across all assessments. Healthy young adults performed slightly better than healthy older adults on all outcomes assessed (Table 3).

All the stroke survivors had ischemic strokes on the left side of the brain. All of them had had a stroke during the past 6 months (time since stroke = 9.3 ± 3.5 years). The average Fugl-Meyer motor score for the affected side was 28.3, while the average Fugl-Meyer motor score for the less affected side was 36.3.

Forearm rotation (pronation and supination)

There were two movement phases in this task: wrist pronation and supination. After applying the Pearson's correlation coefficient analysis, there was a medium negative correlation between the duration of supination with the dominant-side hand task in the PPT [r (Yeudall et al., 1986) = −0.493, $p < 0.05$], both-hands task in the PPT [r (Yeudall et al., 1986) = −0.469, $p < 0.05$], and the assembly task in the PPT [r (Yeudall et al., 1986) = −0.488, $p < 0.05$] (Table 4). There was a moderate-to-high negative correlation between the movement smoothness of pronation and the dominant-side hand task in the PPT [r (Yeudall et al., 1986) = −0.724, $p < 0.01$], medium-to-negative correlation between the smoothness of pronation with both-hands task in the PPT [r (Yeudall et al., 1986) = −0.479, $p < 0.05$], and the assembly task in the PPT [r (Yeudall et al., 1986) = −0.535, $p < 0.05$].

Maximum grip

The purpose of this movement was to understand whether to use affordable sensors to measure maximum gripping force. After the Pearson's correlation coefficient analysis, there was a highly positive correlation between the maximum grip force and Jamar dynamometer [r (Yeudall et al., 1986) = 0.821, $p < 0.01$] (Table 5).

Sequential press

According to the designed task, the finger pressuring force could represent the independence of each digit if the participant could complete the task in sequence. After the Pearson's correlation coefficient analysis of the finger independence, there was a moderate-to-negative correlation between the middle-finger independence and the right-hand subtask of the PPT [r (Yoshida et al., 2019) = −0.615, $p < 0.05$], medium-to-negative correlation between the middle-finger independence, and both-hand task of the PPT [r (Yoshida et al., 2019) = −0.565, $p < 0.05$] (Table 6).

Discussion

Purdue Pegboard Test and device-based processed data

The Purdue Pegboard Test is a standardized and widely used evaluation tool of hand dexterity and upper extremity functions. The movement of the Purdue Pegboard Test could be segmented into the following phases: short lifting, the transition of the objects, picking up the object, and placing the object at the desired spot. If the designed tasks are based on these segmented movements, using the SEHD could offer proper correlations with

TABLE 3 Results of assessment conducted by traditional evaluation tools.

		Purdue Pegboard Test (dominant)		Purdue Pegboard Test (both)		Purdue Pegboard Test (assembly)		Jamar dynamometer (dominant)	
Group	**Number**	**Mean**	**SD**	**Mean**	**SD**	**Mean**	**SD**	**Mean**	**SD**
Healthy young adults	6	16.61	1.10	13.17	1.41	42.67	8.80	30.67	14.53
Healthy elderly	6	15.33	0.63	12.17	0.91	36.61	4.46	23.25	2.87
Stroke survivors	3	11.5	1.32	9.67	0.29	23.17	2.47	14.25	3.88

TABLE 4 Correlation between the Purdue Pegboard Test and SEHD data during forearm rotation movement task.

Correlations

	Duration of supination	LDLJ of pronation	LDLJ of supination	
Purdue (dominant)	Correlation coefficient	−0.493[a]	−0.724 **	−0.498[a]
	Sig. (2-tailed)	0.038	0.001	0.035
	N	18	18	18
Purdue (both)	Correlation coefficient	−0.469[a]	−0.479[a]	−0.421
	Sig. (2-tailed)	0.050	0.044	0.082
	N	18	18	18
Purdue (assembly)	Correlation coefficient	−0.488[a]	−0.535[a]	−0.423
	Sig. (2-tailed)	0.040	0.022	0.082
	N	18	18	18

[a]Correlation is significant at the 0.05 level (2-tailed).

TABLE 5 Correlation between Jamar dynamometer and data from SEHD during maximum grip task.

Correlation

	Maximum grip task	
Jamar dynamometer	Correlation coefficient	0.821[a]
	Sig. (2-tailed)	0.000
	N	18

[a]Correlation is significant at the 0.01 level (2-tailed).

the Purdue Pegboard Test and could be considered a proper reference for clinicians to monitor one's upper extremity functions and/or hand dexterity.

The results showed a medium-to-moderate negative correlation between supination duration and moving forward the tasks. The duration of a movement is one of the indicators of movement ability; the shorter the movement duration, the better the movement ability. According to the calculation of movement smoothness (Balasubramanian et al., 2011), a larger LDLJ meant worse performance of movement smoothness. The results of the studies showed a moderate-to-negative correlation between the pronation and supination of the wrist movement and the traditional Purdue Pegboard Tests of the dominant side, both-hand side, and assembly.

However, the results do not appear to offer a high correlation, which might be due to the following reasons: (A) although there were three groups of participants, most of them were healthy individuals despite differences in age. In addition, the movements were designed according to activities of daily living, which means that these tasks were easy to perform for individuals without any upper extremity disability; (B) the Purdue Pegboard Test results were rendered, which meant that the results of the PPT could not offer details on each segment's upper extremity abilities. Therefore, each individual might apply different strategies during the test, and the same individual might even apply different strategies in each object-picking process; (C) there were ceiling effects and learning effects in healthy individuals conducting the Purdue Pegboard Test (Tseng et al., 2017); (D) movement smoothness (LDLJ) was calculated using the period of the movement unit and the acceleration change during the movement unit. Therefore, LDLJ and the Purdue Pegboard Test might not correlate highly with each other.

TABLE 6 Correlation between Purdue Pegboard Test and data from SEHD during sequential pressing task.

Correlations

		Finger independence (index finger)	Finger independence (middle finger)
Purdue (dominant)	Correlation coefficient	−0.448	−0.615[a]
	Sig. (2-tailed)	0.082	0.011
	N	12	12
Purdue (both)	Correlation coefficient	−0.072	−0.565[a]
	Sig. (2-tailed)	0.790	0.023
	N	12	12

[a]Correlation is significant at the 0.05 level (2-tailed).

Overall, correlation is one of the important indicators for measuring the quality of mobility movements. Although the results of the SEHD may not correlate well with the Purdue Pegboard Test, it can still be considered a useful monitoring device for assessing hand and upper extremity abilities.

Another task related to the Purdue Pegboard Test is using the SEHD for the sequential pressing tasks. Since finger independence is one of the indicators of hand dexterity, the correlation between calculated finger independence and the Purdue Pegboard Test might offer relative references in understanding one's dexterity.

The results show that the middle finger offered a better correlation coefficient with the Purdue Pegboard Test. This may be due to the different roles of the index finger and middle finger. The index finger is the primary guide when performing precise movements, while the middle finger is more supportive and adjustive in the modification of the movement. Finger independence is presented as percentage, with a higher percentage representing poorer finger independence. Therefore, the negative correlations between the Purdue Pegboard Test and percentage of middle finger independence are consistent with our observations.

Jamar dynamometer and device-based processed data

The correlation results between the Jamar dynamometer and the data obtained from the SEHD during the maximum grip task are the most important results that can be derived from this study. This suggests that the application of affordable force sensors on this device can provide a reference for monitoring one's power gripping ability and that this device can be used for the rehabilitation and monitoring of people with hand disabilities. Furthermore, the result also offers the reasonable belief that applying affordable force sensors to the device could provide references in monitoring one's power gripping ability. Therefore, it is possible to use this device in the rehabilitation and monitoring of people with hand disabilities.

Novelty of sensor-embedded holding device

The idea of creating a holding device was to provide a possible solution for the clinical issues in evaluating the hand and UE functions. These issues included 1) undigitized data (Marvin, 2012; Chesworth et al., 2014; Kim et al., 2016), 2) subjective data collection (Marvin, 2012), 3) removal of additional human labor (Bohannon et al., 2006; Sigirtmac and Oksuz, 2022), 4) complicated newer technologies for most of the users (Yusif et al., 2016), and 5) newer devices that were not focused on the force (Tognetti et al., 2006; Lin et al., 2018).

The development of the SEHD was to solve the above problems. The data collected by the SEHD were digitized and could be applied as useful clinical relevant parameters after processing. The shape, appearance, and weight of the SEHD were designed to provide a more intuitive user experience, remove technical barriers for users, and shorten the learning time for users to operate the device. Force sensors that were used in the SEHD could collect appropriate data, and the integration of the IMU and force sensors could provide more parameters related to UE abilities that most of the existing devices could not achieve.

Limitations and future research

The sample size of the study was small, yet the primary purpose of this study was to introduce a novel monitoring device and demonstrate its operability. Studies with larger sample sizes will be considered in future planning. Another limitation would be the choice of the traditional evaluation tools, as such tools might not be able to correlate comprehensively with the SEHD. The concept of the movement tasks for the SEHD was to mimic the partial movement segments of the Purdue Pegboard Test. The PPT is a much complicated movement test, and the score of the PPT is a rendered result that includes UE gross movement, hand dexterity, hand–eye coordination, and control of placement. Therefore, applying other UE movement–related evaluation tools or designing other complex movements for the SEHD might be required.

There are several studies that reveal that grasp is highly related to cognitive rehabilitation (Morganti, 2004; van Vliet et al., 2013) that could be applied to other groups for rehabilitation or training purposes, such as for stroke survivors in order to improve their external focus (Durham et al., 2014) and for people with mild cognitive impairments (Cosgrove, 2016).

Therefore, future research may focus on the following directions: (A) continue to develop the SEHD as a rehabilitation intervention for different populations, such as for people who have suffered stroke, people with mild cognitive impairment, people with carpal tunnel syndrome, and examining the outcomes after an intervention; (B) continue to improve the SEHD's capabilities, such as changing the wired SEHD to a wireless one or changing the sensors to ones with better resolutions for researchers; (C) integrate the SEHD and gamification software to provide a better user experience in different monitoring and rehabilitation settings, such as in clinics, in institutes, or when performing home activities (Lin et al., 2021). With the programmed interface, users can operate the SEHD alone with minimum assistance, which could benefit the users and caregivers.

Conclusion

The purpose of the study was to develop a novel digitized assessment device that could acquire digitized data and process functional parameters from the designed movements in order to present upper extremity functional abilities, such as grip-force and movement abilities. By comparing the processed data with that of other traditional clinical tools, the quantitative functional outcome measurements suggest that the SEHD system can be used as a monitoring tool for users in need. The integrated hardware and software in the SEHD offer proper usability and feasibility for people who need UE rehabilitation, allowing them to understand their upper extremity ability at home or in hospitals.

Based on this research, SEHD processed data could be considered as references for users in understanding their UE functional abilities.

Data availability statement

The original contributions presented in the study are included in the article/Supplementary Material; further inquiries can be directed to the corresponding author.

Ethics statement

The studies involving human participants were reviewed and approved by the Institutional Review Board at the National Cheng Kung University Hospital. The patients/participants provided their written informed consent to participate in this study.

Author contributions

CM conducted this research and wrote the manuscript. FS instructed the study and offered valuable suggestions on the design of the device and study design. PM helped with the data processing and provided recommendations in discussions. Finally, HH provided ideas for study design and gave professional reviews on the clinical prospects. All authors contributed to manuscript revision, and read and approved the submitted version.

Funding

Grant support was provided by the Ministry of Science and Technology (Taiwan). The grant number is MOST 107-2221-E-006-233-MY3.

Acknowledgments

This research was conducted under the guidance of Hsiao-Feng Chieh, Chien-Ju Lin, and other members of the Motion Analysis Laboratory at the National Cheng Kung University. Clinical suggestions were provided by Li-Chieh Kuo. Technical support was provided by DASITEK Co., Taiwan.

Conflict of interest

The authors declare that this research was conducted in the absence of any commercial or financial relationships that could be construed as a potential conflict of interest.

Publisher's note

All claims expressed in this article are solely those of the authors and do not necessarily represent those of their affiliated organizations, or those of the publisher, editors, and reviewers. Any product that may be evaluated in this article, or claim that may be made by its manufacturer, is not guaranteed or endorsed by the publisher.

Supplementary material

The Supplementary Material for this article can be found online at: https://www.frontiersin.org/articles/10.3389/fbioe.2022.976242/full#supplementary-material

References

Ares, F. A., Presso, M., and Aciti, C. (2022). "Prototype of a biomechanical MIDI controller for use in virtual synthesizers," in Argentine Congress of Computer Science (Springer).

Balasubramanian, S., Melendez-Calderon, A., and Burdet, E. (2011). A robust and sensitive metric for quantifying movement smoothness. *IEEE Trans. Biomed. Eng.* 59 (8), 2126–2136. doi:10.1109/tbme.2011.2179545

Bohannon, R. W., Peolsson, A., Massy-Westropp, N., Desrosiers, J., and Bear-Lehman, J. (2006). Reference values for adult grip strength measured with a jamar dynamometer: A descriptive meta-analysis. *Physiotherapy* 92 (1), 11–15. doi:10.1016/j.physio.2005.05.003

Caeiro-Rodríguez, M., Otero-González, I., Mikic-Fonte, F. A., and Llamas-Nistal, M. (2021). A systematic review of commercial smart gloves: Current status and applications. *Sensors* 21 (8), 2667. doi:10.3390/s21082667

Cai M., Kitani K. M., and Sato Y. (2016). Understanding hand-object manipulation with grasp types and object attributes *In Robotics: Science and Systems* 3.

Cano-De-La-Cuerda, R., Molero-Sánchez, A., Carratalá-Tejada, M., Alguacil-Diego, I., Molina-Rueda, F., Miangolarra-Page, J., et al. (2015). Theories and control models and motor learning: Clinical applications in neurorehabilitation. *Neurol. Engl. Ed.* 30 (1), 32–41. doi:10.1016/j.nrleng.2011.12.012

Castiello, U. (2005). The neuroscience of grasping. *Nat. Rev. Neurosci.* 6 (9), 726–736. doi:10.1038/nrn1744

Chen, P-T., Hsu, H-Y., Su, Y-H., Lin, C-J., Chieh, H-F., Kuo, L-C., et al. (2022). Force control strategy of five-digit precision grasping with aligned and unaligned configurations. *Hum. Factors*, 00187208211040914. doi:10.1177/00187208211040914

Chesworth, B. M., Hamilton, C. B., Walton, D. M., Benoit, M., Blake, T. A., Bredy, H., et al. (2014). Reliability and validity of two versions of the upper extremity functional index. *Physiother. Can.* 66 (3), 243–253. doi:10.3138/ptc.2013-45

Chiu, H. Y., Hsu, H. Y., Kuo, L. C., Chang, J. H., and Su, F. C. (2009). Functional sensibility assessment. Part I: Develop a reliable apparatus to assess momentary pinch force control. *J. Orthop. Res.* 27 (8), 1116–1121. doi:10.1002/jor.20859

Chodock, E., Hahn, J., Setlock, C. A., and Lipps, D. B. (2020). Identifying predictors of upper extremity muscle elasticity with healthy aging. *J. biomechanics* 103, 109687. doi:10.1016/j.jbiomech.2020.109687

Cosgrove, J. (2016). *Investigating reach and grasp in Parkinson's disease cognitive impairment*. University of Hull and the University of York.

Crowe, C. S., Massenburg, B. B., Morrison, S. D., Chang, J., Friedrich, J. B., Abady, G. G., et al. (2020). Global trends of hand and wrist trauma: A systematic analysis of fracture and digit amputation using the global burden of disease 2017 study. *Inj. Prev.* 26 (2), i115–i124. doi:10.1136/injuryprev-2019-043495

Domalain, M., Vigouroux, L., Danion, F., Sevrez, V., and Berton, E. (2008). Effect of object width on precision grip force and finger posture. *Ergonomics* 51 (9), 1441–1453. doi:10.1080/00140130802130225

Dowrick, A. S., Gabbe, B. J., Williamson, O. D., and Cameron, P. A. (2005). Outcome instruments for the assessment of the upper extremity following trauma: A review. *Injury* 36 (4), 468–476. doi:10.1016/j.injury.2004.06.014

Durham, K., Sackley, C., Wright, C., Wing, A., Edwards, M., and Van Vliet, P. (2014). Attentional focus of feedback for improving performance of reach-to-grasp after stroke: A randomised crossover study. *Physiotherapy* 100 (2), 108–115. doi:10.1016/j.physio.2013.03.004

Fujiwara, E., dos Santos, M. F. M., and Suzuki, C. K. (2014). Flexible optical fiber bending transducer for application in glove-based sensors. *IEEE Sens. J.* 14 (10), 3631–3636. doi:10.1109/jsen.2014.2330998

Golant, S. M. (2017). A theoretical model to explain the smart technology adoption behaviors of elder consumers (Elderadopt). *J. Aging Stud.* 42, 56–73. doi:10.1016/j.jaging.2017.07.003

Guerra, R., Fonseca, I., Pichel, F., Restivo, M., and Amaral, T. (2014). Hand length as an alternative measurement of height. *Eur. J. Clin. Nutr.* 68 (2), 229–233. doi:10.1038/ejcn.2013.220

Gulde, P., and Hermsdörfer, J. (2018). Smoothness metrics in complex movement tasks. *Front. Neurol.* 9, 615. doi:10.3389/fneur.2018.00615

Halverson, H. M. (1937). Studies of the grasping responses of early infancy: I. *Pedagogical Seminary J. Genet. Psychol.* 51 (2), 371–392. doi:10.1080/08856559.1937.10532507

Harih, G., and Dolšak, B. (2014). Comparison of subjective comfort ratings between anatomically shaped and cylindrical handles. *Appl. Ergon.* 45 (4), 943–954. doi:10.1016/j.apergo.2013.11.011

Harwin, W., and Barrow, A. (2013). *Multi-finger grasps in a dynamic environment*. Springer, 5–30. Multi-finger Haptic Interaction.

Hsiao, P-C., Yang, S-Y., Lin, B-S., Lee, I-J., and Chou, W. (2015). "Data glove embedded with 9-axis IMU and force sensing sensors for evaluation of hand function," in 2015 37th annual international conference of the IEEE Engineering in Medicine and Biology Society (EMBC), Milan, Italy, 25-29 August 2015 (IEEE). doi:10.1109/EMBC.2015.7319426

Hsu, C-H., Lin, Y-C., Hsu, H-Y., Chieh, H-F., Lin, C-J., Ling, S-F., et al. (2021). A novel and clinically feasible instrument for quantifying upper Limb muscle tone and motor function via indirect measure methods. *IEEE J. Transl. Eng. Health Med.* 10, 1–8. doi:10.1109/jtehm.2021.3136754

Hsu, H-Y., Kuan, T-S., Tsai, C-L., Wu, P-T., Kuo, Y-L., Su, F-C., et al. (2021). Effect of a novel perturbation-based pinch task training on sensorimotor performance of upper extremity for patients with chronic stroke: A pilot randomized controlled trial. *Archives Phys. Med. Rehabilitation* 102 (5), 811–818. doi:10.1016/j.apmr.2020.11.004

Huisstede, B. M., Bierma-Zeinstra, S. M., Koes, B. W., and Verhaar, J. A. (2006). Incidence and prevalence of upper-extremity musculoskeletal disorders. A systematic appraisal of the literature. *BMC Musculoskelet. Disord.* 7 (1), 7. doi:10.1186/1471-2474-7-7

Hulley, S. B. (2007). *Designing clinical research*. Lippincott Williams & Wilkins.

Kamimura, T., and Ikuta, Y. (2001). Evaluation of grip strength with a sustained maximal isometric contraction for 6 and 10 seconds. *J. Rehabilitation Med.* 33 (5), 225–229. doi:10.1080/165019701750419626

Kanti Majumdar, K. (2014). *Relationship of activity of daily living with quality of life*. British Medical Bulletin, 757–764. BBB[2][4][2014].

Karnik, A., Adke, D., and Sathe, P. (2020). "Low-cost compact theft-detection system using MPU-6050 and blynk IoT platform," in 2020 IEEE Bombay Section Signature Conference (IBSSC), Mumbai, India, 04-06 December 2020 (IEEE). doi:10.1109/IBSSC51096.2020.9332214

Kim, J-N., Ryu, M-H., Choi, H-R., Yang, Y-S., and Kim, T-K. (2013). Development and functional evaluation of an upper extremity rehabilitation system based on inertial sensors and virtual reality. *Int. J. Distributed Sens. Netw.* 9 (8), 168078. doi:10.1155/2013/168078

Kim, W-S., Cho, S., Baek, D., Bang, H., and Paik, N-J. (2016). Upper extremity functional evaluation by Fugl-Meyer assessment scoring using depth-sensing camera in hemiplegic stroke patients. *PloS one* 11 (7), e0158640. doi:10.1371/journal.pone.0158640

Koester, D., Schack, T., and Westerholz, J. (2016). Neurophysiology of grasping actions: Evidence from ERPs. *Front. Psychol.* 7, 1996. doi:10.3389/fpsyg.2016.01996

Lin, B-S., Hsiao, P-C., Yang, S-Y., Su, C-S., and Lee, I-J. (2017). Data glove system embedded with inertial measurement units for hand function evaluation in stroke patients. *IEEE Trans. Neural Syst. Rehabil. Eng.* 25 (11), 2204–2213. doi:10.1109/tnsre.2017.2720727

Lin, B-S., Lee, I-J., Yang, S-Y., Lo, Y-C., Lee, J., and Chen, J-L. (2018). Design of an inertial-sensor-based data glove for hand function evaluation. *Sensors* 18 (5), 1545. doi:10.3390/s18051545

Lin, C-C., Lin, Y-C., Hsu, H-Y., Lin, Y-S., Su, F-C., and Kuo, L-C. (2021). "Home-based tele-rehabilitation system provides task-oriented training courses based on the stages of stroke," in 2021 IEEE Region 10 Symposium (TENSYMP), Jeju, Korea, 23-25 August 2021 (IEEE). doi:10.1109/TENSYMP52854.2021.9550884

Marvin, K. (2012). Purdue pegboard test (PPT). Dostupno na. Available at: https://strokengineca/en/assessments/purdue-pegboard-test-ppt.

Mathiowetz, V. (2002). Comparison of Rolyan and Jamar dynamometers for measuring grip strength. *Occup. Ther. Int.* 9 (3), 201–209. doi:10.1002/oti.165

Melendez-Calderon, A., Shirota, C., and Balasubramanian, S. (2021). Estimating movement smoothness from inertial measurement units. *Front. Bioeng. Biotechnol.* 8, 558771. doi:10.3389/fbioe.2020.558771

Morganti, F. (2004). *Virtual interaction in cognitive neuropsychology*. Cybertherapy: Ios Press, 55–70.

Nation, U. (2019). *World population ageing 2019: Key messages*. United Nation: World Population Ageing, 1–2.

Ngui, M-H., and Lee, W-K. (2019). "Low power wearable device with GPS and indoor positioning system," in 2019 International Conference on Green and Human Information Technology (ICGHIT), Kuala Lumpur, Malaysia, 5-17 January 2019 (IEEE). doi:10.1109/ICGHIT.2019.00037

Nikkhoo, M., Niu, C-C., Fu, C-J., Lu, M-L., Chen, W-C., Lin, Y-H., et al. (2021). Reliability and validity of a mobile device for assessing head control ability. *J. Med. Biol. Eng.* 41 (1), 45–52. doi:10.1007/s40846-020-00577-w

Onder, G., Penninx, B. W., Lapuerta, P., Fried, L. P., Ostir, G. V., Guralnik, J. M., et al. (2002). Change in physical performance over time in older women: The women's health and aging study. *Journals Gerontology Ser. A Biol. Sci. Med. Sci.* 57 (5), M289–M293. doi:10.1093/gerona/57.5.m289

Quinn, L., Busse, M., and Dal Bello-Haas, V. (2013). Management of upper extremity dysfunction in people with Parkinson disease and huntington disease: Facilitating outcomes across the disease lifespan. *J. Hand Ther.* 26 (2), 148–155. doi:10.1016/j.jht.2012.11.001

Reissner, L., Fischer, G., List, R., Giovanoli, P., and Calcagni, M. (2019). Assessment of hand function during activities of daily living using motion tracking cameras: A systematic review. *Proc. Inst. Mech. Eng. H.* 233 (8), 764–783. doi:10.1177/0954411919851302

Sani, O. G., and Shanechi, M. M. (2021). Motor Control: Sensory feedback can give rise to neural rotations. *Elife* 10, e75469. doi:10.7554/elife.75469

Shi, Y. X., Tian, J. H., Yang, K. H., and Zhao, Y. (2011). Modified constraint-induced movement therapy versus traditional rehabilitation in patients with upper-extremity dysfunction after stroke: A systematic review and meta-analysis. *Archives Phys. Med. rehabilitation* 92 (6), 972–982. doi:10.1016/j.apmr.2010.12.036

Shin, J-H., Kim, M-Y., Lee, J-Y., Jeon, Y-J., Kim, S., Lee, S., et al. (2016). Effects of virtual reality-based rehabilitation on distal upper extremity function and health-related quality of life: A single-blinded, randomized controlled trial. *J. Neuroeng. Rehabil.* 13 (1), 17–10. doi:10.1186/s12984-016-0125-x

Sigirtmac, I. C., and Oksuz, C. (2022). Determination of the optimal cutoff values and validity of the Purdue Pegboard Test. *Br. J. Occup. Ther.* 85 (1), 62–67. doi:10.1177/03080226211008046

Tarchanidis, K. N., and Lygouras, J. N. (2003). Data glove with a force sensor. *IEEE Trans. Instrum. Meas.* 52 (3), 984–989. doi:10.1109/tim.2003.809484

Tognetti, A., Carbonaro, N., Zupone, G., and De Rossi, D. (2006). "Characterization of a novel data glove based on textile integrated sensors," in 2006 International Conference of the IEEE Engineering in Medicine and Biology Society, New York, NY, USA, 30 August 2006 - 03 September 2006 (IEEE). doi:10.1109/IEMBS.2006.260574

Tseng, Y-C., Chang, K-Y., Liu, P-L., and Chang, C-C. (2017). "Applying the purdue pegboard to evaluate precision assembly performance," in 2017 IEEE International Conference on Industrial Engineering and Engineering Management (IEEM), Singapore, 10-13 December 2017 (IEEE). doi:10.1109/IEEM.2017.8290078

Turella, L., and Lingnau, A. (2014). Neural correlates of grasping. *Front. Hum. Neurosci.* 8, 686. doi:10.3389/fnhum.2014.00686

van Vliet, P., Pelton, T. A., Hollands, K. L., Carey, L., and Wing, A. M. (2013). Neuroscience findings on coordination of reaching to grasp an object: Implications for research. *Neurorehabil. Neural Repair* 27 (7), 622–635. doi:10.1177/1545968313483578

Vergara, M., Sancho-Bru, J. L., Gracia-Ibáñez, V., and Pérez-González, A. (2014). An introductory study of common grasps used by adults during performance of activities of daily living. *J. Hand Ther.* 27 (3), 225–234. doi:10.1016/j.jht.2014.04.002

Wang, Q., Chen, W., and Markopoulos, P. (2014). "Literature review on wearable systems in upper extremity rehabilitation," in IEEE-EMBS International Conference on Biomedical and Health Informatics (BHI), Valencia, Spain, 01-04 June 2014 (IEEE). doi:10.1109/BHI.2014.6864424

Yang, Y., Fermuller, C., Li, Y., and Aloimonos, Y. (2015). "Grasp type revisited: A modern perspective on a classical feature for vision," in Proceedings of the IEEE Conference on Computer Vision and Pattern Recognition, Boston, MA, USA, 07-12 June 2015. doi:10.1109/CVPR.2015.7298637

Yeudall, L. T., Fromm, D., Reddon, J. R., and Stefanyk, W. O. (1986). Normative data stratified by age and sex for 12 neuropsychological tests. *J. Clin. Psychol.* 42 (6), 918–946. doi:10.1002/1097-4679(198611)42:6<918::aid-jclp2270420617>3.0.co;2-y

Yoshida, A., Kurimoto, S., Iwatsuki, K., Saeki, M., Nishizuka, T., Nakano, T., et al. (2019). Upper extremity disability is associated with pain intensity and grip strength in women with bilateral idiopathic carpal tunnel syndrome. *NeuroRehabilitation* 44 (2), 199–205. doi:10.3233/nre-182589

Yusif, S., Soar, J., and Hafeez-Baig, A. (2016). Older people, assistive technologies, and the barriers to adoption: A systematic review. *Int. J. Med. Inf.* 94, 112–116. doi:10.1016/j.ijmedinf.2016.07.004

frontiers | Frontiers in Bioengineering and Biotechnology

TYPE Original Research
PUBLISHED 21 November 2022
DOI 10.3389/fbioe.2022.1051747

Check for updates

OPEN ACCESS

EDITED BY
Qichang Mei,
Ningbo University, China

REVIEWED BY
Fu-Lien Wu,
University of Illinois at Urbana-Champaign, United States
Yinghu Peng,
Shenzhen Institutes of Advanced Technology (CAS), China

*CORRESPONDENCE
Xianyi Zhang,
zhangxianyi@mail.sysu.edu.cn

†These authors have contributed equally to this work

SPECIALTY SECTION
This article was submitted to Biomechanics,
a section of the journal Frontiers in Bioengineering and Biotechnology

RECEIVED 23 September 2022
ACCEPTED 09 November 2022
PUBLISHED 21 November 2022

CITATION
Cheng J, Zeng Q, Lai J and Zhang X (2022), Effects of arch support doses on the center of pressure and pressure distribution of running using statistical parametric mapping.
Front. Bioeng. Biotechnol. 10:1051747.
doi: 10.3389/fbioe.2022.1051747

Effects of arch support doses on the center of pressure and pressure distribution of running using statistical parametric mapping

Jiale Cheng[1,2†], Qing Zeng[3,4†], Jiaqi Lai[1,2] and Xianyi Zhang[1,2*]

[1]School of Biomedical Engineering, Shenzhen Campus of Sun Yat-sen University, Shenzhen, China, [2]Key Laboratory of Sensing Technology and Biomedical Instrument of Guangdong Province, School of Biomedical Engineering, Sun Yat-sen University, Guangzhou, China, [3]Department of Rehabilitation Medicine, Zhujiang Hospital, Southern Medical University, Guangzhou, China, [4]School of Rehabilitation Medicine, Southern Medical University, Guangzhou, China

Insoles with an arch support have been used to address biomechanical risk factors of running. However, the relationship between the dose of support and running biomechanics remains unclear. The purpose of this study was to determine the effects of changing arch support doses on the center of pressure (COP) and pressure mapping using statistical parametric mapping (SPM). Nine arch support variations (3 heights * 3 widths) and a flat insole control were tested on fifteen healthy recreational runners using a 1-m Footscan pressure plate. The medial-lateral COP (COP_{ML}) coordinates and the total COP velocity ($COPV_{total}$) were calculated throughout the entirety of stance. One-dimensional and two-dimensional SPM were performed to assess differences between the arch support and control conditions for time series of COP variables and pressure mapping at a pixel level, respectively. Two-way ANOVAs were performed to test the main effect of the arch support height and width, and their interaction on the peak values of the $COPV_{total}$. The results showed that the $COPV_{total}$ during the forefoot contact and forefoot push off phases was increased by arch supports, while the COP medial-lateral coordinates remained unchanged. There was a dose-response effect of the arch support height on peak values of the $COPV_{total}$, with a higher support increasing the first and third valleys but decreasing the third peak of the $COPV_{total}$. Meanwhile, a higher arch support height shifted the peak pressure from the medial forefoot and rearfoot to the medial arch. It is concluded that changing arch support doses, primarily the height, systematically altered the COP velocities and peak plantar pressure at a pixel level during running. When assessing subtle modifications in the arch support, the COP velocity was a more sensitive variable than COP coordinates. SPM provides a high-resolution view of pressure comparisons, and is recommended for future insole/footwear investigations to better understand the underlying mechanisms and improve insole design.

KEYWORDS

center of pressure, pressure distribution, statistical parametric mapping, arch support, running biomechanics

1 Introduction

Running-related injuries primarily result from an accumulation of repetitive stress applied to the body, and technical improvements (e.g., footwear and insoles) could help address biomechanical risk factors such as controlling joint motions and shifting musculoskeletal loading (Willwacher et al., 2022). Among footwear/insole designs, the arch support has been frequently adopted to manage lower limb complaints by improving the dynamic function of lower limbs (Hunt et al., 2017; Peng et al., 2021). Foot posture with a lower arch has been associated with lower limb pathologies including exercise-related injuries, medial tibial stress syndrome (MTSS) and patellofemoral pain (Menz et al., 2013; Neal et al., 2014). Compared with a flat insole control, using an arch support significantly reduces the impact after strike, redistributes plantar pressure and improves lower limb coordination (Fong et al., 2020; Huang et al., 2020; Jafarnezhadgero et al., 2020).

The human foot arch deforms during gait to fulfill its role in storing and recoiling elastic energy and acting as a lever during push-off (Stearne et al., 2016). The amount of arch support determines the allowed arch deformation. To optimize arch support parameters for running, it is essential to establish the dose-response relationship between arch support parameters and running biomechanics. Although the human foot arch deforms in a 3D manner, previous studies mainly evaluated the effect of arch support height alterations on biomechanical risk factors of running-related injuries, such as rearfoot kinematics (Wahmkow et al., 2017) and the center of pressure (COP) medial-lateral displacements during running (Zhang et al., 2022). However, no systematic effects on these biomechanical variables were observed by changing the arch support parameters. From mechanical perspective, changing the doses of the arch support would induce corresponding alterations in running biomechanics at some level. A more sensitive biomechanical variable that changes systematically with the arch support parameter is warranted.

The plantar pressure variables, including the COP and plantar pressure mapping, are subject measures of foot function during gait and excessive pressure on foot tissues have been associated with a higher risk of running-related injuries (De Cock et al., 2008; Fernández-Seguín et al., 2014; Bergstra et al., 2015). There are also other approaches to analyze plantar pressure patterns. For instance, entropy has been used to analyze the complexity of plantar pressure patterns (Liau et al., 2019; Liau et al., 2021). Several experimental studies have shown that plantar pressure variables were sensitive to variations in the rearfoot and forefoot components of the insole. Telfer et al. (2013a) found a linear dose-response effect of rearfoot wedges on the peak pressure of midfoot and lateral rearfoot during running. Zhang et al. (2022) showed a linear dose-response effect of forefoot wedges on the force-time integral under hallux and on the COP medial-lateral displacements during propulsion of running. The COP velocity during the forefoot contact phase of walking was also sensitive to the rearfoot elevation of insoles (Zhang and Li, 2014). It is, therefore, promising to find a systematic relationship between the arch support doses and pressure variables during running using experimental approaches.

It needs to be noted that most previous studies employed traditional subsampling approach to analyze the COP and pressure mapping (Xu et al., 2019; Duan et al., 2022; Xiang et al., 2022), which usually calculates the mean and maximum values of pressure data and divides the foot into a small number of zones. For instance, the mean value of the COP velocity of sub-phases of gait has been used to evaluate gait stability (Zhang and Li, 2014). The foot has been divided into 6 to 10 anatomical regions, and the mean pressure variables of those regions were compared with and without the use of the arch support (Farzadi et al., 2015; Naderi et al., 2019; Fong et al., 2020; Huang et al., 2020). Although this method can effectively reduce the large data set to a manageable size, ignoring most of the data may lead to inaccurate results, potentially leading to misinterpretations of foot function (Pataky and Goulermas, 2008). A systematic review suggested that contradictory results on pressure variables were reported in studies using different methods of subdividing the plantar area (Mann et al., 2016).

Alternatively, statistical parametric mapping (SPM), which originated in the field of neuroimaging (Friston et al., 1994), has been used to analyze one-dimensional (1D) and two-dimensional (2D) data in a continuous manner (Pataky and Goulermas, 2008). This process allows comparisons in more regions of interest, and reduces the likelihood of discarding potentially relevant information (Pataky et al., 2013). Hence, it has been increasing adopted in analyzing cyclical signals, such as cyclical joint angles (Pataky et al., 2013; D'Isidoro et al., 2020) and muscle activity patterns (Nuesch et al., 2019). 1D SPM can analyze time series data, such as the COP trajectories over the stance phase, at each sampling point in the time domain. 2D SPM works by bringing the plantar pressure images from all participants into anatomical correspondence, performing statistical tests at each sample point in the space domain (Booth et al., 2018). Based on a General Linear Model of the data analyses each pixel using standard (univariate) statistical tests under the null hypothesis. This method can generate continuous statistical maps across the entire plantar foot and therefore can detect local pressure alterations at a higher spatial resolution. As hypothesis testing in a continuous manner could

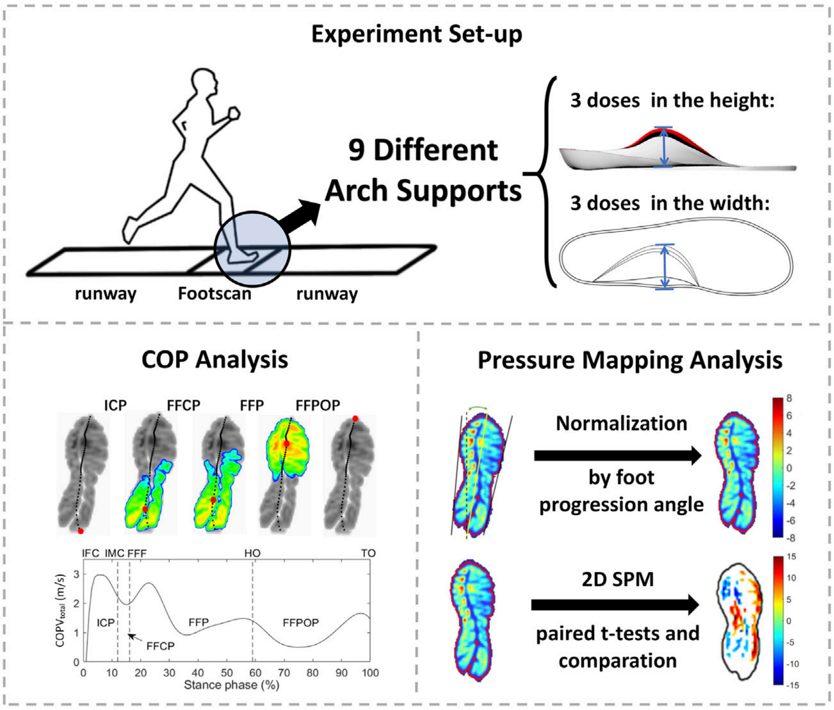

FIGURE 1
The experimental setting. ICP, initial contact phase; FFCP, forefoot contact phase; FFP, foot flat phase; FFPOP, forefoot push off phase; IFC, initial foot contact; IMC, initial metatarsal contact; FFC, forefoot contact; HO, heel-off; TO, toe-off.

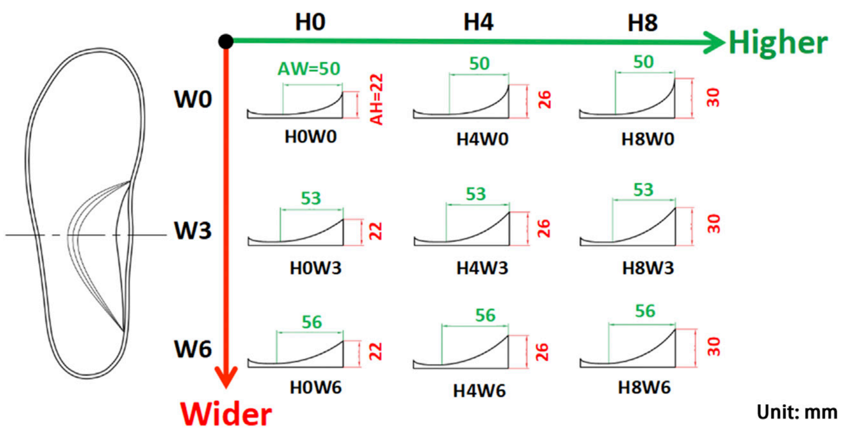

FIGURE 2
Nine variations of the arch support with three doses in the arch support height (AH: H0, H4, and H8 in mm) and three doses in the arch support width (AW: W0, W3, and W6 in mm).

reduce post hoc regional focus bias (Pataky et al., 2011), using SPM may help detect biomechanical variables that are sensitive to subtle insole modification.

The purpose of this study was to determine the acute effect of arch supports varying in the height and width on the COP coordinates, COP velocities and plantar pressure mapping of

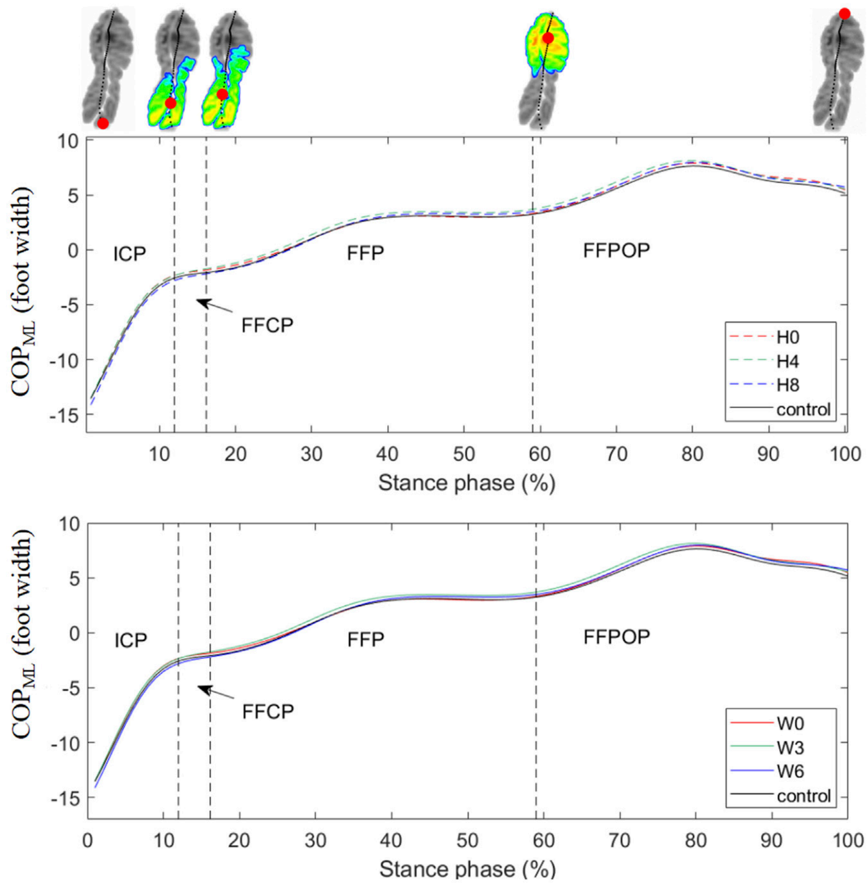

FIGURE 3
Mean curves of the COP_{ML} coordinates during running. Medial displacements of the COP_{ML} were expressed as positive values. H0, H4, and H8 represented the mean data of arch supports of three different heights; W0, W3, and W6 represented the mean data of arch supports of three different widths. Four subphases are indicated with vertical dash lines on the *x*-axis. ICP, initial contact phase; FFCP, forefoot contact phase; FFP, foot flat phase; FFPOP, forefoot push off phase; IFC, initial foot contact; IMC, initial metatarsal contact; FFC, forefoot contact; HO, heel-off; TO, toe-off.

running using SPM. Nine variations of arch supports (3 heights * 3 widths) were designed based on the morphological changes of the arch under different weight bearing conditions. This study hypothesized that using an arch support would alter the COP variables and plantar pressure mapping, and more specifically, that a higher and wider arch support would induce a lateral shift of the COP, a faster COP advancement during push-off, and higher plantar pressure under the medial midfoot.

2 Materials and methods

This study was approved by the Ethics Committee of the Zhujiang Hospital of Southern Medical University and written informed consent was provided by each participant. The experimental setting is shown in Figure 1.

2.1 Participants

The sample size calculation was based on the COP displacement data reported by Zhang et al. (2017) using GPower 3.1 software (University of Kiel, Kiel, Germany), considering a statistical design of the paired-t test, with a power of 80% and an alfa error of 5%. Based on the calculation, a total of 12 participants were needed to detect differences in the COP variables between different conditions. In case of possible bad trials, we recruited 15 young adults (age: 20.0 ± 1.2 years, height: 172.6 ± 4.5 cm, weight: 63.7 ± 4.6 kg) in this study. All participants were recreational runners who ran at least 10 km per week, and had no history of lower limb injuries in the preceding 6 months, and had a neutral foot type, which was assessed using a 6-item foot posture index (Redmond et al., 2008). They ran an average of 4.7 ± 1.3 times per week, 3.5 ± 1.1 km per run, and 14.7 ± 2.7 km in total. All participants had

TABLE 1 Results of tests of within-subject effects from two-way repeated ANOVAs.

Parameter	Effect	F	*p*-value	Best contrast (change% per 4-mm height increase)
1st peak	height	1.204	0.302	Linear (3% reduction)
	width	0.82	0.424	
	height*width	0.239	0.86	
2nd peak	height	1.881	0.17	
	width	2.845	0.066	
	height*width	0.328	0.859	
3rd peak	height	13.542	**0.001**	Linear (6% increase)
	width	1.559	0.219	
	height*width	0.212	0.931	
4th peak	height	1.559	0.219	
	width	0.373	0.69	
	height*width	0.509	0.729	
1st valley	height	11.19	**0.001**	Linear (4% increase)
	width	0.015	0.985	
	height*width	0.446	0.665	
2nd valley	height	0.302	0.675	
	width	0.579	0.564	
	height*width	2.467	0.068	
3rd valley	height	17.994	**0.001**	
	width	2.474	0.093	
	height*width	0.696	0.545	

Bold values show significant differences.

the same shoe size to avoid the effects of shoe size and for the convenience of the following analyses.

2.2 Arch supports

Insoles with a base arch support (H0W0) were digitally designed in Rhinoceros 3D modeling software (Rhino, Washington DC, United States) based on an averaged 3D scan model of the foot in a standing position (shoe size 9), which was provided by a local running shoe company (Li Ning Sports Ltd., Beijing, China). Variations in the arch support height and width were made upon this base arch support. To set a physiologically reasonable value of each variation, the longitudinal arch (LA) dimensions under different weight-bearing conditions were considered. Using a 3D foot scanning system (Yuandian Technology Co., Ltd., Shenzhen, China) on 30 recreational runners, the LA dimensions under three weight-bearing conditions (sitting, double-leg standing and single-leg standing) were compared. As the weight increased, average alterations of 4 mm in the LA height and 3 mm in the LA width were observed. These values were used to set the arch support parameters. A total of 9 variations of arch supports were designed, with the height and width increments setting at 4 mm and 3 mm, respectively (Figure 2). The insoles were made of EVA with a Shore hardness of 60C.

2.3 Data collection

Nine arch supports and a flat insole were put inside neutral running shoes (shoe model: ARBR005-2, Li Ning Sports Ltd., Beijing, China, see Supplementary Figures S1, S2 in

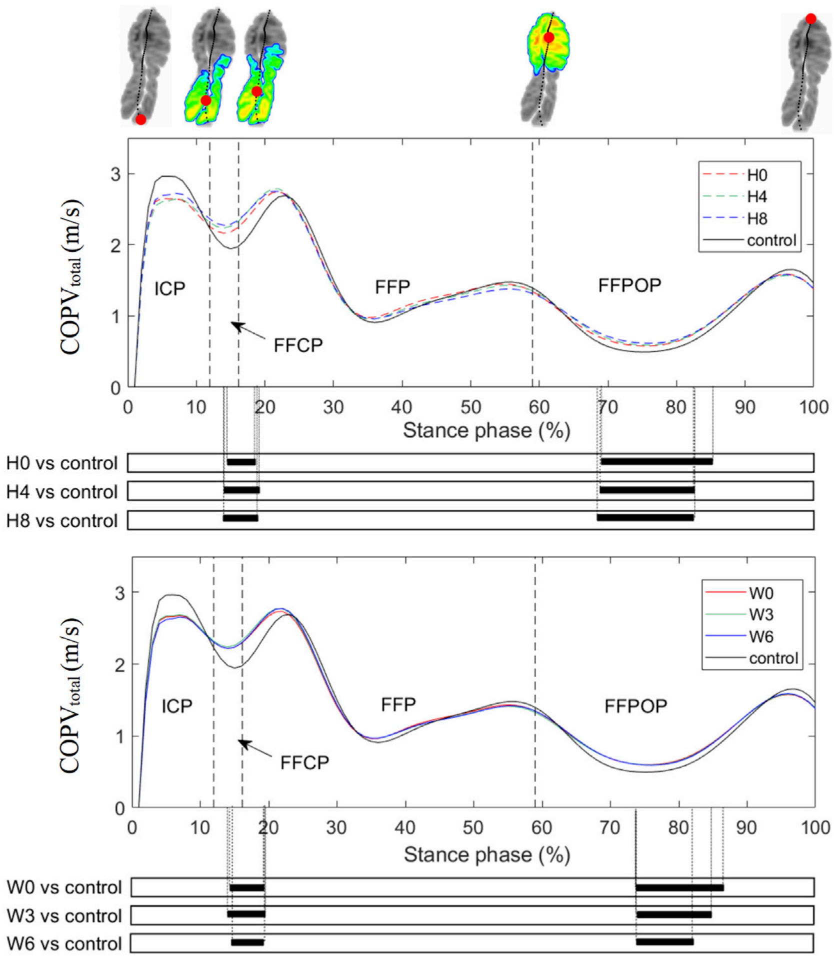

FIGURE 4
Mean curves of the $COPV_{total}$ during running. H0, H4, and H8 represented the mean data of arch supports of three different heights; W0, W3, and W6 represented the mean data of arch supports of three different widths. Four sub-phases are indicated with vertical lines on the *x*-axis. The black bar below the graph represents the time during which the differences between the groups occurred ($p < 0.05$), what was indicated by the SPM {t} statistics. ICP, initial contact phase; FFCP, forefoot contact phase; FFP, foot flat phase; FFPOP, forefoot push off phase; IFC, initial foot contact; IMC, initial metatarsal contact; FFC, forefoot contact; HO, heel-off; TO, toe-off.

Supplementary Material) and tested in a random order. The shoe midsole was made of uniform EVA material with no special structures/designs. Running with the flat insole was defined as the control condition. A 10 min familiarization phase of running was given for each testing condition. Participants were asked to run along a 20 m runway with an integrated 1-m pressure plate (RSscan International, Belgium) at their preferred speeds (3.48 ± 0.01 m/s). The pressure plate has 8,192 resistive sensors (a pixel resolution of 7.62 mm × 5.08 mm) to measure vertical plantar pressure at a frequency of 200 Hz. A laser timer was used to record running speed. A trial was recorded when the running speed was within 5% of the preferred speed of the participant. Five successful steps of each foot were recorded, and data of both feet were pooled together for further analysis. A total of 1,500 time series of the COP trajectory and 1,500 peak pressure images were measured.

2.4 Data and statistical analysis

The COP coordinates were exported from the Footscan software and were filtered with a fourth order low pass Butterworth filter at a cutoff frequency of 50 Hz. The end points were padded through a reflection technique, adding 15 data values at start and end of the data series (De Cock et al., 2008). After filtering, the total COP velocity ($COPV_{total}$)

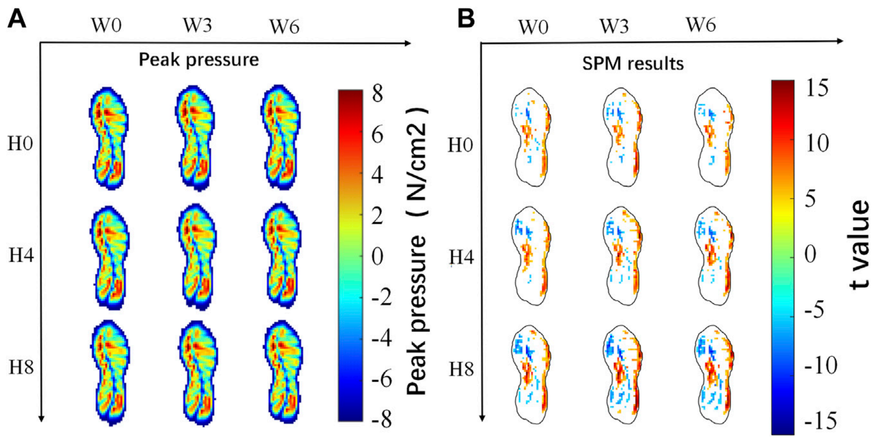

FIGURE 5
Results of plantar pressure analysis of 9 pairs of different arch supports.

was calculated with a simple differentiation and all trials were normalized for the stance time. The stance phase was divided into four sub-phases: initial contact phase (ICP), forefoot contact phase (FFCP), foot flat phase (FFP) and forefoot push off phase (FFPOP) (Chiu et al., 2013b). The ICP is defined as the period from initial foot contact (IFC) to initial metatarsal contact (IMC). The FFCP follows ICP until the entire forefoot contacts the pressure plate. The FFP starts from forefoot contact (FFC) to heel-off (HO). The FFPOP is the period from HO to toe-off (TO).

1D and 2D SPM were performed to assess differences between arch support and control conditions for time series of the COP variables and plantar pressure mapping, respectively. These methods use Random Field Theory to make statistical inferences about continuous 1D/2D data to test where signals may differ in time and space domains (Pataky et al., 2011). The COP trajectory in the medial-lateral direction (COP_{ML}) and $COPV_{total}$ were compared between the arch support and control conditions using 1D SPM paired-samples *t*-test. For this comparison, the average data of arch supports with the same heights (H0, H4 and H8) and same widths (W0, W3, and W6) were calculated. The plantar pressure data was normalized by foot progression angle (Keijsers et al., 2009) and then 2D SPM paired t-tests were performed to compare the normalized pressure mapping between the arch support and control conditions. In short, 1,500 peak pressure images were realigned firstly to ensure anatomical consistency. After realignment, a general linear model was employed to estimate the parameters of a temporal model and to derive the appropriate univariate test statistic SPM{t} at each pixel. The SPM{t} were assembled into SPM. Finally, statistical inferences were made on the basis of the SPM and Random Field Theory (Pataky, 2008). To determine the main effect for the arch support height, width, and their interaction, two-way ANOVAs were performed on the peak values of $COPV_{total}$. Where significant effects of the arch supports were found, linear, quadratic and cubic contrasts were tested to determine if there was a linear trend to the effect. For all statistical analysis, *p*-values less than 0.05 were considered statistically significant.

3 Results

The mean curves of the COP_{ML} during running are illustrated in Figure 3. The 1D SPM results showed no significant difference in the COP_{ML} trajectory between the arch support and control conditions during the entire stance phase.

Mean $COPV_{total}$ curves and the SPM results are illustrated in Figure 4, and comparisons in the anterior-posterior COP velocities ($COPV_{AP}$) and medial-lateral COP velocities ($COPV_{ML}$) are shown in Supplementary Figures S3, S4 in Supplementary Material. The $COPV_{total}$ curve showed a pattern of four peaks and three valleys during all shod running. After heel strike, the $COPV_{total}$ increased rapidly to the first peak and dropped to the first valley before forefoot flat. Then the $COPV_{total}$ fluctuated quickly to reach the second peak and valley and slowly up to the third peak before heel-off. During the FFPOP, the $COPV_{total}$ dropped to the third valley and then raised to the fourth peak till toe-off. Compared with the control, all arch supports showed significant differences in the $COPV_{total}$ during the FFCP and FFPOP of running. Similar trends were seen in the $COPV_{AP}$. In contrast, no significant differences in the $COPV_{ML}$ were observed between conditions.

Results of two-way ANOVAs examining two design factors (height and width of arch suppor) on the peaks and valleys of the $COPV_{total}$ are shown in Table 1. The height of arch support had a main linear effect on the first valley, third peak and third valley of the $COPV_{total}$, with a higher arch support causing an increase in the first and third $COPV_{total}$ valleys and a decrease in the third $COPV_{total}$ peak. In contrast, the width showed no effects on tested variables, and no interaction effect between two design factors was observed.

The mean peak pressure mappings of all arch supports are illustrated in Figure 5A. Overall, high peak pressure was located under the medial forefoot and the lateral rearfoot regions in all conditions. The 2D SPM results comparing the arch support and the control insole are shown in Figure 5B, with the blue area showing a significant decrease, and the red area showing a significant increase ($p < 0.05$). A darker color suggests a larger change. It is noticeable that as the arch support height increased, the peak pressure of the medial forefoot and rearfoot decreased, and the pressure of the medial midfoot and the lateral foot increased accordingly. In contrast, there was few visual differences in the plantar pressure mapping when changing the arch support width.

4 Discussion

This study investigated the acute effects of nine arch support doses on the 1D and 2D pressure data of running in healthy recreational runners using SPM approaches. The COP_{ML} coordinates and $COPV_{total}$ of different conditions were compared throughout the entirety of stance, and the results showed that a higher arch support was more effective in altering the $COPV_{total}$ than the COP_{ML} coordinates. Furthermore, differences in plantar pressure mapping between the arch support and control conditions were illustrated at the pixel level, with a higher arch support reducing the peak pressure of the medial forefoot and rearfoot. These results could contribute to insole optimization in clinical practice and footwear industry.

Among all COP variables during running, the COP displacements in the medial-lateral direction have been most frequently assessed in literature (Mann et al., 2016), and a more laterally directed COP has been associated with the development of overuse injuries (Ghani Zadeh Hesar et al., 2009). However, the effects of the arch support on this variable were inconsistent across studies, probably due to different test populations, statistical methods, and insole configurations. Compared with a flat insole, Naderi et al. (2019) found that an arch support (peak-height of 25 mm) significantly altered the mean COP_{ML} coordinates of running in a population with medial tibial stress syndrome, while Zhang et al. (2022) found that using two arch supports (peak-height of 20 mm and 24 mm) had little effects on the COP_{ML} trajectory of running in a population with symptomatic pronated feet. The results of the current study (arch support peak-height of 22–30 mm) are in line with the latter one, and further showed that changing neither the height nor the width of the arch support failed to alter the COP_{ML} trajectory during running. Although a medial-lateral COP shift has been used to indicate a load transfer between the medial and lateral foot regions, an absence of such shift may not necessarily suggest that the plantar pressure distribution remained unchanged. This can be verified with the statistical differences in the pressure mapping of this study.

Compared to the COP_{ML} coordinates, our results suggested that the COP velocity was more sensitive to subtle modifications of arch supports. The $COPV_{total}$ could partially reflect the progression velocity of the body center of mass over the foot during the stance phase, providing insights for dynamic foot function. Compared to the flat insole, the arch support significantly increased the $COPV_{total}$ during the FFCP and FFPOP of running (Figure 4), affecting the weight shift and progression of gait (Perry and Burnfield, 2010). The arch support has been shown to increase the propulsive force of running (Ng et al., 2021), and this may explain why the COP advanced more rapidly after heel-off. As one prospective study showed that runners who developed overuse injuries had a lower COP velocity at forefoot flat event than healthy controls during running (Ghani Zadeh Hesar et al., 2009), using an arch support may benefit runners at risk. Furthermore, the arch support may allow the foot to supinate more easily, which would increase the arch stiffness to enable a faster forward propulsion (Kelly et al., 2015). The effect of a faster weight shift and propulsion caused by arch supports on reducing injury risks requires further investigation in the future.

Among all COP velocity variables, peak values of the $COPV_{total}$ contain critical information to evaluate shock absorption, weight shift and propulsion of running. Our results showed a quadruple peak pattern of the $COPV_{total}$ curve during all shod running trials, while the third peak that occurred before heel-off was absent during barefoot walking (Cornwall and McPoil, 2000) and running (De Cock et al., 2008). A rapid initial foot pronation after strike can be speculated from the large value of the first $COPV_{total}$ peak, which enables shock absorption (Perry and Burnfield, 2010). This peak value (approximately 3 m/s) was considerably larger than that of barefoot running (approximately 1 m/s) (De Cock et al., 2008), which might be due to the cushioning property of modern running shoes (Malisoux et al., 2020). In contrast, the second $COPV_{total}$ peak, indicating a fast weight shift from the rearfoot to the forefoot, was comparable with that of the barefoot condition. After heel-off, the $COPV_{total}$ dropped to a plateau, where the third $COPV_{total}$ valley occurred, to prepare propulsion. As COP variables can be easily measured and calculated with a pressure measuring system, the peak $COPV_{total}$ may serve as an important measure of foot function in both clinical and footwear industrial settings.

By changing doses of forefoot and rearfoot wedges, previous studies have established linear dose-response relationships between insole doses and peak/mean biomechanical variables during walking (Telfer et al., 2013a; Telfer et al., 2013b) and running (Zhang et al., 2022). Similarly, the current study examined nine arch support doses, and the statistical results partially validated our hypothesis, with the arch support height having a linear main effect on the $COPV_{total}$ peak values, while its width showing little effect and having no interaction effect with the height. More specifically, as the arch support height increased 4 mm, 6% and 4% increase in the first and third valleys of the $COPV_{total}$ were found respectively. As illustrated above, a faster COP velocity during the FFCP and FFPOP may benefit runners, but how fast is optimal has yet to be determined. A higher arch support also slightly decreased the third $COPV_{total}$ peak, which may be because that a higher arch support would increase the contact with the midfoot region during running (Zhao et al., 2021), slowing down the COP velocity before heel-off. Previous studies have shown that the COP velocity during walking served as an indicator for foot mobility and function during the early healing phase after calcaneal fractures (Klopfer-Kramer et al., 2022). The COP velocity in patients with first metatarsophalangeal joint osteoarthritis (Menz et al., 2018) and posterior tibial tendon dysfunction (Wang et al., 2022) was significantly slower than that in healthy individuals during walking. Therefore, these linear dose-response relationships may help future prescription of insoles for runners.

The 2D SPM results showed that a higher arch support reduced the peak plantar pressure of the medial forefoot and rearfoot. Large peak pressure of those regions should be dealt with caution, as excessive pressure were found there in runners with lower limb injuries (Willems et al., 2007; Naderi et al., 2019). This finding confirmed the prediction results of computational studies using a finite element model (Cheung and Zhang, 2008; Peng et al., 2022). And it was partially in agreement with findings of experimental studies. By dividing the foot into 9 to 10 anatomical regions, Fong et al. (2020) found that using an arch support reduced the rearfoot pressure without altering forefoot pressure during running, while Huang et al. (2020) found that the arch support decreased rearfoot pressure and increased the pressure under the second to fourth metatarsals during walking. It needs to be noted that the pressure was recorded by a pressure insole system by Fong et al. and Huang et al. Those studies compared mean pressure values extracted from discrete anatomical regions, while our study used SPM that allows statistical comparisons at the pixel level. It has been suggested that the regional conflation of the former method may produce calculation errors (Pataky et al., 2008). By generating a higher resolution view of pressure distribution comparisons, the current study may provide references for a more precise management of plantar pressure distribution for clinical and industrial purposes in the future.

Several limitations should be noted for this study. Firstly, the participants of this study were young males, and the effect of aging and gender was not considered. Previous studies show that age and gender affect the COP trajectory during walking (Chiu et al., 2013a; Chiu et al., 2013b), and the elderly and females may have different responses to the arch support doses. Secondly, as the participants only wore each insole for a limited time before testing, and it is not clear whether the pressure variables would alter after a longer adaptation. Subsequent studies should examine the long-term effect of using arch supports. Thirdly, only neutral feet were examined in this study. Future studies are required to determine the dose-response relationship between arch supports and pressure variables in other foot types. Fourthly, the insole material used may also have an influence on plantar pressure.

5 Conclusion

Changing arch support doses, primarily the height, affected the COP velocities during loading response and propulsion phases of running, as well as redistributed peak plantar pressure at the pixel level. When assessing subtle modifications in the arch support, the COP velocity was a more sensitive variable than COP coordinates. Furthermore, there was a linear dose-response relationship between the arch support height and peak values of the $COPV_{total}$, and a higher arch support was also more effective in reducing peak plantar pressure of the medial forefoot and rearfoot. The findings of this study would provide insights into the mechanisms of insole interventions and provide potential measures for evaluating foot orthotics and footwear.

Data availability statement

The original contributions presented in the study are included in the article/Supplementary Material, further inquiries can be directed to the corresponding author.

Ethics statement

The studies involving human participants were reviewed and approved by the Ethics Committee of the Zhujiang Hospital of Southern Medical University and written informed consent was provided by each participant. The patients/participants provided their written informed consent to participate in this study.

Author contributions

The corresponding author XZ conceived and designed the study. The author JC and author QZ contributed equally to this work and shared first authorship. The author JC acquired, analysed and interpreted data, and drafted the paper. The author QZ was involved in participants recruitment, provision of clinical expertise and revising the manuscript. The author JL was in charge of 2D SPM analysis of the plantar pressure. All authors read and approved the final manuscript.

Funding

This work was supported by the National Natural Science Foundation of China (No. 32101051) and Shenzhen Science and Technology Program (No. RCBS20210706092410025).

Conflict of interest

The authors declare that the research was conducted in the absence of any commercial or financial relationships that could be construed as a potential conflict of interest.

Publisher's note

Supplementary material

The Supplementary Material for this article can be found online at: https://www.frontiersin.org/articles/10.3389/fbioe.2022.1051747/full#supplementary-material

References

Bergstra, S. A., Kluitenberg, B., Dekker, R., Bredeweg, S. W., Postema, K., Van den Heuvel, E. R., et al. (2015). Running with a minimalist shoe increases plantar pressure in the forefoot region of healthy female runners. *J. Sci. Med. Sport* 18 (4), 463–468. doi:10.1016/j.jsams.2014.06.007

Booth, B. G., Keijsers, N. L. W., Sijbers, J., and Huysmans, T. (2018). Stapp: Spatiotemporal analysis of plantar pressure measurements using statistical parametric mapping. *Gait Posture* 63, 268–275. doi:10.1016/j.gaitpost.2018.04.029

Cheung, J. T., and Zhang, M. (2008). Parametric design of pressure-relieving foot orthosis using statistics-based finite element method. *Med. Eng. Phys.* 30 (3), 269–277. doi:10.1016/j.medengphy.2007.05.002

Chiu, M. C., Wu, H. C., and Chang, L. Y. (2013a). Gait speed and gender effects on center of pressure progression during normal walking. *Gait Posture* 37 (1), 43–48. doi:10.1016/j.gaitpost.2012.05.030

Chiu, M. C., Wu, H. C., Chang, L. Y., and Wu, M. H. (2013b). Center of pressure progression characteristics under the plantar region for elderly adults. *Gait Posture* 37 (3), 408–412. doi:10.1016/j.gaitpost.2012.08.010

Cornwall, M. W., and McPoil, T. G. (2000). Velocity of the center of pressure during walking. *J. Am. Podiatr. Med. Assoc.* 90 (7), 334–338. doi:10.7547/87507315-90-7-334

D'Isidoro, F., Brockmann, C., and Ferguson, S. J. (2020). Effects of the soft tissue artefact on the hip joint kinematics during unrestricted activities of daily living. *J. Biomech.* 104, 109717. doi:10.1016/j.jbiomech.2020.109717

De Cock, A., Vanrenterghem, J., Willems, T., Witvrouw, E., and De Clercq, D. (2008). The trajectory of the centre of pressure during barefoot running as a potential measure for foot function. *Gait Posture* 27 (4), 669–675. doi:10.1016/j.gaitpost.2007.08.013

Duan, Y., Ren, W., Liu, W., Li, J., Pu, F., and Jan, Y. K. (2022). Relationship between plantar tissue hardness and plantar pressure distributions in people with diabetic peripheral neuropathy. *Front. Bioeng. Biotechnol.* 10, 836018. doi:10.3389/fbioe.2022.836018

Farzadi, M., Safaeepour, Z., Mousavi, M. E., and Saeedi, H. (2015). Effect of medial arch support foot orthosis on plantar pressure distribution in females with mild-to-moderate hallux valgus after one month of follow-up. *Prosthet. Orthot. Int.* 39 (2), 134–139. doi:10.1177/0309364613518229

Fernández-Seguín, L. M., Diaz Mancha, J. A., Sánchez Rodríguez, R., Escamilla Martínez, E., Gómez Martín, B., and Ramos Ortega, J. (2014). Comparison of plantar pressures and contact area between normal and cavus foot. *Gait Posture* 39 (2), 789–792. doi:10.1016/j.gaitpost.2013.10.018

Fong, D. T. P., Lue, K. B. K., Chung, M. M. L., Chu, V. W. S., and Yung, P. S. H. (2020). An individually moulded insole with 5-mm medial arch support reduces peak impact and loading at the heel after a one-hour treadmill run. *Gait Posture* 82, 90–95. doi:10.1016/j.gaitpost.2020.08.109

Friston, K. J., Holmes, A. P., Worsley, K. J., Poline, J. P., Frith, C. D., and Frackowiak, R. (1994). Statistical parametric maps in functional imaging: A general linear approach. *Hum. Brain Mapp.* 2 (4), 189–210. doi:10.1002/hbm.460020402

Ghani Zadeh Hesar, N., Van Ginckel, A., Cools, A., Peersman, W., Roosen, P., De Clercq, D., et al. (2009). A prospective study on gait-related intrinsic risk factors for lower leg overuse injuries. *Br. J. Sports Med.* 43 (13), 1057–1061. doi:10.1136/bjsm.2008.055723

Huang, Y. P., Peng, H. T., Wang, X., Chen, Z. R., and Song, C. Y. (2020). The arch support insoles show benefits to people with flatfoot on stance time, cadence, plantar pressure and contact area. *PLoS One* 15 (8), e0237382. doi:10.1371/journal.pone.0237382

Hunt, M. A., Takacs, J., Krowchuk, N. M., Hatfield, G. L., Hinman, R. S., and Chang, R. (2017). Lateral wedges with and without custom arch support for people with medial knee osteoarthritis and pronated feet: An exploratory randomized crossover study. *J. Foot Ankle Res.* 10, 20. doi:10.1186/s13047-017-0201-x

Jafarnezhadgero, A., Mousavi, H., Madadi-Shad, M., and Hijmans, J. M. (2020). Quantifying lower limb inter-joint coordination and coordination variability after four-month wearing arch support foot orthoses in children with flexible flat feet. *Hum. Mov. Sci.* 70, 102593. doi:10.1016/j.humov.2020.102593

Keijsers, N. L., Stolwijk, N. M., Nienhuis, B., and Duysens, J. (2009). A new method to normalize plantar pressure measurements for foot size and foot progression angle. *J. Biomech.* 42 (1), 87–90. doi:10.1016/j.jbiomech.2008.09.038

Kelly, L. A., Lichtwark, G., and Cresswell, A. G. (2015). Active regulation of longitudinal arch compression and recoil during walking and running. *J. R. Soc. Interface* 12 (102), 20141076. doi:10.1098/rsif.2014.1076

Klopfer-Kramer, I., Brand, A., Kroger, I., Wackerle, H., Gabel, J., Dietrich, A., et al. (2022). Development of the center of pressure velocity in the healing process after intra-articular calcaneus fractures. *Gait Posture* 95, 135–140. doi:10.1016/j.gaitpost.2022.04.015

Liau, B., Wu, F. L., Li, Y. M., Lung, C. W., Mohamed, A. A., and Jan, Y. K. (2021). Effect of walking speeds on complexity of plantar pressure patterns, *Complexity*, 2021. 6571336, Artn. doi:10.1155/2021/6571336

Liau, B. Y., Wu, F. L., Lung, C. W., Zhang, X. Y., Wang, X. L., and Jan, Y. K. (2019). Complexity-based measures of postural sway during walking at different speeds and durations using multiscale entropy. *Entropy* 21 (11), 1128. ARTN. doi:10.3390/e21111128

Malisoux, L., Delattre, N., Urhausen, A., and Theisen, D. (2020). Shoe cushioning influences the running injury risk according to body mass: A randomized controlled trial involving 848 recreational runners. *Am. J. Sports Med.* 48 (2), 473–480. doi:10.1177/0363546519892578

Mann, R., Malisoux, L., Urhausen, A., Meijer, K., and Theisen, D. (2016). Plantar pressure measurements and running-related injury: A systematic review of methods and possible associations. *Gait Posture* 47, 1–9. doi:10.1016/j.gaitpost.2016.03.016

Menz, H. B., Auhl, M., Tan, J. M., Buldt, A. K., and Munteanu, S. E. (2018). Centre of pressure characteristics during walking in individuals with and without first metatarsophalangeal joint osteoarthritis. *Gait Posture* 63, 91–96. doi:10.1016/j.gaitpost.2018.04.032

Menz, H. B., Dufour, A. B., Riskowski, J. L., Hillstrom, H. J., and Hannan, M. T. (2013). Association of planus foot posture and pronated foot function with foot pain: The framingham foot study. *Arthritis Care Res. Hob.* 65 (12), 1991–1999. doi:10.1002/acr.22079

Naderi, A., Degens, H., and Sakinepoor, A. (2019). Arch-support foot-orthoses normalize dynamic in-shoe foot pressure distribution in medial tibial stress syndrome. *Eur. J. Sport Sci.* 19 (2), 247–257. doi:10.1080/17461391.2018.1503337

Neal, B. S., Griffiths, I. B., Dowling, G. J., Murley, G. S., Munteanu, S. E., Smith, M. M. F., et al. (2014). Foot posture as a risk factor for lower limb overuse injury: A systematic review and meta-analysis. *J. Foot Ankle Res.* 7, 55. ARTN. doi:10.1186/s13047-014-0055-4

Ng, J. W., Chong, L. J. Y., Pan, J. W., Lam, W. K., Ho, M., and Kong, P. W. (2021). Effects of foot orthosis on ground reaction forces and perception during short sprints in flat-footed athletes. *Res. Sports Med.* 29 (1), 43–55. doi:10.1080/15438627.2020.1755673

Nuesch, C., Roos, E., Egloff, C., Pagenstert, G., and Mundermann, A. (2019). The effect of different running shoes on treadmill running mechanics and muscle activity assessed using statistical parametric mapping (SPM). *Gait Posture* 69, 1–7. doi:10.1016/j.gaitpost.2019.01.013

Pataky, T. C. (2008). Assessing the significance of pedobarographic signals using random field theory. *J. Biomech.* 41 (11), 2465–2473. doi:10.1016/j.jbiomech.2008.05.010

Pataky, T. C., Bosch, K., Mu, T., Keijsers, N. L., Segers, V., Rosenbaum, D., et al. (2011). An anatomically unbiased foot template for inter-subject plantar pressure evaluation. *Gait Posture* 33 (3), 418–422. doi:10.1016/j.gaitpost.2010.12.015

Pataky, T. C., Caravaggi, P., Savage, R., and Crompton, R. H. (2008). Regional peak plantar pressures are highly sensitive to region boundary definitions. *J. Biomech.* 41 (12), 2772–2775. doi:10.1016/j.jbiomech.2008.06.029

Pataky, T. C., and Goulermas, J. Y. (2008). Pedobarographic statistical parametric mapping (pSPM): A pixel-level approach to foot pressure image analysis. *J. Biomech.* 41 (10), 2136–2143. doi:10.1016/j.jbiomech.2008.04.034

Pataky, T. C., Robinson, M. A., and Vanrenterghem, J. (2013). Vector field statistical analysis of kinematic and force trajectories. *J. Biomech.* 46 (14), 2394–2401. doi:10.1016/j.jbiomech.2013.07.031

Peng, Y., Wang, Y., Wong, D. W., Chen, T. L., Chen, S. F., Zhang, G., et al. (2022). Different design feature combinations of flatfoot orthosis on plantar fascia strain and plantar pressure: A muscle-driven finite element analysis with taguchi method. *Front. Bioeng. Biotechnol.* 10, 571192. doi:10.3389/fbioe.2020.571192

Peng, Y., Wong, D. W., Chen, T. L., Wang, Y., Zhang, G., Yan, F., et al. (2021). Influence of arch support heights on the internal foot mechanics of flatfoot during walking: A muscle-driven finite element analysis. *Comput. Biol. Med.* 132, 104355. doi:10.1016/j.compbiomed.2021.104355

Perry, J., and Burnfield, J. (2010). Gait analysis: Normal and pathological function.*The Journal of Bone and Joint Surgery*, 92-B,doi:10.1302/0301-620X.92B8.0921184a

Redmond, A. C., Crane, Y. Z., and Menz, H. B. (2008). Normative values for the foot posture index. *J. Foot Ankle Res.* 1 (1), 6. doi:10.1186/1757-1146-1-6

Stearne, S. M., McDonald, K. A., Alderson, J. A., North, I., Oxnard, C. E., and Rubenson, J. (2016). The foot's arch and the energetics of human locomotion. *Sci. Rep.* 6, 19403. doi:10.1038/srep19403

Telfer, S., Abbott, M., Steultjens, M. P., and Woodburn, J. (2013b). Dose-response effects of customised foot orthoses on lower limb kinematics and kinetics in pronated foot type. *J. Biomech.* 46 (9), 1489–1495. doi:10.1016/j.jbiomech.2013.03.036

Telfer, S., Abbott, M., Steultjens, M., Rafferty, D., and Woodburn, J. (2013a). Dose-response effects of customised foot orthoses on lower limb muscle activity and plantar pressures in pronated foot type. *Gait Posture* 38 (3), 443–449. doi:10.1016/j.gaitpost.2013.01.012

Wahmkow, G., Cassel, M., Mayer, F., and Baur, H. (2017). Effects of different medial arch support heights on rearfoot kinematics. *Plos One* 12 (3), e0172334. doi:10.1371/journal.pone.0172334

Wang, J., Latt, L. D., Martin, R. D., and Mannen, E. M. (2022). Postural control differences between patients with posterior tibial tendon dysfunction and healthy people during gait. *Int. J. Environ. Res. Public Health* 19 (3), 1301. doi:10.3390/ijerph19031301

Willems, T. M., Witvrouw, E., De Cock, A., and De Clercq, D. (2007). Gait-related risk factors for exercise-related lower-leg pain during shod running. *Med. Sci. Sports Exerc.* 39 (2), 330–339. doi:10.1249/01.mss.0000247001.94470.21

Willwacher, S., Kurz, M., Robbin, J., Thelen, M., Hamill, J., Kelly, L., et al. (2022). Running-related biomechanical risk factors for overuse injuries in distance runners: A systematic review considering injury specificity and the potentials for future research. *Sports Med.* 52, 1863–1877. doi:10.1007/s40279-022-01666-3

Xiang, L., Gu, Y., Mei, Q., Wang, A., Shim, V., and Fernandez, J. (2022). Automatic classification of barefoot and shod populations based on the foot metrics and plantar pressure patterns. *Front. Bioeng. Biotechnol.* 10, 843204. doi:10.3389/fbioe.2022.843204

Xu, R., Wang, Z., Ma, T., Ren, Z., and Jin, H. (2019). Effect of 3D printing individualized ankle-foot orthosis on plantar biomechanics and pain in patients with plantar fasciitis: A randomized controlled trial. *Med. Sci. Monit.* 25, 1392–1400. doi:10.12659/msm.915045

Zhang, X., Lam, W. K., and Vanwanseele, B. (2022). Dose-response effects of forefoot and arch orthotic components on the center of pressure trajectory during running in pronated feet. *Gait Posture* 92, 212–217. doi:10.1016/j.gaitpost.2021.11.033

Zhang, X., Li, B., Hu, K., Wan, Q., Ding, Y., and Vanwanseele, B. (2017). Adding an arch support to a heel lift improves stability and comfort during gait. *Gait Posture* 58, 94–97. doi:10.1016/j.gaitpost.2017.07.110

Zhang, X., and Li, B. (2014). Influence of in-shoe heel lifts on plantar pressure and center of pressure in the medial-lateral direction during walking. *Gait Posture* 39 (4), 1012–1016. doi:10.1016/j.gaitpost.2013.12.025

Zhao, X., Wang, M., Fekete, G., Baker, J. S., Wiltshire, H., and Gu, Y. (2021). Analyzing the effect of an arch support functional insole on walking and jogging in young, healthy females. *Technol. Health Care* 29 (6), 1141–1151. doi:10.3233/thc-181373

frontiers | Frontiers in Bioengineering and Biotechnology

TYPE Original Research
PUBLISHED 30 November 2022
DOI 10.3389/fbioe.2022.1022376

Check for updates

OPEN ACCESS

EDITED BY
Qichang Mei,
Ningbo University, China

REVIEWED BY
Robert Peter Matthew,
University of California, San Francisco, United States
Ádám Tibor Schlégl,
University of Pécs, Hungary

*CORRESPONDENCE
Bagen Liao,
Bagenliao@sina.com
Xiaohui Zhang,
Sportsmedzxh@sina.com

SPECIALTY SECTION
This article was submitted to Biomechanics,
a section of the journal Frontiers in Bioengineering and Biotechnology

RECEIVED 18 August 2022
ACCEPTED 18 November 2022
PUBLISHED 30 November 2022

CITATION
Liu Y, Li X, Dou X, Huang Z, Wang J, Liao B and Zhang X (2022), Correlational analysis of three-dimensional spinopelvic parameters with standing balance and gait characteristics in adolescent idiopathic scoliosis: A preliminary research on Lenke V. *Front. Bioeng. Biotechnol.* 10:1022376.
doi: 10.3389/fbioe.2022.1022376

Correlational analysis of three-dimensional spinopelvic parameters with standing balance and gait characteristics in adolescent idiopathic scoliosis: A preliminary research on Lenke V

Yanan Liu[1], Xianglan Li[1], Xiaoran Dou[1], Zhiguan Huang[2], Jun Wang[3], Bagen Liao[1]* and Xiaohui Zhang[1]*

[1]Department of Sports Medicine, Guangzhou Sport University, Guangzhou, China, [2]School of Sports and Health, Guangzhou Sport University, Guangzhou, China, [3]Gosun Medical Imaging Diagnosis Center of Guangdong Province, Guangzhou, China

Background: Adolescent idiopathic scoliosis (AIS), the most common spinal deformity, possibly develops due to imbalanced spinal loading following asymmetric development. Since altered loading patterns may affect standing balance and gait, we investigated whether a correlation exists between balance ability, gait pattern, and the three-dimensional radiographic spinopelvic parameters in AIS patients.

Methods: A cross-sectional observational study was conducted with 34 AIS patients (aged 10–18 years) and an equal number of healthy age and sex-matched teenagers (normal group). We obtained the spinopelvic three-dimensional parameters and balance parameters simultaneously through the EOS imaging system and gait and center of pressure (CoP) characteristics using a plantar pressure measurement mat. Besides determining the intergroup differences in balance and gait parameters, multiple linear regression analyses were performed to identify any correlation between the static plantar pressure and radiographic parameters.

Results: Compared to the normal group, the CoP_x is lower, the CoP path length and 90% confidence ellipse area were significantly higher in AIS patients (AIS: -13.7 ± 5.7 mm, 147.4 ± 58.1 mm, 150.5 ± 62.8 mm^2; normal: -7.0 ± 5.4 mm, 78.8 ± 32.0 mm, 92.1 ± 41.7 mm^2, respectively), correlated with apical vertebra translation, sagittal pelvic tilt, and pelvis axial rotation, respectively. Moreover, AIS patients had a shorter stance phase (61.35 ± 0.97 s vs. 62.39 ± 1.09 s), a longer swing phase (38.66 ± 0.97 s vs. 37.62 ± 1.08 s), and smaller maximum pressure peaks in the gait cycle, especially on the left foot, as compared to healthy subjects. Moreover, the CoP trajectory in AIS patients was different from the latter, and changes in the bipedal trend were not consistent.

Conclusion: The standing balance and gait characteristics of AIS patients are different from those of healthy subjects, as reflected in their three-dimensional spinopelvic radiographic parameters. Trial registration: The study protocol was registered with the Chinese Clinical Trial Registry (Number ChCTR1800018310) and the Human Subject Committee of Guangzhou Sport University (Number: 2018LCLL003).

KEYWORDS

adolescent idiopathic scoliosis, standing balance, 3d parameters, gait, correlation analysis

Introduction

Scoliosis, a three-dimensional deformity of the spine, is characterized by a lateral curvature of ≥10° in the spine in the coronal plane (Altaf et al., 2013), with adolescent idiopathic scoliosis (AIS) being the most common variety encountered in routine pediatric and orthopedic practice (Lonstein et al., 1994). Epidemiological studies show that although 1%–3% of all children between 10 and 16 years of age experience varying degrees of spinal curvatures, most of them do not require cautious intervention (Weinstein et al., 2008). While the life expectancy of AIS patients is not significantly different from the general population (Pehrsson et al., 1992), their quality of life is affected by several multisystem consequences of the deformity, including reduced respiratory function (Koumbourlis et al., 2006), back pain (Wong et al., 2019), degenerative spine disorders (Weinstein et al., 2003), and concerns relating to their body image (Gallant et al., 2018) and mental health (Mitsiaki et al., 2022). Therefore, holistic management strategies for AIS are gradually becoming the focus of research.

Structurally, scoliosis is not only caused by the lateral deviation of the vertebrae but involves a three-dimensional malalignment of the vertebrae leading to geometric and morphological changes in the trunk and pelvis (Cheng et al., 2015). Although the pathogenesis of the malalignment in AIS is still unknown (Lowe et al., 2000) (Kikanloo et al., 2019), existing studies suggest the role of abnormal balance (Nault et al., 2002). Due to the high susceptibility of adolescents to scoliosis, great attention is given to balance and gait disorders in this age group (Mahaudens et al., 2009) (Daryabor et al., 2016) (Yang et al., 2013) (Karimi et al., 2016) (Quervain et al., 2004). It is known that optimal balance is essential for performing both simple everyday tasks and complex movement patterns, such as walking (Saggini et al., 2021). Accordingly, balance dysfunctions can lead to postural instability, walking difficulty, and even, falls. Recent evidence suggests a potential correlation between different gait and balance parameters in AIS patients and that the spine and pelvis play a key role in regulating body balance.

The traditional research on AIS has focused on coronal plane malalignments; fortunately, recent advances in the field of radiography have shifted the attention toward sagittal and axial plane involvements, leading to notable discoveries (Nolte et al., 2020). A balanced three-dimensional spinal alignment serves as a crucial biomechanical foundation to enable flexibility during spinal movements and postural stability while carrying axial loads. Previous studies have reported diminished balance abilities in patients with AIS(Wiernicka et al., 2019) (Beaulieu et al., 2008). Although a few authors have described a relationship between the spinal deformity status and static balance, all these reports studied the deformity from a single plane rather than using a three-dimensional perspective. To the best of our knowledge, no study has explored the association between the balance and imaging acquisition parameters in these patients.

Therefore, the present study aimed to analyze the differences in the balance ability between AIS patients and their age and sex-matched normal individuals (normal group), and whether a correlation exists between their three-dimensional spinopelvic parameters and static balance acquired simultaneously. A secondary objective of the study was to compare the gait characteristics of AIS patients with the normal group subject. We hypothesized that the static balance of AIS patients will be different from that of the normal group subjects.

Materials and methods

Ethics clearance

The study was conducted in accordance with the principles of the Declaration of Helsinki. The study protocol was approved by the Human Subject Committee of Guangzhou Sport University (Number: 2018LCLL003) and the trial was registered with the Chinese Clinical Trial Registry (Number: ChCTR1800018310). The parents or legal guardians of all participants provided informed consent for participating in the study.

Sample size

Using the G*Power software (Germany G*Power version 3.1), we calculated the sample size as 34 using an effect size with a medium value of 0.35, an alpha probability of 0.05, and a beta probability of 0.95.

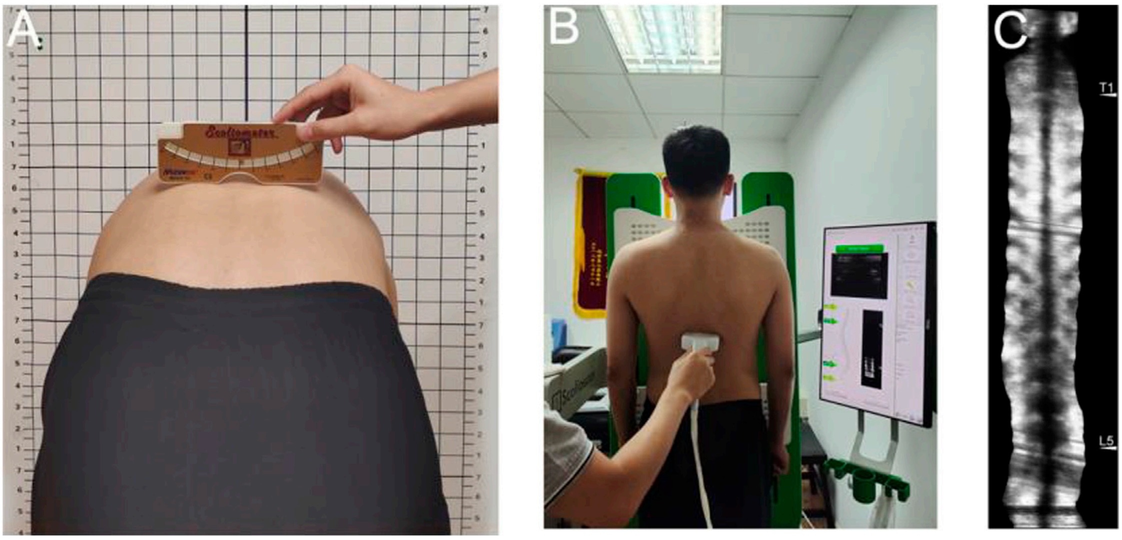

FIGURE 1
Scoliosis screening methods-**(A)** Adam's test and trunk rotation angle measured with a Scoliometer; **(B)** A radiation-free spine ultrasound imaging system; **(C)** Ultrasound imaging.

Participants

We enrolled patients aged 10–18 years diagnosed with AIS by an orthopedist between January 2021 and April 2022 in this study. The patients were included if the diagnosis of AIS was consistent with the curve classification of Lenke V (Slattery and Verma et al., 2018), Cobb's angle between 10° and 40°, and were skeletally immature (defined as 0–3 on the Risser's sign (Wittschieber et al., 2012)). Those with non-idiopathic types of scoliosis (such as neuromuscular or congenital), having a history of treatment with brace or other modalities, or any other musculoskeletal alterations or orthopedic history, a lower limb discrepancy of >1 cm, or malignant and psychiatric diseases, were excluded from the study. An equal number of age and sex-matched healthy teenagers were recruited from the same city as the "normal group" through advertising.

Procedure

Demographic information for every participant was collected. For healthy subjects, we used scoliosis screening methods, including Adam's test, trunk rotation angle measured with a scoliometer, and a radiation-free spine ultrasound imaging system (Scolioscan® SCN801, Hong Kong) to ensure there were no scoliotic deformities (Figure 1). Spinal ultrasonography has been shown to have excellent reliability in the diagnosis of mild to moderate scoliosis (Lv et al., 2019) (Ungi et al., 2020).

In patients with suspected AIS, further examination was performed using a whole-spine biplanar X-ray system (EOS Imaging®, Paris, France). To reduce the potential risk of radiation, posteroanterior views of the upper body and pelvis were taken using the micro-dose method. Subjects were asked to stand in the center of the cabin, with the pelvis located at the isocenter of the platform, and place both fists next to the cheeks with the upper arm at a 40° angle to the body and head facing forward ahead (Zhang et al., 2022). Simultaneously, a 0.5 m plantar pressure measurement mat (Zebris FDM, Germany) was placed under the patient's foot to collect their static plantar center of pressure (CoP) information for 10 s (Figure 2). The following parameters were measured: the mean mediolateral CoP position (CoP_x)—indicates the subject leaning laterally (the right side being positive), the mean anteroposterior CoP position (CoP_y)—indicates the subject leaning anteroposteriorly (forward being positive), the CoP path length—the length of the subject's CoP shift during the test, and the 90% confidence ellipse area—the area including 90% of all CoP points measured and transferred in the test. The center of the base of support (the area between the feet including the soles) is the origin for the CoP measurements. For the normal group, we acquired the aforementioned parameters using the same procedure but without the EOS examination. Afterward, a full 3D reconstruction of the spine was done by a single radiologist using a post-processing software for EOS (sterEOS®) (Courvoisier et al., 2013), which recognized anatomical landmarks and generated a 3D computer model of the full spine based on the synchronized posteroanterior and lateral images (Dubousset et al., 2007) (Figure 2B, C). The

10.3389/fbioe.2022.1022376

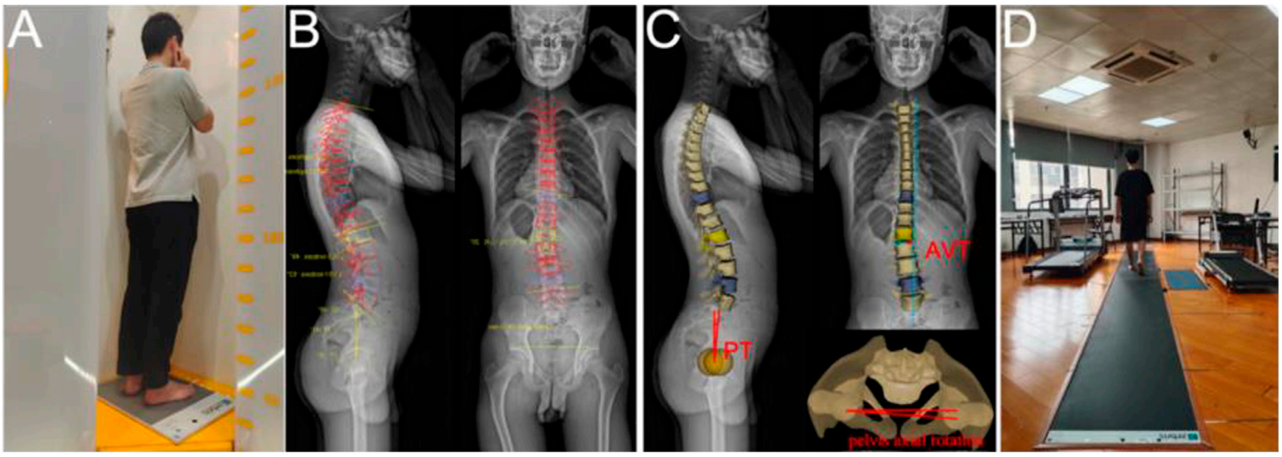

FIGURE 2
(A) is a Patient undergoing EOS imaging while his balance data is collected. **(B)** and **(C)** are the full 3-D recondtruction images of the spine performed by the radiologist using a post-processing software of EOS. **(D)** shows the gaint information of a patient being collected.

following radiographic parameters were collected: 1) coronal: Cobb's angle, coronal balance, apical vertebra translation (AVT), and lateral pelvic tilt; 2) sagittal: thoracic kyphosis (TK), lumbar lordosis (LL), sagittal vertical axis (SVA), pelvic incidence (PI), sacral slope (SS), and sagittal pelvic tilt (PT); 3) axial: axial rotation of apical vertebra, pelvis axial rotation.

Then, all participants were required to walk barefoot through a 6-m plantar pressure measurement mat (Zebris FDM, Germany) at their comfortable pace (Figure.2D). Data for the following spatiotemporal gait parameters were collected: gait speed, cadence, stride length, step width, stance phase, swing phase, maximum pressure curve, and gait line. Both static and dynamic pressure experiments were carried out three times, and the average value was used for statistical analysis.

Statistical analysis

All statistical analyses were performed using SPSS (version 26.0; SPSS IBM Inc, Armonk, NY). The Shapiro–Wilk test was used to check data normality, and independent-samples t-tests were performed to assess the between-group differences in demographic characteristics, balance, and gait data. All values are presented as mean ± standard deviations (SD). A p-value of <0.05 was considered statistically significant.

Additionally, stepwise multiple linear regression analyses were performed to identify any correlation between the balance and radiographic parameters. The entry and removal criteria of the model were the probability of F-values < 0.05 and F > 0.10, respectively. Parameters with an adjusted p-value of <0.05 were reported.

TABLE 1 Demographic characteristics of study participants (n = 34).

Parameters	AIS	Normal	p
Age (years)	13.3 ± 2.2	14.1 ± 1.6	0.315
Height (cm)	162.5 ± 7.3	159.4 ± 4.4	0.203
Weight (kg)	47.5 ± 5.3	47.7 ± 3.8	0.900
BMI (kg/m2)	17.9 ± 0.9	18.8 ± 1.3	0.065

BMI, body mass index

TABLE 2 Static balance parameters in adolescent idiopathic scoliosis (AIS) and normal subjects (n = 34).

Parameters	AIS	Normal	p
CoPx (mm)	−13.7 ± 5.7*	−7.0 ± 5.4	0.029
CoPy (mm)	−28.8 ± 17.9	−22.4 ± 12.9	0.313
CoP path length (mm)	147.4 ± 58.1*	78.8 ± 32.0	0.008
90% confidence ellipse area (mm2)	150.5 ± 62.8*	92.1 ± 41.7	0.004

* means p < 0.05.

Results

We included 34 patients (30 females) with Lenke type V and an equal number of age and sex-matched normal teenagers in the study; both groups were comparable in terms of demographic data (Table 1). The Cobb's angle of the patients who were finally included in our study ranged from 20° to 34°, and the severity was moderate. The spinal and pelvic 3D parameters of the AIS group were as follows: 1) coronal: mean Cobb's angle: 25.0° (21.8°–28.2°), coronal balance: 1.2 ± 1.1 mm, AVT: 1.4 ± 0.7 mm, and lateral pelvic

10.3389/fbioe.2022.1022376

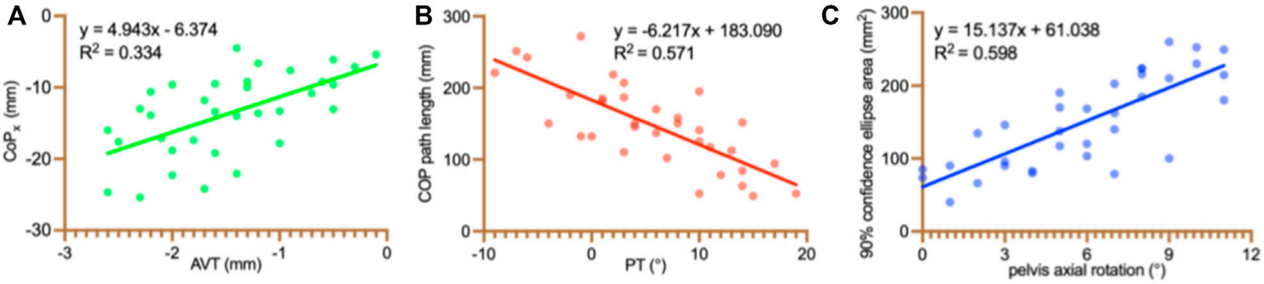

FIGURE 3
Statistically significant relationships between static balance and radiographic parameters. CoP: center of pressure; CoPx: the mean mediolateral CoP position; AVT: apical vertebra translation; PT: Sagittal pelvic tilt.

TABLE 3 Gait parameters in adolescent idiopathic scoliosis (AIS) and normal subjects (n = 34).

Parameters	AIS	Normal	p
Gait speed (km/h)	4.41 ± 0.37	4.13 ± 0.49	0.149
Cadence (step/min)	115.20 ± 5.95	112.54 ± 5.99	0.301
Stride length (cm)	128.62 ± 12.55	122.19 ± 12.03	0.226
Step width (cm)	9.58 ± 2.56	11.19 ± 1.93	0.099
Stance phase (%)	61.35 ± 0.97*	62.39 ± 1.09	0.027
Swing phase (%)	38.66 ± 0.97*	37.62 ± 1.08	0.027

* means $p < 0.05$; The stance phase and the swing phase represent the proportion of the stance phase and the swing phase in the gait cycle, respectively.

tilt: 4.1 ± 3.7 mm. 2) sagittal: TK: 13.2° ± 8.2°, LL: 37.6° ± 11.7°, SVA: −6.7 ± 13.0 mm, PI: 42.2° ± 8.4°, SS: 34.8° ± 8.1°, PT: 5.7° ± 7.1°. 3) axial: axial rotation of apical vertebra: 7.2° ± 2.7° and pelvis axial rotation: 5.9° ± 3.2°.

We also observed a lower CoP_x, a higher CoP path length and 90% confidence ellipse area in the AIS than the normal group. There was no statistically significant difference in the CoP_y value (Table 2).

As per the results of the linear regression analysis for CoP_x and radiographic parameters, AVT was the only remaining variable in the regression analysis, accounting for 33.4% of the variance observed in CoP_x (Figure 3A). Likewise, the linear regression analysis of CoP path length and radiographic parameters revealed that PT was the only remaining variable, leading to a 57.1% variance observed in the CoP path length (Figure 3B). Regarding the 90% confidence ellipse area and radiographic parameters, pelvis axial rotation was the only remaining variable in the regression analysis, accounting for 59.8% of the variance observed in the 90% confidence ellipse area (Figure 3C). Lastly, in the linear regression analysis of CoP_y and radiographic parameters, no variable was remaining.

Regarding the gait parameters, the stance phase formed 61.35 ± 0.97% and 62.39 ± 1.09% of the total gait cycle in the AIS and normal groups, respectively, i.e., the stance phase was significantly reduced in AIS patients compared with the normal group, and the swing phase was correspondingly increased (Table 3). The two maximum pressure peaks of the left foot were smaller in the AIS group than those in the normal group, while that of the right foot was smaller only around the second peak (Figure 4). Figure 5 shows a representation of the gait line for bilateral plantar CoP progressed from the heel to the toe region between the normal and AIS groups. Compared to the normal group, the CoP trajectory of the left foot in the AIS group was initially on the lateral side of the normal group, then transitioned to the medial side gradually, and terminated at the medial side of the normal group. The right foot was just the opposite, i.e., initiating on the inside but ending on the outside.

Discussion

In this study, we observed that the static balance of AIS patients was related to certain three-dimensional spinopelvic parameters, namely AVT, PT, and pelvic axial rotation. Although these Lenke V AIS patients primarily had lumbar scoliosis, the deformity at this level is anatomically related to the pelvis (Mac-thiong et al., 2006), which is an important determinant of lower limb loading pattern. It has been established that abnormal lower limb loading pattern ultimately leads to reduced balance (Márkus et al., 2018). Although many studies have explored the correlation between balance and spinopelvic parameters, most of these studies are limited to a single anatomical plane (Luo et al., 2021) (Ma, 2019) (Burkus et al., 2018); in contrast, we included spinopelvic parameters from all three dimensions. Luo et al. also recorded that PT was positively correlated with almost all baropodometric parameters on the major curve, but not with other parameters (Luo et al., 2021). Therefore, it can be inferred that PT best reflects the influence of sagittal plane balance on the lower limb. A previous study reported that the scoliosis group had a more significant correlation between standing stability and body posture parameters than the non-scoliosis

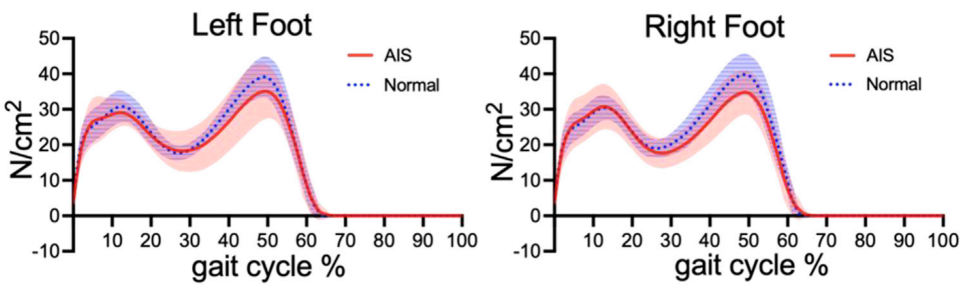

FIGURE 4
Bipedal maximum pressure curves of the two groups during gait cycle.Red indicates Adolesce Idiopathic Scoliosis (AIS) group and Blue indicates normal group. The solid line indicates th maximum pressure curve, and the shaded area is the standard deviation. Expect for the first peak of the right foot, the peak value of AIS group is lower than that of the normal group.

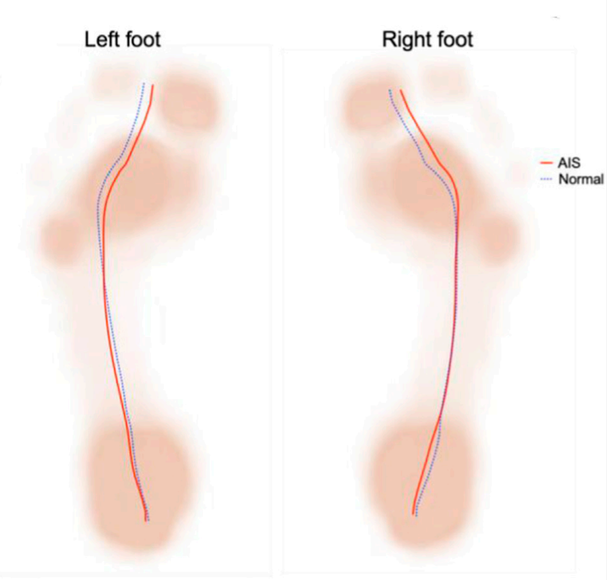

FIGURE 5
The gait line in Adolescent Idiopathic Scoliosis (AIS) and normal groups.Obviously ,the two groups are different, and bipedal asymmetry and Inconsistent change trend.

group (Nault et al., 2002). Our innovative study procedure allowed for the synchronous acquisition of three-dimensional spinopelvic and standing stability parameters. We found that the correlation was multidimensional, i.e., static balance parameters are not only correlated with coronal and sagittal plane parameters, but also with axial plane parameters, which partially supports our study hypothesis. To the best of our knowledge, our results reveal characteristic associations that have rarely been elucidated in previous studies.

Our patients had an increased CoP path length and 90% confidence ellipse area as compared to the normal group, indicating poor static balance. Previous studies have also reported similar findings (Wiernicka, 2019). The CoP_x value was negative in our study, meaning the patients mostly leaned to the left. Catan et al. evaluated 32 girls diagnosed with idiopathic left convex lumbar curves and noticed a significantly higher load on the left foot (Cațan et al., 2020). The predominance of this left-sided imbalance can be attributed to the fact that all of our AIS patients had a thoracolumbar curve, which, anatomically, continues to show a left offset of the trunk and a right offset of the midline of the pelvis in the opposite direction, thus leading to a coronal postural imbalance. Interestingly, our study also highlighted the role of pelvic axial rotation on static balance disturbance, which has been rarely targeted in previous research (Luo et al., 2021) (Ma, 2019). Pelvis axial rotation is the result of the compensation for lumbar scoliosis, and the rotated pelvis is used as an unstable base of support for spine. The more severe the pelvic rotation, the greater the instability and the worse the balance. Notably, the three-dimensional spinopelvic and static balance parameters investigated simultaneously in our AIS patients significantly reduced the potential risks of inconsistent experimental procedures.

Another important finding of our study was the significantly reduced stance phase and a marked increase in the swing phase in AIS patients as compared with the normal group. However, there was no statistically significant between-group difference regarding the gait speed, cadence, stride length, and step width. The results are comparable to the findings of a previous meta-analysis by Kim et al. (Kim et al., 2020). These gait cycle alterations may be related to the significant increase in the electrical activity durations of the quadratus lumborum, erector spinae, and gluteus medius in the AIS group (Mahaudens, 2009); however, the exact mechanism underlying this process are yet to be explored.

The CoP gait line is a curve that directly reflects the nervous control of the ankle-foot complex muscles during walking (Tochigi, 2011) and also reveals the loading pattern and stability in the movement (Teyhen, 2009). We found that the CoP gait line of AIS patients was different from that of healthy individuals, indicating an ankle joint inversion or eversion transition during the stance phase that may lead to inefficient contact loading absorption, ankle injury, and falls. Gao et al. also described similar results (Gao, 2019). The lower peak of the maximal pressure curve in AIS patients compared to healthy individuals, especially in the single stance phase (between the two peaks), may be related to the lower arch in AIS patients, which was more pronounced in the left foot.

Based on these results, it can be recommended that the treatment and management of AIS patients should not only focus on the three-dimensional spinal alignment correction, but also gait and balance dysfunctions. Excellent balance can complete the movement safely and efficiently. Otherwise, the performance of ideal balance and symmetrical gait has a positive effect on maintaining the same activation of bilateral muscles, which may mitigate the deterioration of the curve. These findings further corroborate the importance of monitoring the balance and gait characteristics in AIS patients to understand the progress of the spinal curve.

There were certain limitations to this study. Firstly, AIS patients with Lenke V may be one of the most significant variations in the spinopelvic parameters. Therefore, the characteristics of other types are expected to be clarified by further research. Secondly, the sample size is relatively small, so the heterogeneity of curve severity is not carefully considered. Finally, gait parameters showed differences between the two groups, but the exact causes and mechanisms could not be deciphered from this cross-sectional study. Accordingly, large-scale, multi-centric, and well-designed studies are necessary to provide evidence to devise a more comprehensive clinical treatment for AIS patients.

Conclusion

The standing balance of patients with Lenke V AIS is influenced by their AVT, PT, and pelvis axial rotation. We were able to record important differences in gait spatiotemporal parameters, maximum pressure curve, and gait line between AIS patients and age and sex-matched healthy subjects. We believe these findings may contribute to understanding the etiology of AIS and devising targeted comprehensive treatments.

Data availability statement

The raw data supporting the conclusion of this article will be made available by the authors, without undue reservation.

Ethics statement

The studies involving human participants were reviewed and approved by the Human Subject Committee of Guangzhou Sport University. Written informed consent to participate in this study was provided by the participantsandapos; legal guardian/next of kin. Written informed consent was obtained from the individual(s), and minor(s)' apos; legal guardian/next of kin, for the publication of any potentially identifiable images or data included in this article.

Author contributions

BL and XZ contributed to the study conception and design. Material preparation, data collection was performed by YL, XD, JW, ZH, and XL. The first draft of the manuscript was written by YL and XZ. All authors commented on previous versions of the manuscript. The authors read and approved the final manuscript.

Funding

This research is supported by grants from the Science and Technology Program of Guangdong Province (2019B110210004, 2017A020220003 and 2018A030313786) and Open Fund of the Guangdong Provincial Key Laboratory of Physical Activity and Health Promotion (2021B1212040014), China.

Acknowledgments

We appreciate the contribution of all patients and their parents and medical staff. We thank the Engineering Technology Research Center for Adolescent Scoliosis in Guangdong Province (2019GCZX009) and the Guangzhou Sport University-Klarity United Laboratory for technical support.

Conflict of interest

The authors declare that the research was conducted in the absence of any commercial or financial relationships that could be construed as a potential conflict of interest.

Publisher's note

All claims expressed in this article are solely those of the authors and do not necessarily represent those of their affiliated organizations, or those of the publisher, the editors and the reviewers. Any product that may be evaluated in this article, or claim that may be made by its manufacturer, is not guaranteed or endorsed by the publisher.

Supplementary material

The Supplementary Material for this article can be found online at: https://www.frontiersin.org/articles/10.3389/fbioe.2022.1022376/full#supplementary-material

References

Altaf, F, Gibson, A, Dannawi, Z, and Noordeen, H. (2013). Adolescent idiopathic scoliosis. *Bmj* 346, 2508. doi:10.1136/bmj.f2508

Beaulieu, Marlene, Toulotte, Claire, Gatto, Laura, Rivard, C. H., Teasdale, N., Simoneau, M., et al. (2008). Postural imbalance in non-treated adolescent idiopathic scoliosis at different periods of progression. *Eur. Spine J.* 18 (1), 38–44. doi:10.1007/s00586-008-0831-6

Burkus, M, Tibor Schlégl, Á, O'Sullivan, I, Markus, I., Vermes, C., and Tunyogi-Csapo, M. (2018). Sagittal plane assessment of spino-pelvic complex in a central European population with adolescent idiopathic scoliosis: A case control study. *Scoliosis Spinal Disord.* 13, 10. doi:10.1186/s13013-018-0156-0

Caţan, L, Cerbu, S, Elena, A, Suciu, O., Horhat, D. I., Popoiu, C. M., et al. (2020). Assessment of static plantar pressure, stabilometry, vitamin D and bone mineral density in female adolescents with moderate idiopathic scoliosis. *Int. J. Environ. Res. Public Health* 17 (6), 2167. doi:10.3390/ijerph17062167

Cheng, J C., Castelein, R. M., Chu, W C., Danielsson, A. J., Dobbs, M. B., Grivas, T. B., et al. (2015). Adolescent idiopathic scoliosis. *Nat. Rev. Dis. Prim.* 1, 15030. doi:10.1038/nrdp.2015.30

Courvoisier, A, Ilharreborde, B, Constantinou, B, Aubert, B., Vialle, R., and Skalli, W. (2013). Evaluation of a three-dimensional reconstruction method of the rib cage of mild scoliotic patients. *Spine Deform.* 1 (5), 321–327. doi:10.1016/j.jspd.2013.07.007

Daryabor, A, Arazpour, M, Sharifi, G, Bani, M. A., Aboutorabi, A., and Golchin, N. (2016). Gait and energy consumption in adolescent idiopathic scoliosis: A literature review. *Ann. Phys. Rehabil. Med.* 60 (2), 107–116. doi:10.1016/j.rehab.2016.10.008

Dubousset, J., Charpak, G., Skalli, W., Kalifa, G., and Lazennec, J. Y. (2007). Eos stereo-radiography system: Whole-body simultaneous anteroposterior and lateral radiographs with very low radiation dose. *Rev. Chir. Orthop. Reparatrice Appar. Mot.* 93 (6), 141–143. doi:10.1016/s0035-1040(07)92729-4

Gallant, J. N, ClintonMorgan, D., Stoklosa, J. B., Gannon, S. R., Shannon, C. N., and Bonfield, C. M. (2018). Psychosocial difficulties in adolescent idiopathic scoliosis: Body image, eating behaviors, and mood disorders. *World Neurosurg. x.* 116, 421–4321. doi:10.1016/j.wneu.2018.05.104

Gao, C. C, Chern, J. S, Chang, C. J., Lai, P. L., and Lung, C. W. (2019). Center of pressure progression patterns during level walking in adolescents with idiopathic scoliosis. *PLoS ONE* 14 (4), e0212161. doi:10.1371/journal.pone.0212161

Karimi, M. T, Kavyani, M, and Kamali, M (2016). Balance and gait performance of scoliotic subjects: A review of the literature. *J. Back Musculoskelet. Rehabil.* 29 (3), 403–415. doi:10.3233/bmr-150641

Kikanloo, S. R, Tarpada, S. P, and Cho, W (2019). Etiology of adolescent idiopathic scoliosis: A literature review. *Asian Spine J.* 13 (3), 519–526. doi:10.31616/asj.2018.0096

Kim, D S, Park, S H, Goh, T S, Son, S. M., and Lee, J. S. (2020). A meta-analysis of gait in adolescent idiopathic scoliosis. *J. Clin. Neurosci.* 81, 196–200. doi:10.1016/j.jocn.2020.09.035

Koumbourlis, A. C. (2006). Scoliosis and the respiratory system. *Paediatr. Respir. Rev.* 7 (2), 152–160. doi:10.1016/j.prrv.2006.04.009

Lonstein, J. E. (1994). Adolescent idiopathic scoliosis[J]. *Lancet (london, Engl.* 344 (8934), 12–1407.

Lowe, T. G., Edgar, M., and Margulies, J. Y. (2000). Etiology of idiopathic scoliosis: Current trends in research[J]. *The journal of bone and joint surgery* 82 (8), 68–1157.

Luo, Y, Lin, H, Wang, L, Mengjie, C., and Sun, W. (2021). Evaluation of correlation between sagittal balance and plantar pressure distributions in adolescent idiopathic scoliosis: A pilot study. *Clin. Biomech. (bristol, Avon)* 83, 105308. doi:10.1016/j.clinbiomech.2021.105308

Lv, P, Chen, J, Dong, L, Wang, L., Deng, Y., Li, K., et al. (2019). Evaluation of scoliosis with a commercially available ultrasound system. *J. Ultrasound Med.* 39 (1), 29–36. doi:10.1002/jum.15068

Ma, Q, Lin, H, Wang, L, Zhao, L., Chen, M., Wang, S., et al. (2019). Correlation between spinal coronal balance and static baropodometry in children with adolescent idiopathic scoliosis. *Gait Posture* 75, 93–97. doi:10.1016/j.gaitpost.2019.10.003

Mac-Thiong, J. M, Labelle, H, and Guise, J A. (2006). Comparison of sacropelvic morphology between normal adolescents and subjects with adolescent idiopathic scoliosis. *Stud. Health Technol. Inf.* 123, 195–200.

Mahaudens, P., Banse, X., Mousny, M., and Detrembleur, C. (2009). Gait in adolescent idiopathic scoliosis: Kinematics and electromyographic analysis. *Eur. Spine J.* 18 (4), 512–521. doi:10.1007/s00586-009-0899-7

Márkus, I, Schlégl, Á T, Burkus, M, Jozsef, K., Niklai, B., Than, P., et al. (2018). The effect of coronal decompensation on the biomechanical parameters in lower limbs in adolescent idiopathic scoliosis. *Orthop. Traumatology Surg. Res.* 104 (5), 609–616. doi:10.1016/j.otsr.2018.06.002

Mitsiaki, I, Thirios, A, Panagouli, E, Bacopoulou, F., Pasparakis, D., Psaltopoulou, T., et al. (2022). Adolescent idiopathic scoliosis and mental health disorders: A narrative review of the literature. *Child. (Basel).* 9 (5), 597. doi:10.3390/children9050597

Nault, M. L, Allard, P, Hinse, S, Le Blanc, R., Caron, O., Labelle, H., et al. (2002). Relations between standing stability and body posture parameters in adolescent idiopathic scoliosis. *Spine* 27 (17), 1911–1917. doi:10.1097/00007632-200209010-00018

Nolte, M T., Louie, P K., Harada, G K., Khan, J. M., Ferguson, J., Dewald, C. J., et al. (2020). Sagittal balance in adult idiopathic scoliosis. *Clin. Spine Surg. A Spine Publ.* 33 (2), 53–61. doi:10.1097/bsd.0000000000000940

Pehrsson, K, Larsson, S, Anders, O, and Nachemson, A. (1992). Long-term follow-up of patients with untreated scoliosis a study of mortality, causes of death, and symptoms. *Spine* 17 (9), 1091–1096. doi:10.1097/00007632-199209000-00014

Quervain, K, Müller, R, Stacoff, A., et al. (2004). Gait analysis in patients with idiopathic scoliosis[J] European spine journal and. *Eur. Sect. Cerv. Spine Res. Soc.* 13 (5), 449–456.

Saggini, R., Anastasi, G. P., Battilomo, S., et al. (2021). Consensus paper on postural dysfunction: Recommendations for prevention, diagnosis and therapy[J]. *J. Biol. Regul. Homeost. Agents* 35 (2), 441–456.

Slattery, C, and Verma, K (2018). Classifications in brief: The Lenke classification for adolescent idiopathic scoliosis. *Clin. Orthop. Relat. Res.* 476 (11), 2271–2276. doi:10.1097/corr.0000000000000405

Teyhen, D. S., Stoltenberg, B E., Collinsworth, K M., Giesel, C. L., Williams, D. G., Kardouni, C. H., et al. (2009). Dynamic plantar pressure parameters associated with static arch height index during gait. *Clin. Biomech. (Bristol, Avon.* 24 (4), 391–396. doi:10.1016/j.clinbiomech.2009.01.006

Tochigi, Y, Segal, N A., Vaseenon, T, and Brown, T. D. (2011). Entropy analysis of tri-axial leg acceleration signal waveforms for measurement of decrease of physiological variability in human gait. *J. Orthop. Res.* 30 (6), 897–904. doi:10.1002/jor.22022

Ungi, T, Greer, H, Sunderland, K. R., Wu, V., Baum, Z. M. C., Schlenger, C., et al. (2020). Automatic spine ultrasound segmentation for scoliosis visualization and measurement. *IEEE Trans. Biomed. Eng.* 67 (11), 3234–3241. doi:10.1109/tbme.2020.2980540

Weinstein, S L., Dolan, L A., Cheng, J. C. Y., et al. (2008). Adolescent idiopathic scoliosis[J]. *Lancet (london, Engl.* 371 (9623), 37–1527.

Weinstein, S. L., Dolan, L. A., Spratt, K. F., Peterson, K. K., Spoonamore, M. J., and Ponseti, I. V. (2003). Health and function of patients with untreated idiopathic scoliosis: A 50-year natural history study. *Jama* 289 (5), 559. doi:10.1001/jama.289.5.559

Wiernicka, M, Kotwicki, T, Kamińska, E, Lochynski, D., Kozinoga, M., Lewandowski, J., et al. (2019). Postural stability in adolescent girls with progressive idiopathic scoliosis. *Biomed Res. Int.* 2019, 1–5. doi:10.1155/2019/7103546

Wittschieber, D, Schmeling, A, Schmidt, S, Heindel, W., Pfeiffer, H., and Vieth, V. (2012). The risser sign for forensic age estimation in living individuals: A study of 643 pelvic radiographs. *Forensic Sci. Med. Pathol.* 9 (1), 36–43. doi:10.1007/s12024-012-9379-1

Wong, A Y. L., Samartzis, D, PrudenceCheung, W. H., and Cheung, J. P. Y. (2019). How common is back pain and what biopsychosocial factors are associated with back pain in patients with adolescent idiopathic scoliosis?[J]. *Clin. Orthop. Relat. Res.* 477 (4), 676–686. doi:10.1097/corr.0000000000000569

Yang, J H, Suh, S. W, Sung, P. S., et al. (2013). Asymmetrical gait in adolescents with idiopathic scoliosis[J]. European spine journal: Official publication of the European spine society. *Eur. Sect. Cerv. Spine Res. Soc.* 22 (11), 13–2407.

Zhang, X, Yang, D, Zhang, S, Wang, J., Chen, Y., Dou, X., et al. (2022). Do the three-dimensional parameters of brace-wearing patients with ais change when transitioning from standing to sitting position? A preliminary study on Lenke I[J]. *BMC Musculoskelet. Disord.* 23 (1), 419. doi:10.1186/s12891-022-05380-z

frontiers | Frontiers in Physiology

TYPE Original Research
PUBLISHED 07 December 2022
DOI 10.3389/fphys.2022.1046141

Check for updates

OPEN ACCESS

EDITED BY
Qichang Mei,
Ningbo University, China

REVIEWED BY
Qingguang Liu,
Tongji University, China
Yi Jia,
North University of China, China

*CORRESPONDENCE
Qipeng Song,
songqipeng@sdpei.edu.cn

SPECIALTY SECTION
This article was submitted to Exercise Physiology, a section of the journal Frontiers in Physiology

RECEIVED 16 September 2022
ACCEPTED 28 November 2022
PUBLISHED 07 December 2022

CITATION
Ma X, Lu L, Zhou Z, Sun W, Chen Y, Dai G, Wang C, Ding L, Fong DT-P and Song Q (2022), Correlations of strength, proprioception, and tactile sensation to return-to-sports readiness among patients with anterior cruciate ligament reconstruction.
Front. Physiol. 13:1046141.
doi: 10.3389/fphys.2022.1046141

Correlations of strength, proprioception, and tactile sensation to return-to-sports readiness among patients with anterior cruciate ligament reconstruction

Xiaoli Ma[1], Lintao Lu[2], Zhipeng Zhou[1], Wei Sun[1], Yan Chen[1], Guofeng Dai[2], Cheng Wang[2], Lijie Ding[1], Daniel Tik-Pui Fong[3] and Qipeng Song[1]*

[1]College of Sports and Health, Shandong Sport University, Jinan, China, [2]Department of Orthopedic Surgery, Qilu Hospital, Cheeloo College of Medicine, Shandong University, Jinan, China, [3]School of Sport, Exercise and Health Sciences, Loughborough University, Loughborough, United Kingdom

Objectives: Anterior cruciate ligament reconstruction (ACLR) is the most common surgery for anterior cruciate ligament (ACL) injuries, and the relationships between patients' return to sports (RTS) readiness and different physical functions are inconclusive among patients with ACLR. This study aimed to investigate the correlations of strength, proprioception, and tactile sensation to the RTS readiness among patients with ACLR.

Methods: Forty-two participants who received ACLR for at least 6 months were enrolled in this study. Their strength, proprioception, and tactile sensation were tested, and their RTS readiness was measured with the Knee Santy Athletic Return to Sports (K-STARTS) test, which consists of a psychological scale [Anterior Cruciate Ligament Return to Sports after Injury scale (ACL-RSI)] and seven functional tests. Partial correlations were used to determine their correlations while controlling for covariates (age, height, weight, and postoperative duration), and factor analysis and multivariable linear regressions were used to determine the degrees of correlation.

Results: Knee extension strength was moderately correlated with K-STARTS total, ACL-RSI, and functional scores. Knee flexion strength, knee flexion and extension proprioception, and tactile sensation at the fifth metatarsal were moderately correlated with K-STARTS total and functional scores. Strength has higher levels of correlation with functional scores than proprioception.

Conclusion: Rehabilitation to promote muscle strength, proprioception and tactile sensation should be performed among patients with ACLR, muscle strength has the highest priority, followed by proprioception, with tactile sensation making the least contribution.

KEYWORDS

anterior cruciate ligament reconstruction, neuromuscular control, strength, cutaneous sensation, ACL injury

1 Introduction

The anterior cruciate ligament (ACL) is one of the most important ligaments of the knee joint that prevents the anterior glide of the tibia, maintains the knee joint's stability, and enables the human body to complete a variety of complex and challenging movements (Noyes et al., 2015). ACL injury is one of the most common and devastating knee injuries in rotational and contact sports (Paterno et al., 2010). More than 200,000 ACL tears was reported in the United States annually, particularly among athletes or recreational sportsmen (Lentz et al., 2012). ACL reconstruction (ACLR) is the most common surgery for ACL injuries, and it is considered effective in restoring the function of the knee joint (Leys et al., 2012). A previous study has shown that return to sports (RTS) rates are relatively low after ACLR. Although approximately 81% of individuals who underwent ACLR returned to some form of sports activities, only 55% returned to their pre-injury level of competition (Ardern et al., 2014b).

The Knee Santy Athletic Return to Sports (K-STARTS) test is considered an appropriate and objective measure of functional improvement after ACLR (Blakeney et al., 2018). The K-STARTS test consists of a psychological scale [ACL Return to Sports after Injury scale (ACL-RSI)] and seven functional tests. The ACL-RSI is specific to assess the psychological readiness for RTS after ACLR. Functional tests provide a comprehensive assessment of knee function and reflect the overall motor skill and performance of the lower extremities.

A variety of factors may influence RTS readiness, with inadequate neuromuscular control being at the forefront (Paterno et al., 2010). Decreased strength and impaired sensation are common in weeks, months, and even years after ACLR and may considerably affect the neuromuscular control during locomotion (Kennedy et al., 1982). The ability of muscles to generate adequate force is critical for neuromuscular control (Pijnappels et al., 2008). When an individual moves strenuously (e.g., change of direction, jump, etc.), the muscles around the knee joint work together to maintain the stability of the knee joint, improve neuromuscular control, and help individuals to safely return to the competition. Proprioception refers to the perception of one's own body and movements through information generated inside the body, while tactile information, sensed by receptors in the skin, is concerned with sensory stimuli originating outside the body, such as the physical characteristics of the environment (Song et al., 2021). As primary components of the somatosensory system, proprioception and cutaneous sensation account for about 60–70% of balance control (Li et al., 2019).

The correlations of strength, proprioception, and tactile sensation with RTS readiness remain unclear, although they are considered the primary contributors to neuromuscular control (Song et al., 2021). Several previous studies have indicated that strength is correlated with functional tests (Xergia et al., 2015), and insufficient strength results in a high risk of re-injury (Thomee et al., 2011). Whether the strength is related to the psychological readiness measured by ACL-RSI and the overall RTS readiness measured by K-STARTS is unknown among patients with ACLR. Some studies showed that proprioception is correlated with functional tests (Katayama et al., 2004), whereas others showed non-significant correlations (Muaidi et al., 2009). The correlations of proprioception to psychological readiness for RTS still need to be further investigated. Literature on the correlations of tactile sensation to RTS variables is scarce. Strength training and sensory recovery have been applied to the rehabilitation among patients with ACL injury (Kruse et al., 2012), the necessity of these rehabilitation programs cannot be determined without examining the correlations of strength and sensation with RTS variables. In addition, one study showed a strong correlation between muscle strength and functional performance (r = 0.649, p < 0.05) (Greenberger and Paterno, 1995), and another study detected a moderate correlation between proprioception and functional performance (r = −0.389, p < 0.05) (Katayama et al., 2004). No correlation was detected between cutaneous sensitivity and dynamic balance control (Song et al., 2021). To our knowledge, no one has yet to correlate strength, proprioception and tactile sensation with RTS among patients with ACLR in a single study, the priority of different rehabilitation approaches is difficult to be determined.

This study aimed to investigate the correlations of strength, proprioception, and tactile sensation with RTS variables in patients with ACLR. The following hypotheses were proposed: 1) Strength, proprioception, and tactile sensation are significantly correlated with K-STARTS, ACL-RSI, and functional tests, and 2) Higher levels of correlation existed between strength and RTS for proprioception, while the lowest levels existed between tactile sensations and RTS.

2 Materials and methods

2.1 Participants

An *a priori* power analysis (G*Power Version 3.1) indicated that a minimum of 33 participants are needed to obtain the alpha level of 0.05 and the statistical power of 0.80 based on a previous report, which

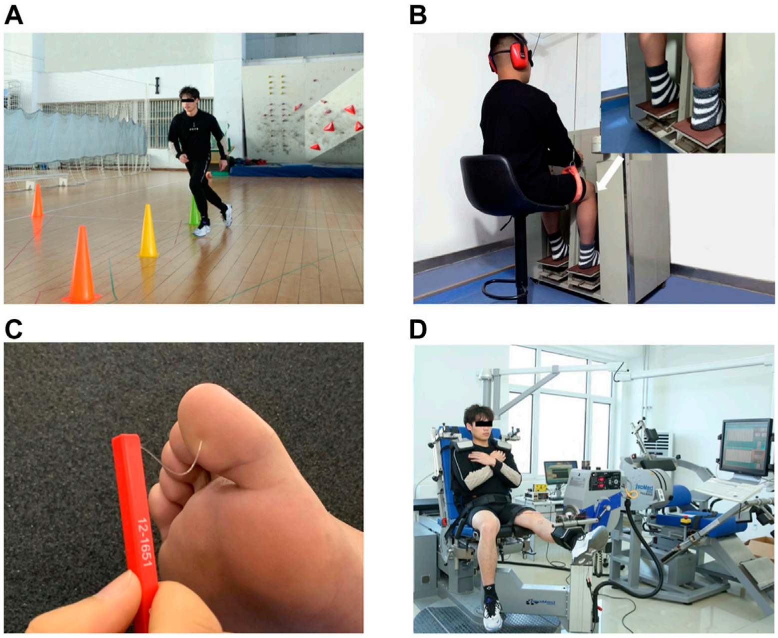

FIGURE 1
Test illustrations. **(A)** K-STARTS tests. **(B)** Proprioception test using a proprioception test device. **(C)** Tactile sensation test with a set of Semmes–Weinstein monofilaments. **(D)** Strength test using the IsoMed 2000 strength-testing system.

detected a r^2 = 0.24 between strength and RTS among 78 young (13–30 years) patients who received ACLR (Della Villa et al., 2021). Patients with high sports demand who had underwent ACLR were enrolled in this study. The inclusion criteria were as follows: 1) aged 18–40 years; 2) regular participation in certain sports before the injury and willing to RTS after ACLR; 3) Tegner≥5; 4) unilateral ACL rupture and ACLR through arthroscopy; 5) without combined meniscus injury; 6) no other lesions; 7) 6–18 months after ACLR. The exclusion criteria were as follows: 1) associated knee ligamentous injuries within 3 months, 2) previous knee surgery, 3) clinically relevant cardiovascular history, 4) clinically relevant neurological and neuromuscular disorders and 5) associated organ diseases that cannot be tolerated. A total of 42 participants were enrolled after the eligibility assessment (female = 12, male = 30, age: 27.6 ± 6.8 years, height: 181.8 ± 9.0 cm, weight: 80.4 ± 8.9 kg, BMI: 24.4 ± 2.7, postoperative duration: 10.3 ± 3.8 months) and were included in the final analysis. Of them, 15, 11, 10, 5 and 1 participated in basketball, soccer, badminton, table tennis and fencing. Human participation was approved by Institutional Review Boards in Shandong Sport University (2022013) and was in accordance with the Declaration of Helsinki.

2.2 Protocol

The participants provided written informed consent and completed a battery of questionnaires, including the International Knee Documentation Committee questionnaire, Tegner, and Visual Analog Scale (VAS). The results were used to determine whether the participants should be included in the study. Multiple measures of strength, proprioception and tactile sensation tests were performed. The order of the K-STARTS, proprioception and tactile sensation tests is randomized and the muscle strength is tested at last to avoid fatigue.

2.3 K-STARTS test

The K-STARTS test had high reliability (intraclass correlation coefficient (ICC) = 0.87, coefficient of variation = 7.8%) in assessing RTS readiness among patients with ACLR (Franck et al., 2021). It consists of an ACL-RSI scale and seven functional tests (Figure 1A). All tests were supervised by two trained research assistants. The ACL-RSI scale consists of 12 psychological questions. The participants were asked to rate the degree of fear for each task using VAS from 0 (no fear at all) to 10 (most fearful). Three points were awarded for ACL-RSI scores of 76% or higher, 2 points for scores between 64% and 75%, 1 point for scores between 56% and 63%, and 0 points for less than 55% (Franck et al., 2021).

The functional scores were determined as follows. 1) Single-leg landing: Participants stood on their affected leg for about 10 s, scored by the Qualitative Assessment of Single-leg Landing (QASLS). The QASLS score ranges between 0 (best) and 10 (worst). Participants with QASLS scores of 0, 1, 2, and ≥3 were given 3, 2, 1, and 0 points, respectively (Franck et al., 2021). 2) Dynamic valgus: a penalty of 3 points was applied if a participant was judged to have a dynamic valgus of the limb during the single-leg loading task. 3) Single, triple, side, and crossover hop tests: the jump distance of each leg in each of the four tests was measured. Hop tests were evaluated using the Limb Symmetry Index (the percentage deficit of the distance hopped on the involved leg compared with the uninvolved contralateral leg). Participants with ≥90%, 80%–90%, and ≤80% distance deficits were given 3, 2, and 1 point, respectively, and 0 point was attributed when pain prevented the test (Blakeney et al., 2018). 4) The Modified Illinois Change of Direction Test (MICODT): the participant sprinted forward as fast as he/she could, following the direction of the arrows and running around the markers. An average time of ≤12.5 s scored 3 points, 12.5–13.5 s scored 2 points, >13.5 s scored 1 point, and 0 point was attributed when pain prevented the test.

2.4 Proprioception test

The participant's knee proprioception threshold was assessed using a proprioception test device (Sunny, AP-II, China; Figure 1B), which showed good test-retest reliability (ICC = 0.74–0.94) (Sun et al., 2015). The device consists of a platform and a pedal. Two electric motors drive the platform at an angular velocity of 0.4°/s. An electronic goniometer in the device recorded the angular displacement of the platform. All participants were seated on a height-adjustable chair with feet on the testing pedal during the test. The hip and knee joints were flexed 90°, respectively, the ankle joint was in a neutral position, and the lower leg was perpendicular to the surface of the platform. The participants wore eye masks and headphones and played soothing music in the headphones to reduce the visual and auditory interference caused by the external environment. Each test movement began by placing the foot on the horizontal platform (position of 0°). The experimenter presses the direction button, and the testing pedal will move in the corresponding direction. Participants were instructed to concentrate on their foot, press the hand switch to stop the movement of the platform when they could sense motion and say (point out) the direction of the joint motion. At least five trials were performed for each direction. The minimal three angles sensed in each direction were used for data analysis.

2.5 Tactile sensation test

The tactile sensation was assessed with a set of Semmes–Weinstein monofilaments (North Coast Medical, Inc., Morgan Hill, CA, United States; Figure 1C), which showed good test-retest reliability (ICC = 0.83–0.86) (Collins et al., 2010). Six monofilaments with different sizes were used in this study: 2.83 (0.07 g), 3.61 (0.4 g), 4.31 (2 g), 4.56 (4 g), 5.07 (10 g), and 6.65 (300 g). The filament size was log10 (10 × force in milligrams). During the assessment, all participants were supine with their eyes closed in a quiet environment. The filaments were randomly applied vertically to the skin on the bases of the great toe, first and fifth metatarsals, arch, and heel on the affected side until they were bent 90° for 1.0–1.5 s. Tactile sensitivity was determined by the initial application of the thin filaments, progressing to the thicker filaments until the participants would be able to detect the touch (Machado et al., 2017). Participants were asked to name the exact location where a monofilament was detected. If a monofilament was perceived correctly on a test location, the tactile sensation threshold was recorded. If a monofilament was not perceived, the next monofilament is tested. The tactile sensation threshold was determined by the thinnest monofilament they could feel (Unver and Akbas, 2018).

2.6 Strength test

The strengths of knee flexion and extension on the affected leg were measured using the IsoMed 2000 strength testing system (D & R Ferstl GmbH, Hemau, Germany; Figure 1D), which showed good test-retest reliability (ICC = 0.77–0.98) (Gonosova et al., 2018). Participant were seated on the dynamometer chair with their knee and hip placed at about 90° and 85°, respectively. Their torso, pelvis, and thigh were secured to the training chair using a lap belt. The chair was adjusted to align each participant's lateral femoral condyle with the axis of rotation of the dynamometer arm and the distal torque pad was affixed to the shank at two finger-widths above the lateral malleolus. The position of the safety valve was adjusted to limit the range of joint movement to prevent accidents and ensure the participant's safety. All participants were instructed to flex and extend the tested leg with the maximal exertion at an angular speed of 60°/s. The reliability at this angular velocity was high (0.87 < ICC < 0.96) (Roth et al., 2017). Three trials were recorded, and at least a 2 min break was taken between two trials. Max knee flexion and extension torques were normalized by body mass.

2.7 Data analysis

Descriptive analysis was used to summarize the means and standard deviations of RTS variables, strength, proprioception, and tactile sensation. The normality of all outcome variables was tested using Shapiro–Wilk tests. A partial correlation (Pearson correlation for normally distributed or Spearman correlation for non-normally distributed data) was used to verify Hypothesis 1 by determining the correlations of the RTS variables with each of the strength, proprioception, and tactile sensation variables while controlling for covariates (age, height, weight, and postoperative duration). Then, a separate exploratory factor analysis was carried out among each

TABLE 1 Descriptive characteristics of outcome variables.

		Mean	SD	Max	Min
RTS variables	K-STARTS	10.45	3.24	16.00	2.00
	ACL-RSI	1.55	0.86	3.00	0.00
	Functional performance	8.90	3.12	14.00	2.00
Strength (N·m/kg)	Knee flexion	1.15	0.49	2.33	0.48
	Knee extension	0.87	0.51	1.82	0.16
Proprioception (°)	Knee flexion	0.92	0.32	1.55	0.27
	Knee extension	0.90	0.35	1.66	0.22
Cutaneous sensitivity (gauge)	Great toe	3.60	0.40	4.31	2.83
	1st metatarsal	3.35	0.52	4.31	2.83
	5th metatarsal	3.64	0.53	4.31	2.83
	Arch	3.65	0.44	4.31	2.83
	Heel	3.75	0.41	4.31	2.83

RTS: return to sports; K-STARTS: knee santy athletic return to sports; ACL-RSI: anterior cruciate ligament return to sports after injury scale.

TABLE 2 Partial correlation outcomes of K-STARTS, ACL-RSI, and functional performance with strength, proprioception, and tactile sensation variables.

		K-STARTS		ACL-RSI		Functional performance	
	Variables	*r*	p	*r*	p	*r*	p
Strength (N·m/kg)	Knee flexion	0.340	0.032	−0.074	0.648	0.374	0.017
	Knee extension	0.415	0.008	0.358	0.023	0.327	0.040
Proprioception (°)	Knee flexion	−0.316	0.047	0.092	0.571	−0.355	0.025
	Knee extension	−0.321	0.044	0.028	0.864	−0.340	0.032
Tactile sensation (gauge)	Great toe	0.220	0.172	0.102	0.532	0.199	0.218
	1st metatarsal	−0.198	0.221	0.243	0.13	−0.276	0.085
	5th metatarsal	−0.395	0.012	0.057	0.725	−0.426	0.006
	Arch	0.059	0.717	0.186	0.252	0.008	0.963
	Heel	0.011	0.948	0.176	0.276	−0.040	0.806

RTS: return to sports, K-STARTS: knee santy athletic return to sports, ACL-RSI: anterior cruciate ligament return to sports after injury scale. The correlations of tactile sensation to ACL-RSI, were analyzed by Spearman correlation. The correlations of the others variables were analyzed by Pearson correlation. The shaded cells represent significant correlation coefficients. The values were adjusted for age, weight, height, and postoperative duration. *r*: correlation coefficient.

category of the variables of interest. Multivariable linear regression was used to verify Hypothesis 2 by exploring the degrees of correlation between each generated factor and RTS variables while controlling for the above-mentioned covariates. The thresholds for the correlation coefficient (r) were as follows: 0–0.1, trivial; 0.1–0.3, weak; 0.3–0.5, moderate; >0.5, strong (Cohen, 1988). All analyses were conducted in SAS 9.4, and the significance level was set at 0.05.

3 Results

Shapiro–Wilk tests showed that most of the tactile sensation and ACL-RSI data were non-normally distributed. Strength, proprioception, K-STARTS, and functional performance data were all normally distributed.

The descriptive characteristics are shown in Table 1. Mean, standard deviation, and minimum and maximum values are reported for the RTS variables, strength, proprioception, and tactile sensation.

Partial correlations are shown in Table 2. Knee flexion strength was moderately correlated with K-STARTS total and functional scores, and knee extension strength was moderately correlated with K-STARTS total, ACL-RSI, and functional scores. Knee flexion proprioception was moderately correlated with K-STARTS total and functional scores, and knee extension proprioception was moderately correlated with K-STARTS

TABLE 3 Factor loadings for the variables among the categories of joint torque, proprioception, and tactile sensation.

		Factor 1	Factor 2	Factor 3
Strength (N·m/kg)	Knee flexion	0.518	--	--
	Knee extension	0.880	--	--
Proprioception (°)	Knee flexion	--	0.793	--
	Knee extension	--	0.759	--
Tactile sensation (gauge)	Great toe	--	--	0.636
	1st metatarsal	--	--	0.798
	5th metatarsal	--	--	0.733
	Arch	--	--	0.719
	Heel	--	--	0.779

total and functional scores. Tactile sensation at the fifth metatarsal was moderately correlated with K-STARTS total and functional scores.

The factor loadings for all the variables of strength, proprioception, and tactile sensation are shown in Table 3. Factor 1 (F1), factor 2 (F2), and factor 3 (F3) were the summaries of strength, proprioception, and tactile sensation, respectively, with a Kaiser Meyer Olkin value of 0.760 and sphericity of <0.001.

The equations for multivariable regression are:

$$\text{K} - \text{STARTS total score} = 10.452 + (1.564 \times \text{F1}) - (0.869 \times \text{F2}) \quad (1)$$

$$\text{Functional score} = 8.905 + (1.369 \times \text{F1}) - (1.038 \times \text{F2}) \quad (2)$$

In Eq. 1, adjusted $r^2 = 0.517$, $p_{F1} = 0.001$, $p_{F2} = 0.048$, $\beta_{F1} = 0.483$, and $\beta_{F2} = 0.268$. In Eq. 2, adjusted $r^2 = 0.520$, $p_{F1} = 0.002$, $p_{F2} = 0.015$, $\beta_{F1} = 0.439$, and $\beta_{F2} = 0.332$. No significant correlations were detected between ACL-RSI and the three factors.

The equations indicated that compared with proprioception, strength has more contribution to K-STARTS total ($\beta_{F1} = 0.483 > \beta_{F2} = 0.268$) and functional scores ($\beta_{F1} = 0.439 > \beta_{F2} = 0.332$).

4 Discussion

This study investigated the correlations of strength, proprioception, and tactile sensation with RTS readiness. The outcomes partly supported Hypothesis 1 that knee strength is correlated with K-STARTS total, ACL-RSI, and functional scores. While proprioception and tactile sensation were only correlated with K-STARTS and functional scores, and not with ACL-RSI. The outcomes supported Hypothesis 2 and pointed out that strength contributed more to K-STARTS total and functional scores than proprioception and that tactile sensation had the least contribution.

The results showed that strength is correlated with K-STARTS total, functional, and ACL-RSI scores. The correlation between strength and functional performance was consistent with previous studies (Myer et al., 2011; Xergia et al., 2015) but inconsistent with another study (Barber et al., 1990). The inconsistencies may be attributed to the different angular velocities in the strength tests. The angular velocity during strength tests was 300°/s in Barber et al.'s study, while 60°/s in the present study. It has been confirmed that isokinetic torque at 60°/s provides valuable information on strength recovery after ACLR (Eitzen et al., 2009). Previous studies supported our outcomes by pointing out that insufficient strength in the quadriceps femoris and hamstrings results in a high risk of re-injury (Callaghan and Oldham, 2004), our study showed a correlation between strength and K-STARTS, which may imply that strength plays an important role in RTS overall readiness. Furthermore, our outcomes also pointed out that knee extension strength was moderately correlated with ACL-RSI. Consistent with our observations, several studies showed a positive correlation between the strength of the affected quadriceps and the psychological readiness, greater quadriceps strength may lead to better confidence in performing functional activities (Lepley et al., 2018). Previous literature has shown that psychological readiness is an important determinant of RTS decisions (Ardern et al., 2014a), and vital element to RTS (Gokeler et al., 2017). Growing evidence supports the impact of psychological dysfunction on RTS among patients with ACLR (Burland et al., 2018). Our outcomes further imply that greater knee strength may enhance confidence in completing specific motor tasks and increase patients' RTS confidence.

Our outcomes indicated that proprioception is correlated with K-STARTS total and functional scores. Our study demonstrates a correlation between proprioception and K-STARTS total score, which may imply that proprioception may influence RTS overall readiness. The correlation between proprioception and the functional score is consistent with some studies (Katayama et al., 2004; Chaput et al., 2022) but inconsistent with another study (Muaidi et al., 2009). The different choices of functional tests may explain the conflict. In the inconsistent study (Muaidi et al., 2009), only a single-legged hop-for-distance test was used. The ACL is a vital sensory organ that contains a variety of sensory nerve endings, provides proprioceptive information, generates protective reflexes, and plays an essential role in stabilizing the knee joint (Bonfim et al., 2003). When the knee flexed or extended, the tension of the surrounding muscles, tendons, and ligaments changes, which excites the mechanoreceptors and transmits information about joint motion and deformation to the CNS; then, the CNS modulates the corresponding muscles around the knee joint through reflex neuromuscular feedback, causing specific muscles to contract and thus maintaining joint stability (Roijezon et al., 2015). Previous studies pointed out that although the mechanical stability of the ACL can be restored in a short period of time, proprioceptive reconstruction takes longer (Lee et al., 2015). Our outcomes support that proprioception is another key to RTS and that proprioception-related rehabilitation should be included in ACLR programs.

Our outcomes also pointed out that tactile sensation at the 5th metatarsal head on the affected side is related to K-STARTS total and functional scores. This finding may be due to the compensation mechanism of tactile sensation with proprioception. Peripheral sensory signals are transmitted along different sensory neurons, such as large type Ia and II sensory neurons responsible for proprioception and small-diameter type III sensory neurons for tactile sensation (Li et al., 2019). Type III sensory neurons are slower and weaker than type Ia and II sensory neurons. Hence, individuals usually rely on proprioception rather than tactile sensation in neuromuscular control during dynamic movement (Song et al., 2021). Proprioception usually decreases with ACLR, and participants may use tactile sensation to compensate for their declined proprioception. This viewpoint is supported by previous studies that observed the compensation between the two senses (Li et al., 2019). Moreover, Impaired balance in the lateral direction is associated with a higher fall risk than impaired anterior-posterior balance (Islam et al., 2004). During locomotion, if the disturbance occurs in the anterior, posterior, or medial direction, the individual can counteract the disturbance by dropping the swinging leg in the appropriate position. However, if the disturbance occurs in the lateral direction, the individual may need the weak lateral foot muscles to maintain balance since it is difficult to drop the swing leg on the lateral of the supporting leg (Mao et al., 2006). It is inferred that the tactile sensation at the lateral part of foot sole, represented by the 5th metatarsal head, is more important than other parts to maintain balance and to facilitate functional performance. To the best of our knowledge, no studies have investigated the correlations of tactile sensation to RTS readiness, and the present study suggests that approaches to increase tactile sensation should be applied to ACLR rehabilitation at least when their proprioception is not well recovered.

Multivariate linear regression revealed that strength contributed more to RTS readiness than proprioception, and tactile sensation contributed the least. ACLR reduces quadriceps strength and impairs knee proprioception (Lepley et al., 2018). It has been pointed out that the recovery of lower extremity strength has a remarkable impact on the RTS of patients in ACLR(Kaya et al., 2019), and proprioceptive training decreases the incidence of ACL injury (Dargo et al., 2017). Our outcomes supported these viewpoints and filled the gap between previous studies by pointing out that strength has higher levels of correlation with RTS than proprioception, which infers that strength training has priority over proprioception rehabilitation in patients with ACLR.

This study has several limitations. First, most of the participants were male, which affects the applicability of the outcomes to female. The MICODT score may be influenced by gender. Second, this study used a passive proprioceptive assessment, and the results might have been different if an active assessment had been used. However, it has been pointed out that participants' performance on active proprioception (usually measured using joint position sense) was more erratic overall compared with passive proprioception (usually measured using threshold to detect passive motion) (Reider et al., 2003), and passive proprioception assessment has better consistency in detecting proprioceptive defects than active assessment in ACL-deficient knees (Friden et al., 1997). Third, the participants had different types of sports, with ball games being the majority, which may have influenced our results.

5 Conclusion

Rehabilitation to promote muscle strength, proprioception, and tactile sensation should be performed among patients with ACLR, muscle strength has the highest priority, followed by proprioception, with tactile sensation making the least contribution to RTS among patients with ACLR.

Data availability statement

The datasets presented in this study can be found in online repositories. The names of the repository/repositories and accession number(s) can be found below: 10.57760/sciencedb.01729.

Ethics statement

The studies involving human participants were reviewed and approved by Institutional Review Boards in Shandong Sport

University (2022013). The patients/participants provided their written informed consent to participate in this study.

Author contributions

XM participated in the design of the study, contributed to data collection and data reduction/analysis and drafted the manuscript; LL and ZZ participated in the design of the study, data reduction/analysis; WS and YC participated in the design of the study, contributed to data collection and data reduction/analysis; GD and CW contributed to data collection and data reduction/analysis; LD participated in data analysis and contributed to statistics; D-PF contributed to data collection and interpretation of results of the study; QS participated in the design of the study, contributed to data analysis and interpretation of results. All authors have read and agreed to the published version of the manuscript.

Funding

This work was supported by the Shandong Young Innovative Talent Team of China (2019–183), and China National Natural Science Foundation (12102235).

Acknowledgments

The authors would like to thank Hao Sun, doctoral student at Loughborough University, and Shanshan Hu, Jingwen Wang, Yaya Pang, Qi Wang, Shiyu Dong, and Boshi Xue, graduate students at Shandong Sport University, for participating in the experiment or data acquisition for this work.

Conflict of interest

The authors declare that the research was conducted in the absence of any commercial or financial relationships that could be construed as a potential conflict of interest.

Publisher's note

References

Ardern, C. L., Österberg, A., Tagesson, S., Gauffin, H., Webster, K. E., and Kvist, J. (2014a). The impact of psychological readiness to return to sport and recreational activities after anterior cruciate ligament reconstruction. *Br. J. Sports Med.* 48 (22), 1613–1619. doi:10.1136/bjsports-2014-093842

Ardern, C. L., Taylor, N. F., Feller, J. A., and Webster, K. E. (2014b). Fifty-five per cent return to competitive sport following anterior cruciate ligament reconstruction surgery: An updated systematic review and meta-analysis including aspects of physical functioning and contextual factors. *Br. J. Sports Med.* 48 (21), 1543–1552. doi:10.1136/bjsports-2013-093398

Barber, S. D., Noyes, F. R., Mangine, R. E., McCloskey, J. W., and Hartman, W. (1990). Quantitative assessment of functional limitations in normal and anterior cruciate ligament-deficient knees. *Clin. Orthop. Relat. Res.* 255, 204–214. doi:10.1097/00003086-199006000-00028

Blakeney, W. G., Ouanezar, H., Rogowski, I., Vigne, G., Guen, M. L., Fayard, J. M., et al. (2018). Validation of a composite test for assessment of readiness for return to sports after anterior cruciate ligament reconstruction: The K-starts test. *Sports Health* 10 (6), 515–522. doi:10.1177/1941738118786454

Bonfim, T. R., Jansen Paccola, C. A., and Barela, J. A. (2003). Proprioceptive and behavior impairments in individuals with anterior cruciate ligament reconstructed knees. *Arch. Phys. Med. Rehabil.* 84 (8), 1217–1223. doi:10.1016/s0003-9993(03)00147-3

Burland, J. P., Toonstra, J., Werner, J. L., Mattacola, C. G., Howell, D. M., and Howard, J. S. (2018). Decision to return to sport after anterior cruciate ligament reconstruction, Part I: A qualitative investigation of psychosocial factors. *J. Athl. Train.* 53 (5), 452–463. doi:10.4085/1062-6050-313-16

Callaghan, M. J., and Oldham, J. A. (2004). Quadriceps atrophy: To what extent does it exist in patellofemoral pain syndrome? *Br. J. Sports Med.* 38 (3), 295–299. doi:10.1136/bjsm.2002.002964

Chaput, M., Onate, J. A., Simon, J. E., Criss, C. R., Jamison, S., McNally, M., et al. (2022). Visual cognition associated with knee proprioception, time to stability, and sensory integration neural activity after ACL reconstruction. *J. Orthop. Res.* 40 (1), 95–104. doi:10.1002/jor.25014

Cohen, J. (1988). *Statistical power analysis for the behavioral sciences*. 2nd ed. Hillsdale, NJ: Lawrence Erlbaum Associates.

Collins, S., Visscher, P., De Vet, H. C., Zuurmond, W. W., and Perez, R. S. (2010). Reliability of the Semmes Weinstein Monofilaments to measure coetaneous sensibility in the feet of healthy subjects. *Disabil. Rehabil.* 32 (24), 2019–2027. doi:10.3109/09638281003797406

Dargo, L., Robinson, K. J., and Games, K. E. (2017). Prevention of knee and anterior cruciate ligament injuries through the use of neuromuscular and proprioceptive training: An evidence-based review. *J. Athl. Train.* 52 (12), 1171–1172. doi:10.4085/1062-6050-52.12.21

Della Villa, F., Straub, R. K., Mandelbaum, B., and Powers, C. M. (2021). Confidence to return to play after anterior cruciate ligament reconstruction is influenced by quadriceps strength Symmetry and injury mechanism. *Sports Health* 13 (3), 304–309. doi:10.1177/1941738120976377

Eitzen, I., Holm, I., and Risberg, M. A. (2009). Preoperative quadriceps strength is a significant predictor of knee function two years after anterior cruciate ligament reconstruction. *Br. J. Sports Med.* 43 (5), 371–376. doi:10.1136/bjsm.2008.057059

Franck, F., Saithna, A., Vieira, T. D., Pioger, C., Vigne, G., Le Guen, M., et al. (2021). Return to sport composite test after anterior cruciate ligament reconstruction (K-starts): Factors affecting return to sport test score in a retrospective analysis of 676 patients. *Sports Health* 13 (4), 364–372. doi:10.1177/1941738120978240

Friden, T., Roberts, D., Zatterstrom, R., Lindstrand, A., Moritz, U., and Moritz, U. (1997). Proprioception after an acute knee ligament injury: A longitudinal study on 16 consecutive patients. *J. Orthop. Res.* 15 (5), 637–644. doi:10.1002/jor.1100150502

Gokeler, A., Welling, W., Zaffagnini, S., Seil, R., and Padua, D. (2017). Development of a test battery to enhance safe return to sports after anterior cruciate ligament reconstruction. *Knee Surg. Sports Traumatol. Arthrosc.* 25 (1), 192–199. doi:10.1007/s00167-016-4246-3

Gonosova, Z., Linduska, P., Bizovska, L., and Svoboda, Z. (2018). Reliability of Ankle⁻Foot complex isokinetic strength assessment using the isomed 2000 dynamometer. *Med. Kaunas.* 54 (3), 43. doi:10.3390/medicina54030043

Greenberger, H. B., and Paterno, M. V. (1995). Relationship of knee extensor strength and hopping test performance in the assessment of lower extremity function. *J. Orthop. Sports Phys. Ther.* 22 (5), 202–206. doi:10.2519/jospt.1995.22.5.202

Islam, M. M., Nasu, E., Rogers, M. E., Koizumi, D., Rogers, N. L., and Takeshima, N. (2004). Effects of combined sensory and muscular training on balance in Japanese older adults. *Prev. Med.* 39 (6), 1148–1155. doi:10.1016/j.ypmed.2004.04.048

Katayama, M., Higuchi, H., Kimura, M., Kobayashi, A., Hatayama, K., Terauchi, M., et al. (2004). Proprioception and performance after anterior cruciate ligament rupture. *Int. Orthop.* 28 (5), 278–281. doi:10.1007/s00264-004-0583-9

Kaya, D., Guney-Deniz, H., Sayaca, C., Calik, M., and Doral, M. N. (2019). Effects on lower extremity neuromuscular control exercises on knee proprioception, muscle strength, and functional level in patients with ACL reconstruction. *Biomed. Res. Int.* 2019, 1694695. doi:10.1155/2019/1694695

Kennedy, J. C., Alexander, I. J., and Hayes, K. C. (1982). Nerve supply of the human knee and its functional importance. *Am. J. Sports Med.* 10 (6), 329–335. doi:10.1177/036354658201000601

Kruse, L. M., Gray, B., and Wright, R. W. (2012). Rehabilitation after anterior cruciate ligament reconstruction: A systematic review. *J. Bone Jt. Surg. Am.* 94 (19), 1737–1748. doi:10.2106/jbjs.K.01246

Lee, S. J., Ren, Y., Kang, S. H., Geiger, F., and Zhang, L. Q. (2015). Pivoting neuromuscular control and proprioception in females and males. *Eur. J. Appl. Physiol.* 115 (4), 775–784. doi:10.1007/s00421-014-3062-z

Lentz, T. A., Zeppieri, G., Jr., Tillman, S. M., Indelicato, P. A., Moser, M. W., George, S. Z., et al. (2012). Return to preinjury sports participation following anterior cruciate ligament reconstruction: Contributions of demographic, knee impairment, and self-report measures. *J. Orthop. Sports Phys. Ther.* 42 (11), 893–901. doi:10.2519/jospt.2012.4077

Lepley, A. S., Pietrosimone, B., and Cormier, M. L. (2018). Quadriceps function, knee pain, and self-reported outcomes in patients with anterior cruciate ligament reconstruction. *J. Athl. Train.* 53 (4), 337–346. doi:10.4085/1062-6050-245-16

Leys, T., Salmon, L., Waller, A., Linklater, J., and Pinczewski, L. (2012). Clinical results and risk factors for reinjury 15 years after anterior cruciate ligament reconstruction: A prospective study of hamstring and patellar tendon grafts. *Am. J. Sports Med.* 40 (3), 595–605. doi:10.1177/0363546511430375

Li, L., Zhang, S., and Dobson, J. (2019). The contribution of small and large sensory afferents to postural control in patients with peripheral neuropathy. *J. Sport Health Sci.* 8 (3), 218–227. doi:10.1016/j.jshs.2018.09.010

Machado, A. S., da Silva, C. B., da Rocha, E. S., and Carpes, F. P. (2017). Effects of plantar foot sensitivity manipulation on postural control of young adult and elderly. *Rev. Bras. Reumatol. Engl. Ed.* 57 (1), 30–36. doi:10.1016/j.rbre.2016.03.007

Mao, D. W., Li, J. X., and Hong, Y. (2006). The duration and plantar pressure distribution during one-leg stance in Tai Chi exercise. *Clin. Biomech.* 21 (6), 640–645. doi:10.1016/j.clinbiomech.2006.01.008

Muaidi, Q. I., Nicholson, L. L., Refshauge, K. M., Adams, R. D., and Roe, J. P. (2009). Effect of anterior cruciate ligament injury and reconstruction on proprioceptive acuity of knee rotation in the transverse plane. *Am. J. Sports Med.* 37 (8), 1618–1626. doi:10.1177/0363546509332429

Myer, G. D., Schmitt, L. C., Brent, J. L., Ford, K. R., Barber Foss, K. D., Scherer, B. J., et al. (2011). Utilization of modified NFL combine testing to identify functional deficits in athletes following ACL reconstruction. *J. Orthop. Sports Phys. Ther.* 41 (6), 377–387. doi:10.2519/jospt.2011.3547

Noyes, F. R., Jetter, A. W., Grood, E. S., Harms, S. P., Gardner, E. J., and Levy, M. S. (2015). Anterior cruciate ligament function in providing rotational stability assessed by medial and lateral tibiofemoral compartment translations and subluxations. *Am. J. Sports Med.* 43 (3), 683–692. doi:10.1177/0363546514561746

Paterno, M. V., Schmitt, L. C., Ford, K. R., Rauh, M. J., Myer, G. D., Huang, B., et al. (2010). Biomechanical measures during landing and postural stability predict second anterior cruciate ligament injury after anterior cruciate ligament reconstruction and return to sport. *Am. J. Sports Med.* 38 (10), 1968–1978. doi:10.1177/0363546510376053

Pijnappels, M., van der Burg, P. J., Reeves, N. D., and van Dieen, J. H. (2008). Identification of elderly fallers by muscle strength measures. *Eur. J. Appl. Physiol.* 102 (5), 585–592. doi:10.1007/s00421-007-0613-6

Reider, B., Arcand, M. A., Diehl, L. H., Mroczek, K., Abulencia, A., Stroud, C. C., et al. (2003). Proprioception of the knee before and after anterior cruciate ligament reconstruction. *Arthroscopy* 19 (1), 2–12. doi:10.1053/jars.2003.50006

Roijezon, U., Clark, N. C., and Treleaven, J. (2015). Proprioception in musculoskeletal rehabilitation. Part 1: Basic science and principles of assessment and clinical interventions. *Man. Ther.* 20 (3), 368–377. doi:10.1016/j.math.2015.01.008

Roth, R., Donath, L., Kurz, E., Zahner, L., and Faude, O. (2017). Absolute and relative reliability of isokinetic and isometric trunk strength testing using the IsoMed-2000 dynamometer. *Phys. Ther. Sport* 24, 26–31. doi:10.1016/j.ptsp.2016.11.005

Song, Q., Zhang, X., Mao, M., Sun, W., Zhang, C., Chen, Y., et al. (2021). Relationship of proprioception, cutaneous sensitivity, and muscle strength with the balance control among older adults. *J. Sport Health Sci.* 10 (5), 585–593. doi:10.1016/j.jshs.2021.07.005

Sun, W., Song, Q., Yu, B., Zhang, C., and Mao, D. (2015). Test-retest reliability of a new device for assessing ankle joint threshold to detect passive movement in healthy adults. *J. Sports Sci.* 33 (16), 1667–1674. doi:10.1080/02640414.2014.1003589

Thomee, R., Kaplan, Y., Kvist, J., Myklebust, G., Risberg, M. A., Theisen, D., et al. (2011). Muscle strength and hop performance criteria prior to return to sports after ACL reconstruction. *Knee Surg. Sports Traumatol. Arthrosc.* 19 (11), 1798–1805. doi:10.1007/s00167-011-1669-8

Unver, B., and Akbas, E. (2018). Effects of plantar sensitivity on balance and mobility in community-dwelling older adults: A Turkish study. *Australas. J. Ageing* 37 (4), 288–292. doi:10.1111/ajag.12558

Xergia, S. A., Pappas, E., and Georgoulis, A. D. (2015). Association of the single-limb hop test with isokinetic, kinematic, and kinetic asymmetries in patients after anterior cruciate ligament reconstruction. *Sports Health* 7 (3), 217–223. doi:10.1177/1941738114529532

frontiers | Frontiers in Physiology

TYPE Original Research
PUBLISHED 09 January 2023
DOI 10.3389/fphys.2022.1064240

OPEN ACCESS

EDITED BY
Kwong Ming (KM) Tse,
Swinburne University of Technology, Australia

REVIEWED BY
Fábio Juner Lanferdini,
Universidade Federal de Santa Maria, Brazil
Luke A. Donnan,
Charles Sturt University, Australia

*CORRESPONDENCE
Xianyi Zhang,
zhangxianyi@mail.sysu.edu.cn

SPECIALTY SECTION
This article was submitted to Exercise Physiology,
a section of the journal
Frontiers in Physiology

RECEIVED 08 October 2022
ACCEPTED 23 December 2022
PUBLISHED 09 January 2023

CITATION
Zhang X and Vanwanseele B (2023), Immediate effects of forefoot wedges on multi-segment foot kinematics during jogging in recreational runners with a symptomatic pronated foot.
Front. Physiol. 13:1064240.
doi: 10.3389/fphys.2022.1064240

Immediate effects of forefoot wedges on multi-segment foot kinematics during jogging in recreational runners with a symptomatic pronated foot

Xianyi Zhang[1,2]* and Benedicte Vanwanseele[3]

[1]School of Biomedical Engineering, Shenzhen Campus of Sun Yat-sen University, Shenzhen, China, [2]Key Laboratory of Sensing Technology and Biomedical Instrument of Guangdong Province, School of Biomedical Engineering, Sun Yat-sen University, Guangzhou, China, [3]Department of Movement Sciences, KU Leuven, Leuven, Belgium

Background: Foot orthoses (FOs) have been used to alter lower limb kinematics and kinetics in pronated feet. A clear relationship between FOs' features, e.g., the amount of wedging and support, and the corresponding biomechanical responses is vital for the design and prescription of FOs. In this study, we sought to determine if changing the level of the forefoot wedge would cause a linear response in the multi-segment foot kinematics during jogging, and if this effect would be enhanced by an arch support.

Methods: Ten pairs of 3D printed FOs with five levels of forefoot wedges and two levels of arch supports were tested on 12 recreational runners with a symptomatic pronated foot. Multi-segment foot kinematic data during jogging was measured using the Oxford Foot Model. Two-way ANOVAs were performed to examine the main effect of the forefoot wedge and arch support, as well as their interaction on peak joint angles. Statistical parametric mapping and paired-t tests were used to identify differences in the foot kinematic traces and the joint range of motion (ROM) between each FO and the control, respectively.

Results: Linear main effects for the forefoot wedge level were found in the forefoot peak dorsiflexion, eversion and rearfoot peak dorsiflexion of jogging. FOs with a medial forefoot wedge caused an average of 2.5° reduction of the forefoot peak abduction during jogging. Furthermore, forefoot wedges showed an opposite effect on the sagittal ROM of the forefoot and rearfoot. Adding an arch support did not improve the kinematic performance of a forefoot wedge during jogging.

Conclusion: This study highlights a linear dose-response effect of a forefoot wedge on forefoot kinematics during jogging, and suggests using a medial forefoot wedge as an anti-pronator component for controlling forefoot motion of a pronated foot.

KEYWORDS

foot orthoses, running biomechanics, multi-segment foot kinematics, pronated foot, dose-response effect

1 Introduction

Foot orthoses (FOs) have been used as a conservative way to manage pain and reduce the risk of overuse injuries in individuals with a pronated foot posture (Banwell et al., 2014; Desmyttere et al., 2021). FOs designed for pronated feet target to restore their normal foot dynamic function, which can be evaluated *via* joint kinematics, kinetics and muscle activities during walking and running (Cherni et al., 2021; Hajizadeh et al., 2022). These corrective effects are usually achieved *via* appropriate configurations of orthotic components (Desmyttere et al., 2021). Thus, a clear relationship between the features of FO components and the corresponding biomechanical responses, i.e., the dose-response effect, is vital for the design and prescription of FOs.

Wedged FO components and arch supports have been used to reduce foot pronation and abnormal joint moments (Nawoczenski and Ludewig, 2004; Braga et al., 2019). Currently, the dose-response relationship between each FO component and foot biomechanics is poorly understood. Most FO studies only examine very limited variations of FOs, normally 1–2 types (Barn et al., 2014; Cherni et al., 2021; Hajizadeh et al., 2022). Only a few studies examined multiple levels of rearfoot wedges and arch supports to determine their dose-response effect on lower limb kinematics during gait. For rearfoot wedges, Telfer et al. (2013) reported a linear effect of rearfoot wedge on the peak and mean rearfoot eversions. For arch supports, Wahmkow et al. (2017) examined four different arch support heights during walking, but found there was no systematic effect on foot kinematics. Studies on the effects of forefoot wedges on kinematics were relatively limited (Nawoczenski and Ludewig, 2004).

Controlling excessive foot pronation involves reducing forefoot abduction, forefoot dorsiflexion and rearfoot eversion (Neville et al., 2016). Currently, most FOs focused on reducing the rearfoot eversion (Banwell et al., 2014; Mo et al., 2019), and consequently a majority of FO studies adopt the rearfoot wedge as the main anti-pronator FO component (Telfer et al., 2013; Cherni et al., 2021; Desmyttere et al., 2021). By comparing pronated feet with and without symptoms, previous studies suggested that the rearfoot peak eversion was comparable between two groups and thus questioned the effectiveness of reducing the rearfoot eversion to manage overuse injuries (Levinger et al., 2010; Kerr et al., 2019; Zhang et al., 2019). Alternatively, it was suggested that excessive forefoot peak abduction, which occurred during propulsion, might be associated with the injury risk in pronated feet, and that regulating forefoot transverse motion could benefit symptomatic pronated feet. The body weight transfers to the forefoot after heel-off of gait stance phase, during which the forefoot orthotic component would theoretically be more effective in altering forefoot kinematics than the rearfoot component (Hsu et al., 2014).

To improve the biomechanical performance of FOs, adding an arch support to other types of FOs has been suggested by several studies (Nakajima et al., 2009; Zhang et al., 2017). It has been shown that the additional use of an arch support improved gait stability and comfort of a heel lift FO (Zhang et al., 2017), and further reduced knee adduction moment of a laterally wedged FO (Nakajima et al., 2009). Using an arch support alone has also been shown to redistribute plantar pressure and reduces impact loading during running (Wang et al., 2020; Peng et al., 2021), while its effect on joint kinematics during running is inconsistent across literature (Wahmkow et al., 2017; Hajizadeh et al., 2020). For a forefoot wedge FO, it remains unclear if changing the arch support parameters would enhance its impact on joint kinematics or not.

Therefore, the primary aim of this study was to examine the dose-response effect of FOs with a forefoot wedge on multi-segment foot kinematics during jogging in recreational runners with a symptomatic pronated foot. We hypothesized a dose-response relationship between forefoot wedges and forefoot kinematics. The secondary aim of this study was to examine if a higher arch support would enhance the biomechanical effect of a forefoot wedge. The insights gained from this work would provide scientific evidence for foot orthoses prescription to manage excessive foot pronation and prevent running-related overuse injuries.

2 Methods

This study was approved by the Medical Ethics Committee of KU Leuven and all participants gave informed consent. The experimental setting is shown in Figure 1.

2.1 Participants

This study recruited 12 recreational runners (5 females and seven males) with a minimal running volume of 10 km per week. These runners also participated in different trials of our previous study, which examined the effect of FOs on the plantar pressure variables during overground running (Zhang et al., 2022a). They had an average age of 25.8 ± 5.5 years, weight of 72.5 ± 9.0 kg, height of 1.79 ± 0.08 m, and training volume of 19.9 ± 7.9 km per week. All participants were diagnosed with some form of lower-leg overuse injuries in the last 6 months before testing, including Achilles tendinopathy, plantar fasciitis, medial tibial stress syndrome, and general knee pain. They were pain free at the time of data acquisition. The most symptomatic leg, which was based on subjective report of one's injury history, was chosen for data collection. Their foot postures were examined *via* foot posture index (FPI), with a FPI value equal or larger than six being classified as a pronated foot posture (Redmond et al., 2008). The average FPI score of all participants was 7.9 ± 1.4.

2.2 Foot orthoses

The FO features were the same as described in our previous study (Zhang et al., 2022a). As shown in Figure 2, ten FOs varied in the forefoot wedges (5 levels: MF4, MF2, NF0, LF2 and LF4 with MF stands for a medial wedge, NF stands for neutral forefoot, and LF stands for a lateral wedge) and the arch supports (2 levels: A20 and A24). The abbreviations of FOs with an arch support height of 20 mm are MF4A20, MF2A20, NF0A20, LF2A20, LF4A20, and those with an arch support height of 24 mm are MF4A24, MF2A24, NF0A24, LF2A24 and LF4A24. All FOs were inserted into a standard neutral running shoe for testing.

2.3 Equipment and procedure

A motion capture system (Vicon MX, Vicon Motion System Ltd., Oxford, England) with 13 cameras was used at a sampling frequency of 150 Hz. Reflective markers were attached to the skin according to the lower limb Plug-in gait model (Kadaba et al.,

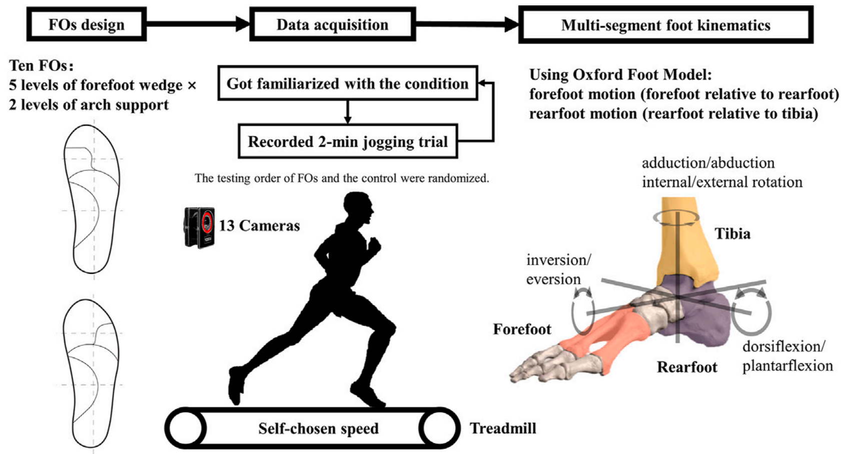

FIGURE 1
The experimental setting.

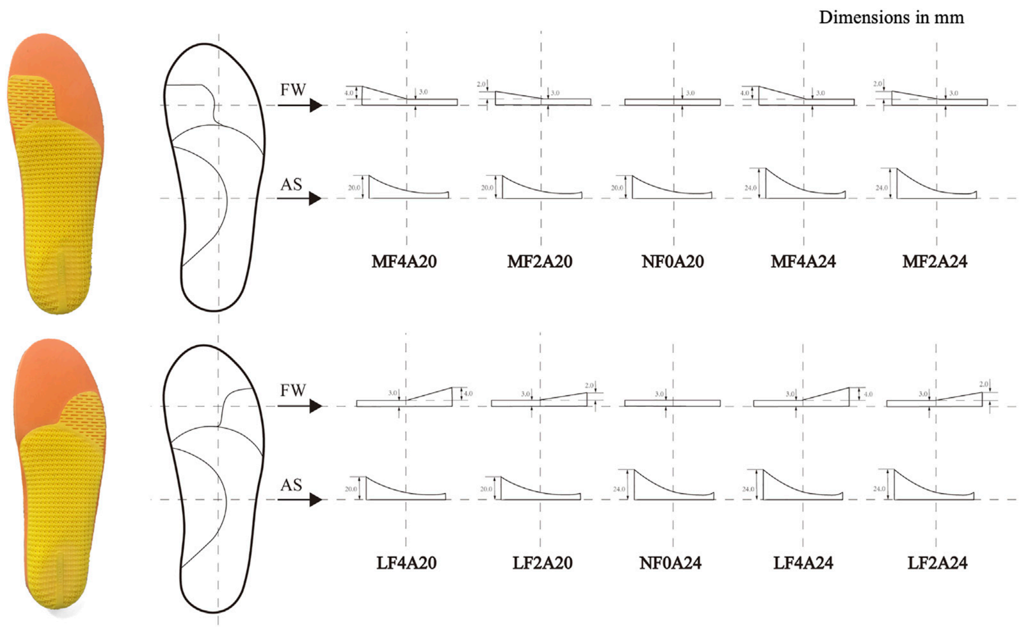

FIGURE 2
Bottom view and dimensions of ten FOs with abbreviations. FW: forefoot wedge, AS: arch support. MF4, MF2, NF0, LF2, LF4 stand for a forefoot wedge with 4 mm medial, 2 mm medial, 0 mm, 2 mm lateral, and 4 mm lateral wedge, respectively; A20 and A24 stand for an arch support with a height of 20 mm and 24 mm, respectively. The base layer in yellow was composed of a conventional three-quarter orthosis with or without a forefoot wedge. Foot orthosis was composed of a 3D printed base layer and flat full-length top layers.

1990) combined with the left/right Oxford Foot Model (Stebbins et al., 2006). Participants wore testing shoes (a neutral shoe model with a uniform EVA midsole) and socks with holes (within 25 mm diameter), and markers attached to the skin *via* a magnetic base through these holes. This allowed the foot marker locations to be consistent between all testing conditions. An instrumented treadmill with integrated force plates (Motekforce Link, Amsterdam, the Netherland) was used to measure the ground reaction forces (GRFs) at a sampling frequency of 900 Hz.

Before the jogging measurements, a static trial of barefoot standing was recorded for each participant. Participants jogged on the treadmill at a self-chosen speed, and this speed was kept constant in all test conditions for the same participant. For each condition, the participant walked and jogged on the treadmill for about 5 min to get familiarized with the condition tested, then a 2-min jogging trial was recorded. The average self-chosen jogging speed was 8.4 ± 0.8 km/h. The foot orthoses were used for both feet. Running trials were repeated for 11 conditions, i.e., shod only (the control) and ten FO

TABLE 1 Results of tests of within-subject effects from two-way ANOVAs.

Parameter	Effect	F	*p*-value	Best contrast
Forefoot peak dorsiflexion	Arch support	0.419	0.531	-
	Forefoot wedge	2.689	0.043	Linear (p = .001)
	Arch support * Forefoot wedge	1.099	0.369	-
Forefoot peak abduction	Arch support	3.035	0.109	-
	Forefoot wedge	1.456	0.232	-
	Arch support * Forefoot wedge	1.125	0.357	-
Forefoot peak eversion	Arch support	0.418	0.531	-
	Forefoot wedge	6.803	<.001	Linear (p = .001)
	Arch support * Forefoot wedge	1.406	0.248	-
Rearfoot peak dorsiflexion	Arch support	2.661	0.131	
	Forefoot wedge	7.891	<.001	Linear (p = .008)
	Arch support * Forefoot wedge	1.048	0.394	-
Rearfoot peak external rotation	Arch support	1.92	0.193	-
	Forefoot wedge	0.811	0.525	-
	Arch support * Forefoot wedge	1.657	0.177	-
Rearfoot peak eversion	Arch support	0.012	0.915	-
	Forefoot wedge	0.653	0.628	-
	Arch support * Forefoot wedge	1.106	0.366	-

conditions. The running strike pattern was visually checked in the Vicon Nexus software, and a rearfoot strike pattern was identified with the center of pressure at foot contact locating at the heel region. All participants adopted a rearfoot strike pattern during all trials. The testing order of FOs and the control was randomized for each participant.

2.4 Data analysis and statistics

Kinematic data was processed in Vicon Nexus software (Vicon MX, Vicon Motion System Ltd., Oxford, England) and low pass filtered at 15 Hz using a fourth order Butterworth filter in MATLAB (The Mathworks Inc., MA, United States). For each trial, the vertical GRF was used to detect the stance phase with a threshold of 50 N. Lower limb segments were defined as previously reported (Stebbins et al., 2006). The following kinematic variables were determined: the forefoot relative to rearfoot: dorsiflexion/plantarflexion, adduction/abduction and inversion/eversion in the sagittal, transverse and frontal planes, respectively; and the rearfoot relative to tibia: dorsiflexion/plantarflexion, internal/external rotation and inversion/eversion in the sagittal, transverse and frontal planes, respectively.

Mean kinematic values and the range of joint motion (ROM) of at least five consecutive steps of each condition of each participant were used for further statistical analysis. Two-way ANOVAs were performed to determine the main effect for the forefoot wedge, arch support, and any interaction effects. Where a significant effect was found, linear contrasts were tested to determine if this effect was linear. (Telfer et al., 2013). For this analysis, all variables were relative to the control. The data of joint ROM were normally distributed. To examine the difference in joint ROM between each FO and the control, a paired *t*-test between them was performed. To compare the time series of forefoot kinematics during the stance phase between each FO and the control, a one-dimensional statistical parametric mapping (SPM) was performed (open-source: www.spm1d.org) in Matlab. *p*-values less than 0.05 were considered statistically significant.

3 Results

3.1 Dose-response effects

Results of two-way ANOVAs are presented in Table 1. Linear main effects for the forefoot wedge level were found in the forefoot peak dorsiflexion, eversion and rearfoot peak dorsiflexion of jogging. In contrast, there was no significant main effect for the arch support level. Moreover, no interaction effects between the forefoot wedge and arch support were found. Figure 3 further illustrated the trends of peak kinematic changes by each FO in relative to the control. A larger medial forefoot wedge linearly reduced the forefoot peak dorsiflexion and eversion but increased the rearfoot peak dorsiflexion.

3.2 Joint range of motion

Table 2 shows that the forefoot sagittal ROM was decreased by all FOs, while the rearfoot sagittal ROM was increased in

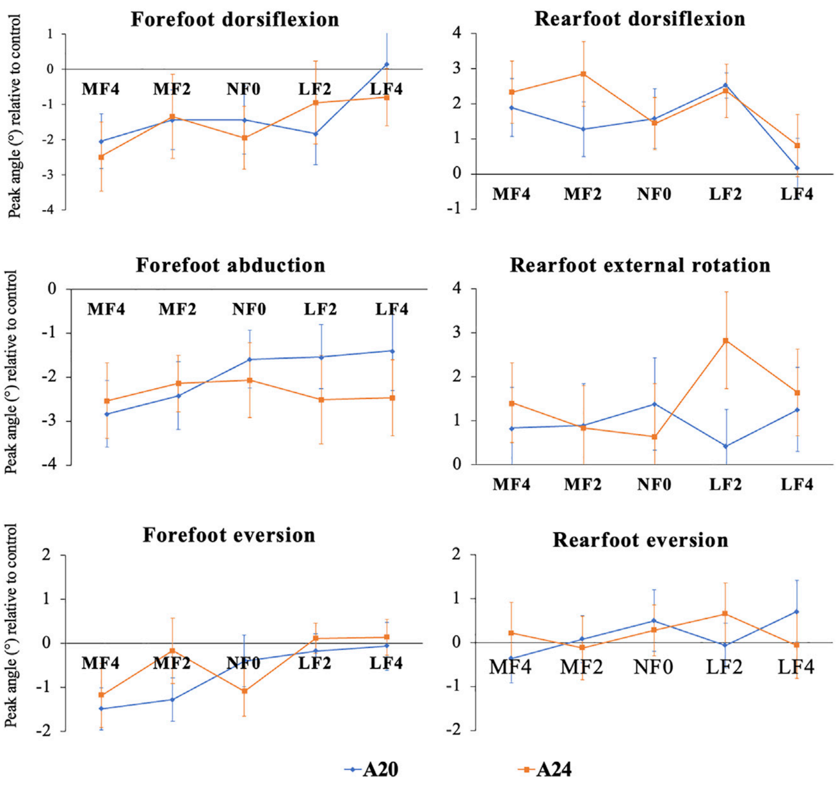

FIGURE 3
Average peak joint angles (± standard error) during the stance phase of jogging. A20 and A24: Arch support height of 20 mm and 24 mm, respectively; MF4, MF2, NF0, LF2 and LF4: forefoot component with 4 mm medial wedge, 2 mm medial wedge, none wedge, 2 mm lateral wedge and 4 mm lateral wedge, respectively. Blue line represents FOs with A20 and orange line represents FOs with A24.

TABLE 2 Comparison of joint ROM (mean ± SD) between FOs and the control during the stance phase of jogging.

Conditions	ROM of forefoot motion (°)			ROM of rearfoot motion (°)		
	Sagittal plane	Transverse plane	Frontal plane	Sagittal plane	Transverse plane	Frontal plane
MF4A20	7.6 ± 1.8 *	2.8 ± 1.2 *	4.1 ± 1.4	22.5 ± 4.3 *	21.2 ± 5.9	18.3 ± 6
MF2A20	7.6 ± 2.2	2.9 ± 1.1 *	4.1 ± 1.8	22.2 ± 4.8	21.5 ± 5.4	18 ± 5.9
NF0A20	7.4 ± 1.9 *	2.7 ± 1.6 *	4.3 ± 1.8	22.5 ± 4.7 *	22.1 ± 6.2	18 ± 5.8
LF2A20	7.4 ± 2.2 *	2.6 ± 1.3 *	3.9 ± 1.7 *	22.1 ± 5.2 *	21.1 ± 5.3	18.3 ± 6
LF4A20	7.7 ± 2.5 *	2.9 ± 1.2 *	4.2 ± 1.8	21.1 ± 4	20.8 ± 5	17.6 ± 6
MF4A24	7.8 ± 1.8 *	2.7 ± 1.3 *	4.8 ± 1.5	22.6 ± 4 *	22.2 ± 4.7	19 ± 5.9 *
MF2A24	8.6 ± 3.7	3.1 ± 2.3	4.7 ± 2.4	23 ± 5.6 *	20.6 ± 5.9	17.5 ± 5.9
NF0A24	7.2 ± 1.9 *	3 ± 1.3	4.5 ± 2	22.9 ± 4.8 *	20.9 ± 5.4	17.8 ± 5.9
LF2A24	8.3 ± 2.1	2.8 ± 1.4 *	4 ± 1.8	22.8 ± 4.4 *	22.3 ± 6	18.3 ± 6.7
LF4A24	8 ± 2.1	2.5 ± 1.4 *	4.1 ± 1.7 *	21.9 ± 4.8	20.7 ± 4.8	17.2 ± 5.2
control	9.3 ± 3.2	3.6 ± 1.2	5.1 ± 2.8	20.7 ± 3.6	20.8 ± 4.2	17.1 ± 5.8

ROM: range of motion. *$p < .05$, vs. control.

comparable degrees. Most FOs reduced the forefoot transverse ROM, but the absolute change was small in value. In contrast, the transverse and frontal rearfoot ROM were not altered by FOs.

3.3 Kinematic patterns

Figure 4 shows the average kinematic traces and the SPM results comparing each FO with A20 and the control. The

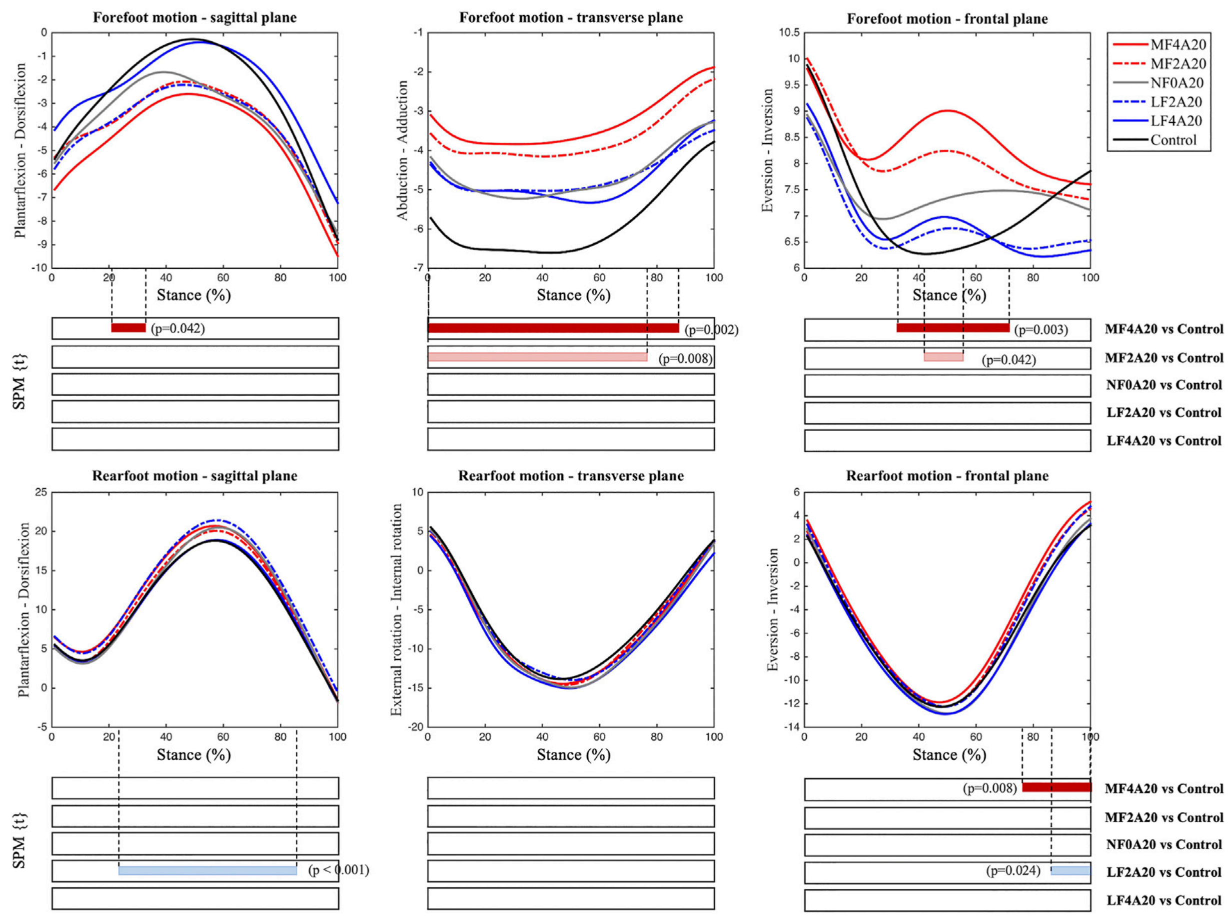

FIGURE 4
Average foot kinematic traces (°) of different FOs with an arch support height of 20 mm and the control during the stance phase of jogging. Shaded bars indicate significant differences ($p < 0.05$) between each FO and the control using SPM.

kinematic patterns using FOs with A20 were comparable with those with A24 (see Supplementary Figure S1). Medial forefoot wedges altered the forefoot motions of three planes, reducing forefoot dorsiflexion, abduction and eversion. Compared to the control, LF2A20 significantly increased the rearfoot dorsiflexion. MF4A20 and LF2A20 reduced the rearfoot eversion during the late stance.

4 Discussion

The purpose of the current study was to examine the immediate effect of FOs with forefoot wedges on multi-segment foot kinematics during jogging in symptomatic pronated feet. As expected, FOs with a forefoot wedge had a significant influence on the forefoot motion, with a medial wedge reducing forefoot peak dorsiflexion, abduction and eversion during jogging. In contrary to our hypothesis, changing the arch support height neither enhanced nor weakened the impact of forefoot wedges on foot kinematics. These findings may provide insights for FOs mechanisms and references for future FOs design and prescription.

Similar to the relationship between rearfoot wedges and rearfoot eversion (Telfer et al., 2013), our results found a linear dose-response effect of forefoot wedges on forefoot eversion during jogging. Less forefoot eversion with a larger medial forefoot wedge agreed with the findings of a previous study on walking (Hsu et al., 2014), and it may also help explain why the COP was shifted more laterally with a medial forefoot wedge (Zhang et al., 2022a). Furthermore, a greater level of a medial forefoot wedge decreased the forefoot peak dorsiflexion but increased the rearfoot peak dorsiflexion, indicating a compensatory motion control mechanism of FOs on different segments of the lower limb kinetic chain. This mechanism was further confirmed by the opposite effects of current FOs on the forefoot and rearfoot ROM in the sagittal plane (Table 2). These findings are aligned with the Howard Dananberg's Sagittal Plane Facilitation Theory (Dananberg, 1986), which suggests that restriction of sagittal plane motion at one site requires compensation by another in the chain. These kinematic alterations in a pronated foot of this study were closer to normal kinematic features of a healthy neutral foot (Hosl et al., 2014). Findings on these dose-response effects of FOs could provide reference values for FO components' parameters to reach desired kinematic alterations, contributing to better FO customization to satisfy individual biomechanical needs.

As aforementioned, reducing the forefoot peak abduction may improve clinical outcomes for symptomatic pronated feet (Levinger et al., 2010; Kerr et al., 2019; Zhang et al., 2019). However, there is no consensus on which FO component can effectively control forefoot abduction (Barn et al., 2014; Garbalosa et al., 2015). Changing FO stiffness with a carbon fiber plate had little effect on forefoot kinematics (Rao et al., 2010; Desmyttere et al., 2021). Both medial and lateral rearfoot wedges failed to reduce the forefoot peak abduction (Telfer et al., 2013). The current study showed that a medial forefoot wedge caused an average reduction of 2.5 on the forefoot peak abduction. The amount of reduction was comparable to other joint angular changes caused by FOs (Desmyttere et al., 2018; Simonsen et al., 2021). Although the clinical significance of this reduction is unclear, it is more than 70% of the mean difference in the forefoot peak abduction between a symptomatic and asymptomatic pronated foot (Zhang et al., 2022b). Future prospective studies are required to investigate the potential clinical effect of this kinematic alteration on reducing complaints in a pronated foot population.

In agreement with our results, a recent study, which used an artificial neural network to predict the deformation of the FO, found that forefoot abduction affected the deformation in the forefoot part of the FO after heel-off of walking in flatfeet (Hajizadeh et al., 2022). However, systematically altering the forefoot peak abduction by changing the level of a forefoot wedge was not supported by the current study. This is not surprising, as the inclination of a medial/lateral forefoot wedge lies in the frontal plane, which only indirectly can manipulate foot motion in the transverse plane motion. An orthotic component in the transverse plane has been adopted in the ankle-foot orthoses to reduce forefoot abduction (Neville et al., 2016). But such component is difficult to be fitted in conventional footwear, which limits its application to FOs. Alternatively, future investigations may implement such modifications in the design of shoe last, which determines the inner space of a shoe, to systematically alter foot motions in the transverse plane.

In contrary to the positive biomechanical effects of adding an arch support to other types of FOs (Nakajima et al., 2009; Zhang et al., 2017), there was no interaction effect between an arch support and a forefoot wedge in this study. It should be noted that former studies evaluated the kinetic responses to FOs, such as the plantar pressure and knee adduction moment, while this study measured multi-segment foot kinematics. Theoretically, the arch support functions to plantarflex the first ray to increase 1st metatarsophalangeal joint (MTPJ), while the medial forefoot wedge functions to dorsiflex the 1st MTPJ. As such, this result is not surprising. Furthermore, using an arch support to modulate foot kinematics in a desirable manner is challenging. By examining prefabricated arch supports of various height, Wahmkow et al. (2017) also did not find a clear systematic effect of the arch support height on foot kinematics. The features of the longitudinal arch (LA), including its static architecture and dynamic deformation of gait, may play an important role in one's biomechanical responses to an arch support. The LA is passively modulated by ligamentous structures and actively modulated by intrinsic and extrinsic foot muscles (Farris et al., 2020). As such, individual characteristics in foot structures may provide additional information to help understand the motion control mechanisms of an arch support in the future.

The results from this study provide further evidence to support the use of FOs in controlling foot pronation during jogging. There were, however, some limitations that should be considered. Firstly, the foot kinematic model relied on skin-mounted markers and was thus susceptible to skin movement artefact. Secondly, a treadmill was used to ensure that each participant ran at a constant jogging speed across all conditions, but most participants habitually ran over ground. Thirdly, the design of FOs in the current study did not consider the 3D foot plantar shape of each participant. Fourthly, this study was conducted on a small sample size and did not consider the gender effects on the results. It should also be noted that the symptoms of participants may not be necessarily due to biomechanical features of a pronated foot. Further prospective studies on a larger sample size is required. Finally, in order to test all FOs in 1 day without fatiguing the participants, they were only given a few minutes to warm up with each FO before testing until they felt comfortable with the testing FO. The FO testing order was randomized, and the observed running strike pattern was consistent across all conditions. Nevertheless, kinematic adaptations may occur with a long-time use of FOs, as it has been documented that muscular adaptations occurred after an 8-week intervention of FOs (Jung et al., 2011).

5 Conclusion

Our results suggested a linear dose-response effect of forefoot wedges on the forefoot peak dorsiflexion, peak eversion and rearfoot peak dorsiflexion during jogging in symptomatic individuals with a pronated foot posture, providing a reference for future FO design and prescription. Regarding foot pronation control, a medial forefoot wedge could be used as an anti-pronator component for restraining forefoot abduction during jogging, with 29%–43% reduction on the peak forefoot abduction. Whether this reduction is of clinical significance still requires further investigation. Furthermore, adding an arch support did not alter the kinematic performance of forefoot wedges, and future studies should consider individual differences in the LA features. This study highlights the multi-segment foot kinematic responses to different configurations of FO components. Understanding these dose-response relationships can further allow a more personalized FO design to better improve lower limb biomechanics for individuals with abnormal foot postures.

Practical implications:

1) FO with a medial forefoot wedge could reduce the peak forefoot abduction in symptomatic pronated feet during jogging.
2) This study found a linear dose-response effect of a forefoot wedge on the forefoot peak dorsiflexion, eversion and rearfoot peak dorsiflexion of jogging.
3) Adding an arch support did not alter the effects of a forefoot wedge on multi-segment foot kinematics.

Data availability statement

The original contributions presented in the study are included in the article/Supplementary Material, further inquiries can be directed to the corresponding author.

Ethics statement

The studies involving human participants were reviewed and approved by Medical Ethics Committee of KU Leuven. The patients/participants provided their written informed consent to participate in this study.

Author contributions

XZ performed data collection, data analysis and writing. BV conceived the study and contributed to the discussion of the results. All authors read and approved the final manuscript.

Funding

This work was supported by the National Natural Science Foundation of China (No. 32101051) and Shenzhen Science and Technology Program (No. RCBS20210706092410025).

Acknowledgments

The authors thank RS Print powered by Materialise NV for providing 3D printed foot orthoses.

Conflict of interest

The authors declare that the research was conducted in the absence of any commercial or financial relationships that could be construed as a potential conflict of interest.

Publisher's note

Supplementary material

The Supplementary Material for this article can be found online at: https://www.frontiersin.org/articles/10.3389/fphys.2022.1064240/full#supplementary-material

References

Banwell, H. A., Mackintosh, S., and Thewlis, D. (2014). Foot orthoses for adults with flexible pes planus: A systematic review. *J. Foot Ankle Res.* 7, 23. doi:10.1186/1757-1146-7-23

Barn, R., Brandon, M., Rafferty, D., Sturrock, R. D., Steultjens, M., Turner, D. E., et al. (2014). Kinematic, kinetic and electromyographic response to customized foot orthoses in patients with tibialis posterior tenosynovitis, pes plano valgus and rheumatoid arthritis. *Rheumatol. Oxf.* 53, 123–130. doi:10.1093/rheumatology/ket337

Braga, U. M., Mendonça, L. D., Mascarenhas, R. O., Alves, C. O. A., Filho, R. G. T., and Resende, R. A. (2019). Effects of medially wedged insoles on the biomechanics of the lower limbs of runners with excessive foot pronation and foot varus alignment. *Gait Posture* 74, 242–249. doi:10.1016/j.gaitpost.2019.09.023

Cherni, Y., Desmyttere, G., Hajizadeh, M., Bleau, J., Mercier, C., and Begon, M. (2021). Effect of 3D printed foot orthoses stiffness on muscle activity and plantar pressures in individuals with flexible flatfeet: A statistical non-parametric mapping study. *Clin. Biomech. (Bristol, Avon)* 92, 105553. doi:10.1016/j.clinbiomech.2021.105553

Dananberg, H. J. (1986). Functional hallux limitus and its relationship to gait efficiency. *J. Am. Podiatr. Med. Assoc.* 76, 648–652. doi:10.7547/87507315-76-11-648

Desmyttere, G., Hajizadeh, M., Bleau, J., and Begon, M. (2018). Effect of foot orthosis design on lower limb joint kinematics and kinetics during walking in flexible pes planovalgus: A systematic review and meta-analysis. *Clin. Biomech. (Bristol, Avon)* 59, 117–129. doi:10.1016/j.clinbiomech.2018.09.018

Desmyttere, G., Hajizadeh, M., Bleau, J., Leteneur, S., and Begon, M. (2021). Anti-pronator components are essential to effectively alter lower-limb kinematics and kinetics in individuals with flexible flatfeet. *Clin. Biomech. (Bristol, Avon)* 86, 105390. doi:10.1016/j.clinbiomech.2021.105390

Farris, D. J., Birch, J., and Kelly, L. (2020). Foot stiffening during the push-off phase of human walking is linked to active muscle contraction, and not the windlass mechanism. *J. R. Soc. Interface* 17, 20200208. doi:10.1098/rsif.2020.0208

Garbalosa, J. C., Elliott, B., Feinn, R., and Wedge, R. (2015). The effect of orthotics on intersegmental foot kinematics and the EMG activity of select lower leg muscles. *Foot (Edinb)* 25, 206–214. doi:10.1016/j.foot.2015.07.005

Hajizadeh, M., Desmyttere, G., Carmona, J. P., Bleau, J., and Begon, M. (2020). Can foot orthoses impose different gait features based on geometrical design in healthy subjects? A systematic review and meta-analysis. *Foot (Edinb)* 42, 101646. doi:10.1016/j.foot.2019.10.001

Hajizadeh, M., Desmyttere, G., Ménard, A. L., Bleau, J., and Begon, M. (2022). Understanding the role of foot biomechanics on regional foot orthosis deformation in flatfoot individuals during walking. *Gait Posture* 91, 117–125. doi:10.1016/j.gaitpost.2021.10.015

Hosl, M., Bohm, H., Multerer, C., and Doderlein, L. (2014). Does excessive flatfoot deformity affect function? A comparison between symptomatic and asymptomatic flatfeet using the Oxford foot model. *Gait Posture* 39, 23–28. doi:10.1016/j.gaitpost.2013.05.017

Hsu, W. H., Lewis, C. L., Monaghan, G. M., Saltzman, E., Hamill, J., and Holt, K. G. (2014). Orthoses posted in both the forefoot and rearfoot reduce moments and angular impulses on lower extremity joints during walking. *J. Biomech.* 47, 2618–2625. doi:10.1016/j.jbiomech.2014.05.021

Jung, D. Y., Koh, E. K., and Kwon, O. Y. (2011). Effect of foot orthoses and short-foot exercise on the cross-sectional area of the abductor hallucis muscle in subjects with pes planus: A randomized controlled trial. *J. Back Musculoskelet. Rehabil.* 24, 225–231. doi:10.3233/BMR-2011-0299

Kadaba, M. P., Ramakrishnan, H. K., and Wootten, M. E. (1990). Measurement of lower extremity kinematics during level walking. *J. Orthop. Res.* 8, 383–392. doi:10.1002/jor.1100080310

Kerr, C. M., Zavatsky, A. B., Theologis, T., and Stebbins, J. (2019). Kinematic differences between neutral and flat feet with and without symptoms as measured by the Oxford foot model. *Gait Posture* 67, 213–218. doi:10.1016/j.gaitpost.2018.10.015

Levinger, P., Murley, G. S., Barton, C. J., Cotchett, M. P., Mcsweeney, S. R., and Menz, H. B. (2010). A comparison of foot kinematics in people with normal- and flat-arched feet using the Oxford Foot Model. *Gait Posture* 32, 519–523. doi:10.1016/j.gaitpost.2010.07.013

Mo, S., Leung, S. H. S., Chan, Z. Y. S., Sze, L. K. Y., Mok, K. M., Yung, P. S. H., et al. (2019). The biomechanical difference between running with traditional and 3D printed orthoses. *J. Sports Sci.* 37, 2191–2197. doi:10.1080/02640414.2019.1626069

Nakajima, K., Kakihana, W., Nakagawa, T., Mitomi, H., Hikita, A., Suzuki, R., et al. (2009). Addition of an arch support improves the biomechanical effect of a laterally wedged insole. *Gait Posture* 29, 208–213. doi:10.1016/j.gaitpost.2008.08.007

Nawoczenski, D. A., and Ludewig, P. M. (2004). The effect of forefoot and arch posting orthotic designs on first metatarsophalangeal joint kinematics during gait. *J. Orthop. Sports Phys. Ther.* 34, 317–327. doi:10.2519/jospt.2004.34.6.317

Neville, C., Bucklin, M., Ordway, N., and Lemley, F. (2016). An ankle-foot orthosis with a lateral extension reduces forefoot abduction in subjects with stage II posterior tibial tendon dysfunction. *J. Orthop. Sports Phys. Ther.* 46, 26–33. doi:10.2519/jospt.2016.5618

Peng, Y., Wong, D. W., Chen, T. L., Wang, Y., Zhang, G., Yan, F., et al. (2021). Influence of arch support heights on the internal foot mechanics of flatfoot during walking: A muscle-driven finite element analysis. *Comput. Biol. Med.* 132, 104355. doi:10.1016/j.compbiomed.2021.104355

Rao, S., Baumhauer, J. F., Tome, J., and Nawoczenski, D. A. (2010). Orthoses alter *in vivo* segmental foot kinematics during walking in patients with midfoot arthritis. *Arch. Phys. Med. Rehabil.* 91, 608–614. doi:10.1016/j.apmr.2009.11.027

Redmond, A. C., Crane, Y. Z., and Menz, H. B. (2008). Normative values for the foot posture index. *J. Foot Ankle Res.* 1, 6. doi:10.1186/1757-1146-1-6

Simonsen, M. B., Hirata, R. P., Næsborg-Andersen, K., Leutscher, P. D. C., Hørslev-Petersen, K., Woodburn, J., et al. (2021). Different types of foot orthoses effect on gait mechanics in patients with rheumatoid arthritis. *J. Biomech.* 139, 110496. doi:10.1016/j.jbiomech.2021.110496

Stebbins, J., Harrington, M., Thompson, N., Zavatsky, A., and Theologis, T. (2006). Repeatability of a model for measuring multi-segment foot kinematics in children. *Gait Posture* 23, 401–410. doi:10.1016/j.gaitpost.2005.03.002

Telfer, S., Abbott, M., Steultjens, M. P., and Woodburn, J. (2013). Dose-response effects of customised foot orthoses on lower limb kinematics and kinetics in pronated foot type. *J. Biomech.* 46, 1489–1495. doi:10.1016/j.jbiomech.2013.03.036

Wahmkow, G., Cassel, M., Mayer, F., and Baur, H. (2017). Effects of different medial arch support heights on rearfoot kinematics. *PLoS One* 12, e0172334. doi:10.1371/journal.pone.0172334

Wang, Y., Lam, W. K., Wong, C. K., Park, L. Y., Tan, M. F., and Leung, A. K. L. (2020). Effectiveness and reliability of foot orthoses on impact loading and lower limb kinematics when running at preferred and nonpreferred speeds. *J. Appl. Biomech.* 37, 66–73. doi:10.1123/jab.2019-0281

Zhang, X., Li, B., Hu, K., Wan, Q., Ding, Y., and Vanwanseele, B. (2017). Adding an arch support to a heel lift improves stability and comfort during gait. *Gait Posture* 58, 94–97. doi:10.1016/j.gaitpost.2017.07.110

Zhang, X., Pauel, R., Deschamps, K., Jonkers, I., and Vanwanseele, B. (2019). Differences in foot muscle morphology and foot kinematics between symptomatic and asymptomatic pronated feet. *Scand. J. Med. Sci. Sports* 29, 1766–1773. doi:10.1111/sms.13512

Zhang, X., Lam, W. K., and Vanwanseele, B. (2022a). Dose-response effects of forefoot and arch orthotic components on the center of pressure trajectory during running in pronated feet. *Gait Posture* 92, 212–217. doi:10.1016/j.gaitpost.2021.11.033

Zhang, X., Yang, F., Zhao, K., and Vanwanseele, B. (2022b). Symptomatic and asymptomatic pronated feet show differences in the forefoot abduction motion during jogging, but not in the arch deformation. *Sports Biomech.*, 1–12. doi:10.1080/14763141.2022.2109506

frontiers | Frontiers in Physiology

TYPE Original Research
PUBLISHED 18 January 2023
DOI 10.3389/fphys.2023.1112708

OPEN ACCESS

EDITED BY
Qichang Mei,
Ningbo University, China

REVIEWED BY
Qiuxia Zhang,
Soochow University, China
Liang Guo,
South China Normal University, China

*CORRESPONDENCE
Qipeng Song,
songqipeng@sdpei.edu.cn

SPECIALTY SECTION
This article was submitted to Exercise Physiology, a section of the journal Frontiers in Physiology

RECEIVED 30 November 2022
ACCEPTED 09 January 2023
PUBLISHED 18 January 2023

CITATION
Hu S, Ma X, Ma X, Sun W, Zhou Z, Chen Y and Song Q (2023), Relationship of strength, joint kinesthesia, and plantar tactile sensation to dynamic and static postural stability among patients with anterior cruciate ligament reconstruction. *Front. Physiol.* 14:1112708.
doi: 10.3389/fphys.2023.1112708

Relationship of strength, joint kinesthesia, and plantar tactile sensation to dynamic and static postural stability among patients with anterior cruciate ligament reconstruction

Shanshan Hu[1], Xiaoli Ma[1], Xiaoyuan Ma[2], Wei Sun[1], Zhipeng Zhou[1], Yan Chen[1] and Qipeng Song[1]*

[1]College of Sports and Health, Shandong Sport University, Jinan, China, [2]Department of Orthopedic Surgery, Qilu Hospital, Cheeloo College of Medicine, Shandong University, Jinan, Shandong, China

Objective: Postural stability is essential for high-level physical activities after anterior cruciate ligament reconstruction (ACLR). This study was conducted to investigate the relationship of muscle strength, joint kinesthesia, and plantar tactile sensation to dynamic and static postural stability among patients with anterior cruciate ligament reconstruction.

Methods: Forty-four patients over 6 months post anterior cruciate ligament reconstruction (age: 27.9 ± 6.8 years, height: 181.7 ± 8.7 cm, weight: 80.6 ± 9.4 kg, postoperative duration: 10.3 ± 3.6 months) participated in this study. Their static and dynamic postural stability, muscle strength, hamstring/quadriceps ratio, joint kinesthesia, and plantar tactile sensation were measured. Partial correlations were used to determine the correlation of the above-mentioned variables with time to stabilization (TTS) and root mean square of the center of pressure (COP-RMS) in anterior-posterior (AP) and mediolateral (ML) directions.

Results: Both TTS_{AP} and TTS_{ML} were related to muscle strength and joint kinesthesia of knee flexion and extension; $COP\text{-}RMS_{AP}$ was correlated with plantar tactile sensations at great toe and arch, while $COP\text{-}RMS_{ML}$ was correlated with joint kinesthesia of knee flexion, and plantar tactile sensation at great toe and heel. Dynamic stability was sequentially correlated with strength and joint kinesthesia, while static stability was sequentially correlated with plantar tactile sensation and joint kinesthesia.

Conclusion: Among patients with anterior cruciate ligament reconstruction, strength is related to dynamic postural stability, joint kinesthesia is related to dynamic and static postural stability, and plantar tactile sensation is related to static postural stability. Strength has a higher level of relationship to dynamic stability than joint kinesthesia, and plantar tactile sensation has a higher level of relationship to static stability than joint kinesthesia.

KEYWORDS

ACLR, body balance, muscle strength, rehabilitation, proprioception

1 Introduction

Anterior cruciate ligament (ACL) injury accounts for approximately 50% of all knee injuries (Kaeding et al., 2017). Approximately 80,000–250,000 ACL ruptures were reported each year in the United States (Cimino et al., 2010; Mall et al., 2014), and more than 500,000 ACL injuries were diagnosed in Europe annually (Bellitti et al., 2022). To restore the mechanical stability of the knee, about 80% of individuals with ACL rupture undertake anterior cruciate ligament reconstruction (ACLR) (Schilaty et al., 2017). In the past 20 years, the rate of ACLR has increased by over 60% (Dodwell et al., 2014). Although the physiological structure of the ligament can be repaired by ACLR, many patients still suffer from postural stability deficits after the surgery (Howells et al., 2011; Logerstedt et al., 2013).

Postural stability is essential for high-level physical activities after ACLR (Ortiz et al., 2014). The reduced postural stability delays the time to return to sports, severely shortening athletes' careers and increasing their psychological burden (Clagg et al., 2015; Gokeler et al., 2017). Static standing is fundamental among many postures, and people who underwent ACLR have persistent deficits in static postural stability (Clark et al., 2014; Sugimoto et al., 2016). These deficits may explain, in part, the increased risk of future knee joint osteoarthritis and additional sport-related injuries (Sugimoto et al., 2016). Additionally, changes in dynamic postural stability can predict the likelihood of re-injury in ACLR patients (Paterno et al., 2010) and the deficit of postural stability increased the risk of injury on the reconstructed or non-reconstructed leg (Dauty et al., 2010). In turn, the re-injury further reduces postural stability, thus forming a pathological circulation (Fulton et al., 2014; Ortiz et al., 2014).

Significant postural stability deficits have been observed among patients with ACLR in both dynamic and static tasks (Colby et al., 1999; Webster and Gribble, 2010; Clark et al., 2014; Sugimoto et al., 2016). In laboratory and clinical practice, static postural stability is usually measured using the root mean square (RMS) of the center of pressure (COP) during standing, while dynamic postural stability is usually measured using the time to stabilization (TTS) during a dynamic task (e.g., single leg jump-landing) (Colby et al., 1999). It has been confirmed that compared to the controls, patients with ACLR have greater RMS of the COP (COP-RMS) (Goetschius et al., 2013; Stensdotter et al., 2016) and longer TTS (Colby et al., 1999; Webster and Gribble, 2010; Patterson and Delahunt, 2013).

Strength, joint kinesthesia, and plantar tactile sensation are three potential factors to maintain postural stability (Song et al., 2021). Joint kinesthesia is one of the proprioception senses, determined by establishing the threshold for detecting passive motion. When a perturbation occurs, signals from proprioceptive and tactile afferents evoke coordinated motor patterns, such as reflexes and automatic postural responses, which rapidly modify the locomotor pattern in response to perturbations (Frigon et al., 2021). These sensory afferents then convey sensory information to the central nervous system (Tahayori and Koceja, 2012) and finally cause muscle contraction that reflexively restores body stability (Wolfson et al., 1994; Gokeler et al., 2012; Song et al., 2021). Sufficient strength of the agonist and antagonist muscles across the joints is needed for good balance during functional activities (Croisier et al., 2008), and persistent muscle weakness may cause further alterations in the hamstring/quadriceps ratio resulting in dynamic instability, and it may increase the risk of further injury (Hohmann et al., 2019). Dysfunction of any part of the peripheral neural pathway may affect postural stability.

Compared to their peers, patients with ACLR has less strength (Schmitt et al., 2012), higher hamstring/quadriceps ratio (Kim et al., 2016), worse proprioception (Bonfim et al., 2003), and reduced plantar tactile sensation (Hoch et al., 2017). However, their relationship with postural stability is unclear. A significant correlation between postural stability and proprioception was detected in one study (Lee et al., 2009), but not in another (Ageberg et al., 2005). One study detected a significant correlation between postural stability with the strength of the quadriceps and hamstrings among patients with ACL injury (Ageberg et al., 2005), but no such correlation was detected in another study (Lee et al., 2009). Some studies indicated hamstring/quadriceps ratio has no relation with knee and body functions among patients with ACL tear (Lee et al., 2015) and ACLR (Hohmann et al., 2019), while some studies believed that dynamic balance depends on the strength balance among thigh muscle groups (White et al., 2003; Park et al., 2012). Additionally, to our knowledge, there is still a gap in the current works of literature regarding the relationship between postural stability and plantar tactile sensation among patients with ACL injuries. Certain rehabilitation methods have been shown to be effective in improving these three potential factors, for example, backward walking (Shen et al., 2019) or exergaming (Sadeghi et al., 2017) to improve joint motor sensation, swimming (Lee and Oh, 2015) or Nordic walking (Bullo et al., 2018) to increase strength, and Tai Chi (Zhang et al., 2021) to improve tactile sensation. Determining the relationship between strength, joint kinesthesia, and plantar tactile sensation with dynamic and static postural stability may help in selecting rehabilitation programs and facilitate the patients with ACLR to return to sports.

This study aimed to investigate the relationship of strength, joint kinesthesia, and plantar tactile sensation to postural stability among patients after ACLR. We hypothesized that 1) Strength, hamstring/quadriceps ratio, joint kinesthesia, and plantar tactile sensation are significantly related to static and dynamic postural stability as measured by the COP-RMS and the TTS. 2) Joint kinesthesia and strength contribute more to postural stability, compares with plantar tactile sensation.

2 Materials and methods

2.1 Participants

An *a priori* power analysis (G*Power Version 3.1) indicated that at least 27 participants are required to obtain an alpha level of 0.05 and a statistical power of 0.80 based on a previous report, which detected an $r^2 = 0.34$ between proprioception and dynamic postural stability among 12 young (20–26 years) patients with ACLR (Lee et al., 2009). The participants were patients with high sports demand who underwent ACLR at a local hospital and rehabilitation center. The inclusion criteria were: 1) ages 18–40 years (Ma et al., 2022); 2) Tegner activity level ≥ 5 (Briggs et al., 2009); 3) regular participation in sports before the injury and willingness to return to sports after ACLR (Niederer et al., 2019); 4) unilateral ACL rupture and at least 6 months after ACLR (Ma et al., 2022); 5) absence of a history of neurological disease or vestibular or visual disturbance (Ma et al., 2022). The exclusion criteria were as follows: 1) associated knee ligamentous injuries within 3 months; 2) previous knee surgery; 3) clinically relevant cardiovascular history; 4) clinically relevant neuromuscular

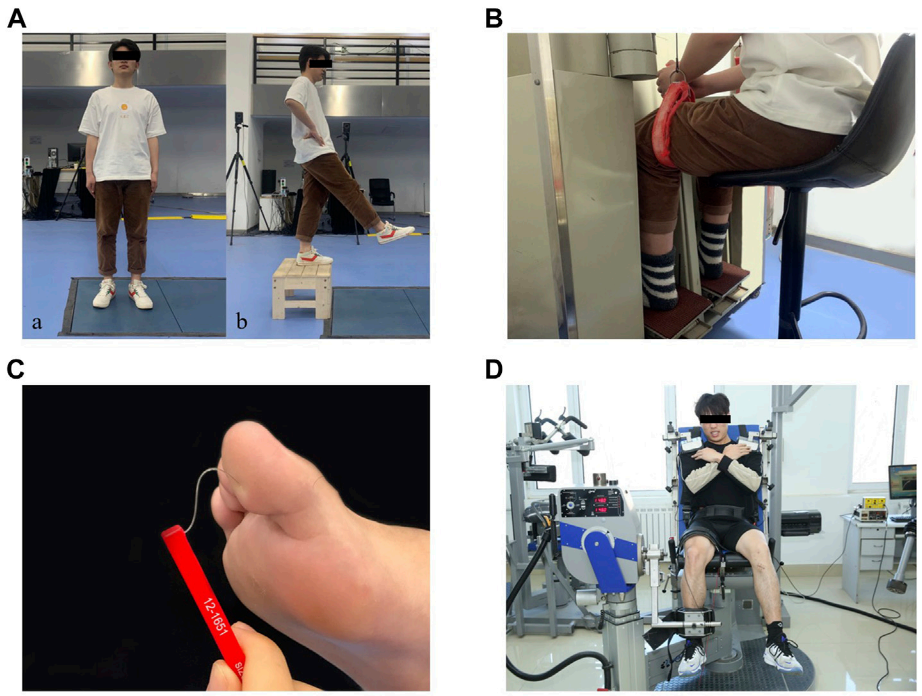

FIGURE 1
Test illustrations: **(Aa)**: Static postural stability test. **(Ab)**: Dynamic postural stability test. **(B)**: Joint kinesthesia test. **(C)**: Plantar tactile sensation test. **(D)**: Muscle strength test.

disorders; and 5) associated organ diseases that cannot be tolerated. A total of 44 participants were enrolled after the eligibility assessment (female = 14, male = 30, age: 27.9 ± 6.8 years, height: 181.7 ± 8.7 cm, weight: 80.6 ± 9.4 kg, BMI: 24.1 ± 3.6 kg/m^2, postoperative duration: 10.3 ± 3.6 months) and included in the final analysis. Among them, 29 had ACLR with autologous hamstring tendons, 6 with autologous bone-patellar tendon-bone, 3 with allogeneic Achilles tendons, and 6 with artificial ligaments. All participants signed a written informed consent before participating in the study. Human participation was approved by the Institutional Review Boards of a local university (2022013) and was in accordance with the Declaration of Helsinki.

2.2 Protocol

The participants completed a battery of functional questionnaires, including the International Knee Documentation Committee questionnaire, Tegner, and Visual Analog Scale. The results were used to determine the participants for inclusion in the study. Dynamic and static postural stability, joint kinesthesia, and plantar tactile sensation were measured in a random order, while strength was measured last to avoid fatigue.

2.3 Static postural stability test

The participants stood upright on both legs with their eyes open on a force plate (AMTI, Inc., Watertown, MA, United States) for 120 s (Figure 1Aa), which showed good test-retest reliability when measuring COP variables [intraclass correlation coefficients (ICC) = 0.78–0.95] (Kouvelioti et al., 2015). They were instructed to look straight ahead with their feet at an angle of 14°, heels 17 cm apart, arms along the sides (McIlroy and Maki, 1997), and stand still during the test. Vertical ground reaction force (GRF) data between 60s and 90s of each trial were used in this study (Hatton et al., 2011). COP data were collected at a sampling rate of 1,000 Hz. Each participant performed three successful trials, and a successful trial was defined as maintaining balance for 120 s without any visible body movement. Each participant had at least a 1 min break between two consecutive trials. The mean value of the three trials were used for data analysis.

2.4 Dynamic postural stability test

Participants performed a jump-landing task to assess their dynamic postural stability (Figure 1Ab), which showed good test-retest reliability (ICC = 0.74–0.90) (Colby et al., 1999). They stood on top of a 35 cm high box in front of the force plate with their feet positioned shoulder width apart, hands at the waist, and looked straight ahead. Once the tester gave the command, participants stepped forward with their reconstructed legs and dropped from the box onto the force plate, and stand still on their reconstructed legs. They were instructed to stabilize as quickly as possible upon landing and to hold a still position for 20 s. Prior to the formal test, all subjects were allowed three practice trials for familiarization with the test procedure. GRF data were collected at a sample rate of 1,000 Hz. Three successful trials were recorded and at least 1 min of rest were given between jump-landing trials. A successful trial was defined as the participant landed without loss of balance or any visible corrections after initial contact (e.g., the other leg touching the ground, sliding the support limb). The mean value of the three trials were used for data analysis.

2.5 Joint kinesthesia test

The participants' joint kinesthesia thresholds during knee flexion and extension of the reconstructed leg were assessed using a joint kinesthesia test device (Sunny, AP-II, China) (Figure 1B), which showed good test-retest reliability (ICC = 0.74–0.94) (Sun et al., 2015). The device consists of an operating platform and a test pedal. The platform was driven by two electric motors at an angular velocity of 0.4°/s. During the test, participants sat in an adjustable chair with their feet placed on the pedals, hips and knees flexed at 90° respectively, ankles in a neutral position, and lower legs perpendicular to the surface of the pedals. They wore blindfolds and headphones with music playing to eliminate visual and auditory stimuli from the testing environment. Participants were instructed to focus their attention on their reconstructed knee and to press the manual switch immediately to stop the movement of the pedal when they could sense the movement and identify the rotation direction. At the start of the trial, the motor was operated to rotate the knee to flexion or extension in a random sequence with random time intervals of 2–10 s. Each trial was started from the horizontal position of the platform. At least five trials were performed in each direction. The mean value of the minimum three angles sensed in each direction were used for data analysis.

2.6 Plantar tactile sensation test

The plantar tactile sensation of the reconstructed leg was assessed with a set of Semmes–Weinstein monofilaments (North Coast Medical, Inc., Morgan Hill, CA, United States) (Figure 1C), which showed good test-retest reliability (ICC = 0.83–0.86) (Collins et al., 2010). Six monofilaments with different sizes were used in this study: 2.83 (0.07 g), 3.61 (0.4 g), 4.31 (2 g), 4.56 (4 g), 5.07 (10 g), and 6.65 (300 g). Filament size = log10 (10 × force in milligrams). The filaments were applied randomly to the skin (bent 90°) on the bases of the great toe, first and fifth metatarsals, arch, and heel. A randomized null stimulus was added to ensure that participants could not anticipate the application of the filaments. Participants lay supine on the treatment table with their eyes closed and the tester selected filaments from thin to thick until they could perceive the stimulation and respond verbally to the correct location of the test area. The plantar tactile sensation threshold was determined by the thinnest monofilament they could feel (Feng et al., 2009).

2.7 Strength test

The strength of knee flexion and extension on the reconstructed leg was measured using a strength testing system (IsoMed 2000, D & R Ferstl GmbH, Germany) (Figure 1D), which showed good test-retest reliability in measuring lower limb strength (ICC = 0.77–0.98) (Gonosova et al., 2018). Participants were seated in a training chair with arms crossed in front of the chest, knees and hips at 90° and 85°, respectively, and secured with a lap belt across the thighs and pelvis and trunk. The lateral femoral condyle of the participant was aligned to the center of rotation of the dynamometer. Their isokinetic knee moments of flexion and extension were measured at 60°/s (Hoffman et al., 1999). Before testing, participants were asked to practice knee extension and flexion movements twice to ensure they understood how to exert force and complete the movements correctly. Once started, they were instructed to try their best to complete one knee extension and flexion movement. During the test, participants were encouraged to exert their maximum strength through verbal stimulation and visual feedback. Three trials were recorded, and at least a 2 min break was taken between two trials. Max knee flexion and extension torques were normalized by body mass (Nm/kg). The mean value of the three trials were used for data analysis.

2.8 Data extraction

Force plate data were used in calculating GRF and COP trajectory. COP was measured in the anterior-posterior (AP) and mediolateral (ML) directions. The GRF and COP data were filtered using a low-pass fourth-order Butterworth digital filter with a cut-off frequency of 50 Hz (Pan et al., 2016). The GRF data from the foot landed on the ground until the body regains stability were used in calculating the TTS (Figure 2). Two time-windows of the last 10 s (10–15, 15–20 s) of the AP and ML components of the GRF were analyzed. The windows with the smallest absolute GRF range for the AP and ML components were regarded as the optimal range of variation values (Ross and Guskiewicz, 2004). The 20 s COP data were collected from each participant after they landed on the ground.

2.9 Variables

The TTS was defined as the time from the foot landed on the ground until the body regains stability, i.e., the starting moment when the smoothed GRF was within the optimal range of variation values for at least 0.5 s (Tulloch et al., 2012).

The vertical ground reaction force data from 60 to 90 s during standing were collected (Hatton et al., 2011). The equations of RMS and mean velocity of the COP were as follows:

$$\text{RMS of COP displacement (AP)} = \sqrt{\frac{\sum (x_i - \bar{x})^2}{N-1}} \tag{1}$$

$$\text{RMS of COP displacement (ML)} = \sqrt{\frac{\sum (y_i - \bar{y})^2}{N-1}} \tag{2}$$

In these equations, $\bar{x}$ and $\bar{y}$ were the mean positions of CoP in the AP and ML directions.

The hamstring/quadriceps ratio was calculated by dividing the peak knee flexion torque by the peak knee extension torque in the strength test.

2.10 Data analysis

Descriptive analysis was used to summarize the means and standard deviations of the variables. The normality of all outcome variables was tested using Shapiro–Wilk test. A partial correlation (Pearson correlation for normally distributed or Spearman correlation for non-normally distributed data) was used to verify Hypothesis #1 by determining the correlations of the stability variables with each of the

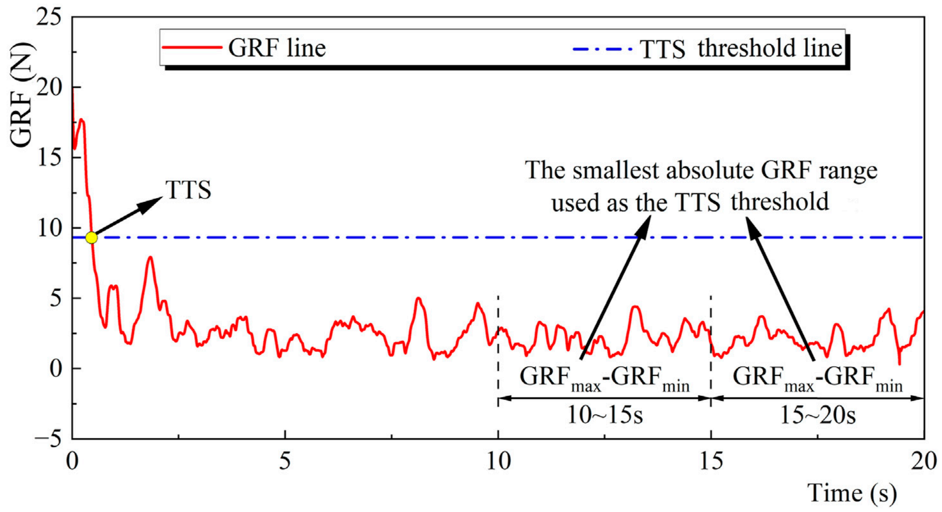

FIGURE 2
Illustration of the TTS calculation. Note: GRF, Ground reaction force; TTS, Time to stabilization.

TABLE 1 Descriptive characteristics of outcome variables.

		Mean	SD	Max	Min
TTS (ms)	Anterior-posterior	843	250	1,377	451
	Mediolateral	544	302	1,428	83
COP-RMS (mm)	Anterior-posterior	0.84	0.52	2.89	0.18
	Mediolateral	0.93	0.59	2.70	0.28
Strength (N·m/kg)	Knee flexion	0.91	0.45	1.82	0.17
	Knee extension	1.21	0.56	2.93	0.44
	Flexion/extension ratio (%)	74.8	27.6	0.35	1.21
Joint kinesthesia (°)	Knee flexion	1.21	0.56	2.93	0.44
	Knee extension	0.96	0.54	2.49	0.22
Plantar tactile sensation (gauge)	Great toe	3.62	0.57	4.31	2.83
	1st metatarsal	3.71	0.41	4.31	2.83
	5th metatarsal	3.62	0.53	4.31	2.83
	Arch	3.78	0.35	4.31	2.83
	Heel	3.83	0.33	4.31	3.61

Abbreviations: TTS, time to stabilization; COP-RMS, root mean square of the center of pressure.

strength, joint kinesthesia, and plantar tactile sensation variables while controlling for covariates (gender, age, height, weight, and postoperative duration). Then, separate exploratory factor analysis was carried out among each category of the variables of interest. Multivariable linear regression was used to verify Hypothesis #2 by exploring the degrees of correlation between each generated factor and the stability variables while controlling for the above-mentioned covariates. The thresholds for the correlation coefficient (r) were as follows: 0–0.1, trivial; 0.1–0.3, weak; 0.3–0.5, moderate; >0.5, strong. All analyses were conducted in SAS 9.4, and the significance level was set at 0.05 (Cohen, 2013).

3 Results

Shapiro–Wilk tests showed that plantar tactile sensation data were non-normally distributed. Strength, joint kinesthesia, TTS, and COP-RMS data were normally distributed.

The descriptive characteristics are shown in Table 1. Mean, standard deviation, minimum value, and maximum value are reported for the TTS, COP-RMS, strength, joint kinesthesia, and plantar tactile sensation.

Partial correlations are shown in Table 2. Both TTS_{AP} and TTS_{ML} were related with strength and joint kinesthesia of knee flexion/

TABLE 2 Partial correlations of dynamic and static postural stability with strength, joint kinesthesia, and plantar tactile sensation.

Variables		Dynamic postural stability				Static postural stability			
		TTS_{AP}		TTS_{ML}		COP-RMS_{AP}		COP-RMS_{ML}	
		r	p	*r*	p	*r*	p	*r*	p
Strength (N·m/kg)	Knee flexion	−0.457	0.002	−0.419	0.005	−0.154	0.317	−0.117	0.448
	Knee extension	−0.446	0.002	−0.437	0.003	−0.056	0.720	0.098	0.525
	Flexion/extension ratio (%)	−0.246	0.108	−0.139	0.368	−0.198	0.198	−0.111	0.473
Joint kinesthesia (°)	Knee flexion	0.385	0.010	0.379	0.011	0.206	0.181	0.422	0.004
	Knee extension	0.393	0.008	0.539	<0.001	0.127	0.411	0.139	0.368
Plantar tactile sensation (gauge)	Great toe	0.270	0.077	0.060	0.699	0.503	<0.001	0.375	0.012
	1st metatarsal	0.107	0.487	0.126	0.014	0.290	0.056	0.198	0.199
	5th metatarsal	0.251	0.104	0.096	0.536	0.016	0.918	0.296	0.051
	Arch	0.280	0.855	0.013	0.931	0.371	0.013	0.194	0.207
	Heel	0.188	0.221	0.294	0.053	0.294	0.053	0.390	0.009

Notes: The correlations of plantar tactile sensation to stability were analyzed by Spearman correlation, others by Pearson correlation. The shaded cells represent significant correlation coefficients. The values were adjusted for gender, age, weight, height, and postoperative duration. Abbreviations: TTS_{AP}, time to stabilization in the anterior-posterior direction; TTS_{ML}, time to stabilization in the mediolateral direction; CoP-RMS_{AP}, root mean square of the center of pressure in the anterior-posterior direction; CoP-RMS_{ML}, root mean square of the center of pressure in the mediolateral direction; r, correlation coefficient.

TABLE 3 Factor loadings for the variables among the strength, joint kinesthesia, and plantar tactile sensation.

		Factor 1	Factor 2	Factor 3
Strength (N·m/kg)	Knee flexion	--	0.788	--
	Knee extension	--	0.863	--
Joint kinesthesia (°)	Knee flexion	--	--	0.973
	Knee extension	--	--	0.844
Plantar tactile sensation (gauge)	Great toe	0.837	--	--
	1st metatarsal	0.547	--	--
	5th metatarsal	0.640	--	--
	Arch	0.744	--	--
	Heel	0.608	--	--

Notes: --, factor loading < 0.500.

extension; COP-RMS_{AP} was correlated with plantar tactile sensations at the great toe and arch, while COP-RMS_{ML} was correlated with joint kinesthesia of knee flexion and plantar tactile sensation at great toe and heel.

The factor loadings for all the variables are shown in Table 3. Factor 1 (F1), factor 2 (F2), and factor 3 (F3) were the summaries of plantar tactile sensation, strength, and joint kinesthesia, respectively, with a Kaiser Meyer Olkin value of 0.718 and a sphericity of < 0.001.

The equations for multivariable regression are:

$$TTS_{AP} = 843.30 - 114.30 \times F2 \tag{3}$$

$$TTS_{ML} = 554.07 - 94.63 \times F2 + 159.45 \times F3 \tag{4}$$

$$COP-RMS_{AP} = 0.84 + 0.24 \times F1 \tag{5}$$

$$COP-RMS_{ML} = 0.93 + 0.23 \times F1 + 0.36 \times F3 \tag{6}$$

In Eq. 3, adjusted $r^2 = 0.249$, $p_{F2} = 0.001$, and $\beta_{F2} = 0.457$; In Eq. 4, adjusted $r^2 = 0.393$, $p_{F2} < 0.001$, $p_{F3} = 0.012$, $\beta_{F2} = 0.529$, and $\beta_{F3} = 0.314$, $\beta_{F2} > \beta_{F3}$ indicated strength contributed more to dynamic postural stability than proprioception. In Eq. 5, adjusted $r^2 = 0.221$, $p_{F1} = 0.001$, and $\beta_{F1} = 0.465$; In Eq. 6, adjusted $r^2 = 0.479$, $p_{F1} < 0.001$, $p_{F3} = 0.002$, $\beta_{F1} = 0.602$, $\beta_{F3} = 0.390$, $\beta_{F1} > \beta_{F3}$ indicated plantar tactile sensation contributed more to static postural stability than proprioception.

4 Discussion

The main purpose of this study was to identify the relationship of dynamic and static postural stability to strength, joint kinesthesia, and plantar tactile sensation, and their degrees of contribution among patients with ACLR. The outcomes partly supported hypothesis #1 by indicating that strength is related to dynamic postural stability, joint kinesthesia is related to dynamic and static postural stability, and plantar tactile sensation is related to static postural stability, while rejected hypothesis #2 by indicating dynamic stability was sequentially correlated with strength and joint kinesthesia, and static stability was sequentially correlated with plantar tactile sensation and joint kinesthesia. The mean and range of results collected in this study were similar and comparable to previous studies investigating postural stability (Colby et al., 1999; Patterson and Delahunt, 2013), strength (Robinson et al., 2022), hamstring/quadriceps ratio (Hohmann et al., 2019), joint kinesthesia (Bonfim et al., 2003), and plantar tactile sensation (Hoch et al., 2017) among patients with ACL reconstruction.

Our results indicated that strength was related to dynamic but not to static postural stability. Previous studies supported our findings (Shiraishi et al., 1996; Kim et al., 2022). Some studies disagreed with our findings and indicated that strength was not related to dynamic postural stability (Novaretti et al., 2018) and was related to static postural stability (Cinar-Medeni et al., 2015), this may be caused by differences in testing protocols. Novaretti et al. (2018) measured the ability to maintain posture under dynamic stress on a circular platform, with up to 20° of tilting. Their protocol is more like a test of static postural control, rather than a dynamic one. Cinar-Medeni et al. (2015) used a single-leg stance task to assess static postural stability, and the movement of transitioning from standing on a double leg to being supported by a single leg may influence postural stability outcomes (Dingenen et al., 2015). The double-legged stance used in this study is considered a standard and reliable posture to assess static postural stability among patients with ACLR (Kouvelioti et al., 2015; Lion et al., 2018). During dynamic activities (e.g., cutting, pivoting, landing, etc.), the knee flexor and extensor contract synchronously to stabilize the knee and thus maintain postural stability (Redler et al., 2021). Compared with dynamic tasks, static standing requires less strength to maintain postural stability and relies more on plantar tactile sensation (Song et al., 2021). This study indicated that strength is correlated to dynamic stability, and our viewpoint is support by previous studies indicating that strength exercise benefits to the recovery of body stability among patients with ACLR (Shaw et al., 2005). Strength training should be employed to improve postural stability among patients with ACLR.

No significant correlations were detected between hamstring/quadriceps ratio and postural stability, agreed by previous studies indicating hamstring/quadriceps ratio has no relation with knee and body functions among patients with ACLR (Hohmann et al., 2019). One of the potential reasons is that with surgical reconstruction of the ACL, static knee stability is restored, and the need to downregulate quadriceps activity reduced with recovery. It has been pointed that a higher hamstring/quadriceps ratio represent a better ability of the hamstrings to stabilize the knee joint (Hiemstra et al., 2004). In our cohort, the hamstring/quadriceps ratio (74.8%) is higher than that among patients with ACL deficits (about 60%–66%) (Myer et al., 2009), agreed by a previous study indicating that patients has higher hamstring/quadriceps ratio after receiving ACLR (Jordan et al., 2015).

The results showed that joint kinesthesia was associated with both dynamic and static postural stability. Our observations were consistent with the previous studies (Borsa et al., 1998; Lee et al., 2009). One study disagreed with us by showing that proprioception was not related to either static or dynamic postural stability among patients with ACLR (Birmingham et al., 2001). They used joint position sense (JPS) to represent joint kinesthesia, unlike the joint kinesthesia in our study. JPS is more complex than joint kinesthesia (Reider et al., 2003). In JPS tests, participants must try to remember the position and then reproduce it accurately. We have reasons to infer that the correlation between JPS and postural stability may be influenced by the memory and learning effect of the participants. Previous studies supported our viewpoint by pointing out that joint kinesthesia is more reliable than position sense in detecting proprioceptive deficits in people with ACL injury or reconstruction (Fischer-Rasmussen and Jensen, 2000; Reider et al., 2003). This study showed that only knee flexion kinesthesia, but not knee extension kinesthesia, is associated with static stability. Knee flexion kinesthesia is provided by mechanoreceptors in the flexor muscles and flexor ligaments, and the ACL is considered agonists of the hamstrings with a knee flexion function (Hohmann et al., 2019). Therefore, it is reasonable to infer that mechanoreceptors in the ACL provide knee flexion kinesthesia. The impaired ACL among patients with ACLR makes the CNS dependent more on kinesthesia signals from the knee flexor muscles. This study further indicated that kinesthesia is correlated to dynamic and static stability, and our viewpoint is support by previous studies indicating that proprioceptive training appeared to decrease the incidence of injury to the knee and specifically the ACL (Cooper et al., 2005). Proprioceptive training should be employed among patients with ACLR.

Impaired postural stability in the ML direction is associated with a higher risk of falls compared to impaired postural stability in the AP direction (Islam et al., 2004). During movement, if the disturbance occurs in the AP direction, individuals can remove the disturbance by swinging their lower limbs to move their feet into the appropriate position. But if the disturbance occurs in the ML direction, it is difficult for them to drop their swing legs on the outside of the supporting leg to maintain postural stability. In addition, Chen et al. (Chen and Qu, 2019) found that ML postural stability deteriorated with decreased ankle proprioception. It is inferred that joint kinesthesia may be limited to ML direction in terms of maintaining postural stability after ACLR.

Our results showed that plantar tactile sensation was related to static postural stability but not dynamic postural stability. To our knowledge, the relationship between plantar tactile sensation and postural stability in the ACLR population has yet to be investigated. Previous findings in other populations were consistent with ours (Nyland et al., 1994; Song et al., 2021). During upright standing, the position of COP changes with slight variation (Meyer et al., 2004). The plantar cutaneous mechanoreceptors transmit spatial and temporal information concerning the pressure variations underfoot to the central nervous system (Kavounoudias et al., 1998), thus reflexively maintaining static postural stability. Unlike during standing still, muscles and tendons were stretched during dynamic locomotion, muscle spindle and Golgi tendon organ were activated, and proprioceptive signals provide movement and position information of body segments (Frigon et al., 2021). Type III sensory neurons, responsive to plantar tactile sensation, conduct slower and weaker signals than type Ia and type II sensory neurons, responsible for proprioception (Li et al., 2019). Therefore, patients with ACLR may rely more on joint kinesthesia rather than plantar tactile sensation to maintain dynamic postural stability.

Cutaneous sensitivity was partially influenced by the mechanical properties of the skin (Strzalkowski et al., 2015). The arch was the softest and thinnest site, followed by the great toe, fifth metatarsal and heel (Strzalkowski et al., 2015). Plantar sensitivity is correlated with plantar pressure distribution (Nurse and Nigg, 2001). The arch and great toe had better sensitivity, and significantly affected the plantar pressure distribution during standing, which were closely related to static postural stability (Zhang and Li, 2013; Song et al., 2021).

Multivariate linear regression showed that dynamic stability was sequentially correlated with strength at a higher level than joint kinesthesia, while static stability was correlated with plantar tactile sensation at a higher level than joint kinesthesia. It needs to be noted that although joint kinesthesia was related to both dynamic and static postural stability, it was outweighed by strength and plantar tactile sensation, respectively. It has been shown that the ACL contains mechanoreceptors (Schultz et al., 1984), which provide proprioceptive information about joint position and movement whilst coordinating muscular reflex stabilization of the knee joint (Mohammadirad et al., 2012). Once the ACL is ruptured, these sensory receptors are damaged, resulting in an altered sensory afferent information and disrupted neurofeedback circuit (Mohammadirad et al., 2012), which may decrease the level joint kinesthesia in relation to dynamic and static postural control.

There are some limitations to this study. First, the reconstruction objects selected by ACLR include autologous tendons, allogeneic tendons, and artificial ligaments. The impact of these three kinds of reconstruction objects on the postural stability of patients with ACLR may be slightly different. Further studies are recommended to subdivide each participant's reconstruction objects and considered the potential influence of these reconstruction objects on postural stability among patients with ACLR. Second, only the effects of strength, joint kinesthesia, and plantar tactile sensation on postural stability among patients with ACLR were investigated in this study. Other factors, such as vision and vestibular system, might also have an impact on postural stability. Third, all the participants in this study were patients with high sports demand, so the findings may only apply to this population.

5 Conclusion

Among patients with ACLR, dynamic stability was sequentially correlated with strength and joint kinesthesia, while static stability was sequentially correlated with plantar tactile sensation and joint kinesthesia. Lower extremity strength training is vital to postural stability recovery since it is firstly related to dynamic stability, and sensations, both joint kinesthesia and plantar tactile sensation, should be emphasized since they related to both dynamic and static stability among patients with ACLR.

Data availability statement

The raw data supporting the conclusion of this article will be made available by the authors, without undue reservation.

Ethics statement

The studies involving human participants were reviewed and approved by Institutional Review Boards of Shandong Sport University. The patients/participants provided their written informed consent to participate in this study.

Author contributions

SH participated in the design of the study and contributed to the collection and analysis of the data and drafted the manuscript. XLM participated in the design of the study, data reduction/analysis. XYM and WS contributed to data collection and data reduction/analysis. ZZ and YC contributed to the data collection and interpretation of results of the study. QS participated in the design of the study and contributed to the interpretation of results and revision of the manuscript. All authors have read and approved the final version of the manuscript, and agree with the order of presentation of the authors.

Funding

This work was supported by Shandong Provincial Youth Talent Induction Team (2019-183), and National Natural Science Foundation of China (12102235).

Acknowledgments

The authors would like to thank Hao Sun, doctoral student at Loughborough University, and Yanhao Liu, Shiyu Dong, Jingwen Wang, Yaya Pang, Qi Wang, Boshi Xue, graduate students at Shandong Sport University, for participating or data acquisition for this work.

Conflict of interest

The authors declare that the research was conducted in the absence of any commercial or financial relationships that could be construed as a potential conflict of interest.

Publisher's note

All claims expressed in this article are solely those of the authors and do not necessarily represent those of their affiliated organizations, or those of the publisher, the editors and the reviewers. Any product that may be evaluated in this article, or claim that may be made by its manufacturer, is not guaranteed or endorsed by the publisher.

References

Ageberg, E., Roberts, D., Holmstrom, E., and Friden, T. (2005). Balance in single-limb stance in patients with anterior cruciate ligament injury: Relation to knee laxity, proprioception, muscle strength, and subjective function. *Am. J. Sports Med.* 33 (10), 1527–1535. doi:10.1177/0363546505274934

Bellitti, P., Borghetti, M., Lopomo, N. F., Sardini, E., and Serpelloni, M. (2022). Smart brace for static and dynamic knee laxity measurement. *Sensors (Basel)* 22 (15), 5815. doi:10.3390/s22155815

Birmingham, T. B., Kramer, J. F., Kirkley, A., Inglis, J. T., Spaulding, S. J., and Vandervoort, A. A. (2001). Knee bracing after ACL reconstruction: Effects on postural control and proprioception. *Med. Sci. Sports Exerc* 33 (8), 1253–1258. doi:10.1097/00005768-200108000-00002

Bonfim, T. R., Jansen, P. C., and Barela, J. A. (2003). Proprioceptive and behavior impairments in individuals with anterior cruciate ligament reconstructed knees. *Arch. Phys. Med. Rehabil.* 84 (8), 1217–1223. doi:10.1016/s0003-9993(03)00147-3

Borsa, P. A., Lephart, S. M., and Irrgang, J. J. (1998). Comparison of performance-based and patient-reported measures of function in anterior-cruciate-ligament-deficient individuals. *J. Orthop. Sports Phys. Ther.* 28 (6), 392–399. doi:10.2519/jospt.1998.28.6.392

Briggs, K. K., Steadman, J. R., Hay, C. J., and Hines, S. L. (2009). Lysholm score and Tegner activity level in individuals with normal knees. *Am. J. Sports Med.* 37 (5), 898–901. doi:10.1177/0363546508330149

Bullo, V., Gobbo, S., Vendramin, B., Duregon, F., Cugusi, L., Di Blasio, A., et al. (2018). Nordic walking can Be incorporated in the exercise prescription to increase aerobic capacity, strength, and quality of life for elderly: A systematic review and meta-analysis. *Rejuvenation Res.* 21 (2), 141–161. doi:10.1089/rej.2017.1921

Chen, X., and Qu, X. (2019). Age-related differences in the relationships between lower-limb joint proprioception and postural balance. *Hum. Factors* 61 (5), 702–711. doi:10.1177/0018720818795064

Cimino, F., Volk, B. S., and Setter, D. (2010). Anterior cruciate ligament injury: Diagnosis, management, and prevention. *Am. Fam. Physician* 82 (8), 917–922.

Cinar-Medeni, O., Baltaci, G., Bayramlar, K., and Yanmis, I. (2015). Core stability, knee muscle strength, and anterior translation are correlated with postural stability in anterior cruciate ligament-reconstructed patients. *Am. J. Phys. Med. Rehabil.* 94 (4), 280–287. doi:10.1097/phm.0000000000000177

Clagg, S., Paterno, M. V., Hewett, T. E., and Schmitt, L. C. (2015). Performance on the modified star excursion balance test at the time of return to sport following anterior cruciate ligament reconstruction. *J. Orthop. Sports Phys. Ther.* 45 (6), 444–452. doi:10.2519/jospt.2015.5040

Clark, R. A., Howells, B., Pua, Y. H., Feller, J., Whitehead, T., and Webster, K. E. (2014). Assessment of standing balance deficits in people who have undergone anterior cruciate ligament reconstruction using traditional and modern analysis methods. *J. Biomech.* 47 (5), 1134–1137. doi:10.1016/j.jbiomech.2013.12.015

Cohen, J. (2013). *Statistical power analysis for the behavioral sciences*. 2nd ed. Hillsdale, NJ: Lawrence Erlbaum Associates.

Colby, S. M., Hintermeister, R. A., Torry, M. R., and Steadman, J. R. (1999). Lower limb stability with ACL impairment. *J. Orthop. Sports Phys. Ther.* 29 (8), 444–451. discussion 452-444. doi:10.2519/jospt.1999.29.8.444

Collins, S., Visscher, P., De Vet, H. C., Zuurmond, W. W., and Perez, R. S. (2010). Reliability of the Semmes Weinstein Monofilaments to measure coetaneous sensibility in the feet of healthy subjects. *Disabil. Rehabil.* 32 (24), 2019–2027. doi:10.3109/09638281003797406

Cooper, R. L., Taylor, N. F., and Feller, J. A. (2005). A randomised controlled trial of proprioceptive and balance training after surgical reconstruction of the anterior cruciate ligament. *Res. Sports Med.* 13 (3), 217–230. doi:10.1080/15438620500222547

Croisier, J. L., Ganteaume, S., Binet, J., Genty, M., and Ferret, J. M. (2008). Strength imbalances and prevention of hamstring injury in professional soccer players: A prospective study. *Am. J. Sports Med.* 36 (8), 1469–1475. doi:10.1177/0363546508316764

Dauty, M., Collon, S., and Dubois, C. (2010). Change in posture control after recent knee anterior cruciate ligament reconstruction? *Clin. Physiol. Funct. Imaging* 30 (3), 187–191. doi:10.1111/j.1475-097X.2010.00926.x

Dingenen, B., Janssens, L., Claes, S., Bellemans, J., and Staes, F. F. (2015). Postural stability deficits during the transition from double-leg stance to single-leg stance in anterior cruciate ligament reconstructed subjects. *Hum. Mov. SciB.V. All rights Reserv.* 41, 46–58. doi:10.1016/j.humov.2015.02.001

Dodwell, E. R., Lamont, L. E., Green, D. W., Pan, T. J., Marx, R. G., and Lyman, S. (2014). 20 years of pediatric anterior cruciate ligament reconstruction in New York State. *Am. J. Sports Med.* 42 (3), 675–680. doi:10.1177/0363546513518412

Feng, Y., Schlosser, F. J., and Sumpio, B. E. (2009). The Semmes Weinstein monofilament examination as a screening tool for diabetic peripheral neuropathy. *J. Vasc. Surg.* 50 (3), 675682–682. e671. doi:10.1016/j.jvs.2009.05.017

Fischer-Rasmussen, T., and Jensen, P. E. (2000). Proprioceptive sensitivity and performance in anterior cruciate ligament-deficient knee joints. *Scand. J. Med. Sci. Sports* 10 (2), 85–89. doi:10.1034/j.1600-0838.2000.010002085.x

Frigon, A., Akay, T., and Prilutsky, B. I. (2021). Control of mammalian locomotion by somatosensory feedback. *Compr. Physiol.* 12 (1), 2877–2947. doi:10.1002/cphy.c210020

Fulton, J., Wright, K., Kelly, M., Zebrosky, B., Zanis, M., Drvol, C., et al. (2014). Injury risk is altered by previous injury: A systematic review of the literature and presentation of causative neuromuscular factors. *Int. J. Sports Phys. Ther.* 9 (5), 583–595.

Goetschius, J., Kuenze, C. M., Saliba, S., and Hart, J. M. (2013). Reposition acuity and postural control after exercise in anterior cruciate ligament reconstructed knees. *Med. Sci. Sports Exerc* 45 (12), 2314–2321. doi:10.1249/MSS.0b013e31829bc6ae

Gokeler, A., Benjaminse, A., Hewett, T. E., Lephart, S. M., Engebretsen, L., Ageberg, E., et al. (2012). Proprioceptive deficits after ACL injury: Are they clinically relevant? *Br. J. Sports Med.* 46 (3), 180–192. doi:10.1136/bjsm.2010.082578

Gokeler, A., Welling, W., Benjaminse, A., Lemmink, K., Seil, R., and Zaffagnini, S. (2017). A critical analysis of limb symmetry indices of hop tests in athletes after anterior cruciate ligament reconstruction: A case control study. *Orthop. Traumatol. Surg. Res.* 103 (6), 947–951. doi:10.1016/j.otsr.2017.02.015

Gonosova, Z., Linduska, P., Bizovska, L., and Svoboda, Z. (2018). Reliability of Ankle⁻Foot complex isokinetic strength assessment using the isomed 2000 dynamometer. *Med. Kaunas.* 54 (3), 43. doi:10.3390/medicina54030043

Hatton, A. L., Dixon, J., Rome, K., and Martin, D. (2011). Standing on textured surfaces: Effects on standing balance in healthy older adults. *Age Ageing* 40 (3), 363–368. doi:10.1093/ageing/afr026

Hiemstra, L. A., Webber, S., MacDonald, P. B., and Kriellaars, D. J. (2004). Hamstring and quadriceps strength balance in normal and hamstring anterior cruciate ligament-reconstructed subjects. *Clin. J. Sport Med.* 14 (5), 274–280. doi:10.1097/00042752-200409000-00005

Hoch, J. M., Perkins, W. O., Hartman, J. R., and Hoch, M. C. (2017). Somatosensory deficits in post-ACL reconstruction patients: A case-control study. *Muscle Nerve* 55 (1), 5–8. doi:10.1002/mus.25167

Hoffman, M., Schrader, J., and Koceja, D. (1999). An investigation of postural control in postoperative anterior cruciate ligament reconstruction patients. *J. Athl. Train.* 34 (2), 130–136.

Hohmann, E., Tetsworth, K., and Glatt, V. (2019). The hamstring/quadriceps ratio is an indicator of function in ACL-deficient, but not in ACL-reconstructed knees. *Arch. Orthop. Trauma Surg.* 139 (1), 91–98. doi:10.1007/s00402-018-3000-3

Howells, B. E., Ardern, C. L., and Webster, K. E. (2011). Is postural control restored following anterior cruciate ligament reconstruction? A systematic review. *Knee Surg. Sports Traumatol. Arthrosc.* 19 (7), 1168–1177. doi:10.1007/s00167-011-1444-x

Islam, M. M., Nasu, E., Rogers, M. E., Koizumi, D., Rogers, N. L., and Takeshima, N. (2004). Effects of combined sensory and muscular training on balance in Japanese older adults. *Prev. Med.* 39 (6), 1148–1155. doi:10.1016/j.ypmed.2004.04.048

Jordan, M. J., Aagaard, P., and Herzog, W. (2015). Rapid hamstrings/quadriceps strength in ACL-reconstructed elite Alpine ski racers. *Med. Sci. Sports Exerc* 47 (1), 109–119. doi:10.1249/MSS.0000000000000375

Kaeding, C. C., Leger-St-Jean, B., and Magnussen, R. A. (2017). Epidemiology and diagnosis of anterior cruciate ligament injuries. *Clin. Sports Med.* 36 (1), 1–8. doi:10.1016/j.csm.2016.08.001

Kavounoudias, A., Roll, R., and Roll, J. P. (1998). The plantar sole is a 'dynamometric map' for human balance control. *Neuroreport* 9 (14), 3247–3252. doi:10.1097/00001756-199810050-00021

Kim, H. J., Lee, J. H., Ahn, S. E., Park, M. J., and Lee, D. H. (2016). Influence of anterior cruciate ligament tear on thigh muscle strength and hamstring-to-quadriceps ratio: A meta-analysis. *PLoS One* 11 (1), e0146234. doi:10.1371/journal.pone.0146234

Kim, J. S., Hwang, U. J., Choi, M. Y., Kong, D. H., Chung, K. S., Ha, J. K., et al. (2022). Correlation between Y-balance test and balance, functional performance, and outcome measures in patients following ACL reconstruction. *Int. J. Sports Phys. Ther.* 17 (2), 193–200. doi:10.26603/001c.31873

Kouvelioti, V., Kellis, E., Kofotolis, N., and Amiridis, I. (2015). Reliability of single-leg and double-leg balance tests in subjects with anterior cruciate ligament reconstruction and controls. *Res. Sports Med.* 23 (2), 151–166. doi:10.1080/15438627.2015.1005292

Lee, B. A., and Oh, D. J. (2015). Effect of regular swimming exercise on the physical composition, strength, and blood lipid of middle-aged women. *J. Exerc Rehabil.* 11 (5), 266–271. doi:10.12965/jer.150242

Lee, D. H., Lee, J. H., Jeong, H. J., and Lee, S. J. (2015). Lack of correlation between dynamic balance and hamstring-to-quadriceps ratio in patients with chronic anterior cruciate ligament tears. *Knee Surg. Relat. Res.* 27 (2), 101–107. doi:10.5792/ksrr.2015.27.2.101

Lee, H. M., Cheng, C. K., and Liau, J. J. (2009). Correlation between proprioception, muscle strength, knee laxity, and dynamic standing balance in patients with chronic anterior cruciate ligament deficiency. *Knee* 16 (5), 387–391. doi:10.1016/j.knee.2009.01.006

Li, L., Zhang, S., and Dobson, J. (2019). The contribution of small and large sensory afferents to postural control in patients with peripheral neuropathy. *J. Sport Health Sci.* 8 (3), 218–227. doi:10.1016/j.jshs.2018.09.010

Lion, A., Gette, P., Meyer, C., Seil, R., and Theisen, D. (2018). Effect of cognitive challenge on the postural control of patients with ACL reconstruction under visual and surface perturbations. *Gait Posture* 60, 251–257. doi:10.1016/j.gaitpost.2017.12.013

Logerstedt, D., Lynch, A., Axe, M. J., and Snyder-Mackler, L. (2013). Symmetry restoration and functional recovery before and after anterior cruciate ligament reconstruction. *Knee Surg. Sports Traumatol. Arthrosc.* 21 (4), 859–868. doi:10.1007/s00167-012-1929-2

Ma, X., Lu, L., Zhou, Z., Sun, W., Chen, Y., Dai, G., et al. (2022). Correlations of strength, proprioception, and tactile sensation to return-to-sports readiness among patients with anterior cruciate ligament reconstruction. *Front. Physiol.* 13, 1046141. doi:10.3389/fphys.2022.1046141

Mall, N. A., Chalmers, P. N., Moric, M., Tanaka, M. J., Cole, B. J., Bach, B. J., et al. (2014). Incidence and trends of anterior cruciate ligament reconstruction in the United States. *Am. J. Sports Med.* 42 (10), 2363–2370. doi:10.1177/0363546514542796

McIlroy, W. E., and Maki, B. E. (1997). Preferred placement of the feet during quiet stance: Development of a standardized foot placement for balance testing. *Clin. Biomech. (Bristol, Avon)* 12 (1), 66–70. doi:10.1016/s0268-0033(96)00040-x

Meyer, P. F., Oddsson, L. I., and De Luca, C. J. (2004). The role of plantar cutaneous sensation in unperturbed stance. *Exp. Brain Res.* 156 (4), 505–512. doi:10.1007/s00221-003-1804-y

Mohammadirad, S., Salavati, M., Takamjani, I. E., Akhbari, B., Sherafat, S., Mazaheri, M., et al. (2012). Intra and intersession reliability of a postural control protocol in athletes with and without anterior cruciate ligament reconstruction: A dual-task paradigm. *Int. J. Sports Phys. Ther.* 7 (6), 627–636.

Myer, G. D., Ford, K. R., Barber Foss, K. D., Liu, C., Nick, T. G., and Hewett, T. E. (2009). The relationship of hamstrings and quadriceps strength to anterior cruciate ligament injury in female athletes. *Clin. J. Sport Med.* 19 (1), 3–8. doi:10.1097/JSM.0b013e318190bddb

Niederer, D., Keller, M., Achtnich, A., Akoto, R., Ateschrang, A., Banzer, W., et al. (2019). Effectiveness of a home-based re-injury prevention program on motor control, return to sport and recurrence rates after anterior cruciate ligament reconstruction: Study protocol for a multicenter, single-blind, randomized controlled trial (PReP). *Trials* 20 (1), 495. doi:10.1186/s13063-019-3610-2

Novaretti, J. V., Franciozi, C. E., Forgas, A., Sasaki, P. H., Ingham, S., and Abdalla, R. J. (2018). Quadriceps strength deficit at 6 Months after ACL reconstruction does not predict return to preinjury sports level. *Sports Health* 10 (3), 266–271. doi:10.1177/1941738118759911

Nurse, M. A., and Nigg, B. M. (2001). The effect of changes in foot sensation on plantar pressure and muscle activity. *Clin. Biomech. (Bristol, Avon)* 16 (9), 719–727. doi:10.1016/s0268-0033(01)00090-0

Nyland, J., Brosky, T., Currier, D., Nitz, A., and Caborn, D. (1994). Review of the afferent neural system of the knee and its contribution to motor learning. *J. Orthop. Sports Phys. Ther.* 19 (1), 2–11. doi:10.2519/jospt.1994.19.1.2

Ortiz, A., Capo-Lugo, C. E., and Venegas-Rios, H. L. (2014). Biomechanical deficiencies in women with semitendinosus-gracilis anterior cruciate ligament reconstruction during drop jumps. *PM R.* 6 (12), 1097–1106. doi:10.1016/j.pmrj.2014.07.003

Pan, J., Liu, C., Zhang, S., and Li, L. (2016). Tai Chi can improve postural stability as measured by resistance to perturbation related to upper limb movement among healthy older adults. *Evid. Based Complement. Altern. Med.* 2016, 9710941. doi:10.1155/2016/9710941

Park, J. S., Nam, D. C., Kim, D. H., Kim, H. K., and Hwang, S. C. (2012). Measurement of knee morphometrics using mri: A comparative study between ACL-injured and non-injured knees. *Knee Surg. Relat. Res.* 24 (3), 180–185. doi:10.5792/ksrr.2012.24.3.180

Paterno, M. V., Schmitt, L. C., Ford, K. R., Rauh, M. J., Myer, G. D., Huang, B., et al. (2010). Biomechanical measures during landing and postural stability predict second anterior cruciate ligament injury after anterior cruciate ligament reconstruction and return to sport. *Am. J. Sports Med.* 38 (10), 1968–1978. doi:10.1177/0363546510376053

Patterson, M. R., and Delahunt, E. (2013). A diagonal landing task to assess dynamic postural stability in ACL reconstructed females. *Knee.V. All rights Reserv.* 20 (6), 532–536. doi:10.1016/j.knee.2013.07.008

Redler, L. H., Sugimoto, D., Bassett, A. J., Kocher, M. S., Micheli, L. J., and Heyworth, B. E. (2021). Effect of concomitant meniscal tear on strength and functional performance in young athletes 6 Months after anterior cruciate ligament reconstruction with hamstring autograft. *Orthop. J. Sports Med.* 9 (11), 23259671211046608. The Author(s) 2021. doi:10.1177/23259671211046608

Reider, B., Arcand, M. A., Diehl, L. H., Mroczek, K., Abulencia, A., Stroud, C. C., et al. (2003). Proprioception of the knee before and after anterior cruciate ligament reconstruction. *Arthroscopy* 19 (1), 2–12. doi:10.1053/jars.2003.50006

Robinson, J. J., Hannon, J., Goto, S., Singleton, S. B., and Garrison, J. C. (2022). Adolescent athletes demonstrate inferior objective profiles at the time of return to sport after ACLR compared with healthy controls. *Orthop. J. Sports Med.* 10 (1), 232596712110635. The Author(s) 2022. doi:10.1177/23259671211063576

Ross, S. E., and Guskiewicz, K. M. (2004). Examination of static and dynamic postural stability in individuals with functionally stable and unstable ankles. *Clin. J. Sport Med.* 14 (6), 332–338. doi:10.1097/00042752-200411000-00002

Sadeghi, H., Hakim, M. N., Hamid, T. A., Amri, S. B., Razeghi, M., Farazdaghi, M., et al. (2017). The effect of exergaming on knee proprioception in older men: A randomized controlled trial. *Arch. Gerontol. Geriatr.* 69, 144–150. doi:10.1016/j.archger.2016.11.009

Schilaty, N. D., Nagelli, C., Bates, N. A., Sanders, T. L., Krych, A. J., Stuart, M. J., et al. (2017). Incidence of second anterior cruciate ligament tears and identification of associated risk factors from 2001 to 2010 using a geographic database. *Orthop. J. Sports Med.* 5 (8), 2325967117724196. doi:10.1177/2325967117724196

Schmitt, L. C., Paterno, M. V., and Hewett, T. E. (2012). The impact of quadriceps femoris strength asymmetry on functional performance at return to sport following anterior cruciate ligament reconstruction. *J. Orthop. Sports Phys. Ther.* 42 (9), 750–759. doi:10.2519/jospt.2012.4194

Schultz, R. A., Miller, D. C., Kerr, C. S., and Micheli, L. (1984). Mechanoreceptors in human cruciate ligaments. A histological study. *J. Bone Jt. Surg. Am.* 66 (7), 1072–1076. doi:10.2106/00004623-198466070-00014

Shaw, T., Williams, M. T., and Chipchase, L. S. (2005). Do early quadriceps exercises affect the outcome of ACL reconstruction? A randomised controlled trial. *Aust. J. Physiother.* 51 (1), 9–17. doi:10.1016/s0004-9514(05)70048-9

Shen, M., Che, S., Ye, D., Li, Y., Lin, F., and Zhang, Y. (2019). Effects of backward walking on knee proprioception after ACL reconstruction. *Physiother. Theory Pract.* 37, 1109–1116. doi:10.1080/09593985.2019.1681040

Shiraishi, M., Mizuta, H., Kubota, K., Otsuka, Y., Nagamoto, N., and Takagi, K. (1996). Stabilometric assessment in the anterior cruciate ligament-reconstructed knee. *Clin. J. Sport Med.* 6 (1), 32–39. doi:10.1097/00042752-199601000-00008

Song, Q., Zhang, X., Mao, M., Sun, W., Zhang, C., Chen, Y., et al. (2021). Relationship of proprioception, cutaneous sensitivity, and muscle strength with the balance control among older adults. *J. Sport Health Sci.* 10 (5), 585–593. doi:10.1016/j.jshs.2021.07.005

Stensdotter, A. K., Tengman, E., and Hager, C. (2016). Altered postural control strategies in quiet standing more than 20 years after rupture of the anterior cruciate ligament. *Gait Posture* 46, 98–103. doi:10.1016/j.gaitpost.2016.02.020

Strzalkowski, N. D., Triano, J. J., Lam, C. K., Templeton, C. A., and Bent, L. R. (2015). Thresholds of skin sensitivity are partially influenced by mechanical properties of the skin on the foot sole. *Physiol. Rep.* 3 (6), e12425. doi:10.14814/phy2.12425

Sugimoto, D., Howell, D. R., Micheli, L. J., and Meehan, W. R. (2016). Single-leg postural stability deficits following anterior cruciate ligament reconstruction in pediatric and adolescent athletes. *J. Pediatr. Orthop. B* 25 (4), 338–342. doi:10.1097/bpb.0000000000000276

Sun, W., Song, Q., Yu, B., Zhang, C., and Mao, D. (2015). Test-retest reliability of a new device for assessing ankle joint threshold to detect passive movement in healthy adults. *J. Sports Sci.* 33 (16), 1667–1674. doi:10.1080/02640414.2014.1003589

Tahayori, B., and Koceja, D. M. (2012). Activity-dependent plasticity of spinal circuits in the developing and mature spinal cord. *Neural Plast.* 2012, 964843. doi:10.1155/2012/964843

Tulloch, E., Phillips, C., Sole, G., Carman, A., and Abbott, J. H. (2012). DMA clinical pilates directional-bias assessment: Reliability and predictive validity. *J. Orthop. Sports Phys. Ther.* 42 (8), 676–687. doi:10.2519/jospt.2012.3790

Webster, K. A., and Gribble, P. A. (2010). Time to stabilization of anterior cruciate ligament-reconstructed versus healthy knees in National Collegiate Athletic Association Division I female athletes. *J. Athl. Train.* 45 (6), 580–585. doi:10.4085/1062-6050-45.6.580

White, K. K., Lee, S. S., Cutuk, A., Hargens, A. R., and Pedowitz, R. A. (2003). EMG power spectra of intercollegiate athletes and anterior cruciate ligament injury risk in females. *Med. Sci. Sports Exerc* 35 (3), 371–376. doi:10.1249/01.MSS.0000053703.65057.31

Wolfson, L., Whipple, R., Derby, C. A., Amerman, P., and Nashner, L. (1994). Gender differences in the balance of healthy elderly as demonstrated by dynamic posturography. *J. Gerontol.* 49 (4), M160–M167. doi:10.1093/geronj/49.4.m160

Zhang, S., and Li, L. (2013). The differential effects of foot sole sensory on plantar pressure distribution between balance and gait. *Gait Posture* 37 (4), 532–535. doi:10.1016/j.gaitpost.2012.09.012

Zhang, T., Mao, M., Sun, W., Li, L., Chen, Y., Zhang, C., et al. (2021). Effects of a 16-week Tai Chi intervention on cutaneous sensitivity and proprioception among older adults with and without sensory loss. *Res. Sports Med.* 29 (4), 406–416. doi:10.1080/15438627.2021.1906673

TYPE Original Research
PUBLISHED 19 January 2023
DOI 10.3389/fbioe.2023.1060059

Check for updates

OPEN ACCESS

EDITED BY
Qichang Mei,
Ningbo University, China

REVIEWED BY
Yijian Zhang,
The First Affiliated Hospital of Soochow University, China
Miha Vodicar,
University Medical Centre Ljubljana, Slovenia

*CORRESPONDENCE
Xueqing Wu,
xueqingwu@buaa.edu.cn
Shuqin Wu,
wushuqin@nuc.edu.cn

†These authors have contributed equally to this work and share first authorship

SPECIALTY SECTION
This article was submitted to Biomechanics, a section of the journal Frontiers in Bioengineering and Biotechnology

RECEIVED 04 October 2022
ACCEPTED 09 January 2023
PUBLISHED 19 January 2023

CITATION
Pei B, Xu Y, Zhao Y, Wu X, Lu D, Wang H and Wu S (2023), Biomechanical comparative analysis of conventional pedicle screws and cortical bone trajectory fixation in the lumbar spine: An in vitro and finite element study.
Front. Bioeng. Biotechnol. 11:1060059.
doi: 10.3389/fbioe.2023.1060059

Biomechanical comparative analysis of conventional pedicle screws and cortical bone trajectory fixation in the lumbar spine: An in vitro and finite element study

Baoqing Pei[1†], Yangyang Xu[1†], Yafei Zhao[2], Xueqing Wu[1]*, Da Lu[1], Haiyan Wang[3] and Shuqin Wu[4]*

[1]Beijing key laboratory for design and evaluation technology of advanced implantable & interventional medical devices, Beijing Advanced Innovation Center for Biomedical Engineering, School of Biological Science and Medical Engineering, Beihang University, Beijing, China, [2]Aerospace center hospital, Beijing, China, [3]School of Basic Medicine, Inner Mongolia Medical University, Hohhot, China, [4]School of Big Data and Information, Shanxi College of Technology, Shanxi, China

Numerous screw fixation systems have evolved in clinical practice as a result of advances in screw insertion technology. Currently, pedicle screw (PS) fixation technology is recognized as the gold standard of posterior lumbar fusion, but it can also have some negative complications, such as screw loosening, pullout, and breakage. To address these concerns, cortical bone trajectory (CBT) has been proposed and gradually developed. However, it is still unclear whether cortical bone trajectory can achieve similar mechanical stability to pedicle screw and whether the combination of pedicle screw + cortical bone trajectory fixation can provide a suitable mechanical environment in the intervertebral space. The present study aimed to investigate the biomechanical responses of the lumbar spine with pedicle screw and cortical bone trajectory fixation. Accordingly, finite element analysis (FEA) and *in vitro* specimen biomechanical experiment (IVE) were performed to analyze the stiffness, range of motion (ROM), and stress distribution of the lumbar spine with various combinations of pedicle screw and cortical bone trajectory screws under single-segment and dual-segment fixation. The results show that dual-segment fixation and hybrid screw placement can provide greater stiffness, which is beneficial for maintaining the biomechanical stability of the spine. Meanwhile, each segment's range of motion is reduced after fusion, and the loss of adjacent segments' range of motion is more obvious with longer fusion segments, thereby leading to adjacent-segment disease (ASD). Long-segment internal fixation can equalize total spinal stresses. Additionally, cortical bone trajectory screws perform better in terms of the rotation resistance of fusion segments, while pedicle screw screws perform better in terms of flexion–extension resistance, as well as lateral bending. Moreover, the maximum screw stress of L4 cortical bone trajectory/L5 pedicle screw is the highest, followed by L45 cortical bone trajectory. This biomechanical analysis can accordingly provide inspiration for the choice of intervertebral fusion strategy.

KEYWORDS

biomechanical phenomena, finite element analysis, biomechanical tests, cortical bone trajectory screws, pedicle screws, hybrid screw strategy

1 Introduction

Numerous intervertebral fusion techniques have arisen as a result of the ongoing upgrading of internal fixation techniques. There are several intervertebral fusion techniques, since internal fixation techniques are always being updated. After short-segment fixation, ASD may emerge, necessitating the selection of yet another surgical strategy. The traditional trajectory for PS requires significant tissue dissection and muscle retraction, whereas the cortical bone trajectory (CBT) screw has the advantages of minimal muscle damage and the preservation of the superior facet joint (Qiu et al., 2022) (Figure 1). Many biomechanical studies have proved that the CBT technique provides greater pull-out strength, rigid insertion torque fixation, and a stable screw structure similar to traditional PS (Matsukawa et al., 2016; Sansur et al., 2016). Less research has been carried out on the impact of various screw implantation strategies on the stability and flexibility of the lumbar spine. The effects of numerous spinal fusion methods on spinal stiffness are still unclear, and research on the benefits and drawbacks of each method is still lacking. Physicians are curious to see whether combining traditional PS and CBT has benefits and how the unique mechanical features function. How to select the correct screw fixation technology to treat degenerative spinal conditions is the problem of the greatest concern for clinicians. For this reason, FEA and IVEs are frequently available.

For the treatment of lumbar instability and ADS surgery, a precise biomechanical analysis of the various surgical modalities is necessary to choose the best option for effective lumbar internal fixation. To define the intricate biomechanical characteristics of the lumbar spine, complementary methods include FEA and IVEs (Xu et al., 2013; Lu and Lu, 2019). In this study, the distribution pattern of the internal fixation system was explored, and the data were analyzed to explore the mechanical references for procedure selection in clinical practice. FEA and IVEs of the T12-S1 vertebral body were performed using different combinations of screw placement techniques to reveal the biomechanical differences between different implantation techniques. The main goals of this study were as follows: 1) to create a workable finite element model (FEM) of the lumbar spine; 2) to simulate screw placement techniques on the models; 3) to compare the stress distribution of the posterior screw–rod system under various screw placement techniques; 4) to create specimen models of various posterior screw–rod systems; and 5) to test the differences in joint mobility and stiffness values between the FEMs and the IVEs.

2 Materials and methods

The research was approved by the Science and Ethics Committee of the School of Biological Science and Medical Engineering at Beihang University (protocol code: BM20220087).

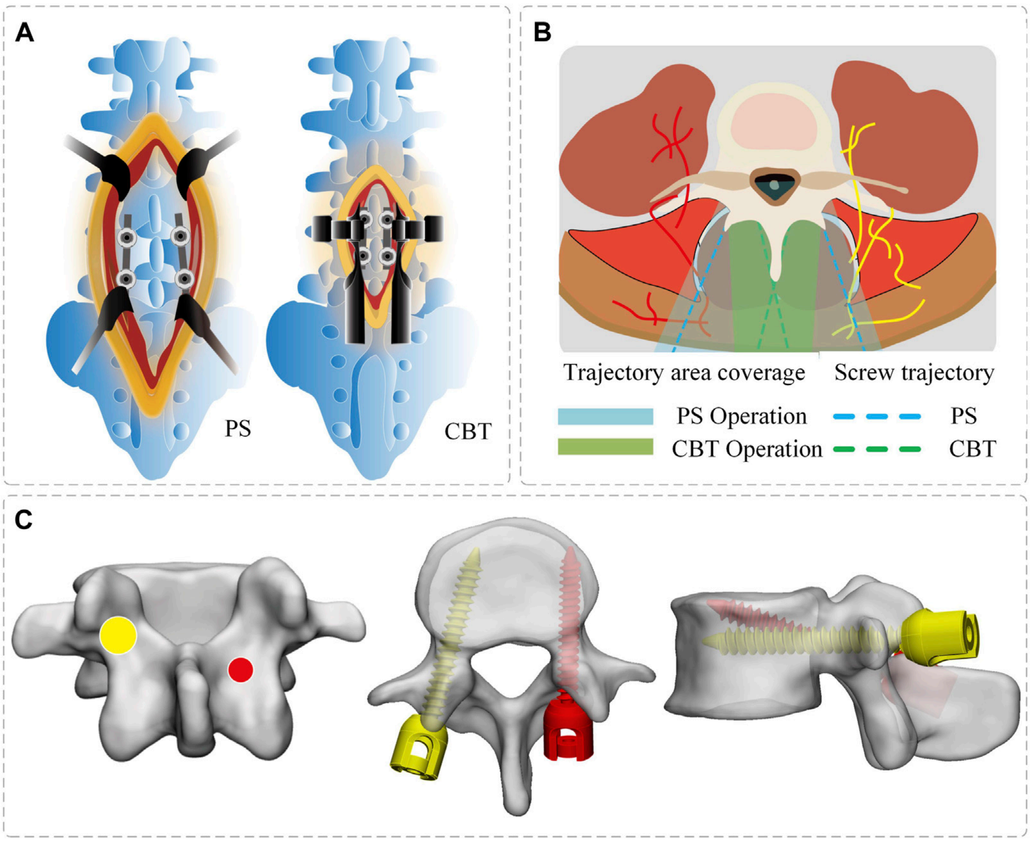

FIGURE 1
Schematic diagram of screw placement. **(A)** Surgical incision in PS/CBT group. **(B)** PS/CBT trajectory area coverage. **(C)** Position of the entry point and screw trajectory (PS—yellow, CBT—red). The screw entry point PS is located at the apex of the herringbone crest and CBT is located at the isthmus of the vertebral arch.

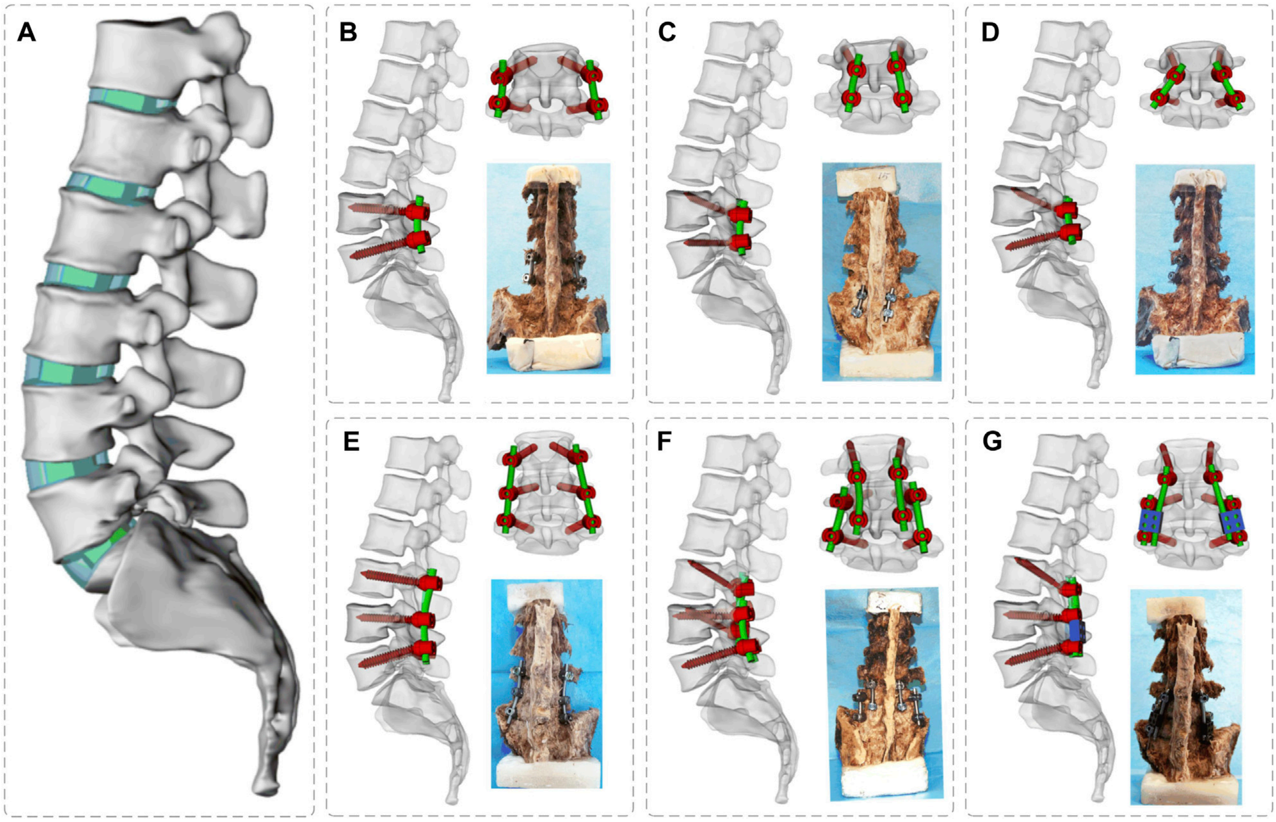

FIGURE 2
Three-dimensional simulation models and spine specimen models for posterior internal fixation of T12-S segment lumbar spine. **(A)** Intact model, **(B)** L45 PS model, **(C)** L45CBT model, **(D)** L4 CBT/L5 PS model, **(E)** L345 PS model, **(F)** L34CBT/L45PS model, and **(G)** L3 CBT-L45 PS model.

2.1 Grouping

In this study, we established one intact model, three common clinical single-segment fusion groups, and three dual-segment fusion groups for the treatment of ASD, with a total of seven groups of models: 1) the intact model, 2) the L45PS model, 3) the L45CBT model, 4) the L4CBT/L5 PS model, 5) the L345 PS model, 6) the L34CBT/L45PS model, and 7) the L3CBT lateral connection L45PS (L3CBT-L45PS) model (Figure 2).

2.2 *In Vitro* specimen biomechanical experiments

2.2.1 Sample selection and processing

Seven adult spine specimens (provided by Beijing Chaoyang Hospital of Capital Medical University) were selected, preserving CT imaging data without obvious imaging abnormalities, such as lumbar spine trauma, tumor, tuberculosis, scoliosis, lumbar spondylolisthesis, ischial cleft, and other diseases. Before the experiment, the specimens were wrapped in multiple layers of cling film and stored at a temperature of −20°C. The specimens were then thawed at a temperature of 4°C for 12–18 h. Using the T12-S1 section of the lumbar spine as the experimental sample, the muscles and soft tissues surrounding the vertebrae were removed in accordance with the anatomical structure, but the ligaments, tiny joints, and intervertebral discs were left in place. The specimens were kept moist with 0.9% saline throughout the testing procedure. The upper end of the L1 vertebral body and the caudal end of the S1 vertebral body was embedded in polymethylmethacrylate (PMMA) using a custom-made embedding cassette mounted on the testing device (Wang et al., 2020a). Screw placement was carried out by orthopedic surgeons from Beijing Chao-yang Hospital of Capital Medical University.

2.2.2 Experimental methods and procedures

The upper end of vertebra L1 is fixedly attached to the front end of a six-degree-of-freedom robotic arm (NX100MH6, Yaskawa Robotic Arm, Kitakyushu, Japan), and the tail vertebra S1 is embedded in a fixed base frame. A moment sensor (Gamma, ATI Industrial Automation, Ontario, Canada) is mounted on the head of the robot arm to record applied forces and moments and provide real-time feedback. The NDI system (Optotrak Certus, North Digital Ltd., Waterloo, Canada) captures the motion path of each vertebral segment by recording the position of several sets of marker points. Motion data acquisition utilizes the 3D spatial coordinate system differences of the NDI system to determine the relative motion position of the vertebral body. In this experiment, five marker points were fixed at T12, L1, L2, L3, L4, L5, and the base (reference point) for capturing the motion path of each segment during lumbar vertebral motion (Figure 3).

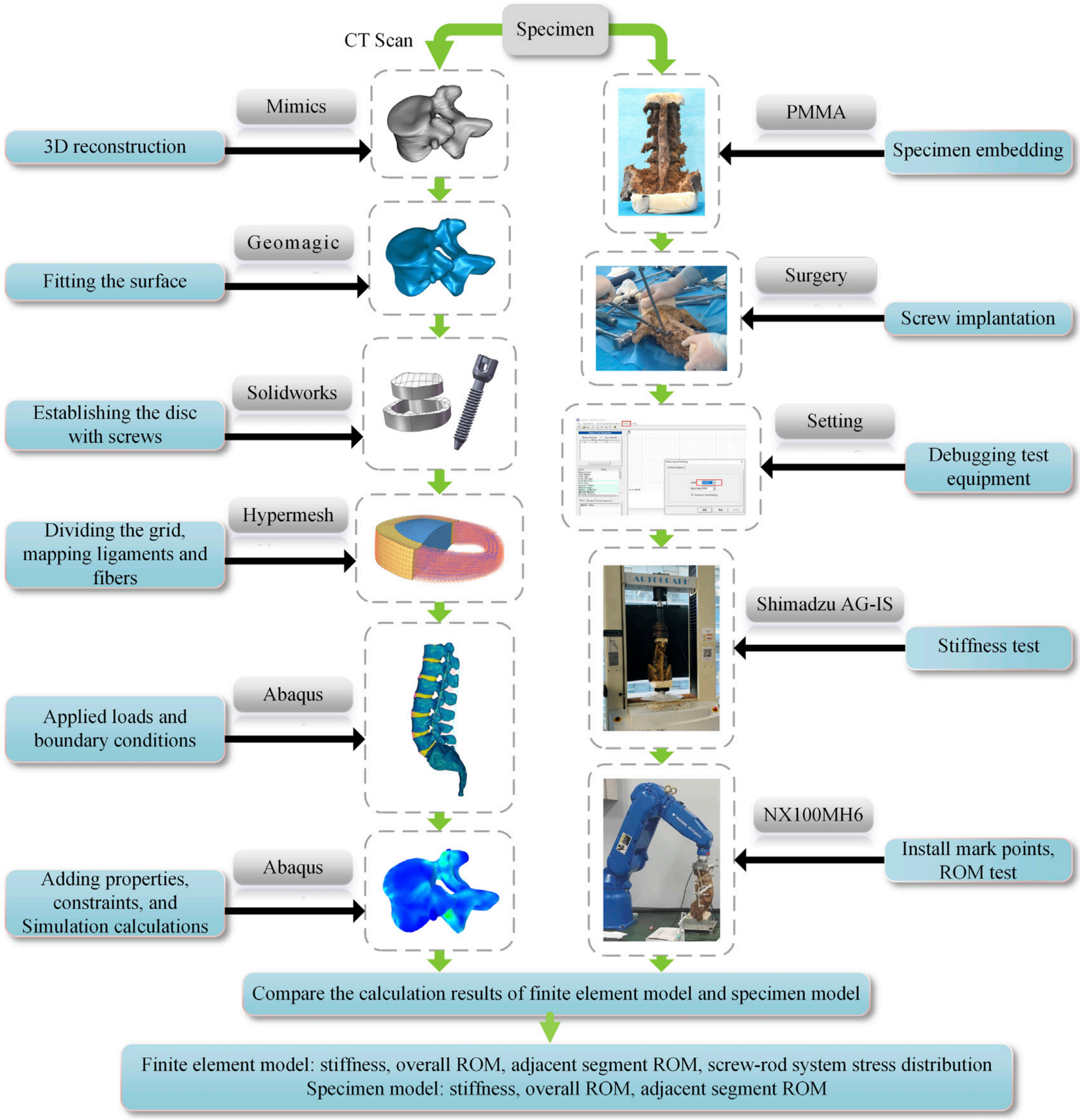

FIGURE 3
Flow chart of FEA and IVE.

The experimental loading method was as follows: a Panjabi pure moment loading control protocol was used with a constant loading rate of 1.0°/s (Panjabi, 2003; Panjabi, 2007). In the experiment, the moment-controlled loading mode was used, and the loading mode procedure was set to 7.5°Nm of forwarding flexion, back extension, left and right lateral bending, and left and right axial rotation. This experiment procedure requires the constant spraying of saline on the specimen to maintain wetness and a room experimental temperature of 25°C.

2.3 Finite element analysis

2.3.1 Finite element model establishing

High-resolution CT scans were performed on the specimens, and the obtained DICOM data were imported into Mimics 21.0 (Materialise, Leuven, Belgium) to obtain the T12-S1 vertebrae by threshold segmentation. To obtain a high-quality vertebral model, the model was processed in Geomagic Studio 2013 (Raindrop Geomagic Inc., Morrisville, NC, United States) for denoising, smoothing, and fitting the surface; the medullary nucleus and fibrous ring matrix were drawn in Solidworks (SolidWorks Corp., Waltham, MA, United States). The entire model was meshed and the ligament and annulus fibrosus fibers were created in Hypermesh (Altair Engineering Inc., Troy, MI, United States). The material properties, set boundaries, loading conditions, and computational conditions were defined, and the FEA was completed in Abaqus (Simulia, Providence, Rhode Island, United States) (Figure 3).

The bone tissue consists of cortical and cancellous elements. The intervertebral disc has a nucleus pulposus, a fibrous annulus matrix, and fibrous annulus fibrosus, which is divided into seven layers (Wang et al., 2019). The model includes the major lumbar ligaments: including the anterior longitudinal ligament (ALL), posterior longitudinal ligament (PLL), ligamentum flavum (FL), supraspinous ligament (SSL), interspinous ligament (ISL), intertransverse ligament

TABLE 1 Material properties of the models.

Structure	Young's modulus (MPa)	Poisson's ratio	Cross-section area (mm^2)
Cortical bone	Ex = 11,300, Ey = 11,300, Ez = 22,300	V_{xy} = 0.484, V_{xz} = 0.203, V_{yz} = 0.203	-
	G_X = 3,800, G_Y = 5,400, G_Z = 5,400		
Cancellous bone	Ex = 140, Ey = 140, Ez = 200	V_{xy} = 0.45, V_{xz} = 0.315, V_{yz} = 0.315	-
	G_X = 48.3, G_Y = 48.3, G_Z = 48.3		
ALL	7.8(<12.0%), 20.0(>12.0%)	0.40	63.7
PLL	10.0(<11.0%), 20.0(>11.0%)	0.30	20
SSL	8.0(<20.0%), 15.0(>20.0%)	0.30	70
ISL	10.0(<14.0%), 11.6(>14.0%)	0.30	70
LF	15.8(<6.2%), 19.5(>6.2%)	0.30	40
TL	10.0(<18.0%), 58.4(>18.0%)	0.30	1.8
CL	7.5(<25.0%), 32.9(>25.0%)	0.30	30
Nucleus pulposus	Hyperelastic, Mooney–Rivlin: C^{10} = 0.18, C^{01} = 0.045	-	-
Annulus fibrosus matrix	Hyperelastic, Mooney–Rivlin: C^{10} = 0.12, C^{01} = 0.03	-	-
Fiber	360–550	0.30	0.15
screw–rods system	110,000	0.28	-

ALL, anterior longitudinal ligament; PLL, posterior longitudinal ligament; SSL, supraspinal ligament; ISL, interspinous ligament; LF, ligamentum flavum; TL, transverse ligaments; CL, capsular ligament.

(TL), and capsular ligament (FC). A 0.25 mm-thick cartilage layer was also added to the surface of each small joint and a 0.5 mm gap was created between the curved small joints (Caruso et al., 2018). PS size (diameter 6.5 mm, length 45 mm), CBT screw size (diameter 5 mm, length 35 mm), and connecting rod size (diameter 5.5 mm) were set. Tetrahedral meshing was performed for all vertebrae, intervertebral discs, articular cartilage, and screw–rod systems, and the material properties of each part of the model and the cross-sectional areas of ligaments and fibers are shown in Table 1.

2.3.2 Boundary conditions

The local muscle force of the lumbar spine was provided by a follower load of 200 N (Rui et al., 2018), and a preload compression force of 400 N body weight was applied at the center of the upper endplate of T12 (Renner et al., 2007). The physical movements of flexion, extension, right and left lateral bending, and right and left axial rotation were replicated using a torque of 7.5 Nm (Alizadeh et al., 2013), small inter-articular contacts were set with a friction factor of 0.1 (Tsouknidas, 2015), and all remaining contacts were "tie" constraints. Fixation constraints were added at the sacrum (Figures 4A,B,C).

2.4 Validation of the models

The ROM of each segmental value measured by the model was compared with the experimental data reported in previous studies to validate the plausibility of the model. Mean ROM values were measured in each motion type and the results were compared with previously published biomechanical experiments and FEA (Chen et al., 2001; Xiao et al., 2012; Biswas et al., 2018; Song et al., 2021). The trends were consistent and there were no significant differences in the data, proving that the model was reasonable (Figure 4D).

3 Results

In this study, the following parameters were evaluated: 1) compressive stiffness in the T12-S segment; 2) overall ROM; 3) ROM of the adjacent segment; 4) ROM of each segment of T12-L5; and 5) Von Mises stress distribution of the screw–rod system.

3.1 Stiffness

The results of the FEM group and the IVE group showed that the stiffness of dual-segment internal fixation was stronger than that of single-segment internal fixation, and both were greater than that of the intact model, showing a specific variation pattern. The FEM group's changing trend in single-segment internal fixation stiffness was significantly less, but the changing trend in the IVE group was clear. The results reveal that the FEM group followed the same pattern as the IVE group: L34CBT/L45PS (FEA: 115.81 N/mm, IVE: 98.12 N/mm)> L3CBT-L45PS (FEA: 114.67 N/mm, IVE: 90.44 N/mm)> L345PS (FEA: 107.77 N/mm, IVE: 87.74 N/mm)> L4CBT/L5PS (FEA: 78.27 N/mm, IVE: 65.46 N/mm)> L45CBT (FEA: 77.35 N/mm, IVE: 59.98 N/mm)> L45PS(FEA: 76.79 N/mm, IVE: 48.59 N/mm)> Intact. (Figure 5B).

3.2 Overall range of motion

FEM group: Compared with the intact model, the L45CBT significantly decreased ROM in flexion–extension and lateral bending conditions, but decreased ROM less in rotation. L4CBT/L5PS rotational ROM decreased the most, but ROM was decreased less in flexion and extension and lateral bending conditions. L345PS,

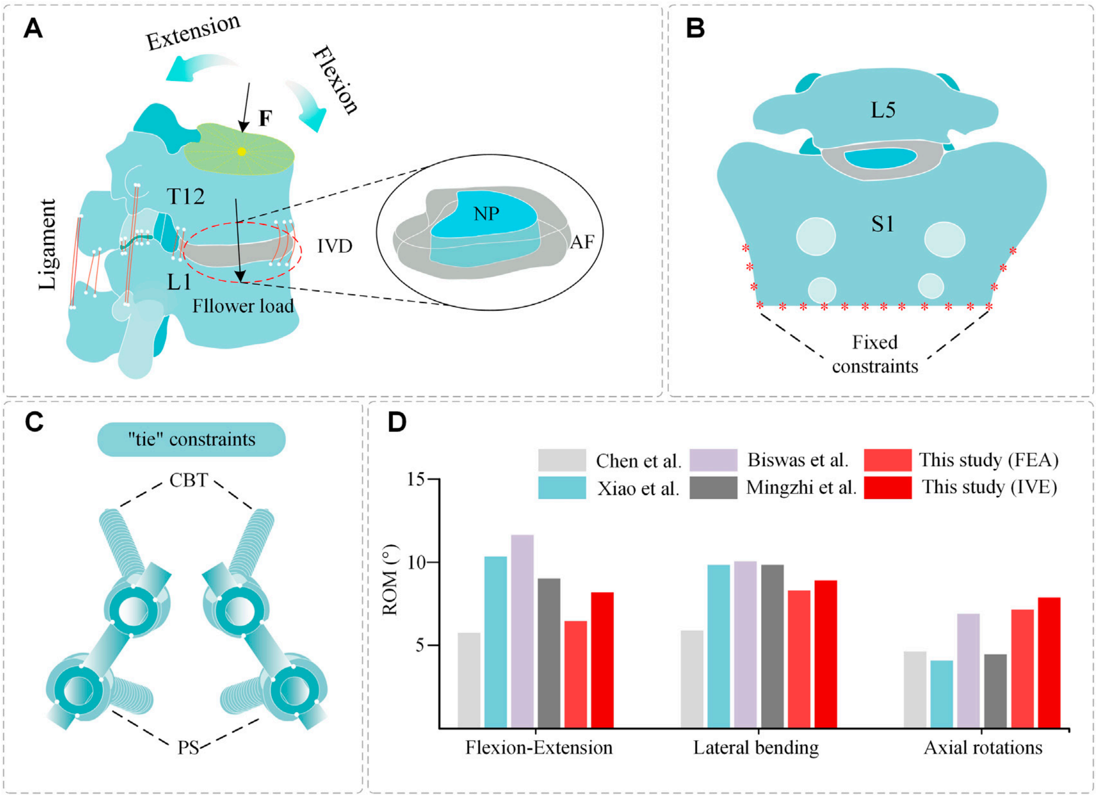

FIGURE 4
Spinal composition, constraint setting, and validation. **(A)** Spinal constraint setting: compression force F, follower load. **(B)** Spinal constraint setting: S1 fixed constraints. **(C)** Hybrid placement of screws and "tie" constrains. **(D)** Comparison of ROM, between this study and the results reported in the previous literature.

L34CBT/L45PS, and L3CBT-L45PS displayed similar ROM performance in flexion and extension and lateral bending, and L345PS rotational ROM was less decreased. IVE group: Compared with the intact model, the overall ROM of the L45CBT was significantly reduced in flexion–extension and lateral bending conditions, but less in rotation. L45PS rotational ROM loss was significant, but ROM was decreased less in flexion and extension and lateral bending conditions. L34CBT/L45PS had a significant decrease in flexion–extension and rotational ROM. L3CBT-L45PS showed a significant decrease in ROM in lateral bending, and a slightly greater decrease in ROM in the two-segment internal fixation approach than in the single-segment internal fixation approach (Figure 5D).

3.3 Adjacent-segment range of motion

Following internal fixation surgery, both the FEM group and the IVE group saw varying degrees of ROM loss in adjacent-segment mobility.

FEM group: Compared with the intact model, the adjacent-segment (L3) ROM of the single-segment fusion (L4-L5) was decreased. In the three conditions of flexion–extension, lateral bending, and rotational ROM, L45PS decreased by 80.1%, 73.3%, and 72.7%; L45CBT decreased by 80.9%, 70.1%, and 72.6%; and L4CBT/L5PS decreased by 72.6%, 62.5%, and 67.4%, respectively. Compared with the intact model, the adjacent-segment (L2) ROM of the dual-segment fusion (L3-L5) was decreased. L345PS decreased by 63.0%, 65.5%, and 53.7%; L3CBT-L45PS decreased by 61.6%, 65.9%, and 44.2%; and L34CBT/L45PS decreased by 54.8%, 61.8%, and 48.3% (Figure 6A).

The ROM of the adjacent segments between the single/dual-segment internal fixation is determined by the L3 segment and L2 segment, and since they are not the same segment, the single-segment internal fixation L2 segment was analyzed to facilitate a better comparison with the dual-segment internal fixation surgical approach. The outcomes demonstrated comparable changes in adjacent-segment ROM with the identical fusion segment, and the surgical technique used had no appreciable impact on adjacent-segment ROM. However, there was a difference between single-segment and dual-segment internal fixation, and dual-segment internal fixation resulted in a greater loss of adjacent-segment ROM (Figure 6B).

IVE group: Compared with the intact model, the adjacent-segment (L3) ROM of the single-segment fusion (L4-L5) was decreased. In the three conditions of flexion–extension, lateral bending, and rotation ROM, L45PS decreased by 56.0%, 52.7%, and 47.1%; L45CBT decreased by 63.8%, 55.6%, and 36.2%; and L4CBT/L5PS decreased by 44.1%, 47.5%, and 49.0%, respectively. Compared with the intact model, the adjacent-segment (L2) ROM of the dual-segment fusion (L3-L5) was decreased.

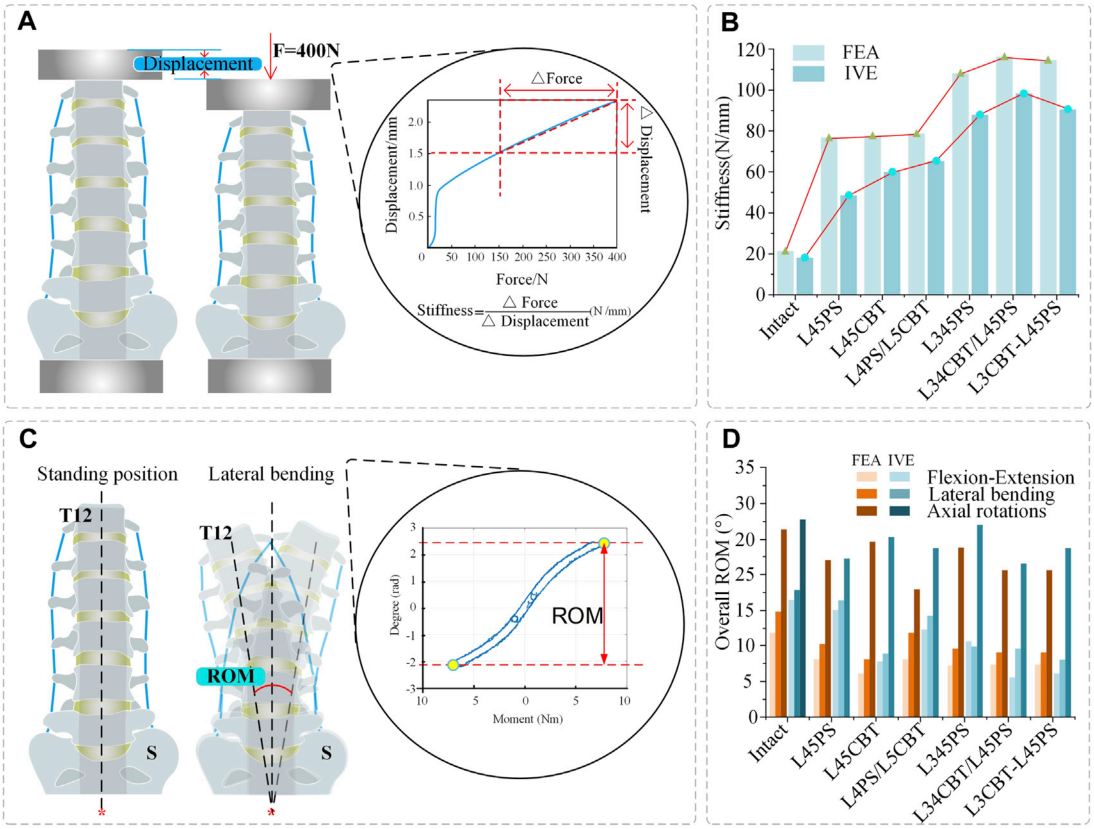

FIGURE 5
Stiffness and overall ROM. **(A)** Stiffness calculation (force–displacement curve). **(B)** Comparison of stiffness, between FEMs and IVEs under different conditions. **(C)** ROM measurement. **(D)** Comparison of overall ROM, between FEMs and IVEs under different operations.

L345PS decreased by 58.0%, 48.0%, and 46.8%; L3CBT-L45PS decreased by 61.1%, 61.9%, and 40.8%; and L34CBT/L45PS ROM decreased by 38.2%, 32.7%, and 37.2% (Figure 6C).

The same analysis was performed for the L2-segment ROM. L45PS decreased by 29.5%, 6.0%, and 15.4%; L45CBT decreased by 34.3%, 7.9%, and 16.7%; and L4CBT/L5PS decreased by 37.7%, 17.9%, and 33.8% (Figure 6D). With L45PS as the basis for the screw–rod lengthening procedure, L345PS, L34CBT/L45PS, and L3CBT-L45PS were decreased by 5.8%–18.7%, with a somewhat greater reduction in the ROM of IVE.

The results show that for adjacent-segment ROM, the pure CBT better preserved rotation, and the hybrid screw decreased the loss of flexion–extension and lateral bending ROM. The longer the fixed segment, the more ROM is lost.

3.4 Range of motion of each segment

For all segments of the FEM group, the ROM was read after internal fixation surgery, and as compared with the intact model, all segments' ROM showed a decline under various conditions. For non-fixed segments, the ROM of dual-segment internal fixation is smaller than that of single-segment internal fixation under flexion–extension and lateral bending conditions. Under rotation conditions, the ROM of the model with CBT screws was found to be smaller than that of simple PS screw fixation (Figure 7).

3.5 Von Mises stress of the screw–rod system

The stress data were collected by choosing 50 points from each area of the screw–rod system stress concentration and computing the average value as the screw–rod system's final stress value to exclude the influence of force singularities. L4CBT/L5PS and L45CBT had the highest stress values among the six conditions. L34CBT/L45PS bears more stress in rotations, L4CBT/L5PS bears more stress in extension, right lateral flexion, and left rotation, L45CBT bears more stress in flexion and left rotation, and L3CBT-L45PS bears more stress in rotation (Figure 8).

The stress is mostly centered in the connecting rod's center and the screw body's caudal end and its precise position is where the cortical bone comes into contact with the screw, as shown by the stress cloud figure. The PS screw's stress distribution is mostly focused in the back half of the screw body, whereas the CBT screw's stress distribution is concentrated in the head and tail of the screw, and the entire CBT screw is under severe stress. The upper screw is significantly more stressed than the lower screw. The middle layer of three-layer screws experiences the least stress, with the majority of the stress occurring in the top and lower layer. Axial rotation considerably increases the load on the screw below. The values obtained in the studies were all well below the maximum stress values for titanium, and as a consequence, there is no risk of rupture under normal settings when analyzing the risk of fracture of the screws employed in the stabilizing system (Figure 9).

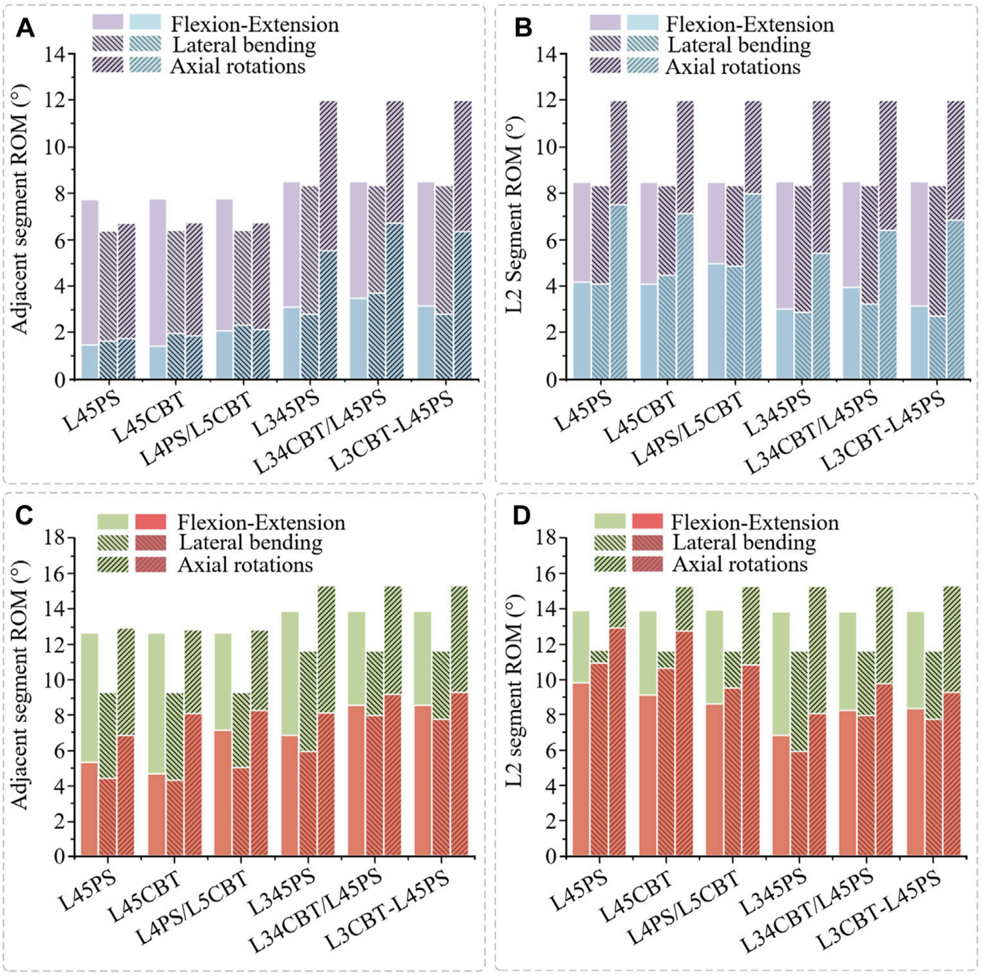

FIGURE 6
Adjacent-segment ROM and L2-segment ROM. **(A)** Comparison of adjacent-segment ROM, between postoperative FEMs (blue column) and the intact FEM (purple column). **(B)** Comparison of L2-segment ROM, between postoperative FEMs (blue column) and the intact FEM (purple column). **(C)** Comparison of adjacent-segment ROM, between postoperative IVEs (red column) and the intact IVE (green column). **(D)** Comparison of L2-segment ROM, between postoperative IVEs (red column) and the intact IVE (green column).

4 Discussion

A frequent and essential surgical approach for the treatment of spinal problems such as degenerative spine conditions is the internal fixation technique. Long and six screws both demonstrated improved lumbar spine sagittal stability. According to Spiegl et al. (2021), older individuals with mid-thoracic spinal instability treated with extended segmental stabilization had a much lower risk of subsequent vertebral fractures over time. Santoni et al. (2009) first introduced the CBT screw internal fixation approach in 2009, using screws along the caudal head sagittal and lateral paths. Later, Takata et al. (2014) presented a novel surgical technique that eliminates soft tissue stripping and shortens the incision length by fusing the upper portion with CBT screws and the lower segment with traditional pedicle screws. Numerous authors have also looked into the bone purchase of CBT screws. Using a human lumbar spine model, Santoni et al. (2009) examined the uniaxial tension of CBT screws and compared the axial pullout force of CBT screws with standard pedicle screws. Although lumbar pedicle screw fixation has the benefit of improving biomechanical stability, screw loosening and fracture can still happen as ASD progresses. The biomechanical examination of the various surgical procedures is crucial for successfully fusing the spine since it enables us to choose the best surgical strategy. There is no consensus regarding the evaluation of different spinal fusion methods leading to spinal stiffness. Additionally, little research has been conducted on the benefits and drawbacks of different fusion procedures (Park et al., 2009). In this experiment, a combination of FEA and IVE was used, and the experimental data were then cross-checked to increase their accuracy. This study's findings provide guidance for the decision-making process in terms of the best pedicle screw therapy for ADS.

The stiffness results of the FEM group and the IVE group were similar: L34CBT/L45PS > L3CBT-L45PS > L345PS > L4CBT/L5PS > L45CBT > L45PS > Intact. This study demonstrates that hybrid screw placement and CBT may both produce greater stiffness and improved stability. The researchers also discovered that compared with short-segment fixation, long-segment fixation produced higher stiffness (Kahaer et al., 2022b). The overall stress is decreased by lengthening the internal fixation system, and several biomechanical studies have demonstrated that the use of hybrid screws enhances the biomechanical stability of the joint. The spine's flexibility is greatly

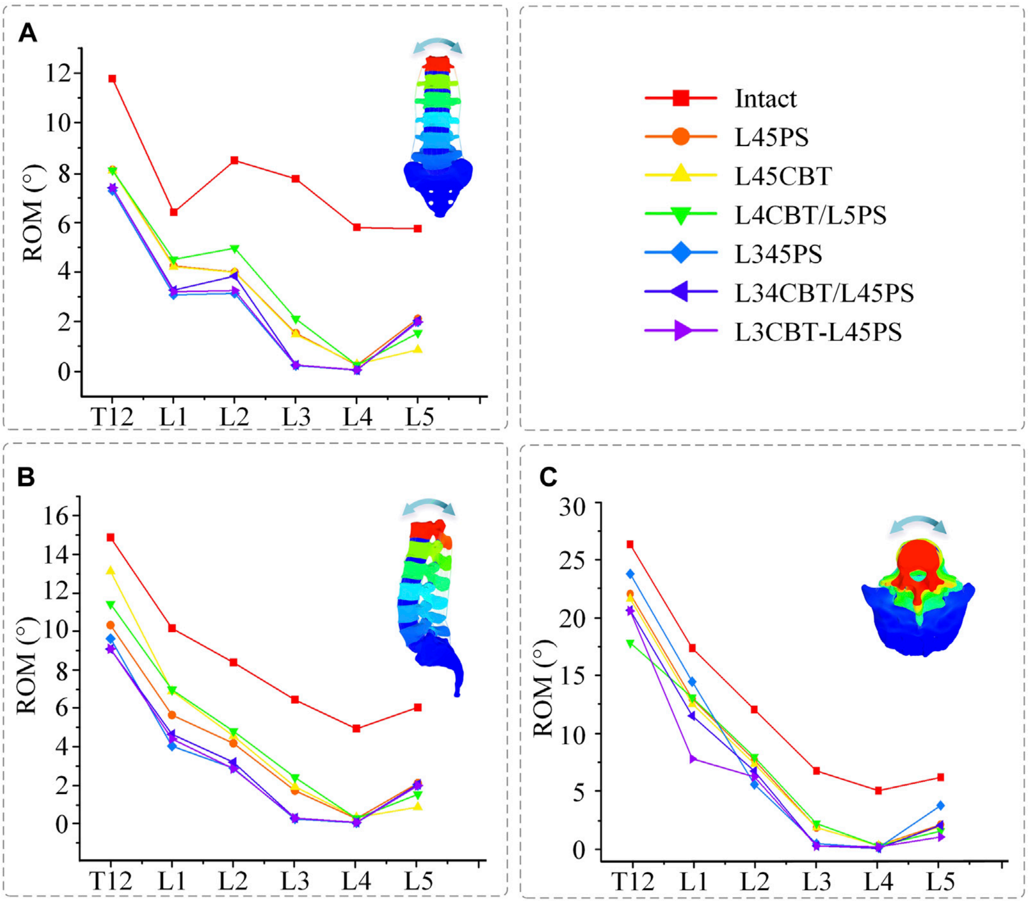

FIGURE 7
ROM for each segment between postoperative FEMs and the intact FEM. **(A)** Flexion–extension conditions. **(B)** Lateral bending conditions. **(C)** Axial rotation conditions.

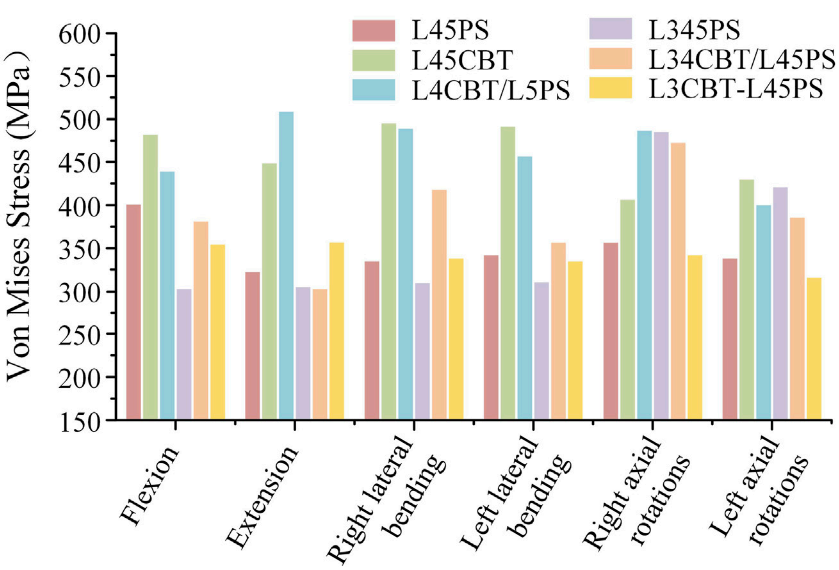

FIGURE 8
The stress value of screw–rod systems in six postoperative FEMs under different conditions.

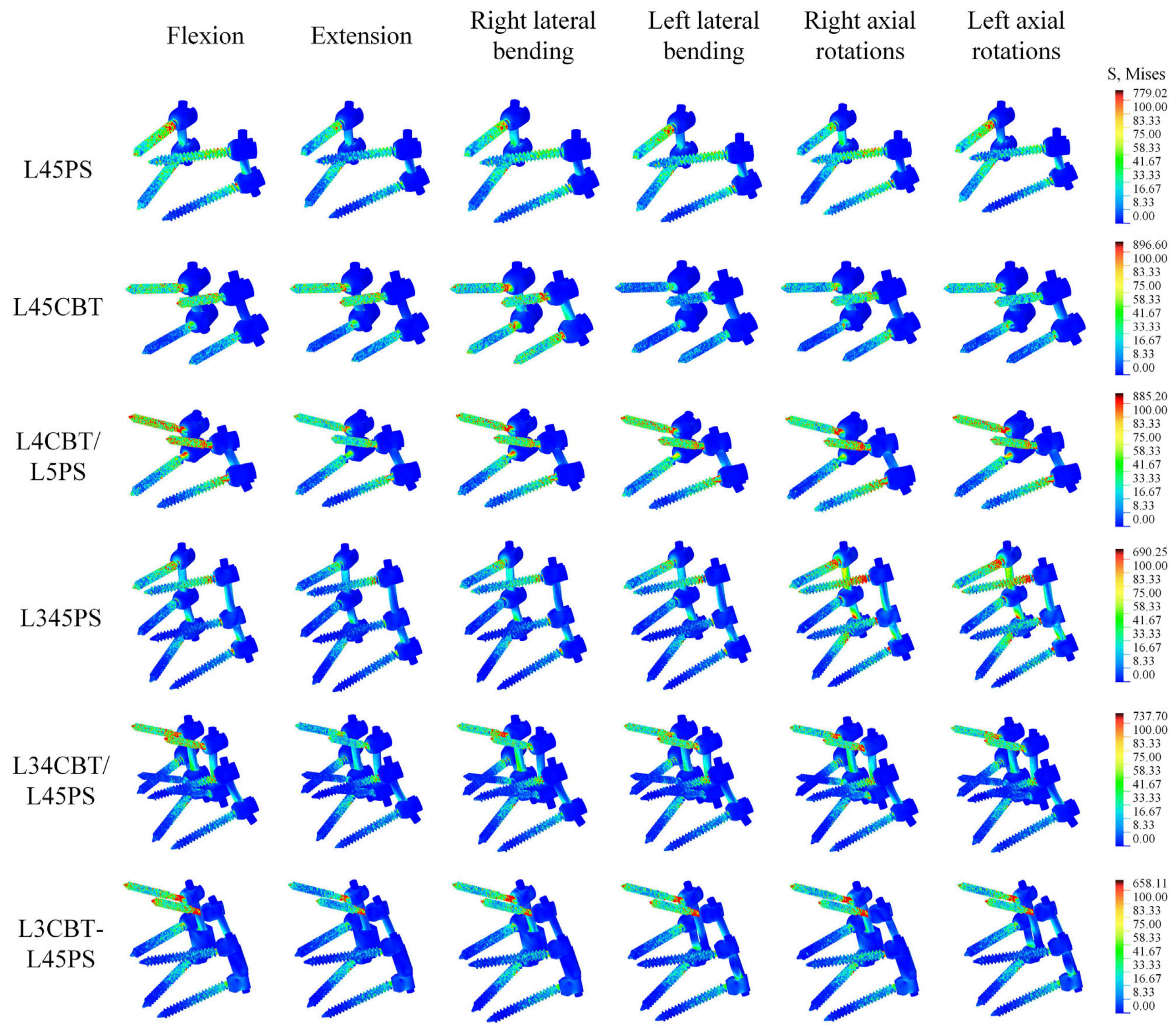

FIGURE 9
The stress distribution of screw–rod systems in six postoperative FEMs under different conditions. According to the indicator diagram, red indicates the stress concentration area, while blue shows the stress dispersion area.

decreased by posterior fixation, and its stiffness is significantly increased. The longer the fused segment, the stiffer the spine becomes; hence, the dual-segment internal fixation strategy is stiffer than the single-segment approach. Excessive stiffness may result in excessive spinal motion and may cause ASD (Goto et al., 2003; Dai et al., 2007). At present, the term stability is misused. A stable system is one that does not undergo a large displacement under small perturbations (Liang et al., 2020). Clinically, an ROM less than 5° was considered to be a successful fusion in terms of the FDA definition (Boustani et al., 2012). Focusing only on more stiff constructions is not scientific. In order to reduce the incidence of ASD, changes in ROM must be taken into account.

In this study, the results are consistent between the FEM group and IVE group when comparing the three groups of single-segment internal fixation techniques, as determined by the total ROM loss rate. For fused segments, L45PS has high rotational resistance, whereas L45CBT has high flexion, extension, and lateral bending resistance. Comparing the three groups of two-segment internal fixation modalities, the FEM group had stronger rotational resistance with hybrid screws and similar results in the three groups for both flexion and extension and lateral bending resistance. Due to the domino connection of the screw–rod system, which leads to instability of the fused segment in the rotating state, L34CBT/L45PS and L3CBT-L45PS have greater resistance to flexion and extension as well as lateral bending in the IVE group. According to this study, L34CBT/L45PS is more effective than L3CBT-L45PS and L345PS when ASD develops as a result of single-segment fixation. Zhang et al. (2022) came to the conclusion that while the fused segment's flexion and extension mobility were relatively low in the CBT screw group, its rotational ROM was higher than that of the PS screw, and comparable findings were found in the current investigation. Spinal flexibility is greatly decreased by posterior fixation. In a study by Elmasry et al. (2017), a posterior fixation system was discovered to have greater stiffness. According to the adjacent-segment ROM, there was no difference between the single-segment internal fixation groups and barely any difference between the dual-segment internal fixation groups. Dual-segment internal fixation had higher stability than single-segment internal fixation, but it also resulted in a substantial loss of adjacent-segment ROM. The hybrid screw design decreased the rate of ROM loss in flexion and extension and lateral bending, whereas the pure CBT treatment better maintained rotation better.

The L345PS screws were substantially more stressed than the other two groups in rotation for the dual-segment internal fixation, but the L34CBT/L45PS and L3CBT-L45PS screws were significantly more stressed than the L345PS in flexion-extension and lateral bending. For PS and CBT screws, the head and tail of the screw should be reinforced for stiffness since the stress distribution was focused in these areas where the screw made contact with the cortical bone. The upper screw stress is significantly greater than the lower screw stress, and extending the nail bar system can effectively reduce the total stress. The authors of various investigations on this subject came to the conclusion that most broken screws (78%–90%) happen in the caudal area (Chen et al., 2005; Kwon et al., 2006). Studies on the lumbar spine by Natarajan et al. revealed that the screw's caudal area experiences the highest degree of von Mises stress, which is around 5–6 times larger than that in the screw head location and rod. (Natarajan et al., 2018). Therefore, it may be said that the rod in the same location has a higher likelihood of failing than the caudal position of the screw in posterior internal fixation.

Bone density is a risk factor for the development of postoperative ASD (Yuan et al., 2022). There is a greater surgical failure rate in patients with osteoporosis (Wu et al., 2012; Kim et al., 2015); however, osteoporosis has little effect on the ROM of the lumbar spine (Yang et al., 2009; Liu et al., 2022), so better stability should be considered when internal fixation is performed in osteoporotic patients. Our results suggest that long-segment fixation results in greater stiffness but is concomitant with a greater loss of ROM. Therefore, short-segment fixation is recommended as the first clinical option whenever possible. On this basis, CBT should be further chosen because it can provide higher stability, avoiding the occurrence of secondary operations due to the failure of screw–rod systems. Although PS is still the dominant technique for spinal internal fixation in clinical practice, CBT has a distinct advantage of reducing the incidence of ASD, thereby effectively avoiding screw–rod systems and the prolongation of surgery (Sakaura et al., 2016). Furthermore, even if a patient has developed an ASD, CBT should also be prioritized by clinicians as extended screw–rod systems, because it can provide a better retention of rotation and higher resistance to flexion, extension, and lateral bending compared with other surgical procedures. By reviewing the literature (Kahaer et al., 2022a), different scholars have conducted similar experiments with the hybrid screw and also pointed out that the hybrid screw can provide greater stability, but none of them studied the adjacent-segment ROM and did not point out the relationship with ASD development, which is also an essential highlight of this paper. The hybrid screw approach in particular has been poorly studied, and although its long-term efficacy still requires clinical validation, it is admittedly an innovation.

Both FEM and IVE methods have advantages and disadvantages. FEA has been used to analyze the biomechanical parameters within the spine and connective soft tissues that are difficult to capture by experimental techniques (Alizadeh et al., 2013; Chang et al., 2020). The use of FEA can solve some practical issues and play a significant role in clinical practice because of its relative simplicity (Wang et al., 2020b). However, due to the complexity of human structures, FEA approaches have their limitations. Different material properties and model simplifications could cause experimental results to be inaccurate. IVE can yield relatively realistic results, but its widespread use is limited by the fact that its physical specimens are scarce, expensive, and not reusable. Many scholars are currently using FEA to conduct studies, despite the inevitably great limitations of simple FEA studies; IVE is a crucial research method that will make the experimental results more accurate. Biomechanical characteristics obtained by IVE are closer to *in vitro* biomechanical characteristics (Iliescu et al., 2021). FEA and IVE are still the dominant methods for studying spinal biomechanics. In this study, FEA and specimen experiments were used to verify each other for lumbar internal fixation, and the experimental design was complete and scientific.

In this study, there are a few issues: 1) Muscles and paravertebral soft tissues were not included in the FEM and IVE, and body weight loads and muscle forces were used to calculate the loading torque. 2) The sample size should be increased to account for statistical analysis. 3) Due to the limited experimental settings, significant stress indicators were not examined in the specimen experiments. 4) The bone quality of the specimens was not taken into account for bone quality, and there were individual differences between specimens.

5 Conclusion

In this study, the biomechanical responses of the lumbar spine with PS and CBT fixation were investigated. Our results show that long-segment fixation produces greater stiffness than short-segment fixation, but is more likely to lead to ASD. Using a hybrid screw combination technology can considerably increase the spine's biomechanical stability. For non-fused segments, the CBT approach provides the better retention of rotation and higher resistance to flexion, extension, and lateral bending compared with the PS technique. However, there are differences between single-segment and dual-segment internal fixation, and the ROM of adjacent segments is lost more strongly reduced by dual-segment internal fixation. Thus, the hybrid screw is an approach to consider, and is perhaps a better surgical option after clinical validation. In summary, an alternative to take into account is the hybrid screw, if internal fixation lengthening is carried out. This study can provide a better understanding of the biomechanical response to single-versus dual-segment internal fixation by different surgical procedures. A direction for future work could be to carry out statistical analysis on a larger sample of clinical data and verify the biomechanical results of this study.

Data availability statement

The raw data supporting the conclusion of this article will be made available by the authors, without undue reservation.

Ethics statement

The research was approved by the Science and Ethics Committee of the School of Biological Science and Medical Engineering at Beihang University (protocol code: BM20220087).

Author contributions

Conceptualization, BP and XW; methodology, YX; software, YX and DL; validation, YZ and HW; investigation, BP; resources, BP; data curation, YZ and HW; writing—original draft preparation, BP, YX, and XW; writing-review and editing, BP, YX, and XW; visualization, SW; supervision, SW; project administration, XW; funding acquisition, BP All authors have read and agreed to the published version of the manuscript.

Funding

This research was funded by the Defense Industrial Technology Development Program (JCKY2021601B021).

Conflict of interest

The authors declare that the research was conducted in the absence of any commercial or financial relationships that could be construed as a potential conflict of interest.

Publisher's note

All claims expressed in this article are solely those of the authors and do not necessarily represent those of their affiliated organizations, or those of the publisher, the editors and the reviewers. Any product that may be evaluated in this article, or claim that may be made by its manufacturer, is not guaranteed or endorsed by the publisher.

References

Alizadeh, M., Kadir, M. R. A., Fadhli, M. M., Fallahiarezoodar, A., Azmi, B., Murali, M. R., et al. (2013). The use of X-shaped cross-link in posterior spinal constructs improves stability in thoracolumbar burst fracture: A finite element analysis. *J. Orthop. Res.* 31 (9), 1447–1454. doi:10.1002/jor.22376

Biswas, J. K., Rana, M., Majumder, S., Karmakar, S. K., and Roychowdhury, A. (2018). Effect of two-level pedicle-screw fixation with different rod materials on lumbar spine: A finite element study. *J. Orthop. Sci.* 23 (2), 258–265. doi:10.1016/j.jos.2017.10.009

Boustani, H. N., Rohlmann, A., van der Put, R., Burger, A., and Zander, T. (2012). Which postures are most suitable in assessing spinal fusion using radiostereometric analysis? *Clin. Biomech.* 27 (2), 111–116. doi:10.1016/j.clinbiomech.2011.08.012

Caruso, G., Lombardi, E., Andreotti, M., Lorusso, V., Gildone, A., Padovani, S., et al. (2018). Minimally invasive fixation techniques for thoracolumbar fractures: Comparison between percutaneous pedicle screw with intermediate screw (PPSIS) and percutaneous pedicle screw with kyphoplasty (PPSK). *Eur. J. Orthop. Surg. Traumatology* 28 (5), 849–858. doi:10.1007/s00590-018-2122-1

Chang, D.-G., Suk, S.-I., Kim, J.-H., Song, K.-S., Suh, S.-W., Kim, S.-Y., et al. (2020). Long-term outcome of selective thoracic fusion using rod derotation and direct vertebral rotation in the treatment of thoracic adolescent idiopathic scoliosis: More than 10-year follow-up data. *Clin. Spine Surg.* 33 (2), E50–E57. doi:10.1097/Bsd.0000000000000833

Chen, C.-S., Chen, W.-J., Cheng, C.-K., Jao, S.-H. E., Chueh, S.-C., and Wang, C.-C. (2005). Failure analysis of broken pedicle screws on spinal instrumentation. *Med. Eng. Phys.* 27 (6), 487–496. doi:10.1016/j.medengphy.2004.12.007

Chen, C.-S., Cheng, C.-K., Liu, C.-L., and Lo, W.-H. (2001). Stress analysis of the disc adjacent to interbody fusion in lumbar spine. *Med. Eng. Phys.* 23 (7), 485–493. doi:10.1016/s1350-4533(01)00076-5

Dai, L. Y., Jiang, S. D., Wang, X. Y., and Jiang, L. S. (2007). A review of the management of thoracolumbar burst fractures. *Surg. Neurol.* 67 (3), 221–231. doi:10.1016/j.surneu.2006.08.081

Elmasry, S., Asfour, S., and Travascio, F. (2017). Effectiveness of pedicle screw inclusion at the fracture level in short-segment fixation constructs for the treatment of thoracolumbar burst fractures: A computational biomechanics analysis. *Comput. methods biomechanics Biomed. Eng.* 20 (13), 1412–1420. doi:10.1080/10255842.2017.1366995

Goto, K., Tajima, N., Chosa, E., Totoribe, K., Kubo, S., Kuroki, H., et al. (2003). Effects of lumbar spinal fusion on the other lumbar intervertebral levels (three-dimensional finite element analysis). *J. Orthop. Sci.* 8 (4), 577–584. doi:10.1007/s00776-003-0675-1

Iliescu, D. M., Micu, S.-I., Ionescu, C., Bulbuc, I., Bordei, P., Obada, B., et al. (2021). Axial and para-axial loading response evaluation on human cadaver-harvested lumbar vertebral blocks: *In vitro* experiment with possible clinical implications for clinical practice. *Exp. Ther. Med.* 22 (4), 1192. doi:10.3892/etm.2021.10626

Kahaer, A., Maimaiti, X., Maitirouzi, J., Wang, S., Shi, W., Abuduwaili, N., et al. (2022a). Biomechanical investigation of the hybrid modified cortical bone screw–pedicle screw fixation technique: Finite-element analysis. *Front. Surg.* 9 (1), 911742. doi:10.3389/fsurg.2022.911742

Kahaer, A., Zhou, Z., Maitirouzi, J., Wang, S., Shi, W., Abuduwaili, N., et al. (2022b). Biomechanical investigation of the posterior pedicle screw fixation system at level L4-L5 lumbar segment with traditional and cortical trajectories: A finite element study. *J. Healthc. Eng.* 2022, 1–11. doi:10.1155/2022/4826507

Kim, J.-B., Park, S.-W., Lee, Y.-S., Nam, T.-K., Park, Y.-S., and Kim, Y.-B. (2015). The effects of spinopelvic parameters and paraspinal muscle degeneration on S1 screw loosening. *jkns* 58 (4), 357–362. doi:10.3340/jkns.2015.58.4.357

Kwon, B. K., Elgafy, H., Keynan, O., Fisher, C. G., Boyd, M. C., Paquette, S. J., et al. (2006). Progressive junctional kyphosis at the caudal end of lumbar instrumented fusion: Etiology, predictors, and treatment. *Spine* 31 (17), 1943–1951. doi:10.1097/01.brs.0000229258.83071.db

Liang, Z., Cui, J., Zhang, J., He, J., Tang, J., Ren, H., et al. (2020). Biomechanical evaluation of strategies for adjacent segment disease after lateral lumbar interbody fusion: Is the extension of pedicle screws necessary? *BMC Musculoskelet. Disord.* 21 (1), 117. doi:10.1186/s12891-020-3103-1

Liu, Z.-X., Gao, Z.-W., Chen, C., Liu, Z.-Y., Cai, X.-Y., Ren, Y.-N., et al. (2022). Effects of osteoporosis on the biomechanics of various supplemental fixations co-applied with oblique lumbar interbody fusion (OLIF): A finite element analysis. *BMC Musculoskelet. Disord.* 23, 794. doi:10.1186/s12891-022-05645-7

Lu, T., and Lu, Y. (2019). Comparison of biomechanical performance among posterolateral fusion and transforaminal, extreme, and oblique lumbar interbody fusion: A finite element analysis. *World Neurosurg.* 129 (2), e890–e899. doi:10.1016/j.wneu.2019.06.074

Matsukawa, K., Yato, Y., Imabayashi, H., Hosogane, N., Asazuma, T., and Chiba, K. (2016). Biomechanical evaluation of lumbar pedicle screws in spondylolytic vertebrae: Comparison of fixation strength between the traditional trajectory and a cortical bone trajectory. *J. Neurosurg. Spine* 24 (6), 910–915. doi:10.3171/2015.11.SPINE15926

Natarajan, R. N., Watanabe, K., and Hasegawa, K. (2018). Biomechanical analysis of a long-segment fusion in a lumbar spine—A finite element model study. *J. biomechanical Eng.* 140 (9), 091011. doi:10.1115/1.4039989

Panjabi, M. M. (2003). Clinical spinal instability and low back pain. *J. Electromyogr. Kinesiol.* 13 (4), 371–379. doi:10.1016/s1050-6411(03)00044-0

Panjabi, M. M. (2007). Hybrid multidirectional test method to evaluate spinal adjacent-level effects. *Clin. Biomech.* 22 (3), 257–265. doi:10.1016/j.clinbiomech.2006.08.006

Park, W. M., Park, Y.-S., Kim, K., and Kim, Y. H. (2009). Biomechanical comparison of instrumentation techniques in treatment of thoracolumbar burst fractures: A finite element analysis. *J. Orthop. Sci.* 14 (4), 443–449. doi:10.1007/s00776-009-1341-z

Qiu, L., Niu, F., Wu, Z., Zhang, W., Chen, F., Tan, J., et al. (2022). Comparative outcomes of cortical bone trajectory screw fixation and traditional pedicle screws in lumbar fusion: A meta-analysis. *World Neurosurg.* 164, e436–e445. doi:10.1016/j.wneu.2022.04.129

Renner, S. M., Natarajan, R. N., Patwardhan, A. G., Havey, R. M., Voronov, L. I., Guo, B. Y., et al. (2007). Novel model to analyze the effect of a large compressive follower pre-load on range of motions in a lumbar spine. *J. Biomechanics* 40 (6), 1326–1332. doi:10.1016/j.jbiomech.2006.05.019

Rui, Z., Niu, W. X., Wang, Z. P., Pei, X. L., He, B., Zeng, Z. L., et al. (2018). The effect of muscle direction on the predictions of finite element model of human lumbar spine. *BioMed Res. Int.* 2018 (3), 1–6. doi:10.1155/2018/4517471

Sakaura, H., Miwa, T., Yamashita, T., Kuroda, Y., and Ohwada, T. (2016). Posterior lumbar interbody fusion with cortical bone trajectory screw fixation versus posterior lumbar interbody fusion using traditional pedicle screw fixation for degenerative lumbar spondylolisthesis: A comparative study. *J. Neurosurg. Spine SPI* 25 (5), 591–595. doi:10.3171/2016.3.spine151525

Sansur, C. A., Caffes, N. M., Ibrahimi, D. M., Pratt, N. L., Lewis, E. M., Murgatroyd, A. A., et al. (2016). Biomechanical fixation properties of cortical versus transpedicular screws in the osteoporotic lumbar spine: An *in vitro* human cadaveric model. *J. Neurosurg. Spine* 25 (4), 467–476. doi:10.3171/2016.2.SPINE151046

Santoni, B., Hynes, R., McGilvray, K., Rodriguez-Canessa, G., Lyons, A., Henson, M., et al. (2009). Cortical bone trajectory for lumbar pedicle screws. *Spine J.* 9 (5), 366–373. doi:10.1016/j.spinee.2008.07.008

Song, M., Sun, K., Li, Z., Zong, J., Tian, X., Ma, K., et al. (2021). Stress distribution of different lumbar posterior pedicle screw insertion techniques: A combination study of finite element analysis and biomechanical test. *Sci. Rep.* 11 (1), 1–15. doi:10.1038/s41598-021-90686-6

Spiegl, U. J., Holbing, P. L., Jarvers, J. S., N, V. D. H., Pieroh, P., Osterhoff, G., et al. (2021). Midterm outcome after posterior stabilization of unstable Midthoracic spine fractures in the elderly. *BMC Musculoskelet. Disord.* 22 (1), 188. doi:10.1186/s12891-021-04049-3

Takata, Y., Matsuura, T., Higashino, K., Sakai, T., Mishiro, T., Suzue, N., et al. (2014). Hybrid technique of cortical bone trajectory and pedicle screwing for minimally invasive spine reconstruction surgery: A technical note. *J. Med. Investigation* 61, 388–392. doi:10.2152/jmi.61.388

Tsouknidas, A. (2015). The effect of pedicle screw implantation depth and angle on the loading and stiffness of a spinal fusion assembly. *Bio-Medical Mater. Eng.* 25 (3), 425–433. doi:10.3233/BME-151537

Wang, W., Wu, B. L., Duan, R. M., Yuan, Y. S., Qu, M. J., Zhang, S., et al. (2020a). Treatment of thoracolumbar fractures through different short segment pedicle screw fixation techniques: A finite element analysis. *Orthop. Surg.* 12 (2), 601–608. doi:10.1111/os.12643

Wang, W., Pei, B., Pei, Y., Li, H., Fan, Y., Wu, X., et al. (2020b). Biomechanical effects of over lordotic curvature after spinal fusion on adjacent intervertebral discs under continuous compressive load. *Clin. Biomech.* 73 (3), 149–156. doi:10.1016/j.clinbiomech.2020.01.002

Wang, W., Pei, B., Pei, Y., Shi, Z., Lu, S., Wu, X., et al. (2019). Biomechanical effects of posterior pedicle fixation techniques on the adjacent segment for the treatment of thoracolumbar burst fractures: A biomechanical analysis. *Comput. Methods Biomechanics Biomed. Eng.* 22 (9), 1083–1092. doi:10.1080/10255842.2019.1631286

Wu, Z.-x., Gong, F.-t., Liu, L., Ma, Z.-s., Zhang, Y., Zhao, X., et al. (2012). A comparative study on screw loosening in osteoporotic lumbar spine fusion between expandable and conventional pedicle screws. *Archives Orthop. Trauma Surg.* 132 (4), 471–476. doi:10.1007/s00402-011-1439-6

Xiao, Z., Wang, L., Gong, H., and Zhu, D. (2012). Biomechanical evaluation of three surgical scenarios of posterior lumbar interbody fusion by finite element analysis. *Biomed. Eng. online* 11 (1), 31–11. doi:10.1186/1475-925X-11-31

Xu, H., Ju, W., Xu, N., Zhang, X., Zhu, X., Zhu, L., et al. (2013). Biomechanical comparison of transforaminal lumbar interbody fusion with 1 or 2 cages by finite-element analysis. *Oper. Neurosurg.* 73 (2), 198–205. doi:10.1227/01.neu.0000430320.39870.f7

Yang, Z., Griffith, J. F., Leung, P. C., and Lee, R. (2009). Effect of osteoporosis on morphology and mobility of the lumbar spine. *Spine* 34 (3), E115–E121. doi:10.1097/BRS.0b013e3181895aca

Yuan, C., Zhou, J., Wang, L., and Deng, Z. (2022). Adjacent segment disease after minimally invasive transforaminal lumbar interbody fusion for degenerative lumbar diseases: Incidence and risk factors. *BMC Musculoskelet. Disord.* 23, 982. doi:10.1186/s12891-022-05905-6

Zhang, S., Liu, Z., Lu, C., Zhao, L., Feng, C., Wang, Y., et al. (2022). Oblique lateral interbody fusion combined with different internal fixations for the treatment of degenerative lumbar spine disease: A finite element analysis. *BMC Musculoskelet. Disord.* 23 (1), 206–210. doi:10.1186/s12891-022-05150-x

Frontiers in Bioengineering and Biotechnology

TYPE Original Research
PUBLISHED 14 March 2023
DOI 10.3389/fbioe.2023.1148342

Check for updates

OPEN ACCESS

EDITED BY
Qichang Mei,
Ningbo University, China

REVIEWED BY
Snehal Shetye,
United States Food and Drug Administration, United States
Xun Sun,
Tianjin Hospital, China

*CORRESPONDENCE
Yong Hai,
yong.hai@ccmu.edu.cn
Yuzeng Liu,
beijingspiine2010@163.com

†These authors have contributed equally to this work and share first authorship

SPECIALTY SECTION
This article was submitted to Biomechanics, a section of the journal Frontiers in Bioengineering and Biotechnology

RECEIVED 20 January 2023
ACCEPTED 06 March 2023
PUBLISHED 14 March 2023

CITATION
Yang H, Pan A, Hai Y, Cheng F, Ding H and Liu Y (2023), Biomechanical evaluation of multiple pelvic screws and multirod construct for the augmentation of lumbosacral junction in long spinal fusion surgery.
Front. Bioeng. Biotechnol. 11:1148342.
doi: 10.3389/fbioe.2023.1148342

Biomechanical evaluation of multiple pelvic screws and multirod construct for the augmentation of lumbosacral junction in long spinal fusion surgery

Honghao Yang†, Aixing Pan†, Yong Hai*, Fengqi Cheng†, Hongtao Ding and Yuzeng Liu*

Department of Orthopedic Surgery, Beijing Chao-Yang Hospital, Beijing, China

Background: Posterior long spinal fusion was the common procedure for adult spinal deformity (ASD). Although the application of sacropelvic fixation (SPF), the incidence of pseudoarthrosis and implant failure is still high in long spinal fusion extending to lumbosacral junction (LSJ). To address these mechanical complications, advanced SPF technique by multiple pelvic screws or multirod construct has been recommended. This was the first study to compare the biomechanical performance of combining multiple pelvic screws and multirod construct to other advanced SPF constructs for the augmentation of LSJ in long spinal fusion surgery through finite element (FE) analysis.

Methods: An intact lumbopelvic FE model based on computed tomography images of a healthy adult male volunteer was constructed and validated. The intact model was modified to develop five instrumented models, all of which had bilateral pedicle screw (PS) fixation from L1 to S1 with posterior lumbar interbody fusion and different SPF constructs, including No-SPF, bilateral single S2-alar-iliac (S2AI) screw and single rod (SS-SR), bilateral multiple S2AI screws and single rod (MS-SR), bilateral single S2AI screw and multiple rods (SS-MR), and bilateral multiple S2AI screws and multiple rods (MS-MR). The range of motion (ROM) and stress on instrumentation, cages, sacrum, and S1 superior endplate (SEP) in flexion (FL), extension (EX), lateral bending (LB), and axial rotation (AR) were compared among models.

Results: Compared with intact model and No-SPF, the ROM of global lumbopelvis, LSJ, and sacroiliac joint (SIJ) was decreased in SS-SR, MS-SR, SS-MR, and MS-MR in all directions. Compared with SS-SR, the ROM of global lumbopelvis and LSJ of MS-SR, SS-MR, and MS-MR further decreased, while the ROM of SIJ was only decreased in MS-SR and MS-MR. The stress on instrumentation, cages, S1-SEP, and sacrum decreased in SS-SR, compared with no-SPF. Compared with SS-SR, the stress in EX and AR further decreased in SS-MR and MS-SR. The most significantly decreased ROM and stress were observed in MS-MR.

Conclusion: Both multiple pelvic screws and multirod construct could increase the mechanical stability of LSJ and reduce stress on instrumentation, cages, S1-SEP, and sacrum. The MS-MR construct was the most adequate to reduce the risk of lumbosacral pseudarthrosis, implant failure, and sacrum fracture. This study may provide surgeons with important evidence for the application of MS-MR construct in the clinical settings.

KEYWORDS

sacropelvic fixation, multiple screw, multirod construct, lumbosacral junction, finite element, Biomechanics, spinal fusion, spinal deformity

Introduction

Adult spinal deformity (ASD) is a heterogeneous spectrum of abnormalities causing spinal malalignment in sagittal and coronal plane (Kim et al., 2020). With prolonged life expectancy, the prevalence of ASD is up to 68% in the elderly population (Ames et al., 2016). Patients with ASD commonly complain of low back pain, radiculopathy, disability, and poor health-related quality of life (HRQoL) (Pellisé et al., 2015; Yang et al., 2023). As a reliable and lasting solution, surgical treatment for ASD has gained popularity in the last decade (Safaee et al., 2020). The primary goals of surgery are to improve HRQoL through restoration of spinal alignment and resolution of neurological deficit.

Posterior long spinal fusion was the most common surgical procedure for ASD. However, if the construct was extended to the sacrum, a high incidence of mechanical complications including pseudoarthrosis (19.0%–83.0%) and implant failure (23.7%–56.0%) has been reported due to the sacral cancellous nature, complex anatomy, and substantial shear forces at the lumbosacral junction (LSJ) (Kim et al., 2006a; Kim et al., 2006b; Kim et al., 2010; Finger et al., 2014; Guler et al., 2015; Hallager et al., 2017; Eastlack et al., 2022). Strategies for addressing this concern predominantly included anterior column support and sacropelvic fixation (SPF) to enhance the fusion rate at the LSJ and increase construct stiffness. SPF traditionally involves iliac screw or S2-alar-iliac (S2AI) screw. S2AI fixation has increased in prevalence in recent years owing to various advantages over iliac screw placements (Jain et al., 2016; Hasan et al., 2020). S2AI screw could get a stronger anchor through additional purchase in the sacrum and sacroiliac joint (SIJ). Also, S2AI was in-line with S1 screws; therefore, the need for medial-to-lateral connectors could be avoided.

Although the application of SPF, the incidence of implant failure is still unsatisfactory, with reported rates ranging from 12.0% to 46.9% (Park et al., 2021b; Gao et al., 2021). In recent cohort studies, advanced SPF technique by multiple pelvic screws or multirod construct has been recommended following long spinal fusion to stabilize the LSJ further, protect the primary rod and screws, and reduce the persistent motion of SIJ (Uotani et al., 2021; Lee et al., 2022a; Lee et al., 2022b). However, there was only one small-size cohort study reporting the application of combining the multiple pelvic screws and multirod construct, without any control groups (Shen et al., 2018). Whether this kind of construct could further decrease the risk of mechanical complications remains unknown. Understanding the biomechanical advantages of this construct could provide surgeons with some valuable guidance to solve the arising problems of mechanical complications in long spinal fusion surgery.

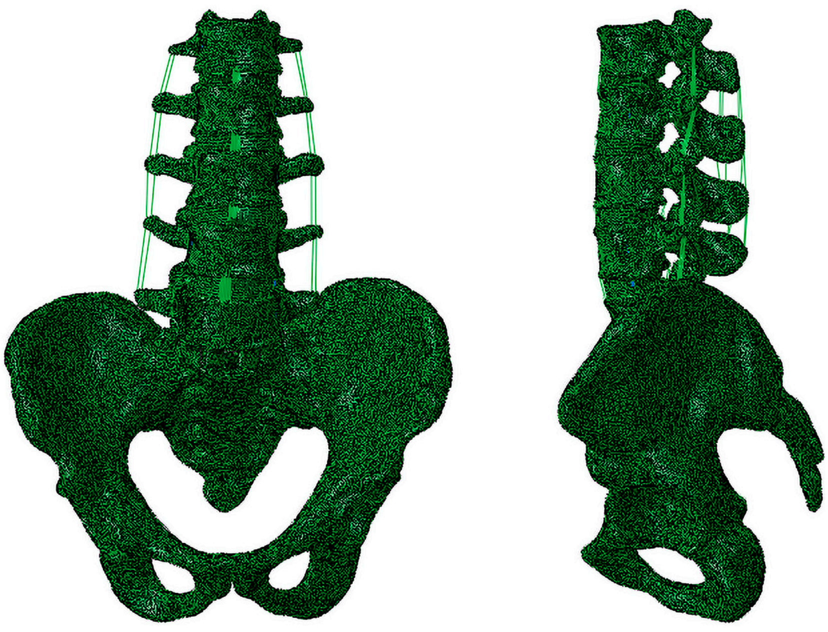

FIGURE 1
The intact lumbopelvic finite element model.

TABLE 1 Material properties of the lumbopelvic finite element model.

Components	Young's modulus (MPa)	Poisson's ratio	Element type	Reference
Lumbar vertebra cortical bone	12000	0.30	C3D8R	Kawahara et al. (2003)
Lumbar vertebra cancellous bone	100	0.30	C3D4	
Sacrum cortical bone	6140	0.30	C3D6	Hakim and King (1979)
Sacrum cancellous bone	1400	0.30	C3D4	
Ilium cortical bone	17000	0.30	C3D6	Dalstra and Huiskes (1995)
Ilium cancellous bone	132	0.20	C3D4	
Sacrum cartilage	54	0.40	C3D8H	Sohn et al. (2018)
Ilium cartilage	54	0.40	C3D8H	
Pubic symphysis	5	0.45	C3D10	Shi et al. (2014)
Endplate	100	0.30	C3D4	Shirazi-Adl et al. (1984)
Annulus fiber	450	0.30	T3D2	
Annulus matrix	$C_{10} = 0.18$, $C_{01} = 0.045$	0.30	C3D8H	Schmidt et al. (2007)
Nucleus pulposus	$C_{10} = 0.12$, $C_{01} = 0.03$	0.50	C3D8H	

This was the first study to compare the biomechanical performance of combining the multiple pelvic screws and multirod construct to other advanced SPF constructs for the augmentation of LSJ in long spinal fusion surgery through finite element (FE) analysis.

Materials and methods

Construction of the intact FE model

A healthy 30-year male volunteer (175 cm tall and 68 kg) was recruited. History of low back pain, leg pain, spinal degeneration, deformity, infection, trauma, tumours, and abnormality of bone mass was ruled out. The study protocol was approved by the Research Ethics Committee of Beijing Chao-Yang Hospital (2022-11-02-4), and informed consent was obtained from the participant. A 128-slice spiral computed tomography (CT) scan (SOMATOM Definition AS+, Siemens, Germany) from L1 to pelvic with a thickness of 0.625 mm was performed for the participant. The tomographic images were imported into Mimics Research 21.0 (Materialise, Belgium) for three-dimensional (3D) reconstruction in Digital Imaging and Communications in Medicine format (DICOM). Through region growing, threshold segmentation, and manual mask editing, a basic 3D lumbopelvic contour model was generated and stored in STL format. Subsequently, the above data were imported into Geomagic Studio 12 (Geomagic, United States) to construct the bony contour of lumbopelvic model by smoothing, denoising, and reverse-engineering, and the geometric model was saves as STP format. Next, Hypermesh 17.0 (Altair Engineering, United States) was used for pre-processing procedures of FE analysis, including meshing, material properties assignment, definition of interaction, and application of loading and boundary conditions.

The lumbopelvic geometric model was composed of the vertebral body, intervertebral disc, and posterior elements. The vertebral body included cortical bone, cancellous bone, and cartilaginous endplates. The intervertebral disc was consisted of nucleus pulposus and annulus fibrosus, a ground matrix reinforced by fibres. The thickness of the cortical bone and endplate was set as 1.0 mm and 0.5 mm, respectively. The nucleus pulposus accounted for around 50% of the intervertebral disc volume, and the thickness of the articular cartilage was assumed to be 0.2 mm. A frictionless surface contact between facet joints was assigned, and the SIJ interaction was modelled as surface-to-surface contact with a frictional coefficient of 0.4 (Kiapour et al., 2020). Ligaments included anterior longitudinal ligament, posterior longitudinal ligament, ligamentum flavum, capsular ligament, intertransverse ligament, interspinous ligament, supraspinous ligament, anterior sacroiliac ligament, posterior sacroiliac ligament, interosseous sacroiliac ligament, sacrospinous ligament, sacrotuberous ligament, superior pubic ligament, arcuate pubic ligament, inguinal ligament, and the iliolumbar ligament were generated using hyper-elastic, tension-only, two-node Truss elements (T3D2). The insertion locations of ligaments were referenced from the anatomical attachment points. The intact FE model included 173,636 nodes and 738,423 elements (Figure 1). The properties of all components in the lumbopelvic model were listed in Table 1 and Table 2, according to the literature (Hakim and King, 1979; Shirazi-Adl et al., 1984; Dalstra and Huiskes, 1995; Zheng et al., 1997; Kawahara et al., 2003; Rohlmann et al., 2006; Phillips et al., 2007; Schmidt et al., 2007; Shi et al., 2014; Sohn et al., 2018).

Generation of the instrumented model

The instrumented model was posterior bilateral pedicle screw fixation from L1 to S1 with posterior lumbar interbody fusion

TABLE 2 Material properties of the lumbar and pelvic ligaments.

Ligament	Stiffness coefficient (N/mm)	Reference
Anterior longitudinal ligament	1864	Rohlmann et al. (2006)
Posterior longitudinal ligament	236	
Ligamentum flavum	58	
Capsular ligament	384	
Intertransverse ligament	11	
Interspinous ligament	15	
Supraspinous ligament	34	
Anterior sacroiliac ligament	700	Zheng et al. (1997)
posterior sacroiliac ligament	400	
Interosseous sacroiliac ligament	2800	
Sacrospinous ligament	1400	
Sacrotuberous ligament	1500	
Superior pubic ligament	500	
Arcuate pubic ligament	500	
Inguinal ligament	250	Phillips et al. (2007)
Iliolumbar ligament	1000	

(PLIF) and SPF. There was no any facetectomy, laminectomy, or discectomy from L1 to L4. Regarding to PLIF, resections of the spinous processes, laminectomy, and inferior facetectomy were performed at L5. The intervertebral disc and endplates of L5/S1 were removed, and two cube-shaped fusion cages were implanted. The instrumentation for SPF was different among the instrumented models (Figure 2).

(1) No-SPF: SPF was not performed and only bilateral pedicle screws were inserted at S1.
(2) Bilateral single S2AI screw and single rod (SS-SR): The primary rod was anchored to single S2AI screw, and there was no any accessory rods.
(3) Bilateral multiple S2AI screws and single rod (MS-SR): The primary rod was anchored to dual S2AI screws, and there was no any accessory rods.
(4) Bilateral single S2AI screw and multiple rods (SS-MR): The primary rod was anchored to S1-PS. Medial accessory rod was used, with distal end anchored to single S2AI screw and proximal end connected to the ipsilateral primary rod by rod-rod connector.
(5) Bilateral multiple S2AI screws and multiple rods (MS-MR): The primary rod was anchored to S1-PS. Medial accessory rod was used, with distal end anchored to dual S2AI screws and proximal end connected to the ipsilateral primary rod by rod-rod connector.

SolidWorks (Dassault Systems, United States) was used to design and assemble the screws, rods, cages, and connecters in instrumented models. The rods were simulated by fitting lines passing though centres of screw caps. C3D8R was applied to mesh these implants. Ti6Al4V and PEEK were assigned to the materials of the posterior instrumentation and cages, respectively. The contact surface of screw-rod, screw-vertebral body, and cage-endplate were set as tie constraints.

Validation of the intact FE model

The ROM of each lumbar segment and SIJ in this intact FE model was compared to the data in several *in vitro* studies under equivalent loading conditions (Panjabi et al., 1994; Lindsey et al., 2014; Cook et al., 2015; Cross et al., 2018; Ntilikina et al., 2020; Sayed et al., 2021). For the validation of ROM of each lumbar segment, the S1 was constrained, and pure moments of 7.5 Nm in flexion (FL), extension (EX), lateral bending (LB), and axial rotation (AR) were applied to the superior endplate (SEP) of L1. For the validation of ROM of SIJ, the right ilium was fixed, and pure moments of 7.5 Nm in six directions were applied to L4-SEP.

The intradiscal pressure (IDP) of each lumbar segment was compared to the data in a cadaveric test by Hsiao et al. (Hsiao et al., 2022). Pure moments of 7.5 Nm with and without an axial load of 500 N in FL, EX, and LB were applied to the superior endplate of L1.

Validation of the instrumented FE models

As MS-SR, SS-MR, and MS-MR were relatively novel instrumented models, no cadaveric study using these three models was reported. There were two cadaveric studies using the instrumented models of No-SPF and

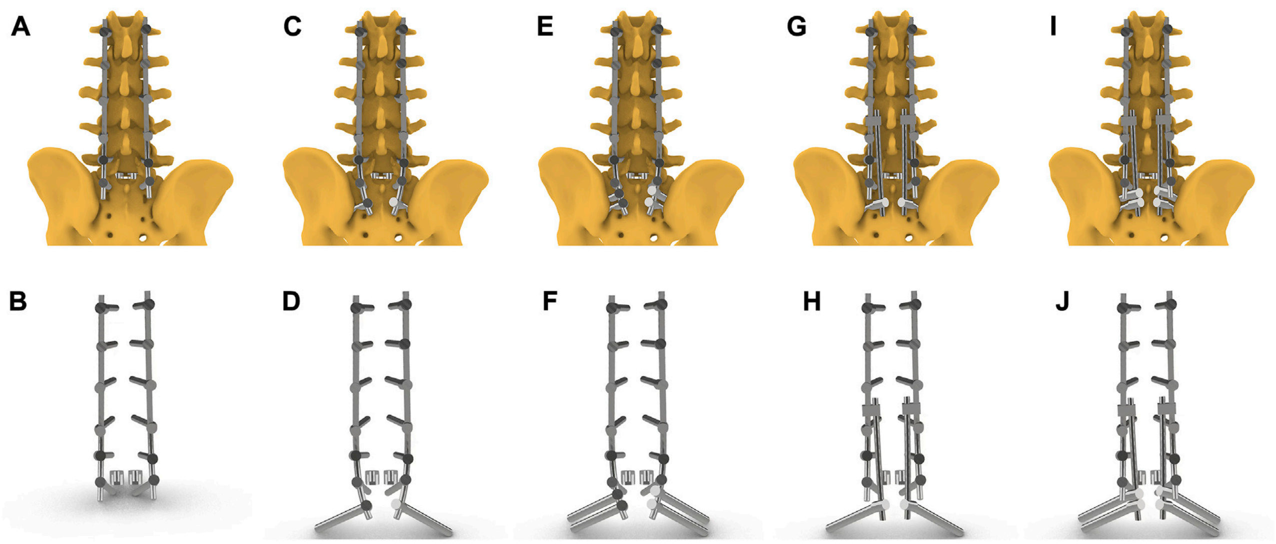

FIGURE 2
Five instrumented models including instrumentations and cages. **(A, B)** No-SPF: SPF was not performed and only bilateral pedicle screws were inserted at S1; **(C, D)** SS-SR: The primary rod was anchored to single S2AI screw, and there was no any accessory rods. **(E, F)** MS-SR: The primary rod was anchored to dual S2AI screws, and there was no any accessory rods; **(G, H)** SS-MR: The primary rod was anchored to S1-PS. Medial accessory rod was used, with distal end anchored to single S2AI screw and proximal end connected to the ipsilateral primary rod by rod-rod connector; **(I, J)** The primary rod was anchored to S1-PS. Medial accessory rod was used, with distal end anchored to dual S2AI screws and proximal end connected to the ipsilateral primary rod by rod-rod connector.

SS-SR, and both were performed by Pereira et al. (de Andrada Pereira et al., 2021; de Andrada Pereira et al., 2022). After carefully reviewing the cadaveric specimen information in these studies, we confirmed that the cadaveric specimen were not reused. Only anterior lumbar interbody fusion was performed at L5/S1 in the cadaveric instrumented models by Pereira et al., without any laminectomy or facetectomy, which may impact the stability and stress distribution of spine. To make our validation more reliable, we restored the lamina and facet joints but the interbody fusion cages were preserved before pure moments of 7.5 Nm were applied.

The ROM of L2-S1 and LSJ in the No-SPF and SS-SR models was compared to the data in the studies by Pereira et al. (de Andrada Pereira et al., 2021; de Andrada Pereira et al., 2022). The rod strains on lumbosacral rod (between L5-PS and S1-PS) and S1-S2 rod were also validated. Consistent with the protocol by Pereira et al., the rod trains were measured on the posterior surface, at the middle level, on the right side.

Loading and boundary condition

The loads and boundary conditions were set in Abaqus 6.10 (Dassault Systems, France) for FE analysis. In all the FE models, the iliac was fully constrained in all degrees of freedom. A load of 500 N and a pure moment of 7.5 Nm was applied to the nodes coupled with L1-SEP to simulate flexion, extension, lateral bending and axial rotation under the physiological compressive load

Data analysis

The global ROM, the ROM of LSJ, the maximum von-Mises stress (VMS) on instrumentation, the S1-PS, the lumbosacral rods, the cages, the sacrum, and S1-SEP in FL, EX, LB, and AR were compared among the intact model and instrumented models.

Results

Validation of the intact and instrumented FE models

The ROM of each lumbar segment and SIJ in the current intact FE model was consistent with the data from the literature (Figure 3). The IDP of each lumbar segment in the intact FE model was also consistent with the data from the study by Hsiao et al. (Supplementary Figure S1). (Hsiao et al., 2022). The ROM of L2-S1 and LSJ in the No-SPF and SS-SR instrumented models was consistent with the data from the studies by Pereira et al. (Supplementary Figure S2). (de Andrada Pereira et al., 2021; de Andrada Pereira et al., 2022). The rod strains on lumbosacral rod and S1-S2 rod were also well validated (Supplementary Figure S3). The validations suggested that the intact and instrumented lumbopelvic models in the present study were effective and reliable, which could be used for further analysis.

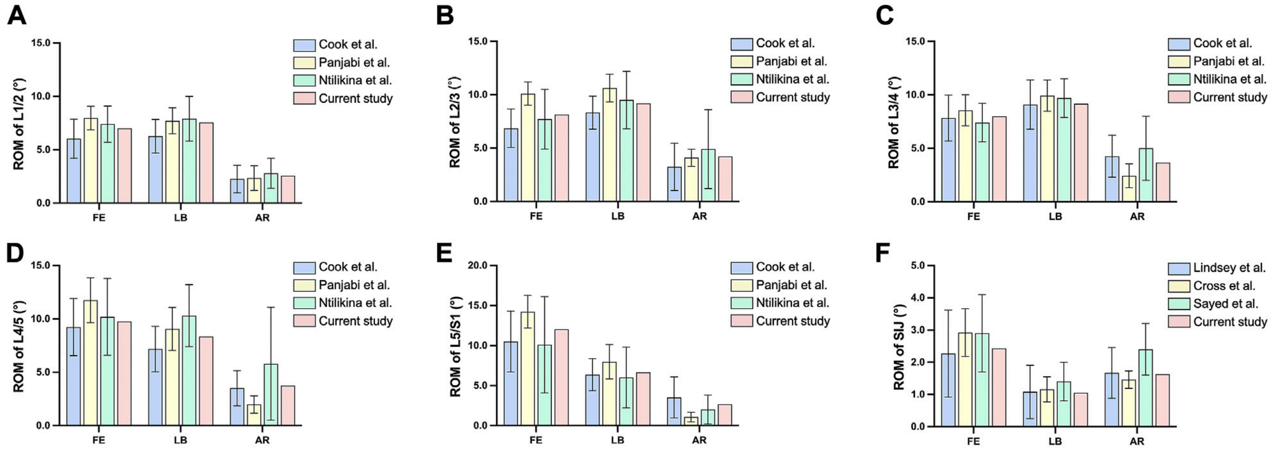

FIGURE 3
Comparison of the range of motion between the intact model and *in vitro* studies. **(A)** range of motion of L1/2; **(B)** range of motion of L2/3; **(C)** range of motion of L3/4; **(D)** range of motion of L4/5; **(E)** range of motion of L5/S1; **(F)** range of motion of sacroiliac joint.

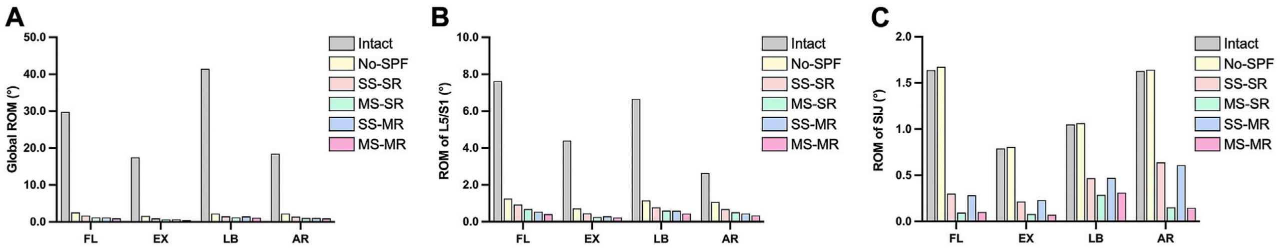

FIGURE 4
Comparison of the range of motion among intact and instrumented models. **(A)** the global range of motion; **(B)** the range of motion of lumbosacral junction; **(C)** the range of motion of sacroiliac joint.

Global ROM

The global ROM of intact model, No-SPF, SS-SR, MS-SR, SS-MR, and MS-MR in all directions was demonstrated in Figure 4A. Compared with intact model, the global ROM of No-SPF decreased in all directions; compared with No-SPF, the ROM of SS-SR decreased by 32.97%, 39.25%, 31.43%, and 38.21% in FL, EX, LB, and AR, respectively. Compared with SS-SR, the ROM further decreased in MS-SR, SS-MR, and MS-MR. The most significant decreased ROM was observed in MS-MR, ranging from 27.30% in LB to 54.21% in EX, compared with SS-SR. In FL, EX, and AR, the ROM was similar between MS-SR and SS-MR; however, in LB, the ROM was similar between SS-SR and SS-MR, as well as between MS-SR and MS-MR.

ROM of lumbosacral junction

The ROM of LSJ of intact model, No-SPF, SS-SR, MS-SR, SS-MR, and MS-MR in all directions was demonstrated in Figure 4B. Compared with intact model, the ROM of No-SPF decreased in all directions; compared with No-SPF, the ROM of SS-SR decreased by 25.81%, 37.62%, 32.81%, and 36.18% in FL, EX, LB, and AR, respectively. Compared with SS-SR, the ROM further decreased in MS-SR, SS-MR, and MS-MR. The most significant decreased ROM was observed in MS-MR, ranging from 43.25% in LB to 55.29% in FL, compared with SS-SR. The ROM of SS-MR decreased by 20.71% in FL and 13.91% in AR but increased by 17.00% in EX, compared with MS-SR. In LB, the ROM was similar between MS-SR and SS-MR.

ROM of sacroiliac joint

The ROM of SIJ of intact model, No-SPF, SS-SR, MS-SR, SS-MR, and MS-MR in all directions was demonstrated in Figure 4C. Compared with intact model, the ROM of No-SPF slightly increased in all directions. Compared with No-SPF, the ROM of SS-SR decreased by 82.03%, 73.36%, 55.83%, and 61.07% in FL, EX, LB, and AR, respectively. Compared with SS-SR, the ROM of MS-SR further decreased by 68.11%, 62.33%, 38.30%, and 76.09% in FL, EX, LB, and AR, respectively. The ROM was similar between SS-SR and SS-MR, as well as between MS-SR and MS-MR.

10.3389/fbioe.2023.1148342

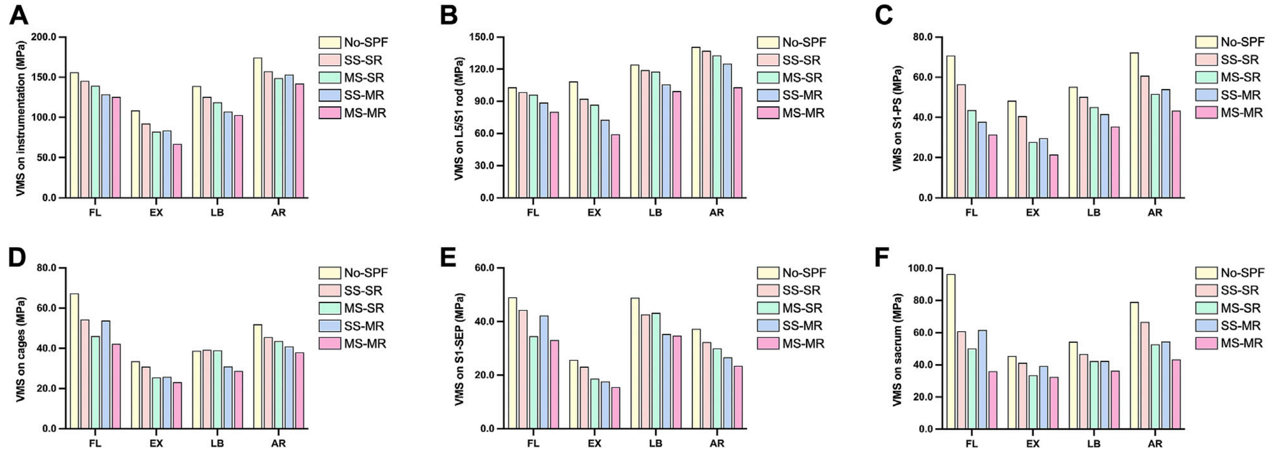

FIGURE 5
Comparison of the maximum von-Mises stress among instrumented models. **(A)** instrumentation; **(B)** lumbosacral rods; **(C)** S1-pedicle screws; **(D)** cages; **(E)** S1-superior endplate; **(F)** sacrum.

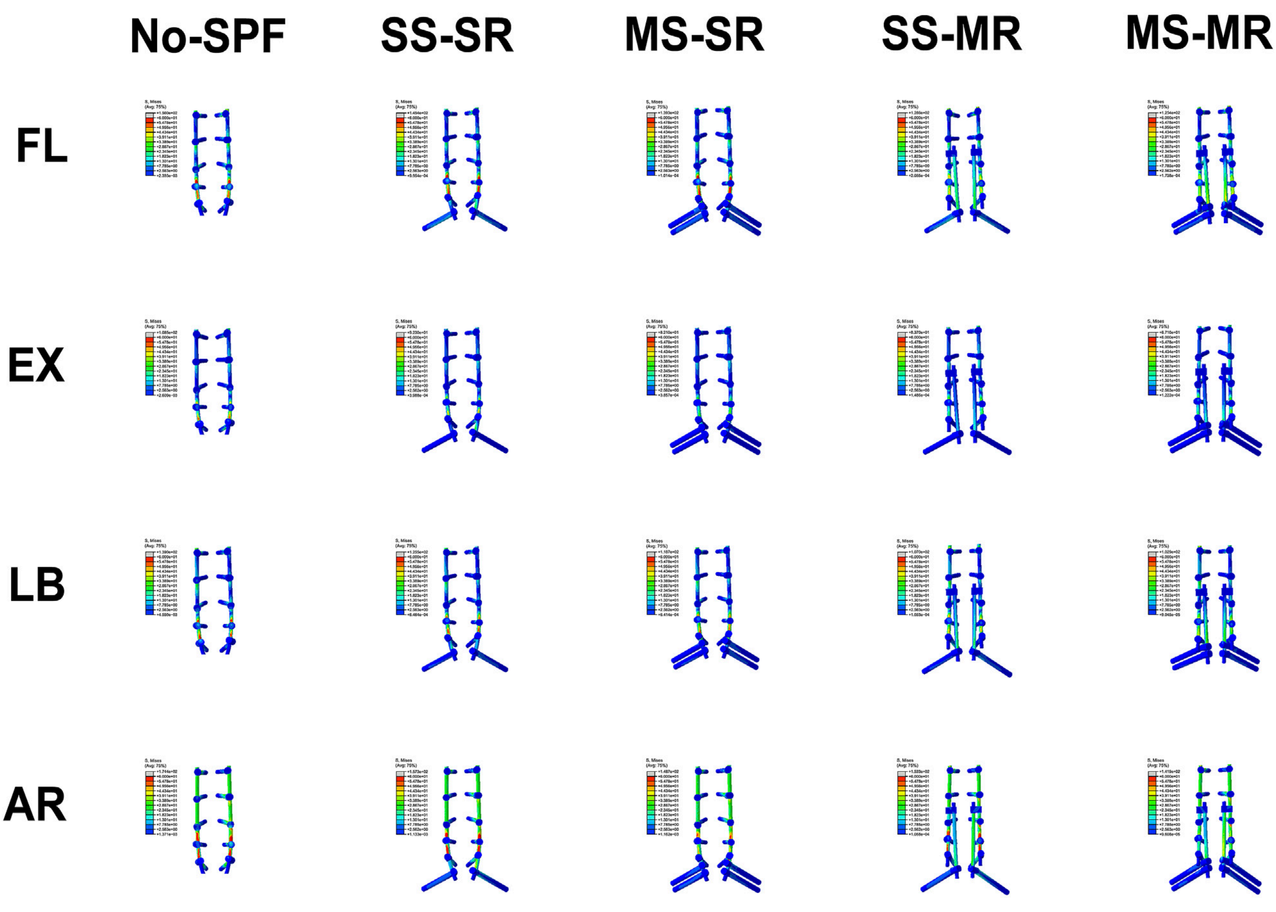

FIGURE 6
Von-Mises stress on instrumentation of different instrumented models in flexion, extension, lateral bending, and axial rotation.

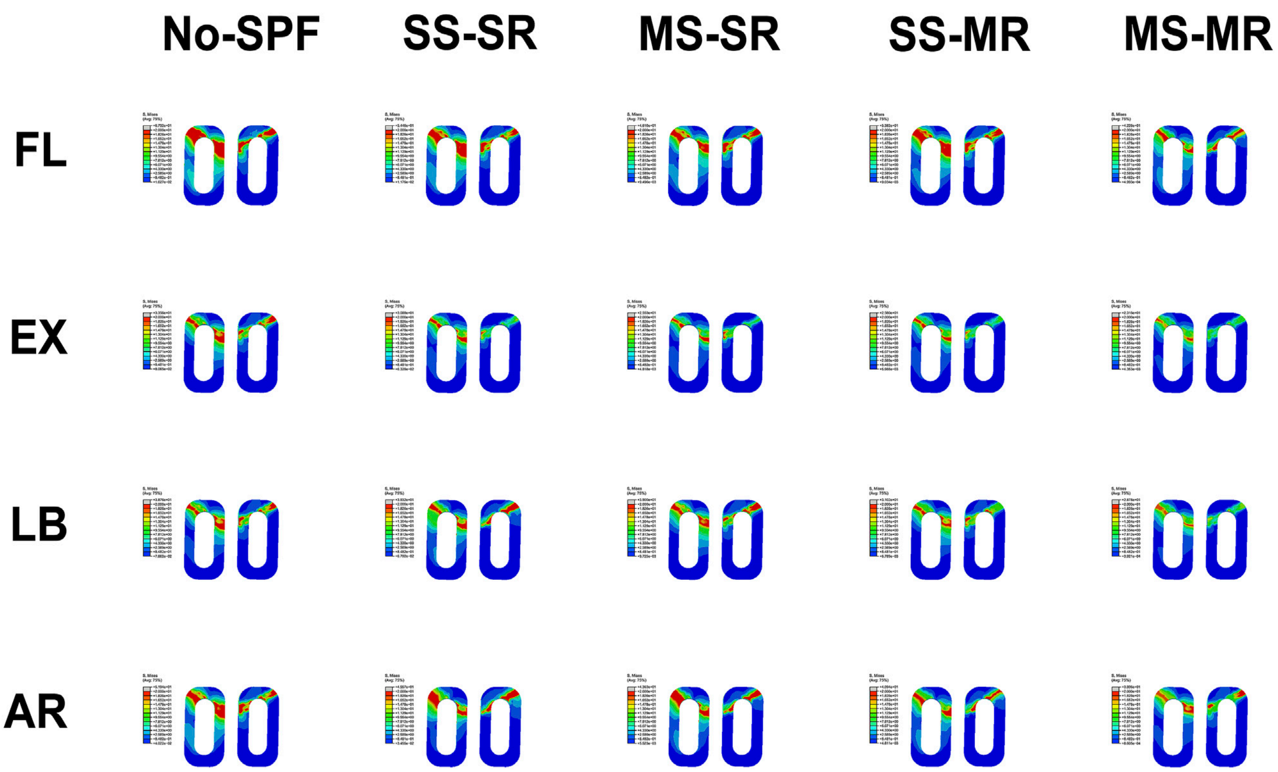

FIGURE 7
Von-Mises stress on cages of different instrumented models in flexion, extension, lateral bending, and axial rotation.

Maximum von-Mises stress on instrumentation

The maximum VMS on instrumentation in No-SPF, SS-SR, MS-SR, SS-MR, and MS-MR in all directions was demonstrated in Figure 5A and Figure 6. Compared with No-SPF, the maximum VMS on SS-SR decreased by 6.79%, 14.93%, 9.71%, and 9.79% in FL, EX, LB, and AR, respectively. Compared with SS-SR, the maximum VMS further decreased in MS-SR, SS-MR, and MS-MR in all directions. The most significantly decreased maximum VMS was observed in MS-MR, ranging from 9.82% in AR to 27.30% in EX, compared with SS-SR. In FL and LB, the maximum VMS gradually decreased from MS-SR to MS-MR; however, in EX and AR, the VMS on SS-MR was slightly greater than MS-SR.

Maximum von-Mises stress on lumbosacral rods

The maximum VMS on lumbosacral rods in No-SPF, SS-SR, MS-SR, SS-MR, and MS-MR in all directions was demonstrated in Figure 5B. Compared with No-SPF, the maximum VMS on SS-SR significantly decreased in EX. The maximum VMS was similar between SS-SR and MS-SR in all directions; however, the maximum VMS on both SS-MR and MS-MR were significantly lower than MS-SR. The most significantly decreased maximum VMS was observed in MS-MR, ranging from 16.54% in LB to 35.85% in EX, compared with SS-SR. Compared with SS-MR, the maximum VMS on MS-MR further decreased by 9.64%, 18.44%, 5.90%, and 17.67% in FL, EX, LB, and AR, respectively.

Maximum von-Mises stress on S1-PS

The maximum VMS on S1-PS in No-SPF, SS-SR, MS-SR, SS-MR, and MS-MR in all directions was demonstrated in Figure 5C. Compared with No-SPF, the maximum VMS on SS-SR decreased by 20.09%, 16.06%, 8.98%, and 15.97% in FL, EX, LB, and AR, respectively. Compared with SS-SR, the maximum VMS further decreased in MS-SR, SS-MR, and MS-MR. The most significantly decreased maximum VMS was observed in MS-MR, ranging from 28.71% in AR to 47.03% in EX, compared with SS-SR. In FL and LB, the maximum VMS gradually decreased from MS-SR to MS-MR; however, in EX and AR, the VMS on SS-MR was slightly greater than MS-SR. This trend was similar to that of global instrumentation.

Maximum von-Mises stress on cages

The maximum VMS on cages in No-SPF, SS-SR, MS-SR, SS-MR, and MS-MR in all directions was demonstrated in Figure 5D and Figure 7. Compared with No-SPF, the maximum VMS on SS-SR decreased in FL, EX, and AR. Compared with SS-SR, in FL, the maximum VMS significantly decreased in MS-SR and MS-MR but comparative in SS-MR; in EX, the maximum VMS significantly decreased in MS-SR, SS-MR, and MS-MR; in LB, the maximum VMS significantly decreased in SS-MR and MS-MR but comparative in MS-SR; in AR, the maximum VMS gradually decreased from MS-SR to MS-MR. The most significantly decreased maximum VMS was observed in MS-MR, ranging from 16.48% in AR to 26.81% in LB, compared with SS-SR. The maximum VMS in EX was similar between MS-SR and SS-MR.

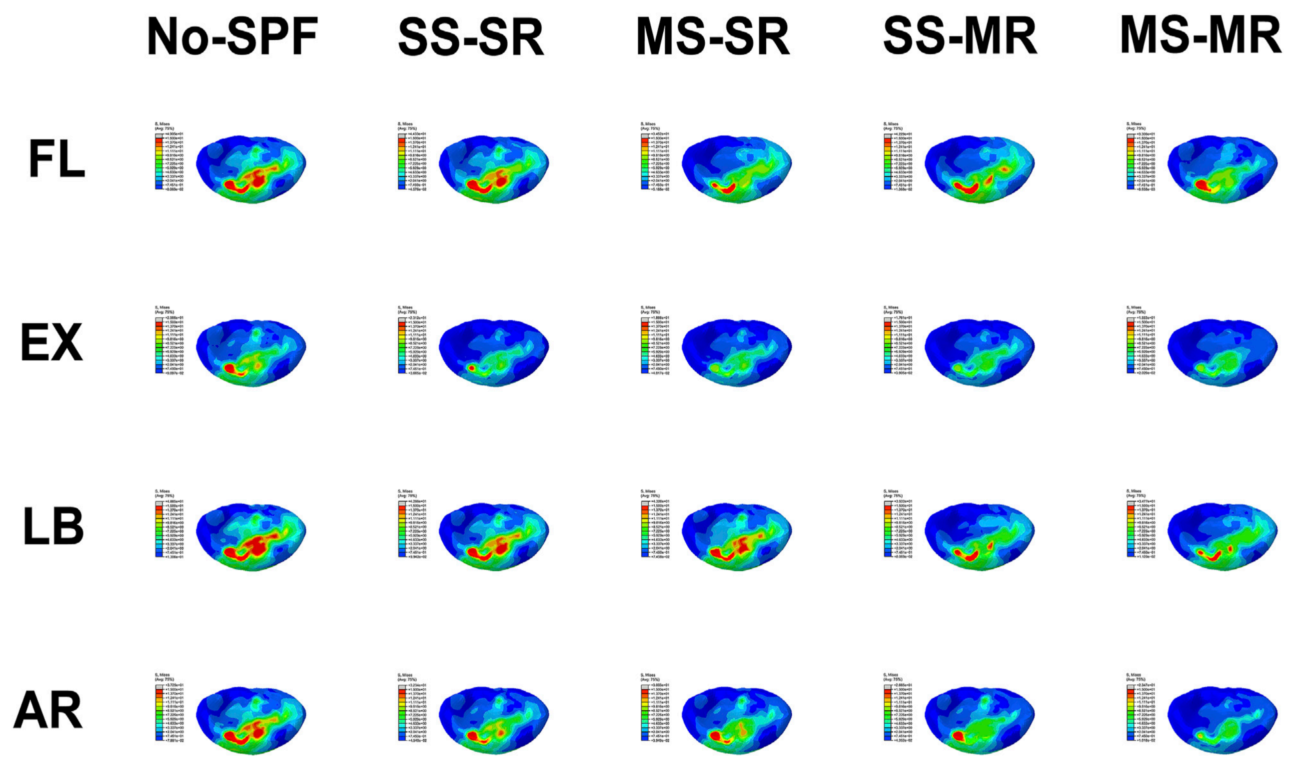

FIGURE 8
Von-Mises stress on S1-superior endplate of different instrumented models in flexion, extension, lateral bending, and axial rotation.

Maximum von Mises stress on S1-SEP

The maximum VMS on S1-SEP in No-SPF, SS-SR, MS-SR, SS-MR, and MS-MR in all directions was demonstrated in Figure 5E and Figure 8. Compared with No-SPF, the maximum VMS on SS-SR decreased by 9.62%, 9.90%, 12.67%, and 13.18% in FL, EX, LB, and AR, respectively. Compared with SS-SR, in FL, the maximum VMS significantly decreased in MS-SR and MS-MR but comparative in SS-MR; in EX, the maximum VMS significantly decreased in MS-SR, SS-MR, and MS-MR; in LB, the maximum VMS significantly decreased in SS-MR and MS-MR but comparative in MS-SR; in AR, the maximum VMS gradually decreased from MS-SR to MS-MR. This trend was consistent with that of cages. The most significantly decreased maximum VMS was observed in MS-MR, ranging from 18.50% in LB to 32.83% in EX, compared with SS-SR.

Maximum von Mises stress on sacrum

The maximum VMS on the sacrum in No-SPF, SS-SR, MS-SR, SS-MR, and MS-MR in all directions was demonstrated in Figure 5F and Figure 9. Compared with No-SPF, the maximum VMS on SS-SR decreased by 36.90%, 9.37%, 13.96%, and 15.57% in FL, EX, LB, and AR, respectively. Compared with SS-SR, in EX, LB, and AR, the maximum VMS further decreased in MS-SR, SS-MR, and MS-MR; however, in FL, the maximum VMS was comparative in SS-MR. The most significantly decreased maximum VMS was observed in MS-MR, ranging from 21.32% in EX to 40.85% in FL, compared with SS-SR. Compared with SS-MR, the maximum VMS on MS-MR further decreased by 41.69%, 17.25%, 14.38%, and 20.58% in FL, EX, LB, and AR, respectively.

Discussion

The substantial biomechanical shear forces of LSJ, poor bone quality of sacrum, and complex sacral anatomy make long spinal fusion challenging to achieve solid lumbosacral fusion, which impacts patients' HRQoL and usually needs revision surgery (Kim et al., 2010). Also, the large lever arms and cantilever forces result in high stress on the base of the construct, increasing the risk of implant failure. Therefore, SPF has been proposed following long spinal fusion ending at S1 (Guler et al., 2015; El Dafrawy et al., 2019). Although SPF indeed reinforces the construct stiffness, 12.0%–46.9% of implant failure rate has been reported by previous studies (Park et al., 2021b; Gao et al., 2021). To reduce the incidence of mechanical complications, multiple pelvic screws or multirod construct have been applied as an advanced SPF technique (Uotani et al., 2021; Lee et al., 2022a; Lee et al., 2022b; Tang et al., 2022). The current study revealed that both multiple pelvic screws and multirod construct could increase the mechanical stability of LSJ, reduce strain on the lumbosacral rod, and protect the S1-PS and sacrum. The combination of these two constructs could further improve these effects. This study may play a role of pre-clinical evaluation of MS-MR construct and could provide surgeons with more information about its advantages over the other advanced SPF constructs.

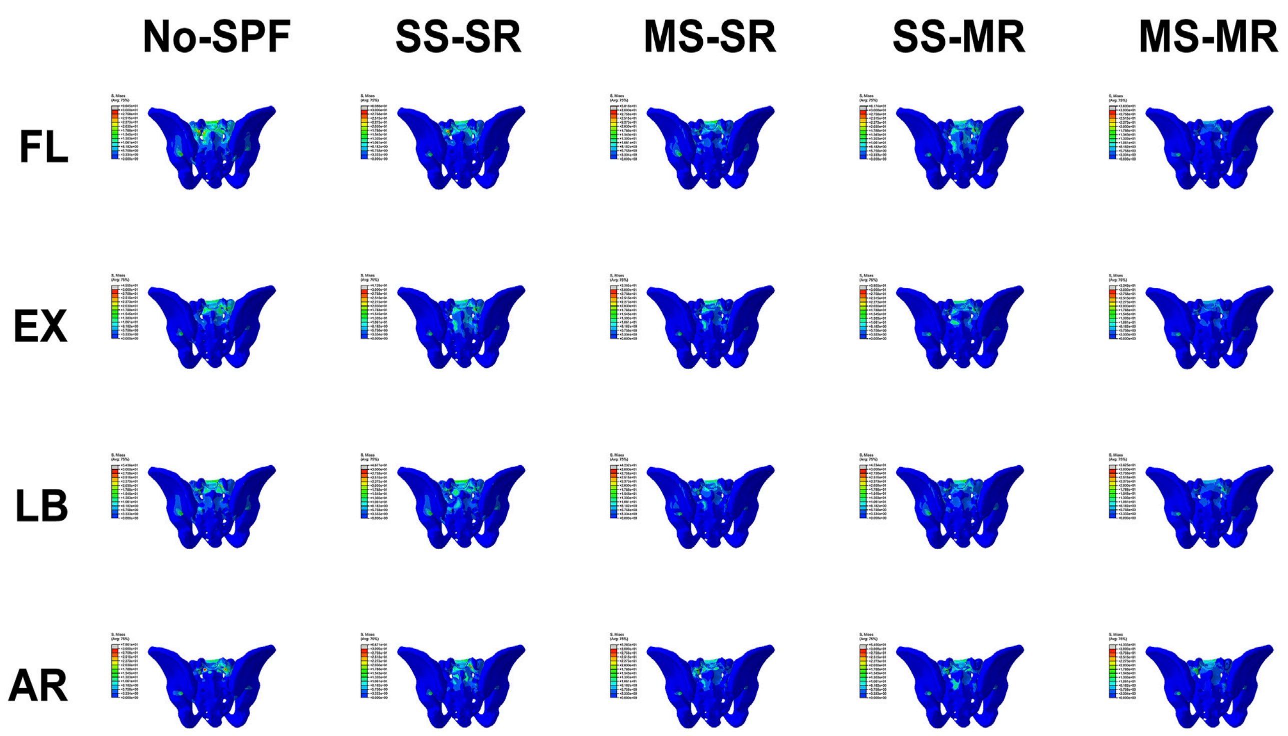

FIGURE 9
Von-Mises stress on sacrum of different instrumented models in flexion, extension, lateral bending, and axial rotation.

The LSJ is the most mobile and anteriorly inclined segment in the lumbar spine (Park et al., 2021a). These biomechanical characteristics induce a risk of pseudarthrosis in this region, which could predispose the implant to mechanical failure (Park et al., 2021b). Several studies reported a high incidence of lumbosacral pseudarthrosis with S1-PS alone (19.0%–83.0%) or additional SPF (10.5%–33.3%) (Kim et al., 2006a; Kim et al., 2006b; Finger et al., 2014; Guevara-Villazón et al., 2020; Eastlack et al., 2022). A meta-analysis by Han et al. reported that there was no significant difference in the pseudarthrosis rate between patients with or without SPF (Han et al., 2021). Therefore, advanced SPF technique by multiple pelvic screws or multirod construct was tried to solve this problem. Cadaveric studies have shown that four-rod constructs could significantly reduce the flexibility and motion of LSJ in FL, EX, and AR (Kelly et al., 2008; Wang et al., 2013; Godzik et al., 2019; Ntilikina et al., 2020). Consistent with previous studies, the current study additionally indicated that both the multiple pelvic screws and multirod construct could decrease the ROM of LSJ in FL, EX, LB, and AR compared with the SS-SR model. The ROM decreased most in the MS-MR model. In this construct, there were four rods crossing the LSJ, and the caudal anchors of the four rods were independent, which may contribute to its superior biomechanical characteristics. Therefore, we considered that additional pelvic screws and accessory rods had the potential to stabilize the LSJ further and achieve solid fusion. Priority should be given to the MS-MR construct for patients with high risks of pseudarthrosis.

Anterior column support using fusion cages could enhance the fusion rate and prevent implant failure at LSJ (Jung et al., 2019; Lee et al., 2020). However, osteoporosis is a risk factor for cage subsidence, with a high prevalence of 32.8% in ASD patients undergoing long spinal fusion (Gupta et al., 2021; Yang et al., 2021). Therefore, an appropriate biomechanical environment is paramount to a solid interbody fusion for ASD patients. The current study detected similar trends in the VMS variation on cage and S1-SEP. Compared with No-SPF and SS-SR, the VMS decreased the most in the MS-MR model. The VMS on cages in all directions decreased, ranging from 25.75% to 37.23% compared with No-SPF and 16.48%–26.81% compared with SS-SR; the VMS on S1-SEP in all directions decreased, ranging from 28.82% to 39.48% compared with No-SPF and 18.50%–32.83% compared with SS-SR. This finding indicated that the MS-MR construct could facilitate lumbosacral fusion by reducing the risk of cage subsidence. For patients with risk factors of cages subsidence, such as osteoporosis and age >60 years, the MS-MR could be considered.

The high incidence of lumbosacral and pelvic implant failure is a major concern for long spinal fusion. Substantial rates ranging from 23.7% to 56.0% have been reported by previous cohort studies (Guler et al., 2015; Hallager et al., 2017; Eastlack et al., 2022). Among the implant failure, rod fracture (RF) was the most common complication, and 28.0%–81.3% of RF occurred at lumbosacral rods (Devlin et al., 1991; Lertudomphonwanit et al., 2018; Rabinovich et al., 2021). The culprits of RF were pseudarthrosis and the increasing fatigue cracks under external stress (Yamanaka et al., 2015; Sardi et al., 2022). We reviewed and synthesised the data of all published clinical studies comparing the mechanical complication rate between two-rod construct and multirod construct, and a significantly lower incidence of pseudarthrosis (14.2% vs. 35.0%) and RF (15.8% vs. 32.9%) was detected in patients undergoing multirod construct (Hyun et al., 2014; Han et al., 2017; Merrill et al., 2017; Guevara-Villazón et al., 2020; Yamato et al., 2020; Bourghli et al., 2021; Dinizo et al., 2021; Lamas et al., 2021; Rabinovich et al., 2021; Lyu et al., 2022). There are two options to anchor the distal end of accessory rods, including domino connectors and multiple pelvic screws. The way of stress dispersal was different between the two options. Domino connector is the most popular option, in which the accessory rods were anchored to the primary rods instead of the vertebra, just as satellite rods. The stress of primary rods was transferred to the accessory rods, but it would be finally transferred back at the region distal to the accessory rods, resulting in RF or screw breakage at LSJ (Palumbo et al., 2015; Shen et al., 2018). However, by multiple pelvic screws, the accessory rods were directly anchored to the pelvis. The four rods crossing the LSJ are more mechanically independent, similar to two separate spinal constructs, providing the majority of cantilever force (Ramey et al., 2021). Cadaveric studies by Ntilikina et al. (2020) and Godzik et al. (2019) reported that accessory rods connected by domino connector could significantly decrease the strain of primary rods in FL, EX, LB, and the strain of S1-PS in AR. Nevertheless, the protective effect of accessory rods connected by multiple pelvic screws is still unknown. VMS was used in the current study. VMS is an equivalent stress value based on distortion energy to decide if a material will fail (yield) under a given loading condition. For spine and spinal instrumentation, a higher VMS on bone or internal fixation suggests a greater amount of deformation on it, which makes it more prone to instrumentation failure or fracture. We found that the VMS on instrumentation was decreased with the additional use of either S2AI screws or accessory rods. The VMS mainly concentrated on the L5-S1 rod, and the MS-MR model decreased the VMS in all directions, especially in EX, compared with No-SPF (45.40%) and SS-SR (35.85%). Also, both multiple pelvic screws and multirod constructs could protect the S1-PS and sacrum, and this effect provided by the MS-MR model was the most significant. This finding indicated that MS-MR could enhance the construct stiffness, reduce the risk of RF and screw breakage at LSJ, and reduce the risk of sacrum fracture. Additionally, the less stress values on MS-MR construct may indicate its superior durability, which could provide patients with long-term benefits.

The persistent motion of SIJ may result in further stress on the SPF and induce delayed failures (Eastlack et al., 2022). Tang et al., 2022 reported that the dual S2AI screws could mitigate postoperative SIJ pain and play an anti-rotation role. Consistent with their study, the current study revealed that the additional S2AI screw could further decrease the ROM of SIJ, especially in AR. This advantage may be associated with reduced VMS on instrumentation.

In addition to pseudarthrosis, postoperative residual sagittal and/or coronal malalignment are risk factors for implant failure following long spinal fusion for ASD (Lee et al., 2022b; Martin et al., 2022). For complex cases with preoperative several sagittal and coronal malalignment, three-column osteotomy (3-CO) and sequential correction techniques are usually needed (Lau et al., 2021; Shi et al., 2021). Therefore, a secure foundation and stiff construct that could accommodate powerful deformity correction and maintenance are essential. The dual pelvic screws could provide a stronger pelvic anchorage, and the accessory rods could reinforce the spinal construct, facilitating the restoration of spinopelvic alignment. For patients who need undergoing 3-CO at lumbar vertebra and extending the instrumentation into the upper thoracic region, some modifications could be made to the MS-MR construct presented in this study: the distal end of the primary rods should be extended and anchored to S2/ilium by pelvic screws; the proximal end of the accessory rods should be anchored to the distal adjacent vertebra of the upper instrumented vertebra by PS or cortical bone trajectory screw. More importantly, all the four rods should cross both the LSJ and the osteotomy site. These modifications made the four rods completely mechanically independent, constructing two separate spinopelvic fixation constructs. According to the spine instrumentation nomenclature provided by Ramey et al. the accessory rods in this kind of construct should be defined as “secondary rods” (Ramey et al., 2021). S2AI screw and iliac screw are two commonly used pelvic screws to achieve SPF. However, various advantages of S2AI screw over iliac screw have been demonstrated. The systematic review of biomechanical studies by Hirase et al. suggested that the stress on instrumentations and surrounding iliac bone was lower in S2AI screw fixation than iliac screw (Hirase et al., 2022). The meta-analysis by Gao et al. reported that using S2AI screw could adequately maintain the deformity correction and significantly decrease the risk of mechanical complications compared with the iliac screw (Gao et al., 2021). Also, the placement of S2AI screw does not require dissection as extensive as iliac screw; therefore, the incidence of skin breakdown and would infection was lower. Accordingly, when surgeons decide to implant multiple pelvic screws, we advocated S2AI screw as routine instrumentation.

The current biomechanical research may facilitate surgeons to better understand the mechanism of mechanical complications in long spinal fusion surgery and improve the instrumentation scenario or device designs. However, several limitations should be noted. First, as constructing a real ASD patient-specific lumbopelvic model and simulating the correction procedures (e.g., multi-level decompression, laminectomy, facetectomy, or osteotomies) remain technically challenging, the FE model was developed using the CT images from a healthy volunteer as an alternative. Therefore, the abnormal spinal loading caused by ASD and the individual variation of degeneration were not considered. This methodology was consistent with the previous FE studies focusing on the performance of different instrumentations and instrumentation-related problems in ASD (Buell et al., 2019; He et al., 2021; Oe et al., 2021; Leszczynski et al., 2022; Son et al., 2022). Further studies should construct and use ASD patient-specific FE models to elucidate the clinical significance of the various instrumentations. Second, boundary conditions were assigned based on the literature. However, the actual mechanical environment was patient-specific. Therefore, a discrepancy may exist between the FE model and clinical observations. Third, some simplifications were made in the construction of FE models. The paraspinal muscles and surrounding soft tissues were not simulated, and the nucleus pulposus was assigned with a hyperplastic material, which may affect the flexibility of the spine and misrepresent the stress distribution on some spinal components. Biphasic materials composed of a solid phase embedded in a fluid media may be more appropriate and realistic for the modelling of intervertebral disc (Elmasry et al., 2017). Also, bone mineral density could influence the stress pattern in SEP and cage, but it was not considered a variable in the current study. Finally, although FE analysis has the advantage of eliminating anatomical variability and has been shown to be a reliable method to perform biomechanical comparisons among spinal instrumentations, the actual clinical effects of MS-MR construct still need to be verified by cadaveric tests as well as clinical trials with large sample size and long-term follow-up.

Conclusion

Both multiple pelvic screws and multirod construct could increase the mechanical stability of LSJ and reduce stress on construct, cages, S1-SEP, and sacrum. The MS-MR construct was the most adequate to reduce the risk of lumbosacral pseudarthrosis, RF, screw breakage, and sacrum fracture. This study may provide surgeons with important evidence for the application of MS-MR construct in the clinical settings.

Data availability statement

The raw data supporting the conclusion of this article will be made available by the authors, without undue reservation.

Ethics statement

The studies involving human participants were reviewed and approved by the Research Ethics Committee of Beijing Chao-Yang Hospital. The patients/participants provided their written informed consent to participate in this study.

Author contributions

HY, AP, and YH contributed to conception and design of the study. HY and YL organized the database. FC performed the statistical analysis. HY wrote the first draft of the manuscript. AP, FC, and HD wrote sections of the manuscript. All authors contributed to manuscript revision, read, and approved the submitted version.

Funding

This study was supported by the Beijing Natural Science Foundation No. 20L2211.

Conflict of interest

The authors declare that the research was conducted in the absence of any commercial or financial relationships that could be construed as a potential conflict of interest.

Publisher's note

Supplementary material

The Supplementary Material for this article can be found online at: https://www.frontiersin.org/articles/10.3389/fbioe.2023.1148342/full#supplementary-material

References

Ames, C. P., Scheer, J. K., Lafage, V., Smith, J. S., Bess, S., Berven, S. H., et al. (2016). Adult spinal deformity: Epidemiology, health impact, evaluation, and management. *Spine Deform.* 4 (4), 310–322. doi:10.1016/j.jspd.2015.12.009

Bourghli, A., Boissiere, L., Kieser, D., Larrieu, D., Pizones, J., Alanay, A., et al. (2021). Multiple-rod constructs do not reduce pseudarthrosis and rod fracture after pedicle subtraction osteotomy for adult spinal deformity correction but improve quality of life. *Neurospine* 18 (4), 816–823. doi:10.14245/ns.2142596.298

Buell, T. J., Bess, S., Xu, M., Schwab, F. J., Lafage, V., Ames, C. P., et al. (2019). Optimal tether configurations and preload tensioning to prevent proximal junctional kyphosis: A finite element analysis. *J. Neurosurg. Spine* 30, 574–584. doi:10.3171/2018.10.Spine18429

Cook, D. J., Yeager, M. S., and Cheng, B. C. (2015). Range of motion of the intact lumbar segment: A multivariate study of 42 lumbar spines. *Int. J. Spine Surg.* 9, 5. doi:10.14444/2005

Cross, W. W., 3rd, Berven, S. H., Slater, N., Lehrman, J. N., Newcomb, A., and Kelly, B. P. (2018). *In vitro* biomechanical evaluation of a novel, minimally invasive, sacroiliac joint fixation device. *Int. J. Spine Surg.* 12 (5), 587–594. doi:10.14444/5072

Dalstra, M., and Huiskes, R. (1995). Load transfer across the pelvic bone. *J. Biomech.* 28 (6), 715–724. doi:10.1016/0021-9290(94)00125-n

de Andrada Pereira, B., Lehrman, J. N., Sawa, A. G. U., Lindsey, D. P., Yerby, S. A., Godzik, J., et al. (2021). Biomechanical effects of a novel posteriorly placed sacroiliac joint fusion device integrated with traditional lumbopelvic long-construct instrumentation. *J. Neurosurg. Spine* 35, 320–329. doi:10.3171/2020.11.Spine201540

de Andrada Pereira, B., Wangsawatwong, P., Lehrman, J. N., Sawa, A. G. U., Lindsey, D. P., Yerby, S. A., et al. (2022). Biomechanics of a laterally placed sacroiliac joint fusion device supplemental to S2 alar-iliac fixation in a long-segment adult spinal deformity construct: A cadaveric study of stability and strain distribution. *J. Neurosurg. Spine* 36 (1), 42–52. doi:10.3171/2021.3.Spine202175

Devlin, V. J., Boachie-Adjei, O., Bradford, D. S., Ogilvie, J. W., and Transfeldt, E. E. (1991). Treatment of adult spinal deformity with fusion to the sacrum using CD instrumentation. *J. Spinal Disord.* 4 (1), 1–14.

Dinizo, M., Passias, P., Kebaish, K., Errico, T. J., and Raman, T. (2021). The approach to pseudarthrosis after adult spinal deformity surgery: Is a multiple-rod construct necessary? *Glob. Spine J.*, 21925682211001880. doi:10.1177/21925682211001880

Eastlack, R. K., Soroceanu, A., Mundis, G. M., Jr., Daniels, A. H., Smith, J. S., Line, B., et al. (2022). Rates of loosening, failure, and revision of iliac fixation in adult deformity surgery. *Spine (Phila Pa 1976)* 47 (14), 986–994. doi:10.1097/brs.0000000000004356

El Dafrawy, M. H., Raad, M., Okafor, L., and Kebaish, K. M. (2019). Sacropelvic fixation: A comprehensive review. *Spine Deform.* 7 (4), 509–516. doi:10.1016/j.jspd.2018.11.009

Elmasry, S., Asfour, S., and Travascio, F. (2017). Effectiveness of pedicle screw inclusion at the fracture level in short-segment fixation constructs for the treatment of thoracolumbar burst fractures: A computational biomechanics analysis. *Comput*

Methods Biomech. Biomed. Engin 20 (13), 1412–1420. doi:10.1080/10255842.2017.1366995

Finger, T., Bayerl, S., Onken, J., Czabanka, M., Woitzik, J., and Vajkoczy, P. (2014). Sacropelvic fixation versus fusion to the sacrum for spondylodesis in multilevel degenerative spine disease. *Eur. Spine J.* 23 (5), 1013–1020. doi:10.1007/s00586-014-3165-6

Gao, Z., Sun, X., Chen, C., Teng, Z., Xu, B., Ma, X., et al. (2021). Comparative radiological outcomes and complications of sacral-2-alar iliac screw versus iliac screw for sacropelvic fixation. *Eur. Spine J.* 30 (8), 2257–2270. doi:10.1007/s00586-021-06864-7

Godzik, J., Hlubek, R. J., Newcomb, A., Lehrman, J. N., de Andrada Pereira, B., Farber, S. H., et al. (2019). Supplemental rods are needed to maximally reduce rod strain across the lumbosacral junction with TLIF but not ALIF in long constructs. *Spine J.* 19 (6), 1121–1131. doi:10.1016/j.spinee.2019.01.005

Guevara-Villazón, F., Boissiere, L., Hayashi, K., Larrieu, D., Ghailane, S., Vital, J. M., et al. (2020). Multiple-rod constructs in adult spinal deformity surgery for pelvic-fixated long instrumentations: An integral matched cohort analysis. *Eur. Spine J.* 29 (4), 886–895. doi:10.1007/s00586-020-06311-z

Guler, U. O., Cetin, E., Yaman, O., Pellise, F., Casademut, A. V., Sabat, M. D., et al. (2015). Sacropelvic fixation in adult spinal deformity (ASD); a very high rate of mechanical failure. *Eur. Spine J.* 24 (5), 1085–1091. doi:10.1007/s00586-014-3615-1

Gupta, A., Cha, T., Schwab, J., Fogel, H., Tobert, D. G., Razi, A. E., et al. (2021). Osteoporosis is under recognized and undertreated in adult spinal deformity patients. *J. Spine Surg.* 7 (1), 1–7. doi:10.21037/jss-20-668

Hakim, N. S., and King, A. I. (1979). A three dimensional finite element dynamic response analysis of a vertebra with experimental verification. *J. Biomech.* 12 (4), 277–292. doi:10.1016/0021-9290(79)90070-8

Hallager, D. W., Karstensen, S., Bukhari, N., Gehrchen, M., and Dahl, B. (2017). Radiographic predictors for mechanical failure after adult spinal deformity surgery: A retrospective cohort study in 138 patients. *Spine (Phila Pa 1976)* 42 (14), E855–e863. doi:10.1097/brs.0000000000001996

Han, B., Yin, P., Hai, Y., Cheng, Y., Guan, L., and Liu, Y. (2021). The comparison of spinopelvic parameters, complications, and clinical outcomes after spinal fusion to S1 with or without additional sacropelvic fixation for adult spinal deformity: A systematic review and meta-analysis. *Spine (Phila Pa 1976)* 46 (17), E945–e953. doi:10.1097/brs.0000000000004003

Han, S., Hyun, S. J., Kim, K. J., Jahng, T. A., Lee, S., and Rhim, S. C. (2017). Rod stiffness as a risk factor of proximal junctional kyphosis after adult spinal deformity surgery: Comparative study between cobalt chrome multiple-rod constructs and titanium alloy two-rod constructs. *Spine J.* 17 (7), 962–968. doi:10.1016/j.spinee.2017.02.005

Hasan, M. Y., Liu, G., Wong, H. K., and Tan, J. H. (2020). Postoperative complications of S2AI versus iliac screw in spinopelvic fixation: A meta-analysis and recent trends review. *Spine J.* 20 (6), 964–972. doi:10.1016/j.spinee.2019.11.014

He, Z., Zhang, M., Li, W., Long, Z., Wang, L., Li, Q. Q., et al. (2021). Finite element analysis of an improved correction system for spinal deformity. *Vivo* 35 (4), 2197–2205. doi:10.21873/invivo.12491

Hirase, T., Shin, C., Ling, J., Phelps, B., Haghshenas, V., Saifi, C., et al. (2022). S2 alar-iliac screw versus traditional iliac screw for spinopelvic fixation: A systematic review of comparative biomechanical studies. *Spine Deform.* 10 (6), 1279–1288. doi:10.1007/s43390-022-00528-2

Hsiao, C. K., Tsai, Y. J., Yen, C. Y., Li, Y. C., Hsiao, H. Y., and Tu, Y. K. (2022). Biomechanical effect of hybrid dynamic stabilization implant on the segmental motion and intradiscal pressure in human lumbar spine. *Bioeng. (Basel)* 10 (1), 31. doi:10.3390/bioengineering10010031

Hyun, S. J., Lenke, L. G., Kim, Y. C., Koester, L. A., and Blanke, K. M. (2014). Comparison of standard 2-rod constructs to multiple-rod constructs for fixation across 3-column spinal osteotomies. *Spine* 39 (22), 1899–1904. doi:10.1097/BRS.0000000000000556

Jain, A., Brooks, J. T., Kebaish, K. M., and Sponseller, P. D. (2016). Sacral alar iliac fixation for spine deformity. *JBJS Essent. Surg. Tech.* 6 (1), e10. doi:10.2106/jbjs.St.15.00074

Jung, J. M., Hyun, S. J., Kim, K. J., and Jahng, T. A. (2019). Rod fracture after multiple-rod constructs for adult spinal deformity. *J. Neurosurg. Spine* 32, 407–414. doi:10.3171/2019.9.Spine19913

Kawahara, N., Murakami, H., Yoshida, A., Sakamoto, J., Oda, J., and Tomita, K. (2003). Reconstruction after total sacrectomy using a new instrumentation technique: A biomechanical comparison. *Spine (Phila Pa 1976)* 28 (14), 1567–1572. doi:10.1097/01.brs.0000076914.32408.85

Kelly, B. P., Shen, F. H., Schwab, J. S., Arlet, V., and Diangelo, D. J. (2008). Biomechanical testing of a novel four-rod technique for lumbo-pelvic reconstruction. *Spine (Phila Pa 1976)* 33 (13), E400–E406. doi:10.1097/BRS.0b013e31817615c5

Kiapour, A., Joukar, A., Elgafy, H., Erbulut, D. U., Agarwal, A. K., and Goel, V. K. (2020). Biomechanics of the sacroiliac joint: Anatomy, function, biomechanics, sexual dimorphism, and causes of pain. *Int. J. Spine Surg.* 14 (1), 3–13. doi:10.14444/6077

Kim, H. J., Yang, J. H., Chang, D. G., Suk, S. I., Suh, S. W., Song, K. S., et al. (2020). Adult spinal deformity: Current concepts and decision-making strategies for management. *Asian Spine J.* 14 (6), 886–897. doi:10.31616/asj.2020.0568

Kim, J. H., Horton, W., Hamasaki, T., Freedman, B., Whitesides, T. E., Jr., and Hutton, W. C. (2010). Spinal instrumentation for sacral-pelvic fixation: A biomechanical comparison between constructs ending with either S2 bicortical, bitriangulated screws or iliac screws. *J. Spinal Disord. Tech.* 23 (8), 506–512. doi:10.1097/BSD.0b013e3181c37438

Kim, Y. J., Bridwell, K. H., Lenke, L. G., Cho, K. J., Edwards, C. C., 2nd, et al. (2006a). Pseudarthrosis in adult spinal deformity following multisegmental instrumentation and arthrodesis. *J. Bone Jt. Surg. Am.* 88 (4), 721–728. doi:10.2106/jbjs.E.00550

Kim, Y. J., Bridwell, K. H., Lenke, L. G., Rhim, S., and Cheh, G. (2006b). Pseudarthrosis in long adult spinal deformity instrumentation and fusion to the sacrum: Prevalence and risk factor analysis of 144 cases. *Spine (Phila Pa 1976)* 31 (20), 2329–2336. doi:10.1097/01.brs.0000238968.82799.d9

Lamas, V., Charles, Y. P., Tuzin, N., and Steib, J. P. (2021). Comparison of degenerative lumbar scoliosis correction and risk for mechanical failure using posterior 2-rod instrumentation versus 4-rod instrumentation and interbody fusion. *Eur. Spine J.* 30 (7), 1965–1977. doi:10.1007/s00586-021-06870-9

Lau, D., Haddad, A. F., Fury, M. T., Deviren, V., and Ames, C. P. (2021). Multilevel pedicle subtraction osteotomy for correction of severe rigid adult spinal deformities: A case series, indications, considerations, and literature review. *Oper. Neurosurg. Hagerst.* 20 (4), 343–354. doi:10.1093/ons/opaa419

Lee, K. Y., Lee, J. H., Kang, K. C., Shin, S. J., Shin, W. J., Im, S. K., et al. (2020). Strategy for obtaining solid fusion at L5-S1 in adult spinal deformity: Risk factor analysis for nonunion at L5-S1. *J. Neurosurg. Spine* 33, 323–331. doi:10.3171/2020.2.Spine191181

Lee, N. J., Marciano, G., Puvanesarajah, V., Park, P. J., Clifton, W. E., Kwan, K., et al. (2022a). Incidence, mechanism, and protective strategies for 2-year pelvic fixation failure after adult spinal deformity surgery with a minimum six-level fusion. *J. Neurosurg. Spine* 38, 208–216. doi:10.3171/2022.8.Spine22755

Lee, N. J., Park, P. J., Puvanesarajah, V., Clifton, W. E., Kwan, K., Morrissette, C. R., et al. (2022b). How common is acute pelvic fixation failure after adult spine surgery? A single-center study of 358 patients. *J. Neurosurg. Spine* 38, 91–97. doi:10.3171/2022.7.Spine22498

Lertudomphonwanit, T., Kelly, M. P., Bridwell, K. H., Lenke, L. G., McAnany, S. J., Punyarat, P., et al. (2018). Rod fracture in adult spinal deformity surgery fused to the sacrum: Prevalence, risk factors, and impact on health-related quality of life in 526 patients. *Spine J.* 18 (9), 1612–1624. doi:10.1016/j.spinee.2018.02.008

Leszczynski, A., Meyer, F., Charles, Y. P., Deck, C., Bourdet, N., and Willinger, R. (2022). Influence of double rods and interbody cages on range of motion and rod stress after spinopelvic instrumentation: A finite element study. *Eur. Spine J.* 31 (6), 1515–1524. doi:10.1007/s00586-022-07149-3

Lindsey, D. P., Perez-Orribo, L., Rodriguez-Martinez, N., Reyes, P. M., Newcomb, A., Cable, A., et al. (2014). Evaluation of a minimally invasive procedure for sacroiliac joint fusion - an *in vitro* biomechanical analysis of initial and cycled properties. *Med. Devices (Auckl)* 7, 131–137. doi:10.2147/mder.S63499

Lyu, Q., Lau, D., Haddad, A. F., Deviren, V., and Ames, C. P. (2022). Multiple-rod constructs and use of bone morphogenetic protein–2 in relation to lower rod fracture rates in 141 patients with adult spinal deformity who underwent lumbar pedicle subtraction osteotomy. *J. Neurosurg. Spine* 36 (2), 1–11. doi:10.3171/2021.3.SPINE201968

Martin, C. T., Polly, D. W., Holton, K. J., San Miguel-Ruiz, J. E., Albersheim, M., Lender, P., et al. (2022). Acute failure of S2-alar-iliac screw pelvic fixation in adult spinal deformity: Novel failure mechanism, case series, and review of the literature. *J. Neurosurg. Spine* 36 (1), 53–61. doi:10.3171/2021.2.Spine201921

Merrill, R. K., Kim, J. S., Leven, D. M., Kim, J. H., and Cho, S. K. (2017). Multi-rod constructs can prevent rod breakage and pseudarthrosis at the lumbosacral junction in adult spinal deformity. *Glob. Spine J.* 7 (6), 514–520. doi:10.1177/2192568217699392

Ntilikina, Y., Charles, Y. P., Persohn, S., and Skalli, W. (2020). Influence of double rods and interbody cages on quasistatic range of motion of the spine after lumbopelvic instrumentation. *Eur. Spine J.* 29 (12), 2980–2989. doi:10.1007/s00586-020-06594-2

Oe, S., Narita, K., Hasegawa, K., Natarajan, R. N., Yamato, Y., Hasegawa, T., et al. (2021). Longer screws can reduce the stress on the upper instrumented vertebra with long spinal fusion surgery: A finite element analysis study. *Glob. Spine J.* 21925682211018467, 21925682211018467. doi:10.1177/21925682211018467

Palumbo, M. A., Shah, K. N., Eberson, C. P., Hart, R. A., and Daniels, A. H. (2015). Outrigger rod technique for supplemental support of posterior spinal arthrodesis. *Spine J.* 15 (6), 1409–1414. doi:10.1016/j.spinee.2015.03.004

Panjabi, M. M., Oxland, T. R., Yamamoto, I., and Crisco, J. J. (1994). Mechanical behavior of the human lumbar and lumbosacral spine as shown by three-dimensional load-displacement curves. *J. Bone Jt. Surg. Am.* 76 (3), 413–424. doi:10.2106/00004623-199403000-00012

Park, S. J., Park, J. S., Lee, C. S., and Lee, K. H. (2021a). Metal failure and nonunion at L5-S1 after long instrumented fusion distal to pelvis for adult spinal deformity: Anterior versus transforaminal interbody fusion. *J. Orthop. Surg. Hong. Kong)* 29 (3), 230949902110542. doi:10.1177/23094990211054223

Park, S. J., Park, J. S., Nam, Y., Yum, T. H., Choi, Y. T., and Lee, C. S. (2021b). Failure types and related factors of spinopelvic fixation after long construct fusion for adult spinal deformity. *Neurosurgery* 88 (3), 603–611. doi:10.1093/neuros/nyaa469

Pellisé, F., Vila-Casademunt, A., Ferrer, M., Domingo-Sàbat, M., Bagó, J., Pérez-Grueso, F. J., et al. (2015). Impact on health related quality of life of adult spinal deformity (ASD) compared with other chronic conditions. *Eur. Spine J.* 24 (1), 3–11. doi:10.1007/s00586-014-3542-1

Phillips, A. T., Pankaj, P., Howie, C. R., Usmani, A. S., and Simpson, A. H. (2007). Finite element modelling of the pelvis: Inclusion of muscular and ligamentous boundary conditions. *Med. Eng. Phys.* 29 (7), 739–748. doi:10.1016/j.medengphy.2006.08.010

Rabinovich, E. P., Buell, T. J., Wang, T. R., Shaffrey, C. I., and Smith, J. S. (2021). Reduced occurrence of primary rod fracture after adult spinal deformity surgery with accessory supplemental rods: Retrospective analysis of 114 patients with minimum 2-year follow-up. *J. Neurosurg. Spine* 35 (4), 504–515. doi:10.3171/2020.12.Spine201527

Ramey, W. L., Jack, A. S., and Chapman, J. R. (2021). The lexicon of multirod constructs in adult spinal deformity: A concise description of when, why, and how. *J. Neurosurg. Spine* 36, 1023–1029. doi:10.3171/2021.10.Spine21745

Rohlmann, A., Bauer, L., Zander, T., Bergmann, G., and Wilke, H. J. (2006). Determination of trunk muscle forces for flexion and extension by using a validated finite element model of the lumbar spine and measured *in vivo* data. *J. Biomech.* 39 (6), 981–989. doi:10.1016/j.jbiomech.2005.02.019

Safaee, M. M., Ames, C. P., and Smith, J. S. (2020). Epidemiology and socioeconomic trends in adult spinal deformity care. *Neurosurgery* 87 (1), 25–32. doi:10.1093/neuros/nyz454

Sardi, J. P., Lazaro, B., Smith, J. S., Kelly, M. P., Dial, B., Hills, J., et al. (2022). Rod fractures in thoracolumbar fusions to the sacrum/pelvis for adult symptomatic lumbar scoliosis: Long-term follow-up of a prospective, multicenter cohort of 160 patients. *J. Neurosurg. Spine* 38, 217–229. doi:10.3171/2022.8.Spine22423

Sayed, D., Amirdelfan, K., Naidu, R. K., Raji, O. R., and Falowski, S. (2021). A cadaver-based biomechanical evaluation of a novel posterior approach to sacroiliac joint fusion: Analysis of the fixation and center of the instantaneous Axis of rotation. *Med. Devices (Auckl)* 14, 435–444. doi:10.2147/mder.S347763

Schmidt, H., Heuer, F., Drumm, J., Klezl, Z., Claes, L., and Wilke, H. J. (2007). Application of a calibration method provides more realistic results for a finite element model of a lumbar spinal segment. *Clin. Biomech. (Bristol, Avon)* 22 (4), 377–384. doi:10.1016/j.clinbiomech.2006.11.008

Shen, F. H., Qureshi, R., Tyger, R., Lehman, R., Singla, A., Shimer, A., et al. (2018). Use of the "dual construct" for the management of complex spinal reconstructions. *Spine J.* 18 (3), 482–490. doi:10.1016/j.spinee.2017.08.235

Shi, B., Liu, D., Zhu, Z., Wang, Y., Li, Y., Liu, Z., et al. (2021). Sequential correction technique in degenerative scoliosis with type C coronal imbalance: A comparison with traditional 2-rod technique. *J. Neurosurg. Spine* 36, 1005–1011. doi:10.3171/2021.10.Spine21768

Shi, D., Wang, F., Wang, D., Li, X., and Wang, Q. (2014). 3-D finite element analysis of the influence of synovial condition in sacroiliac joint on the load transmission in human pelvic system. *Med. Eng. Phys.* 36 (6), 745–753. doi:10.1016/j.medengphy.2014.01.002

Shirazi-Adl, S. A., Shrivastava, S. C., and Ahmed, A. M. (1984). Stress analysis of the lumbar disc-body unit in compression. A three-dimensional nonlinear finite element study. *Spine (Phila Pa 1976)* 9 (2), 120–134. doi:10.1097/00007632-198403000-00003

Sohn, S., Park, T. H., Chung, C. K., Kim, Y. J., Jang, J. W., Han, I. B., et al. (2018). Biomechanical characterization of three iliac screw fixation techniques: A finite element study. *J. Clin. Neurosci.* 52, 109–114. doi:10.1016/j.jocn.2018.03.002

Son, D. M., Lee, S. B., Lee, S. J., Park, T. H., Jang, J. E., Jeong, S. J., et al. (2022). Biomechanical comparison of multilevel lumbar instrumented fusions in adult spinal deformity according to the upper and lower fusion levels: A finite element analysis. *Biomed. Res. Int.* 2022, 1–9. doi:10.1155/2022/2534350

Tang, Z., Hu, Z., Zhu, Z., Qiao, J., Mao, S., Ling, C., et al. (2022). The utilization of dual second sacral alar-iliac screws for spinopelvic fixation in patients with severe kyphoscoliosis. *Orthop. Surg.* 14 (7), 1457–1468. doi:10.1111/os.13348

Uotani, K., Tanaka, M., Sonawane, S., Ruparel, S., Fujiwara, Y., Arataki, S., et al. (2021). Comparative study of bilateral dual sacral-alar-iliac screws versus bilateral single sacral-alar-iliac screw for adult spine deformities. *World Neurosurg.* 156, e300–e306. doi:10.1016/j.wneu.2021.09.048

Wang, T., Liu, H., Zheng, Z., Li, Z., Wang, J., Shrivastava, S. S., et al. (2013). Biomechanical effect of 4-rod technique on lumbosacral fixation: An *in vitro* human cadaveric investigation. *Spine (Phila Pa 1976)* 38(15), E925–E929. doi:10.1097/BRS.0b013e3182967968

Yamanaka, K., Mori, M., Yamazaki, K., Kumagai, R., Doita, M., and Chiba, A. (2015). Analysis of the fracture mechanism of Ti-6Al-4V alloy rods that failed clinically after spinal instrumentation surgery. *Spine (Phila Pa 1976)* 40 (13), E767–E773. doi:10.1097/brs.0000000000000881

Yamato, Y., Hasegawa, T., Togawa, D., Yoshida, G., Banno, T., Arima, H., et al. (2020). Long additional rod constructs can reduce the incidence of rod fractures following 3-column osteotomy with pelvic fixation in short term. *Spine Deform.* 8 (3), 481–490. doi:10.1007/s43390-020-00071-y

Yang, H., Liu, J., Hai, Y., and Han, B. (2023). What are the benefits of lateral lumbar interbody fusion on the treatment of adult spinal deformity: A systematic review and meta-analysis deformity. *Glob. Spine J.* 13 (1), 172–187. doi:10.1177/21925682221089876

Yang, H., Liu, J., and Hai, Y. (2021). Is instrumented lateral lumbar interbody fusion superior to stand-alone lateral lumbar interbody fusion for the treatment of lumbar degenerative disease? A meta-analysis. *J. Clin. Neurosci.* 92, 136–146. doi:10.1016/j.jocn.2021.08.002

Zheng, N., Watson, L. G., and Yong-Hing, K. (1997). Biomechanical modelling of the human sacroiliac joint. *Med. Biol. Eng. Comput* 35 (2), 77–82. doi:10.1007/bf02534134

frontiers | Frontiers in Bioengineering and Biotechnology

TYPE Original Research
PUBLISHED 14 March 2023
DOI 10.3389/fbioe.2023.1049100

Check for updates

OPEN ACCESS

EDITED BY
Qichang Mei,
Ningbo University, China

REVIEWED BY
Jan Kubicek,
VSB-Technical University of Ostrava, Czechia
Steve Laslovich,
Hawaii Pacific University, United States

*CORRESPONDENCE
Jian Li,
hxlijian.china@163.com
Yan Xiong,
luyibingli@163.com

SPECIALTY SECTION
This article was submitted to Biomechanics, a section of the journal Frontiers in Bioengineering and Biotechnology

RECEIVED 20 September 2022
ACCEPTED 14 February 2023
PUBLISHED 14 March 2023

CITATION
Li J, Tang J, Yao L, Fu W, Deng Q, Xiong Y and Li J (2023), The validity of the Ligs digital arthrometer at different loads to evaluate complete ACL ruptures.
Front. Bioeng. Biotechnol. 11:1049100.
doi: 10.3389/fbioe.2023.1049100

The validity of the Ligs digital arthrometer at different loads to evaluate complete ACL ruptures

Junqiao Li, Jiexi Tang, Lei Yao, Weili Fu, Qian Deng, Yan Xiong* and Jian Li*

Department of Orthopedics, Orthopedic Research Institute, West China Hospital, Sichuan University, Chengdu, China

Objective: The Ligs Digital Arthrometer is a recently launched versatile arthrometer that can be used for the quantitative assessment of knee and ankle joint laxity. This study aimed to evaluate the validity of the Ligs Digital Arthrometer for the diagnosis of complete anterior cruciate ligament (ACL) ruptures at different loads.

Materials and Methods: From March 2020 to February 2021, we included 114 normal subjects and 132 subjects diagnosed with complete ACL ruptures by magnetic resonance imaging (MRI) and eventually confirmed by arthroscopy in the study. Anterior knee laxity was independently measured by the same physical therapist using the Ligs Digital Arthrometer. Recorded anterior knee laxity and calculated the side-to-side difference (SSD) at 30, 60, 90, 120, and 150 N loads, respectively. The receiver operating characteristic (ROC) curve was used to determine the optimal laxity threshold, and the diagnostic value was evaluated by the area under the curve (AUC).

Results: The demographic data of the subjects were comparable between the two groups ($p > 0.05$). The mean values of anterior knee laxity measured by the Ligs Digital Arthrometer between the complete ACL ruptures group and the control group were significantly different at 30, 60, 90, 120, and 150 N loads ($p < 0.001$ for all). According to the results of ROC curve analysis, the optimal laxity threshold for the diagnosis of complete ACL ruptures was 1.1 mm SSD (Se = 66.7%, Sp = 69.3%) at 30 N, 1.3 mm (Se = 74.2%, Sp = 82.5%) at 60 N, 1.6 mm (Se = 79.5%, Sp = 94.7%) at 90 N, 1.9 mm (Se = 84.1%, Sp = 92.1%) at 120 N and 2.1 mm (Se = 85.6%, Sp = 91.2%) at 150 N. The AUC order at different loads from high to low was 150 N (0.948 [0.923–0.973])>120 N (0.933 [0.903–0.963])>90 N (0.902 [0.862–0.943]) >60 N (0.846 [0.799–0.893])>30 N (0.720 [0.657–0.783]).

Conclusion: The Ligs Digital Arthrometer proved to be of high diagnostic value in complete ACL ruptures at 90 N, 120 N, and 150 N loads. The diagnostic value improved with the increase of load in a certain range. Based on the results of this study, as a portable, digital and versatile new arthrometer, the Ligs Digital Arthrometer was a valid and promising tool for diagnosing complete ACL ruptures.

KEYWORDS

anterior cruciate ligament, knee laxity, quantitative assessment, Ligs digital arthrometer, diagnostic value

1 Introduction

Anterior cruciate ligament (ACL) ruptures are the most common type of knee injury with more than 250,000 ACL ruptures annually in the United States. Up to 65% of patients with ACL ruptures undergo anterior cruciate ligament reconstruction (ACLR) surgery; however, some patients with ACL ruptures can be treated with conservative therapy and rehabilitation training instead of operative therapy (Musahl and Karlsson, 2019; Kakavas et al., 2021). Considering this diversity of treatments, clinical diagnosis and evaluation after ACL ruptures are of great significance for selecting proper treatment. Therefore, the objective quantification assessment of anterior knee laxity using an arthrometer is necessary for ACL ruptures (Rohman and Macalena, 2016; Ryu et al., 2018).

Current arthrometers mainly include the KT-1000/KT-2000, Rolimeter and GNRB. Although the KT-1000/KT-2000 (MEDmetric Corp, San Diego, United States) is the most widely used arthrometer with generally supportive diagnostic validity, it can only provide specific loads to diagnose ACL ruptures. Additionally, precision is relatively low at 1 mm and a reading error exists because an artificial reading is required (Robert et al., 2009; Rohman and Macalena, 2016; Saravia et al., 2020). The Rolimeter (Aircast Europa, Neubeuern, Germany) is a device that requires the examiner to record anterior knee laxity by performing the Lachman test at maximal manual force, but this device has several drawbacks including an uncontrolled load and poor repeatability (Balasch et al., 1999; Papandreou et al., 2005; Rohman and Macalena, 2016). The GNRB (Genourob, Laval, France) is a computerized arthrometer with high precision that can provide a constant thrust load and automatically record the corresponding knee laxity, and has been proven to have good validity by several studies (Robert, et al., 2009; Klouche et al., 2015; Rohman and Macalena, 2016; Ryu, et al., 2018; Saravia, et al., 2020). Moreover, as a stress radiography system, the Telos device (GmbH, Hungen, Germany) can directly evaluate anterior tibial translation with high repeatability and no interference with soft tissue. However, it requires the operator to measure radiographs, which is expensive and includes a certain amount of radiation exposure for patients (Jorn et al., 1998; Beldame et al., 2012; Lefevre et al., 2014; Bouguennec et al., 2015; Rohman and Macalena, 2016; Ryu, et al., 2018).

The recently launched Ligs Digital Arthrometer (Innomotion Inc., Shanghai, China) is a versatile arthrometer with portable, digital and radiation-free characteristics that can be used for the quantitative assessment of knee and ankle joint laxity. It has a built-in pressure sensor with an accuracy of 1 N and can provide continuous or constant loads as required. During the measurement, the push rod of the Ligs Digital Arthrometer applies vertical load on the tibia from the rear of the lower leg parallel to the tibial tubercle. The relative displacement is automatically collected in real time by a displacement sensor on the top of the push rod, with a precision of 0.1 mm and a sampling frequency of 30 Hz. Collected data are processed and analysed using the built-in PC system to obtain a force-displacement curve displayed on the screen. In addition, it can perform simultaneous stress radiography with the assistance of radiological equipment when necessary.

At present, the Ligs Digital Arthrometer has been reported in the literature for the quantitative assessment of chronic ankle instability and knee laxity after ACLR (Chen et al., 2022; Zhou et al., 2022). However, there are no studies concerning the application of the Ligs Digital Arthrometer in the diagnosis of ACL ruptures. Therefore, the purpose of this study was to evaluate the validity of the Lig Digital Arthrometer for the diagnosis of complete ACL ruptures at different loads using arthroscopic assessment as the reference standard.

FIGURE 1
The presentation of the Ligs Digital Arthrometer.

2 Materials and methods

A cross-sectional study from March 2020 to February 2021 was conducted. This study was approved by the Ethics Committee on Biomedical Research, West China Hospital of Sichuan University (No. 2016–99 11/1/2016). All subjects understood the purpose and significance of this study and signed an informed consent form.

2.1 Inclusion and exclusion criteria

Subjects in the experimental group included the patients in our hospital between 18 and 60 years of age, who were diagnosed with complete ACL ruptures by magnetic resonance imaging (MRI) and eventually confirmed by arthroscopy. The exclusion criteria were as follows: 1) ACL avulsion fracture; 2) concomitant PCL injury; 3) previous surgery and primary disease in the involved knee; 4) previous injury, surgery and primary disease in the contralateral knee; or 5) refusal to participate in the research. Meanwhile, normal people aged between 18 and 60 years were recruited as the control group. The exclusion criteria were as follows: 1) previous injury, surgery and primary disease in either knee; or 2) refusal to participate in the research.

2.2 Measurement of anterior knee laxity

Anterior knee laxity was independently measured by the same physical therapist after strict training using the Ligs Digital Arthrometer (Figure 1). In the experimental group, the healthy

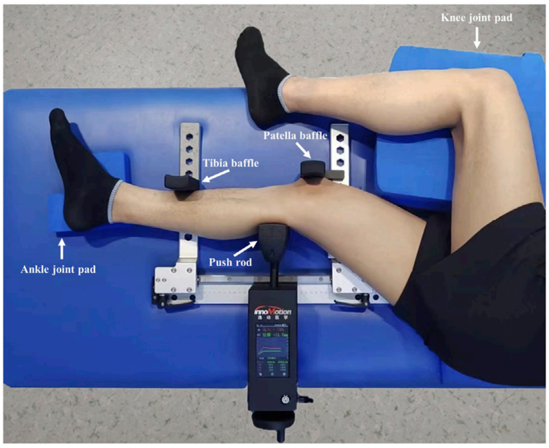

FIGURE 2
The measurement of anterior knee laxity by the Ligs Digital Arthrometer.

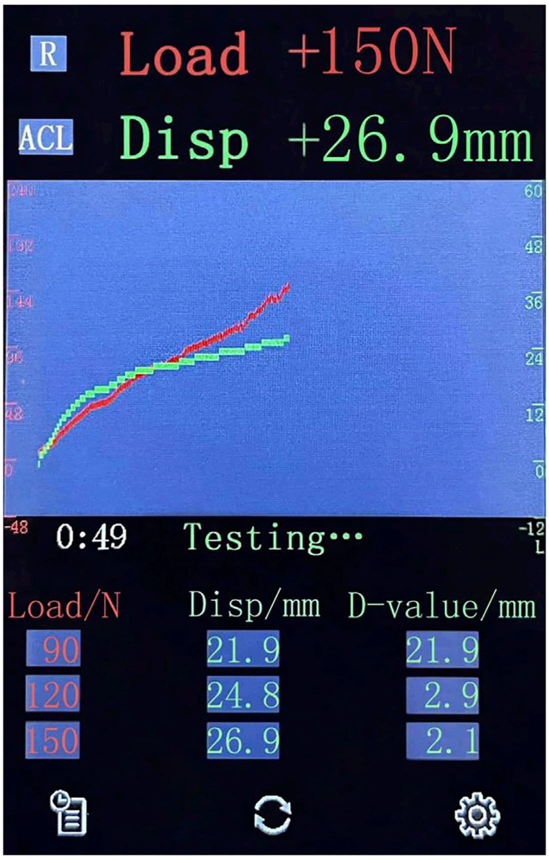

FIGURE 3
The display interface of the Ligs Digital Arthrometer for data collection. Load, the applied load; Disp, anterior displacement of the knee; D-value, the difference value of displacement between the current load and the prior load.

knee was measured followed by the involved knee. In the control group, the operator first measured the left knee followed by the right knee.

The subject was placed in the standard lateral decubitus position with the involved lower limb on the Ligs Digital Arthrometer. The involved knee flexed at 30° with neutral rotation, and a pad was used to support the ankle joint to keep the tibia horizontal without internal and external rotation. Meanwhile, the contralateral lower limb was bent and placed in front of the body, and the knee joint was supported with a pad to keep it in a relaxed state. The operator aimed the centre of the push rod at the level of the tibial tubercle from the rear of the lower leg, then adjusted the upper bracket to make the patella close to the groove of the patella baffle, and then moved the lower bracket to the end to fix the lower tibia using the tibia baffle (Figure 2).

Before each measurement, the operator reset the arthrometer and instructed the patient to relax the muscles of the lower limbs. During the measurement, a forward load ranging from 0 to 150 N was manually applied to the tibia at a constant speed. If the subject experienced any significant discomfort, the measurement procedure was stopped immediately or at any time upon the subject's request. The contralateral knee joint was measured by the same method.

In the present study, the anterior knee laxity corresponding to the loads of 30, 60, 90, 120, and 150 N was automatically recorded and a force-displacement curve was generated (Figure 3). Each knee joint was measured three times, and the average of the three measurements was determined. After the measurement, the side-to-side difference (SSD) of anterior knee laxity at the corresponding load was calculated.

2.3 Data collection

The sex ratio, age, height, weight, BMI and SSD in anterior knee laxity at 30, 60, 90, 120, and 150 N loads were recorded for all subjects. Besides, we recorded the time from injury to measurement and the concomitant injuries of the medial collateral ligament (MCL), anterolateral ligament (ALL) and meniscuses for patients with complete ACL ruptures. A total of 246 subjects were enrolled in this study, which included 132 subjects with complete ACL ruptures in the experimental group and 114 normal subjects in the control group. The mean age of the subjects was 31.04 ± 5.35 years (range, 19 to 44 years) with a sex distribution of 171 males and 75 females.

2.4 Statistical analysis

A post hoc power analysis using G*Power software version 3.1.9.2 (Franz, Universitat Kiel, Germany) with a given effect size of 0.8 and α = 0.05 revealed a power of 1.

Data were analysed using the Statistical Package for Social Sciences (SPSS) version 26.0 (IBM Corp., Armonk, New York, United States). Categorical variables were expressed as frequencies and analysed using the chi-square test. Continuous variables were expressed as means and standard deviations. The normality of continuous variable distributions was analysed using the Shapiro–Wilk test. If the distribution was normal, the parametric Student's t-test was used for the quantitative variables. Otherwise, the non-parametric Mann–Whitney *U* test was used. The optimal laxity thresholds of the Ligs Digital Arthrometer at 30, 60, 90, 120, and 150 N loads were determined according to receiver operating

TABLE 1 Demographic data of the subjects in two groups.

Variables	Experimental group (n = 132)	Control group (n = 114)	*p*-value
Sex ratio, male/female	92/40	79/35	0.946
Age, y	30.52 ± 4.94	31.65 ± 5.01	0.076
Height, cm	171.45 ± 6.24	170.34 ± 6.16	0.162
Weight, kg	68.78 ± 8.62	67.54 ± 11.37	0.332
Body mass index, kg/m^2	23.39 ± 2.75	23.17 ± 3.03	0.550

*Data are given as the mean ± standard deviation or the number of subjects.

characteristic (ROC) curve analysis. The sensitivity (Se), specificity (Sp), positive predictive value (PPV), negative predictive value (NPV), positive likelihood ratio (LR+), negative likelihood ratio (LR-) and Youden's index were calculated. Furthermore, the diagnostic value was evaluated by the area under the curve (AUC) with a 95% CI. Specifically, the diagnostic value corresponding to different AUCs can be divided into null (AUC = 0.5), poorly informative (0.5<AUC<0.7), fairly informative (0.7<AUC<0.9), highly informative (0.9<AUC<1), and perfect (AUC = 1) (Klouche, et al., 2015). A *p*-value <0.05 was considered statistically significant for all analyses.

3 Results

A total of 132 subjects, including 92 males and 40 females, were finally diagnosed with complete ACL ruptures by arthroscopy in the experimental group, and 46 cases were accompanied with MCL injuries (including 36 cases of grade I, 8 cases of grade II and 2 cases of grade III), 74 cases were accompanied with ALL abnormalities, 52 cases were accompanied with lateral meniscus injuries, and 46 cases were accompanied with medial meniscus injuries (including 7 cases of bucket handle tears). The mean time from injury to measurement was 8.69 ± 8.22 weeks and ranged from 1 to 42 weeks. The 114 normal subjects in the control group included 79 males and 35 females. The demographic data of the subjects were comparable between the two groups (Table 1). All the subjects were able to tolerate the maximum load of 150 N during the measurement.

The mean SSD of anterior knee laxity measured by the Ligs Digital Arthrometer at 30 N was 1.58 ± 1.07 mm in the experimental group and 0.84 ± 0.59 mm in the control group ($p < 0.001$). The mean SSD at 60 N was 2.65 ± 1.71 mm in the experimental group and 0.90 ± 0.67 mm in the control group ($p < 0.001$). At 90 N, the mean SSD was 3.37 ± 2.02 mm in the experimental group and 0.94 ± 0.70 mm in the control group ($p < 0.001$). At 120 N, the mean SSD was 4.08 ± 2.30 mm in the experimental group and 1.01 ± 0.71 mm in the control group ($p < 0.001$). At 150 N, the mean SSD was 4.63 ± 2.52 mm in the experimental group and 1.10 ± 0.79 mm in the control group ($p < 0.001$) (Figure 4).

According to the ROC curve analysis, the optimal laxity threshold for the diagnosis of complete ACL ruptures by the Ligs Digital Arthrometer was 1.1 mm SSD (Se = 66.7%, Sp = 69.3%) at 30 N, 1.3 mm (Se = 74.2%, Sp = 82.5%) at 60 N, 1.6 mm (Se = 79.5%, Sp = 94.7%) at 90 N, 1.9 mm (Se = 84.1%, Sp = 92.1%) at 120 N, and 2.1 mm (Se = 85.6%, Sp = 91.2%) at 150 N (Table 2).

The AUC analysis showed that the measurements of the Ligs Digital Arthrometer were fairly informative at 30 N and 60 N loads, and highly informative at 90 N, 120 N, and 150 N loads. The AUC order at different loads from high to low was 150 N (0.948 [0.923–0.973])>120 N (0.933 [0.903–0.963])>90 N (0.902 [0.862–0.943])>60 N (0.846 [0.799–0.893])>30 N (0.720 [0.657–0.783]) (Figure 5).

4 Discussion

Clinical examination and MRI are the two main methods that are used to evaluate ACL ruptures (Kaeding et al., 2017). Although MRI is widely used as the preferred imaging method for the diagnosis of ACL ruptures with excellent sensitivity and specificity, it cannot be used to evaluate the severity of knee instability after injury (Koch et al., 2021; Shantanu et al., 2021). The anterior drawer test and Lachman test are commonly used physical examination to evaluate anterior knee laxity, but results are susceptible to patients' pain, muscular tension and inherent knee laxity (Rohman and Macalena, 2016). In addition, the differences in clinician experience and applied manual force will lead to a certain degree of subjectivity in results and an inaccurate quantitative assessment of anterior knee laxity. In view of this problem, arthrometers have gradually become an important auxiliary device for the diagnosis of ACL ruptures and the quantitative evaluation of anterior knee laxity.

As a new versatile arthrometer, one advantage of the Ligs Digital Arthrometer is the ability to quantitatively assess the laxity of knee and ankle joints, by combining different fixation suites. A recent study by Chen et al. showed that the Ligs Digital Arthrometer is useful for quantifying the ankle laxity in chronic ankle instability with high diagnostic accuracy and excellent reliability (Chen et al., 2022). In terms of rehabilitation after ACLR, Zhou et al. assessed knee laxity after ACLR using the Ligs Digital Arthrometer to assist the guidance of return-to-sports decision-making (Zhou et al., 2022). Second, the Ligs Digital Arthrometer generates a force-displacement curve by delivering continuous loads and recording the laxity with a precision up to 0.1 mm, which allows the diagnosis of ACL ruptures based on the differential laxity of a force-displacement curve (Rohman and Macalena, 2016). Furthermore, another potential advantage of the Ligs Digital Arthrometer is that it can provide a specific load for simultaneous stress radiography. The imaging protocol of this approach is similar to that of the Telos

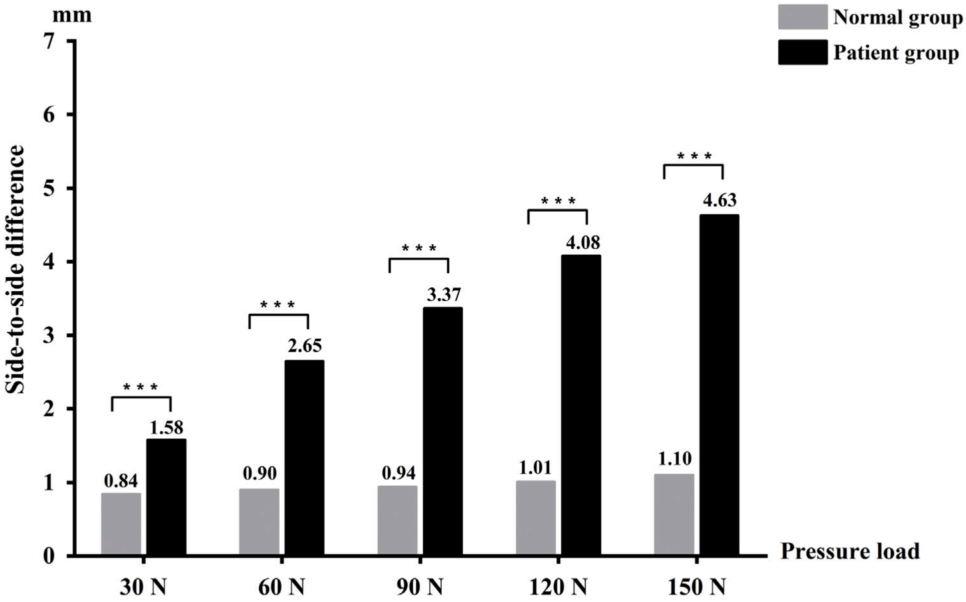

FIGURE 4
The side-to-side difference between the two groups in anterior knee laxity measured by the Ligs Digital Arthrometer.

TABLE 2 Results of the ROC curve analysis for the Ligs Digital Arthrometer.

Variables	30 N	60 N	90 N	120 N	150 N
SSD threshold, mm	1.1	1.3	1.6	1.9	2.1
Youden's index	0.36	0.57	0.74	0.76	0.77
Se	66.7%	74.2%	79.5%	84.1%	85.6%
Sp	69.3%	82.5%	94.7%	92.1%	91.2%
PPV	0.68	0.78	0.93	0.93	0.92
NPV	0.64	0.72	0.81	0.83	0.85
LR+	2.17	4.24	15.00	10.65	9.73
LR−	0.48	0.31	0.22	0.17	0.16

SSD, side-to-side difference; Se, sensitivity; Sp, specificity; PPV, positive predictive value; NPV, negative predictive value; LR+, positive likelihood ratio; LR-, negative likelihood ratio.

device, which can directly evaluate the anterior tibial translation to avoid soft-tissue effects.

Therefore, for the diagnosis of ACL ruptures, the Ligs Digital Arthrometer can apply continuous loads to the patients, automatically record knee laxity with a higher accuracy on the screen, and provide a force-displacement curve when compared with the KT-1000 (Robert et al., 2009; Rohman and Macalena, 2016; Saravia et al., 2020). Although the GNRB can automatically measure knee laxity and has surface electrodes to control hamstring relaxation, the measurement is limited to the knee joint, and the instrument is not capable of realizing stress radiography like the Ligs Digital Arthrometer (Robert et al., 2009). In addition, the Telos device is specialized for stress radiography and cannot perform radiation-free arthrometry (Bouguennec et al., 2015).

The application of several arthrometers, such as the KT-1000, Genucom, Rolimeter, GNRB and the Stryker knee laxity tester, for the diagnosis of ACL ruptures has been previously reported (Mouton et al., 2016). The results of a meta-analysis showed that the sensitivity of the KT-1000 at 69 N was 54% for the diagnosis of ACL ruptures. The sensitivity and specificity of the KT-1000 were 78% and 92% at 89 N, respectively, while it had a better sensitivity of 93% and a better specificity of 93% at the maximum manual force. For the Genucom Knee Analysis System, the sensitivity was 74% and the specificity was 82%, while the Stryker Knee Laxity Tester had a sensitivity of 82% and a specificity of 90% (Van Eck, et al., 2013). Moreover, Panisset et al. found that the Rolimeter with SSD>5 mm had a 67.5% sensitivity and an 84.3% specificity for complete ACL ruptures (Panisset et al., 2012). For ACL-deficient knees, Ganko et al. found that the Rolimeter had a better sensitivity of 89% and a better specificity of 95% with SSD>3 mm

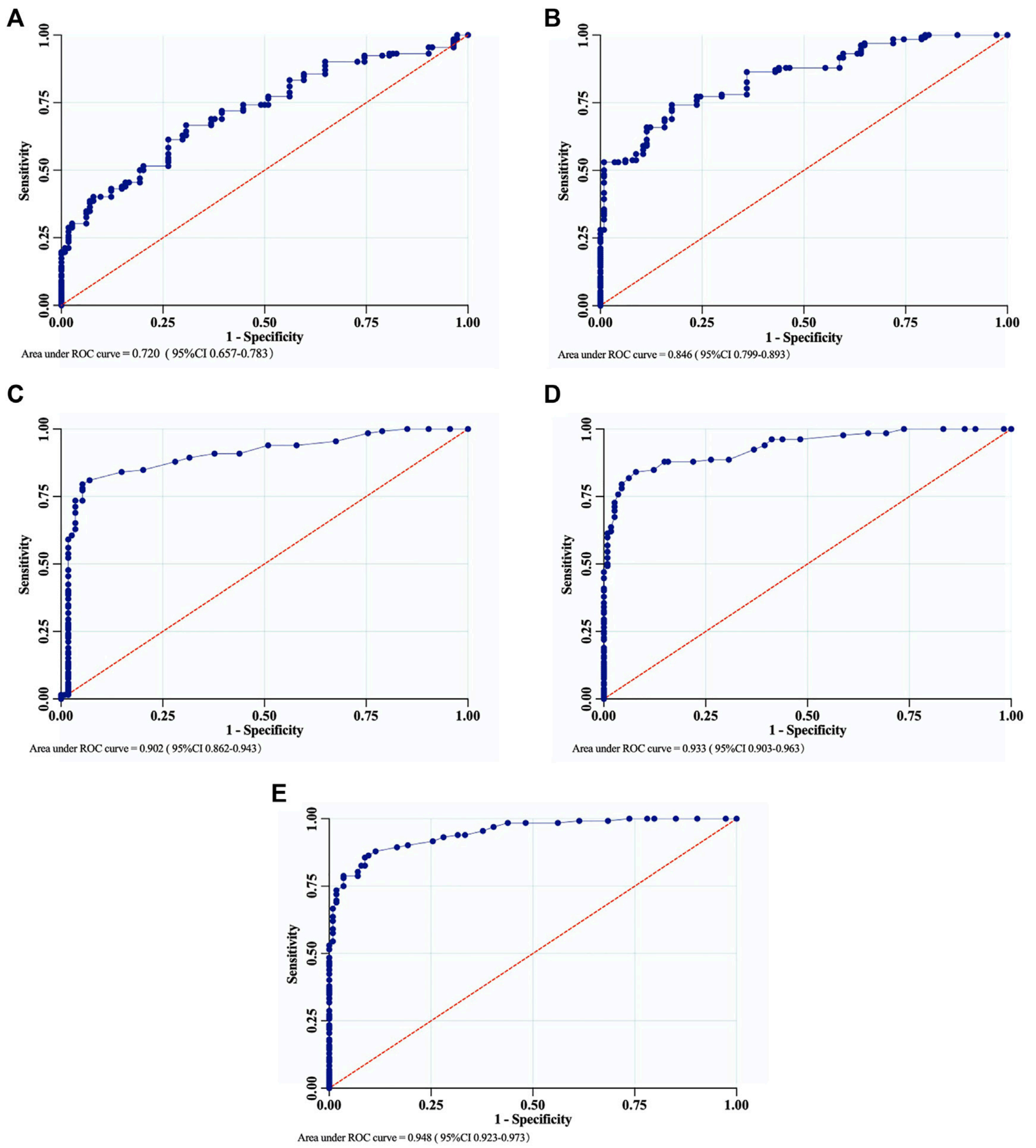

FIGURE 5
The ROC curves of the Ligs Digital Arthrometer for the diagnosis of complete ACL ruptures. **(A)** 30 N; **(B)** 60 N; **(C)** 90 N; **(D)** 120 N; **(E)** 150 N.

diagnostic threshold (Ganko et al., 2000). Similarly, Passler et al. reported that the sensitivity and specificity of the Rolimeter for the diagnosis of ACL deficiency were 93% and 87%, respectively (Pässler et al., 1998) (Table 3).

Furthermore, the validity of the GNRB for the diagnosis of ACL ruptures has been confirmed by several studies. Robert et al. found that the GNRB with SSD>3 mm had a sensitivity of 70% and a specificity of 99% at 134 N for the diagnosis of complete ACL ruptures, and at 134 N, it provided a sensitivity of 80% and a specificity of 87% with a 1.5 mm SSD diagnostic threshold in partial ACL ruptures (Robert, et al., 2009). A study by Klouche et al. reported the diagnostic value of the GNRB at different loads in complete ACL ruptures, and the GNRB with a 1.9 mm SSD threshold, had the highest diagnostic value at 200 N with a sensitivity of 92% and a specificity of 98% (Klouche, et al., 2015). Likewise, Saravia et al. found that the GNRB at 134 N delivered a sensitivity of 90.7% and a specificity of 40.3% with a threshold of 3 mm SSD for complete ACL ruptures. The threshold at 6.8 mm SSD offered a higher sensitivity (74.4%) and specificity (93.8%) with an AUC of 0.863 (Saravia, et al., 2020). Furthermore, Beldame et al. evaluated the validity of the GNRB in diagnosing complete ACL ruptures at loads of 89 N to 250 N (Beldame, et al., 2012). These results demonstrated that the GNRB with a 1.5 mm SSD threshold, had a sensitivity of 48.6% and specificity of 93.1% at 89 N, a sensitivity of 59.4% and specificity of 93.1% at 134 N, a sensitivity of 59.4% and specificity of 91.4% at 150 N, and a sensitivity of 62.2% and specificity of 75.9% at 250 N. For the diagnosis of partial ACL ruptures, Lefevre et al. found that the optimal

TABLE 3 Results of the ROC curve analysis for different arthrometers.

Study	Arthrometer	Type of ACL rupture	Load	Se	Sp	Threshold
Van Eck et al. (2013) (meta-analysis)	KT-1000	Complete	69 N	54%	N/A	N/A
			89 N	78%	92%	N/A
			Maximum manual force	93%	93%	N/A
Van Eck et al. (2013) (meta-analysis)	Genucom	Complete	Maximum manual force	74%	82%	N/A
Van Eck et al. (2013) (meta-analysis)	Stryker	Complete	Maximum manual force	82%	90%	N/A
Panisset et al. (2012)	Rolimeter	Complete	Maximum manual force	67.5%	84.3%	5.0 mm
Ganko et al. (2000)	Rolimeter	ACL deficiency	Maximum manual force	89%	95%	3.0 mm
Pässler et al. (1998)	Rolimeter	ACL deficiency	Maximum manual force	93%	87%	N/A
Robert et al. (2009)	GNRB	Complete	134 N	70%	99%	3.0 mm
		Partial	134 N	80%	87%	1.5 mm
Klouche et al. (2015)	GNRB	Complete	89 N	92.2%	88.9%	1.0 mm
			134 N	92.2%	96.3%	1.5 mm
			200 N	92.2%	98.1%	1.9 mm
			250 N	90.6%	98.1%	2.1 mm
Saravia et al. (2020)	GNRB	Complete	134 N	90.7%	40.3%	3.0 mm
				74.4%	93.8%	6.8 mm
Beldame et al. (2012)	GNRB	Complete	89 N	48.6%	93.1%	1.5 mm
			134 N	59.4%	93.1%	
			150 N	59.4%	91.4%	
			250 N	62.2%	75.9%	
Lefevre et al. (2014)	GNRB	Partial	134 N	83.2%	64.3%	2.0 mm
			250 N	84%	81%	2.5 mm
Mouton et al. (2016)	GNRB	All types	200 N	75%	95%	1.2 mm

ACL, anterior cruciate ligament; Se, sensitivity; Sp, specificity; N/A, not available.

SSD threshold of the GNRB was 2.5 mm with an AUC of 0.89, which had 84% sensitivity and 81% specificity (Lefevre, et al., 2014). Besides, Mouton et al. reported that the sensitivity and specificity of the GNRB at 200 N were 75% and 95%, respectively, with a threshold of 1.2 mm when diagnosing all ACL rupture types (Mouton et al., 2015) (Table 3).

To our knowledge, this study was the first to report the application of the Ligs Digital Arthrometer in the diagnosis of complete ACL ruptures. In the present study, the Ligs Digital Arthrometer provided a high diagnostic value at 90, 120, and 150 N loads. Simultaneously, we found that the diagnostic value improved with an increasing applied load in a certain range, which was similar to the results of previous studies (Highgenboten et al., 1992; Van Eck et al., 2013; Klouche, et al., 2015). Especially at 150 N load, the Ligs Digital Arthrometer delivered a better validity (Se 85.6% and Sp 91.2% at a 2.1 mm SSD threshold with an AUC of 0.95) for the diagnosis of complete ACL ruptures.

According to the findings of Lee et al., the diagnostic value of an arthrometer at the 30° knee flexion was significantly superior to that at the 45°, 60°, and 90° knee positions (Lee et al., 2019). Therefore, the 30° knee position, similar to the Lachman test, was used to measure anterior knee laxity by the Ligs Digital Arthrometer in the present study, which was helpful in increasing its diagnostic validity. During the measurement, the knee joint should be in neutral rotation because the anterior knee laxity measured in this state was considered as the intermediate displacement between the medial and lateral compartment (Papandreou, et al., 2005). Otherwise, the internal rotation of the knee joint decreased anterior knee laxity, while the external rotation resulted in an increase (Saravia, et al., 2020). Moreover, Ryu et al. found that meniscal tears or grade I MCL injuries accompanied by ACL ruptures may increase the laxity of the involved knee and improve the reliability of diagnostic tools (Ryu, et al., 2018). Besides, the method of SSD measurement was used to interpret the results to minimize the effect of inherent knee laxity and female hormones on the measurements of female subjects, which showed better consistency than absolute single-knee translation measurement (Rohman and Macalena, 2016).

Several limitations of the present study should be mentioned. First, we evaluated the validity of the Ligs Digital Arthrometer in complete ACL ruptures by only using the SSD values at specific loads, without further attempts to use the differential laxity of a force-displacement curve. Second, due to the small sample size of patients with partial ACL ruptures, no independent statistical analysis could be conducted to evaluate the validity of the Ligs Digital Arthrometer for diagnosing partial ACL ruptures. Moreover, further studies are needed to determine the reliability of the Ligs Digital Arthrometer in patients with ACL ruptures.

5 Conclusion

The Ligs Digital Arthrometer proved to be of high diagnostic value in complete ACL ruptures at 90 N, 120 N, and 150 N loads. The diagnostic value improved with increasing load in a certain range. Based on the results of this study, as a portable, digital and versatile new arthrometer, the Ligs Digital Arthrometer was a valid and promising tool for diagnosing complete ACL ruptures.

Data availability statement

The raw data supporting the conclusion of this article will be made available by the authors, without undue reservation.

Ethics statement

The studies involving human participants were reviewed and approved by the Biomedical Ethics Committee of West China Hospital, Sichuan University. The patients/participants provided their written informed consent to participate in this study.

Author contributions

JL and WF contributed to the conception and design of this study. QD and JT contributed to the data collection. LY performed the statistical analysis. YX and JL supervised the progress of the study. JL wrote the first draft of the manuscript. JT contributed to the manuscript review and revising. All authors have read and approved the submitted version.

Funding

This study received the funding from 1.3.5 Project for Disciplines of Excellence, West China Hospital, Sichuan University (ZYGD21005).

Acknowledgments

We would like to thank all participants in the study.

Conflict of interest

The authors declare that the research was conducted in the absence of any commercial or financial relationships that could be construed as a potential conflict of interest.

Publisher's note

All claims expressed in this article are solely those of the authors and do not necessarily represent those of their affiliated organizations, or those of the publisher, the editors and the reviewers. Any product that may be evaluated in this article, or claim that may be made by its manufacturer, is not guaranteed or endorsed by the publisher.

References

Balasch, H., Schiller, M., Friebel, H., and Hoffmann, F. (1999). Evaluation of anterior knee joint instability with the Rolimeter. *Knee Surg. Sport. Tr. A* 7 (4), 204–208. doi:10.1007/s001670050149

Beldame, J., Mouchel, S., Bertiaux, S., Adam, J. M., Mouilhade, F., Roussignol, X., et al. (2012). Anterior knee laxity measurement: Comparison of passive stress radiographs telos® and "lerat", and gnrb® arthrometer. *Orthop. Traumatol-Sur.* 98 (7), 744–750. doi:10.1016/j.otsr.2012.05.017

Bouguennec, N., Odri, G., Graveleau, N., and Colombet, P. (2015). Comparative reproducibility of telos™ and gnrb® for instrumental measurement of anterior tibial translation in normal knees. *Orthop. Traumatol-Sur.* 101 (3), 301–305. doi:10.1016/j.otsr.2015.01.007

Chen, Y., Cao, S., Wang, C., Ma, X., and Wang, X. (2022). Quantitative analysis with load–displacement ratio measured via digital arthrometer in the diagnostic evaluation of chronic ankle instability: A cross-sectional study. *J. Orthop. Surg. Res.* 17 (1), 287. doi:10.1186/s13018-022-03177-3

Ganko, A., Engebretsen, L., and Ozer, H. (2000). The rolimeter: A new arthrometer compared with the kt-1000. *Knee Surg. Knee Surg. Sport. Tr. A* 8 (1), 36–39. doi:10.1007/s001670050008

Highgenboten, C. L., Jackson, A. W., Jansson, K. A., and Meske, N. B. (1992). Kt-1000 arthrometer: Conscious and unconscious test results using 15, 20, and 30 pounds of force. *Am. J. Sport. Med.* 20 (4), 450–454. doi:10.1177/036354659202000415

Jorn, L. P., Fridén, T., Ryd, L., and Lindstrand, A. (1998). Simultaneous measurements of sagittal knee laxity with an external device and radiostereometric analysis. *J. Bone Jt. Surg. Br.* 80 (1), 169–172. doi:10.1302/0301-620x.80b1.0800169

Kaeding, C. C., Léger-St-Jean, B., and Magnussen, R. A. (2017). Epidemiology and diagnosis of anterior cruciate ligament injuries. *Clin. Sport. Med.* 36 (1), 1–8. doi:10.1016/j.csm.2016.08.001

Kakavas, G., Malliaropoulos, N., Bikos, G., Pruna, R., Valle, X., Tsaklis, P., et al. (2021). Periodization in anterior cruciate ligament rehabilitation: A novel framework. *Med. Prin. Pract.* 30 (2), 101–108. doi:10.1159/000511228

Klouche, S., Lefevre, N., Cascua, S., Herman, S., Gerometta, A., and Bohu, Y. (2015). Diagnostic value of the gnrb® in relation to pressure load for complete acl tears: A prospective case-control study of 118 subjects. *Orthop. Traumatol-Sur.* 101 (3), 297–300. doi:10.1016/j.otsr.2015.01.008

Koch, J. E., Ben-Elyahu, R., Khateeb, B., Ringart, M., Nyska, M., Ohana, N., et al. (2021). Accuracy measures of 1.5-tesla mri for the diagnosis of acl, meniscus and articular knee cartilage damage and characteristics of false negative lesions: A level iii prognostic study. *BMC Musculoskel. Dis.* 22 (1), 124. doi:10.1186/s12891-021-04011-3

Lee, H-J., Park, Y.-B., and Kim, S. H. (2019). Diagnostic value of stress radiography and arthrometer measurement for anterior instability in anterior cruciate ligament injured knees at different knee flexion position. *Arthroscopy* 35 (6), 1721–1732. doi:10.1016/j.arthro.2019.01.046

Lefevre, N., Bohu, Y., Naouri, J., Klouche, S., and Herman, S. (2014). Validity of gnrb® arthrometer compared to telos™ in the assessment of partial anterior cruciate ligament tears. *Knee Surg. Sport. Tr. A* 22 (2), 285–290. doi:10.1007/s00167-013-2384-4

Mouton, C., Theisen, D., Meyer, T., Agostinis, H., Nührenbörger, C., Pape, D., et al. (2015). Combined anterior and rotational knee laxity measurements improve the diagnosis of anterior cruciate ligament injuries. *Knee Surg. Sport. Tr. A* 23 (10), 2859–2867. doi:10.1007/s00167-015-3757-7

Mouton, C., Theisen, D., and Seil, R. (2016). Objective measurements of static anterior and rotational knee laxity. *Curr. Rev. Musculoske.* 9 (2), 139–147. doi:10.1007/s12178-016-9332-0

Musahl, V., and Karlsson, J. (2019). Anterior cruciate ligament tear. *New Engl. J. Med.* 380 (24), 2341–2348. doi:10.1056/NEJMcp1805931

Panisset, J., Ntagiopoulos, P., Saggin, P., and Dejour, D. (2012). A comparison of telos™ stress radiography versus rolimeter™ in the diagnosis of different patterns of anterior cruciate ligament tears. *Orthop. Traumatol-Sur* 98 (7), 751–758. doi:10.1016/j.otsr.2012.07.003

Papandreou, M. G., Antonogiannakis, E., Karabalis, C., and Karliaftis, K. (2005). Inter-rater reliability of rolimeter measurements between anterior cruciate ligament injured and normal contra lateral knees. *Knee Surg. Sport. Tr. A* 13 (7), 592–597. doi:10.1007/s00167-004-0597-2

Pässler, H., Ververidis, A., and Monauni, F. (1998). Beweglichkeitswertung an knien mit vkb-schaden mit hilfe des kt 1000 und aircast rolimeter. *Hefte zur Z. Unfallchirurg* 272, 731–732.

Robert, H., Nouveau, S., Gageot, S., and Gagniere, B. (2009). A new knee arthrometer, the gnrb®: Experience in acl complete and partial tears. *Orthop. Traumatol-Sur* 95 (3), 171–176. doi:10.1016/j.otsr.2009.03.009

Rohman, E. M., and Macalena, J. A. (2016). Anterior cruciate ligament assessment using arthrometry and stress imaging. *Curr. Rev. Musculoske.* 9 (2), 130–138. doi:10.1007/s12178-016-9331-1

Ryu, S. M., Na, H. D., and Shon, O. J. (2018). Diagnostic tools for acute anterior cruciate ligament injury: Gnrb, lachman test, and telos. *Knee Surg. Relat. Res.* 30 (2), 121–127. doi:10.5792/ksrr.17.014

Saravia, A., Cabrera, S., Molina, C. R., Pacheco, L., and Muñoz, G. (2020). Validity of the genourob arthrometer in the evaluation of total thickness tears of anterior cruciate ligament. *J. Orthop.* 22, 203–206. doi:10.1016/j.jor.2020.03.041

Shantanu, K., Singh, S., Srivastava, S., and Saroj, A. K. (2021). The validation of clinical examination and mri as a diagnostic tool for cruciate ligaments and meniscus injuries of the knee against diagnostic arthroscopy. *Cureus* 13 (6), e15727. doi:10.7759/cureus.15727

Van Eck, C. F., Loopik, M., Van den Bekerom, M. P., Fu, F. H., and Kerkhoffs, G. M. (2013). Methods to diagnose acute anterior cruciate ligament rupture: A meta-analysis of instrumented knee laxity tests. *Knee Surg. Sport. Tr. A* 21 (9), 1989–1997. doi:10.1007/s00167-012-2246-5

Zhou, L., Xu, Y., Zhang, J., Guo, L., Zhou, T., Wang, S., et al. (2022). Multiplanar knee kinematics-based test battery helpfully guide return-to-sports decision-making after anterior cruciate ligament reconstruction. *Front. Bioeng. Biotechnol.* 10, 974724. doi:10.3389/fbioe.2022.974724

frontiers | Frontiers in Bioengineering and Biotechnology

TYPE Review
PUBLISHED 27 April 2023
DOI 10.3389/fbioe.2023.1145937

Check for updates

OPEN ACCESS

EDITED BY
Qichang Mei,
Ningbo University, China

REVIEWED BY
Ye Ma,
Ningbo University, China
Shinya Aoi,
Osaka University, Japan

*CORRESPONDENCE
Alessandro Scano,
alessandro.scano@stiima.cnr.it

RECEIVED 16 January 2023
ACCEPTED 11 April 2023
PUBLISHED 27 April 2023

CITATION
Beltrame G, Scano A, Marino G, Peccati A, Molinari Tosatti L and Portinaro N (2023), Recent developments in muscle synergy analysis in young people with neurodevelopmental diseases: A Systematic Review.
Front. Bioeng. Biotechnol. 11:1145937.
doi: 10.3389/fbioe.2023.1145937

Recent developments in muscle synergy analysis in young people with neurodevelopmental diseases: A Systematic Review

Giulia Beltrame[1], Alessandro Scano[2]*, Giorgia Marino[3], Andrea Peccati[4], Lorenzo Molinari Tosatti[2] and Nicola Portinaro[1,4]

[1]Residency Program in Orthopedics and Traumatology, Universitá degli Studi di Milano, Milan, Italy, [2]Institute of Intelligent Industrial Systems and Technologies for Advanced Manufacturing (STIIMA), Italian Council of National Research (CNR), Milan, Italy, [3]Physiotherapy Unit, Humanitas Clinical and Research Center—IRCCS, Milan, Italy, [4]Department of Pediatric Surgery, Fondazione IRCCS Ca' Granda, Ospedale Maggiore Policlinico, Milan, Italy

The central nervous system simplifies motor control by sending motor commands activating groups of muscles, known as synergies. Physiological locomotion can be described as a coordinated recruitment of four to five muscle synergies. The first studies on muscle synergies in patients affected by neurological diseases were on stroke survivors. They showed that synergies can be used as biomarkers for motor impairment as they vary in patients with respect to healthy people. Likewise, muscle synergy analysis has been applied to developmental diseases (DD). The need for a comprehensive view of the present findings is crucial for comparing results achieved so far and promote future directions in the field. In the present review, we screened three scientific databases and selected thirty-six papers investigating muscle synergies extracted from locomotion in children affected by DD. Thirty-one articles investigate how cerebral palsy (CP) influences motor control, the currently exploited method in studying motor control in CP and finally the effects of treatments in these patients in terms of synergies and biomechanics; two articles investigate how muscle synergies vary in Duchenne muscular dystrophy (DMD), and three other articles assess other developmental pathologies, such as chronic and acute neuropathic pain. For CP, most of the studies demonstrate that the number of synergies is lower and that the synergy composition varies in the affected children with respect to normal controls. Still, the predictability of treatment's effects and the etiology of muscle synergy variation are open questions, as it has been reported that treatments minimally modify synergies, even if they improve biomechanics. The application of different algorithms in extracting synergies might bring about more subtle differences. Considering DMD, no correlation was found between non-neural muscle weakness and muscle modules' variation, while in chronic pain a decreased number of synergies was observed as a possible consequence of plastic adaptations. Even if the potential of the synergistic approach for clinical and rehabilitation practices is recognized, there is not full consensus on protocols nor widely accepted guidelines for the systematic clinical adoption of the method in DD. We critically commented on the current findings, on the methodological issues and the relative open points, and on the clinical impact of muscle synergies in neurodevelopmental diseases to fill the gap for applying the method in clinical practice.

KEYWORDS

muscle synergies, neurodevelopmental diseases, cerebral palsy, biomarkers, rehabilitation, review

Introduction

Locomotion requires the central nervous system (CNS) to coordinate a vast number of variables due to the redundant degrees of freedom of the musculoskeletal system. It has been theorized that the central nervous system simplifies the motor control by sending motor commands through a linear combination of motor synergies, each composed of a group of muscles that activates together. Muscle synergies can be considered as an efficient and parsimonious way to control and simplify spatiotemporal patterns of muscle activation by reducing the degrees of freedom to be coordinated (Bizzi et al., 1991; d'Avella and Bizzi, 2005; Cheung et al., 2009; Niemitz, 2010; Zaaimi et al., 2018).

Muscle synergy analyses have been applied to several fields of research. Pioneeristic studies on stroke survivors have shown synergistic control in both the affected and unaffected upper limb (Cheung et al., 2009). In severely impaired patient merged and fractionated motor modules were found; in mildly affected patients, synergy muscle weightings were similar in composition between cases and controls, but the activation timing profiles may change, showing more variability or overlapping of temporal coefficients across modules in the control group (Cheung et al., 2012).

Adult locomotion can be described as the subsequent activation of four to five muscle synergies (Ivanenko et al., 2004; Cappellini et al., 2006). Differences in modular organization have an impact on functional consequences as impairment in self-selected walking speed, propulsive asymmetry and step length asymmetry (Clark et al., 2010). The biomechanical implications found in post stroke patients associated with synergies' variation impose to know more about how muscle synergies vary also in other neurological pathologies, especially in developmental diseases (DD). In clinical settings, a better understanding on how muscles synergies vary among healthy children and children affected by cerebral palsy as well as by other DD would provide a deeper insight on the possible therapeutical options and their outcomes.

Cerebral palsy (CP) is the most common cause of chronic disability in childhood, occurring in about 2–2.5 per 1,000 live births (Jan 2006). CP is the clinical presentation of a wide variety of cerebral cortical and sub-cortical lesions occurring in the pre-natal, peri-natal and post-natal periods, up to the first 2 years of life (Jan 2006). It represents a group of permanent motor and cognitive disorders due to a non-progressive damage to the developing brain, without a univocal etiology, eventually resulting in inabilities to selectively control muscles. From a clinical point of view, the most important classification relates motor abilities and functional limitations with the Gross Motor Function Classification System (GMFCS), which is a scale of five levels, ranging from walking without limitations (level I) to being on a wheelchair (level V) (Palisano et al., 1997; Rosenbaum et al., 2008). The therapeutical options directly correlate to the level of disability, ranging from physical therapy, drugs for spasticity, orthopedic and neurosurgical interventions. Many patients require a combination of the previously mentioned therapies. The therapeutic challenge relies on providing an individualized treatment plan which is patient-oriented, goal-oriented and cost-effective (Pavone et al., 2016). This is the reason why there has been a growing interest in muscle synergy analysis which has the potential to provide a quantitative method for gait assessment in clinics. The current knowledge on the topic demonstrates that the number of muscle synergies is lower in CP than in healthy subjects and it decreases when the GMCSF level increases (Kim et al., 2021). The most affected synergies are those related to the knee-foot and the knee-hip couples, which result to be impaired in most patients (Thelen et al., 2003; Czupryna and Nowotny, 2012). In addition, children affected by CP show a higher stride-to-stride variability, which is not observed in healthy controls (Kim et al., 2018; Yu et al., 2019; Bekius et al., 2021). Bekius and others have recently summarized the evolution in the use of muscle synergies as biomarkers for evaluating locomotion in children affected by CP (Bekius et al., 2020). However, many articles have been published since then. Furthermore, even if CP is the most common cause of gait impairment in children, other DD affect locomotion and the evaluation of other pathologies presenting different pathogeneses might help in defining when muscle synergy analysis is useful in clinical practice.

Duchenne muscular dystrophy (DMD) is an X-linked degenerative muscular disease, affecting 1 in 3,500–6,000 male births. The absence of the protein dystrophin is responsible for the infiltration of the muscular tissue with non-contractile fibrofatty tissue (Sussman, 2002). The typical clinical sign is muscular weakness which influences walking ability. According to the few studies focusing on the relation between muscle weakness and motor control, muscle synergies do not change significantly between the DMD group and the control group (Goudriaan et al.,2018; Vandekerckhove et al., 2020).

Other pathologies that affect gait have been analyzed by exploiting muscle synergies analysis. Hemophilic arthropathy is a systemic arthropathy mostly caused by hemophilia and characterized by repetitive hemarthroses as well as progressive joint involvement (Cruz-Montecinos et al., 2019). Affected children show a higher total variance accounted for (tVAF) of muscle synergies compared to the control group (Cruz-Montecinos et al., 2019). Toddlers affected by Down syndrome need to compensate the increased joint laxity and the decreased muscle tone by using different strategies of muscle synergies, in terms of rhythmicity of their muscle bursts (Chang et al., 2009). Spinal cord injuries impose the coactivation of flexors and extensors (Fox et al., 2013).

In the present review, we collected the state of art on muscles synergy analysis in DD, with a special interest in CP given the increasing number of published papers on the topic, integrating the previous findings with the latest pieces of evidence, focusing on the new trends on synergies analysis and extraction. Novel work not only brought further pieces of evidence regarding pathological gait, but also proposed new techniques, including the use of recently released algorithms or multi-modal approaches that may shed light

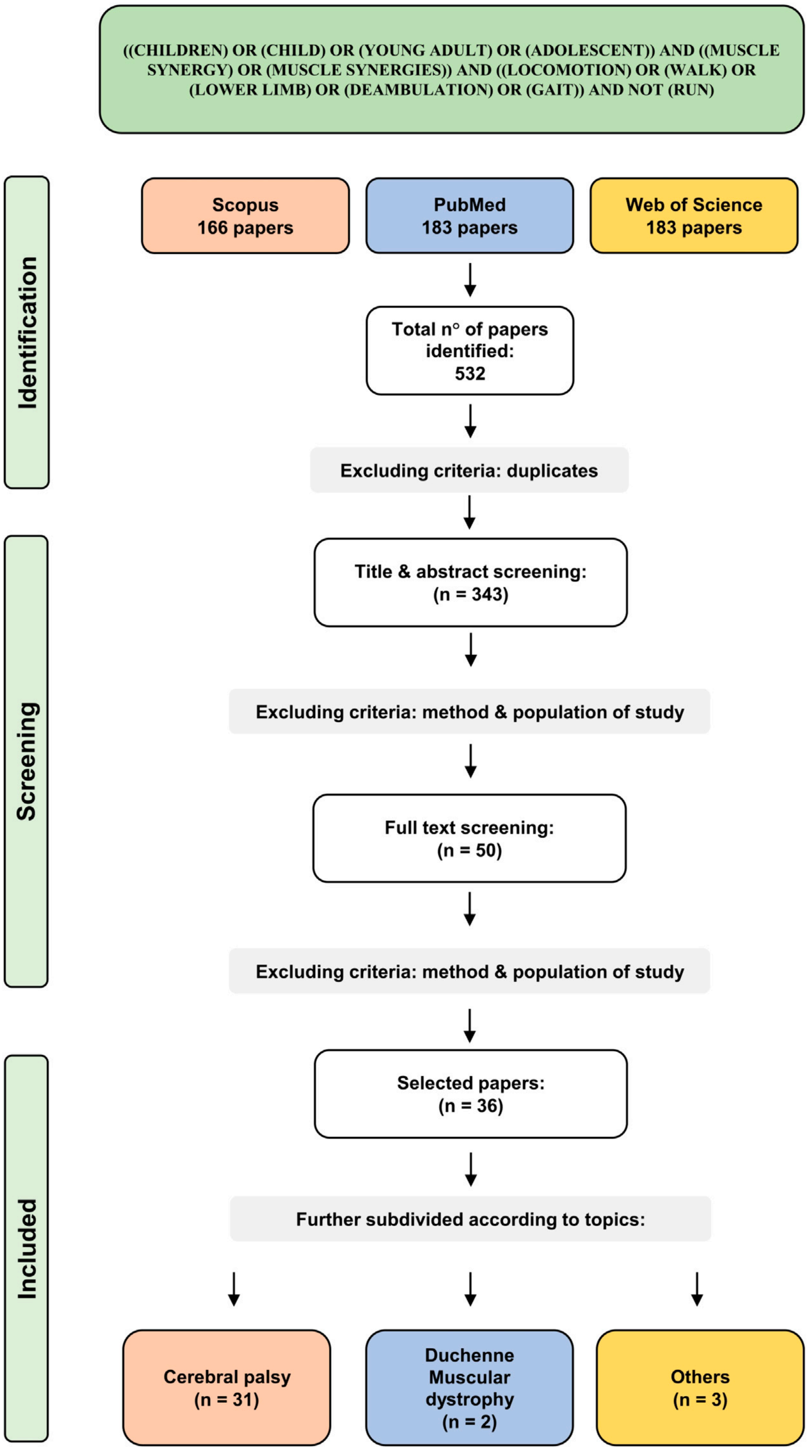

FIGURE 1
Prisma flowchart of the included studies.

on mechanisms of recovery that have not been fully understood yet. Regarding the methodology of synergy extraction, in the present review we focused on all data processing steps such as normalization and data structure, which are of great interest since the technical methodology may impact the clinical interpretation. Many open points have been lately suggested to improve the field of muscle synergies analysis in DD, such as the need of standardizing the synergy extraction methods, the need of expanding the use of novel computational approaches that increase interpretation power, as well as the need of understanding the etiology of muscle synergy

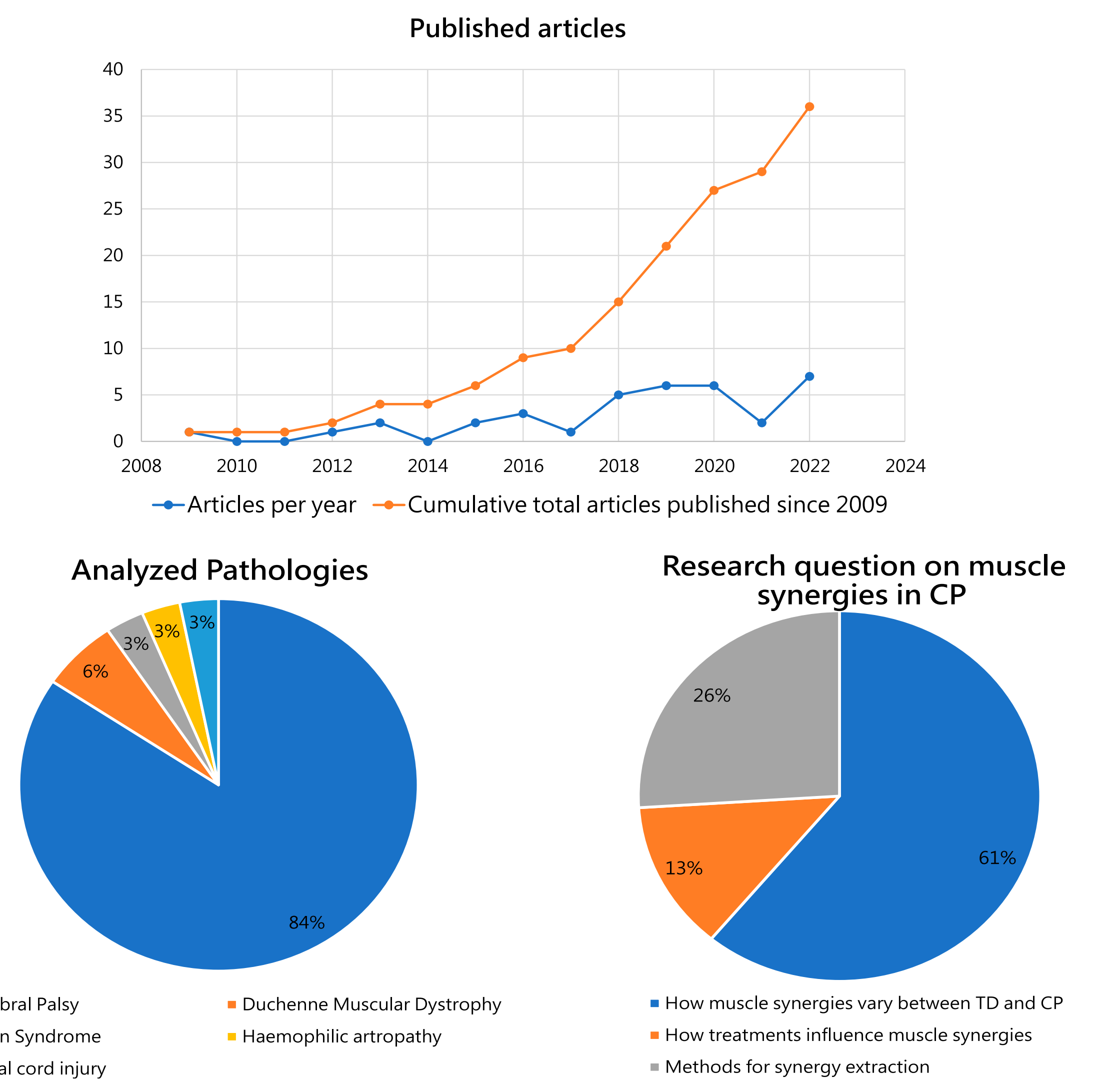

FIGURE 2
Upper panel: Number of studies on muscle synergies investigating children affected by developmental diseases per year, since 2009, is reported in blue. Cumulative number of articles published on muscle synergy analysis in children affected by DD eligible for this review is shown in orange. Lower left panel: The percentages of studies exploiting muscle synergy analysis for the considered developmental diseases. Lower right: The main research questions analyzed in the available articles on muscle synergies in CP.

variation and the prediction of the effects of rehabilitation treatments on synergies. To better understand what is known on muscle synergy analysis in other DD, we also extended the investigation to the role of muscle synergies in other developmental pathologies, other than CP. With these aims, we performed a systematic review, screening three main databases to provide a comprehensive summary of the current knowledge on muscles synergies analysis in DD.

2 Materials and methods

This review was conducted according to the international guidelines established by PRISMA (Preferred Reporting Items for Systematic Reviews and Meta-Analyses) (Liberati et al., 2009).

2.1 Research questions

The papers that have been considered for this review exploit multi-channel EMG signals recorded from lower limb muscles during walking in TD (typically developed) children and children affected by DD. The main research question of the review is to investigate how muscle synergies vary between typically developed children and children affected by DD during locomotion. Particularly, reviewers are interested in investigating the differences in muscle synergies between TD and CP groups. A focus is also dedicated to how rehabilitative treatments and interventions influence muscle synergies in CP to investigate the effects of longitudinal studies.

Reviewers intend also to emphasize which processing steps have been used to extract muscle synergies in DD, in order to evaluate

TABLE 1 Aim of the study, population, analyzed muscles, data processing, data structure, extracted synergies, main results of the articles investigating how muscle synergies vary in children affected by Cerebral Palsy (CP) in respect to healthy subjects. Acronyms: CP: cerebral palsy, TD: typically developed, HC: healthy controls, GMFCS: Gross Motor Function Classification System, BW: backward walking, FW: forward walking, SDR: selective dorsal rhizotomy, BoNT-A: Botulinum Toxin Type-A, GM: gluteus maximum; Gmed: Gluteus medius; BF: biceps femoris; ST: semitendinosus; SM: semimebranosus; RF: rectus femoris; VL: vastus lateralis; VM: vastus medialis; TA: tibialis anterior; PL: peroneus longus; EHL: extensor hallucis longus; SO: Soleus; ES: erector spinae; TFL; tensor fasciae latae; MG: medial gastrocnemius; LG: lateral gastrocnemius; GR: gracilis; RA: rectus abdominis, NMF: Non-negative matrix factorization, RMSE: Root mean square error, HP: high pass filter, LP: low pass filter, WNMF: weighted-NMF, Walk-DMC: dynamic motor control index during walking, VAF: Variance Accounted For.

Study	Aim of the study	Population	Analyzed muscles	Data processing				Extracted SYNERGIES		Data structure	Main results
				Processing	Threshold	Normalization	Algorithm	Healthy controls	Cerebral palsy		
Kim et al. (2022)	To examine if external environmental changes to the walking task influence muscle synergies in children with cerebral palsy (CP) and/or typical development (TD)	**CP:** n = 6 GMFCS I; n = 2	TA, EHL, LG, SO RF VL, ST. BF	HP = 35 Hz LP = 5 Hz	VAF >90%	Norm_window	NMF	**1:** TA + HL + RF + VL	**1:** TA + EHL + RF + VL + ST + SM	Concatenated_all	Muscle synergies in children with CP are more sensitive to changes in the external walking environment than in typically developing children
		GMFCS II; age 11–18yo						**2:** MG + SO + PL	**2:** MG + SO + PL + ndTA EHL + RF		
		TD: n = 8; age 11–18yo						**3:** ndTA + EHL + RF + VL	**3:** ndMG + SO + PL		
								4: ndMG + SO + PL	**4:** nd MG + SO + PL		
								No changes at walking environment changes	Alterations at treadmill walking speed variation		
Ettema et al. (2022)	To evaluate the effects of prolonged walking on signs of muscle fatigue and complexity of neuromuscular control in children with CP	**CP:** n = 10; GMFCS I – II; age 6–18yo; no surgery within 6 months **TD:** n = 15; age 6–18yo	RF, VL, ST, GM, LG, PL, TA and SO	HP = 20Hz; LP = 10 Hz	VAF1 Synergies	Norm_all	NMF	**1:** LG + MG + SOL + PL	**1:** starts earlier	Single_stride	Children with CP presented signs of muscle fatigue after prolonged walking, while no effects were found for TD. Still muscle fatigue is not associated to changes in muscle synergies' complexity
								2: ST + SM	**2:** almost the same		
								3: VL + RF	**3:** the 2nd peak is delayed		
								4: TA + GL + SOL + PL	**4:** the 2nd peak is delayed and prolonged in time		
									Same weighting, different timings		
Spomer et al. (2022)	To evaluate the effect that altered biomechanics have on synergies. (*Emulated equinus EE; CP equinus CP-Q; emulated equinus crouch EEC; CP equinus crouch CP-EEC; emulated mid crouch and crouch EmidC; CP mid crouch and crouch CP-EmidC*)	2 **CP** subjects matched to every healthy subjects for emulated gait **HC:** n = 14; mean age: 23yo	GM, BF, ST, SM, VM, SO, TA and MG	HP = 20Hz; LP = 10 Hz	VAF1 VAFn	Normalized to the 95th percentile of maximum activation	NMF	**1:** Glu + VL + RF	***EE:*** 1: TA; 2: BF + ST + SM; 3: GL + GM	Single_stride	Altered gait patterns are not primarily driving the changes in synergies observed in CP
								2: ST + SM + BF	***CP -E***: TA; 2: ST + GM + LG + VL		
								3: SOL + MG + LG	***EEC:*** 1: TA; 2: BF + ST; 3–4: TA + GL + GM + VL		
									CP-EC:1.: TA; 2.: ST + SM + VAL + GM + GL		
									EmidC: 1.: TA; 2.: ST + LG + MG + TA; 3.: GM + GL + TA; 4.: VL		
									CP-EmidC: 1.: TA; 2.: ST + SM + VL + GM + GL		
Goudriaan et al. (2022)	To determine if muscle synergy structure differs between gait patterns	**CP**: n = 188; age 3–17yo **TD**: n = 57; age 4–17yo	RF, VL, BF, ST, SM, TA, MG, LG, SO and GMed	HP = 20 Hz LP = 10 Hz	VAF>90% (and others) VAF1	Normalized to its average amplitude	WNMF	n/a	In all pathways: **Stance phase:** VL + BF + ST + SM + Glu **Push off**: MG + SO + Glu **Swing phase:** RF + TA	Concatenated_all	Synergy structure was similar between gait patterns, although weights differed in the more impaired children (crouch and jump gait) when compared to the other patterns
Kim et al. (2021)	To conduct a larger study incorporating more muscles and gait cycles to prove that children	**CP**: n = 10; age 14.9 ± 3.8 yo; GMFCS I – II; no surgery within 6 months	TA, EHL, LG, SO, RF, VL, ST and BF	HP = 35 Hz LP = 6 Hz	VAF>90%	Norm_all	NMF	T1: TA + EHL T2: SO + PL + MG T3: nd HL + TA + ST + RF + VL T4: RF + VL + TA +	7 CP specific clusters + T1 – 3 – 4 – 5 – 6 + N: MG + SO + PL	Concatenated_all	A greater CP-specificity of muscle synergies was related to poorer performance. CP-

(Continued on following page)

10.3389/fbioe.2023.1145937

TABLE 1 (*Continued*) Aim of the study, population, analyzed muscles, data processing, data structure, extracted synergies, main results of the articles investigating how muscle synergies vary in children affected by Cerebral Palsy (CP) in respect to healthy subjects. Acronyms: CP: cerebral palsy, TD: typically developed, HC: healthy controls, GMFCS: Gross Motor Function Classification System, BW: backward walking, FW: forward walking, SDR: selective dorsal rhizotomy, BoNT-A: Botulinum Toxin Type-A, GM: gluteus maximum; Gmed: Gluteus medius; BF: biceps femoris; ST: semitendinosus; SM: semimebranosus; RF: rectus femoris; VL: vastus lateralis; VM: vastus medialis; TA: tibialis anterior; PL: peroneus longus; EHL: extensor hallucis longus; SO: Soleus; ES: erector spinae; TFL; tensor fasciae latae; MG: medial gastrocnemius; LG: lateral gastrocnemius; GR: gracilis; RA: rectus abdominis, NMF: Non-negative matrix factorization, RMSE: Root mean square error, HP: high pass filter, LP: low pass filter, WNMF: weighted-NMF, Walk-DMC: dynamic motor control index during walking, VAF: Variance Accounted For.

Study	Aim of the study	Population	Analyzed muscles	Data processing				Extracted SYNERGIES		Data structure	Main results
				Processing	Threshold	Normalization	Algorithm	Healthy controls	Cerebral palsy		
	with CP have greater stride-to-stride variability	**TD**: n = 10; age 15.0 ± 3.2 yo						EHL + ST T5: nd HL + TA + ST + RF + VL T6: MG + SO + PL + CP 1 – 7 – 10 + N: MG + SO + PL			specific synergies can influence motor dysfunction
Bekius et al. (2021)	How muscle synergies differ in children with CP vs. TD children with the same walking ability, before and after the onset of independent walking	**CP:** n = 20; age 6.5–45.5months **TD:** n = 20; age 6.3–53.5 months	TA, GM, LG, SO, RF, VM, VL, BF, TFL, MG, ES	HP = 30 Hz LP = 10 Hz	VAF>85% or +8% + 80% single muscle	Maximum of mean value	NMF	**Supported walking:** 3–4 synergies **Indipendent walking:** 3–4-5 synergies	**Supported walking:** 2–3-4 synergies **Indipendent walking:** 3–4 synergies	averaged	Early brain lesions result in early alterations of neuromuscular control, specific for the most affected side in asymmetric CP
Cappellini et al. (2020)	To consider how to intervene according to how much the dysfunction of gait can be related to spinal neuronal networks vs supraspinal dysfunction	n/a	n/a	n/a	n/a	n/a	n/a	n/a	n/a	n/a	Physical therapy interventions, recent advances in biotechnology and neuromodulation of the locomotor circuitry might promote early motor recovery in children with CP
Short et al. (2020)	To evaluate the relationships between cortical and muscle activation	**CP:** n = 9; age 16.0 ± 2.7 yo; GMFCS I – II **TD:** n = 12; age 4.8 ± 3.0 yo	TA, MG, SO, PL, RF, VL, ST, SM and EHL	HP = 35 Hz LP = 5 Hz	VAF>90%	Normalized single stride	NMF	**1:** TA + EHL + RF + VL + ST	Same 5 synergies as TD children, but synergy n.3 appears later, while the 5th one is anticipated	Averaged_all	Differences reflecting the unilateral injury that primarily disrupts distal control and its cortical representation in the sensorimotor brain regions in CP
								2: RF + VL + ST + SM			
								3: MG + SO + PL			
								4: RF			
								5: ST + SM + EHL (action of MG of the non-dominant leg)			
Steele et al. (2019)	To prove if EMG recordings and muscle synergies are repeatable between visits	**CP:** 20 children with bilateral CP	RF, ST, SM, VL, TM, MG	HP = 25 Hz LP = 10 Hz	VAF>95%	Norm all	NMF	n/a	n/a	Averaged all	The inter-visit variance ratios of EMG data for children with CP were similar to previously reported results for typically developing children and unimpaired adults
Yu et al. (2019)	To assess the relationship between GMFCS levels and the gait synergistic control	**CP:** n = 18, age 4–6 yo; GMFCS I – II – III; No suergery within 1 year **TD:** n = 8; age 4.43 ± 1.36 years	TA, SO, LG, VL, RF, ST, BF and TFL	HP = 50 Hz LP = 10 Hz	Forced to four	Norm_all	NMF	4 synergies per leg	GMFCS I – II: Same 4 synergies as described in TD children, different pattern of activity: Synergies n1 n2 last longer, without evident peaks Synergy n3 does not show the first peak GMFCS III: Merging synergies/new synergies	Single_stride	Children at GMFCS levels I and II and the TD children had similar synergy structures, with different synergy activations. Children GMFCS level III could not access all four basic synergies on both sides
								1: VL + RF + TFL			
								2: SO + LG			
								3: TA			
								4: ST + SM + BF			

(Continued on following page)

TABLE 1 (*Continued*) Aim of the study, population, analyzed muscles, data processing, data structure, extracted synergies, main results of the articles investigating how muscle synergies vary in children affected by Cerebral Palsy (CP) in respect to healthy subjects. Acronyms: CP: cerebral palsy, TD: typically developed, HC: healthy controls, GMFCS: Gross Motor Function Classification System, BW: backward walking, FW: forward walking, SDR: selective dorsal rhizotomy, BoNT-A: Botulinum Toxin Type-A, GM: gluteus maximum; Gmed: Gluteus medius; BF: biceps femoris; ST: semitendinosus; SM: semimebranosus; RF: rectus femoris; VL: vastus lateralis; VM: vastus medialis; TA: tibialis anterior; PL: peroneus longus; EHL: extensor hallucis longus; SO: Soleus; ES: erector spinae; TFL; tensor fasciae latae; MG: medial gastrocnemius; LG: lateral gastrocnemius; GR: gracilis; RA: rectus abdominis, NMF: Non-negative matrix factorization, RMSE: Root mean square error, HP: high pass filter, LP: low pass filter, WNMF: weighted-NMF, Walk-DMC: dynamic motor control index during walking, VAF: Variance Accounted For.

Study	Aim of the study	Population	Analyzed muscles	Data processing				Extracted SYNERGIES		Data structure	Main results
				Processing	Threshold	Normalization	Algorithm	Healthy controls	Cerebral palsy		
Booth et al. (2019)	To establish if muscle synergies are modified when children with CP are challenged to improve aspects of gait with real-time biofeedback	**CP:** n = 25; age 5–16yo; GMFCS I II; no surgery within 1year **TD:** n = 27; age 5–16yo	GMed, RF, VL, ST, TA, MG, SO and PL	HP = 20 Hz LP = 10 Hz	VAF>90%	Mean muscle activation	NMF	4 synergies solution for VAF >90% in 13 children 1 child with 5 synergies	3 synergies solution for VAF >90% in 13 children; the others: 2–3 synergies No significant interaction effect of feedback on composition muscle weightings and timings vs. kinetic and kinematic parameters	Concatenated_all	Children with CP can selectively adapt and improve aspects of gait when challenged with biofeedback
Cappellini et al. (2018)	To evaluate muscle synergies in hemiplegic and diplegic children vs. typically developed peers during forward walking (FW) and backward walking (BW)	**CP:** n = 14; age 3–11.1 yo; GMFCS I – II – III; No surgery within 1year **TD:** n = 14; age 3.3 – 11.8yo	LG, MG, SO, TA, BF, ST, TFL, GM, RF, VL and VM	HP = 30 Hz LP = 10 Hz	VAF linear fit (RMSE<10^{-4})	Norm_all	NMF	**FW:** SOL + LG + MG: late stance **BW:** BF + ST: mid swing	**FW:** SOL + LG + MG at whole stance. Different CoA: plantarflexors and TA between legs **BW: d**ifferent CoA: RF, VL, VM, Glu, BF, ST, TA Different CoA: ST + SM between legs	Concatenated_all	BW highlights prominent gait asymmetries in children with CP, giving a more comprehensive assessment of the gait pathology No relevant gait asymmetries have been found during FW.
Hashiguchi et al. (2018)	To compare the number of muscle synergies between children with CP and TD children and clarified whether certain clinical parameters differed accordingly	**CP:** n = 13; GMFCS I – II – III **TD:** n = 10; age: 6 – 18yo	TA, LG, SO, Gmed, RF, VM, BF and ST	HP = 20 Hz LP = 10 Hz	VAF >90%	Norm_all	NMF	4–5 synergies	2–3-4 synergies	Concatenated_all	Children with cerebral palsy had significantly fewer synergies than children developing typically. The extent of spasticity and gait kinetics differed according to the number of synergies
Cappellini et al. (2016)	To evaluate spatiotemporal alpha-motoneuron activation during walking by mapping the electromyographic activity profiles from several, simultaneously recorded muscles	**CP**: n = 35; age 2 – 12yo; GMFCS I – II – III; no surgery within 1year **TD:** n = 7; age1 – 1.2 yo; n = 26 age 1–2 – 12yo	BF, GM, LG, MG, RF, SO, VL, ST, TA, TFL and VM	HP = 30 Hz LP = 10 Hz	VAF linear fit (RMSE<10^{-4})	Norm_all	NMF	SO + LG + MG: late stance TA: 2 peaks in ST + BF	SO + LG + MG ++: whole stance TA: 1 peak at early swing RF + VL + VM ++ (vs. ST BF: shifted later) Wider EMG bursts: ST, SM, BF, VL, SO, LG, MG	Concatenated_all	Early injuries to developing motor regions of the brain substantially affect the maturation of the spinal locomotor output and consequently the future locomotor behavior
Shuman et al. (2016)	To evaluate the repeatability of synergy complexity and structure in unimpaired individuals and individuals with cerebral palsy (CP)	**CP:** n = 5; age 10.2 ± 2.3 **TD:** n = 5, age 10.3 ± 3.5	GMed, ST, SM, BF, VL, RF, GL, SO, TA	HP = 40 Hz LP = 4 Hz	VAF 1	Norm_all	NMF	n/a	n/a	Single_stride	Synergies are repeatable between days in both groups
Tang et al. (2015)	To explore the mechanism of lower extremity dysfunction of CP children through muscle synergy analysis	**CP:** n = 12; age 5.75 ± 1.83 yo; no history of surgery **TD:** n = 8; age 6.05 ± 1.66yo **HC:** n = 10; age 24.5 ± 1.08 yo	TA, SO, LG, VL, RF, ST, BF and TFL	HP = 50 Hz LP = 10 Hz	VAF >95%	Norm to unit variance	NMF	**HC:** 4 synergies per leg 1: VL + RF + TFL 2: ST + SM + BF 3: SO + LG 4: TA **TD:** 3 synergies, asymmetrically recruited between legs	The higher the GMCSF level, the lower the number of "classical" synergies exploited, which are replaced by CP-related synergies. In toe-walkers: SO + LG + TA	Single_stride	Fewer mature synergies were recruited in the CP group and many abnormal synergies specific to the CP group appeared with a larger difference in structure and symmetry between two legs of one subject and different subjects

(Continued on following page)

10.3389/fbioe.2023.1145937

10.3389/fbioe.2023.1145937

TABLE 1 (*Continued*) Aim of the study, population, analyzed muscles, data processing, data structure, extracted synergies, main results of the articles investigating how muscle synergies vary in children affected by Cerebral Palsy (CP) in respect to healthy subjects. Acronyms: CP: cerebral palsy, TD: typically developed, HC: healthy controls, GMFCS: Gross Motor Function Classification System, BW: backward walking, FW: forward walking, SDR: selective dorsal rhizotomy, BoNT-A: Botulinum Toxin Type-A, GM: gluteus maximum; Gmed: Gluteus medius; BF: biceps femoris; ST: semitendinosus; SM: semimebranosus; RF: rectus femoris; VL: vastus lateralis; VM: vastus medialis; TA: tibialis anterior; PL: peroneus longus; EHL: extensor hallucis longus; SO: Soleus; ES: erector spinae; TFL; tensor fasciae latae; MG: medial gastrocnemius; LG: lateral gastrocnemius; GR: gracilis; RA: rectus abdominis, NMF: Non-negative matrix factorization, RMSE: Root mean square error, HP: high pass filter, LP: low pass filter, WNMF: weighted-NMF, Walk-DMC: dynamic motor control index during walking, VAF: Variance Accounted For.

Study	Aim of the study	Population	Analyzed muscles	Data processing				Extracted SYNERGIES		Data structure	Main results
				Processing	Threshold	Normalization	Algorithm	Healthy controls	Cerebral palsy		
Steele et al. (2015)	To evaluate if individuals with CP demonstrate reduced complexity of neuromuscular control during gait and if changes are related to functional ability	**CP:** n = 549; no previous surgery **TD:** n = 84; age: 3.9 – 70yo	RF, ST, SM, BF, MG and TA	HP = 20 Hz LP = 10 Hz	VAF1, walk-DMC	Norm single stride	NMF	3 synergies equals a VAF >90% for 60% of individuals	1–2 synergies equals a VAF >90% in 80% of CP patients: 1: ST + SM + MG (++ in early stance) 2: RF + TA (– in late swing)	Single_stride	Individuals with CP use a simplified control strategy during gait compared with unimpaired individuals, similarly, to stroke survivors
								1: BF + ST + SM			
								2: MG			
								3: RF + TA			
Li et al. (2013)	To find the difference of lower-limb muscle synergies between CP children and adults	**CP:** n = 8; no previous surgery **HC:** n = 5	TA, SO, LG, VL, RF, ST, BF and TFL	n/a	VAF	Norm sub-maximal	NMF	All subjects exploit 5 "classical" synergies per leg	A combination of 3 "classical" synergies per leg + specific CP synergies	n/a	Four or five muscle synergies were required for adult subject's vs. two, three or four for cerebral palsy
								1: VL + RF + TFL	1: TA + SOL + LG		
								2: ST + SM + BF	2: VL + RF + TSF + BF + ST		
								3: SO + LG			
								4: TA			
								5: VL + RF			
Zwaan et al. (2012)	To evaluate the role of EMG in studying the thigh and the extensor synergies	**CP:** n = 39; age 2–13yo pre and post SDR n = 38; age 3–20yo (GMFCS I-II-III) **TD:** n = 30; age 6–11yo	VM, ST and MG	HP = 20 Hz LP = 2 Hz	n/a	n/a	Cross correlation	**Thigh synergy**: VM vs. ST **Extensor synergy:** GM vs. VM	The extensor synergy is more expressed	Averaged_all	The EMG is sensitive enough to represent an aberrant motor control in CP
Sorek et al. (2022)	To evaluate the influence of the number of muscles and strides on estimating motor control accuracy during treadmill-gait, in individuals with cerebral palsy (CP)	**CP:** 44 children and adolescents	GMed, ST, RF, VL, MG, SO, TA, PL	HP = 20 Hz LP = 10 Hz	VAF1, VAF >90%	Norm_to_mean amplitude	WNMF	n/a	n/a	Concatenated_all	Differing numbers of muscles and strides did not influence the group mean tVAF1 value, but it influenced the tVAF-threshold value. Using different number of muscles or strides can lead to a large measurement error in the individual tVAF1 value
Rabbi et al. (2022)	To estimate muscle synergies from EMG measured from a small set of muscles	**CP:** 6 children **TD:** 6 children	LG, MG, SO, TA, RF, SM, BF, VL, VM	HP = 30 Hz LP = 6 Hz	VAFn, R^2, RMSE, Kolmogorov-Smirnov test	Norm_all	NMF	n/a	n/a	Concatenated_all	Muscle activation patterns of unmeasured muscles can be estimated from EMG measured from three to four muscles using muscle synergy extrapolation method
d'Avella et al. (2022)	A commentary on "Muscle structure and gait patterns in children with spastic cerebral palsy"	n/a	n/a	n/a	n/a	n/a	n/a	n/a	n/a	n/a	Spatiotemporal decomposition of combined kinematic and EMG data and extracting task-specific features of motor variability affecting performance might provide compact and discriminative representations of individual motor control strategies

(Continued on following page)

TABLE 1 (*Continued*) Aim of the study, population, analyzed muscles, data processing, data structure, extracted synergies, main results of the articles investigating how muscle synergies vary in children affected by Cerebral Palsy (CP) in respect to healthy subjects. Acronyms: CP: cerebral palsy, TD: typically developed, HC: healthy controls, GMFCS: Gross Motor Function Classification System, BW: backward walking, FW: forward walking, SDR: selective dorsal rhizotomy, BoNT-A: Botulinum Toxin Type-A, GM: gluteus maximum; Gmed: Gluteus medius; BF: biceps femoris; ST: semitendinosus; SM: semimebranosus; RF: rectus femoris; VL: vastus lateralis; VM: vastus medialis; TA: tibialis anterior; PL: peroneus longus; EHL: extensor hallucis longus; SO: Soleus; ES: erector spinae; TFL; tensor fasciae latae; MG: medial gastrocnemius; LG: lateral gastrocnemius; GR: gracilis; RA: rectus abdominis, NMF: Non-negative matrix factorization, RMSE: Root mean square error, HP: high pass filter, LP: low pass filter, WNMF: weighted-NMF, Walk-DMC: dynamic motor control index during walking, VAF: Variance Accounted For.

Study	Aim of the study	Population	Analyzed muscles	Data processing				Extracted SYNERGIES		Data structure	Main results
				Processing	Threshold	Normalization	Algorithm	Healthy controls	Cerebral palsy		
Falisse et al. (2020)	To evaluate the ability of a predictive simulation platform to differentiate the effects of musculoskeletal and motor control impairments on the impaired walking pattern	one CP subject aged 10-15y	GMed, RF, BF, ST, TA, GL, VL, SO	n/a	n/a	Personalized muscle-tendon parameters	n/a	n/a	n/a	n/a	The altered muscle-tendon properties rather than reduced neuromuscular control complexity and spasticity were the primary cause of the crouch gait pattern
Kim et al. (2018)	To investigate the variability of muscle synergy in children with CP vs. TD, by extracting them from individual strides and allowing the n. of synergies to vary for each stride. Clustering and discriminant analyses were then applied	**CP:** n = 20; age 12.5 ± 3.3 yo; GMFCS I – II; no surgery within 1year **TD:** n = 8; age 12.0 ± 2.6 yo	TA, MG, RF, ST and SM	HP = 35 Hz LP = 5 Hz	VAF >90% (and other); VAF1; walk-DMC	Normalized single stride	NMF	4 clusters of synergies to describe 5 strides	10 clusters of synergies to describe 5 strides. One cluster is CP specific: TA + RF of non-dominant leg TA + RF + ST + SM of dominant leg During stance (0%–40% of the gait cycle)	Single_stride	Children with CP utilize the same synergies as those with TD in some strides while at other times exhibiting distinct synergies do not present in those with TD
Shuman et al. (2017)	To evaluate how EMG signal processing impacts synergy outputs during gait, by evaluating the impacts of two common processing steps for synergy analyses: low pass (LP) filtering and unit variance scaling	**CP:** n = 40 (GMFCS I), n = 40 (GMFCS II = n = 33 (GMFCS III); age 10.9 ± 5.8 yo **TD:** n = 73; age 10.5 ± 3.5yo	RF, ST, BF, MG, TA	HP = 40 Hz LP = 4-6-8-10–20-30–40 Hz	VAF >90%; tVAF; Z-score of tVAF	Norm_all; unit variance	NMF	TA + RF ST + BF	TA + MG TA + RF ST + BF	Concatenated_all	Unit variance scaling caused comparatively small changes in tVAF. Synergy weights and activations were impacted less than tVAF by LP filter choice and unit variance normalization
van der Krogt et al. (2016)	To determine the effect of different choices in the EMG analysis (filtering, normalization, and stride selection) on the outcome of synergy analysis the effects on synergies before and after botulinum neurotoxin (BoNT-A) treatment	68 ambulant children with CP (9.3yo) Pre and post treatment with botulinum toxin - A	RF, VL, ST. TA, MG	HP = 20 Hz LP = 2-3-10–25 Hz	VAF; VAF1	Norm_all_not_ normalized; Norm_pre_treatment	NMF	n/a	VAF decreased strongly with increasing filter frequency, and when including individual strides rather than the mean. No main effect of normalization was found. VAF increased slightly after BoNT-A	Single stride; averaged_all; concatenated_all	Synergy outcomes strongly depend on EMG processing method, and may help in making deliberate choices during data analysis

* analyzed muscles are not reported because no clear information about the extracted synergies have been indicated.

10.3389/fbioe.2023.1145937

TABLE 2 Aim of the study, Population, Analyzed muscles, Data processing, Data structure and main results of the articles investigating how muscle synergies vary in children affected by CP after treatments. **Acronyms: SDR: selective dorsal rhizotomy, BTA Botulinum Toxin Type-A Injection, SEMLS: single-event multilevel orthopedic surgery; CONS: conservative treatment, ORTHO: single-level orthopedic surgery, CP: cerebral palsy, GMFCS: Gross Motor Function Classification System, HP: high pass filter, LP: low pass filter, VAF: Variance Accounted For, Walk-DMC: dynamic motor control index during walking, NMF: Non-negative matrix factorization, WNMF: weighted-NMF, Gmed: Gluteus medius; BF: biceps femoris; ST: semitendinosus; SM: semimembranosus; RF: rectus femoris; VL: vastus lateralis; VM: vastus medialis; TA: tibialis anterior; G: gastrocnemius; S: soleus; MG: medial gastrocnemius.**

Study	Aim	Population	Analyzed muscles	Data processing				Data structure	Main results
				Processing	Threshold	Normalization	Algorithm		
Pitto et al. (2020)	To predict and compare the functional outcome of a series of candidate interventions	**BTA**: n = 25; age 8.3 ± 2.1yo **SEMLS:** n = 21; age 11.5 ± 3.1yo	RF, VL, BF, TA, Gmed, SM, G, S, ST	HP = 40Hz; LP = 6 Hz	VAF_based bootstrap procedure	To have unitary standard deviation	NMF	Concatenated_all	Subject-specific muscle synergies computed from pre-treatment EMG data could be used with confidence to represent the post-treatment motor control of children with CP during walking
Shuman et al. (2019)	To understand if synergies change after treatment, or are associated with treatment outcomes	**BTA**: n = 52, age 6y10 m (±2y11 m) **SDR**: n = 38, age 9y4m (±2 years) **SELMS**: n = 57, age 12y2m (±3y1m)	Gmed, RF, VL, SM, ST, TA, G, S, BF, ST	HP = 20Hz; LP = 10 Hz	VAF >90%; VAF1; walk-DMC	Norm_all	WNMF	Concatenated_all	There were minimal changes in synergies after treatment despite changes in walking patterns
Oudenhoven et al. (2019)	To identify factors associated with long- term improvement after selective dorsal rhizotomy	**SDR:** n = 36	RF, VL, ST, TA, MG	HP = 20Hz; LP = 2 Hz	VAF >90%	Norm_single stride	NMF	Concatenated_all	Gait quality improved after SDR, with a large variation between patients. Gait improved more in children with GMFCS I and II compared to III
Shuman et al. (2018)	To determine whether patient-specific differences in muscle synergies were associated with changes in gait after treatment	Center 1 **CONS:** n = 76, age 6y8m (±2 years,7 m) **ORTHO:** n = 39, age 6y11 m (±3y4m) **SEMLS:** n = 176, age 10y0m (±3y5m) **SDR:** n = 182, age 5y7m (±2y0m) Center 2 **BTA**: n = 60, 6y9m (±2y11 m) **SEMLS:** n = 59, 12y1m (±3y1m) **SDR:** n = 44, 9y1m (±2y0m)	RF, SM, G, TA Four additional muscles: Gmed, VL, ST, S	HP = 20 Hz LP = 10 Hz	VAF1; walk-DMC	Norm_all	WNMF-NMF	Concatenated_all	Children with less impaired motor control were more likely to have improvements in walking speed and gait kinematics after treatment, independent of treatment group

10.3389/fbioe.2023.1145937

TABLE 3 Aim of the study, population, analyzed muscles, data processing, data structure, extracted synergies, main results of the articles investigating how muscle synergies vary in children affected by other developmental diseases in respect to healthy controls. **Acronyms: DMD: Duchenne muscular dystrophy, CP: cerebral palsy, PWHA: people with hemophilic arthropathy, ISCI: Incomplete Spinal Cord Injury, ID: intellectual disability, DS: Down Syndrome, TD: typical development, GMFCS: Gross Motor Function Classification System, GM: gluteus maximum; Gmed: Gluteus medius; BF: biceps femoris; ST: semitendinosus; SM: semimebranosus; RF: rectus femoris; VL: vastus lateralis; VM: vastus medialis; TA: tibialis anterior; SO: Soleus; ES: erector spinae; MG: medial gastrocnemius; LG: lateral gastrocnemius; RA: rectus abdominis, NMF: Non-negative matrix factorization, RMSE: Root mean square error, HP: high pass filter, LP: low pass filter, WNMF: weighted-NMF, Walk-DMC: dynamic motor control index during walking, VAF: Variance Accounted For.**

Study	Aim	Population	Analyzed muscles	Data processing				Data structure	Extracted SYNERGIES		Main results
				Processing	Threshold	Normalization	Algorithm		TD	DD	
Vandekerckhove et al. (2020)	To determine if synergies are altered in Duchenne muscular dystrophy and if these alterations could be linked to muscle weakness	**DMD:** n = 22; age 6–10yo; non-previous limb surgery	GMed, RF, ST, SM, TA and MG	HP = 20 Hz LP = 10 Hz	VAF >90% (and others); VAF1	Normalized to its averaged amplitude	NMF	Single_step	Early stance and late swing: Glu + ST	Increased activity of RF	Synergy weights and activations do not change in DMD
		TD: n = 22; age 7–10yo	SO, VL, BF						Mid stance: MG + LG	Decreased activity of LG and MG	
									End stance and swing: TA + RF		
Goudriaan et al. (2018)	To compare the impact of muscle weakness on muscle synergies	**CP:** n = 15; mean age 8.9yo; GMFCS I-II; no previous surgery	RF, VL, ST, SM, BF, MG, SO, TA and Gmed	HP = 20 Hz	VAF1	Normalized to its averaged amplitude	NMF	Concatenated_all	Mean tVAF1: 0.65	Mean tVAF1 in DMD: 0.65	Non-neural muscle weakness has little influence on complexity of motor control during gait
		DMD: n = 15; mean age 8.7yo		LP = 10 Hz						Mean tVAF1 in CP: 0.60	
		TD: n = 15; mean age 8.6yo									
Cruz-Montecinos et al. (2019)	To assess how haemophilic arthropathy affects the complexity of neuromuscular control during gait and their relation	**PWHA:** n = 13; age 18–45yo	MG, LG, SO, TA, VL, VM, RF, ST, BF, GM and Gmed	HP = 20 Hz LP = 10 Hz	VAF >90% or <+5%; walk-DMC	Norm_all	NMF	Concatenated_all	Acceptance synergy: VL + VM + RF; ST + BF	Acceptance synergy: VL + VM + (less) RF; SM + BF (more)	PWHA reduces the complexity of neuromuscular control. The higher the number of joints involved, the more limited the synergies are
		TD: n = 13; age 18 – 45yo							Push off synergy: MG + LG + SOL	Push off synergy: MG + LG + SOL; VL + ST	While considering 1 synergy in PWHA it can describe a higher tVAF value
									Swing synergy: TA + RF	Swing synergy: TA + RF	
									Deceleration synergy: TA and ST + SM + BF	Deceleration synergy: TA and ST + SM + BF	

(Continued on following page)

10.3389/fbioe.2023.1145937

TABLE 3 (*Continued*) Aim of the study, population, analyzed muscles, data processing, data structure, extracted synergies, main results of the articles investigating how muscle synergies vary in children affected by other developmental diseases in respect to healthy controls. Acronyms: **DMD: Duchenne muscular dystrophy, CP: cerebral palsy, PWHA: people with hemophilic arthropathy, ISCI: Incomplete Spinal Cord Injury, ID: intellectual disability, DS: Down Syndrome, TD: typical development, GMFCS: Gross Motor Function Classification System, GM: gluteus maximum; Gmed: Gluteus medius; BF: biceps femoris; ST: semitendinosus; SM: semimebranosus; RF: rectus femoris; VL: vastus lateralis; VM: vastus medialis; TA: tibialis anterior; SO: Soleus; ES: erector spinae; MG: medial gastrocnemius; LG: lateral gastrocnemius; RA: rectus abdominis, NMF: Non-negative matrix factorization, RMSE: Root mean square error, HP: high pass filter, LP: low pass filter, WNMF: weighted-NMF, Walk-DMC: dynamic motor control index during walking, VAF: Variance Accounted For.**

Study	Aim	Population	Analyzed muscles	Data processing				Data structure	Extracted SYNERGIES		Main results
				Processing	Threshold	Normalization	Algorithm		TD	DD	
Fox et al. (2013)	To examine neuromuscular control of reciprocal locomotor tasks in children with ISCIs as well as children without neurological injuries	**ISCI:** n = 5; age 3–13yo	TA, MG, VM, RF, ST, SM and GM	HP = 30 Hz LP = 4 Hz	VAF >90%	Normalized to that muscle's mean value during that trial	NMF	Single stride	Early stance: VM + Glu	Stance: MG + TA	Children with ISCIs most often required two modules and relied on synergistic muscle coactivation across the flexion and extension phases of each task
		TD: n = 5; age matched							Late stance: MG	Swing: ST, SM	
									Early swing and late swing-stance: TA + RF		
									Swing and early stance: ST, SM		
Chang et al. (2009)	To compare the emergence of muscle activity patterns of toddlers with Typically Development (TD) to those of toddlers with Down Syndrome (DS)	**DS:** n = 8	TA, MG, LG, RF, BF, RA, ES	n/a	n/a	n/a	n/a	n/a			Both TD and DS groups similarly demonstrated the need for a prolonged period of practice (6 months) to acquire a rhythmic and stable muscle activation pattern during independent walking
		TD: n = 8									By 6 months, TD show an efficient synergy among muscles, allowing increased relaxation time between bursts. Toddlers with DS improved the rhythmicity of their muscle burst, sustaining longer bursts but timing remained inconsistent

how reliable is the comparison between studies, and which steps can be made to improve the understanding of the results and the interpretative power of the recorded data.

2.2 Bibliographic research criteria

With the above-mentioned aims, a collection of articles was obtained by screening the databases PubMed, Scopus, and Web of Science (WOS), applying a query based on the following keywords: "CHILDREN", "YOUNG ADULT", "ADOLESCENT", "MUSCLE SYNERGY", "LOCOMOTION", "WALK", "LOWER LIMB", "DEAMBULATION", "GAIT", and excluding "RUN".

The formal logical query was [(CHILDREN) OR (CHILD) OR (YOUNG ADULT) OR (ADOLESCENT)] AND [(MUSCLE SYNERGY) OR (MUSCLE SYNERGIES)] AND [(LOCOMOTION) OR (WALK) OR (LOWER LIMB) OR (DEAMBULATION) OR (GAIT)] AND NOT (RUN). Databases were searched up to 5 January 2023.

2.3 Eligibility criteria

To be included in the final review, the screened papers had to satisfy the following criteria: (A) to include the specified query in the abstract and/or title and/or in the keywords (B) to evaluate muscle synergies with algorithms for synergy extraction (C) to have enrolled volunteers younger than 18 years old (D) to have recruited children affected by developmental diseases (E) to be available in English.

After exclusion of duplicate articles, one of the authors of the review performed a title and abstract screening on the residual articles. Thereafter, the reviewer assessed the eligibility of the remaining articles by a full-text screening. Other authors cross-checked the papers until full agreement was found on all doubts about inclusions. The selected works had to satisfy the inclusion criteria "A and B and C and D and E".

3 Results

3.1 Selected papers

As a result of the screening, 183 papers were found on PubMed, 166 on Scopus, 183 on Web of Science. The total number of articles was 532. After duplicate removal, 343 articles were screened. Title and abstract allowed to exclude 293 papers, mainly due to different target populations (i.e., age, diagnosis) or study design (i.e., no muscle synergy analysis, not involving lower limb, not analyzing locomotion). Full-text screening of the remaining 50 articles excluded 14 articles because of different target study purpose. In the end, 36 papers were included in the review. Selected articles were subdivided into three macro categories according to the pathologies analyzed: "Cerebral palsy", "Duchenne muscular dystrophy" and "others". The PRISMA chart for the study is reported in Figure 1.

Since 2018, a general increase in interest on muscle synergy analysis in children with disability was found. In 2019 and 2020, a total of 12 articles were published on the topic. The reduction of papers observed in 2021 is probably explainable with the COVID-19 pandemic rather than with a deflection of interest. In 2022, 7 articles were published on the topic, the highest number of eligible papers in a single year. Details on the number of published articles and on the cumulative number of articles are reported on the top of Figure 2.

The first article in our screening was published in 2009 and focuses on children with Down Syndrome. It aims at comparing the muscle activity patterns in toddlers with normal development and those affected by trisomy 21 (Chang et al., 2009), showing minimal differences between cases and controls. In the following years, literature has focused mainly on analyzing muscle synergies in CP: 31 out of the 36 articles included in the present review investigate the influences of CP on muscle synergies. Five articles investigate other DD to determine variation of muscle synergies from the ones observed in normally developed children (Figure 2, lower left panel).

The articles investigating muscle synergies in CP were further categorized according to their main research questions (Figure 2, lower right panel). The majority of the studies focus on differences between muscle synergies between TD and CP (a), agreeing in finding major differences in synergy composition at increased GMCSF level. 13% of the included studies focus on how treatment interferes with muscle synergies (b), demostrating important amelioration in gait biomechanics, but without clear changes in synergy structure. Lastly, 26% of the included articles focus on methods of synergy extraction (c), ranging from the role of EMG for muscle synergy analysis (Zwaan et al., 2012) to the recent work by d'Avella et al. posing questions on future directions for the field (D'Avella et al., 2022).

Reflecting our organization of the articles, Table 1 summarizes the articles that investigate how muscle synergies vary in children affected by CP and the methods of synergy extraction.

Table 2 focuses on how longitudinal treatments influence muscle synergies in children affected by CP. Table 3 presents the articles showing how muscle synergies vary in other developmental diseases, and the methods of synergy extraction.

3.2 What is known on muscle synergies in developmental diseases

3.2.1 Cerebral palsy

Since the first pilot studies that investigated muscles synergies in DD, it was clear that the kinetic and the kinematic variables observed in children affected by CP were different from those observed in typically developing children and this was reflected into muscle synergy patterns. In fact, children affected by CP use simplified control strategies during gait, exploiting fewer muscle synergies compared to normally developing children (Li et al., 2013; Steele et al., 2015; Tang et al., 2015; Hashiguchi et al., 2018). In addition, children affected by CP use some synergies exploited by healthy peers as well as specific synergies which are unique and repeatable over multiple gait cycles and between days (Shuman et al., 2016; Kim et al., 2018; Steele et al., 2019).

Two or three muscles synergies are sufficient to describe locomotion in CP. The observed motor modules are either

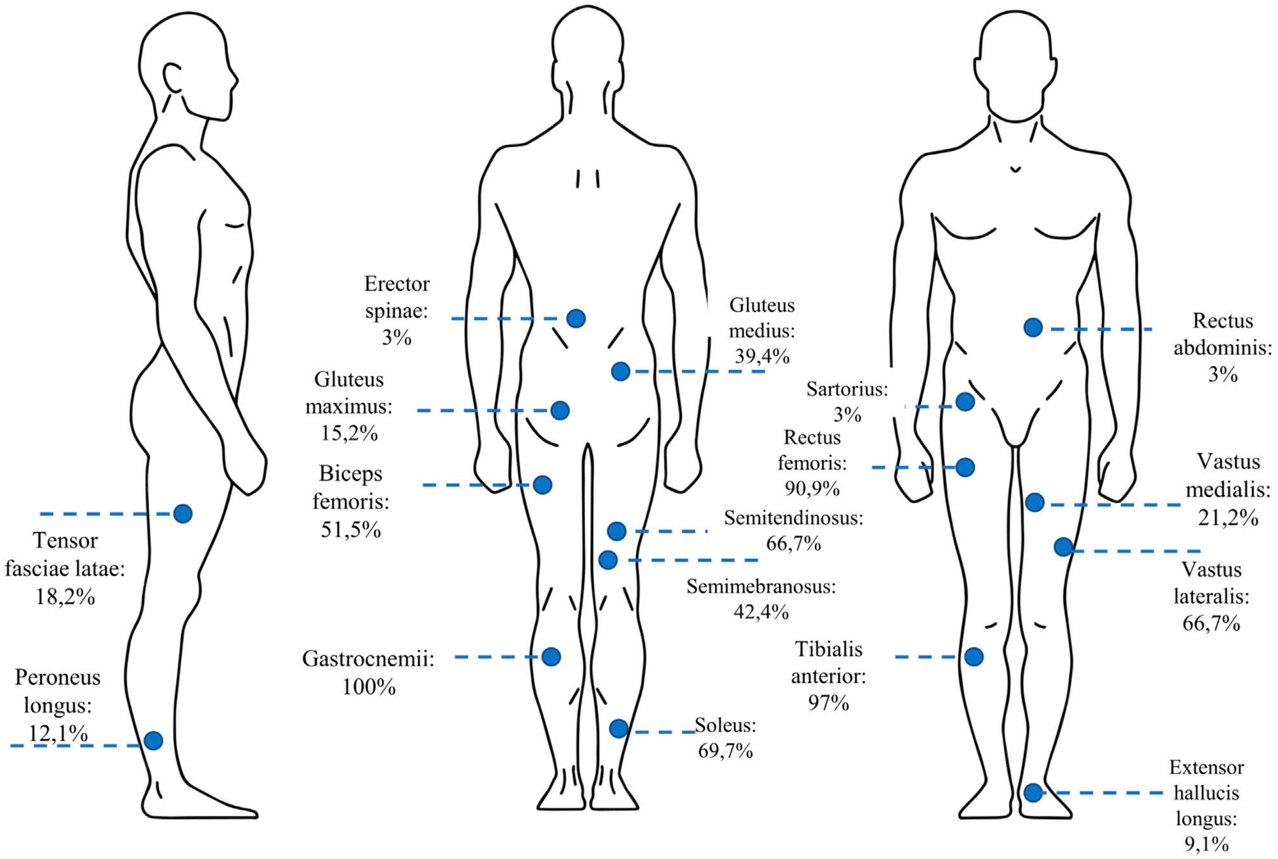

FIGURE 3
The percentage of the studies in which each of the lower-limb muscles was selected for muscle synergy analysis.

similar to the healthy ones, or they are the result of merging synergies, giving rise to "CP-specific" motor modules. On the contrary, some modules are often retained: the most repeatable synergies across different CP subjects are the ones with high loadings for the triceps surae in the late stance phase and the one showing the coactivation of the tibialis anterior-rectus femoris with the hamstrings, as it is reported in the previous tables.

According to literature (Table 1), gait kinematic and muscles fatigability are not primary driving changes for muscle synergy composition, while the severity of the disease (represented as a high GMFCS level) negatively interferes with the number and composition of the exploited synergies. Indeed, according to many studies, the differences in muscle synergies observed in TD children and children affected by CP are not related to the fatiguability of the muscular tissue nor to impaired biomechanics (Yu et al., 2019; Falisse et al., 2020; Ettema et al., 2022; Goudriaan et al., 2022; Spomer et al., 2022). To support the hypothesis, it is noteworthy to consider that different treatment approaches have shown minimal changes in synergies, even if gait pattern, movement quality and speed improved significantly after treatment (Table 2). These results are coherent with the fact that CP results from a cortical and/or subcortical brain lesions in the perinatal period, causing impairments in motor controls since the very beginning (Cappellini et al., 2016; Cappellini et al., 2020; Short et al., 2020; Bekius et al., 2021).

3.2.2 Other developmental diseases

Two studies focus on Duchenne muscular dystrophy (DMD), demonstrating no differences in the recruitment of muscles synergies (Goudriaan et al., 2018; Vandekerckhove et al., 2020) between cases and controls. Cruz-Montecinos and others studied how muscle synergies change in children affected by hemophilic arthropathy, showing that there is a direct correlation between the number of affected joints and the impaired neuromuscular control (Cruz-Montecinos et al., 2019). Chang et al. demonstrated that toddlers affected by Down syndrome do not correctly adapt to external changes (Chang et al., 2009) whereas Fox et al. showed that children affected by incomplete spinal cord injury used fewer muscles synergies compared to healthy peers (Fox et al., 2013). More details are reported in Table 3.

3.3 Analyzed muscles

One of the important methodological aspects that must be considered in understanding muscle synergy variation is the

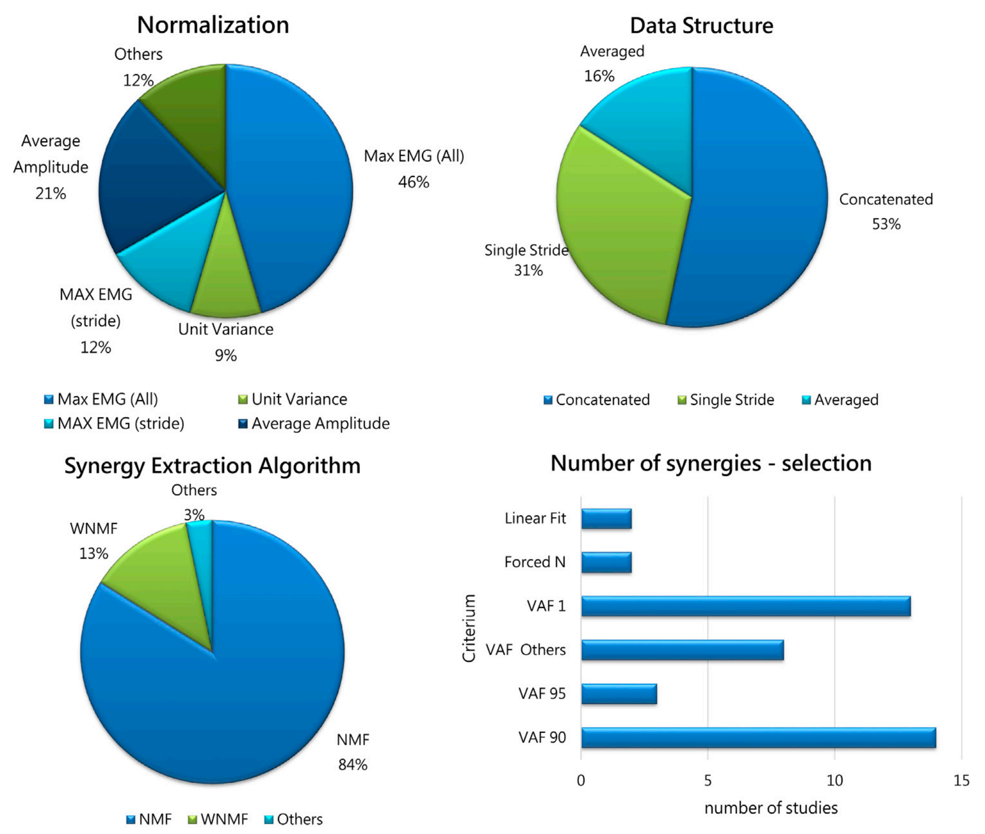

FIGURE 4
Upper-left panel: The percentage of Normalization Approaches adopted in the selected studies. Max EMG (All): normalization on the Maximum pre-processed EMG value on all trials; Average Amplitude: normalization on the average value for each channel; Unit Variance: normalization to achieve unit variance for each channel; Max EMG (Stride): normalization on single gait cycles; Others includes approaches used in single studies (maximum of mean value, normalized to the 95th percentile of maximum activation). Upper-left panel: Data Structure occurrences before synergy extraction: Concatenated (53%); Single Stride (31%); Averaged strides (16%). Lower-left panel: The percentage of Algorithms used in the selected studies. Acronyms: NMF: non-negative matrix factorization; WNM: weighted non-negative matrix factorization; Others: EMG cross correlation. Lower-right panel: The percentage of criteria for selecting the number of synergies used in previous studies: VAF threshold was adopted by most of the studies (almost 90%); 2 studies used the linear fit, and 2 forced *a priori* the number of extracted synergies.

number and type of analyzed muscles, as remarked by Steele and others (Steele et al., 2013) and, more recently, by Sorek and others (Sorek et al., 2022), that show how the selection and the number of selected muscles may impact on the extracted synergies. The studies included in the present review analyzed mainly the following muscles: gastrocnemii (100%), the soleus (69,7%), the rectus femoris (90,9%), the biceps femoris (69,7%), the semitendinosus (90,9%), the gluteus maximus (15,2%) and medius (39,4%), the tibialis anterior (97%). Figure 3 shows a detailed chart of the muscles selected in the screened studies.

The selection of the muscles is coherent with what observed in reference studies of the field such as those by Ivanenko and others, who described human locomotion as a subsequent activation of 4–5 muscle synergies (extracted with Principal Component Analysis—PCA), that include the previously mentioned muscles (Ivanenko et al., 2004), and Clark and others (Clark et al., 2010), that described healthy locomotion with four to five synergies when using Non-negative Matrix Factorization (NMF) for extracting muscle synergies.

3.4 Data processing

In Tables 1–3, the details for data processing for all the studies included in the screening are reported.

3.4.1 EMG processing

EMG processing includes the steps needed to obtain EMG envelopes before synergies are extracted. The first step is signal filtering. In our screening, we noticed that 20 Hz is the most used frequency for high-pass filtering (in agreement with EMG filtering recommendations, de Luca et al., 2010), while 10 Hz is frequently adopted for low-pass filtering as a typical cut-off frequency for achieving envelopes in muscle synergy analysis. However, even lower frequencies are used in many studies; it is known that EMG pre-processing may impact on muscle synergy outcomes. In fact, the high pass filtering reduces motion artefacts, but may slightly impact also on useful EMG signal; the low pass filtering influences the smoothness and regularity of EMG envelopes and may impact synergy number and composition.

10.3389/fbioe.2023.1145937

In their work, Hug and others (Hug et al., 2012) observed that a wide variety of low-pass filters have been used in literature aiming at extracting muscle synergies during walking and they observed that the smoothing procedure influences the amount of VAF explained, and, as a consequence, the number of extracted synergies. They suggested caution when comparing the number of synergies from studies that adopt different filtering. They also suggested that when different velocities are compared, the low-pass cut-off frequency should be adapted to provide the same smoothing EMG profiles, even if this approach was rarely adopted.

In their paper, Shuman and others investigated low pass (LP) filtering and unit variance scaling influence synergy extraction (Shuman et al., 2017), by applying LP filters to the EMG data with cutoff frequencies ranging from 4 to 40 Hz. They showed that the total variance accounted for (tVAF) by a given number of synergies was sensitive to LP filter choice and decreased in both TD and CP groups with increasing LP cutoff frequency. They also concluded that the change in tVAF derived from filtering can alter the number of synergies selected for further analyses. Synergy weights and activations were impacted less than tVAF by LP filter choice. These results demonstrate that EMG signal processing methods impact outputs of synergy analysis and z-score based measures can assist in reporting and comparing results across studies and clinical centers.

The issue was investigated also by another work (van der Krogt et al., 2016), that studied what is the effect of different choices in the EMG filtering, on the outcome of synergy analysis in CP, by comparing low-pass filtering at 2, 3, 10, or 25 Hz. They found that the VAF decreased significantly with increasing filter frequency impacting on the number of extracted synergies.

3.4.2 EMG normalization

Normalization of EMG envelopes is needed to allow inter-subject and inter-session comparisons, and to account for muscles that intrinsically produce less activity due to their properties. Normalization analyses included several approaches that are summarized in Figure 4 (upper-left panel). The most frequent approach is to normalize with respect to the maximum EMG value found in all the dataset for each muscle (46%). This approach was already in use for upper-limb studies (d'Avella et al., 2003), and is particularly effective when a reasonable high number of strides or walking conditions are available. Other approaches aim at normalizing EMG signals by the average value found for that muscle in all the trials (21%), to refer normalization to single strides rather than global approaches (12%) or to achieve unit variance for each channel (9%). Other approaches were also used (12%), and include normalizing on the 95% of mean of the peaks for each channel. No study employed the Maximum Voluntary Contraction (MVC) as it is hardly measured, especially on patients.

According to the available studies, non-uniformity in normalizing methods is however tolerable as it was reported that no main effect of normalization was found when EMG data were either not normalized, normalized to their own maximum, or normalized to the pre-treatment maximum (van der Krogt et al. 2016). Also, Cappellini (Cappellini et al., 2018), concluded that the choice of the normalization approach had minimal effect.

3.4.3 Data structure

Some data structure methods were used in previous works. Most of the studies documented time normalization before analysis (typically, each stride was resampled to 100 or 101 samples) in order to organize data in matrices before synergy extraction. However, different choices were made on how to organize data structure before synergy extraction. In fact, about half of the papers (53%) concatenated EMG from different strides, as suggested in Oliveira's work (Oliveira et al., 2014), achieving a "large" matrix that accounts for all the strides. This approach allows to keep track of single-stride variability, by concatenating strides rather than averaging. The authors suggest that concatenation is the best approach to use and this is reflected in the adoption of this method in more than half of the studies. On the contrary, about a third of the papers (31%) extracted synergies directly from single strides. Another approach, used in 16% of the papers, used averaged EMG envelopes before extracting synergies. Details are reported in Figure 4 (upper-right panel).

3.4.4 Algorithms for synergy extraction

The algorithms employed for muscle synergy extraction are reported in Figure 4 (lower-left panel). A vast majority of the studies used non-negative matrix factorization (NMF) (Lee & Seung 1999). In few studies, a variation of NMF was employed to account for missing or corrupted data (weighted NMF or WNMF, Shuman et al., 2018). WNMF preserves the properties of NMF but helps in saving data when they are not recorded properly, which may happen in clinical scenarios. One of the first available paper extracted synergies using an EMG cross correlation approach (Zwaan et al., 2012). The NMF method found wide use as it is frequently employed in the literature and allows to compare findings between works. However, it was used only for the extraction of the spatial synergies, while the dual temporal synergy model implemented with NMF was never adopted. Even if standardization is desirable, some aspects are not uniformly applied (such as convergence criteria and number of replicates), which may lead to slightly different extracted synergies. Moreover, while algorithms such as NMF and WNMF are well established and suit well to clinical scenarios, several other models are available such as spatiotemporal or time-varying synergies (d'Avella and Tresch, 2002), space-by-time synergies (Delis et al., 2014), kinematic-muscular synergies (Scano et al., 2022) that were never applied to these scenarios, and their potential in improving clinical interpretation was not explored. It is believable that these computational approaches may shed light into the mechanisms of motor control that have not been assessed yet in this field. In fact, we believe that exploiting the potential of all the available methods will help to shade light on the neuro-motor control (e.g.,: using spatiotemporal decomposition or space-by-time) and on the functional outcomes occurring due to modified control in which the modifications take place after treatments or surgery. When biomechanics alterations are found after treatments, the kinematic-muscular synergistic approach may allow to detect how biomechanics is related to muscle patterns and the key to the understanding of the modifications rely on the use of synergies in the task space, rather than in their spatial composition.

3.4.5 Selection of the number of synergies

The methods used to select the number of extracted synergies are reported in Figure 4 (lower-right panel). The Variance Accounted For (VAF) threshold approaches are used in many studies and included VAF 90 and VAF 95, used as fixed thresholds for extracting the number of synergies; VAF1 (Steele et al., 2015) shows the amount of variance achieved with one synergy, as an index of the complexity of motor control, also used to compute the walk-DMC (the z-score of the unaccounted variance by a single synergy). The group "Others" includes other VAF-based criteria, including various VAF thresholds (85% and lower, adding further synergies only if they explain a minimum level of variance, 5% or 8% usually), bootstrap-based procedures, or VAFn associated to various orders of factorization. Two studies employed the linear fit technique (Cappellini et al., 2016; Cappellini et al., 2018), and two studies forced *a priori* the number of extracted synergies (Yu et al., 2019; Ettema et al., 2022).

4 Discussion

4.1 Muscle synergies in physiological locomotion

Human gait can be defined as a series of alternating rhythmic movements of lower extremities that results in forward body progression preserving energy (Perry and Burnfield, 2010). The gait cycle can be divided into 2 main phases: the *stance phase*, starting when the foot touches the ground and the *swing phase*, when the same foot leaves the ground. Most of the works identify four muscle synergies to describe the gait cycle of an healthy adult: the coactivation of the glutei and the quadriceps, in the early stance, guarantees the correct body support; triceps surae assure postural stability and forward propulsion in late stance; the rectus femoris and the tibialis anterior contribute to foot clearance in early and mid-swing, while the hamstrings are involved in leg deceleration in late swing and in the correct leg positioning prior to the subsequent heel strike (Lacquaniti et al., 2012). An additional fifth synergy has been described by some authors as the coactivation of the ileo-psoas and the erector spinae in late stance and early swing (Ivanenko et al., 2004). Since the first studies proving that stroke survivors present a lower number of muscle synergies than healthy controls, an increasing interest has been directed to understand if the same results are observable in DD affecting children (Clark et al., 2010; Cheung et al., 2012).

4.2 CP-specific muscle synergies

Most of the studies that investigate how muscle synergies change in children affected by DD focus on CP and generally agree on finding a lower number of muscle synergies with a different activation timing profile when compared to synergies exploited by TD children. In 2020, Bekius published a systematic review on the use of muscle synergy analysis during walking in children with CP (Bekius et al., 2020). The increasing interest in this field is shown by the fact that since then, fourteen more studies have been published on the topic and were deemed eligible for this review. The 31 included studies aimed at understanding how muscle synergies change between CP and TD, in terms of number, spatial composition, temporal recruitment and in terms of correlation with the GMFCS level; if treatments restore healthy-like muscle synergies; and, lastly, which methodological issues need to be resolved by the scientific community, which is one of the point underlined in a recent commentary (D'Avella et al. 2022). Indeed, the most recent works proposed new techniques, including the use of recently released algorithms or multi-modal approaches that may shed light on mechanisms of recovery that have not been fully understood yet. For this reason, in the present review we focused on relevant data processing steps such as normalization and data structure, which are of great interest since the technical methodology may impact the clinical interpretation.

According to most of the studies included in the present review, children affected with CP recruit from two to four muscle synergies during gait. The recruited synergies are either "CP-specific", eventually resulting from healthy subject's merging synergies, or "standard synergies", observed also in healthy controls (Kim et al., 2021). The relative amount of "CP-specific" and "standard" muscle synergies varies in accordance with the severity of the disease. The higher the GMFCS level, the lower is the number of "standard synergies". The greater the number of "CP-specific synergies", the poorer the gait performance.

As shown in Table 1, most of the patients affected with CP present the coactivation of the triceps surae during the whole stance and the coactivation of the tibialis anterior with rectus femoris and hamstrings in late stance. The activation of the triceps surae during the whole stance causes ankle plantarflexion and knee flexion as well as hip flexion as a compensatory mechanism to maintain balance, as the center of mass displaces anteriorly. The latter posture is typical of toe walkers (Kelly et al., 1997) The rectus femoris-tibialis anterior couple is not able to provide knee extension and foot clearance for the correct heel strike. The coactivation of the hamstrings together with the physiological synergy composed of the tibialis anterior and the rectus femoris is responsible for the impaired knee extension and the accentuated hip flexion. The earlier activation of the medial hamstrings in late swing and early stance is responsible for the impairment in knee extension. The continuous firing of the rectus femoris causes hip flexion, eventually associated to triceps surae insufficiency typical of crouch gait (Li et al., 2013; Tang et al., 2015; Cappellini et al., 2018; Kim et al., 2018; Yu et al., 2019).

The previously mentioned results are visible as early as a child starts walking, as demonstrated by Dominici et al. (2011) who found that neonates already show patterns of stepping that are retained later (Dominici et al. 2011). Bekius et al. investigated specifically muscle synergies variation before and after the onset of independent walking in both TD and CP children (Bekius et al., 2021). They showed that children with CP recruit less synergies already in supported walking as well as in the first years of independent walking, underlining the need of an early rehabilitation program which might promote an early motor recovery as proposed by Cappellini et al. (2020). Another demonstration of the consistency of muscle synergies relies on finding that CP patients show the same modules among different study sessions, besides a greater stride-to-stride variability when compared to healthy controls (Li et al., 2013; Steele et al., 2015; Goudriaan et al., 2018; Hashiguchi et al., 2018; Yu et al., 2019; Kim et al., 2021).

The presence of different muscle synergies already in the support walking is consistent with the fact that altered gait patters are not the primary cause of changes in muscle synergies, nor the muscle fatigue observed after prolonged walking (Ettema et al., 2022; Spomer et al., 2022). One of the studies included in the review states that the primary cause of crouch gait relies on altered muscle-tendon properties, rather than on reduced neuromuscular control complexity and spasticity (Falisse et al., 2020). On the other hand, the majority of the articles that investigate this issue have reported that in CP toddlers different muscle synergies rely on the abnormal development of brain regions which are responsible for the maturation of the spinal locomotor output and of the locomotor behavior (Cappellini et al., 2018; Bekius et al., 2021). Accordingly, the muscle synergies result to be mined since the first steps of the child and they remain rather consistent throughout life, being the result of a central nervous system impairment (Cappellini et al., 2016; Bekius et al., 2020; Short et al., 2020).

4.3 The effect of treatments on CP-specific muscle synergies

Few papers investigate the effects of treatments on children with CP: only 4 out of the 31 included articles address the topic. The limited number of studies limit the interpretation of how treatments may intervene in reshaping muscle synergies. However, some common lines are accepted. First, a general consensus has been reached in finding amelioration in gait pattern following treatments, particularly in children with GMFCS level I and II. However, while biomechanics and kinematics improve, none of the studies have proved clear changes in muscle synergies weighting, while they have proved limited effects regarding temporal activation (Shuman et al., 2019). The currently described non-alteration in spatial synergies can be justified according to the most accepted findings at the moment: muscle synergies are encoded before the child acquires the ability to walk (Dominici et al., 2011; Bekius et al., 2021). When the child starts walking, the previously occurred brain lesions impair the neuromuscular control system, resulting into faulty muscle recruitment (Cappellini et al., 2018; Bekius et al., 2021). Orthopedic treatments generally occur later in time and, indeed, they eventually improve gait patterns, without modifying synergies, encoded long before (Shuman et al., 2018; Oudenhoven et al., 2019; Shuman et al., 2019). Noteworthy, some authors have shown that children with CP can selectively adapt and improve aspects of gait when challenged with bio feedbacks (Booth et al., 2019; Cappellini et al., 2020) as well as they show worse performance when challenged with environmental changes (Kim et al., 2022).

Interestingly, a slightly higher number of studies have employed muscle synergies for assessing rehabilitation protocols of upper limbs, especially in stroke patients, showing that the number and spatial structure of synergies eventually rarely change in these patients following treatments. Consequently, as already proposed in a previous review (Bekius et al., 2020), the temporal structure of synergies could be a target for treating lower limb impairments in CP patients. Furthermore, we would like to extend this concept and propose that the space related performance achievable with each synergy could be a training target too. Assuming that no changes occur following treatment, the same pre-treatment synergies can be recruited with different timings or, more precisely, with a different biomechanical function. This assessment can be achieved with correlation analysis, factor analysis, or with the Mixed-Matrix Factorization (MMF) algorithm (Scano et al., 2022).

4.4 How muscle synergies vary in other developmental diseases

The choice of including other neurodevelopmental diseases than CP was associated to the need of better understanding the etiology of the variation of muscle synergies in children affected by DD. According to what observed so far in CP, the CP specific muscle synergies potentially result from brain lesions. If this is the case, we expected not to find any differences in other pathologies which do not directly mine the nervous system.

Two of the articles included in the present review analyze muscle synergies in children affected by Duchenne muscular dystrophy. The absence of the protein dystrophin is responsible for the infiltration of the muscular tissue with non-contractile fibrofatty tissue leading to muscular weakness. While weakness in CP has neural and non-neural components, in DMD weakness can be considered as a predominantly non-neural problem. As in CP, non-neural muscle weakness has little influence on complexity of motor control during gait. Both studies agreed on not finding any differences in synergy weights and activation within respect to healthy controls (Goudriaan et al., 2018; Vandekerckhove et al., 2020).

Other studies have focused on how muscle synergies change in different pathologies ranging from Down syndrome and spinal cord injuries to hemophilic arthropathy.

Three groups of authors have respectively investigated the role of muscle synergy analysis in intellectual disability, incomplete spinal cord injuries and Down syndrome. People with intellectual disability exploit the same muscle synergies as healthy peers during motor tasks, but they have limited ability to use somatosensory information and to adapts their postural muscle responses to repeated external perturbation, which is consistent with what observed in children exposed to acute painful stimuli (Blomqvist et al., 2014; Van den Hoorn et al., 2015). Children with incomplete spinal cord injuries most often rely on synergistic muscle coactivation across the flexion and extension phases of different motor tasks, presenting different muscle synergies when compared to healthy peers (Fox et al., 2013).

Lastly, the paper on the emergence of neuromuscular patterns during walking in toddlers affected by Down syndrome and typically developed toddlers demonstrated that a period of 6 months of practice is needed to acquire a rhythmic and stable muscle activation pattern during independent walking. Still, following the first 6 months, typically developed toddlers present efficient synergies among muscles, allowing increased relaxation time between muscular bursts, while toddlers affected by Down disease present inconsistent timing of muscular activation (Chang et al., 2009).

Another study on hemophilic arthropathy demonstrated that the disease reduces the complexity of the neuromuscular control, probably due to chronic painful stimuli (Cruz-Montecinos et al., 2019). Differently, acute noxious stimulations did not show any changes in motor control (Van den Hoorn et al., 2015). In the previously two mentioned cases, the different afferent information might cause an impaired neuromuscular response. In both cases the problem occurs when the child has already started walking, experiencing the four muscle synergies that underlie locomotion. We believe that the reason why this happens is because chronic pain might cause a plastic rearrangement in the corticospinal tract up to select muscles differently. On the other hand, acute pain does not allow a plastic rearrangement.

4.5 Muscle synergy extraction methods

Pipelines for muscle synergy extraction employed in previous studies require several steps for analysis. Typically, these steps include preprocessing (filtering and aligning), segmentation, normalization (in time and on EMG amplitude), organization of the data in a specific data structure before synergy extraction (in a compatible way with the factorization algorithm), synergy extraction, implementation of the algorithm for comparison between extracted synergies to address the research questions. For the aims of this paper, a systematic revision of five steps has been made: pre-processing, data normalization, data structure, algorithms for synergy extraction, and algorithms for determining the number of synergies to extract.

EMG preprocessing is a crucial step needed before synergies are extracted. In particular, the frequencies adopted in literature for the low-pass filtering fall in a wide range (from 4 to 40 Hz as reported already in Shuman et al., 2017). When changing the cut-off frequency, not only EMG envelopes show different shapes, but also the VAF curve are modified and the number of extracted synergies may be misinterpreted. Setting specific guidelines, as it was done for other fields of research in which EMG analysis is performed, would increase inter-study comparison and data operability. Some adaptions proposed include the adaption of the filtering low-pass frequency according to the velocity (Hug et al., 2012), but this suggestion was rarely adopted in further studies.

EMG amplitude normalization is needed to allow inter-subject and inter-session comparison, and to account for reduced signals coming from muscles having lower volume and activation that would explain very little variance if EMG data were not normalized. In fact, lower EMG signals may be due to intrinsic features inherent to that muscle (number of motor units activated; detection area; muscle geometry, and others) rather than muscle non-use. Interestingly, it was found that non-uniform approaches for normalization were employed in literature. In more than half of the studies, researchers normalized each EMG activity with respect to the maximum EMG value found in all trials for that session. This approach seems the most similar in measuring MVC, which cannot be applied to these scenarios as MVC cannot be easily and reliably measured. However, other approaches were used in several works, including single-stride normalization, normalization to achieve unit variance on each channel, and others. The issue of which procedures should be adopted for normalization is an open question in muscle synergy analysis and it may constitute a source of bias for inter-study comparison, as well as a limiting factor for generalizing results. Few papers considered this issue and verified whether normalization may alter results (van der Krogt et al., 2016; Cappellini et al., 2018). There is a general agreement in stating that the choice of the normalization approach has a minimal effect, probably due to the fact that tests on patients include generally a limited number of conditions. Shuman and others suggested that some approaches based on z-scores may reduce the effect of normalization (Shuman et al., 2017). However, these conclusions cannot be generalized to other studies and a uniform choice of EMG normalization is one of the gaps to fill for generating optimal and commonly accepted guidelines for inter-study comparisons. We also noted that while the normalization itself may account only for slight differences, its “cascade” effects when non-uniform approaches are used for filtering, data structure, etc. might become relevant. Novel approaches available for the field such as the recently released MMF will pose further questions for researchers, such as how to filter and normalize data coming from different domains when they are factorized together (such as the case of kinematics and EMG).

Similarly, data structure used for extraction show relevant differences between studies. In nearly half of the studies (53%), data from various strides were concatenated. This approach preserves the variability between steps, but may capture noise-related features of the movement. According to Oliveira’s work (Oliveira et al. 2014), concatenating is the best method for structuring data in locomotion. About a third of the studies extracted synergies from single strides instead. While this process captures inter-stride variability, it may also interpolate noise and generate noise-driven synergies (D’Avella et al., 2022), thus misinterpreting the synergies underlying gait, especially when very few steps are available. Lastly, in a minor number of papers, data were averaged. This approach allows to remove noise, but loses sensibility in quantifying single stride variability. It is worthy to note that the choice of the approach impacts on VAF curves; thus, it impacts most of the VAF-based metrics used to select the number of synergies.

The results reported in our screening refer mainly to the NMF algorithm and its variation WNMF, which are the state-of-the-art for synergy extraction (especially in this field). Regarding the employed algorithms so far, the screened studies are uniform. Non-negative matrix factorization is considered the most appropriate method for extraction of muscle synergies in walking and running (Rabbi et al., 2022) and all the studies (except one) employed it (or its variation WNMF) to extract synergies. This can be now considered as a consolidated standard, allowing fair comparison of the results between studies. However, this uniform and use of NMF and WNMF so far can be seen also as an opportunity. In fact, other algorithmic approaches can be used in future work and they might open a variety of novel insights. It was already suggested that spatial-temporal synergies may relate better with the patients’ clinical functioning level (d’Avella et al., 2022); the time-varying algorithm might help in showing subtle changes which might not be detected with the standard NMF, as it was already found in studies regarding the upper-limb (Berger et al., 2020). Considering kinematic and EMG waveforms together as proposed with the mixed matrix factorization (Scano et al., 2022) might improve the interpretation of the data and provide links between muscle synergies and their motor outcome, thus providing further elements to verify how stable synergies can be related to improved motor outcome after treatments. In fact, considering the little modifications of synergies found in pathology, the MMF algorithm opens the way to the study of biomechanics or kinematics and muscle synergies in the same factorization, providing novel keys of interpretation encompassing both motor coordination and functional outcomes. Lastly, the use of temporal models, rarely employed in this field of research, could enhance the comprehension of the mechanisms connected to temporal recruitment of coordinated muscles. The development and the application of novel algorithms might help in understanding the neurophysiological mechanisms underlying the disease and are probably one of the main ways to pursue future researches. We also suggest that clinical applications are probably not following the rate at which novel methods are made available, missing promising directions and valuable tools toward the development of the field.

While the choice of the number of synergies is a further source of uncertainty, the number of synergies for walking are well-established and determined in physiological gait. However, when pathological gait is analyzed, the number of synergies might be altered and thus also the determination of the number of synergies should be standardized in a definitive way. Most of the screened studies employed VAF threshold algorithms, with quite consistent threshold levels adopted between studies, often coupled with the VAF1 criterium that measures the complexity of motor control. However, according to previous literature, the linear fit model was suggested as a valid alternative method for determining the appropriate number of synergies (Borzelli et al., 2013), as it is potentially less sensitive to VAF shifting found when changing the filtering parameters. To determine the minimum number of basic activity patterns n that best accounts for the EMG data variance, the best linear fit is based on a linear regression procedure (D'Avella et al. 2006) by varying the number of basic patterns from 1 to 8 and selecting the smallest n such that a linear fit of the VAF vs. n curve had a residual mean square below a specific threshold. The performance of the linear fit for this aim should be tested more.

Methods for further analysis (after synergy extraction) are very study-specific and are not reported in detail since they depend heavily on the purpose of the study and cannot be compared systematically. However, future work should also focus on how synergy analysis methods could be used to maximize the interpretation of the extracted synergies.

Lastly, recent studies in muscle synergy analysis from other fields suggest to repeat the selection of the number of synergies according to multiple criteria to confirm the solidity of the results, for example, by adopting multiple VAF thresholds (Pale et al., 2020). This approach might be meaningful especially when selecting the number of synergies for patients.

4.6 Future directions for the clinical application of muscle synergies

A growing interest in muscle synergy analysis in DD has been demonstrated with a growing number of published papers. In 2022, 7 articles were published on muscle synergy analysis in CP and since the last systematic review conducted by Bekius and others (Bekius et al., 2020), fourteen publicly studies have become available on the main databases. The novel works brough to light some important questions which are still open, as the optimization of the extraction methods and the prediction of the effects of rehabilitation treatments on muscle synergies. This review offers a summary on the currently open points in the field and compare the aims, the methodology and the results of the study conducted so far, with all the technical aspects in terms of data extraction.

In the following paragraphs, we summarize some of the main points that we believe will be considered for a more effective application of the method in the future, to exploit its potential and foster a systematic use of muscle synergies in clinical practice.

4.6.1 The selection of the study population

The choice of the best experimental design and methods relies not only on applying the most suitable synergy extraction model, but also on selecting the most suitable study population, in terms of inclusion-exclusion criteria, matching and grouping.

One of the main exclusion criteria observed in most of the study protocols are previous surgeries. Still, none of the studies have proved changes in muscle synergies weighting and temporal activation following treatment (Shuman et al., 2018; Oudenhoven et al., 2019; Shuman et al., 2019). We see in this discrepancy an opportunity to better understand the role of previous surgeries in the study design. One of the points that needs to be clarified is if the GMCSF level does not change at all besides the already proved post-surgical biomechanical amelioration. This point might help in understating if surgery is indeed a confounding factor as it is considered now and which surgical interventions, ranging from tendon transfers to injections, must be eventually considered as confounding factors.

Apart from surgeries, we have noticed a high level of variance in the criteria of selecting the study population, even among the most refined studies. Goudriaan focused on the gait patterns (Goudriaan et al., 2022), Bekius matched cases and control based on the walking abilities (Bekius et al., 2021), whereas Kim et al. decided to include only unilateral CP patients (Kim et al., 2018; Kim et al., 2021). All the previous aspects are of great importance; the possibility of studying muscle synergies according to the gait patterns (Goudriaan et al., 2022; Spomer et al., 2022) might be a starting point to consider customized rehabilitation protocols, as it is the case for studying only unilateral CP patients (Kim et al., 2021). Still, even if the high variance among the study designs is of great importance in offering different points of view, it makes harder to compare the clinical results.

Some considerations can be made on the selection of cases and controls. Besides the selection protocol, the case-control matching is generally based on the age of the patients, and then cases are further subdivided according to the GMFCS level. The subdivisions of the patients according to the severity of the disease has demonstrated a direct correlation between the GMFCS level and the walking impairment which strengthens the clinical role of the GMFCS scale by adding to it a neuro-engineering based value, represented by muscle synergies. This concept is especially true for GMFCS level I and II which indeed present a lower number of CP-specific muscle synergies compared to GMFCS III and IV (Yu et al., 2019).

On the other hand, we believe that the age of the patient is one of the interesting fields that should be investigated more in depth. According to Bekius and others muscle synergies do not change before and after the onset of independent walking (Bekius et al., 2021). These results are coherent with the fact that CP is caused by a non-progressive brain lesion and with the thesis that muscles synergies impairments are mainly due to brain lesion occurring very early in life (Cappellini et al., 2020; Short et al., 2020). We think that it would be of interest to evaluate a same cohort of patients at different ages to assess if any changes occur as the patient gets older and therefore, if there is a more suitable time for treatments.

4.6.2 The acquisition session

A limiting factor to the systematic adoption of synergies in clinical practice is the time-consuming procedures needed for acquiring data and the "transparency" of the equipment and apparatus when worn by patients. An interesting approach to simplify synergy extraction protocols and to ease the adoption of synergies has been offered by Rabbi et al. who have proposed a new model of extracting muscle synergies based on limiting to the minimum the number of the analyzed muscles in CP children and to reconstruct the EMG signal of the missing muscles from what is observed in TD children, thus increasing the clinical applicability of the employed methods. This approach reduces the time needed for data acquisition and therefore patients' stress, making muscle synergy analysis more applicable also in clinical practice (Rabbi et al., 2022). Besides the need of analyzing more subjects to validate the previously mentioned method, we believe that reducing the number of probes is a promising approach, even if there are some muscles that must be always recorded in CP patients, being the ones forming the CP-specific synergies, as the tibialis anterior, rectus femoris, medial hamstrings and gastrocnemii.

Furthermore, even if some muscles are considered more meaningful and therefore they are more used among the studies, we need to bear in mind that the number of muscles and the muscles analyzed can interfere with the results. The same is true for the number of strides that should be high enough to make normalization choices meaningful, and in order not to capture trial specific features rather than synergies, as well as to deepen the analysis on temporal components (Bekius et al., 2020) that may benefit from the availability of multiple strides. For all these reasons, we must be careful in choosing the right minimum number of muscles as well as the right minimum number of strides.

4.6.3 The role of muscle synergies in clinical practice

We believe that the great push fostering the application of muscle synergy analysis in clinical practice does not aim only at diagnosing and describing quantitatively the disease, but also at understanding the underlying neurophysiological mechanism for offering the best therapeutical option.

The latest studies have tried to understand both the etiology of muscle synergy variation and the effect of treatments on muscle synergies and biomechanics.

According to Spomer and others, children emulating CP gait exploit neither the same synergies of CP children nor the usual synergies, proving that biomechanics is not the unique cause of altered motor performance (Spomer et al., 2022). The role of biomechanics has been investigated by Falisse et al. who identified few causes of CP motor impairments as control impairments, spasticity, bone deformities and altered tendon properties (Falisse et al., 2020). Muscle fatigue is not involved in muscle synergy changes as proved by studies on CP as well as on Duchenne muscular dystrophy (Goudriaan et al., 2018; Vandekerckhove et al., 2020; Ettema et al., 2022), whereas the cortex plays a crucial role in determining altered muscle synergies, as demonstrated by Cappellini et al. (2020). As follow, we can agree on defining CP as a disease with a non-univocal etiology, at least for what it is known so far.

Considering synergy extraction protocols, non-negative matrix factorization can be considered as a consolidated standard, allowing comparison of the results between studies. However, the perspective from the standard spatial synergy model already explored cannot probably fully explain the mechanisms underlying the pathology. Algorithms "free" from non-negative input constrains such as MMF for kinematic-muscular synergies (Scano et al., 2022) have not been employed yet and may shed light on the neurophysiological mechanisms underlying pathology, and might help in correlating gait patterns, GMFCS level and muscle synergies. Such models foster multi-modal approaches: they include spatio-temporal features and allow to link muscular variables to the outcome variables. Moreover, d'Avella and others have recently focused on the current pitfalls and challenges in synergies extraction that should be addressed in future work (d'Avella et al., 2022). They include the avoidance of extracting noise-dependent synergies, matching pairs of temporal or weighting activation profiles at their best, discriminating power dependence on the type of synergistic model. Novel directions focus also on improving the knowledge of the mechanisms underlying the pathology: it has been recommended that techniques such as magnetic resonance imaging should be employed to provide a more discriminative representations of individual motor control strategy (d'Avella et al., 2022). Such issues should be solved with the purpose of trying to extract task-specific features of motor variability affecting performances and to correlate synergies with anatomopathological information (D'Avella et al., 2022).

Four of the thirty-one studies on CP focus on treatment outcomes. Even if Spomer showed that biomechanics is not the unique cause of altered motor performance in CP patients (Spomer et al., 2022), it is also true that, according to the published studies, biomechanics is the main aspect that changes in the post treatment period (Shuman et al., 2018; Oudenhoven et al., 2019; Shuman et al., 2019). A more refined analysis on temporal components (Bekius et al., 2020) may also clarify better whether synergies are not modified, but still used in new ways after treatment. Again, four articles are a limited number to make any conclusions on what happens following treatment, which constitutes one of the main directions for future research. Some relevant models such as the spatio-temporal one (d'Avella and Tresch, 2002) might find subtle differences among pretreatment and post treatment synergies, which cannot be revealed by the NMF model, which does not capture time-varying features.

Lastly, since it remains controversial how muscle synergies and clinical observation convey the same information on motor impairment, it is possible to work more on multi-modal approaches by linking features from the synergy domain to items of clinical scales, as recently proposed for upper-limb investigations by combining factor analysis with linear regression methods (Maistrello et al., 2021). These approaches represent a promising way to integrate clinical assessments and synergies and to understand how they relate.

4.6.4 The role of muscle synergies in other developmental diseases

According to what observed in literature, the application of muscle synergies in developmental diseases other than CP did not show any differences in cases and controls in DMD (Goudriaan et al., 2018; Vandekerckhove et al., 2020) and in intellectual disability (Blomqvist et al., 2014). Few differences were observed in chronic painful stimuli, as in hemophilic arthropathy (Cruz-Montecinos et al., 2019), while no changes were spotted in acute noxious stimuli (Van den Hoorn et al., 2015). The possibility of analyzing other pathologies in the present review helped in better understanding the etiology of altered muscle synergies in patients. DMD is characterized by a peripheral weakness which apparently does not interfere with the recruitment of muscles by the CNS. On the other hand, chronic pain might cause a plastic rearrangement in the corticospinal tract up to cause a selection of different muscles. According to this, we believe that it might be less useful applying muscle synergies in those pathologies in which there is not an impairment and/or rearrangement of the motor control at a central level, as it happens in CP, which is mainly caused by cortical and subcortical lesions, and in chronic pain, which causes neurological plastic rearrangement.

5 Conclusion

The current review of literature demonstrates that there is an increasing interest in applying muscle synergy analysis in children affected by developmental diseases. The scientific community aims at understanding how the neuromotor control is impaired in developmental diseases, with a special interest in CP. Indeed, the main changes in muscle synergies appear to have a neurological origin and treatments appear to influence gait biomechanics, but to have very little effects on muscle synergies. All the studies included in the review agree on finding a lower number of muscle synergies in CP children during locomotion. They also show an indirect correlation between the number of synergies and the GMFCS level. In Duchenne muscular dystrophy the weakness has a non-neural origin and, accordingly, no changes in muscle synergies were observed. On the other hand, patient affected by incomplete spinal cord injuries present fewer muscle synergies than healthy peers, as it is for children affected by intellectual disability and by chronic painful condition, possibly due to plastic changes in response to the afferent information conveyed to the cortex.

There are many aspects that must be still determined: the application of new, potentially useful protocols that are based on synergies, also for clinical decision making; the focus on different aged population to better understand if there is a perfect timing for treatment; the design of longer follow-up studies which might highlight changes as a result of the plasticity of the CNS.

Even though many scientific results have been achieved, the neurophysiological mechanism of DD, particularly of the CP, are still not completely known, and there is the need to translate the researches' results to provide the best clinical care for DD patients.

Author contributions

Authors' contributions: Conceptualization, AS, GB, and NP; methodology, GB and AS; software n.a.; validation, GB, AS, and NP; formal analysis, GB and AS; investigation, GB and AS; resources, NP and LM; data curation, GB, AS, and GM; writing—original draft preparation, GB and AS; writing—review and editing, GB, AS, GM, NP, LM, and AP; visualization, GB, AS, and GM; supervision, AS and NP; project administration, AS, NP, and LM; funding acquisition, AS, NP, and LM. All authors have read and agreed to the published version of the manuscript.

Funding

The study was partially funded by the Fondazione Ariel (Milano, Italy).

Conflict of interest

The authors declare that the research was conducted in the absence of any commercial or financial relationships that could be construed as a potential conflict of interest.

Publisher's note

All claims expressed in this article are solely those of the authors and do not necessarily represent those of their affiliated organizations, or those of the publisher, the editors and the reviewers. Any product that may be evaluated in this article, or claim that may be made by its manufacturer, is not guaranteed or endorsed by the publisher.

References

Bekius, A., Bach, M. M., van der Krogt, M. M., de Vries, R., Buizer, A. I., and Dominici, N. (2020). Muscle synergies during walking in children with cerebral palsy: A systematic review. *Front. physiology* 11, 632. doi:10.3389/fphys.2020.00632

Bekius, A., Zandvoort, C. S., Kerkman, J. N., van de Pol, L. A., Vermeulen, R. J., Harlaar, J., et al. (2021). Neuromuscular control before and after independent walking onset in children with cerebral palsy. *Sensors* 21 (8), 2714. doi:10.3390/s21082714

Berger, D. J., Masciullo, M., Molinari, M., Lacquaniti, F., and d'Avella, A. (2020). Does the cerebellum shape the spatiotemporal organization of muscle patterns? Insights from subjects with cerebellar ataxias. *J. Neurophysiology* 123 (5), 1691–1710. doi:10.1152/jn.00657.2018

Bizzi, E., Mussa-Ivaldi, F. A., and Giszter, S. (1991). Computations underlying the execution of movement: A biological perspective. *Sci. (New York, N.Y.)* 253 (5017), 287–291. doi:10.1126/science.1857964

Blomqvist, S., Wester, A., and Rehn, B. (2014). Postural muscle responses and adaptations to backward platform perturbations in young people with and without intellectual disability. *Gait posture* 39 (3), 904–908. doi:10.1016/j.gaitpost.2013.11.018

Booth, A. T. C., van der Krogt, M. M., Harlaar, J., Dominici, N., and Buizer, A. I. (2019). Muscle synergies in response to biofeedback-driven gait adaptations in children with cerebral palsy. *Front. physiology* 10, 1208. doi:10.3389/fphys.2019.01208

Borzelli, D., Berger, D. J., Pai, D. K., and d'Avella, A. (2013). Effort minimization and synergistic muscle recruitment for three-dimensional force generation. *Front. Comput. Neurosci.* 7, 186. doi:10.3389/fncom.2013.00186

Cappellini, G., Ivanenko, Y. P., Martino, G., MacLellan, M. J., Sacco, A., Morelli, D., et al. (2016). Immature spinal locomotor output in children with cerebral palsy. *Front. Physiology* 7, 478. doi:10.3389/fphys.2016.00478

Cappellini, G., Ivanenko, Y. P., Poppele, R. E., and Lacquaniti, F. (2006). Motor patterns in human walking and running. *J. neurophysiology* 95 (6), 3426–3437. doi:10.1152/jn.00081.2006

Cappellini, G., Sylos-Labini, F., Dewolf, A. H., Solopova, I. A., Morelli, D., Lacquaniti, F., et al. (2020). Maturation of the locomotor circuitry in children with cerebral palsy. *Front. Bioeng. Biotechnol.* 8, 998. doi:10.3389/fbioe.2020.00998

Cappellini, G., Sylos-Labini, F., MacLellan, M. J., Sacco, A., Morelli, D., Lacquaniti, F., et al. (2018). Backward walking highlights gait asymmetries in children with cerebral palsy. *J. neurophysiology* 119 (3), 1153–1165. doi:10.1152/jn.00679.2017

Chang, C. L., Kubo, M., and Ulrich, B. D. (2009). Emergence of neuromuscular patterns during walking in toddlers with typical development and with Down syndrome. *Hum. Mov. Sci.* 28 (2), 283–296. doi:10.1016/j.humov.2008.12.002

Cheung, V. C., Piron, L., Agostini, M., Silvoni, S., Turolla, A., and Bizzi, E. (2009). Stability of muscle synergies for voluntary actions after cortical stroke in humans. *Proc. Natl. Acad. Sci. U. S. A.* 106 (46), 19563–19568. doi:10.1073/pnas.0910114106

Cheung, V. C., Turolla, A., Agostini, M., Silvoni, S., Bennis, C., Kasi, P., et al. (2012). Muscle synergy patterns as physiological markers of motor cortical damage. *Proc. Natl. Acad. Sci. U. S. A.* 109 (36), 14652–14656. doi:10.1073/pnas.1212056109

Clark, D. J., Ting, L. H., Zajac, F. E., Neptune, R. R., and Kautz, S. A. (2010). Merging of healthy motor modules predicts reduced locomotor performance and muscle coordination complexity post-stroke. *J. neurophysiology* 103 (2), 844–857. doi:10.1152/jn.00825.2009

Cruz-Montecinos, C., Pérez-Alenda, S., Cerda, M., and Maas, H. (2019). Neuromuscular control during gait in people with haemophilic arthropathy. *Haemoph. official J. World Fed. Hemophilia* 25 (2), e69–e77. doi:10.1111/hae.13697

Czupryna, K., and Nowotny, J. (2012). Foot and knee behaviour during gait in response to the use of additional means of treatment in celebral palsied children. *Ortop. Traumatol. Rehabil.* 14 (5), 7–465. doi:10.5604/15093492.1005088

d'Avella, A., and Bizzi, E. (2005). Shared and specific muscle synergies in natural motor behaviors. *Proc. Natl. Acad. Sci. U. S. A.* 102 (8), 3076–3081. doi:10.1073/pnas.0500199102

d'Avella, A., Ivanenko, Y., and Lacquaniti, F. (2022). Muscle synergies in cerebral palsy and variability: Challenges and opportunities. *Dev. Med. child neurology* 64 (4), 404–405. doi:10.1111/dmcn.15106

d'Avella, A., Portone, A., Fernandez, L., and Lacquaniti, F. (2006). Control of fast-reaching movements by muscle synergy combinations. *J. Neurosci. official J. Soc. Neurosci.* 26 (30), 7791–7810. doi:10.1523/JNEUROSCI.0830-06.2006

d'Avella, A., Saltiel, P., and Bizzi, E. (2003). Combinations of muscle synergies in the construction of a natural motor behavior. *Nat. Neurosci.* 6 (3), 300–308. doi:10.1038/nn1010

d'Avella, A., and Tresch, M. C. (2002). "Modularity in the motor system: Decomposition of muscle patterns as combinations of time-varying synergies," in *Advances in neural information processing systems*. Editors T. G. Dietterich, S. Becker, and Z. Ghahramani (Cambridge, Massachusetts: MIT Press), 141–148.

De Luca, C. J., Gilmore, L. D., Kuznetsov, M., and Roy, S. H. (2010). Filtering the surface EMG signal: Movement artifact and baseline noise contamination. *J. biomechanics* 43 (8), 1573–1579. doi:10.1016/j.jbiomech.2010.01.027

Delis, I., Panzeri, S., Pozzo, T., and Berret, B. (2014). A unifying model of concurrent spatial and temporal modularity in muscle activity. *J. neurophysiology* 111 (3), 675–693. doi:10.1152/jn.00245.2013

Dominici, N., Ivanenko, Y. P., Cappellini, G., d'Avella, A., Mondì, V., Cicchese, M., et al. (2011). Locomotor primitives in newborn babies and their development. *Sci. (New York, N.Y.)* 334 (6058), 997–999. doi:10.1126/science.1210617

Ettema, S., Oudenhoven, L. M., Roeleveld, K., Buizer, A. I., and van der Krogt, M. M. (2022). The effect of prolonged walking on muscle fatigue and neuromuscular control in children with cerebral palsy. *Gait posture* 93, 7–13. doi:10.1016/j.gaitpost.2022.01.004

Falisse, A., Pitto, L., Kainz, H., Hoang, H., Wesseling, M., Van Rossom, S., et al. (2020). Physics-based simulations to predict the differential effects of motor control and musculoskeletal deficits on gait dysfunction in cerebral palsy: A retrospective case study. *Front. Hum. Neurosci.* 14, 40. doi:10.3389/fnhum.2020.00040

Fox, E. J., Tester, N. J., Kautz, S. A., Howland, D. R., Clark, D. J., Garvan, C., et al. (2013). Modular control of varied locomotor tasks in children with incomplete spinal cord injuries. *J. neurophysiology* 110 (6), 1415–1425. doi:10.1152/jn.00676.2012

Goudriaan, M., Papageorgiou, E., Shuman, B. R., Steele, K. M., Dominici, N., Van Campenhout, A., et al. (2022). Muscle synergy structure and gait patterns in children with spastic cerebral palsy. *Dev. Med. child neurology* 64 (4), 462–468. doi:10.1111/dmcn.15068

Goudriaan, M., Shuman, B. R., Steele, K. M., Van den Hauwe, M., Goemans, N., Molenaers, G., et al. (2018). Non-neural muscle weakness has limited influence on complexity of motor control during gait. *Front. Hum. Neurosci.* 12, 5. doi:10.3389/fnhum.2018.00005

Goudriaan, M., Van den Hauwe, M., Simon-Martinez, C., Huenaerts, C., Molenaers, G., Goemans, N., et al. (2018). Gait deviations in Duchenne muscular dystrophy-Part 2. Statistical non-parametric mapping to analyze gait deviations in children with Duchenne muscular dystrophy. *Gait posture* 63, 159–164. doi:10.1016/j.gaitpost.2018.04.038

Hashiguchi, Y., Ohata, K., Osako, S., Kitatani, R., Aga, Y., Masaki, M., et al. (2018). Number of synergies is dependent on spasticity and gait kinetics in children with cerebral palsy. *Pediatr. Phys. Ther. official Publ. Sect. Pediatr. Am. Phys. Ther. Assoc.* 30 (1), 34–38. doi:10.1097/PEP.0000000000000460

Hug, F., Turpin, N. A., Dorel, S., and Guével, A. (2012). Smoothing of electromyographic signals can influence the number of extracted muscle synergies. *Clin. neurophysiology official J. Int. Fed. Clin. Neurophysiology* 123 (9), 1895–1896. doi:10.1016/j.clinph.2012.01.015

Ivanenko, Y. P., Poppele, R. E., and Lacquaniti, F. (2004). Five basic muscle activation patterns account for muscle activity during human locomotion. *J. physiology* 556, 267–282. doi:10.1113/jphysiol.2003.057174

Jan, M. M. (2006). Cerebral palsy: Comprehensive review and update. *Ann. Saudi Med.* 26 (2), 123–132. doi:10.5144/0256-4947.2006.123

Kelly, I. P., Jenkinson, A., Stephens, M., and O'Brien, T. (1997). The kinematic patterns of toe-walkers. *J. Pediatr. Orthop.* 17 (4), 478–480. doi:10.1097/01241398-199707000-00013

Kim, Y., Bulea, T. C., and Damiano, D. L. (2018). Children with cerebral palsy have greater stride-to-stride variability of muscle synergies during gait than typically developing children: Implications for motor control complexity. *Neurorehabilitation neural repair* 32 (9), 834–844. doi:10.1177/1545968318796333

Kim, Y., Bulea, T. C., and Damiano, D. L. (2022). External walking environment differentially affects muscle synergies in children with cerebral palsy and typical development. *Front. Hum. Neurosci.* 16, 976100. doi:10.3389/fnhum.2022.976100

Kim, Y., Bulea, T. C., and Damiano, D. L. (2021). Greater reliance on cerebral palsy-specific muscle synergies during gait relates to poorer temporal-spatial performance measures. *Front. physiology* 12, 630627. doi:10.3389/fphys.2021.630627

Lacquaniti, F., Ivanenko, Y. P., and Zago, M. (2012). Patterned control of human locomotion. *J. physiology* 590 (10), 2189–2199. doi:10.1113/jphysiol.2011.215137

Lee, D. D., and Seung, H. S. (1999). Learning the parts of objects by non-negative matrix factorization. *Nature* 401 (6755), 788–791. doi:10.1038/44565

Li, F., Wang, Q., Cao, S., Wu, D., Wang, Q., and Xiang, C. (2013). "Lower-limb muscle synergies in children with cerebral palsy," in *International IEEE/EMBS conference on neural engineering*, 1226–1229.

Liberati, A., Altman, D. G., Tetzlaff, J., Mulrow, C., Gøtzsche, P. C., Ioannidis, J. P., et al. (2009). The PRISMA statement for reporting systematic reviews and meta-analyses of studies that evaluate health care interventions: Explanation and elaboration. *PLoS Med.* 6 (7), e1000100. doi:10.1371/journal.pmed.1000100

Maistrello, L., Rimini, D., Cheung, V. C., Pregnolato, G., and Turolla, A. (2021). Muscle synergies and clinical outcome measures describe different factors of upper limb motor function in stroke survivors undergoing rehabilitation in a virtual reality environment. *Sensors* 21 (23), 8002. doi:10.3390/s21238002

Niemitz, C. (2010). The evolution of the upright posture and gait-a review and a new synthesis. *Die Naturwiss.* 97 (3), 241–263. doi:10.1007/s00114-009-0637-3

Oliveira, A. S., Gizzi, L., Farina, D., and Kersting, U. G. (2014). Motor modules of human locomotion: Influence of EMG averaging, concatenation, and number of step cycles. *Front. Hum. Neurosci.* 8, 335. doi:10.3389/fnhum.2014.00335

Oudenhoven, L. M., van der Krogt, M. M., Romei, M., van Schie, P. E. M., van de Pol, L. A., van Ouwerkerk, W. J. R., et al. (2019). Factors associated with long-term improvement of gait after selective dorsal rhizotomy. *Archives Phys. Med. Rehabilitation* 100 (3), 474–480. doi:10.1016/j.apmr.2018.06.016

Pale, U., Atzori, M., Müller, H., and Scano, A. (2020). Variability of muscle synergies in hand grasps: Analysis of intra-and inter-session data. *Sensors* 20 (15), 4297. doi:10.3390/s20154297

Palisano, R., Rosenbaum, P., Walter, S., Russell, D., Wood, E., and Galuppi, B. (1997). Development and reliability of a system to classify gross motor function in children with cerebral palsy. *Dev. Med. child neurology* 39 (4), 214–223. doi:10.1111/j.1469-8749.1997.tb07414.x

Pavone, V., Testa, G., Restivo, D. A., Cannavò, L., Condorelli, G., Portinaro, N. M., et al. (2016). Botulinum Toxin treatment for limb spasticity in childhood cerebral palsy. *Front. Pharmacol.* 7, 29. doi:10.3389/fphar.2016.00029

Perry, J., and Burnfield, J. M. (2010). "Gait analysis," in *Normal and pathological function* (Thorofare: SLACK Inc.), 152–153.

Pitto, L., van Rossom, S., Desloovere, K., Molenaers, G., Huenaerts, C., De Groote, F., et al. (2020). Pre-treatment EMG can be used to model post-treatment muscle coordination during walking in children with cerebral palsy. *PLOS ONE* 15 (2), 0228851. doi:10.1371/journal.pone.0228851

Rabbi, M. F., Diamond, L. E., Carty, C. P., Lloyd, D. G., Davico, G., and Pizzolato, C. (2022). A muscle synergy-based method to estimate muscle activation patterns of children with cerebral palsy using data collected from typically developing children. *Sci. Rep.* 12 (1), 3599. doi:10.1038/s41598-022-07541-5

Rosenbaum, P. L., Palisano, R. J., Bartlett, D. J., Galuppi, B. E., and Russell, D. J. (2008). Development of the gross motor function classification system for cerebral palsy. *Dev. Med. child neurology* 50 (4), 249–253. doi:10.1111/j.1469-8749.2008.02045.x

Scano, A., Mira, R. M., and d'Avella, A. (2022). Mixed matrix factorization: A novel algorithm for the extraction of kinematic-muscular synergies. *J. Neurophysiology* 127 (2), 529–547. doi:10.1152/jn.00379.2021

Short, M. R., Damiano, D. L., Kim, Y., and Bulea, T. C. (2020). Children with unilateral cerebral palsy utilize more cortical resources for similar motor output during treadmill gait. *Front. Hum. Neurosci.* 14, 36. doi:10.3389/fnhum.2020.00036

Shuman, B., Goudriaan, M., Bar-On, L., Schwartz, M. H., Desloovere, K., and Steele, K. M. (2016). Repeatability of muscle synergies within and between days for typically developing children and children with cerebral palsy. *Gait posture* 45, 127–132. doi:10.1016/j.gaitpost.2016.01.011

Shuman, B. R., Goudriaan, M., Desloovere, K., Schwartz, M. H., and Steele, K. M. (2019). Muscle synergies demonstrate only minimal changes after treatment in cerebral palsy. *J. NeuroEngineering Rehabilitation* 16 (1), 46. doi:10.1186/s12984-019-0502-3

Shuman, B. R., Goudriaan, M., Desloovere, K., Schwartz, M. H., and Steele, K. M. (2018). Associations between muscle synergies and treatment outcomes in cerebral palsy are robust across clinical centers. *Archives Phys. Med. rehabilitation* 99 (11), 2175–2182. doi:10.1016/j.apmr.2018.03.006

Shuman, B. R., Schwartz, M. H., and Steele, K. M. (2017). Electromyography data processing impacts muscle synergies during gait for unimpaired children and children with cerebral palsy. *Front. Comput. Neurosci.* 11, 50. doi:10.3389/fncom.2017.00050

Sorek, G., Goudriaan, M., Schurr, I., and Schless, S. H. (2022). Influence of the number of muscles and strides on selective motor control during gait in individuals with cerebral palsy. *J. Electromyogr. Kinesiol. official J. Int. Soc. Electrophysiol. Kinesiol.* 66, 102697. doi:10.1016/j.jelekin.2022.102697

Spomer, A. M., Yan, R. Z., Schwartz, M. H., and Steele, K. M. (2022). Synergies are minimally affected during emulation of cerebral palsy gait patterns. *J. biomechanics* 133, 110953. doi:10.1016/j.jbiomech.2022.110953

Steele, K. M., Rozumalski, A., and Schwartz, M. H. (2015). Muscle synergies and complexity of neuromuscular control during gait in cerebral palsy. *Dev. Med. Child Neurology* 57, 1176–1182. doi:10.1111/dmcn.12826

Steele, K. M., Munger, M. E., Peters, K. M., Shuman, B. R., and Schwartz, M. H. (2019). Repeatability of electromyography recordings and muscle synergies during gait among children with cerebral palsy. *Gait posture* 67, 290–295. doi:10.1016/j.gaitpost.2018.10.009

Steele, K. M., Tresch, M. C., and Perreault, E. J. (2013). The number and choice of muscles impact the results of muscle synergy analyses. *Front. Comput. Neurosci.* 7, 105. doi:10.3389/fncom.2013.00105

Sussman, M. (2002). Duchenne muscular dystrophy. *J. Am. Acad. Orthop. Surg.* 10 (2), 138–151. doi:10.5435/00124635-200203000-00009

Tang, L., Li, F., Cao, S., Zhang, X., Wu, D., and Chen, X. (2015). Muscle synergy analysis in children with cerebral palsy. *J. neural Eng.* 12 (4), 046017. doi:10.1088/1741-2560/12/4/046017

Thelen, D. D., Riewald, S. A., Asakawa, D. S., Sanger, T. D., and Delp, S. L. (2003). Abnormal coupling of knee and hip moments during maximal exertions in persons with cerebral palsy. *Muscle and nerve* 27 (4), 486–493. doi:10.1002/mus.10357

van den Hoorn, W., Hodges, P. W., van Dieën, J. H., and Hug, F. (2015). Effect of acute noxious stimulation to the leg or back on muscle synergies during walking. *J. neurophysiology* 113 (1), 244–254. doi:10.1152/jn.00557.2014

van der Krogt, M. M., Oudenhoven, L., Buizer, A. I., Dallmeijer, A., Dominici, N., and Harlaar, J. (2016). The effect of EMG processing choices on muscle synergies before and after BoNT-A treatment in cerebral palsy. *Gait Posture* 49, 31. Poster session presented at ESMAC 2016, Seville, Spain. doi:10.1016/j.gaitpost.2016.07.095

Vandekerckhove, I., De Beukelaer, N., Van den Hauwe, M., Shuman, B. R., Steele, K. M., Van Campenhout, A., et al. (2020). Muscle weakness has a limited effect on motor control of gait in Duchenne muscular dystrophy. *PloS one* 15 (9), e0238445. doi:10.1371/journal.pone.0238445

Yu, Y., Chen, X., Cao, S., Wu, D., Zhang, X., and Chen, X. (2019). Gait synergetic neuromuscular control in children with cerebral palsy at different gross motor function classification system levels. *J. neurophysiology* 121 (5), 1680–1691. doi:10.1152/jn.00580.2018

Zaaimi, B., Dean, L. R., and Baker, S. N. (2018). Different contributions of primary motor cortex, reticular formation, and spinal cord to fractionated muscle activation. *J. neurophysiology* 119 (1), 235–250. doi:10.1152/jn.00672.2017

Zwaan, E., Becher, J. G., and Harlaar, J. (2012). Synergy of EMG patterns in gait as an objective measure of muscle selectivity in children with spastic cerebral palsy. *Gait posture* 35 (1), 111–115. doi:10.1016/j.gaitpost.2011.08.019

Frontiers in Sports and Active Living

TYPE Systematic Review
PUBLISHED 17 May 2023
DOI 10.3389/fspor.2023.1144484

Effects of exercise treatment on functional outcome parameters in mid-portion achilles tendinopathy: a systematic review

MyoungHwee Kim*, Chiao-I Lin, Jakob Henschke, Andrew Quarmby, Tilman Engel and Michael Cassel

University Outpatient Clinic, Sports Medicine & Sports Orthopaedics, University of Potsdam, Potsdam, Germany

Check for updates

OPEN ACCESS

EDITED BY
Giuseppe D'Antona,
University of Pavia, Italy

REVIEWED BY
Saúl Martín Rodríguez,
University of Las Palmas de Gran Canaria, Spain
Iker J. Bautista,
Catholic University of Valencia San Vicente Mártir, Spain

*CORRESPONDENCE
MyoungHwee Kim
zokimro@gmail.com

RECEIVED 14 January 2023
ACCEPTED 24 April 2023
PUBLISHED 17 May 2023

CITATION
Kim M, Lin C-I, Henschke J, Quarmby A, Engel T and Cassel M (2023) Effects of exercise treatment on functional outcome parameters in mid-portion achilles tendinopathy: a systematic review.
Front. Sports Act. Living 5:1144484.
doi: 10.3389/fspor.2023.1144484

Exercise interventions are evident in the treatment of mid-portion Achilles tendinopathy (AT). However, there is still a lack of knowledge concerning the effect of different exercise treatments on improving a specific function (e.g., strength) in this population. Thus, this study aimed to systematically review the effect of exercise treatments on different functional outcomes in mid-portion AT. An electronic database of Pubmed, Web of Science, and Cochrane Central Register of Controlled Trials were searched from inception to 21 February 2023. Studies that investigated changes in plantar flexor function with exercise treatments were considered in mid-portion AT. Only randomized controlled trials (RCTs) and clinical controlled trials (CCTs) were included. Functional outcomes were classified by kinetic (e.g., strength), kinematic [e.g., ankle range of motion (ROM)], and sensorimotor (e.g., balance index) parameters. The types of exercise treatments were classified into eccentric, concentric, and combined (eccentric plus concentric) training modes. Quality assessment was appraised using the Physiotherapy Evidence Database scale for RCTs, and the Joanna Briggs Institute scale for CCTs. The search yielded 2,260 records, and a total of ten studies were included. Due to the heterogeneity of the included studies, a qualitative synthesis was performed. Eccentric training led to improvements in power outcomes (e.g., height of countermovement jump), and in strength outcomes (e.g., peak torque). Concentric training regimens showed moderate enhanced power outcomes. Moreover, one high-quality study showed an improvement in the balance index by eccentric training, whereas the application of concentric training did not. Combined training modalities did not lead to improvements in strength and power outcomes. Plantarflexion and dorsiflexion ROM measures did not show relevant changes by the exercise treatments. In conclusion, eccentric training is evident in improving strength outcomes in AT patients. Moreover, it shows moderate evidence improvements in power and the sensorimotor parameter "balance index". Concentric training presents moderate evidence in the power outcomes and can therefore be considered as an alternative to improve this function. Kinematic analysis of plantarflexion and dorsiflexion ROM might not be useful in AT people. This study expands the knowledge what types of exercise regimes should be considered to improve the functional outcomes in AT.

KEYWORDS

exercise treatments, eccentric training, concentric training, combined training, kinetic parameters, kinematic parameters, sensorimotor parameters, mid-portion achilles tendinopathy

Introduction

Achilles tendinopathy is a type of degenerative tendon disease that causes functional impairment and morbidity (1). According to epidemiological data, a prevalence of 2.16 cases per 1,000 patient-years was estimated in the general population and 6.2%–9.5% in athlete population (2, 3). According to its anatomical location, it is divided into two primary categories: insertional, which occurs at the calcaneus Achilles tendon junction, and mid-portion, which occurs 2–6 cm proximal to the calcaneus (4). The characteristic of mid-portion tendinopathy is diffuse or localized swelling, degenerated tendon morphology and pain caused by repetitive loading without adequate compensation of the plantar flexor muscle function (1, 5).

In consequence, one of the most effective management strategies for mid-portion AT have been proposed to be exercise-based therapy (6). To date, several exercise interventions have been reported for AT, such as the "Alfredson protocol" which is also known as heavy eccentric calf training (7), concentric training (8), the "Stanish protocol" (9), and the "Silbernagel protocol" (10). These interventions can be classified as three different loading protocols: eccentric, concentric, and combined (eccentric plus concentric) training, respectively. Among those, eccentric loading has emerged as one of the primary conservative approaches for AT rehabilitation over the past twenty years. It is hypothesized to influence the formation in carboxyterminal propeptide of type I collagen, boosting tendon volume and tensile strength (11, 12). Eccentric exercises may also have the potential to reduce the neovascularization and related nerve ingrowth being responsible for pain development (13). A recent meta-analysis examined the relationship between eccentric exercise treatments and tendon volume in healthy and pathological tendons (14). In healthy tendons no significant immediate volume changes following acute exercise interventions were apparent. In pathological tendons, immediate and short-term volume reductions were reported, while no long-term adaptations were found as investigated in one study only. Based on the limited number of studies examining long-term changes in tendon morphology, the proclaimed effect of eccentric training on tendon volume remains inconclusive (14).

Research indicates that both concentric and combined exercise treatments can also be effective in improving plantar flexor functions such as power (e.g., height of countermovement jump) (10) in the AT population, which is believed to occur through the strengthening of the affected tendon (9). Therefore, it remains unclear whether the effects of eccentric loading are different from other types of loadings, such as slow concentric loading (15). The primary cause for these similar adaptations may be explained by the "time-under-tension" hypothesis, which states that positive adaptations could be achieved regardless of contraction type, as long as the mechanical strain is performed slowly and heavy enough (16, 17). Since the tendinopathic regions can be subjected to mechanical strain that restores normal fibril alignment and cell morphology, different types of loading may have a comparable impact to eccentric exercise.

In conclusion, different types of exercise treatments have reported positive findings in varying functional outcomes in addition to eccentric training (8–10). Nevertheless, there is a lack of knowledge concerning the effect of specific exercise treatments for improving specific functional outcomes (e.g., strength) in mid-portion AT. Being able to differentiate the effects of different types of exercises on functional outcomes might allow for more tailored treatment in people with AT. Therefore, the purpose of this systematic review was to analyze the effect of various exercise treatments (eccentric, concentric, combined) on different functional outcomes (strength, power, range of motion, balance) in people with mid-portion AT.

Methods

Data sources and search criteria

The Preferred Reporting Items for Systematic Reviews and Meta-Analyses (PRISMA) guidelines were used to conduct and report this study (18). The electronic databases Pubmed, Web of Science, and Cochrane Central Register of Controlled Trials were searched for relevant studies from inception to 21 February 2023. The search was performed by combining the three main categories: intervention, pathology, and anatomical location (**Table 1** shows the search terms used in Pubmed). Each search term was mapped to the "title and abstract" heading that has this feature in the databases. Quotation marks were not used to allow any word variations. Filters such as article type (clinical trial, RCTs, etc.) and language (English) were also applied. Animal studies were excluded using a filter or adding the Boolean operator "NOT" if there was no filter for this. This study was not pre-registered.

Eligibility criteria

Studies investigating direct functional measures of kinetic, kinematic, and sensorimotor outcomes were included following exercise treatments in mid-portion AT (mean age ≥18 years) diagnosed by clinical or sonography method. The kinetic parameters included analysis of forces such as strength (5), power, or ground reaction force outcomes. The kinematic parameters included outcomes of segmental movement

TABLE 1 Search terms used in pubmed.

Combiners	Terms
Intervention[#]	Exercise OR training OR therapy OR rehabilitation
	AND
Anatomical location[#]	Achilles tendon OR triceps surae OR calcan* OR plantarflex*
	AND
Pathology[#]	Tendinopathy OR tendinitis OR tendinosis OR Achillodynia OR paratenonitis OR peritendinitis

[#]Quotation marks were not used.
[*]Truncation symbol used to allow for word variations searching.

characteristics such as joint moments, angles, positions, accelerations, velocities, or range of motion [ROM] (10). The sensorimotor parameters included any sensorimotor-related analysis such as balance (8), reflex, or muscle activity measures. Studies that measured a minimum of one outcome in kinetic, kinematic or sensorimotor parameters with exercise interventions were considered. Exercise interventions that were prescribed with specific guidelines (e.g., volume, type, progression, and training period) that loaded the Achilles tendon for more than four weeks were considered. The interventions might be described as eccentric, concentric, combined (eccentric & concentric), or isometric training. At least one group should have conducted an exercise intervention as a single treatment. Other non-exercise treatments (e.g., manual therapy, injections, electrotherapy, etc.) were not considered, including sports activity, and co-interventions with exercise treatments were also excluded. Studies that did not measure the outcomes at the end point of an exercise intervention were excluded to minimize biases. Included study designs were randomized controlled trials (RCTs) or controlled clinical trials (CCTs).

Study selection

Once all the searched articles were combined in an Excel file, two authors (MH, CIL) independently screened titles and abstracts for eligibility based on the inclusion and exclusion criteria. After the procedure, the remaining articles underwent full-text reviews to determine the final inclusion. The corresponding authors were contacted for inaccessible articles to acquire the full text. During the process, disagreements between the authors were resolved by discussion.

Methodological quality assessment

The Physiotherapy Evidence Database (PEDro) scale was used to assess the quality of the RCTs. This scale has shown good validity and reliability in evaluating RCTs (19). The PEDro scale consists of 11 criteria. Without the first criterion asking about the eligibility of a respective study, the rest 10 criteria were calculated for the total score. Studies with scores of ≥6 were considered "high-quality", 4–5 were considered "medium-quality", and scores <4 were considered "low-quality" (20).

For assessing non-randomized clinical controlled trials (CCTs), the Joanna Briggs Institute (JBI) non-randomized experimental studies tool was used. This tool has 9 criteria to assess the quality of studies. There is no standardized total scoring for the tool. Hence, same as the PEDro scale, studies were classified as "high-quality", "medium-quality", and "low-quality" based on the score criteria explained above.

Two reviewers (MH, CIL) assessed the methodological quality independently, and discrepancies were resolved by discussion. In the case of unreached agreements, the third reviewer (JH) was involved.

Data extraction

Two reviewers (MH, CIL) independently extracted data using a standardized form. Characteristics including study information (i.e., author, year, design), participant [i.e., sample size, sex, mean age (years), mean duration of symptoms, diagnosis method of AT], interventions (i.e., duration, type of intervention, sets/repetitions, frequency, progression, pain allowance during exercise), outcomes of function measures (name, scale), and results [mean ± standard deviation (SD), *p*-value] were extracted. If there was no applicable mean and SD, mean difference (MD) and confidence interval (CI) were extracted. For studies that did not provide any numeric data, at least *p*-values were taken. Disagreements between the authors were resolved by discussion.

Data synthesis and analysis

A qualitative synthesis was performed to analyze the change of plantar flexor function measures due to the clinical heterogeneity of outcome parameters and exercise interventions. Subgroup analysis was performed according to exercise intervention types [eccentric, concentric, and combined (eccentric plus concentric) training]. To enable synthesis of outcome parameters within each pre-defined category (i.e., kinetic, kinematic, sensorimotor), outcomes were sub-categorized by task features (e.g., strength, power, balance index) considering the exercise treatments applied. Where studies covered several relevant tasks, the results from the single study were categorized accordingly. Finally, the levels of evidence (21) based on the methodological quality assessment was added. To indicate changes in the outcomes, delta changes from pre to post exercise were calculated in percentage (%) where possible.

Results

Study selection

The search found a total of 2,260 studies which excluded 329 duplicates by automatic title matchings and 37 more duplicates were removed by manual confirmation using Excel. Following 1,867 articles were excluded by the title and abstract screening process. The remaining 27 articles were gone through a full-text eligibility check. Among them, 9 studies were removed due to inappropriate outcome parameters, 1 study for not providing no original data, 3 studies for missing responses from the authors, 1 study for no suitable study design, 2 studies for no suitable subjects, and 1 study for co-intervention allowance. Six corresponding authors were contacted for inaccessible articles, and three authors provided the full text. Finally, 10 articles were included in this study (**Figure 1**). Detailed information on the included and excluded articles is shown in the **Supplementary File S2**.

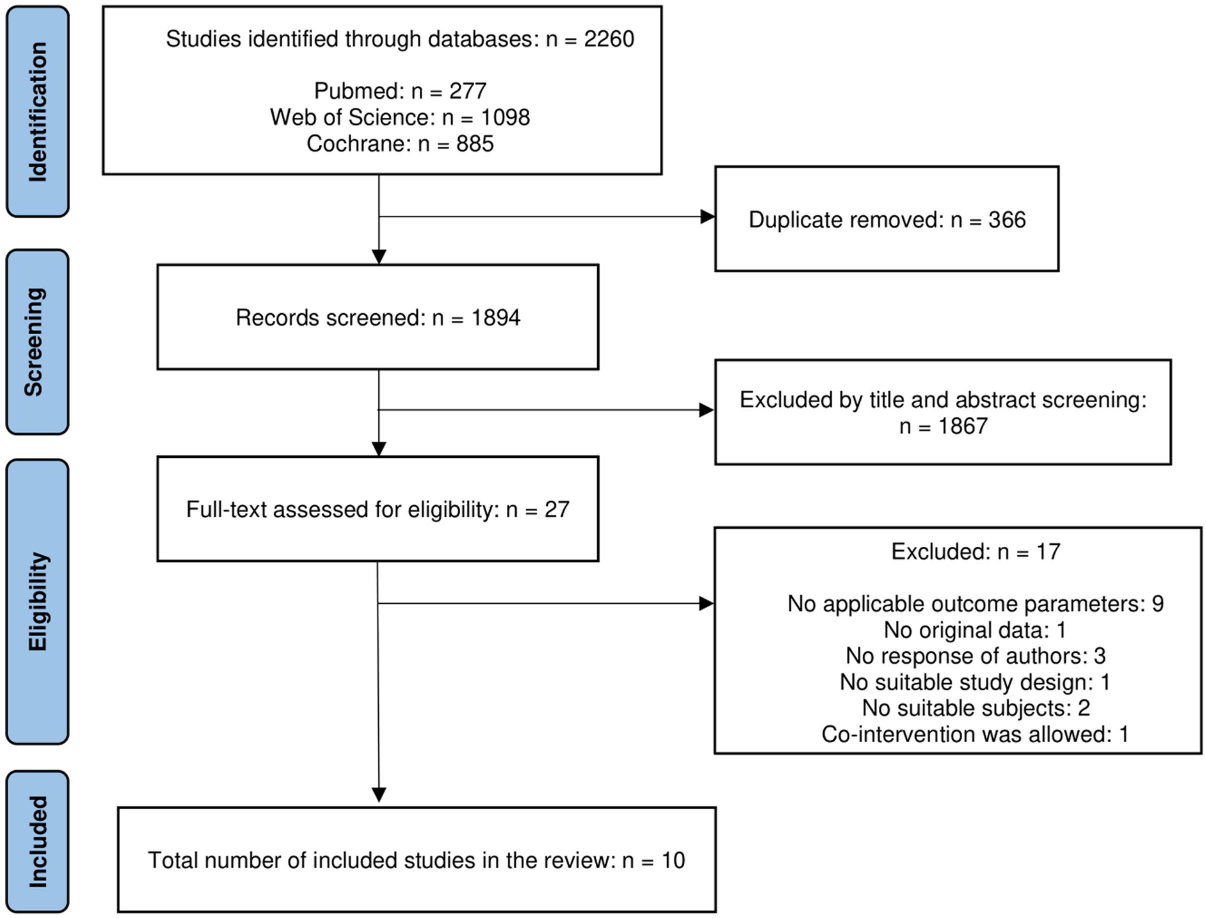

FIGURE 1
Study selection flowchart according to the PRISMA statements.

Methodological quality

A total of eight RCTs studies were included (8–10, 22–27). The mean quality score of the PEDro scale was 6 ± 0.83 points, ranging from 5 to 7 points. Six studies were ranked as high-quality (67%) (8, 10, 22, 24–26), and three studies were medium-quality (33%) (9, 23, 27). All the eight studies performed blinding of the assessors but blinding of therapists was performed by two studies covering the group assignments (8, 26). Blinding of subjects was not conducted in all the studies due to the nature of exercise treatments. Subjects' allocation was concealed by two studies (25–27), whereas six studies acquired data from more than 85% of subjects initially allocated to the groups (8–10, 22, 24, 26) (**Table 2**).

In comparison to the RCTs, two CCTs were appraised (7, 28). The mean quality score was 7, and both studies scored 7 points that were ranked as high-quality (100%). These studies clearly stated the effect of exercise treatments with pre- and post-measurements. The outcomes were measured in a reliable way using machine devices, and it was measured in the same way for the intervention and control groups. However, none of the studies were satisfied with conducting appropriate statistical analysis because the number and type of dependent and independent variables were not considered (**Table 3**).

Characteristics of exercise treatments

The exercise treatments used in the included studies can be categorized into three types based on the loading mode: eccentric, concentric, and combined training. Eccentric exercise was widely applied in 6 studies (7–9, 23, 25, 26, 28), concentric training was applied in 3 studies (8–10), and combined training was also applied in 3 studies (10, 22, 24). Among the eccentric training protocols, three studies applied the "Alfredson protocol" (7, 26, 28), while the others implemented "supervised eccentric training" (8, 25), "modified Alfredson protocol" (23), and "Stanish and Curwin protocol" (9). There were no other special names used for the concentric mode training protocols. Combined training protocols were named the "Silbernagel protocol" or "physiotherapy exercise protocol" that mainly utilized the combination of eccentric and concentric contraction modes. The intervention period was mostly 12 weeks, except for two studies that implemented an 8 week training intervention

TABLE 2 Physiotherapy evidence database (PEDro) scale assessment for randomized controlled trials (RCTs).

Study (year)	1†	2	3	4	5	6	7	8	9	10	11	Total score‡	Quality assessment
Niesen- Vertommen et al. (9)	N	Y	N	N	N	N	Y	Y	N	Y	Y	5	Medium
Silbernagel et al. (10)	Y	Y	N	Y	N	N	Y	Y	N	Y	Y	6	High
Silbernagel et al. (22)	Y	Y	N	Y	N	N	Y	Y	Y	Y	Y	7	High
Tumilty et al. (26)	Y	Y	Y	N	N	Y	Y	Y	N	N	Y	6	High
Stergioulas et al. (25)	Y	Y	Y	Y	N	N	Y	N	Y	Y	Y	7	High
YU et al. (8)	Y	Y	N	Y	N	Y	Y	Y	N	Y	Y	7	High
Stefansson et al. (23)	Y	Y	N	Y	N	N	Y	N	N	Y	Y	5	Medium
Solomons et al. (24)	Y	Y	N	Y	N	N	N	Y	Y	Y	Y	6	High

Y, criterion satisfied; N, criterion not satisfied.
1. Eligibility criteria were specified.
2. Subjects randomly allocated to groups.
3. Allocation was concealed.
4. Groups similar at baseline regarding most important prognostic indicators.
5. Blinding of subjects.
6. Blinding of all therapists.
7. Blinding of all assessors who measured at least one key outcome.
8. Measures of key outcomes were obtained from more than 85% of those initially allocated to groups.
9. All subjects for whom outcome measures were available or, where this was not the case, data for at least one key outcome was analysed by "intention to treat".
10. Comparison results between groups.
11. Measured at least one key outcome at two time points and measures of variability.
†Not calculated in overall score.
‡Out of ten.

TABLE 3 Joanna briggs institute (JBI) non-randomized experimental studies tool assessment for clinical controlled trials (CCTs).

Study (year)	1	2	3	4	5	6	7	8	9	Total score	Study quality
Alfredson et al. (7)	Y	N	Y	Y	Y	Y	Y	Y	N	7	High
Alfredson et al. (28)	Y	N	Y	Y	Y	Y	Y	Y	N	7	High

Y, criterion satisfied; N, criterion not satisfied.
1. Is it clear in the study what is the "cause" and what is the "effect" (i.e. there is no confusion about which variable comes first)?
2. Were the participants included in any comparisons similar?
3. Were the participants included in any comparisons receiving similar treatment/care, other than the exposure or intervention of interest?
4. Was there a control group?
5. Were there multiple measurements of the outcome both pre and post the intervention/exposure?
6. Was follow up complete and if not, were differences between groups in terms of their follow up adequately described and analyzed?
7. Were the outcomes of participants included in any comparisons measured in the same way?
8. Were outcomes measured in a reliable way?
9. Was appropriate statistical analysis used?

period (8, 25). The overview of the exercise treatment types is summarized in **Table 4**.

Characteristics of included studies

The total number of females and males was 48 (24%) and 137 (68%), respectively, with 16 (8%) unknown sex. The mean age of the subjects was 38 years, ranging from 20 ± 2 years (8) to 48 ± 7 years (22). Seven studies reported their subjects were in their 40 s (7, 10, 22–24, 26, 28), whereas one study reported them to by in their 30 s (9) and the other two in their 20 s (8, 25). The mean duration of symptoms was 16.5 months, ranging from 3.7 ± 1 (9) to 48 ± 6.8 months (22), except one study that did not report the symptom duration (26). Ultrasonography was performed to diagnose AT with or without the clinical methods in six studies (7, 8, 22, 23, 25, 28), whereas the other four studies only utilized the clinical methods (9, 26)' such as reported pain (10, 24). The detailed characteristics of the included studies are summarized in **Tables 5**.

TABLE 4 Overview of the exercise treatment types that have been included in this study.

Eccentric training	Eccentric loadings of the plantarflexor muscle-tendon unit that were named "eccentric training", "Alfredson protocol," or "Stanish and Curwin protocol"
Concentric training	Concentric loadings of the plantarflexor muscle-tendon unit that were named "concentric training"
Combined training	Combination of eccentric and concentric loadings of the plantarflexor that were named "Silbernagel protocol" or "physiotherapy exercise protocol," which also includes balance and/or plyometric or isometric loadings

Kinetic parameters

Plantar flexor strength

Two high-quality studies using eccentric training showed significant improvements in concentric & eccentric torque at 12 weeks measurement point (26), concentric peak torque at 90°/sec (+11%) & at 225°/sec (+15%), and eccentric peak torque at 90°/sec (+18%) (7). One high-quality study also showed improvements in

TABLE 5 Characteristics of the included studies.

Study (year)	Study characteristics	Participants (n)†	Intervention‡	Kinetic, kinematic, and sensorimotor outcomes	Results
Niesen-Vertommen et al. (9)	RCT A: ET B: CT	Group A; $N = 8$ (4 female, 4 male) Mean age: 35.3 ± 2.9 years Mean symptom duration: 3.7 ± 1 months Group B; $N = 9$ (3 female, 6 male) Mean age: 33 ± 2.5 years Mean symptom duration: 3.8 ± 1.1 months Diagnosis: clinical method	12 weeks Group A; • Stanish and Curwin protocol • Fast eccentric + slow concentric loading • 5 × 10 repetitions • Once daily, 6 days a week • Load was increased by resistance (speed and load) • Pain was not allowed Group B; • Concentric + eccentric loading • 5 × 10 repetitions • Once daily, 6 days a week • Load was increased by resistance (speed and load) • Pain was not allowed	Plantarflexion concentric torque (Nm) Plantarflexion eccentric torque (Nm)	Improved by both groups ($P < 0.001$). No difference between the groups Improved by both groups ($P < 0.001$). No difference between the groups
Alfredson et al. (7)	CCT A: ET B: Surgery	Group A; $N = 15$ (3 female, 12 male) Mean age: 44.3 ± 7 years Mean symptom Duration: 18.3 months Diagnosis: clinical + ultrasound method	12 weeks Group A; • Alfredson protocol • Eccentric loading • 3 × 15 repetitions (straight & bent knee) • Twice daily • Load was increased using backpack or weight machine • Pain was allowed	Plantarflexion concentric peak torque at 90°/sec, 225°/sec (Nm) Plantarflexion eccentric peak torque at 90°/sec (Nm)	Improved; 69.1 ± 24.6 vs 76.9 ± 20.6 ($P < 0.05$, +11%), 30.9 ± 10.4 vs 35.5 ± 11.3 ($P < 0.05$, +15%) Improved; 152 ± 57.4 vs 179.2 ± 56.9 ($P < 0.01$, +18%)
Alfredson et al. (28)	CCT A: ET B: Surgery	Group A; $N = 14$ (2 female, 12 male) Mean age: 44.2 ± 7.1 years Mean symptom Duration: 17.8 months Diagnosis: clinical + ultrasound method	12 weeks Group A; • Alfredson protocol	Plantarflexion concentric peak torque (Nm) Plantarflexion eccentric peak torque (Nm)	Baseline deficits were resolved compared to the contralateral side by the concentric peak torque ($P < 0.01$) Baseline deficits were resolved compared to the contralateral side by the eccentric peak torque ($P < 0.05$)
Silbernagel et al. (10)	RCT A: Combined B: CT	Group A; $N = 22$ (5 female, 17 male) mean age: 47 ± 14.7 years Mean symptom Duration: 20 ± 25.4 months Group B; $N = 18$ (4 female, 14 male) mean age: 41 ± 10.2 years Mean symptom Duration: 41 ± 55.9 months Diagnosis: Clinical method	12 weeks Group A; • Silbernagel protocol • Progressing from eccentric-concentric to eccentric and balance loading • 3 × 15 repetitions • Starting from 3 times a day to once daily from at 4 weeks • Load was increased using speed, load (backpack), and type of exercises • Pain was allowed Group B; • Concentric + eccentric loading • 2 × 30 repetitions • 3 times a day • Load was increased using sets, repetitions, and form of the exercise (two to one leg) • Pain was allowed • 2 × 30 s stretching	CMJ height (cm) Plantarflexion ROM (degrees)	Both groups improved. A; 13 ± 7 vs 14 ± 7.9 ($P < 0.05$, +8%), B; 15 ± 3.6 vs 16 ± 2.9 ($P < 0.05$, +7%). No difference between the groups No change by either group A; 72 ± 6.9 vs 73 ± 5 (+1%), B; 73 ± 6.6 vs 72 ± 5.7 (- 1%)

(*Continued*)

TABLE 5 (Continued)

Study (year)	Study characteristics	Participants (n)[†]	Intervention[‡]	Kinetic, kinematic, and sensorimotor outcomes	Results
Silbernagel et al. (22)	RCT A: Combined + adjusted sports activity B: Combined	Group B; $N = 19$ (11 female, 8 male) mean age: 48 ± 6.8 years Mean symptom Duration: 24.4 months Diagnosis: clinical + ultrasound method	12 weeks Group B; • Silbernagel protocol • Progressing from eccentric-concentric to eccentric, balance, and plyometric loading	Plantarflexion toe-raise test (J) Plantarflexion eccentric-concentric toe raise Drop CMJ height (cm) CMJ height (cm) Dorsiflexion ROM	No change; 1,716 ± 1,021 vs 2,051 ± 1,020 (+20%) No change; 277 ± 144 vs 303 ± 183 (+9%) No change; 9.9 ± 5.2 vs 10.3 ± 5.1 (+4%) No change; 10.3 ± 5.1 vs 10.3 ± 4.6 (=0%) No change; 34 ± 5.3 vs 33 ± 5.4 (- 3%)
Tumilty et al. (26)	Pilot RCT A: ET + placebo B: ET + low-level laser therapy	Group A; $N = 10$ (4 female, 6 male) mean age: 42.5 ± 8.5 years Mean symptom Duration: unknown Diagnosis: Clinical method	12 weeks Group A; • Alfredson protocol	Plantarflexion concentric torque (Nm) Plantarflexion eccentric torque (Nm)	MD (CI, P) Improved; −84.2 (−125.8–−42.5, $P = 0.001$) Improved; −79.2 (−132.8–−25.6, $P = 0.009$)
Stergioulas et al. (25)	RCT A: ET + low-level laser therapy B: ET + placebo	Group B; $N = 20$ (7 female, 13 male) Mean age: 28.8 ± 4.8 years Mean Symptom duration: 9.4 ± 2.7 months Diagnosis: clinical + ultrasound method	8 weeks Group B; • Supervised eccentric protocol • Eccentric loading • 12 × 12 repetitions (knee-straight, knee-flexed) • 4 times per week • Load was increased by exercise volume and a backpack (4 kg) • Pain was allowed • Stretching of gastrocnemius and soleus muscles (15 s × 5 times, before and after the program)	Dorsiflexion ROM (degrees)	No change
Yu et al. (8)	RCT A: ET B: CT	Group A; $N = 16$ (16 male) mean age: 20.1 ± 1.8 years Mean symptom Duration: 11.3 months Group B; $N = 16$ (16 male) mean age: 20.4 ± 1.3 years Mean symptom Duration: 12.1 months Diagnosis: ultrasound method	8 weeks Group A; • Supervised eccentric protocol • Eccentric loading • 3 × 15 repetitions • Three times a week (50 min each time) • Load was increased weekly using weighted backpacks (5–10 lbs) and form of the exercise (two to one leg) • Pain was not allowed Group B; • Supervised concentric protocol • Concentric loading • 3 × 15 repetitions • Three times a week (50 min each time) • Load was increased using elastic band • Pain was not allowed • Stretching Hamstring and calf muscles was performed	Plantarflexion concentric peak torque (Nm) Plantarflexion eccentric peak torque (Nm) Total balance index Sargent jump	Improved only by the group A; 56.9 ± 7.3 vs 66.4 ± 11.8 ($P < 0.05$, +17%), B; 63.2 ± 6.3 vs 71.2 ± 10.3 (+13%) Improved only by the group A; 37 ± 6.9 vs 44.7 ± 10.1 ($P < 0.05$, +21%), B; 36.7 ± 11.7 vs 43.9 ± 12.2 (+20%) Improved only by the group A; 36.4 ± 8.5 vs 8 ± 5.4 ($P < 0.05$, −78%), B; 29 ± 16 vs 22.5 ± 7.5; Group difference was found ($P < 0.05$) Improved by both groups A; 53.1 ± 4.3 vs 68 ± 3.5 ($P < 0.05$, +28%), B; 54.6 ± 4.7 vs 64.4 ± 4.5 ($P < 0.05$, +18%), but significant differences were found between the groups in favor of the group A
Stefansson et al. (23)	RCT A: ET B: pressure massage C: ET + pressure massage	Group A; $N = 16$ (Sex unknown) Mean age: 46 ± 12.9 years Mean symptom duration: 28.8 ± 39.7 months Diagnosis: clinical + ultrasound method	12 weeks Group A; • Modified Alfredson protocol • Gradual increase of sets from one to six days	Dorsiflexion ROM with knee-straight (degrees) Dorsiflexion ROM with knee-bent (degrees)	No change; 34.3 ± 6.2 vs 35.6 ± 4.8 (+4%) No change; 37.4 ± 6.1 vs 38.8 ± 4.7 (+4%)

(*Continued*)

TABLE 5 (Continued)

Study (year)	Study characteristics	Participants (n)†	Intervention‡	Kinetic, kinematic, and sensorimotor outcomes	Results
Solomons et al. (24)	RCT A: Combined B: Combined + sham intramuscular stimulation C: Combined + intramuscular dry needling treatment	Group A; *N* = 8 (5 female, 3 male) Mean age: 47 ± 7.2 years Mean symptom duration: 7.6 ± 7.5 months	12 weeks Group A; • Physiotherapy exercise training • Isometric loading to concentric + eccentric loading • Sets/repetitions were not stated • Frequency was not stated • Load, range and speed were increased gradually • Pain was allowed	Dorsiflexion ROM with knee-straight (degrees) Dorsiflexion ROM with knee-bent (degrees)	No change; 34 ± 4.8 vs 37 ± 1.8 (+9%) No change; 42 ± 4.6 vs 43 ± 2.4 (+2%)

MD, mean difference; CI, confidence interval; ET, eccentric training; CT, concentric training; MVC, maximal voluntary contraction; wk, week; RCT, randomized controlled trial; CCT, controlled clinical trial; ROM, range of motion; CS, cohort study; CMJ, counter movement jump; Nm, newton meter; J, joules; w, watt; cm, centimeter; N, newtons.
†Data are only from exercise intervention groups; co-interventions were not considered.
‡Duration of intervention; loading mode; sets/repetitions; frequency; rate of progression; pain allowed during exercises.

concentric (+17%) & eccentric (+21%) peak torque at 8 weeks by eccentric training (8). Moreover, one medium-quality study with eccentric training reported an improvement in concentric & eccentric torque at 12 weeks (9). One high-quality study showed the baseline eccentric & concentric peak torque deficits were resolved when compared with the contralateral side by eccentric training at 12 weeks (28). One medium-quality study using concentric training showed an improvement in concentric & eccentric torque at 12 weeks (9), whereas one high-quality study reported an insignificant improvement in concentric (+13%) & eccentric (+20%) peak torque at 8 weeks (8). One high-quality study with combined training reported an insignificant improvement in toe-raise test at 12 weeks (+20%) (22).

Plantar flexor power

One high-quality study using eccentric training showed an improvement (+28%) in sargent jump at 8 weeks (8). Two high-quality studies using concentric training showed improvements (+18%) in sargent jump at 8 weeks (8), and countermovement jump (+7%) at 12 weeks (10). One high-quality study with combined training reported an improvement (+8%) in countermovement jump (10), whereas one high-quality study showed an insignificant improvement in eccentric-concentric toe raise (+9%), drop countermovement jump (+4%), and countermovement jump (=0%) at 12 weeks (22).

Kinematic parameters

Ankle range of motion

One high-quality (25) showed no change in dorsiflexion ROM at 8 weeks by eccentric training, and one moderate-quality study (23) reported insignificant improvement dorsiflexion ROM in knee-straight (+4%) and knee-bend positions (+4%) by eccentric training at 12 weeks. By use of concentric training one high-quality study reported insignificant decrease in plantarflexion ROM (−1%) at 12 weeks (10). Three high-quality studies with combined training reported insignificant improvement in plantarflexion ROM (+1%) (10), insignificant decrease in dorsiflexion ROM (−3%) (22), and insignificant improvement in knee-straight (+9%) and knee-bend (+2%) dorsiflexion ROM (24) at 12 weeks.

Sensorimotor parameters

Balance index

One high-quality study using eccentric training showed an improvement (−78%) in total balance index, while concentric training showed an insignificant improvement (−22%) at 8 weeks (8).

Discussion

The purpose of this systematic review was to analyze the effect of various exercise treatments (eccentric, concentric, combined) on different functional outcomes (strength, power, range of motion, balance) in the subjects of mid-portion AT. A variety of exercise interventions were categorized into eccentric, concentric, and combined training modes, and the effects on functional outcomes were investigated. In kinetic parameters, eccentric training showed moderate to strong evidence in power and strength outcomes, respectively. Concentric training showed conflicting evidence in strength outcomes but moderate evidence in power outcomes. Combined training revealed moderate evidence of no improvement in strength outcomes and conflict evidence of power outcomes. Concerning kinematic parameters, only plantarflexion and dorsiflexion ROM measures were available by the exercise treatments that no study reported improvements. Regarding sensorimotor parameters, eccentric training showed moderate evidence in the balance index. In contrast, moderate evidence of insignificant improvement was revealed by concentric training. There was no study that applied combined training to measure a sensorimotor parameter.

Kinetic parameters with the exercise treatments

For improving kinetic parameters of strength outcomes such as peak torque or power outcomes such as height of sargent jump, eccentric training was found to have strong and moderate evidence, respectively. For subjects who are not responsive to this type of loading training, however, concentric training could be an option since moderate evidence was found to improve power outcomes. Nevertheless, eccentric training should be the primary choice to improve power outcomes as the high-quality RCT study that directly compared supervised eccentric training vs. concentric training showed a significant difference of the sargent jump in favor of the eccentric training group, despite the concentric training group has significantly improved after the training (8). The possibility of greater mechanical load from eccentric loading over concentric loading has been proposed (8), as eccentric loading may cause the tendon to extend more and result in greater mechanical strain on the tendon (29–31). However, the actual efficacy of eccentric over concentric loading for improving kinetic parameters in AT remains inconclusive. It is argued that positive adaptations can be achieved through heavy mechanical strain regardless of the type of contraction (16, 17). Additional research has demonstrated that eccentric loadings do not cause more stress on the Achilles tendon compared to concentric exercises, suggesting that this mechanism may not be a contributing factor (32). In eccentric training, stimulating collagen synthesis and remodeling in the tendon were suggested as one possible hypothesis (33) which might eventually lead to an increased plantar flexor strength capacity, and pain reduction was deemed to be involved with tendon structure re-organization mechanism (12). Contrarily, a recent systematic review (34) and the overall inference from the available literature (35) support the idea that tendon structure does not change considerably during the course of treatment and the alterations do not lead to improvements in pain or function (34). Together, these findings imply that clinical advancements during rehabilitation take place via a mechanism different from structural adaptation. One other hypothesis is the elimination of new blood vessels in the tendon that may contribute to pain (12, 36). During the heel-drop eccentric loadings, the flow in the neovessels was stopped when compared to the resting position. Thus, the effect of cessations might directly affect the neovessels which were relevant for the resolution of pain (12, 36). Regarding concentric training, it is possible that this form of loading increases blood flow and oxygen delivery to the Achilles tendon that may enhance healing (37). In conclusion, both of the training regimes could bring positive improvements to kinetic parameters for AT, but further high-quality studies are required to confirm the effects with concentric training.

The result of no improvement in strength outcomes and conflicting evidence of power outcomes by combined training was unexpected because it is generally believed to bring more advantages compared to isolated eccentric or concentric training since contraction mode is known to affect training gains (38). Nevertheless, these results may be explained by the aberrant neural commands that are seen in AT due to the pathological condition (39). The eccentric and concentric combined contractions are similar to the movements that are involved in daily walking or running, since they incorporate stretch-shortening cycles (SSC). SSC is defined as pre-activated muscle contraction that undergoes an eccentric lengthening followed by a concentric contraction (40). It increases mechanical overload on the tendon through elevated stress. During SSC, Achilles tendon force reached 12.5 times as body weight (41), generating tendon strain as low as 4.1% to as high as 12.8% (42, 43). By nature, the Achilles tendon always undergoes SSC during functional tasks. However, the uncoordinated motor activities in AT (39) could impose higher stress on the Achilles tendon (44, 45) following this kind of activity. Thus, the combined exercise treatment, like the "Silbernagel protocol" (22), may not be as effective as eccentric loading protocols in improving kinetic outcomes.

Kinematic parameters with the exercise treatments

This study identified the lack of kinematic outcome parameters except for the outcome of plantarflexion and dorsiflexion ROM by the exercise treatments in five studies (10, 22–25) that reported no improvements. Although decreased ankle dorsiflexion is regarded as natural history following the onset of AT (46), the assessment of the ankle ROM to analyze the effect of exercise treatments requires caution in this population. There were studies that showed increased dorsiflexion ROM as a risk factor for AT that may impose higher loads on the Achilles tendon (47). In contrast, with currently available evidence, it is unclear whether decreased ankle ROM after an exercise treatment represents a functional improvement in AT. In this review, one study measured plantarflexion (10), and four studies examined dorsiflexion ROM following the exercise treatments (22–25). Since no significant changes were reported, the assessment of ankle ROM may not be a defining factor of recovery in AT. However, from a clinical point of view, a higher ankle ROM can be caused by higher compliancy of the tendon, which may be a sign of impaired loading capacity. Overall, the limited availability of kinematic outcome parameters, in line with the uncertainty in the role of ankle ROM in exercise treatments for mid-portion AT, highlights the need for more comprehensive evaluations for future studies.

Sensorimotor parameters with the exercise treatments

In terms of the sensorimotor outcome parameters, only the total balance index measurement was available from one high-quality RCT study that compared eccentric training to concentric training (8). While the eccentric training showed an improvement, the concentric training showed no notable change, which resulted in a significant group difference. Under eccentric contractions, the muscle is actively extended through external stress, which differs from concentric contractions in several neurological ways (48, 49). Motor unit discharge rates were more varied during eccentric contractions than concentric contractions (50), which is derived from the high motor unit discharge rate variability, and selective recruitment of motor unit threshold. This supports the belief that eccentric loadings inspire different patterns of brain activity compared to concentric loadings, suggesting a distinct neuromuscular processing strategy. According to Latella et al. (2019), the long-lasting influence on the cortical process by eccentric loading reflects the complexity of the motor control required to conduct the movements (51). That means eccentric contractions require challenging motor control (52), which provokes the neuromuscular system more than concentric contractions. During eccentric contractions, cortical excitability appears to be heightened, and a larger brain region seems to be engaged (53).

Limitations

There were a couple of limitations of the study. One limitation was the stage of the tendon pathology. The continuum model of tendon pathology was suggested by Cook and Purdam (1), and thereby diagnostic subgroups might have existed between the included studies (relatively short duration of symptom [3.7 months (9)], and low age [in the 20 s (8, 25)] compared to the other studies).

It is also worth mentioning the modalities of exercise treatments. There were exercise protocols engaged in both eccentric and concentric loading components, but those protocols were named as either "eccentric" or "concentric" training following the mainstream of the loading mode (9, 10). Moreover, the combined training protocols also have involved balance (10, 22), plyometric (22, 54), and isometric (24) loading components. These combinations of training modes make it difficult to determine which type of loading protocol is beneficial for which type of functional outcomes.

Moreover, the present study excluded the endurance measurements such as heel raise tests that counting the number of repetitions a subject can perform until experiencing fatigue or discomfort. It was deemed unsuitable for inclusion since it does not directly assess the pre-defined categories of kinetic, kinematic, or sensorimotor parameters. However, future research may consider to include this test to provide a more comprehensive overview of the effect of different exercise treatments on various functional outcomes in mid-portion AT.

Lastly, this study has illustrated the need for assessing outcome measures in the kinematic and sensorimotor outcome parameters. Measurements in broad outcome variables, including joint moments, angles, and positions in the kinematic parameter, and reflex and muscle activities in the sensorimotor parameter with exercise treatments will provide a clear picture of what loading types should be considered to improve these functional outcomes.

Clinical implications

It is worth to underline the total volume reduced eccentric training protocol (8). Unlike the traditional Alfredson protocol (7), which is widely accepted as the gold standard of exercise treatment for AT subjects, the total volume reduced eccentric training was conducted three times a week for eight weeks but showed significant improvements in strength, power, and balance outcomes (8). Being considered the time efficiency and the burden of compliance with the Alfredson protocol, the result is certainly meant for the subjects. The Alfredson protocol requires a high amount of training volume, but there is no rationale for this much training volume (55). It can be extra work and even can induce delayed-onset muscle soreness. Future studies should consider applying total volume reduced eccentric training protocol with the outcomes of kinetic and sensorimotor parameters.

During exercise interventions, the pain was not a required feature since the studies showed improvements in the functional outcomes without allowance of pain (8, 9). In contrast, Alfredson protocol (7) allows some degree of pain while conducting the protocol. Although it is debatable whether pain should be allowed during an exercise intervention to lead to a functional improvement, training-induced pain ought to be informed for subjects before conducting any exercise treatments.

Conclusion

This is the first study to investigate the effect of different exercise treatments on the different functional outcome parameters in mid-portion AT. Eccentric training showed moderate to strong evidence in the kinetic parameters of power and strength outcomes, respectively. Also, moderate evidence was found in the sensorimotor parameters of the balance index through eccentric training. Concentric training showed moderate evidence in the power outcomes, so it could be considered for the subjects who are not responsive to eccentric training to improve this function. In contrast, combined training modalities did not lead to improvements in strength and power outcomes. In terms of kinematic parameters, there were only plantarflexion and dorsiflexion ROM measures examined showing no changes by different training modes (eccentric, concentric, and combined). Thus, ankle ROM measurement is not recommended with the subjects of mid-portion AT. This study identified supportive evidence of eccentric training in the functional outcomes of strength and power as well as the sensorimotor ability "balance index". Concentric training modalities can be considered optional in order to improve the outcome of power. Future studies applying the different training modalities with kinematic outcome parameters such as joint moments and angles instead of plantarflexion and dorsiflexion ROM will expand the knowledge what types of exercise treatments should be considered to improve the function.

Data availability statement

The original contributions presented in the study are included in the article/**Supplementary Material**, further inquiries can be directed to the corresponding author.

Author contributions

MK: Conceptualization, data curation, formal analysis, investigation, methodology, project administration, resources, roles/writing - original draft, and writing - review & editing. C-IL: data curation and investigation. JH and AQ: methodology and writing - review & editing. TE: conceptualization and writing - review & editing. MC: conceptualization, writing - review & editing, resources, project administration, and project supervision. All authors contributed to the article and approved the submitted version.

Funding

Deutsche Forschungsgemeinschaft (DFG, German Research Foundation) — Projektnummer 491466077.

Conflict of interest

The authors declare that the research was conducted in the absence of any commercial or financial relationships that could be construed as a potential conflict of interest.

Publisher's note

Supplementary material

The Supplementary Material for this article can be found online at: https://www.frontiersin.org/articles/10.3389/fspor.2023.1144484/full#supplementary-material.

References

1. Cook JL, Rio E, Purdam CR, Docking SI. Revisiting the continuum model of tendon pathology: what is its merit in clinical practice and research? *Br J Sports Med.* (2016) 50:1187–91. doi: 10.1136/bjsports-2015-095422

2. Albers IS, Zwerver J, Diercks RL, Dekker JH, van den Akker-Scheek I. Incidence and prevalence of lower extremity tendinopathy in a Dutch general practice population: a cross sectional study. *BMC Musculoskelet Disord.* (2016) 17(1):16. doi: 10.1186/s12891-016-0885-2

3. Lopes AD, Hespanhol LC, Yeung SS, Costa LOP. What are the main running-related musculoskeletal injuries? *Sports Med.* (2012) 42(10):891–905. doi: 10.1007/BF03262301

4. Singh A, Calafi A, Diefenbach C, Kreulen C, Giza E. Noninsertional tendinopathy of the Achilles. *Foot Ankle Clin.* (2017) 22(4):745–60. doi: 10.1016/j.fcl.2017.07.006

5. van der Vlist AC, Breda SJ, Oei EHG, Verhaar JAN, de Vos RJ. Clinical risk factors for Achilles tendinopathy: a systematic review. *Br J Sports Med.* (2019) 53 (21):1352–61. doi: 10.1136/bjsports-2018-099991

6. Murphy MC, Travers MJ, Chivers P, Debenham JR, Docking SI, Rio EK, et al. Efficacy of heavy eccentric calf training for treating mid-portion Achilles tendinopathy: a systematic review and meta-analysis. *Br J Sports Med.* (2019) 53 (17):1070–7. doi: 10.1136/bjsports-2018-099934

7. Alfredson H, Pietilä T, Jonsson P, Lorentzon R. Heavy-load eccentric calf muscle training for the treatment of chronic Achilles tendinosis. *Am J Sports Med.* (1998) 26 (3):360–6. doi: 10.1177/03635465980260030301

8. Yu J, Park D, Lee G. Effect of eccentric strengthening on pain, muscle strength, endurance, and functional fitness factors in male patients with achilles tendinopathy. *Am J Phys Med Rehabil.* (2013) 92(1):68–76. doi: 10.1097/PHM.0b013e31826eda63

9. Niesen-Vertommen S, Taunton J, Clement D, Mosher R. The effect of eccentric versus concentric exercise in the management of Achilles tendonitis. *Clin J Sport Med.* (1992) 2:109–13. doi: 10.1097/00042752-199204000-00006

10. Silbernagel KG, Thomeé R, Thomeé P, Karlsson J. Eccentric overload training for patients with chronic Achilles tendon pain—a randomised controlled study with reliability testing of the evaluation methods. *Scand J Med Sci Sports.* (2001) 11 (4):197–206. doi: 10.1034/j.1600-0838.2001.110402.x

11. Langberg H, Ellingsgaard H, Madsen T, Jansson J, Magnusson SP, Aagaard P, et al. Eccentric rehabilitation exercise increases peritendinous type I collagen synthesis in humans with Achilles tendinosis. *Scand J Med Sci Sports.* (2006) 17 (1):61–6. doi: 10.1111/j.1600-0838.2006.00522.x

12. Ohberg L, Alfredson H. Effects on neovascularisation behind the good results with eccentric training in chronic mid-portion Achilles tendinosis? *Knee Surg Sports Traumatol Arthrosc.* (2004) 12(5):465–70. doi: 10.1007/s00167-004-0494-8

13. de Vos RJ, Weir A, Tol JL, Verhaar JAN, Weinans H, van Schie HTM. No effects of PRP on ultrasonographic tendon structure and neovascularisation in chronic midportion Achilles tendinopathy. *Br J Sports Med.* (2011) 45(5):387–92. doi: 10.1136/bjsm.2010.076398

14. Merza E, Pearson S, Lichtwark G, Ollason M, Malliaras P. Immediate and long-term effects of mechanical loading on Achilles tendon volume: a systematic review and meta-analysis. *J Biomech.* (2021) 30(118):110289. doi: 10.1016/j.jbiomech.2021.110289

15. Kjaer M, Heinemeier KM. Eccentric exercise: acute and chronic effects on healthy and diseased tendons. *J Appl Physiol (1985).* (2014) 116(11):1435–8. doi: 10.1152/japplphysiol.01044.2013

16. Hasani F, Haines T, Munteanu SE, Schoch P, Vicenzino B, Malliaras P. LOAD-intensity and time-under-tension of exercises for men who have Achilles tendinopathy (the LOADIT trial): a randomised feasibility trial. *BMC Sports Sci Med Rehabil.* (2021) 13(1). doi: 10.1186/s13102-021-00279-z

17. Beyer R, Kongsgaard M, Hougs Kjær B, Øhlenschlæger T, Kjær M, Magnusson SP. Heavy slow resistance versus eccentric training as treatment for Achilles

tendinopathy: a randomized controlled trial. *Am J Sports Med*. (2015) 43(7):1704–11. doi: 10.1177/0363546515584760

18. Page MJ, McKenzie JE, Bossuyt PM, Boutron I, Hoffmann TC, Mulrow CD, et al. The PRISMA 2020 statement: an updated guideline for reporting systematic reviews. *Int J Surg*. (2021) 88:105906. doi: 10.1016/j.ijsu.2021.105906

19. Yamato TP, Maher C, Koes B, Moseley A. The PEDro scale had acceptably high convergent validity, construct validity, and interrater reliability in evaluating methodological quality of pharmaceutical trials. *J Clin Epidemiol*. (2017) 86:176–81. doi: 10.1016/j.jclinepi.2017.03.002

20. Maher CG, Sherrington C, Herbert RD, Moseley AM, Elkins M. Reliability of the PEDro scale for rating quality of randomized controlled trials. *Phys Ther*. (2003) 83 (8):713–21. doi: 10.1093/ptj/83.8.713

21. van Tulder M, Furlan A, Bombardier C, Bouter L. Updated method guidelines for systematic reviews in the cochrane collaboration back review group. *Spine (Phila Pa 1976)*. (2003) 28(12):1290–9. doi: 10.1097/01.BRS.0000065484.95996.AF

22. Silbernagel KG, Thomeé R, Eriksson BI, Karlsson J. Continued sports activity, using a pain-monitoring model, during rehabilitation in patients with achilles tendinopathy: a randomized controlled study. *Am J Sports Med*. (2007) 35 (6):897–906. doi: 10.1177/0363546506298279

23. Stefansson SH, Brandsson S, Langberg H, Arnason A. Using pressure massage for Achilles tendinopathy: a single-blind, randomized controlled trial comparing a novel treatment versus an eccentric exercise protocol. *Orthop J Sports Med*. (2019) 7(3). doi: 10.1177/232596711983428. Available from: https://journals.sagepub.com/doi/pdf/10.1177/2325967119834284.

24. Solomons L, Lee JJY, Bruce M, White LD, Scott A. Intramuscular stimulation vs sham needling for the treatment of chronic midportion Achilles tendinopathy: a randomized controlled clinical trial. *PLoS One*. (2020) 15(9 September). doi: 10.1371/journal.pone.0238579

25. Stergioulas A, Stergioula M, Aarskog R, Lopes-Martins RAB, Bjordal JM. Effects of low-level laser therapy and eccentric exercises in the treatment of recreational athletes with chronic achilles tendinopathy. *Am J Sports Med*. (2008) 36(5):881–7. doi: 10.1177/0363546507312165

26. Tumilty S, Munn J, Abbott JH, McDonough S, Hurley DA, Baxter GD. Laser therapy in the treatment of achilles tendinopathy: a pilot study. *Photomed Laser Surg*. (2008) 26(1):25–30. doi: 10.1089/pho.2007.2126

27. Hasani F, Haines TP, Munteanu SE, Vicenzino B, Malliaras P. Efficacy of different load intensity and time-under-tension calf loading protocols for Achilles tendinopathy (the LOADIT trial): protocol for a randomised pilot study. *Pilot Feasibility Stud*. (2020) 6(1):1–12. doi: 10.1186/s40814-020-00639-5

28. Alfredson H, Nordström P, Pietilä T, Lorentzon R. Bone mass in the calcaneus after heavy loaded eccentric calf-muscle training in recreational athletes with chronic Achilles tendinosis. *Calcif Tissue Int*. (1999) 64(5):450–5. doi: 10.1007/PL00005827

29. Alfredson H. The chronic painful Achilles and patellar tendon: research on basic biology and treatment. *Scand J Med Sci Sports*. (2005) 15(4):252–9. doi: 10.1111/j.1600-0838.2005.00466.x

30. Mafi N, Lorentzon R, Alfredson H. Superior short-term results with eccentric calf muscle training compared to concentric training in a randomized prospective multicenter study on patients with chronic Achilles tendinosis. Knee surgery, sports traumatology. *Arthroscopy*. (2001) 9(1):42–7. doi: 10.1007/s001670000148

31. Allison GT, Purdam C. Eccentric loading for Achilles tendinopathy–strengthening or stretching? *Br J Sports Med*. (2009) 43(4):276–9. doi: 10.1136/bjsm.2008.053546

32. Rees JD, Lichtwark GA, Wolman RL, Wilson AM. The mechanism for efficacy of eccentric loading in Achilles tendon injury; an in vivo study in humans. *Rheumatology*. (2008) 47(10):1493–7. doi: 10.1093/rheumatology/ken262

33. Woodley BL, Newsham-West RJ, David Baxter G, Woodley B. Chronic tendinopathy: effectiveness of eccentric exercise. *ACP J Club*. (2007) 41:188–99. doi: 10.1136/bjsm.2006.029769

34. Drew BT, Smith TO, Littlewood C, Sturrock B. Do structural changes (e.g., collagen/matrix) explain the response to therapeutic exercises in tendinopathy: a systematic review. *Br J Sports Med*. (2014) 48(12):966–72. doi: 10.1136/bjsports-2012-091285

35. de Vos RJ, Heijboer MP, Weinans H, Verhaar JAN, van Schie HTM. Tendon structure's lack of relation to clinical outcome after eccentric exercises in chronic midportion Achilles tendinopathy. *J Sport Rehabil*. (2012) 21(1):34–43. doi: 10.1123/jsr.21.1.34

36. Knobloch K, Alfredson H. Eccentric training in Achilles tendinopathy: is it harmful to tendon microcirculation? *Br J Sports Med*. (2007) 41(6):e2. doi: 10.1136/bjsm.2006.030437

37. Couppé C, Svensson RB, Silbernagel KG, Langberg H, Magnusson SP, … KS journal of orthopaedic, et al. Eccentric or concentric exercises for the treatment of tendinopathies? *J Orthop Sports Phys Ther*. (2015) 45(11):853–63. doi: 10.2519/jospt.2015.5910

38. Morrissey MC, Harman EA, Johnson MJ. Resistance training modes: specificity and effectiveness. *Med Sci Sports Exerc*. (1995) 27(5):648–60. doi: 10.1249/00005768-199505000-00006

39. Chang YJ, Kulig K. The neuromechanical adaptations to Achilles tendinosis. *J Physiol*. (2015) 593(15):3373–87. doi: 10.1113/JP270220

40. Baur H, Müller S, Hirschmüller A, Cassel M, Weber J, Mayer F. Comparison in lower leg neuromuscular activity between runners with unilateral mid-portion Achilles tendinopathy and healthy individuals. *J Electromyogr Kinesiol*. (2011) 21(3):499–505. doi: 10.1016/j.jelekin.2010.11.010

41. Komi P v., Fukashiro S, Jarvinen M. Biomechanical loading of Achilles tendon during normal locomotion. *Clin Sports Med*. (1992) 11(3):521–31. doi: 10.1016/S0278-5919(20)30506-8

42. Magnusson SP, Hansen P, Aagaard P, Brønd J, Dyhre-Poulsen P, Bojsen-Moller J, et al. Differential strain patterns of the human gastrocnemius aponeurosis and free tendon, in vivo. *Acta Physiol Scand*. (2003) 177(2):185–95. doi: 10.1046/j.1365-201X.2003.01048.x

43. Finni T, Hodgson JA, Lai AM, Edgerton VR, Sinha S. Nonuniform strain of human soleus aponeurosis-tendon complex during submaximal voluntary contractions in vivo. *J Appl Physiol*. (2003) 95(2):829–37. doi: 10.1152/japplphysiol.00775.2002

44. Grigg NL, Wearing SC, O'Toole JM, Smeathers JE. Achilles tendinopathy modulates force frequency characteristics of eccentric exercise. *Med Sci Sports Exerc*. (2013) 45(3):520–6. doi: 10.1249/MSS.0b013e31827795a7

45. Wyndow N, Cowan SM, Wrigley Tv, Crossley KM. Neuromotor control of the lower limb in Achilles tendinopathy: implications for foot orthotic therapy. *Sports Med*. (2010) 40(9):715–27. doi: 10.2165/11535920-000000000-00000

46. Becker J, James S, Wayner R, Osternig L, Chou LS. Biomechanical factors associated with achilles tendinopathy and medial tibial stress syndrome in runners. *Am J Sports Med*. (2017) 45(11):2614–21. doi: 10.1177/0363546517708193

47. Yeh CH, Calder JD, Antflick J, Bull AMJ, Kedgley AE. Maximum dorsiflexion increases Achilles tendon force during exercise for midportion Achilles tendinopathy. *Scand J Med Sci Sports*. (2021) 31:1674–82. doi: 10.1111/sms.13974

48. Duchateau J, Enoka RM. Neural control of lengthening contractions. *J Exp Biol*. (2016) 219(Pt 2):197–204. doi: 10.1242/jeb.123158

49. Papitsa A, Paizis C, Papaiordanidou M, Martin A. Specific modulation of presynaptic and recurrent inhibition of the soleus muscle during lengthening and shortening submaximal and maximal contractions. *J Appl Physiol (1985)*. (2022) 133 (6):1327–40. doi: 10.1152/japplphysiol.00065.2022

50. Duchateau J, Baudry S. Insights into the neural control of eccentric contractions. *J Appl Physiol*. (2014) 116:1418–25. doi: 10.1152/japplphysiol.00002.2013

51. Latella C, Goodwill AM, Muthalib M, Hendy AM, Major B, Nosaka K, et al. Effects of eccentric versus concentric contractions of the biceps brachii on intracortical inhibition and facilitation. *Scand J Med Sci Sports*. (2019) 29(3):369–79. doi: 10.1111/sms.13334

52. Perrey S. Brain activation associated with eccentric movement: a narrative review of the literature. *Eur J Sport Sci*. (2018) 18(1):75–82. doi: 10.1080/17461391.2017.1391334

53. Fang Y, Siemionow V, Sahgal V, Xiong F, Yue GH. Distinct brain activation patterns for human maximal voluntary eccentric and concentric muscle actions. *Brain Res*. (2004) 1023(2):200–12. doi: 10.1016/j.brainres.2004.07.035

54. Silbernagel KG, Thomeé R, Eriksson BI, Karlsson J, Silbernagel G. Full symptomatic recovery does not ensure full recovery of muscle-tendon function in patients with Achilles tendinopathy. *Br J Sports Med*. (2007) 41:276–80. doi: 10.1136/bjsm.2006.033464

55. Munteanu SE, Scott LA, Bonanno DR, Landorf KB, Pizzari T, Cook JL, et al. Effectiveness of customised foot orthoses for achilles tendinopathy: a randomised controlled trial. *Br J Sports Med*. (2015) 49(15):989–94. doi: 10.1136/bjsports-2014-093845

frontiers | Frontiers in Bioengineering and Biotechnology

TYPE Mini Review
PUBLISHED 17 May 2023
DOI 10.3389/fbioe.2023.1127289

Check for updates

OPEN ACCESS

EDITED BY
Qichang Mei,
Ningbo University, China

REVIEWED BY
Yunfei Hou,
Peking University People's Hospital, China
Zixiang Gao,
Eötvös Loránd University, Hungary

*CORRESPONDENCE
Yan-Song Qi,
malaqinfu@126.com
Yong-Sheng Xu,
xys_sportsmedicine@126.com

†These authors have contributed equally to this work and share first authorship

SPECIALTY SECTION
This article was submitted to Biomechanics, a section of the journal Frontiers in Bioengineering and Biotechnology

RECEIVED 19 December 2022
ACCEPTED 27 March 2023
PUBLISHED 17 May 2023

CITATION
Zhang Z-H, Qi Y-S, Wei B-G, Bao H-R-C and Xu Y-S (2023), Application strategy of finite element analysis in artificial knee arthroplasty.
Front. Bioeng. Biotechnol. 11:1127289.
doi: 10.3389/fbioe.2023.1127289

Application strategy of finite element analysis in artificial knee arthroplasty

Zi-Heng Zhang[1,2†], Yan-Song Qi[1*†], Bao-Gang Wei[1], Hu-Ri-Cha Bao[1] and Yong-Sheng Xu[1*]

[1]Orthopedics Center, Inner Mongolia People's Hospital, Hohhot, China, [2]Graduate School, Inner Mongolia Medical University, Hohhot, China

Artificial knee arthroplasty, as the most effective method for the treatment of end-stage joint diseases such as knee osteoarthritis and rheumatoid arthritis, is widely used in the field of joint surgery. At present, Finite element analysis (FEA) has been widely used in artificial knee replacement biomechanical research. This review presents the current hotspots for the application of FEA in the field of artificial knee replacement by reviewing the existing research literature and, by comparison, summarizes guidance and recommendations for artificial knee replacement surgery. We believe that lower contact stress can produce less wear and complications when components move against each other, in the process of total knee arthroplasty (TKA), mobile-bearing prostheses reduce the contact surface stress of the tibial-femoral joint compared with fixed-bearing prostheses, thus reducing the wear of the polyethylene insert. Compared with mechanical alignment, kinematic alignment reduces the maximum stress and maximum strain of the femoral component and polyethylene insert in TKA, and the lower stress reduces the wear of the joint contact surface and prolongs the life of the prosthesis. In the unicompartmental knee arthroplasty (UKA), the femoral and tibial components of mobile-bearing prostheses have better conformity, which can reduce the wear of the components, while local stress concentration caused by excessive overconformity of fixed-bearing prostheses should be avoided in UKA to prevent accelerated wear of the components, the mobile-bearing prosthesis maintained in the coronal position from 4° varus to 4° valgus and the fixed-bearing prosthesis implanted in the neutral position (0°) are recommended. In revision total knee arthroplasty (RTKA), the stem implant design should maintain the best balance between preserving bone and reducing stress around the prosthesis after implantation. Compared with cemented stems, cementless press-fit femoral stems show higher fretting, for tibial plateau bone defects, porous metal blocks are more effective in stress dispersion. Finally, compared with traditional mechanical research methods, FEA methods can yield relatively accurate simulations, which could compensate for the deficiencies of traditional mechanics in knee joint research. Thus, FEA has great potential for applications in the field of medicine.

KEYWORDS

artificial knee replacement, artificial joint prosthesis, finite element analysis, bionics, biomechanics, kinematics, prosthesis design

Introduction

FEA is a computer simulation of the physical forces in real working conditions through models and study parameters. In Rybicki et al. (1972) and Brekelmans et al. (1972) applied FEA in orthopaedics for the first time, which greatly promoted the application of FEA technology in orthopaedics. In artificial knee arthroplasty, also known as knee joint surface replacement, artificial biomaterials are used to replace diseased cartilage and bone of the knee joint after worn and damaged components of the articular surface are removed (Price et al., 2018). This procedure is the most effective means for the treatment of end-stage knee osteoarthritis (Ferket et al., 2017; Price et al., 2018). However, biomechanical problems such as prosthesis loosening, periprosthetic fracture and prosthesis wear after knee arthroplasty remain to be solved (Wang et al., 2021). At present, FEA models can be observed at any angle, and operations on the model, such as determining the osteotomy thickness, analysing the stress of different prosthetic materials (Castellarin et al., 2023), and measuring the alignment between prostheses, can be simulated. FEA methods can overcome the shortcomings of traditional mechanical research methods, such as the long cycles, non-repeatable operations and high costs. This paper summarizes the application of FEA in TKA, UKA and RTKA in the context of the operation scheme, prosthesis design and material selection to provide a reference for biomechanical research on knee arthroplasty.

Application of FEA in TKA

The option of TKA provides an effective means of functional reconstruction in patients with severe physical knee dysfunction (Carr et al., 2012). Although the process of TKA is becoming increasingly mature, surgeons also remain troubled by postoperative prosthesis loosening, periprosthetic fracture, and prosthesis wear due to a poor knee mechanical environment. FEA can simulate the occurrence of these problems in a computer. Much research has been conducted, focus mainly on prosthesis material and component design and component alignment, among other factors (Innocenti et al., 2016; Park et al., 2021).

Application of FEA in prosthesis material and design

According to the mode of connection between the polyethylene insert and metal tibial component, TKA prostheses can be divided into fixed- and mobile-bearing prostheses based on whether the polyethylene insert and metal tibial component are locked. In fixed-bearing prostheses, the polyethylene insert is fixed to the tibial component through a locking mechanism; in mobile-bearing prostheses, a movable joint is formed with the femoral component, and a certain degree of movement between the polyethylene insert and the tibial component is allowed, comparing the two designs, it was found that the former insert allows for longitudinal rotation of the tibial or allows for anterior-posterior displacement between the insert and the tibial. Due to the rotation and displacement effect between the mobile insert and the tibial component, the tibial component can better fit the femoral component without sacrificing the natural rotation and displacement between the tibial and the femur, in fixed-bearing prostheses, the polyethylene insert locks on the tibial component, limiting the relative motion between the components (Ranawat et al., 2004). Depending on the degree of restriction on the knee joint, TKA prostheses can be divided into constrained condylar knee (CCK) prosthesis and the rotating hinge knee (RHK). CCK is designed to restrict knee motion through the postcam and femoral box and is considered a semirestricted prosthesis (Andreani et al., 2020; Athwal et al., 2021). RHK connects the femoral prosthesis to the tibial prosthesis via a rotating shaft, thereby achieving maximum restraint (Clement et al., 2023). The contact pressure and contact area of the tibiofemoral joint after TKA are related to the prosthesis design, with the contact stress being inversely proportional to the contact area. Greenwald and Heim (2005) compared the tibial-thigh contact area of fixed- and mobile-bearing prostheses by three-dimensional finite element gait analysis. The results showed that the contact area of the mobile-bearing prosthesis polyethylene insert was 400–800 mm^2, while that of the fixed-bearing prosthesis polyethylene insert was 200–250 mm^2. The findings confirmed that the contact area of the tibiofemoral joint of the mobile-bearing prosthesis was higher than that of the fixed-bearing prosthesis; thus, the contact stress of the mobile-bearing prosthesis was lower than that of the fixed-bearing prosthesis because the contact pressure was inversely proportional to the contact area Castellarin et al. (2023) (Table 1). Stukenborg-Colsman et al. (2002) performed an FEA study on cadavers and reached the same conclusion: compared with fixed-bearing prostheses, mobile-bearing prostheses maximized the contact area of the tibiofemoral joint and reduced the peak contact pressure, so that the mobile-bearing prosthesis polyethylene insert provides more movement for the prosthesis and minimizes polyethylene wear compared to the fixed-bearing prosthesis model (Heesterbeek et al., 2018; Andreani et al., 2020), resulting in improved implant survival and performance. For CCK and RHK prostheses, Samiezadeh et al. (2019) performed FEA on both and found that the CCK prosthesis should produce 16.9 MPa interprosthetic stress at the bone-prosthesis interface of 37.6 MPa, while the RHK bone-prosthesis interface stress was 13.7 MPa, a decrease of 18.9%, and the average stress of the CCK polyethylene insert was 9.6 MPa, while the RHK was 2.6 MPa, a decrease of 72.7%.

In summary, the low degree of matching achieved with a fixed-bearing prosthesis can reduce the stress at the interface between the knee joint bone and prosthesis and reduce loosening of the prosthesis, but at the cost of relatively high contact pressure with the knee joint and increased wear of the polyethylene insert. The contradiction between free rotation and low joint contact pressure is a problem that cannot be solved by fixed-bearing prostheses. The high degree of matching achieved with mobile-bearing prostheses can reduce the stress at the interface between the knee joint bone and the prosthesis and reduce the contact pressure, thus reducing the wear of the polyethylene insert; additionally, mobile-bearing prostheses can rotate freely, which can reduce loosening of the prosthesis and compensate for this disadvantage of fixed-plateau prostheses. At present, most FEA studies have shown that mobile-

TABLE 1 Application of FEA in TKA.

Refence	Experimental design	Conclusion
Greenwald and Heim (2005)	Fixed-bearing prosthesis vs. mobile-bearing prosthesis	The tibiofemoral joint contact area of mobile-bearing prostheses is higher than that of fixed-bearing prostheses. The contact stress of mobile-bearing prostheses is lower than that of fixed-bearing prostheses.
Stukenborg-Colsman et al. (2002)	Fixed-bearing prosthesis vs. mobile-bearing prosthesis	Compared with fixed-bearing prostheses, mobile-bearing prostheses maximize the tibiofemoral joint contact area and reduce the peak contact pressure. The greater the tibiofemoral joint contact stress, the more serious the wear of the polyethylene insert.
Brihault et al. (2016)	All-polyethylene tibial component vs. metal-backed tibial component	The stress distribution of all-polyethylene tibial components under the plateau is obviously higher than that of metal-backed tibial components.
Tokunaga et al. (2016)	All-polyethylene tibial component vs. metal-backed tibial component	The stress of metal tibial components is lower than that of all-polyethylene tibial components, and the stress distribution is more balanced.
Castellarin et al. (2019)	Asymmetric insert vs. symmetric insert	During standing and squatting movements, lower tibial contact stress was observed in those with asymmetric spacers than those with symmetric spacers.
Klasan et al. (2022)	Kinematic alignment vs. mechanical alignment	Lower contact pressure on the polyethylene insert was observed with kinematic alignment than mechanical alignment.
Song et al. (2021)	Kinematic alignment vs. mechanical alignment	Lower contact pressure on the polyethylene insert was observed with kinematic alignment group than mechanical alignment.

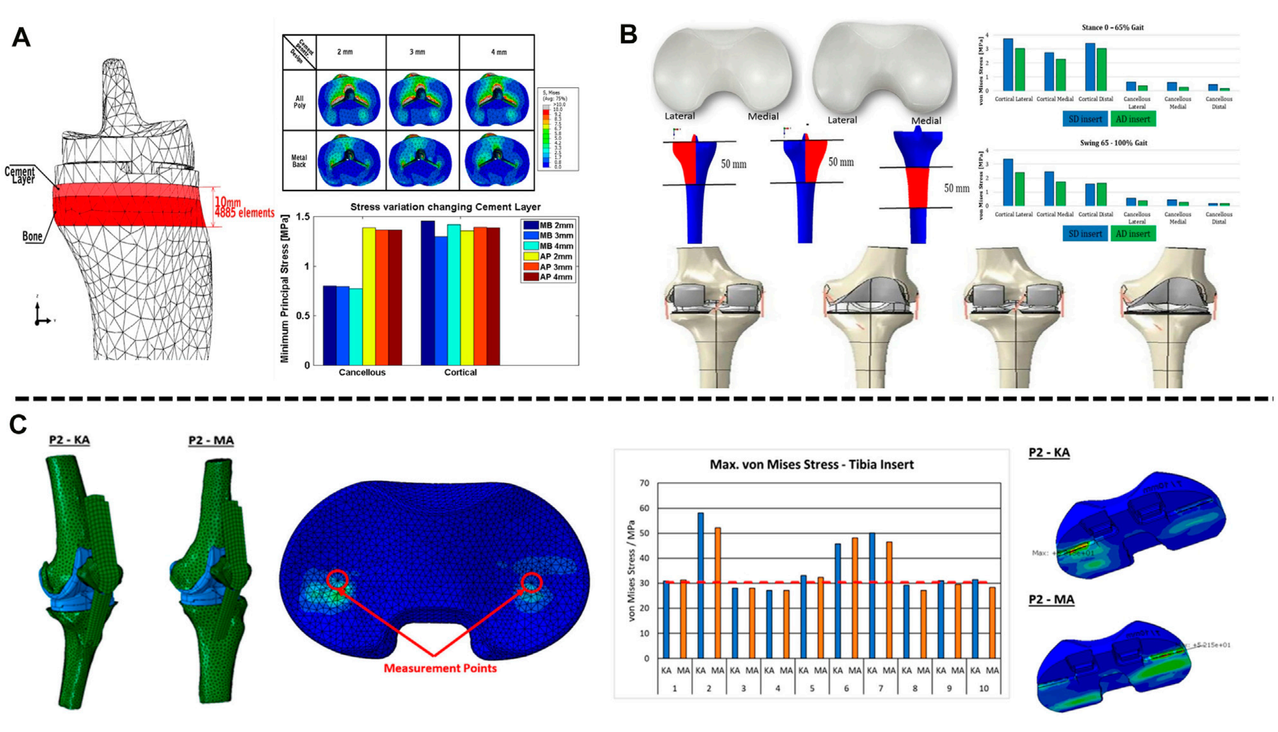

FIGURE 1
Application of FEA in TKA. **(A)** Contact stress behaviour of all-polyethylene and metal backed-tibial components at the proximal tibia. **(B)** Mechanical difference between symmetric and asymmetric inserts in the proximal tibial cortex. **(C)** Effects of mechanical alignment and kinematic alignment on the surface contact stress of inserts in TKA. **(A)** Reprinted with permission from ref. Brihault et al. (2016) (Copyright 2023; Springer Nature Switzerland AG.). **(B)** Reprinted with permission from ref. Castellarin et al. (2019) (Copyright 2023; Springer Nature Switzerland AG). **(C)** Reprinted with permission from ref. Klasan et al. (2022) (Copyright 2022; MDPI, Basel, Switzerland).

bearing prostheses can improve the degree of joint matching, reduce the contact surface stress of the tibiofemoral joint, and thus reduce polyethylene wear. However, the postoperative efficacy and prosthesis survival rate after the clinical application of the two types of prostheses have not been compared in this context, and further long-term follow-up studies are required (Hantouly et al., 2022). For CCK and RHK prostheses, the latter is better in terms of stress performance, and the 2-year clinical follow-up also confirms that the use of RHK provides good results compared to CCK (Hermans et al., 2019).

Artificial joint prostheses of different materials show different biomechanical characteristics in artificial joint replacement. Current tibial components consist of two main material options, all-polyethylene tibial components and metal-backed tibial components, which differ in material and component method, resulting in differences in prosthesis-bone and component-component stresses. It was found that while a significant increase in measured strain was observed for both the all-polyethylene and metal-backed tibial components in the simulated load distribution, the all-polyethylene tibial component showed a more pronounced stress rise at the proximal tibia (Small et al., 2010). Brihault et al. (2016) compared the stress distribution and fretting of tibial plateau prostheses made of different materials when the knee joint flexed 120°. The research results showed that the stress distribution of the all-polyethylene tibial component under the plateau was significantly higher than that of the metal-backed tibial component, with fretting five times higher than that of the metal-backed tibial component (Figure 1A). Tokunaga et al. (2016) established a standing finite element model to compare the stress distribution of the metal-backed tibial component and all-polyethylene tibial component. The results showed a significant increase in proximal tibial cortical stresses in the standing alignment after implantation of the all-polyethylene tibial component and a posterior shift in tibial loading with increased resection depth. For clinical outcomes, metal-backed tibial components and all-polyethylene tibial components did not show any significant differences in most of the outcome scores included, but statistically significant differences were found in complication and revision rates. A meta-analysis showed a revision rate of 1.85% in the metal-backed tibial component group compared with 2.02% in the all-polyethylene tibial component group (Longo et al., 2017). Surgeons tend to prefer metal-backed prostheses when selecting the appropriate tibial component for their patients. With advances in material science, all-polyethylene tibial components will have better mechanical properties and value for future applications given their cost and modular design advantages (Gioe and Maheshwari, 2010; AbuMoussa et al., 2019). The polyethylene insert between the femoral and tibial plateau plays a buffering role in knee joint movement, and polyethylene inserts of different design types have different biomechanical effects. The available polyethylene inserts included symmetrical and asymmetrical designs, and to compare the postoperative mechanical results of both, Castellarin et al. (2019) retrospectively analysed 303 patients treated with TKA by the FEA method. Under the condition of the same tibial and femoral components, symmetric and asymmetric polyethylene inserts were used in 151 and 152 patients, respectively. During standing and squatting, the contact stress in the tibial component was lower in those with asymmetric inserts (Figure 1B), at the 2-year follow-up, the asymmetric polyethylene insert group was able to perform certain routine movements better and without any pain, while patients in the symmetrically designed polyethylene group reported pain, validating the FEA results (Castellarin et al., 2021).

In addition to the material and design of the prosthesis, the type matching of the tibial component also affects the service life of the polyethylene insert after TKA. Completo et al., 2010 constructed a finite element model and paired a No. 3 femoral component with No. 2.5, 3, and 4 tibial components, and the corresponding polyethylene insert size (10 mm) was used to study the stress at each flexion angle. The results showed that the interface stress of the No. 3 femoral component paired with the No. 3 tibial component was significantly higher than that of the No. 4 tibial component. Such increased stress accelerates the wear of the polyethylene insert, which in turn affects the life of the prosthesis.

Application of FEA in component alignment

The success of TKA is closely related to the recovery of the lower extremity force line (Srivastava et al., 2012; Panni et al., 2018; Johnston et al., 2019). Poor alignment of the lower limbs and misalignment of the prosthesis can lead to abnormal wear of the polyethylene liner and premature loosening of the components, thus affecting the life of the components. The force line of the lower limb is formed by the connection of the centre of the femoral head to the centre of the tibial at the ankle joint. Normally, the axis passes through the centre of the knee joint, which is called the mechanical axis of the neutral position. In a normal knee joint, the tibia is 3° varus and the femur is 9° valgus relative to the force line of the lower extremity, respectively, with respect to the force line, and the midpoint of the tibial intercondylar ridge may shift inwards or outwards with respect to the lower extremity force line during disease (Yilmaz et al., 2016). Current finite element studies on component alignment have focused on component angulation and alignment theory. For tibial component alignment angles, scholars used a fixed-bearing TKA model in computer simulations to investigate tibial stress distribution and component micromovement when tibial components were placed in translation and rotation and found that tibial stress and ligament tension increased when laterally offset, and tibial stress and component micromovement were greatest when reaching 6 mm and that stress and micromovement were acceptable when controlling errors to within 2 mm acceptable (Mizu-Uchi et al., 2022). Mell et al. (2022) predicted by the model that tibial component rotation at 15° alignment can cause severe wear up to 5 mm^3/million cycles, almost twice as much as neutral alignment. For femoral components, scholars modelled femoral components in −3°, 0°, 3°, 5° and 7° flexion to study patellar contact stress and ligament tension and found that patellar contact stress and ligament tension decreased and knee flexion range increased with 3° flexion alignment (Koh et al., 2022). At present, there are two alignment methods in TKA: including early mechanical alignment (MA) and later kinematic alignment (KA). The traditional view is that the lower limb force line of patients after TKA should be reconstructed to a position where the deviation from the neutral position force line is less than 3°; however, KA holds that osteotomy and prosthesis placement should be based on the motion axis of the patient's knee joint in the normal or prelesion state. MA aims to restore the mechanical axis of the leg (Insall et al., 1985), whereas KA aligns the rotational axis of the component with the three kinematic axes of the knee joint by aligning the component to the natural joint line

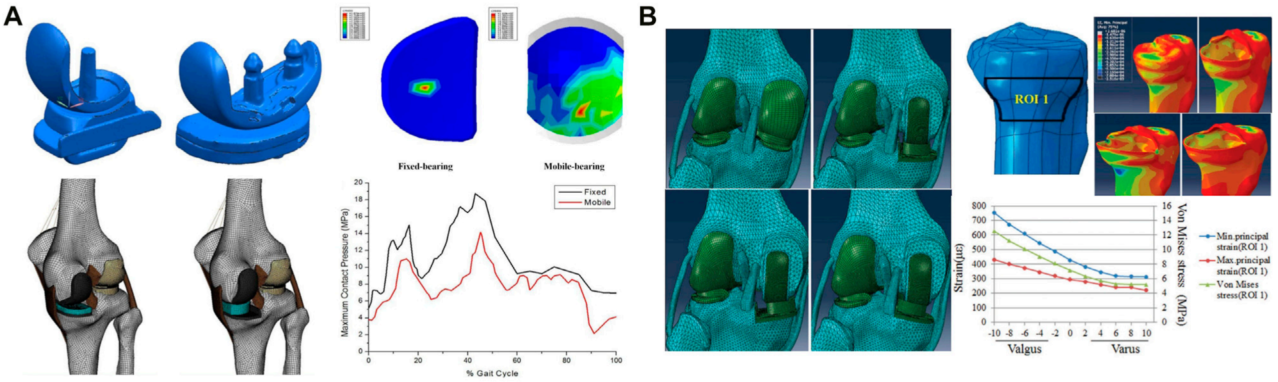

FIGURE 2
Application of FEA in UKA. **(A)** Comparison of the effect of fixed- and mobile-bearing UKA prostheses on the surface stress of the insert. **(B)** Stress analysis of the proximal tibial cortex under the condition of varus and valgus UKA tibial components. **(A)** Reprinted with permission from ref. Kwon et al. (2014) (Copyright 1999-2023; John Wiley & Sons, Inc.). **(B)** Reprinted with permission from ref. Zhu et al. (2015) (Copyright 2023; The Chinese Medical Association).

TABLE 2 Application of FEA in UKA.

Refence	Experimental design	Conclusion
Zhu et al. (2015)	Mobile-bearing prosthesis	The recommended angle of coronal alignment of the tibial component is between 4° varus and 4° valgus.
Ma et al. (2022)	Fixed-bearing prosthesis	The coronal arrangement of the femoral component should be neutral (0°).
Innocenti et al. (2016)	Fixed-bearing prosthesis	The coronal arrangement of the tibial component should be neutral (0°).
Kwon et al. (2014)	Fixed-bearing prosthesis vs. mobile-bearing prosthesis	The contact pressure of the polyethylene liner is lower on mobile-bearing prostheses than on fixed-bearing prostheses.
Koh et al. (2019)	Fixed-bearing prosthesis vs. mobile-bearing prosthesis	The contact pressure of the polyethylene liner is lower on mobile-bearing prostheses than fixed-bearing prostheses.
Sano et al. (2020)	All-polyethylene tibial component vs. metal-backed tibial component	The stress of metal tibial components is lower than that of all-polyethylene tibial components, and the stress distribution is more balanced.

(Howell et al., 2010). The two alignment methods have variability in different correction situations. Thus, the artificial knee joint can simulate the normal biomechanical state of the human knee joint as much as possible after the operation. Kang et al. (2020) studied ligament-preserving prostheses and found that KA had better mobility and even stress distribution than MA. Klasan et al. (2022) established a finite element model for 10 patients with knee osteoarthritis to simulate TKA with mechanical alignment and kinematic alignment. The results showed a larger contact area and lower contact pressure on the polyethylene insert in TKA patients treated with kinematic alignment than in those treated with mechanical alignment (Figure 1C), but there was no significant difference in von Mises stress between the polyethylene insert and the tibia. Therefore, the pressure distribution on the contact surface of the artificial joint was more uniform, and the stress was lower, reducing the wear of the joint contact surface and prolonging the life of the prosthesis. In addition, Song et al. (2023) found that when the knee joint was valgus, the contact stress on the polyethylene insert was higher with KA than with MA. Generally, the best method for alignment in TKA remains controversial. Before the emergence of KA, MA was the “gold standard” in TKA. KA can maximize the biomechanics of the knee joint, thus achieving better surgical results and functional recovery. However, when simulating patients with valgus deformity and severe flexion deformity, the contact stresses on the polyethylene surface of the KA prosthesis increased compared to MA, probably because valgus requires excessive soft tissue release for balancing and soft tissue release is not available in the flexion deformity model (Nakamura et al., 2017; Klasan et al., 2022), and further experiments and studies are needed.

Application of FEA for alignment in UKA

Compared with TKA, UKA is a new type of minimally invasive surgery. In UKA, only the injured surface is replaced, such as damaged cartilage in the medial or lateral compartment of the knee joint (Price and Svard, 2011; Hansen et al., 2019). This technique does not require removal of the anterior and posterior cruciate ligament and retains the proprioceptive sensation and function of the knee joint (Cameron and Jung, 1988; Vince and

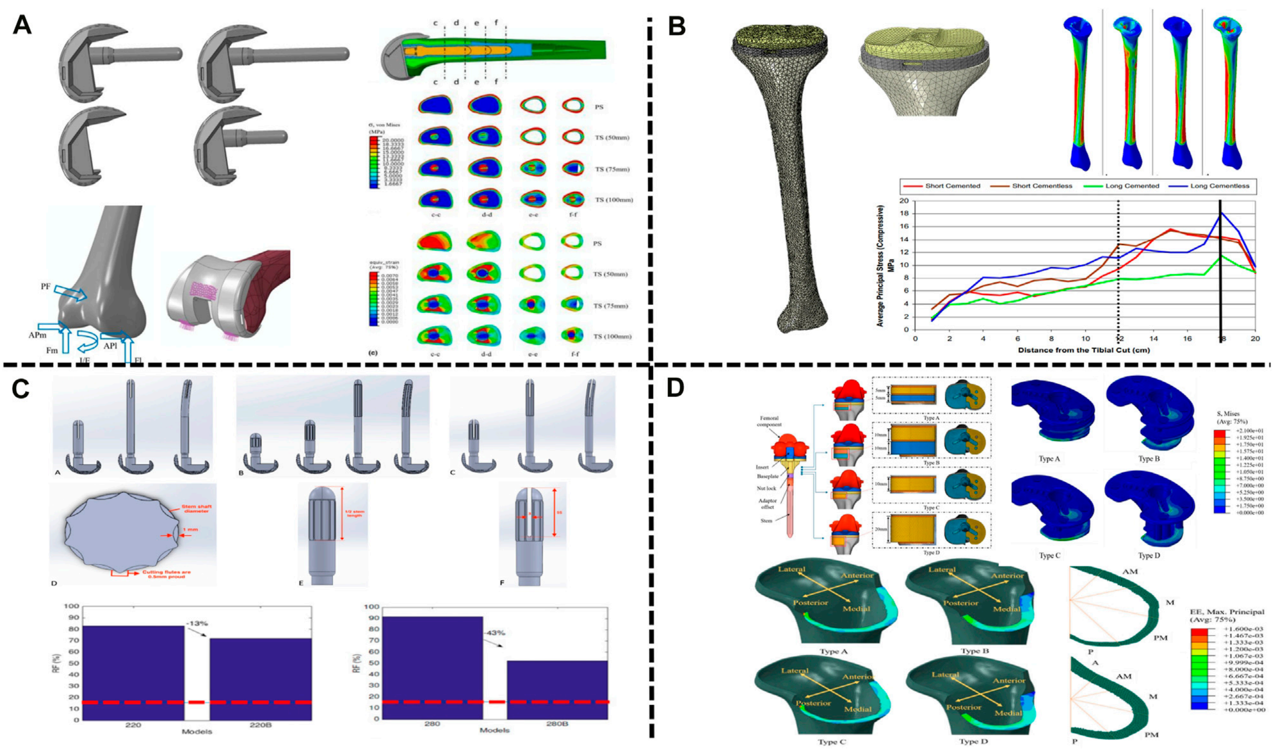

FIGURE 3
Application of FEA in RTKA. **(A)** Contact stress of different types of femoral implants. **(B)** Cortical bone stress of cemented and cementless press-fit tibial components. **(C)** Comparison between straight and bowed stem implants. **(D)** RTKA bone defect metal augmentation block design. **(A)** Reprinted with permission from ref. Conlisk et al. (2018) (Copyright 2023; Springer Nature Switzerland AG). **(B)** Reprinted with permission from ref. El-Zayat et al. (2016) (Copyright 2023; Springer Nature Switzerland AG). **(C)** Reprinted with permission from ref. Innocenti et al. (2022) (Copyright 2022; MDPI, Basel, Switzerland). **(D)** Reprinted with permission from ref. Kang et al. (2019) (Copyright 2022; MDPI, Basel, Switzerland).

TABLE 3 Application of FEA in RTKA.

Refence	Experimental design	Conclusion
Conlisk et al. (2018)	Comparison of the effects of short-, medium-, and long-stem implants	The femoral stress was decreased by 11%, 26%, and 29% with short-, medium-, and long-stem implants, respectively. A medium-length (75 mm) femoral stem implant can keep the best balance between retaining bone and reducing stress around the prosthesis after implantation.
El-Zayat et al. (2016)	Press-fit stem implant vs. cemented stem implant	Compared with cemented prostheses, during the gait cycle and during squatting, press-fit stem implants resulted in a larger stress distribution and more easily led to fretting.
Innocenti et al. (2022)	Straight stem implant vs. bowed stem implant	The overall stress distribution of bowed stem implants is lower than that of straight stem implants.
Innocenti et al. (2018)	Bone cement vs. porous metal vs. solid metal	The stress produced by porous metal and bone cement is significantly lower than that produced by solid metal (e.g., Ti and CoCr). In addition, the characteristic of porous metal allowing bone ingrowth further reduces the occurrence of loosening.
Kang et al. (2019)	Single-metal block augmentation vs. double metal block augmentation	Bimetal augmentation blocks can obviously reduce the stress distribution compared with single-metal augmentation blocks.

Cyran, 2004). This strategy has the advantages of causing less injury and allowing quick recovery (Scott and Santore, 1981; Berend et al., 2005). However, UKA is a technically demanding surgical method, and attention must be paid to the size of the components, the osteotomy and postoperative alignment because overcorrection or overloosening may lead to adverse results, these include primarily bearing dislocations (in mobile-bearing designs), aseptic mechanical loosening, polyethylene wear (in fixed-bearing designs), progression of osteoarthritis in unreplaced compartments, periprosthetic fractures and unexplained pain (Shee et al., 1990; Kim et al., 2016). Resulting in a typical 10-year survival rate of 80% to 85% for the prosthesis (Crawford et al., 2020), and ways to reduce these adverse events to improve prosthesis longevity need to be continuously explored.

Similar to the TKA prosthesis design, the UKA prosthesis has both fixed- and mobile-bearing prostheses, with the mobile-bearing prosthesis allowing the femoral condyle to roll on the polyethylene surface and allowing the polyethylene insert to slide freely on the surface of the tibial component; the fixed-bearing prosthesis locks the polyethylene insert to the tibial component, more closely resembling the movement of the femoral condyle on the meniscal surface (Weale et al., 2000; Hernigou and Deschamps, 2004). For medial compartment osteoarthritis, both prostheses have good clinical results (Neufeld et al., 2018). Mobile-bearing prostheses use the spherical articular surface to limit the range of motion of the femur relative to the articular surface while using a curved surface with the same curvature to maximize the contact surface (Figure 2A) and reduce the pressure on the lateral meniscus by 1/3 (Kwon et al., 2014). In contrast, the design concept of fixed-bearing prostheses is the opposite. Fixed-bearing prostheses more closely imitate the motion mode of the normal knee joint by setting the active area between the femoral component and the polyethylene insert. Kwon et al. (2014) used a finite element model to simulate the complete gait and compare the contact pressure and stress of fixed-bearing and mobile-bearing prostheses. While the results showed that the contact pressure on the polyethylene insert was lower for mobile-bearing prostheses than fixed-bearing prostheses, UKA with fixed-bearing prostheses will increase the overall risk of progressive knee osteoarthritis due to the high pressure in the contralateral chamber. Danese et al. (2019) and Sano et al. (2020) relied on FEA to investigate the stress distribution in the material and shape of the prosthesis. It was found that fixed-bearing prostheses may lead to excessive wear of polyethylene inserts due to local stress concentrations and that mobile-bearing prostheses are closer to the normal knee joint (Koh et al., 2019; Koh et al., 2020), a finding confirmed by studies by Pena et al. (2006) and Li et al. (2006). Zhu et al. (2015) studied the coronal arrangement of the tibial component on mobile-bearing prostheses. The von Mises stress and compressive strain of the proximal part of the medial tibial cortex increased significantly when the tibial component was more than 4° valgus, and the compressive strain at the keel notch of the tibial prosthesis was higher than the maximum threshold when the tibial component was more than 4° varus (Figure 2B). Therefore, Dai et al. (2018) verified the effect of bone stress, ligament tension and polyethylene liner stress distribution in the tibial component from neutral to 6° varus by using a finite element model of mobile-bearing prosthesis and found that neutral alignment to 3° varus exhibited lower stresses, which supported the above findings, the recommended angle of the tibial component of mobile-bearing prostheses on the coronal plane is between 4° varus and 4° valgus. Innocenti et al. (2016) studied the coronal plane of fixed-bearing prostheses and established a model in which the femoral and tibial components had different varus and valgus angles while the posterior inclination of the tibial component was 6°. The results showed that during the gait cycle, the stress caused by tibial component varus and valgus on the polyethylene insert was greater than that in the neutral position, Sekiguchi et al. (2019) simulated knee kinematics and cruciate ligament tension in weight-bearing knee flexion and gait motion and found that the preferred tibial component alignment was neutral in the coronal plane and that varus or valgus alignment resulted in the onset of instability. Kang et al. (2018b) observed that as the fixed-bearing UKA femoral component was progressively valgus from a neutral alignment, the contact pressure on the polyethylene insert increased, and the contact stress on the lateral compartment also increased. Therefore, it is recommended that the femoral component be placed in neutral alignment. Ma et al. (2022) simulated the stress changes on the polyethylene insert and the cartilage surface of the lateral compartment for femoral components with 3°, 6° and 9° of valgus and found that the stresses on the polyethylene surface increased significantly when the femoral prosthesis was valgus, the stresses on the lateral cartilage surface and the medial collateral ligament increased significantly at >6° (Kang et al., 2018a), and the stresses on the lateral intertrochanteric cartilage surface decreased during the transition from valgus to neutral alignment, thus confirming the above findings. Park et al. (2019) modelled a fixed-bearing UKA femoral component in the range from 10° of flexion to 10° of extension and found that the lateral intertrochanteric contact stresses increased in flexion, suggesting that the femoral component be placed in the sagittal neutral alignment. Thus, in terms of the coronal arrangement of the tibial component of fixed-bearing prostheses, the neutral position (0°) is recommended.

In summary, FEA results show that good shape matching can be achieved with the femoral and tibial components of mobile-bearing prostheses, which can reduce the wear of the components, while fixed-bearing prostheses should be avoid in UKA to prevent the local stress concentration and subsequently accelerated insert wear caused by excessive fitting. Additionally, the FEA shows that for optimal clinical and biomechanical results, fixed-bearing prostheses should be placed with the tibial component in a neutral (0°) alignment and the femoral component in a neutral alignment while maintaining a reduced sagittal plane flexion angle. For mobile-bearing prostheses, 4° varus to 4° valgus alignment is recommended by scholars.

Materials included metal-backed and all-polyethylene tibial components. Walker et al. (2011) found a stress concentration at the proximal tibia due to the all-polyethylene component by comparing all-polyethylene and metal-backed tibial components. In contrast, the metal-backed tibial component showed a 6-fold reduction in stress. Sano et al. (2020) compared the stresses in the proximal tibia with the metal-backed UKA prosthesis by FEA, and with consistent bone density and alignment, the metal-backed implant had a stress distribution that was more uniform than that of polyethylene, reducing the stress concentration in the proximal tibial cortex. Koh et al. (2019) compared the polyethylene surface contact stresses of the two prostheses and found that the metal-backed component reduced the contact stresses and had lower wear (Table 2).

Application of FEA in RTKA

RTKA is expected to increase with the increase in primary knee arthroplasty for the active patient population (Lombardi et al., 2019). RTKA is associated with high operative difficulty, great trauma to patients, long recovery periods and complex clinical management in the perioperative period, is a challenging procedure with often unsatisfactory outcomes compared to primary knee arthroplasty (Bae et al., 2013). Due to the rapid increase in the number of patients treated with primary knee arthroplasty annually, RTKA has gradually become the focus of future research in the field of joint surgery (Mason and Fehring, 2006). The causes of surgical failure have been studied by FEA, and the design of procedures and prostheses used in RTKA have been further optimized from a biomechanical point of view. Understanding the effects of materials and prosthesis design from a biomechanical perspective is the current focus of FEA.

Application of FEA in stem implant design

Adequate fixation is the basis of RTKA, and modular implants with stems can reduce stress concentrations and improve the outcome. However, there are no biomechanical-based guidelines to determine the appropriate stem length, according to the fixation mode, prostheses can be divided into cemented and cementless prostheses (cementless press-fit prostheses). The femoral condylar surface of most prostheses is fixed with bone cement, and the stem implant can be fixed with bone cement or compression without cement. Cementless prostheses can be more easily revised, but cemented prostheses should be used in patients with obvious osteoporosis or metaphyseal deformity. Conlisk et al. (2018) analysed cemented prostheses with the finite element method. They constructed four kinds of femoral components with different lengths, namely, a femoral component without a stem implant and with a short-stem implant (50 mm), a medium-stem implant (75 mm) and a long-stem implant (100 mm) (Figure 3A). Bori et al. (2022) considered that a medium-length stem (75 mm) is the best choice between bone preservation and stress reduction, especially in osteoporotic patients, and can help reduce the risk of periprosthetic fractures. Each stem implant was implanted into the femur, and the stress and strain around the femur were analysed during the gait cycle (Wang et al., 2021). The use of components with stem implants could reduce the stress around the prosthesis, and the stress on the femur could be reduced by 11%, 26%, and 29% with the use of the short-, medium- and long-stem implants, especially in osteoporotic patients, and can help reduce the risk of periprosthetic fracturesth (Bori et al., 2022). However, in the combined case of preserving bone and balancing stresses, medium-stem implants (75 mm) are considered to maintain the best balance between preserving bone during surgery and reducing stress around the prosthesis after implantation, especially in osteoporotic patients, and can help reduce the risk of periprosthetic fracturesth (Bori et al., 2022) (Table 3).

El-Zayat et al. (2016) compared the stress distribution on the femur between cemented and cementless stem implants by FEA. Compared with the cemented component, found that the presence of cement reduced peri-stem bone stress during the gait cycle, while the cementless stem showed higher micromotion, which may explain pain at the tip of the intramedullary stem implant reported after RTKA (Figure 3B). Innocenti et al. (2022) further analysed the influence of the shape of the stem implant on the stress distribution with the use of different fixation methods on the basis of the study by El-Zayat et al. (2016). It was found that due to the existence of the anterior femoral arch, the overall stress distribution of the bowed stem implant was lower than that of the straight stem implant; intramedullary stems with a slotted tip also resulted in lower stress than solid stems in the medullary cavity (Figure 3C). These findings are consistent with those reported by Barrack et al. (2004). In RTKA, the presence of bone cement reduces the stress along each area of the prosthesis. In summary, the length of the stem implant should maintain the best balance between preserving the bone and reducing the stress around the prosthesis after implantation, and compared with cemented stem implants, press-fit stem implants show more fretting. In addition, bowed stem implants more closely mimic the anatomical structure, and the use of stems with a slotted tip can help reduce the stress distribution at the distal end and reduce the occurrence of tip pain after the operation. These findings will help orthopaedic surgeons select the most suitable prosthesis for use in RTKA.

Application of FEA in augmentation block material selection

Augmentation blocks are one of the options for the reconstruction of nonenclosed bone defects, and the technique is based on the size of the defect, the patient's age and life expectancy (Qiu et al., 2012), but the mechanical performance varies between materials. Innocenti et al. (2018) and Liu et al. (2021) used a finite element model to analyse the biomechanics of augmentation blocks of different materials (bone cement, porous metal and solid metal). The results showed that augmentation blocks of any material can cause a change in stress, especially in the area near the bone defect, in which the stress produced by porous metal and bone cement is significantly lower than that produced by solid metal (e.g., Ti and CoCr). In addition, porous metal allows bone ingrowth, which further reduces the occurrence of loosening. Kang et al. (2019) further found that in large-area (10–20 mm) bone defects, compared with a single-metal augmentation block, found that the peak stress of a single-metal augmentation block was on average 1.4 times higher than that of bimetal augmentation blocks. In addition, customized metal augmentation blocks can achieve complete contact with cortical bone, thereby allowing better stress transfer and reducing the risk of bone resorption caused by stress shielding and cement failure (Figure 3D). At present, the main methods for the treatment of bone defects in RTKA include bone cement, bone cement with screw reinforcement, metal augmentation blocks, pressed bone transplantation and structural allografting (Huten et al., 2021), depending on the location and size of the defect (Mancuso et al., 2017). Comparing the cement-screw technique and metal augmentation block, Zheng et al. (2020) determined the role of screws in repair by building a finite element model of tibial bone defects and found that, compared with bone cement alone, the use of cement screws decreased stresses on the cancellous bone and cement boundary by 10%, while vertical screws provided better stability than oblique screws. Zhao et al. (2022) found that vertical screws had better stability than screws parallel to the proximal tibial cortical bone for either one or two screws, supporting the above findings. Ma et al. (2023) found that longer screws may not achieve better stability with consistent defect conditions, but thicker screws reduced stresses in the area of the bone defect and achieved better stability. Liu et al. (2020) modelled 5 mm and 10 mm bone defects and found that for 5 mm defects, both methods provided good stability for the implants. However, for the 10 mm defect, the maximum micromovement of the augmentation block (128 μm) was less than that of the cement-screw technique (155 μm). Because metal augmentation blocks are easy to use and transfer stress well, they are increasingly used in the treatment of bone defects. In addition, basis of porous metal augmentation blocks, scholars suggest that the biomechanical properties of bone can be improved by tailoring the shape to reduce bone resorption (Liu et al., 2021), customized metal augmentation blocks can be used to optimize the treatment of bone defects (Bao et al., 2013) (Table 3).

Conclusion and outlook

We have compared different surgical approaches, prosthesis types, prosthesis materials and component alignments by summarizing the current applications of finite element techniques in the field of TKA, UKA and RTKA to provide a mechanical theoretical and research reference for clinical purposes. By reviewing the above studies, it was found that the contact surface stress of the tibiofemoral joint is lower with mobile-bearing prostheses than fixed-bearing prostheses in TKA and thus reduces polyethylene insert wear. Compared with mechanical alignment, TKA with kinematic alignment reduces the maximum stress and strain of the femoral component and polyethylene insert and thus reduces the wear of the joint contact surface and prolongs the life of the prosthesis. However, the gap in the practical application of the two is relatively small in current clinical research, and further study is needed. Asymmetric metal-backed tibial components are less stressful between components and to the underside of the tibial plateau than symmetric all polyethylene tibial components. In addition, mismatching of the prosthesis type leads to an increase in stress, accelerates the wear of the polyethylene insert and affects the service life of the prosthesis. In UKA, while the femoral and tibial components of mobile-bearing prostheses are more formable, which can reduce the wear of the prosthesis insert, fixed-bearing prostheses should be avoided to prevent the local stress concentration and subsequently accelerated wear caused by excessive formation. From an FEA perspective, it is recommended that the tibial component of the mobile-bearing prostheses is arranged from 4° varus to 4° valgus on the coronal plane, while that of fixed-bearing prostheses should maintain a neutral position (0°). In RTKA, the length of the stem should maintain the best balance between preserving bone and reducing stress around the prosthesis after implantation, a 95 mm to 100 mm stem implant can help with better fixation, but a medium stem (75 mm) is more appropriate to preserve as much bone as possible. Compared with the cemented stem implants, press-fit stem implants show more fretting. In addition, bowed stem implants are more similar in shape to the anatomical structure, and stems with slotted tips in the medullary cavity are beneficial for reducing the stress distribution at the distal end, thus reducing the occurrence of tip pain after surgery. For periprosthetic bone defect repair, should take into account the location and size of the defect, and using the cement-screw technique is more suitable for smaller defects. If the defect is larger, double porous metal augmentation blocks are more appropriate.

In the future, FEA can be used to carry out relatively accurate calculations and simulations in knee arthroplasty; FEA has been further studied from the perspectives of prosthesis material and design, knee joint alignment and operation scheme, provide an important reference for the accurate diagnosis and treatment of knee diseases, the design of artificial knee prosthesis and the study of knee biomechanics.

Author contributions

Z-HZ wrote the manuscript. Y-SQ and B-GW participated in critical revision of the manuscript for intellectual content and sorted out and screened the relevant literatures. H-R-CB and Y-SX designed the outline and revised the paper. All authors have read and approved the final version of this manuscript.

Funding

This study was supported by the National Natural Science Foundation of China (grant numbers: 82172444, 81960399), the Science and Technology Program of Inner Mongolia (grant numbers: 2021GG0127, 2022YFSH0053), and the Medical and Health Science and Technology Program of Health Commission of Inner Mongolia (grant number: 202201050).

Acknowledgments

We thank American Journal Experts for their language editing, which greatly improved the manuscript.

Conflict of interest

The authors declare that the research was conducted in the absence of any commercial or financial relationships that could be construed as a potential conflict of interest.

Publisher's note

References

AbuMoussa, S., White, C. C. T., Eichinger, J. K., and Friedman, R. J. (2019). All-Polyethylene versus metal-backed tibial components in total knee arthroplasty. *J. Knee Surg.* 32 (8), 714–718. doi:10.1055/s-0039-1683979

Andreani, L., Pianigiani, S., Bori, E., Lisanti, M., and Innocenti, B. (2020). Analysis of biomechanical differences between condylar constrained knee and rotating hinged implants: A numerical study. *J. Arthroplasty* 35 (1), 278–284. doi:10.1016/j.arth.2019.08.005

Athwal, K. K., Willinger, L., Manning, W., Deehan, D., and Amis, A. A. (2021). A constrained-condylar fixed-bearing total knee arthroplasty is stabilised by the medial soft tissues. *Knee Surg. Sports Traumatol. Arthrosc.* 29 (2), 659–667. doi:10.1007/s00167-020-05995-6

Bae, D. K., Song, S. J., Heo, D. B., Lee, S. H., and Song, W. J. (2013). Long-term survival rate of implants and modes of failure after revision total knee arthroplasty by a single surgeon. *J. Arthroplasty* 28 (7), 1130–1134. doi:10.1016/j.arth.2012.08.021

Bao, H. R., Zhu, D., Gu, G., and Gong, H. (2013). The effect of complete radial lateral meniscus posterior root tear on the knee contact mechanics: A finite element analysis. *J. Orthop. Sci.* 18 (2), 256–263. doi:10.1007/s00776-012-0334-5

Barrack, R. L., Stanley, T., Burt, M., and Hopkins, S. (2004). The effect of stem design on end-of-stem pain in revision total knee arthroplasty. *J. Arthroplasty* 19 (7), 119–124. doi:10.1016/j.arth.2004.06.009

Berend, K. R., Lombardi, A. V., Jr., Mallory, T. H., Adams, J. B., and Groseth, K. L. (2005). Early failure of minimally invasive unicompartmental knee arthroplasty is associated with obesity. *Clin. Orthop. Relat. Res.* 440, 60–66. doi:10.1097/01.blo.0000187062.65691.e3

Bori, E., Armaroli, F., and Innocenti, B. (2022). Biomechanical analysis of femoral stems in hinged total knee arthroplasty in physiological and osteoporotic bone. *Comput. Methods Programs Biomed.* 213, 106499. doi:10.1016/j.cmpb.2021.106499

Brekelmans, W. A., Poort, H. W., and Slooff, T. J. (1972). A new method to analyse the mechanical behaviour of skeletal parts. *Acta Orthop. Scand.* 43 (5), 301–317. doi:10.3109/17453677208998949

Brihault, J., Navacchia, A., Pianigiani, S., Labey, L., De Corte, R., Pascale, V., et al. (2016). All-polyethylene tibial components generate higher stress and micromotions than metal-backed tibial components in total knee arthroplasty. *Knee Surg. Sports Traumatol. Arthrosc.* 24 (8), 2550–2559. doi:10.1007/s00167-015-3630-8

Cameron, H. U., and Jung, Y. B. (1988). A comparison of unicompartmental knee replacement with total knee replacement. *Orthop. Rev.* 17 (10), 983–988.

Carr, A. J., Robertsson, O., Graves, S., Price, A. J., Arden, N. K., Judge, A., et al. (2012). Knee replacement. *Lancet* 379 (9823), 1331–1340. doi:10.1016/S0140-6736(11)60752-6

Castellarin, G., Pianigiani, S., and Innocenti, B. (2019). Asymmetric polyethylene inserts promote favorable kinematics and better clinical outcome compared to symmetric inserts in a mobile bearing total knee arthroplasty. *Knee Surg. Sports Traumatol. Arthrosc.* 27 (4), 1096–1105. doi:10.1007/s00167-018-5207-9

Castellarin, G., Bori, E., and Innocenti, B. (2021). Experimental and clinical analysis of the use of asymmetric vs symmetric polyethylene inserts in a mobile bearing total knee arthroplasty. *J. Orthop.* 23, 25–30. doi:10.1016/j.jor.2020.12.031

Castellarin, G., Bori, E., Rapallo, L., Pianigiani, S., and Innocenti, B. (2023). Biomechanical analysis of different levels of constraint in TKA during daily activities. *Arthroplasty* 5 (1), 3. doi:10.1186/s42836-022-00157-0

Clement, N. D., Avery, P., Mason, J., Baker, P. N., and Deehan, D. J. (2023). First-time revision knee arthroplasty using a hinged prosthesis: Temporal trends, indications, and risk factors associated with re-revision using data from the national joint registry for 3,855 patients. *Bone Jt. J.* 105-B (1), 47–55. doi:10.1302/0301-620X.105B1.BJJ-2022-0522.R1

Completo, A., Rego, A., Fonseca, F., Ramos, A., Relvas, C., and Simoes, J. (2010). Biomechanical evaluation of proximal tibia behaviour with the use of femoral stems in revision TKA: An *in vitro* and finite element analysis. *Clin. Biomech. (Bristol, Avon)* 25 (2), 159–165. doi:10.1016/j.clinbiomech.2009.10.011

Conlisk, N., Howie, C. R., and Pankaj, P. (2018). Optimum stem length for mitigation of periprosthetic fracture risk following primary total knee arthroplasty: A finite element study. *Knee Surg. Sports Traumatol. Arthrosc.* 26 (5), 1420–1428. doi:10.1007/s00167-016-4367-8

Crawford, D. A., Berend, K. R., and Thienpont, E. (2020). Unicompartmental knee arthroplasty: US and global perspectives. *Orthop. Clin. North Am.* 51 (2), 147–159. doi:10.1016/j.ocl.2019.11.010

Dai, X., Fang, J., Jiang, L., Xiong, Y., Zhang, M., and Zhu, S. (2018). How does the inclination of the tibial component matter? A three-dimensional finite element analysis of medial mobile-bearing unicompartmental arthroplasty. *Knee* 25 (3), 434–444. doi:10.1016/j.knee.2018.02.004

Danese, I., Pankaj, P., and Scott, C. E. H. (2019). The effect of malalignment on proximal tibial strain in fixed-bearing unicompartmental knee arthroplasty: A comparison between metal-backed and all-polyethylene components using a validated finite element model. *Bone Jt. Res.* 8 (2), 55–64. doi:10.1302/2046-3758.82.BJR-2018-0186.R2

El-Zayat, B. F., Heyse, T. J., Fanciullacci, N., Labey, L., Fuchs-Winkelmann, S., and Innocenti, B. (2016). Fixation techniques and stem dimensions in hinged total knee arthroplasty: A finite element study. *Arch. Orthop. Trauma Surg.* 136 (12), 1741–1752. doi:10.1007/s00402-016-2571-0

Ferket, B. S., Feldman, Z., Zhou, J., Oei, E. H., Bierma-Zeinstra, S. M., and Mazumdar, M. (2017). Impact of total knee replacement practice: Cost effectiveness analysis of data from the osteoarthritis initiative. *BMJ* 356, j1131. doi:10.1136/bmj.j1131

Gioe, T. J., and Maheshwari, A. V. (2010). The all-polyethylene tibial component in primary total knee arthroplasty. *J. Bone Jt. Surg. Am.* 92 (2), 478–487. doi:10.2106/JBJS.I.00842

Greenwald, A. S., and Heim, C. S. (2005). Mobile-bearing knee systems: Ultra-high molecular weight polyethylene wear and design issues. *Instr. Course Lect.* 54, 195–205.

Hansen, E. N., Ong, K. L., Lau, E., Kurtz, S. M., and Lonner, J. H. (2019). Unicondylar knee arthroplasty has fewer complications but higher revision rates than total knee arthroplasty in a study of large United States databases. *J. Arthroplasty* 34 (8), 1617–1625. doi:10.1016/j.arth.2019.04.004

Hantouly, A. T., Ahmed, A. F., Alzobi, O., Toubasi, A., Salameh, M., Elmhiregh, A., et al. (2022). Mobile-bearing versus fixed-bearing total knee arthroplasty: A meta-analysis of randomized controlled trials. *Eur. J. Orthop. Surg. Traumatol.* 32 (3), 481–495. doi:10.1007/s00590-021-02999-x

Heesterbeek, P. J. C., van Houten, A. H., Klenk, J. S., Eijer, H., Christen, B., Wymenga, A. B., et al. (2018). Superior long-term survival for fixed bearing compared with mobile bearing in ligament-balanced total knee arthroplasty. *Knee Surg. Sports Traumatol. Arthrosc.* 26 (5), 1524–1531. doi:10.1007/s00167-017-4542-6

Hermans, K., Vandenneucker, H., Truijen, J., Oosterbosch, J., and Bellemans, J. (2019). Hinged versus CCK revision arthroplasty for the stiff total knee. *Knee* 26 (1), 222–227. doi:10.1016/j.knee.2018.10.012

Hernigou, P., and Deschamps, G. (2004). Alignment influences wear in the knee after medial unicompartmental arthroplasty. *Clin. Orthop. Relat. Res.* 423, 161–165. doi:10.1097/01.blo.0000128285.90459.12

Howell, S. M., Howell, S. J., and Hull, M. L. (2010). Assessment of the radii of the medial and lateral femoral condyles in varus and valgus knees with osteoarthritis. *J. Bone Jt. Surg. Am.* 92 (1), 98–104. doi:10.2106/JBJS.H.01566

Huten, D., Pasquier, G., and Lambotte, J. C. (2021). Techniques for filling tibiofemoral bone defects during revision total knee arthroplasty. *Orthop. Traumatol. Surg. Res.* 107 (1S), 102776. doi:10.1016/j.otsr.2020.102776

Innocenti, B., Pianigiani, S., Ramundo, G., and Thienpont, E. (2016). Biomechanical effects of different varus and valgus alignments in medial unicompartmental knee arthroplasty. *J. Arthroplasty* 31 (12), 2685–2691. doi:10.1016/j.arth.2016.07.006

Innocenti, B., Fekete, G., and Pianigiani, S. (2018). Biomechanical analysis of augments in revision total knee arthroplasty. *J. Biomech. Eng.* 140 (11), 111006. doi:10.1115/1.4040966

Innocenti, B., Bori, E., and Pianigiani, S. (2022). Biomechanical analysis of the use of stems in revision total knee arthroplasty. *Bioeng. (Basel)* 9 (6), 259. doi:10.3390/bioengineering9060259

Insall, J. N., Binazzi, R., Soudry, M., and Mestriner, L. A. (1985). Total knee arthroplasty. *Clin. Orthop. Relat. Res.* 192, 13–22. doi:10.1097/00003086-198501000-00003

Johnston, H., Abdelgaied, A., Pandit, H., Fisher, J., and Jennings, L. M. (2019). The effect of surgical alignment and soft tissue conditions on the kinematics and wear of a fixed bearing total knee replacement. *J. Mech. Behav. Biomed. Mater* 100, 103386. doi:10.1016/j.jmbbm.2019.103386

Kang, K. T., Son, J., Baek, C., Kwon, O. R., and Koh, Y. G. (2018a). Femoral component alignment in unicompartmental knee arthroplasty leads to biomechanical change in contact stress and collateral ligament force in knee joint. *Arch. Orthop. Trauma Surg.* 138 (4), 563–572. doi:10.1007/s00402-018-2884-2

Kang, K. T., Son, J., Koh, Y. G., Kwon, O. R., Kwon, S. K., Lee, Y. J., et al. (2018b). Effect of femoral component position on biomechanical outcomes of unicompartmental knee arthroplasty. *Knee* 25 (3), 491–498.

Kang, K. S., Tien, T., Lee, M., Lee, K. Y., Kim, B., and Lim, D. (2019). Suitability of metal block augmentation for large uncontained bone defect in revision total knee arthroplasty (TKA). *J. Clin. Med.* 8 (3), 384. doi:10.3390/jcm8030384

Kang, K. T., Koh, Y. G., Nam, J. H., Kwon, S. K., and Park, K. K. (2020). Kinematic alignment in cruciate retaining implants improves the biomechanical function in total knee arthroplasty during gait and deep knee bend. *J. Knee Surg.* 33 (3), 284–293. doi:10.1055/s-0039-1677846

Kim, K. T., Lee, S., Lee, J. I., and Kim, J. W. (2016). Analysis and treatment of complications after unicompartmental knee arthroplasty. *Knee Surg. Relat. Res.* 28 (1), 46–54. doi:10.5792/ksrr.2016.28.1.46

Klasan, A., Kapshammer, A., Miron, V., and Major, Z. (2022). Kinematic alignment in total knee arthroplasty reduces polyethylene contact pressure by increasing the contact area, when compared to mechanical alignment-A finite element analysis. *J. Pers. Med.* 12 (8), 1285. doi:10.3390/jpm12081285

Koh, Y. G., Park, K. M., Lee, H. Y., and Kang, K. T. (2019). Influence of tibiofemoral congruency design on the wear of patient-specific unicompartmental knee arthroplasty using finite element analysis. *Bone Jt. Res.* 8 (3), 156–164. doi:10.1302/2046-3758.83.bjr-2018-0193.r1

Koh, Y. G., Lee, J. A., Lee, H. Y., Chun, H. J., Kim, H. J., and Kang, K. T. (2020). Anatomy-mimetic design preserves natural kinematics of knee joint in patient-specific mobile-bearing unicompartmental knee arthroplasty. *Knee Surg. Sports Traumatol. Arthrosc.* 28 (5), 1465–1472. doi:10.1007/s00167-019-05540-0

Koh, Y. G., Lee, J. A., Lee, H. Y., Suh, D. S., Park, J. H., and Kang, K. T. (2022). Finite element analysis of femoral component sagittal alignment in mobile-bearing total knee arthroplasty. *Biomed. Mater Eng.* 33 (3), 195–207. doi:10.3233/BME-211280

Kwon, O. R., Kang, K. T., Son, J., Kwon, S. K., Jo, S. B., Suh, D. S., et al. (2014). Biomechanical comparison of fixed- and mobile-bearing for unicomparmental knee arthroplasty using finite element analysis. *J. Orthop. Res.* 32 (2), 338–345. doi:10.1002/jor.22499

Li, M. G., Yao, F., Joss, B., Ioppolo, J., Nivbrant, B., and Wood, D. (2006). Mobile vs. fixed bearing unicondylar knee arthroplasty: A randomized study on short term clinical outcomes and knee kinematics. *Knee* 13 (5), 365–370. doi:10.1016/j.knee.2006.05.003

Liu, Y., Zhang, A., Wang, C., Yin, W., Wu, N., Chen, H., et al. (2020). Biomechanical comparison between metal block and cement-screw techniques for the treatment of tibial bone defects in total knee arthroplasty based on finite element analysis. *Comput. Biol. Med.* 125, 104006. doi:10.1016/j.compbiomed.2020.104006

Liu, Y., Chen, B., Wang, C., Chen, H., Zhang, A., Yin, W., et al. (2021). Design of porous metal block augmentation to treat tibial bone defects in total knee arthroplasty based on topology optimization. *Front. Bioeng. Biotechnol.* 9, 765438. doi:10.3389/fbioe.2021.765438

Lombardi, A. V., Jr., MacDonald, S. J., Lewallen, D. G., and Fehring, T. K. (2019). Four challenges in revision total knee arthroplasty: Exposure, safe and effective component removal, bone deficit management, and fixation. *Instr. Course Lect.* 68, 217–230.

Longo, U. G., Ciuffreda, M., D'Andrea, V., Mannering, N., Locher, J., and Denaro, V. (2017). All-polyethylene versus metal-backed tibial component in total knee arthroplasty. *Knee Surg. Sports Traumatol. Arthrosc.* 25 (11), 3620–3636. doi:10.1007/s00167-016-4168-0

Ma, P., Muheremu, A., Zhang, S., Zheng, Q., Wang, W., and Jiang, K. (2022). Biomechanical effects of fixed-bearing femoral prostheses with different coronal positions in medial unicompartmental knee arthroplasty. *J. Orthop. Surg. Res.* 17 (1), 150. doi:10.1186/s13018-022-03037-0

Ma, J., Xu, C., Zhao, G., Xiao, L., and Wang, J. (2023). The optimal size of screw for using cement-screw technique to repair tibial defect in total knee arthroplasty: A finite element analysis. *Heliyon* 9 (3), e14182. doi:10.1016/j.heliyon.2023.e14182

Mancuso, F., Beltrame, A., Colombo, E., Miani, E., and Bassini, F. (2017). Management of metaphyseal bone loss in revision knee arthroplasty. *Acta Biomed.* 88 (2S), 98–111. doi:10.23750/abm.v88i2-S.6520

Mason, J. B., and Fehring, T. K. (2006). Removing well-fixed total knee arthroplasty implants. *Clin. Orthop. Relat. Res.* 446, 76–82. doi:10.1097/01.blo.0000214413.06464.ce

Mell, S. P., Wimmer, M. A., Jacobs, J. J., and Lundberg, H. J. (2022). Optimal surgical component alignment minimizes TKR wear - an *in silico* study with nine alignment parameters. *J. Mech. Behav. Biomed. Mater* 125, 104939. doi:10.1016/j.jmbbm.2021.104939

Mizu-Uchi, H., Ma, Y., Ishibashi, S., Colwell, C. W., Jr., Nakashima, Y., and D'Lima, D. D. (2022). Tibial sagittal and rotational alignment reduce patellofemoral stresses in posterior stabilized total knee arthroplasty. *Sci. Rep.* 12 (1), 12319. doi:10.1038/s41598-022-15759-6

Nakamura, S., Tian, Y., Tanaka, Y., Kuriyama, S., Ito, H., Furu, M., et al. (2017). The effects of kinematically aligned total knee arthroplasty on stress at the medial tibia: A case study for varus knee. *Bone Jt. Res.* 6 (1), 43–51. doi:10.1302/2046-3758.61.BJR-2016-0090.R1

Neufeld, M. E., Albers, A., Greidanus, N. V., Garbuz, D. S., and Masri, B. A. (2018). A comparison of mobile and fixed-bearing unicompartmental knee arthroplasty at a minimum 10-year follow-up. *J. Arthroplasty* 33 (6), 1713–1718. doi:10.1016/j.arth.2018.01.001

Panni, A. S., Ascione, F., Rossini, M., Braile, A., Corona, K., Vasso, M., et al. (2018). Tibial internal rotation negatively affects clinical outcomes in total knee arthroplasty: A systematic review. *Knee Surg. Sports Traumatol. Arthrosc.* 26 (6), 1636–1644. doi:10.1007/s00167-017-4823-0

Park, K. K., Koh, Y. G., Park, K. M., Park, J. H., and Kang, K. T. (2019). Biomechanical effect with respect to the sagittal positioning of the femoral component in unicompartmental knee arthroplasty. *Biomed. Mater Eng.* 30 (2), 171–182. doi:10.3233/BME-191042

Park, H. J., Bae, T. S., Kang, S. B., Baek, H. H., Chang, M. J., and Chang, C. B. (2021). A three-dimensional finite element analysis on the effects of implant materials and designs on periprosthetic tibial bone resorption. *PLoS One* 16 (2), e0246866. doi:10.1371/journal.pone.0246866

Pena, E., Calvo, B., Martinez, M. A., and Doblare, M. (2006). A three-dimensional finite element analysis of the combined behavior of ligaments and menisci in the healthy human knee joint. *J. Biomech.* 39 (9), 1686–1701. doi:10.1016/j.jbiomech.2005.04.030

Price, A. J., and Svard, U. (2011). A second decade lifetable survival analysis of the Oxford unicompartmental knee arthroplasty. *Clin. Orthop. Relat. Res.* 469 (1), 174–179. doi:10.1007/s11999-010-1506-2

Price, A. J., Alvand, A., Troelsen, A., Katz, J. N., Hooper, G., Gray, A., et al. (2018). Knee replacement. *Lancet* 392 (10158), 1672–1682. doi:10.1016/s0140-6736(18)32344-4

Qiu, Y. Y., Yan, C. H., Chiu, K. Y., and Ng, F. Y. (2012). Review article: Treatments for bone loss in revision total knee arthroplasty. *J. Orthop. Surg. Hong. Kong* 20 (1), 78–86. doi:10.1177/230949901202000116

Ranawat, C. S., Komistek, R. D., Rodriguez, J. A., Dennis, D. A., and Anderle, M. (2004). *In vivo* kinematics for fixed and mobile-bearing posterior stabilized knee prostheses. *Clin. Orthop. Relat. Res.* 418 (418), 184–190. doi:10.1097/00003086-200401000-00030

Rybicki, E. F., Simonen, F. A., and Weis, E. B., Jr. (1972). On the mathematical analysis of stress in the human femur. *J. Biomech.* 5 (2), 203–215. doi:10.1016/0021-9290(72)90056-5

Samiezadeh, S., Bougherara, H., Abolghasemian, M., D'Lima, D., and Backstein, D. (2019). Rotating hinge knee causes lower bone-implant interface stress compared to constrained condylar knee replacement. *Knee Surg. Sports Traumatol. Arthrosc.* 27 (4), 1224–1231. doi:10.1007/s00167-018-5054-8

Sano, M., Oshima, Y., Murase, K., Sasatani, K., and Takai, S. (2020). Finite-Element analysis of stress on the proximal tibia after unicompartmental knee arthroplasty. *J. Nippon. Med. Sch.* 87 (5), 260–267. doi:10.1272/jnms.JNMS.2020_87-504

Scott, R. D., and Santore, R. F. (1981). Unicondylar unicompartmental replacement for osteoarthritis of the knee. *J. Bone Jt. Surg. Am.* 63 (4), 536–544. doi:10.2106/00004623-198163040-00004

Sekiguchi, K., Nakamura, S., Kuriyama, S., Nishitani, K., Ito, H., Tanaka, Y., et al. (2019). Effect of tibial component alignment on knee kinematics and ligament tension in medial unicompartmental knee arthroplasty. *Bone Jt. Res.* 8 (3), 126–135. doi:10.1302/2046-3758.83.BJR-2018-0208.R2

Shee, C. D., Wright, A. M., and Cameron, I. R. (1990). The effect of aminophylline on function and intracellular pH of the rat diaphragm. *Eur. Respir. J.* 3 (9), 991–996. doi:10.1183/09031936.93.03090991

Small, S. R., Berend, M. E., Ritter, M. A., and Buckley, C. A. (2010). A comparison in proximal tibial strain between metal-backed and all-polyethylene anatomic graduated component total knee arthroplasty tibial components. *J. Arthroplasty* 25 (5), 820–825. doi:10.1016/j.arth.2009.06.018

Song, Y. D., Nakamura, S., Kuriyama, S., Nishitani, K., Ito, H., Morita, Y., et al. (2021). Biomechanical comparison of kinematic and mechanical knee alignment techniques in a computer simulation medial pivot total knee arthroplasty model. *J. Knee Surg.* doi:10.1055/s-0041-1740392

Srivastava, A., Lee, G. Y., Steklov, N., Colwell, C. W., Jr., Ezzet, K. A., and D'Lima, D. D. (2012). Effect of tibial component varus on wear in total knee arthroplasty. *Knee* 19 (5), 560–563. doi:10.1016/j.knee.2011.11.003

Stukenborg-Colsman, C., Ostermeier, S., Hurschler, C., and Wirth, C. J. (2002). Tibiofemoral contact stress after total knee arthroplasty: Comparison of fixed and mobile-bearing inlay designs. *Acta Orthop. Scand.* 73 (6), 638–646. doi:10.3109/17453670209178028

Tokunaga, S., Rogge, R. D., Small, S. R., Berend, M. E., and Ritter, M. A. (2016). A finite-element study of metal backing and tibial resection depth in a composite tibia following total knee arthroplasty. *J. Biomech. Eng.* 138 (4), 041001. doi:10.1115/1.4032551

Vince, K. G., and Cyran, L. T. (2004). Unicompartmental knee arthroplasty: New indications, more complications? *J. Arthroplasty* 19 (4), 9–16. doi:10.1016/j.arth.2004.02.022

Walker, P. S., Parakh, D. S., Chaudhary, M. E., and Wei, C. S. (2011). Comparison of interface stresses and strains for onlay and inlay unicompartmental tibial components. *J. Knee Surg.* 24 (2), 109–115. doi:10.1055/s-0031-1280873

Wang, J. Y., Qi, Y. S., Bao, H. R. C., Xu, Y. S., Wei, B. G., Wang, Y. X., et al. (2021). The effects of different repair methods for a posterior root tear of the lateral meniscus on the biomechanics of the knee: A finite element analysis. *J. Orthop. Surg. Res.* 16 (1), 296. doi:10.1186/s13018-021-02435-0

Weale, A. E., Murray, D. W., Baines, J., and Newman, J. H. (2000). Radiological changes five years after unicompartmental knee replacement. *J. Bone Jt. Surg. Br.* 82 (7), 996–1000. doi:10.1302/0301-620x.82b7.10466

Yilmaz, B., Kesikburun, S., Koroglu, O., Yasar, E., Goktepe, A. S., and Yazicioglu, K. (2016). Effects of two different degrees of lateral-wedge insoles on unilateral lower extremity load-bearing line in patients with medial knee osteoarthritis. *Acta Orthop. Traumatol. Turc* 50 (4), 405–408. doi:10.1016/j.aott.2016.06.004

Zhao, G., Yao, S., Ma, J., and Wang, J. (2022). The optimal angle of screw for using cement-screw technique to repair tibial defect in total knee arthroplasty: A finite element analysis. *J. Orthop. Surg. Res.* 17 (1), 363. doi:10.1186/s13018-022-03251-w

Zheng, C., Ma, H. Y., Du, Y. Q., Sun, J. Y., Luo, J. W., Qu, D. B., et al. (2020). Finite element assessment of the screw and cement technique in total knee arthroplasty. *Biomed. Res. Int.* 2020, 3718705. doi:10.1155/2020/3718705

Zhu, G. D., Guo, W. S., Zhang, Q. D., Liu, Z. H., and Cheng, L. M. (2015). Finite element analysis of mobile-bearing unicompartmental knee arthroplasty: The influence of tibial component coronal alignment. *Chin. Med. J. Engl.* 128 (21), 2873–2878. doi:10.4103/0366-6999.168044

Frontiers in
Bioengineering and Biotechnology

Accelerates the development of therapies, devices, and technologies to improve our lives

A multidisciplinary journal that accelerates the development of biological therapies, devices, processes and technologies to improve our lives by bridging the gap between discoveries and their application.

Discover the latest Research Topics

See more →

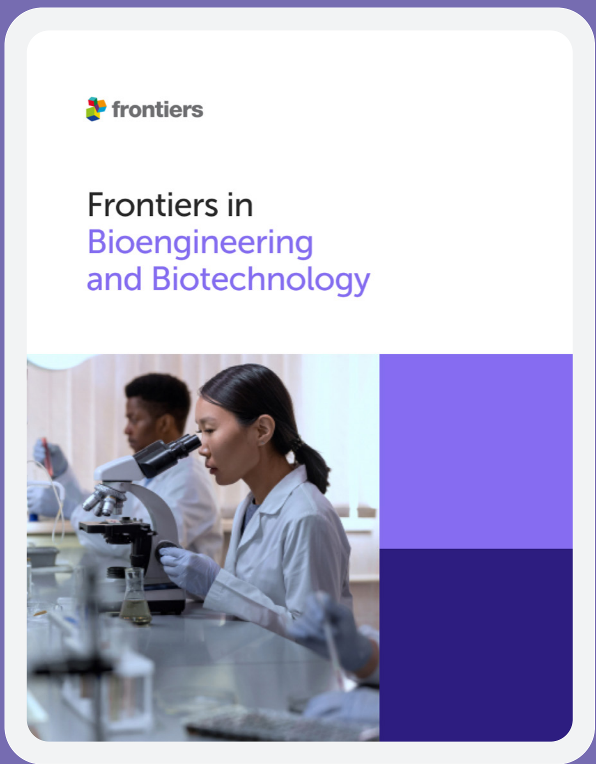

Frontiers

Avenue du Tribunal-Fédéral 34
1005 Lausanne, Switzerland
frontiersin.org

Contact us

+41 (0)21 510 17 00
frontiersin.org/about/contact